Bei Zeng, Xie Chen, Duan-Lu Zhou,
Xiao-Gang Wen

Quantum Information Meets Quantum Matter

From Quantum Entanglement to Topological Phase in Many-Body Systems

February 11, 2022

Springer

Preface

After decades of development, quantum information science and technology has now come to its golden age. It is not only widely believed that quantum information processing offers the secure and high rate information transmission, fast computational solution of certain important problems, which are at the heart of the modern information technology. But also, it provides new angles, tools and methods which help in understanding other fields of science, among which one important area is the link to modern condensed matter physics.

For a long time, people believe that all phases of matter are described by Landau's symmetry-breaking theory, and the transitions between those phases are described by the change of those symmetry-breaking orders. However, after the discovery of fractional quantum Hall effect, it was realized in 1989 that the fractional quantum Hall states contain a new type of order (named topological order) which is beyond Landau symmetry breaking theory. Traditional many-body theory for condensed matter systems is mostly based on various correlation functions, which suite Landau symmetry breaking theory very well. But this kind of approaches is totally inadequate for topological orders, since all different topological orders have the similar short-range correlations.

The traditional condensed matter theory mostly only consider two kinds of many-body states: product states (such as in various mean-field theories) and states obtained by filling orbitals (such as in Fermi liquid theory). Those two types of states fail to include the more general topologically ordered states. So the big question is, can we understand what is missing in the above two types of states, so that they fail to capture the topological order?

What quantum information science brings is the information-theoretic understanding of correlation, and a new concept called 'entanglement', which is a pure quantum correlation that has no classical counterpart. Such input from quantum information science led to a recent realization that the new topological order in some strongly correlated systems is nothing but the pattern of many-body entanglement. The study of topological order and the related new quantum phases is actually a study of patterns of entanglement. The non-trivial patterns of entanglement is the root of many highly novel phenomena in topologically ordered phases (such

as fractional quantum Hall states and spin liquid states), which include fractional charge, fractional statistics, protected gapless boundary excitations, emergence of gauge theory and Fermi statistics from purely bosonic systems, etc.

The connection between quantum information science and condensed matter physics is not accidental, but has a very deep root. Quantum theory has explained and unified many microscopic phenomena, ranging from discrete spectrum of Hydrogen atom, black-body radiation, to interference of electron beam, *etc* . However, what quantum theory really unifies is information and matter. We know that a change or frequency is a property of information. But according to quantum theory, frequency corresponds to energy. According to the theory of relativity, energy correspond to mass. Energy and mass are properties of matter. In this sense frequency leads to mass and information becomes matter.

But do we believe that matter (and the elementary particles that form the matter) all come from qubits? Is it possible that qubits are the building blocks of all the elementary particles? If matter were formed by simple spin-0 bosonic elementary particles, then it was quite possible that the spin-0 bosonic elementary particles, and the matter that they form, all came from qubits. We can simply view the space as a collection of qubits and the 0-state of qubits as the vacuum. Then the 1-state of qubit will correspond to a spin-0 bosonic elementary particle in space. But our world is much more complicated. The matter in our world is formed by particles that have two really strange properties: Fermi statistics and fractional angular momentum (spin-1/2). Our world also have light, which correspond to spin-1 particles that strangely only have two components. Such spin-1 particles are called gauge bosons.

Can space formed by simple qubits produce spin-1/2 fermions and spin-1 gauge bosons? In the last 20 years (and as explained in this book), we start to realize that although qubits are very simple, their organization – their quantum entanglement – can be extremely rich and complex. The long-range quantum entanglement of qubits make it possible to use simple qubits to produce spin-1/2 fermions and spin-1 gauge bosons, as well as the matter formed by those elementary particles.

Thousands of research papers studying the properties of quantum entanglement has been published in the past two decades. Notable progress includes, but not limited to, extensive study of correlation and entanglement properties in various strongly-correlated systems, development of concepts of entanglement area law which results in a new tool called tensor network method, the role of entanglement play in quantum phase transitions, the concept of long range entanglement and its use in the study of topological phase of matter. Also, extensive attentions have been attracted on the new states of quantum matter and the emergence of fractional quantum numbers and fractional/Fermi statistics, with many published papers during the last decades along these directions.

It is not possible to include all these exciting developments in a single book. The scope of this book is rather, to introduce some general concepts and basic ideas and methods that the viewpoints of quantum information scientists have on condensed matter physics. The style of quantum information theorists treating physics problem is typically more mathematical than usual condensed matter physicists. One may understand this as traditional mathematical physics with tools added from quan-

tum information science. Typical models are studied, but more general perspectives are also emphasized. For instance, one important problem widely studied is the so-called 'local Hamiltonian problem', which is based on the real physical situations where Hamiltonians involve only local interactions with respect to certain lattice geometry. General theory regarding this problem is developed, which provides powerful tools in understanding the common properties of these physical systems.

This book aims to introduce the quantum information science viewpoints on condensed matter physics to graduate students in physics (or interested researchers). We keep the writing in a self-consistent way, requiring minimum background in quantum information science. Basic knowledge in undergraduate quantum physics and condensed matter physics is assumed. We start slowly from the basic ideas in quantum information theory, but wish to eventually bring the readers to the frontiers of research in condensed matter physics, including topological phases of matter, tensor networks, and symmetry-protected topological phases.

Structure of the Book

The book has five parts, each includes several chapters. We start from Part I for introducing the basic concepts in quantum information that will be later used in the book. Quantum information science is a very large field and many new ideas and concepts are developed. For a full reference one may turn to other classical sources such as 'Quantum Computation and Quantum Information' by Nielsen & Chuang and Preskill's lecture notes for the course of 'Quantum Computation' at Caltech. The goal of this part is to introduce minimum knowledge that will quickly bring the readers into the more exiting topics of application of quantum information science to condensed matter physics.

Three main topics are discussed: Chapter 1 summarizes useful tools in the theory of correlation and entanglement. It introduces the basic idea of correlation from information-theoretic viewpoint, and the basic idea of entanglement and how to quantify it. Chapter 2 discusses quantum information viewpoint of quantum evolution and introduces the idea of quantum circuits, and the important concept of circuit depth. Chapter 3 summarizes useful tools in the theory of quantum error correction, and the toric code is introduced for the first time.

Then Part II starts from Chapter 4, discussing a general viewpoint of the local Hamiltonian problem, which is at the heart of the link between quantum information science and condensed matter physics. A local Hamiltonian involves only geometrically local few-body interactions. We discuss the ways of determining the ground-state energy of local Hamiltonians, and their hardness. Theories have been developed in quantum information science to show that even with the existence of a quantum computer, there is no efficient way of finding the ground-state energy for a local Hamiltonian in general. However, for practical cases, special structures may lead to simpler method, such as Hartree's mean-field theory. A special kind of local Hamiltonians, called the frustration-free Hamiltonian, where the ground state of the Hamiltonian also minimizes the energy of each local term of the Hamiltonian,

is also introduced. These Hamiltonians play important role in later chapters of the book.

In Chapter 5, we start to focus our attention on systems of infinite size (i.e. the thermodynamic limit), which are the central subject of study in condensed matter physics. We introduce important notions for the discussion of such quantum many-body systems, like locality, correlation, gap, etc. In particular, we discuss in depth the notion of many-body entanglement, which is one of the most important distinction between quantum and classical many-body systems, and is the key to the existence of topological order, a subject which we study in detail in this book. We discuss the important concepts of entanglement area law, and the topological entanglement entropy. We study the topological entanglement entropy from an information-theoretic viewpoint, which leads to generalizations of topological entanglement entropy that can also be used to study systems without topological order. The corresponding information-theoretic quantity, called the quantum conditional mutual information, provides a universal detector of non-trivial entanglement in many-body systems.

Entanglement is especially important for the description and understanding of systems with a special type of order – topological order. Topological order has emerged as an exciting research topic in condensed matter physics for several decades. People have approached the problem using various methods but many important issues still remain widely open. Recent developments show that quantum information ideas can contribute greatly to the study of topological order, the topological entanglement entropy discussed in Chapter 5 is such an example. Part III will further discuss the entanglement properties of topological order in detail.

In Chapter 6, we give a full review of the basic ideas of topological order from the perspective of modern condensed matter theory. Through this part, we hope to give readers a general idea of what topological order is, why physicists are interested in it, and what the important issues are to be solved. This chapter is devoted to the basic concepts and the characteristic properties of topological order. After setting the stage up on both the quantum information and condensed matter physics side, we are then ready to show that how the combination of these two leads to new discoveries.

In Chapter 7, we are going to show how quantum information ideas can be used to reformulate and characterize topological order and what we have learned from this new perspective, which leads to a microscopic theory of topological order. A new formulation of the basic notion of phase and phase transition in terms of quantum information concepts is given, based on the concept of local unitary equivalence between systems in the same gapped phase. We are going to introduce the concept of gapped quantum liquids, and show that topological order corresponds to stable gapped quantum liquids. We also show that symmetry-breaking orders correspond to unstable quantum liquids. This allows us to study both symmetry-breaking and topological order in a same general framework. We also discuss the concept of long-range entanglement, and show that topological orders are patterns of long-range entanglement.

After that, in part IV, we study gapped phases in one and two dimension (1D and 2D) using the tensor network formalism. First, we focus on one dimensional systems in Chapter 8. It turns out the matrix product state – the one dimensional version of the tensor network representation – provides a complete and precise characterization of 1D gapped systems so that we can actually classify all gapped phases in 1D. In particular, we show, after a careful introduction to the matrix product formalism, that there is no topological order in 1D and all gapped states in 1D belong to the same phase (if no symmetry is required). In Chapter 9, we move on to two dimensions, where things become much more complicated and also more interesting. The tensor product state is introduced, whose similarity and difference with matrix product states is emphasized. Apart from the short range entangled phases like symmetry breaking phases, the tensor network states can also represent topological phases in 2D. We discuss examples of such tensor product states and how the topological order is encoded in the local tensors. In Chapter 10, global symmetry is introduced into the system. It was realized that short range entangled states can be in different phases even when they have the same symmetry. Examples of such 'Symmetry Protected Topological (SPT) Phases' are introduced both in 1D and 2D. Moreover, we show that 1D SPT can be fully classified using the matrix product state formalism and a systematic construction exists for SPT states in 2D and higher dimensions in interacting bosonic systems.

The last part (Chapter 11) is devoted to an overview of physics and an outlook how many-body entanglement may influence how we view our world. We outline the developement of our world views in the last a few hundreds of years: from all matter being fromed by particles to the discovery of wave-like matter (electromanetics waves and gravitational waves), and to the unification of particle-like matter and wave-like matter by quantum theory. We feel that we are in the process of a new revolution where quantum information, matter, interactions, and even space itself will be all unified. To make sush a point, we discuss some simple examples of more general highly entangled quantum states of matter, which can be gapless. This leads to a unification of light and electrons (or all elementary particles) by qubits that form the space. Those examples demonstrate a unification of information and matter, the central theme of this book.

The unified theme of quantum information and quantum matter represents a totally new world in physics. This book tries to introduce this new world to the reader. However, we can only scratch the surface of this new world at this stage. A lot of new developments are needed to truly reveal this exciting new world. Even a new mathematical language is needed for such a unified understanding of information and matter. A comprehensive theory of highly entangled quantum states of matter requires such a mathematical theory which is yet to be developed.

February 2018

Bei Zeng
Xie Chen
Duan-Lu Zhou
Xiao-Gang Wen

Acknowledgements

This is an incomplete list of people that we owe thanks to. Updated list will be included in the published version of Springer.

B.Z. X.-G.W. X.C. would like to thank Institute for Advanced Study at Tsinghua University (IASTU), Beijing, for hospitality. Part of the book has been written during our visit to IASTU for the past five years.

We are grateful to Jianxin Chen, Runyao Duan, David Gosset, Zheng-Cheng Gu, Jame Howard, Zhengfeng Ji, Joel Klassen, Chi-Kwong Li, Yiu Tung Poon, Yi Shen, Changpu Sun, Zhaohui Wei, Zhan Xu, and Nengkun Yu for valuable discussions during writing the first draft of the book.

We appreciate the comments received for Version 1 and Version 2 of the book draft, from Oliver Buerschaper, Abdulah Fawaz, Nicole Yunger Halpern, Junichi Iwasaki, Zeyang Li, David Meyer, Mikio Nakahara, Tomotoshi Nishino,Fernando Pastawski, Mehdi Soleimanifar, Dawson Wang, and Youngliang Zhang.

We appreciate the comments received for Version 3 of the book draft, from Stephen Kwaku Amponsah, Zhi-An Jia, Oleg Kabermik, David Meyer, Mikio Nakahara, Hal Tasaki, Julien Vidal, Mark Wilde, and Mingli Yuan.

We are grateful to Haijing Song for making part of the figures in Chapters 7 and 10, and Zheng An for making part of the figures in Chapters 8 and 9.

We acknowledge volunteers from Swarma Club for making part of the figures in Chapter 11. They are: Song Cheng (Figures 11.9, 11.11(b)),Yanping Dai (Figures 11.4(a,b,c), 11.26(c)),Lei Dong (Figures 11.1, 11.2(a,c)), Yueyuan Hou (Figure 11.6(c),11.25(c)), Weiyi Qiu (Figures 11.7(a),11.26(a), 11.14(a,b,c,d)), Jiannan Wang (Figure 11.3?11.2(b), 11.3, 11.5(a)), Yizhuang You (Figures 11.5(d), 11.10, 11.11(a), 11.25(a,b), 11.26(c)) , Yanbo Zhang (Figures11.5(b), 11.6(a) 11.8(c), 11.11(a), 11.13, 11.26(b)), Yongjie Zhang (Figure 11.25(g)), and Bin Zhao (Figure 11.11(a)).

More comments are welcome.

Contents

Part I
Basic Concepts in Quantum Information Theory

Chapter 1
Correlation and Entanglement

Abstract In this chapter we discuss correlation and entanglement in many-body systems. We start from introducing the concepts ofone independence and correlation in probability theory, which leads to some understanding of the concepts of entropy and mutual information, which are of vital importance in modern information theory. This builds a framework that allows us to look at the theory of a new concept, called quantum entanglement, which serves as a fundamental object that we use to develop new theories for topological phase of matter later in this book.

1.1 Introduction

The concept of correlation is used ubiquitously in almost every branch of sciences. Intuitively, correlations describe the dependence of certain properties for different parts of a composite object. If these properties of different parts are independent of each other, then we say that there do not exist correlations between (or among) them. If they are correlated, then how to characterize the correlation, both qualitatively and quantitatively, becomes an essential task.

Different branches of science usually have their own way of characterizing correlation, in particular related to things that scientists in different fields do care about. For instance, in many-body physics, people usually characterize correlations in terms of correlation functions $\langle O_i O_j \rangle - \langle O_i \rangle \langle O_j \rangle$, where O_i is some observable on the site i, and $\langle \cdot \rangle$ denotes the expectation value with respect to the quantum state of the system. The behavior of these correlation functions gives lots of useful information such as the correlation length.

In this chapter we would like to treat correlation in a more formal way. It will later become clearer that doing so does help with a better understanding of many-body physics. In other words, there is something beyond just correlation function to look at, which turns out to provide new information and characterization of some rather interesting new physical phenomena, such as the topological phase of matter.

We start looking at correlation in terms of elementary probability theory. First of all it is the formal mathematical language of characterizing the concept of independence and correlation. This formal language will then be further linked to the concept of entropy and mutual information, which are key concepts in information theory. Physicists are indeed familiar with the concept of entropy, which is in some sense a measure of how chaotic a system is, or how lack of knowledge we are regarding the system. By looking at it slight differently, it is then a measure of how much information the system carries – in other words, because the lack of knowledge, the system carries some 'information' to tell.

What might be quite surprising to physicists is that the concept of 'entropy' lays the foundation to modern information theory, which eventually guarantees the correct output of our computers that we rely on for our everyday research, and fast communication via cell phone or Internet that we rely on to exchange opinions with our colleagues. Sitting in this information age, we are proud to know that the basic concept in physics helps making all this possible. On the other hand, it is also of vital importance to know 'how'. One simple reason is that we physicists are always curious, which is the essential inert driving force of our research. But most importantly, one can borrow the ideas back from information theory to add new ingredient to our theory of fundamental physics.

One important success in quantum information is the development of the theory of entanglement. 'Entanglement' is widely heard nowadays but what we would like to emphasize here is that there is nothing mysterious, in a sense that almost all quantum many-body systems are entangled. Perhaps you are still quite happy with mean-field theory, which is valid in most cases, where no entanglement needs to be considered. This does not mean that the system is not entangled, but just perhaps not strongly entangled. On the other hand, you may also be aware of the headache in the theory for strongly-correlated systems, where the systems turn out to be highly entangled.

We would also like to introduce the theory of entanglement in a more formal manner, which naturally follows the information theoretic point of view. One good thing is that this will explain the difference between 'classical correlation' and 'quantum entanglement'. More importantly, it builds on a framework of 'tensor product structure' of Hilbert space for many-body systems, which is natural but not emphasized in the traditional framework of many-body theory. It will later become clearer that this 'tensor product structure' will indeed bring new concepts for understanding many-body physics.

We will start our discussion from the simplest case, where we only consider two objects and their independence/correlation. We look at the classical correlation case first, and then move to the case of quantum systems, where the concept of entanglement can be naturally introduced. Following up all that, we move into looking at the theory for many-body systems, in terms of both classical correlation and quantum entanglement.

1.2 Correlations in classical probability theory

In this section, we introduce the concepts of independence and correlation in probability theory, and further link it to vital concepts in modern information theory, such as entropy and mutual information.

1.2.1 Joint probability without correlations

We start from looking at the simplest case: two independent objects A and B. Due to conventions of information theory, instead we usually discuss two people, Alice and Bob, performing some joint experiments. In this case, assume that Alice has total d_A possible outcomes, and let us denote the set of these possible outcomes by $\Omega = \{\omega_i, i = 0, 1, \cdots, d_A - 1\}$. For example, the simplest case is that Alice has only two possible outcomes, where $\Omega = \{\omega_0, \omega_1\}$.

Similarly, assume that Bob has total d_B possible outcomes, and denote the set of these possible outcomes for Bob by $\Lambda = \{\lambda_m, m = 0, 1, \cdots, d_B - 1\}$. Again the simplest case is that Bob has only two possible outcomes, i.e. $\Lambda = \{\lambda_0, \lambda_1\}$.

A joint possible outcome for Alice and Bob is (ω_i, λ_m). All such joint possible outcomes form a set that we denote by $\Omega \times \Lambda$, which is the Cartesian product of two sets Ω and Λ. For instance, when $\Omega = \{\omega_0, \omega_1\}$ and $\Lambda = \{\lambda_0, \lambda_1\}$, we have $\Omega \times \Lambda = \{(\omega_0, \lambda_0), (\omega_0, \lambda_1), (\omega_1, \lambda_0), (\omega_1, \lambda_1)\}$. In general, the set $\Omega \times \Lambda$ contains total $d_A d_B$ elements.

The joint probability distribution $p_{AB}(\omega_i, \lambda_m)$ for the joint experiment Alice and Bob perform needs to satisfy the following conditions.

$$p_{AB}(\omega_i, \lambda_m) \geq 0, \tag{1.1}$$

$$\sum_{i=0}^{d_A-1} \sum_{m=0}^{d_B-1} p_{AB}(\omega_i, \lambda_m) = 1. \tag{1.2}$$

The probability for Alice to get the outcome $\omega_i \in \Omega$ is then

$$p_A(\omega_i) = \sum_{m=0}^{d_B-1} p_{AB}(\omega_i, \lambda_m). \tag{1.3}$$

Similarly, the probability for Bob to get the outcome $\lambda_m \in \Lambda$ is

$$p_B(\lambda_m) = \sum_{i=0}^{d_A-1} p_{AB}(\omega_i, \lambda_m). \tag{1.4}$$

As an example, let us again consider the simplest case where $\Omega = \{\omega_0, \omega_1\}$ and $\Lambda = \{\lambda_0, \lambda_1\}$, so $\Omega \times \Lambda = \{(\omega_0, \lambda_0), (\omega_0, \lambda_1), (\omega_1, \lambda_0), (\omega_1, \lambda_1)\}$. One possible choice of the joint probability distribution could be

$$p_{AB}(\omega_0,\lambda_0)=\frac{1}{12},\ p_{AB}(\omega_0,\lambda_1)=\frac{1}{4},\ p_{AB}(\omega_1,\lambda_0)=\frac{1}{6},\ p_{AB}(\omega_1,\lambda_1)=\frac{1}{2}. \quad (1.5)$$

It is easy to check that $\sum_{i=0}^{1}\sum_{m=0}^{1} p_{AB}(\omega_i,\lambda_m)=1$, and for Alice,

$$\begin{aligned} p_A(\omega_0) &= \sum_{m=0}^{1} p_{AB}(\omega_0,\lambda_m)=\frac{1}{12}+\frac{1}{4}=\frac{1}{3},\\ p_A(\omega_1) &= \sum_{m=0}^{1} p_{AB}(\omega_1,\lambda_m)=\frac{1}{6}+\frac{1}{2}=\frac{2}{3}. \end{aligned} \quad (1.6)$$

For Bob,

$$\begin{aligned} p_B(\lambda_0) &= \sum_{i=0}^{1} p_{AB}(\omega_i,\lambda_0)=\frac{1}{12}+\frac{1}{6}=\frac{1}{4},\\ p_B(\lambda_1) &= \sum_{i=0}^{1} p_{AB}(\omega_i,\lambda_1)=\frac{1}{4}+\frac{1}{2}=\frac{3}{4}. \end{aligned} \quad (1.7)$$

Now let us try to examine under which circumstances a joint probability distribution $p_{AB}(\omega_i,\lambda_m)$ has some correlation between the outcomes of Alice's and Bob's or not. Note that when Bob gets the outcome λ_m, the probability for Alice to get the outcome ω_i is then

$$p_{A|B}(\omega_i,\lambda_m)=\frac{p_{AB}(\omega_i,\lambda_m)}{p_B(\lambda_m)}. \quad (1.8)$$

Here $p_{A|B}$ is called the conditional probability distribution for A, conditionally on the outcome of B. Similarly one can write down the conditional probability distribution $p_{B|A}$ for B, conditionally on the outcome of A. That is, when Alice gets the outcome ω_i, the conditional probability for Bob to get the outcome λ_m is

$$p_{B|A}(\lambda_m,\omega_i)=\frac{p_{AB}(\omega_i,\lambda_m)}{p_A(\omega_i)}. \quad (1.9)$$

Now suppose that the joint distribution $p_{AB}(\omega_i,\lambda_m)$ has no correlation at all, then from Alice's point of view, her outcome is independent of Bob's outcome. In other words, whatever Bob's outcome is, the probability distribution of Alice's outcome should be just the same. This means that the conditional probability $p_{A|B}(\omega_i,\lambda_m)$ should not depend on λ_m, i.e.

$$p_{A|B}(\omega_i,\lambda_m)=p_{A|B}(\omega_i,\lambda_n),\forall i,m,n. \quad (1.10)$$

Similarly, from Bob's point of view, one should have

$$p_{B|A}(\lambda_m,\omega_i)=p_{B|A}(\lambda_m,\omega_j),\forall i,j,m. \quad (1.11)$$

We will show that the condition of (1.10) and (1.11) implies that the joint probability distribution equals the product of the probability distributions of each party,

i.e.

$$p_{AB}(\omega_i,\lambda_m) = p_A(\omega_i)\, p_B(\lambda_m), \forall i,m, \tag{1.12}$$

and vice versa. In other words, the conditions (1.11) and (1.12) are just equivalent.

To see this, we first show how to go from (1.11) to (1.12). For $\forall m,i$, we have for $\forall j$,

$$p_{B|A}(\omega_i,\lambda_m) = p_{B|A}(\omega_j,\lambda_m) = \frac{p_{AB}(\omega_j,\lambda_m)}{p_A(\omega_j)}. \tag{1.13}$$

Then

$$p_{B|A}(\omega_i,\lambda_m) = \frac{\sum_{j=0}^{d_A-1} p_{AB}(\omega_j,\lambda_m)}{\sum_{j=0}^{d_A-1} p_A(\omega_j)} = p_B(\lambda_m). \tag{1.14}$$

Inserting (1.14) into (1.9), we will obtain (1.12). To show the converse of going from (1.12) to (1.11): Inserting (1.12) to (1.9), we get $p_{B|A}(\omega_i,\lambda_m) = p_B(\lambda_m)$, which is independent of the index i, i.e., we have (1.11).

Because the indices of A and B can be reversed, we also obtain the equivalence between (1.10) and (1.12). Therefore, the three conditions (1.10), (1.11) and (1.12) are essentially equivalent. In other words, Alice's outcome is independent of Bob's indicates that Bob's outcome is independent of Alice's and vice versa, and both imply that the joint probability distribution equals the product of the probability distributions of each party. We summarize these results in the box below, which will be our starting point for talking about independent probability distributions.

Box 1.1 Independent probability distribution

The following statements are equivalent:

1. There is no correlation in the joint probability distribution $p_{AB}(\omega_i,\lambda_m)$.
2. The probability for Bob's outcome is independent of Alice's outcome:

$$p_{B|A}(\omega_i,\lambda_m) = p_{B|A}(\omega_j,\lambda_m), \forall i,j,m.$$

3. The probability for Alice's outcome is independent of Bob's outcome:

$$p_{A|B}(\omega_i,\lambda_m) = p_{A|B}(\omega_i,\lambda_n), \forall i,m,n.$$

4. The joint probability equals the product of probabilities for the two parties:

$$p_{AB}(\omega_i,\lambda_m) = p_A(\omega_i)\, p_B(\lambda_m), \forall i,m.$$

As an example, one can show that the joint probability distribution given in Eq. (1.5) has no correlation. One can also show that the joint probability distribution given below in Eq. (1.15) does have some correlation.

$$p_{AB}(\omega_0,\lambda_0) = \frac{1}{6},\ p_{AB}(\omega_0,\lambda_1) = \frac{1}{3},\ p_{AB}(\omega_1,\lambda_0) = \frac{1}{4},\ p_{AB}(\omega_1,\lambda_1) = \frac{1}{4}. \tag{1.15}$$

1.2.2 Correlation functions

When the condition given in Eq.(1.12) does not hold, then there must be correlation between the outcomes of Alice and Bob. We would like to examine this condition further by relating it to correlation functions. We first introduce a random variable $X(\Omega)$, which is a real function whose domain is the set of all possible outcomes of Alice. The average value of this random variable can then be given by

$$E(X) = \sum_{i=0}^{d_A-1} p_A(\omega_i) X(\omega_i). \tag{1.16}$$

Sometimes for simplicity one will write Eq. (1.16) as

$$E(X) = \sum_{x\in X} p(x)x, \tag{1.17}$$

where the sum runs over all possible values in X, and indeed $p(x) = p(X(\omega_i) = x) = p_A(\omega_i)$. Here we assume that the correspondence between ω_i and x is one-to-one.

Similarly, a random variable $Y(\Lambda)$, a real function whose domain is the set of all possible outcomes of Bob, has the average value

$$E(Y) = \sum_{m=0}^{d_B-1} p_B(\lambda_m) Y(\lambda_m), \tag{1.18}$$

and for simplicity we can write

$$E(Y) = \sum_{y\in Y} p(y)y, \tag{1.19}$$

where the sum runs over all possible values in Y, and indeed $p(y) = p(Y(\lambda_i) = y) = p_B(\lambda_i)$.

Note that the direct product of random variables X and Y is a random variable defined on $\Omega \times \Lambda$. Let us write the joint probability distribution

$$p(x,y) = p(X(\omega_i) = x, Y(\lambda_m) = y) = p_{AB}(\omega_i, \lambda_m), \tag{1.20}$$

then the average value of the random variable $X \times Y$ is (denoted by $E(X,Y)$)

$$E(X,Y) = \sum_{y\in Y}\sum_{x\in X} p(x,y)xy. \tag{1.21}$$

As an example, again consider that $\Omega = \{\omega_0, \omega_1\}$. Choose a random variable variable $X(\omega_0) = 0$ and $X(\omega_1) = 1$. A variable like this is called a 'bit', i.e.

Box 1.2 Bit

A bit is a random variable with only two possible values 0 or 1.

Bit is an important concept in information theory – for instance we know that the capacity of our hard drive is measured in terms of 'Gigabytes', which is 10^9 bytes, and 1 byte is actually 8 bits. We will soon be clear what '8 bits' mean. Let us continue the discussion of the above example and further consider $\Lambda = \{\lambda_0, \lambda_1\}$, and another random variable Y which is also a 'bit', i.e. $Y(\lambda_0) = 0$ and $Y(\lambda_1) = 1$. Then the possible values of $X \times Y$ will be $\{(0,0),(0,1),(1,0),(1,1)\}$. And when no confusion arises, we can simply write it as $\{00,01,10,11\}$. Those are all the possible values of 2 bits. In general, if we have N bits, then we have the following:

Box 1.3 N Bits

A possible value of N bits is a binary string of length N, i.e. $x_N x_{N-1} \ldots x_1$, where each x_i is a bit, i.e. $x_i \in \{0,1\}$. There are total 2^N possible values.

Now let us come back to the discussion of the correlation between two random variables X and Y. It is naturally captured by the 'correlation function', which is given by

$$C(X,Y) = E(X,Y) - E(X)E(Y). \tag{1.22}$$

One direct observation is that if the joint distribution $p_{AB}(\omega_i, \lambda_m)$ given by Eq. (1.20) has no correlation, then we should have $C(X,Y) = 0$. To see this, we start from (1.12). Inserting (1.12) into (1.21), we get $E(X \times Y) = E(X)E(Y)$, i.e. $C(X,Y) = 0$.

Indeed, the converse is also true. To show this, note that $\forall j,n$, we take $X(\omega_i) = \delta_{ij}$ and $Y(\lambda_m) = \delta_{mn}$. Then $E(X,Y) = p_{AB}(\omega_j, \lambda_n)$, $E(X) = p_A(\omega_j)$, and $E(Y) = p_B(\lambda_n)$. Hence $C(X,Y) = 0$ implies that $p_{AB}(\omega_j, \lambda_n) = p_A(\omega_j)\, p_B(\lambda_n)$, i.e. the joint probability distribution p_{AB} does not have correlation.

We summarize these observations as below.

Box 1.4 Correlated joint probability distribution

A joint probability distribution p_{AB} does not have correlation if and only if $C(X,Y) = 0,\ \forall X,Y$.

In other words, Eq.(1.12) holds for the joint probability distribution p_{AB} if and only if for any random variables $X(\Omega)$ and $Y(\Lambda)$, the correlation function between them vanishes.

This fact clarifies the role of correlation functions in characterizing and quantifying of correlations. That is, if all the correlation functions vanish, then indeed no correlation exists. However, if one correlation function does not vanish, then the joint probability distribution cannot have the form of Eq.(1.12) hence there must exist some correlation between the outcomes of Alice and Bob.

As an example, one can take both the distributions given in Eq. (1.5) and given in Eq. (1.15). Choose the random variables as the bits discussed above, $X(\omega_0) = 0, X(\omega_1) = 1$ and $Y(\lambda_0) = 0, Y(\lambda_1) = 1$, compute the correlations functions using Eq. (1.22). Then one will get the values 0 (with no correlation) and $-1/24$ (with correlation), respectively.

1.2.3 Mutual information

We have seen that correlation functions can indeed give some information of correlation in the system consisting of two subsystems – one is the system of Alice and the other is of Bob. However, we know that a single correlation function, associated with two given random variables $X(\Omega)$ and $Y(\Lambda)$, is not sufficient to characterize the correlation in the system. One indeed has to look at all the correlation functions in some sense, or has to determine which observables are essentially related to the physics phenomena one cares about.

Interestingly, in the context of information theory established by Shannon, there is a concept which nicely quantifies the degree of correlation with operational meaning for information transmission task between the two subsystems. The concept is called mutual information, which is defined for two random variables $X(\Omega)$ and $Y(\Lambda)$, given by

$$I(X{:}Y) = \sum_{y\in Y}\sum_{x\in X} p(x,y)\log\left(\frac{p(x,y)}{p(x)p(y)}\right). \tag{1.23}$$

Note that similar to the correlation functions, mutual information is defined on two random variables $X(\Omega)$ and $Y(\Lambda)$, however unlike the correlation functions, it does not depend on the choice of $X(\Omega)$ and $Y(\Lambda)$. In other words, what only matters is the joint probability distribution of $X \times Y$ but not the values of the variables $X(\Omega)$ and $Y(\Lambda)$. Therefore, for any two random variables $X(\Omega)$ and $Y(\Lambda)$, Eq.(1.23) returns a single value. In this sense, one can also say that the mutual information is essentially just for the joint probability distribution.

Intuitively, mutual information measures the information that X and Y share. Or in other words, how correlated they are in a sense that how much knowing one of these two variables reduces the uncertainty about knowing the other. For instance, if X and Y are independent, then knowing X does not give any information about Y and vice versa, so their mutual information should be zero. This can be seen from Eq.(1.23) given that Eq.(1.12) now holds. On the other extreme, if X and Y are identical, which is a case of 'perfect correlation', then all information conveyed by X is shared with Y. Or in other words, knowing X determines the value of Y and vice versa. In this case, the mutual information should be the same as the uncertainty contained in Y (or X) alone.

We will need to clarify what it means by 'uncertainty contained in X or Y.' We know in physics uncertainty is quantified by entropy. Information theory does borrow the same concept. For any variable $X(\Omega)$, Shannon's entropy is given by

$$H(X) = -\sum_{x \in X} p(x) \log p(x), \tag{1.24}$$

where, just for convenience, 2 is taken as the base of the log function. Again, this quantity of entropy only depends on the probability distribution of X, but not the very values of X, so this is essentially the entropy (or uncertainty) of the probability distribution.

Now back to the case of 'perfect correlation,' which means mathematically

$$p(x,y) = \begin{cases} 0 & \text{if } x \neq y \\ p(x) = p(y) & \text{otherwise} \end{cases} \tag{1.25}$$

Eq. (1.23) then becomes

$$I(X{:}Y) = \sum_{x \in X} p(x) \log \left(\frac{p(x)}{p(x)p(x)} \right) = H(X). \tag{1.26}$$

That is, the mutual information should be the same as the uncertainty contained in X (or Y) alone.

We would like to look at a simple example of Shannon's entropy in case the random variable X is a bit and the probability distribution is given by

$$p(0) = p, \quad p(1) = 1 - p. \tag{1.27}$$

This gives

$$H(p) = -p \log p - (1-p) \log(1-p). \tag{1.28}$$

The function $H(p)$ is called the 'binary entropy function.' A figure of this function is shown in Fig. 1.1. It vanishes only for $p = 0$ and $p = 1$, and reaches the maximum value only at $p = \frac{1}{2}$ where one has the most 'uncertainty': the probability of getting values 0 and 1 is just half and half.

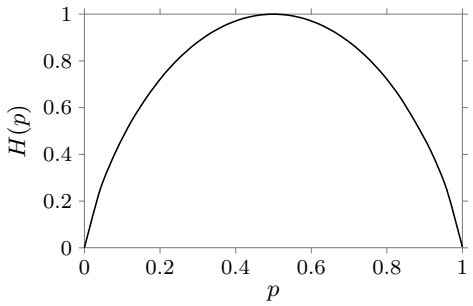

Fig. 1.1 Binary entropy function $H(p)$

In the language of Shannon entropy, for the joint probability distribution $p(x,y)$ of two random variables, the entropy will be (denoted by $H(X,Y)$)

$$H(X,Y) = -\sum_{x\in X}\sum_{y\in Y} p(x,y)\log p(x,y). \tag{1.29}$$

The quantity $H(X|Y=y)$ will then be the entropy of X conditional on the variable of Y taking the value y, i.e.

$$H(X|Y=y) = -\sum_{x\in X} p(x|y)\log p(x|y), \tag{1.30}$$

where $p(x|y) = p_{A|B}(\omega_i,\lambda_m)$, as given in Eq. (1.8). The conditional entropy $H(X|Y)$ is then given by

$$\begin{aligned} H(X|Y) &= \sum_{y\in Y} p(y)H(X|Y=y) = -\sum_{y\in Y}\sum_{x\in X} p(y)p(x|y)\log p(x|y) \\ &= -\sum_{x\in X}\sum_{y\in Y} p(x,y)\log\frac{p(x,y)}{p(y)}. \end{aligned} \tag{1.31}$$

In terms of all these quantities, the mutual information can then be written as

$$\begin{aligned} I(X{:}Y) &= H(X)+H(Y)-H(X,Y) \\ &= H(X)-H(X|Y) \\ &= H(Y)-H(Y|X) \\ &= H(X,Y)-H(X|Y)-H(Y|X). \end{aligned} \tag{1.32}$$

These relationship can be viewed as in Fig. 1.2, which nicely gives intuitively the meaning of all these quantities.

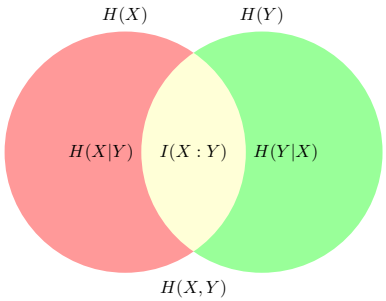

Fig. 1.2 Mutual information: $H(X)$ and $H(Y)$ are plotted as the regions inside two circles, and the mutual information $I(X{:}Y)$ is just their overlap. The quantities $H(X,Y)$, $H(X|Y)$ and $H(Y|X)$ are also illustrated.

Finally, we summarize the meaning of mutual information below.

Box 1.5 Mutual information
The mutual information $I(X{:}Y)$ given by Eqs. (1.23) and (1.32) quantifies the correlation of the joint distribution $p(x,y)$.

1.3 Quantum entanglement

In this section, we move our discussion of correlation into the quantum realm. It will soon become clear that there is much more to expect in the quantum case, due to the superposition principle. Our discussion will eventually lead to a formal study of the concept of entanglement.

1.3.1 Pure and mixed quantum states

In quantum mechanics, the state of a quantum system S is represented by a normalized vector $|\psi\rangle$ in the Hilbert space $\mathscr{H}$. Hence if $|\psi_1\rangle$ and $|\psi_2\rangle$ are two orthogonal quantum states, then any coherent superposition of the two states

$$c_1|\psi_1\rangle + c_2|\psi_2\rangle,$$

where c_1 and c_2 are two complex number satisfying $|c_1|^2 + |c_2|^2 = 1$, is also a quantum state. This obvious property for vectors in a Hilbert space is called the superposition principle of quantum states in quantum mechanics, which is a fundamental feature distinguished from classical mechanics.

Let us take a look at the simplest quantum system – a two-level system, which could be a spin-$1/2$ particle (here we only care about the internal states instead of the spatial wavefunction), or a two-level atom (where all the higher excited states are ignored if they never enter into the dynamics we care about). The Hilbert space of the system is then only two-dimensional, with two orthonormal basis states that we denote as $|0\rangle$ and $|1\rangle$ (which could represent, for instance, spin up and spin down for the spin-$1/2$ particle, or ground state and the excited state for the two-level atom).

Any quantum state in this two-dimensional Hilbert space is called 'quantum bit,' or in short 'qubit.'

Box 1.6 Qubit
A qubit is a quantum state in a two-dimensional Hilbert space with orthonormal basis states $|0\rangle$ and $|1\rangle$, which has the form $|\psi\rangle = \alpha|0\rangle + \beta|1\rangle$, where $|\alpha|^2 + |\beta|^2 = 1$.

Unlikely 'bit,' which has only two possible values 0 and 1, a qubit could be in any kind of superposition of the basis states $|0\rangle$ and $|1\rangle$. This is a direct consequence of the quantum superposition principle.

Since $|\alpha|^2 + |\beta|^2 = 1$, we may write $|\psi\rangle$ as

$$|\psi\rangle = e^{i\gamma}\left(\cos\frac{\theta}{2}|0\rangle + e^{i\phi}\sin\frac{\theta}{2}|1\rangle\right), \tag{1.33}$$

where γ, θ, ϕ are real. And by ignoring the overall phase $e^{i\gamma}$ we can simply write

$$|\psi\rangle = \cos\frac{\theta}{2}|0\rangle + e^{i\phi}\sin\frac{\theta}{2}|1\rangle. \tag{1.34}$$

This means that $|\psi\rangle$ corresponds to a point on the unit three-dimensional sphere defined by θ and φ, called the Bloch sphere, as shown in Fig. 1.3.

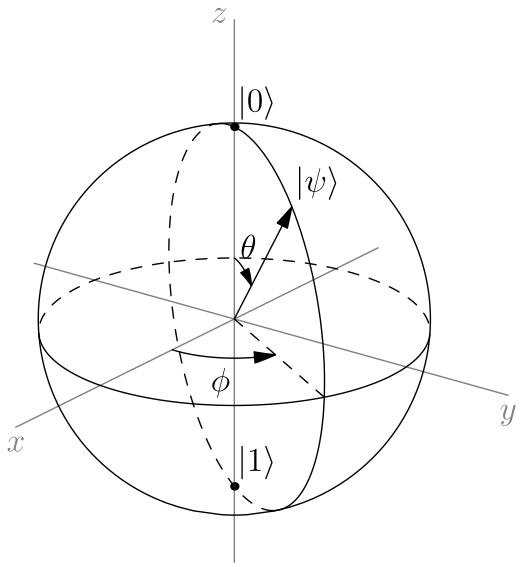

Fig. 1.3 Bloch sphere.

To understand further about the quantum superposition principle, and how a qubit could be different from a bit in terms of probability distribution, let us look at the consequence of quantum measurement. When a quantum measurement of an observable (i.e. a Hermitian operator) M is made on the system S, we will get one of the eigenvalues of the operator M. We know that M can be written as

$$M = \sum_i c_i |\phi_i\rangle\langle\phi_i|, \tag{1.35}$$

where each c_i is an eigenvalue of M and $|\phi_i\rangle$ is the corresponding eigenvector. We know that since M is Hermitian, $\{|\phi_i\rangle\}$ can always be chosen as an orthonormal basis of the Hilbert space, that is,

$$\langle\phi_i|\phi_j\rangle = \delta_{ij} \tag{1.36}$$

and

$$\sum_i |\phi_i\rangle\langle\phi_i| = I. \tag{1.37}$$

The probability of getting the value c_i is then

$$p_i = \langle\psi|\phi_i\rangle\langle\phi_i|\psi\rangle, \tag{1.38}$$

and the identity of Eq.(1.37) directly gives $\sum_i p_i = 1$. That is to say, when a measurement is involved, a quantum state is associated with a classical probability distribution, and the correlations discussed in probability theory naturally generalize to the quantum domain.

Let us look at an example of the qubit case, where $|\psi\rangle = \alpha|0\rangle + \beta|1\rangle$ is a qubit state. Suppose we measure an operator whose eigenvectors are $|0\rangle$ and $|1\rangle$, with eigenvalues $1, -1$, respectively, i.e. $|0\rangle\langle 0| - |1\rangle\langle 1|$, which is nothing but the Pauli operator σ_z. For simplicity we will write it as Z and its matrix form in the basis $\{|0\rangle, |1\rangle\}$ is

$$Z = \sigma_z = \begin{pmatrix} 1 & 0 \\ 0 & -1 \end{pmatrix}. \tag{1.39}$$

When measuring Z, the probabilities p_0 of getting $|0\rangle$ and p_1 of getting $|1\rangle$ are

$$p_0 = |\alpha|^2 = p,\ p_1 = |\beta|^2 = 1 - p, \tag{1.40}$$

respectively.

However, a qubit is indeed different from a bit. To see this, let W be a bit with probabilities of $p(W = 0) = |\alpha|^2, p(W = 1) = 1 - |\alpha|^2$. Let us consider an example where $\alpha = \beta = \frac{1}{\sqrt{2}}$, so $p(W = 0) = p(W = 1) = \frac{1}{2}$. For a corresponding qubit state $|\psi\rangle = \frac{1}{\sqrt{2}}(|0\rangle + |1\rangle)$, measuring the Pauli operator will return, $|0\rangle$ or $|1\rangle$ with probability $\frac{1}{2}$. In this sense, the qubit state $|\psi\rangle$ is similar to the bit W.

However, this is more to do for the qubit. Let us write the Pauli operator σ_x as X and σ_y as Y, i.e.

$$X = \sigma_x = \begin{pmatrix} 0 & 1 \\ 1 & 0 \end{pmatrix}, \quad \text{and} \quad Y = \sigma_y = \begin{pmatrix} 0 & -i \\ i & 0 \end{pmatrix}. \tag{1.41}$$

It is then straightforward to observe that $|\psi\rangle = \frac{1}{\sqrt{2}}(|0\rangle + |1\rangle)$ is an eigenvector of X with eigenvalue 1, therefore if we measure X, we will get a definite value 1. However, when measuring Y, we will again get each eigenvalue of Y of probability half and half.

This example also shows that the probability distribution of a pure quantum state must be associated with a chosen measurement. In this sense the chosen measurement is an analog of a random variable in the classical case. However, it is different from the classical case, where all the random variables share a single probability distribution. In the quantum case, if the state happens to be the eigenstate of the measurement, then the measurement returns a definite value (i.e. no uncertainty); while if not, there exists some amount of uncertainty. So it is not consistent to assign a certain value of uncertainty to a pure quantum state unless the measurement is specified.

In general, one can further put some probability distribution 'on top of' quantum states, that is, a quantum system may be in the state $|\psi_i\rangle$ with probability p_i, which is represented by a density operator

$$\rho = \sum_i p_i |\psi_i\rangle\langle\psi_i|, \tag{1.42}$$

where $p_i \geq 0$ and $\sum_i p_i = 1$.

When the system definitely stays in a state $|\psi\rangle$, then the state is a pure state. Otherwise the state is a mixed state. Note that any state ρ will satisfy

1. ρ is Hermitian.
2. $\mathrm{Tr}\,\rho = \sum_i p_i = 1$.
3. ρ is positive (may be written as $\rho \geq 0$), i.e. for any $|\psi\rangle$, $\langle\psi|\rho|\psi\rangle = \sum_i p_i |\langle\psi_i|\psi\rangle|^2 \geq 0$, or all the eigenvalues of ρ are positive. Consequently, ρ has a spectral decomposition $\rho = \sum_k \alpha_k |\phi_k\rangle\langle\phi_k|$, where $\alpha_k \geq 0$ are eigenvalues of ρ and $|\phi_k\rangle$s are the corresponding eigenvectors which form an orthonormal basis.
4. $\mathrm{Tr}\,\rho^2 \leq 1$, where the equality is satisfied if and only if the state is a pure state.

For a two-dimensional Hilbert space, note that all the three Pauli operators X, Y, Z, together with the identity operator

$$I = \begin{pmatrix} 1 & 0 \\ 0 & 1 \end{pmatrix} \tag{1.43}$$

form a basis for 2×2 matrices. Denote

$$\sigma = (\sigma_x, \sigma_y, \sigma_z) = (X, Y, Z), \tag{1.44}$$

then a general quantum state ρ of a qubit can be written as

$$\rho = \frac{I + \mathbf{r} \cdot \sigma}{2}, \tag{1.45}$$

where $\mathbf{r} = (r_x, r_y, r_z)$ with $r_x^2 + r_y^2 + r_z^2 \leq 1$.

Now we introduce a measure of uncertainty for a state ρ, i.e. the von Neumman entropy

$$S(\rho) = -\mathrm{Tr}\,(\rho \log \rho), \tag{1.46}$$

which is a generalization of the Shannon entropy. This is in a sense that when writing in its spectral decomposition $\rho = \sum_k \alpha_k |\phi_k\rangle\langle\phi_k|$, we have $S(\rho) = H(\alpha_k) = -\sum_k \alpha_k \log \alpha_k$.

1.3.2 Composite quantum systems, tensor product structure

Now we consider the case of composite quantum systems. Assume we have two quantum systems, one for Alice and the other for Bob. We denote Alice's Hilbert space by $\mathscr{H}_A$, whose dimension is d_A with an orthonormal basis $\{|i_A\rangle\} : i = 0, 1, \ldots d_A - 1$. Similarly, we denote Bob's Hilbert space by $\mathscr{H}_B$, whose dimension is d_B with an orthonormal basis $\{|m_B\rangle\} : m = 0, 1, \ldots d_B - 1$.

In this case, the basis for the total Hilbert space of both Alice and Bob will be the Cartesian product of $\{|i_A\rangle\}$ and $\{|m_B\rangle\}$, i.e. $\{|i_A\rangle\} \times \{|m_B\rangle\}$, which is of dimension $d_A d_B$. The corresponding Hilbert space is denoted by $\mathscr{H}_A \otimes \mathscr{H}_B$, where $\otimes$ is called the tensor product of two spaces. Therefore, any pure state $|\psi_{AB}\rangle \in \mathscr{H}_A \otimes \mathscr{H}_B$ can be written as

$$|\psi_{AB}\rangle = \sum_{im} c_{im} |i_A\rangle |m_B\rangle, \tag{1.47}$$

where each term $|i_A\rangle|m_B\rangle$ is sometimes written as $|i_A\rangle \otimes |m_B\rangle$ to emphasize the tensor product structure of $\mathscr{H}_A \otimes \mathscr{H}_B$, or sometimes just for simplicity written as $|i_A m_B\rangle$ or even just $|im\rangle$ if no confusion arises.

Compared to the case of classical joint probability of two systems, the difference is that the quantum case deals with a linear space but the classical case only deals with a certain basis. This is again a natural consequence of quantum superposition principle. Therefore, any composite quantum system always has tensor product structure of its Hilbert space, i.e.

Box 1.7 Composite quantum system
The Hilbert space of a composite quantum system is a *tensor product* of the Hilbert spaces of all its subsystems.

As an example, let us consider the simplest case that both $\mathscr{H}_A$ and $\mathscr{H}_B$ are two-dimensional, with orthonormal basis $\{|0_A\rangle, |1_A\rangle\}$ and $\{|0_B\rangle, |1_B\rangle\}$, respectively. The basis for the Hilbert space $\mathscr{H}_A \otimes \mathscr{H}_B$ is then given by

$$\{|00\rangle,\ |01\rangle,\ |10\rangle,\ |11\rangle\}, \tag{1.48}$$

i.e. the basis for 2 qubits. That is, any two qubit state $|\psi_{AB}\rangle$ can be written in the form

$$|\psi_{AB}\rangle = c_{00}|00\rangle + c_{01}|01\rangle + c_{10}|10\rangle + c_{11}|11\rangle. \tag{1.49}$$

Similarly, we can write a basis for any n-qubit state.

Box 1.8 Computational basis for an N-qubit state
A basis for an N-qubit state are all the 2^N binary strings of length n, i.e. $|x_N x_{N-1}\ldots x_1\rangle$, where each x_i is a bit, i.e. $x_i \in \{0,1\}$. This basis is called the 'computational basis.'

The way to find the quantum state ρ_B for the system B from the state $|\psi_{AB}\rangle$ given the equation (1.47) is to 'ignore' the subsystem A, i.e. to trace (or integrate) over the subsystem A. That is,

$$\rho_B = \mathrm{Tr}_A\,|\psi_{AB}\rangle\langle\psi_{AB}| = \sum_i \langle i_A|\psi_{AB}\rangle\langle\psi_{AB}|i_A\rangle = \sum_i c_{im}c_{in}^*|m_B\rangle\langle n_B|, \tag{1.50}$$

where c_{in}^* is the complex conjugate of c_{in}. And the density matrix ρ_B is called the reduced density matrix for the system B.

On the other hand, any density matrix ρ_B of the subsystem B can be regarded as reduced state from a pure composite state, i.e. the system B plus an auxiliary system A. That is, for any state ρ_B with spectral decomposition $\rho_B = \sum_i p_i|\phi_{i_B}\rangle\langle\phi_{i_B}|$, we can construct a pure state

$$|\psi_{AB}\rangle = \sum_i \sqrt{p_i}|i_A\rangle \otimes |\phi_{i_B}\rangle, \tag{1.51}$$

with $\langle i_A|j_A\rangle = \delta_{ij}$, such that $\rho_B = \mathrm{Tr}_A\,(|\psi_{AB}\rangle\langle\psi_{AB}|)$. This process is called quantum state purification.

Notice that for another orthonormal basis $\{|\varphi_{i_A}\rangle\}$ of $\mathscr{H}_A$, we can rewrite

$$\begin{aligned}|\psi_{AB}\rangle &= \sum_i\sum_j |\varphi_{j_A}\rangle\langle\varphi_{j_A}|\sqrt{p_i}|i_A\rangle \otimes |\phi_{i_B}\rangle \\ &= \sum_j\sum_i \sqrt{p_i}\langle\varphi_{j_A}|i_A\rangle|\varphi_{j_A}\rangle \otimes |\phi_{i_B}\rangle \\ &= \sum_j \sqrt{q_j}|\varphi_{j_A}\rangle \otimes |\xi_{j_B}\rangle,\end{aligned}$$

where

$$\sum_i \langle\varphi_{j_A}|i_A\rangle\sqrt{p_i}|\phi_{i_B}\rangle = \sqrt{q_j}|\xi_{j_B}\rangle. \tag{1.52}$$

This implies that the state

$$\rho_B = \mathrm{Tr}_A\,(|\psi_{AB}\rangle\langle\psi_{AB}|) = \sum_j q_j|\xi_{j_B}\rangle\langle\xi_{j_B}|.$$

Therefore any mixed state ρ_B can be regarded as the reduced state of the pure state $|\psi_{AB}\rangle$. Different realizations of the ensemble ρ_B correspond to different measurement bases on the auxiliary system A. However, these different realizations can not be distinguished by any measurements on the system, in this sense the mixed state ρ_B is uniquely defined.

1.3.3 Pure bipartite state, Schmidt decomposition

For a pure bipartite state

$$|\psi_{AB}\rangle = \sum_{i=0}^{d_A-1}\sum_{m=0}^{d_B-1} c_{im}|i_A\rangle|m_B\rangle, \tag{1.53}$$

where $\{|i_A\rangle\}$ and $\{|m_B\rangle\}$ are orthonormal bases of $\mathscr{H}_A$ and $\mathscr{H}_B$ respectively, by choosing carefully the basis of subsystems A and B, one can write the state $|\psi_{AB}\rangle$ in an important standard form, namely, the Schmidt decomposition.

Box 1.9 Schmidt decomposition

The state $|\psi_{AB}\rangle$ can be written in the form

$$|\psi_{AB}\rangle = \sum_{i=1}^{n_s} \sqrt{\lambda_i}|\varphi_{i_A}\rangle|\phi_{i_B}\rangle, \tag{1.54}$$

where $\lambda_i > 0$, $\sum_i \lambda_i = 1$, $n_s \leq \min\{d_A, d_B\}$, and $\langle\varphi_{i_A}|\varphi_{j_A}\rangle = \langle\phi_{j_B}|\phi_{i_B}\rangle = \delta_{ij}$.

Let us show why this works. For the state $|\psi_{AB}\rangle$, we get the reduced density matrix ρ_A of particle A, and assume its spectral decomposition is $\rho_A = \sum_{i=1}^{n_s} \lambda_i|\varphi_{i_A}\rangle\langle\varphi_{i_A}|$ with $\lambda_i > 0$, $\sum_i \lambda_i = 1$, and $\langle\varphi_{i_A}|\varphi_{j_A}\rangle = \delta_{ij}$. Now the state $|\psi_{AB}\rangle$ can be written as $|\psi_{AB}\rangle = \sum_{i=1}^{n_s} c_i|\varphi_{i_A}\rangle|\phi_{i_B}\rangle$, where $|\phi_{i_B}\rangle$ is a normalized vector, and c_i is the corresponding coefficient. Note that we can always take $c_i \geq 0$ by choosing the phase factor of $|\phi_{i_B}\rangle$. The reduced state for particle A is then

$$\rho_A = \sum_{ij} |\varphi_{i_A}\rangle c_i c_j^* \langle\phi_{j_B}|\phi_{i_B}\rangle\langle\varphi_{j_A}|. \tag{1.55}$$

Comparing the above equation with the spectral decomposition of ρ_A, we get $\langle\phi_{j_B}|\phi_{i_B}\rangle = \delta_{ij}$ and $c_i = \sqrt{\lambda_i}$. Obviously, $n_s \leq \min\{d_A, d_B\}$. This completes our proof.

The Schmidt decomposition plays a key role in characterization of correlations in a pure bipartite quantum state. The coefficients $\{\lambda_i\}$ are called Schmidt coefficients, and the basis $|\varphi_{i_A}\rangle$ and $|\phi_{i_B}\rangle$ are called Schmidt basis.

When a joint projective measurement $\{P_{i_A m_B} = |\varphi_{i_A}\rangle\langle\varphi_{i_A}| \otimes |\phi_{m_B}\rangle\langle\phi_{m_B}|\}$ is performed, then we get a joint probability distribution

$$p_{AB}(i,m) = \langle\psi_{AB}|P_{i_A m_B}|\psi_{AB}\rangle. \tag{1.56}$$

Because there are many different choices of projective measurements, a single bipartite state $|\psi_{AB}\rangle$ corresponds to infinite many numbers of joint probability distributions. And there is no correlation in the state $|\psi_{AB}\rangle$ if none of the joint probability distributions has any correlation. We summarize this observation below.

Box 1.10 Pure state correlation and projective measurement

A state $|\psi_{AB}\rangle$ has no correlation if $\forall$ projective measurement $P_{i_A m_B}$, the joint probability distribution $p_{AB}(i,m)$ has no correlation.

In other words, no correlation can be retrieved from the joint system by any kind of projective measurement.

Recall that each Hermitian operator corresponds to a random variable in classical probability theory. Then for two observables O_A acting locally on the subsystem A, and O_B acting locally on subsystem B, the correlation function is given by

$$C(O_A, O_B) = \langle O_A \otimes O_B \rangle - \langle O_A \otimes I_B \rangle \langle I_A \otimes O_B \rangle, \tag{1.57}$$

where $\langle \cdot \rangle = \langle \psi_{AB}| \cdot |\psi_{AB}\rangle$ is the average value of some observable.

We now ready to state the conditions under which a bipartite pure state is without correlation.

Box 1.11 Bipartite pure state without correlation

A state $|\psi_{AB}\rangle$ has no correlations if and only if

1. $|\psi_{AB}\rangle = |\psi_A\rangle \otimes |\psi_B\rangle$, or
2. $\forall O_A, O_B, C(O_A, O_B) = 0$.

Note that a pure state of the form $|\psi_A\rangle \otimes |\psi_B\rangle$ is called a product state. We now show the necessary and sufficient condition 1. For the 'if' part: if $|\psi_{AB}\rangle = |\psi_A\rangle \otimes |\psi_B\rangle$, then for $\forall |i_A\rangle, |m_B\rangle$, $p_{AB}(i,m) = |\langle \psi_A | i_A \rangle|^2 |\langle \psi_B | m_B \rangle|^2 = p_A(i)\, p_B(m)$. For the 'only if' part: if the basis of the projective measurement is chosen as the Schmidt basis of $|\psi_{AB}\rangle$, then we get $p_{AB}(i,j) = \lambda_i \delta_{ij}$. Hence the condition for $|\psi_{AB}\rangle$ to have no correlations is $n_s = 1$, i.e., it is a product state.

We then further show the equivalence of the conditions 1 and 2. The part from 1 to 2 is straightforward. For the part from 2 to 1: we start from the Schmidt decomposition $|\psi_{AB}\rangle = \sum_i \sqrt{\lambda_i} |\varphi_{i_A}\rangle \otimes |\phi_{i_B}\rangle$. We take $M_{i_A} = |\varphi_{i_A}\rangle\langle\varphi_{i_A}|$ and $N_{m_B} = |\phi_{m_B}\rangle\langle\phi_{m_B}|$. Then $C(M_{i_A}, N_{m_B}) = \delta_{im}\lambda_i - \lambda_i \lambda_m = 0$, which implies that $\lambda_m = \delta_{im}$. Therefore there exists some m such that $\lambda_m = 1$, so $|\psi_{AB}\rangle$ is a product state.

1.3.4 Mixed bipartite state

We consider the correlations in a mixed bipartite state ρ_{AB}. Now the average value of observable O_{AB} is defined as $\langle O_{AB} \rangle = \mathrm{Tr}_{AB}(O_{AB}\rho_{AB})$. For example,

$$p_{AB}(i,m) = \mathrm{Tr}_{AB}(P_{i_A m_B}\rho_{AB}).$$

Similar to the pure state case, we have the following observation for a bipartite state to have no correlation.

Box 1.12 Correlation and projective measurement

A state ρ_{AB} has no correlation if $\forall$ projective measurement $P_{i_A m_B}$, the joint probability distribution $p_{AB}(i,m)$ has no correlations.

Again, similar as the pure state case, the conditions under which a bipartite state ρ_{AB} has no correlation can be given by

Box 1.13 Bipartite state without correlation

A state ρ_{AB} has no correlations if and only if

1. $\rho_{AB} = \rho_A \otimes \rho_B$, or
2. $\forall O_A, O_B, C(O_A, O_B) = 0$

Let us first show the condition 2. For the 'if' part: $\forall |\varphi_{i_A}\rangle, |\phi_{m_B}\rangle$, we take two types of operators: $O_A = \sum_i x_i |\varphi_{i_A}\rangle\langle\varphi_{i_A}|$ and $O_B = \sum_m y_m |\phi_{m_B}\rangle\langle\phi_{m_B}|$. Then we have

$$C(O_A, O_B) = \sum_{im} x_i y_m \left(p_{AB}(i,m) - p_A(i)\, p_B(m)\right) = 0.$$

Since x_i and y_m can take arbitrary values, we obtain $p_{AB}(i,m) = p_A(i)\, p_B(m)$. The 'only if' part can be shown in a similar way.

The equivalence of conditions 1 and 2 can be shown by noticing that

$$\mathrm{Tr}_{AB}\left(O_A \otimes O_B \left(\rho_{AB} - \rho_A \otimes \rho_B\right)\right) = C(O_A, O_B).$$

Similar as the case of classical joint probability, we have the concept of quantum mutual information which measures the total amount of correlation between A and B.

Box 1.14 Quantum mutual information

The correlation in a bipartite state ρ_{AB} is measured by the quantum mutual information:

$$I(A{:}B) = S_A + S_B - S_{AB},$$

Here for simplicity we write S_A for $S(\rho_A)$, S_B for $S(\rho_B)$, and S_{AB} for $S(\rho_{AB})$.

If ρ_{AB} is a pure state, then $S_{AB} = 0$ and $S_A = S_B = H(\{\lambda_i\})$, where λ_i is the Schmidt coefficients of the state. Hence $I(A{:}B) = 2H(\{\lambda_i\})$.

1.3.5 Bell's inequalities

When correlation exists in a bipartite system, there must be two local measurements on the two parties respectively, with dependent measurement results. This is the case for both classical and quantum bipartite systems. This similarity in classical and quantum correlations naturally raises the following question: is there any feature of correlation in a quantum state that is distinct from that in a classical probability distribution? The Bell's inequalities give an affirmative answer to this question. Here we look at one of those inequalities, called the CHSH (Clauser-Horne-Shimony-Holt) inequality.

Let us consider a bipartite system with subsystems A and B. Let a, c be local dichotomic variables of A, and b, d be local dichotomic variables of B. Here a dichotomic variable is a random variable that takes one of the two possible values ± 1.

Note that

$$v(a)v(b)+v(a)v(d)+v(c)v(b)-v(c)v(d)=\pm 2, \tag{1.58}$$

where $v(x)$ is the value of the dichotomic variable x, which could be ± 1.

We now obtain the CHSH inequality

$$|\langle ab\rangle+\langle ad\rangle+\langle cb\rangle-\langle cd\rangle|\leq 2. \tag{1.59}$$

This CHSH inequality is indeed built on the hidden variable assumption. That is, if some hidden variable λ is given, the values of the dichotomic variables a, b, c, and d are specified.

In the quantum situation, a system with dichotomic variables may correspond to a qubit, and the above bipartite system can correspond to a two-qubit system. A dichotomic variable will map to the component of the Pauli operator along a space direction, e.g., a corresponds to $\boldsymbol{\sigma}\cdot\mathbf{n}_a$. Here $\mathbf{n}_a$ is a unit vector on the Bloch sphere.

Thus the quantum version of the CHSH inequality becomes

$$\begin{aligned}
&|\langle\boldsymbol{\sigma}_A\cdot\mathbf{n}_a\boldsymbol{\sigma}_B\cdot\mathbf{n}_b\rangle+\langle\boldsymbol{\sigma}_A\cdot\mathbf{n}_a\boldsymbol{\sigma}_B\cdot\mathbf{n}_d\rangle+\langle\boldsymbol{\sigma}_A\cdot\mathbf{n}_c\boldsymbol{\sigma}_B\cdot\mathbf{n}_b\rangle-\langle\boldsymbol{\sigma}_A\cdot\mathbf{n}_c\boldsymbol{\sigma}_B\cdot\mathbf{n}_d\rangle|\\
&\leq|\langle\boldsymbol{\sigma}_A\cdot\mathbf{n}_a\boldsymbol{\sigma}_B\cdot(\mathbf{n}_b+\mathbf{n}_d)\rangle|+|\langle\boldsymbol{\sigma}_A\cdot\mathbf{n}_c\boldsymbol{\sigma}_B\cdot(\mathbf{n}_b-\mathbf{n}_d)\rangle|\\
&\leq|\mathbf{n}_b+\mathbf{n}_d|+|\mathbf{n}_b-\mathbf{n}_d|\\
&\leq\sqrt{2(|\mathbf{n}_b+\mathbf{n}_d|^2+|\mathbf{n}_b-\mathbf{n}_d|^2)}=2\sqrt{2}.
\end{aligned} \tag{1.60}$$

In fact, the maximum value $2\sqrt{2}$ can be reached for a singlet state

$$|\psi_{AB}\rangle=\frac{1}{\sqrt{2}}(|01\rangle-|10\rangle), \tag{1.61}$$

for some $\mathbf{n}_a$, $\mathbf{n}_b$, $\mathbf{n}_c$, and $\mathbf{n}_d$ which are in the same plane with $\mathbf{n}_a\perp\mathbf{n}_b$, $\mathbf{n}_c\perp\mathbf{n}_d$, and $\mathbf{n}_a\perp(\mathbf{n}_b-\mathbf{n}_d)$. For instance, one choice could be that $\mathbf{n}_a$, $\mathbf{n}_b$, $\mathbf{n}_c$, and $\mathbf{n}_d$ are in

the $x-z$ plane of the Bloch sphere with angles to the z axis as $\theta_a = 0$, $\theta_b = \pi/2$, $\theta_c = \pi/4$ and $\theta_d = -\pi/4$.

Comparing the CHSH inequality Eq. (1.59) with its quantum version Eq. (1.60), we then conclude that the quantum correlation is stronger than its classical counterpart.

1.3.6 Entanglement

Bell inequality implies that a pure bipartite quantum state can have correlations beyond its classical counterpart. This special type of correlation is called entanglement. Entanglement is originated from the superposition principle of quantum states. It is the key resource for quantum information processing.

For a pure bipartite state $|\psi_{AB}\rangle$, it is natural to state the following.

Box 1.15 Bipartite product state

A pure bipartite state $|\psi_{AB}\rangle$ is a product state if it can be written as $|\psi_A\rangle \otimes |\psi_B\rangle$ for some $|\psi_A\rangle \in \mathscr{H}_A$ and $|\psi_B\rangle \in \mathscr{H}_B$, otherwise it is entangled.

Traditionally, entanglement for a pure bipartite state $|\psi_{AB}\rangle$ is measured by the von Neumann entropy of its the subsystem.

Box 1.16 von Neumann entropy as entanglement measure

The entanglement for a pure bipartite state $|\psi_{AB}\rangle$ is given by the von Neumann entropy of the subsystem state ρ_A or ρ_B:

$$S(|\psi_{AB}\rangle) = -\operatorname{Tr}\rho_A \log \rho_A = -\operatorname{Tr}\rho_B \log \rho_B.$$

In terms of the Schmidt coefficients $\{\lambda_i\}$ of the state $|\psi_{AB}\rangle$, we have $E(|\psi_{AB}\rangle) = H(\{\lambda_i\})$. Therefore, for any bipartite pure state $\rho_{AB} = |\psi_{AB}\rangle\langle\psi_{AB}|$, its mutual information $I(A{:}B) = 2H(\{\lambda_i\})$ is twice its entanglement. Since the mutual information measures the total correlation, this in some sense means that for ρ_{AB}, half of the correlation is 'quantum' and the other half is 'classical.'

To see what this might possibly mean, let us write the mutual information for any bipartite state ρ_{AB} as the following.

$$\begin{aligned} I(A{:}B) &= S_A + S_B - S_{AB} \\ &= S_A - S_{A|B} \\ &= S_B - S_{B|A} \\ &= S_{AB} - S_{A|B} - S_{B|A}. \end{aligned} \tag{1.62}$$

Here the quantum conditional entropy is given by

$$S_{A|B} = S_{AB} - S_B$$
$$S_{B|A} = S_{AB} - S_A.$$

This looks very similar as Eq. (1.32) for the classical case. Or in other words, the picture given by Fig. 1.2 is in some sense still valid for the quantum case. We need to emphasize that there is an essential difference though: in the classical case, the conditional entropy can never be negative, but the quantum conditional entropy could be.

Any entangled pure state $|\psi_{AB}\rangle$ is an example, where $S_{AB} = 0$ and $S_B = S_A > 0$, therefore $S_{A|B} = S_{B|A} < 0$. This sounds strange that how such a 'partial information' could be negative, which could mean that the more you know then the less you know. This puzzle was solved by quantum information scientists to associate this negative quantity with future potential to transmit quantum information.

It is beyond the scope of the book to go into detail of this operational meaning for quantum mutual information, which would explain that a pure state contains both classical and quantum correlation when used for quantum information transmission. Because there is only a constant factor '2' between its total correlation and entanglement, in most cases it is both qualitatively and quantitatively fine that we simply say 'all the correlation' in a bipartite pure state is just 'quantum,' i.e. entanglement, at least for the discussion of this book. Therefore in the rest of the book, we will simply use the word 'entanglement' when talking about correlation in bipartite pure state.

Indeed 'almost all' bipartite pure states are entangled, in a sense that a very small amount of states can be written into the form of $|\psi_{AB}\rangle = |\psi_A\rangle \otimes |\psi_B\rangle$. Take the two-qubit case as an example. A general state can be written as

$$|\psi\rangle = c_{00}|00\rangle + c_{01}|01\rangle + c_{10}|10\rangle + c_{11}|11\rangle, \tag{1.63}$$

where $|c_{00}|^2 + |c_{01}|^2 + |c_{00}|^2 + |c_{01}|^2 = 1$.

If $|\psi\rangle$ can be written as $|\psi_A\rangle \otimes |\psi_B\rangle$, then we will have $|\psi_A\rangle = a_0|0\rangle + a_1|1\rangle$ and $|\psi_B\rangle = b_0|0\rangle + b_1|1\rangle$, then

$$|\psi\rangle = |\psi_A\rangle \otimes |\psi_B\rangle = a_0b_0|00\rangle + a_0b_1|01\rangle + a_1b_0|10\rangle + a_1b_1|11\rangle, \tag{1.64}$$

which means one must have

$$c_{00} = a_0b_0,\ c_{01} = a_0b_1,\ c_{10} = a_1b_0,\ c_{11} = a_1b_1. \tag{1.65}$$

However, this is cannot be true in general for c_{ij} satisfying only $|c_{00}|^2 + |c_{01}|^2 + |c_{10}|^2 + |c_{11}|^2 = 1$.

One interesting consequence of entanglement is that an unknown quantum state cannot be 'copied'. In other words, there does not exist an apparatus $\mathscr{A}$ which realizes the following mapping:

$$\mathscr{A} : (\alpha|0\rangle + \beta|1\rangle) \otimes |0\rangle \rightarrow (\alpha|0\rangle + \beta|1\rangle) \otimes (\alpha|0\rangle + \beta|1\rangle) \tag{1.66}$$

for any α, β. To see why this is case, we know that quantum mechanics is linear. Therefore, if $\mathscr{A}$ can copy the basis states $|0\rangle$ and $|1\rangle$, i.e.

$$\mathscr{A} : |00\rangle \rightarrow |00\rangle, \; |10\rangle \rightarrow |11\rangle, \tag{1.67}$$

then it must map $(\alpha|0\rangle + \beta|1\rangle) \otimes |0\rangle$ to $\alpha|00\rangle + \beta|11\rangle$, however we know that $\alpha|00\rangle + \beta|11\rangle$ is entangled and

$$\alpha|00\rangle + \beta|11\rangle \neq (\alpha|0\rangle + \beta|1\rangle) \otimes (\alpha|0\rangle + \beta|1\rangle) \tag{1.68}$$

in general.

This then leads to an important fact which is called the 'no-cloning theorem'.

Box 1.17 The no-cloning theorem

An unknown quantum state cannot be cloned.

Having said that 'all the correlation in a bipartite pure state is just quantum', a mixed bipartite state ρ_{AB}, however, should contain both classical correlation and quantum correlation (entanglement). Here classical correlation means the correlation with origin of classical probability, i.e. from mixing pure bipartite states. If initially there is no entanglement in all these pure bipartite states, then a mixing of them should only result in classical correlation, but no quantum entanglement. Therefore, a widely-used definition of entanglement for a general bipartite state is then given as follows.

Box 1.18 Separable states

A state ρ_{AB} is separate if and only if it can be written in the form:

$$\rho_{AB} = \sum_i p_i |\varphi_{i_A}\rangle\langle\varphi_{i_A}| \otimes |\phi_{i_B}\rangle\langle\phi_{i_B}|$$

Otherwise, it is called entangled.

The degree of entanglement is a more subtle problem, which has different definitions in different contexts, and often is very hard to calculate. As an example, the entanglement of formation is defined as

$$E_F(\rho_{AB}) = \min_{\sum_i p_i |\psi_{i_{AB}}\rangle\langle\psi_{i_{AB}}| = \rho_{AB}} \sum_i p_i E(|\psi_{i_{AB}}\rangle).$$

According to the definition, it is obvious that the entanglement of formation for a state ρ_{AB} is zero if and only if it is separable.

1.4 Correlation and entanglement in many-body quantum systems

Now let us move on to discuss many-body quantum systems. We start from a simplest case where there are only three systems A,B,C, i.e. the Hilbert space is now the tensor product of the three systems, $\mathscr{H} = \mathscr{H}_A \otimes \mathscr{H}_B \otimes \mathscr{H}_C$. We first start to examine a paradox which shows many-body quantum correlation is stronger than the classical correlation.

1.4.1 The GHZ paradox

To further demonstrate the essential differences between classical correlation and quantum correlation, Greenberg, Horne, and Zeilinger find that there exists remarkable correlations in the following state

$$|GHZ\rangle = \frac{1}{\sqrt{2}}\left(|000\rangle + |111\rangle\right). \tag{1.69}$$

Hence the above state is called the GHZ state.

The correlation in the GHZ state can be described as follows. First, let us observe that it is the unique common eigenstate with eigenvalues being 1 of the following observables:

$$\{Z_A \otimes Z_B \otimes I_C, I_A \otimes Z_B \otimes Z_C, X_A \otimes X_B \otimes X_C\}. \tag{1.70}$$

Then we use the above set of observables as the generator to generate the following group:

$$\begin{aligned}\{&I_A \otimes I_B \otimes I_C, Z_A \otimes Z_B \otimes I_C, I_A \otimes Z_B \otimes Z_C, Z_A \otimes I_B \otimes Z_C,\\ &X_A \otimes X_B \otimes X_C, -Y_A \otimes Y_B \otimes X_C, -Y_A \otimes X_B \otimes Y_C, -X_A \otimes Y_B \otimes Y_C\}.\end{aligned} \tag{1.71}$$

Obviously, the GHZ state is also the eigenstate with eigenvalue being 1 for all the observables in the group.

Now let us return to the classical world. If we take a measurement of a Pauli operator Λ with $\Lambda \in \{X,Y,Z\}$, we always get its value, 1 or -1. Then the value of a Pauli matrix $v(\Lambda)$ can take a value 1 or -1. The quantum theory, in the viewpoint of classical world, implies that

$$v(X_A)v(X_B)v(X_C) = 1, \tag{1.72}$$
$$-v(Y_A)v(Y_B)v(X_C) = 1, \tag{1.73}$$
$$-v(Y_A)v(X_B)v(Y_C) = 1, \tag{1.74}$$
$$-v(X_A)v(Y_B)v(Y_C) = 1. \tag{1.75}$$

However, this is impossible because the product of the above four equations leads to $-1 = 1$. This reflects that it is no longer true in the quantum world that there always exists a value for a local observable, as in the classical world. Therefore, the correlation in the GHZ state can not be simulated by any classical theory.

This GHZ paradox can be viewed as a many-body analogy of the Bell's inequalities, which show quantum correlation is stronger than classical correlation. Note that GHZ paradox has an even simpler form than the Bell's inequalities. This indicates that in the many-body case, quantum system will more easily behave in a nonclassical manner.

1.4.2 Many-body correlation

Similar to the bipartite case, we can discuss the correlation for a tripartite state ρ_{ABC}

Box 1.19 Tripartite states without correlation
A state ρ_{ABC} acting on $\mathscr{H}$ has no correlations if and only if it can be written as $\rho_{ABC} = \rho_A \otimes \rho_B \otimes \rho_C$.

Naturally, the degree of the total correlation in a state ρ_{ABC} equals the generalized mutual information of the state, i.e.,

$$C_T(\rho_{ABC}) = \mathscr{I}(\rho_{ABC}) = S_A + S_B + S_C - S_{ABC}. \tag{1.76}$$

In general, this total correlation $C_T(\rho_{(ABC})$ must contain both bipartite correlation and tripartite correlation. And we also know that the bipartite correlations are given by the quantum mutual information $I(A{:}B)$, $I(B{:}C)$, $I(A{:}C)$ respectively. So one simple guess will be that the true tripartite correlation $C_{tri}(\rho_{ABC})$ should be given by

$$\begin{aligned} C_{tri}(\rho_{ABC}) &= C_T(\rho_{ABC}) - (I(A{:}B) + I(B{:}C) + I(A{:}C)) \\ &= S_{AB} + S_{AC} + S_{BC} - S_A - S_B - S_C - S_{ABC}, \end{aligned} \tag{1.77}$$

which can be viewed in the graphical manner as illustrated in Fig. 1.4.

Unfortunately, this does not work as $C_{tri}(\rho_{ABC})$ could sometimes be negative. Indeed, this is even the case of classical joint probability distribution. As an example, consider a three-qubit system with the quantum state

$$\rho^c_{ABC} = \frac{1}{2}(|000\rangle\langle 000| + |111\rangle\langle 111|). \tag{1.78}$$

We note that $C_T(\rho^c_{ABC}) = 2$, but $I(A{:}B) = I(B{:}C) = I(A{:}C) = 1$.

To solve the above paradox, for the tripartite state ρ_{ABC}, let us write its one-particle reduced density matrices (1-RDMs) as $\{\rho_A, \rho_B, \rho_C\}$, and two particle reduced density matrices (2-RDMs) as $\{\rho_{AB}, \rho_{BC}, \rho_{AC}\}$. Now define

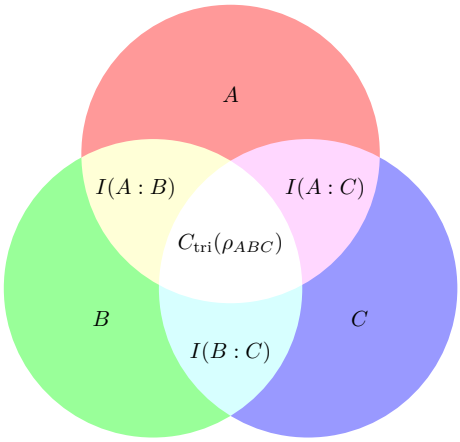

Fig. 1.4 An inituitive distribution of correlations in a tripartite quantum state ρ_{ABC}. The true three-body correlation is the overlap of A,B,C, and the two-body correlations between A and B, between A and C, between B and C are represented by the mutual information $I(A:B)$, $I(A:C)$, $I(B:C)$ respectively.

$$\mathbb{L}_1 = \{\sigma_{ABC} | \sigma_A = \rho_A, \sigma_B = \rho_B, \sigma_C = \rho_C\}, \tag{1.79}$$

$$\mathbb{L}_2 = \{\sigma_{ABC} | \sigma_{AB} = \rho_{AB}, \sigma_{BC} = \rho_{BC}, \sigma_{CA} = \rho_{CA}\}, \tag{1.80}$$

$$\mathbb{L}_3 = \{\sigma_{ABC} | \sigma_{ABC} = \rho_{ABC}\}. \tag{1.81}$$

That is, $\mathbb{L}_k$ is the set of all tripartite states σ_{ABC} that has the same k-RDMs as those of ρ_{ABC}.

The idea of $\mathbb{L}_k$ can naturally be generalized to the case of the N-particle case. That is, given an n-particle state ρ, we have

$$\mathbb{L}_k = \{\sigma | \sigma \text{ has the same } k\text{-RDMs as those of } \rho\}, \tag{1.82}$$

for $k = 1,\ldots,N$.

Now the question is which state in $\mathbb{L}_k$ is the best inference of the global state ρ given only the information of k-RDMs. This is given by the principle of maximum entropy.

Box 1.20 The principle of maximum entropy

For a given set of k-RDMs, the best inference of the N-particle state is the one with the maximum von Neumann entropy in $\mathbb{L}_k$.

In fact, this state with maximum entropy is unique and let us denote it by ρ_k^*. What the principle of maximum entropy says is that ρ_k^* contains all the information that is contained in the k-RDMs, but no more. In this sense, the more information we get by knowing ρ compared to knowing only its k-RDMs is given by the decrease

of the uncertainty of our knowledge of the state ρ, i.e.,

$$\Delta S = S(\rho_k^*) - S(\rho). \tag{1.83}$$

Similarly the more information we get by knowing the k-RDMs compared to knowing only its $(k-1)$-RDMs is given by

$$C_k = S(\rho_{k-1}^*) - S(\rho_k^*), \tag{1.84}$$

where C_k measures the degree of k-particle correlation that cannot be learned from the information in $(k-1)$-RDMs. In this sense, we will call C_k the irreducible k-particle correlation.

Now let us come back to the problem of decomposing the correlations in a tripartite quantum state into bipartite correlation and tripartite correlation. We can now solve our paradox raised in Eq. (1.77) by using the concept of the irreducible k-particle correlations. That is, for a three-particle state ρ_{ABC}, the state with maximum entropy in $\mathbb{L}_k$ for $k = 1,2,3$ are

$$\rho_1^* = \text{argmax}\{S(\sigma) : \sigma \in \mathbb{L}_1(\rho_{ABC})\}, \tag{1.85}$$
$$\rho_2^* = \text{argmax}\{S(\sigma) : \sigma \in \mathbb{L}_2(\rho_{ABC})\}, \tag{1.86}$$
$$\rho_3^* = \text{argmax}\{S(\sigma) : \sigma \in \mathbb{L}_3(\rho_{ABC})\}. \tag{1.87}$$

In fact, it is easy to prove that $\rho_1^* = \rho_A \otimes \rho_B \otimes \rho_C$ and $\rho_3^* = \rho_{ABC}$. The total correlation in the tripartite state ρ_{ABC} is

$$\begin{aligned} C_T(\rho_{ABC}) &= S(\rho_1^*) - S(\rho_3^*), \\ &= S_A + S_B + S_C - S_{ABC}. \end{aligned} \tag{1.88}$$

The total correlation can be further decomposed into the irreducible bipartite correlation and irreducible tripartite correlation. The degrees of irreducible bipartite correlation and tripartite correlation are

$$C_2(\rho_{ABC}) = S(\rho_1^*) - S(\rho_2^*), \tag{1.89}$$
$$C_3(\rho_{ABC}) = S(\rho_2^*) - S(\rho_3^*). \tag{1.90}$$

According to the above definitions, $C_T(\rho_{ABC})$, $C_2(\rho_{ABC})$ and $C_3(\rho_{ABC})$ are non-negative, and

$$C_T(\rho_{ABC}) = C_2(\rho_{ABC}) + C_3(\rho_{ABC}). \tag{1.91}$$

Therefore the paradox discussed above is resolved. For the state ρ_c, $C_T(\rho_c) = 2$, $C_2(\rho_c) = 2$, and $C_3(\rho_c) = 0$.

It is interesting to see how the irreducible tripartite correlation arise in a tripartite quantum state. The simplest example with irreducible tripartite correlation is the *GHZ* state:

$$|GHZ\rangle = \frac{1}{\sqrt{2}}(|000\rangle + |111\rangle). \tag{1.92}$$

According to a simple calculation, $C_3(|GHZ\rangle) = 1$. In fact, it is impossible to specify the relative phase between the components $|000\rangle$ and $|111\rangle$ from only biparticle correlation, which is the physical reason for the irreducible tripartite correlation in the GHZ state.

Now let us look at the states where $C_3(\rho_{ABC}) = 0$, i.e. states with no irreducible tripartite correlation, or in other words states contain only irreducible bipartite correlation. This will mean that

$$\rho_{ABC} = \rho_2^*. \tag{1.93}$$

Given that ρ_2^* is unique, this means that the state ρ_{ABC} is uniquely determined by its 2-RDMs. This does not mean that there are no other states with the same 2-RDMs as ρ_{ABC}, but there are no other state with the same 2-RDMs and a larger entropy than that of ρ_{ABC}. We call these states 2-correlated, meaning that they only contain 2-particle irreducible correlations, but no more.

If the state satisfying Eq.(1.93) is a pure state $|\psi_{ABC}\rangle$, then it really means the state is uniquely determined by its 2-RDMs, in a sense that there is no other state, pure or mixed, which has the same 2-RDMs as $|\psi_{ABC}\rangle$. Surprisingly, it is shown that almost all tripartite pure states are uniquely determined by their 2-RDMs (i.e. 2-correlated). It turns out that the only three-qubit state with non-zero irreducible tripartite correlation are those equivalent to

$$\alpha|000\rangle + \beta|111\rangle, \tag{1.94}$$

with $\alpha, \beta \neq 0$.

Obviously the above discussion can be generalized to the case of many-body systems with n-particles. Notice that we always have $C_k \geq 0$ and $\sum_{i=1}^{k} C_k = S(\rho) - S(\rho_1^*)$, which is the total correlation given by the generalized mutual information. In this sense, C_k gives a hierarchy of correlations contained in the state ρ.

1.4.3 Many-body entanglement

For a pure tripartite state $|\psi_{ABC}\rangle$, it is natural to state the following.

Box 1.21 Tripartite product state
A pure tripartite state $|\psi_{ABC}\rangle$ is a product state if it can be written as $|\psi_A\rangle \otimes |\psi_B\rangle \otimes |\psi_C\rangle$ for some $|\psi_A\rangle \in \mathscr{H}_A$, $|\psi_B\rangle \in \mathscr{H}_B$ and $|\psi_C\rangle \in \mathscr{H}_C$, otherwise it is entangled.

However, tripartite situation is more complicated than the bipartite case. For instance, $|\psi_{ABC}\rangle$ may be written as

$$|\psi_{ABC}\rangle = |\psi_A\rangle \otimes |\psi_{BC}\rangle, \tag{1.95}$$

where $|\psi_{BC}\rangle$ is an entangled bipartite state in $\mathscr{H}_B \otimes \mathscr{H}_C$. In this case, there is indeed no entanglement between the subsystem A and the subsystems BC.

In case we are only interested in tripartite states that contain 'genuine' entanglement, we will need the following statement.

Box 1.22 Genuine entangled state

A pure tripartite state $|\psi_{ABC}\rangle$ is genuinely entangled, if it cannot be written as a product state with respect to any bipartition of the system.

To quantify the entanglement in a pure tripartite state $|\psi_{ABC}\rangle$, one idea is that we can quantify its 'bipartite' entanglement with respect to any bipartition, using von Neumann entropy. As we will see in later chapters, in many practical cases, this provides important information, such as the entanglement area law. There are also various entanglement measures used in different scenarios for quantifying pure state entanglement. Here we discuss one with geometric meaning, namely the geometric measure of entanglement.

Box 1.23 Geometric measure of entanglement

For a pure tripartite state $|\psi_{ABC}\rangle$, consider a tripartite product state $|\alpha\rangle = |\alpha_A\rangle \otimes |\alpha_B\rangle \otimes |\alpha_C\rangle$. The geometric measure of entanglement $E_G(|\psi_{ABC}\rangle)$ is then revealed by the maximal overlap

$$\Lambda_{\max}(|\psi_{ABC}\rangle) = \max_{|\alpha\rangle} |\langle\alpha|\psi_{ABC}\rangle|, \tag{1.96}$$

and is given by

$$E_G(|\psi_{ABC}\rangle) = -\log \Lambda^2_{\max}(|\psi_{ABC}\rangle). \tag{1.97}$$

Geometrically, $E_G(|\psi_{ABC}\rangle)$ measures how far $|\psi_{ABC}\rangle$ is from the set of product states $\{|\alpha\rangle\}$. And $E_G(|\psi_{ABC}\rangle) = 0$ if and only if $|\psi_{ABC}\rangle$ itself is a product state. As an example, for the GHZ state

$$|GHZ\rangle = \frac{1}{\sqrt{2}}(|000\rangle + |111\rangle), \tag{1.98}$$

the maximal overlap

$$\Lambda^2_{\max}(|GHZ\rangle) = \frac{1}{\sqrt{2}}, \tag{1.99}$$

with the maximum at either $\alpha = |000\rangle$ or $\alpha = |111\rangle$, hence the geometric measure of entanglement is

$$E_G(|GHZ\rangle) = 1. \tag{1.100}$$

And E_G has a natural generalization to a system with more than three particles, which is similarly given by the maximal overlap with a product state.

For mixed many-body states, one can also similarly discuss entanglement with respect to any bipartition. However, similar to the bipartite case, in most practical cases, we are more concerned with 'total' correlation rather than just 'quantum' correlation for mixed states, so with respect to any bipartition, we quantify correlation using mutual information. And when we talk about correlation beyond just the bipartite ones, we look at the 'irreducible' tripartite correlations as discussed in Sec. 1.4.2. The case for many-body systems with more than three particles can be dealt with similarly.

1.5 Summary and further reading

In this chapter we have discussed the basic concepts of correlation and entanglement for many-body quantum systems. We start from introducing concepts of independence and correlation in probability theory, which lead to some understanding of the concepts of entropy and mutual information, which are vital in modern information theory. Historically, these concepts are introduced by Shannon, who is considered as the founding father of electronic communications age, in his 1948 paper 'a mathematical theory of communication' [16], which builds the foundation for information theory.

We then continue to examine the correlation in quantum systems. It turns out that quantum systems possess 'somewhat more' correlation beyond the classical one, which is then called quantum entanglement. Historically, this issue was first raised by Einstein, Podolsky and Rosen in 1935 [6], where they discussed the so called 'EPR paradox', which is a thought experiment revealing what they believed to be incompleteness of quantum mechanics, that is, quantum mechanics cannot be reproduced from some hidden variables. The word 'entanglement' was first mentioned by Schrödinger in 1935 [15], where he described a famous cat that is unfortunately both alive and dead due to quantum entanglement, which later adopts the name 'Schrödinger's cat'.

A more serious study of quantum entanglement beyond just thought experiment starts from the study of Bell's inequalities. It was first proposed by Bell in 1964 [3]. It comes in a form of 'Bell's theorem', which states that no hidden variable theory can reproduce all of the predictions of quantum mechanics, or in other words, quantum correlation is beyond classical correlation. There are many subsequent inequalities following Bell's work, and the CHSH inequality presented in this chapter is discussed in [5].

The operational meaning of partial quantum information (negative quantum conditional entropy) was given in [8]. The no-cloning theorem is proved in [18]. The GHZ paradox has a spirit similar to the Bell's theorem, but looking at more than two particles such that inequalities are no longer necessary, is originally proposed in [7].

The principle of maximum entropy is advocated by Jaynes in the study on the foundation of statistical mechanics [10]. The irreducible correlation is first proposed in [11] for full rank states, and then later generalized to non-full rank states in [19]. Their work provides a quantum analog of the information hierarchy idea as studied [1, 14].

The idea of separable state is originally from [17]. The entanglement of formation was proposed in [4]. There are many aspects of quantum entanglement that have not been mentioned is this chapter. As already mentioned, we have only chosen those very basic facts and those will be used to study many-body physics later in this book. In fact, entanglement theory is an active bunch of study in the frontier of quantum information and quantum foundation. For a general review of quantum entanglement emphasizing on mathematical aspects, we direct the reader to [9]. For readers interested in more on entanglement theory in many-body systems, we refer to [2].

Furthermore, it is also not the goal of this part of the book (i.e. Chap. 1,2 and 3) to introduce the general theory of quantum information and computation. Again, we will only introduce those very basic facts and those will be used to study many-body physics in later parts of this book. For readers interested in quantum information and computation in general, there are many good references, such as the book by Nielsen and Chuang [12]. There also various good resources available online, for instance the lecture notes by Preskill at Caltech [13].

References

1. S. Amari. Information geometry on hierarchy of probability distributions. *IEEE Transactions on Information Theory*, 47:1701–1711, 2001.
2. L. Amico, R. Fazio, A. Osterloh, and V. Vedral. Entanglement in many-body systems. *Reviews of Modern Physics*, 80:517–576, April 2008.
3. J. S. Bell. On the einstein podolsky rosen paradox. *Physics*, 1(3):195–200, 1964.
4. C. H. Bennett, D. P. Divincenzo, J. A. Smolin, and W. K. Wootters. Mixed-state entanglement and quantum error correction. *Physical Review A*, 54:3824–3851, November 1996.
5. J. F. Clauser, M. A. Horne, A. Shimony, and R. A. Holt. Proposed Experiment to Test Local Hidden-Variable Theories. *Physical Review Letters*, 23:880–884, October 1969.
6. A. Einstein, B. Podolsky, and N. Rosen. Can Quantum-Mechanical Description of Physical Reality Be Considered Complete? *Physical Review*, 47:777–780, May 1935.
7. D. M. Greenberger, M. Horne, and A. Zeilinger. Going beyond Bell's theorem. In M. Kafatos, editor, *Bell's Theorem, Quantum Theory, and Conceptions of the Universe*, pages 69–72, Dordrecht, 1989. Kluwer Academic.
8. M. Horodecki, J. Oppenheim, and A. Winter. Partial quantum information. *Nature*, 436:673–676, August 2005.
9. R. Horodecki, P. Horodecki, M. Horodecki, and K. Horodecki. Quantum entanglement. *Reviews of Modern Physics*, 81:865–942, April 2009.
10. E. T. Jaynes. Information theory and statistical mechanics. *Phys. Rev.*, 106:620–630, 1957.
11. N. Linden, S. Popescu, and W. K. Wootters. Almost Every Pure State of Three Qubits Is Completely Determined by Its Two-Particle Reduced Density Matrices. *Physical Review Letters*, 89(20):207901, October 2002.
12. M. Nielsen and I. Chuang. *Quantum computation and quantum information*. Cambridge University Press, Cambridge, England, 2000.

13. J. Preskill. Lecture notes for physics 219 at caltech.
14. E. Schneidman, S. Still, M. J. Berry, and W. Bialek. Network Information and Connected Correlations. *Physical Review Letters*, 91(23):238701, December 2003.
15. E. Schrödinger. Die gegenwärtige Situation in der Quantenmechanik. *Die Naturwissenschaften*, 48,49:807–812,823–828,844–849, 1935. English translation in Proc. Am. Phil. Soc. **124**, 323–338 (1980).
16. C. E. Shannon. A mathematical theory of communication. *Bell Labs Technical Journal*, 27:379–423, 1948.
17. R. F. Werner. Quantum states with Einstein-Podolsky-Rosen correlations admitting a hidden-variable model. *Physical Review A*, 40:4277–4281, October 1989.
18. W. K. Wootters and W. H. Zurek. A single quantum cannot be cloned. *Nature*, 299:802, October 1982.
19. D. L. Zhou. Irreducible Multiparty Correlations in Quantum States without Maximal Rank. *Physical Review Letters*, 101(18):180505, October 2008.

Chapter 2
Evolution of Quantum Systems

Abstract In this chapter we discuss in general a quantum system with Hilbert space $\mathscr{H}_S$, whose quantum state is described by a density matrix ρ_S, under time evolution. In the ideal case, the evolution of the wave function $|\psi_S\rangle \in \mathscr{H}_S$ is unitary. This unitary evolution gives rise to the circuit model of quantum computation, where the computational procedure is to 'apply' unitary operations to the quantum state carrying information of the computation. However, as discussed in Chapter 1, in the general case, the system S interacts with the environment. Then the quantum state ρ_S of the system comes from part of a larger system $\mathscr{H}_S \otimes \mathscr{H}_E$, which is composed of both the system and its environment.

2.1 Introduction

The time evolution of a wave function is governed by the Schrödinger's equation and hence is unitary. One may just feel that in principle this is the end of the story as there is nothing more than just unitary to talk about. This is indeed, the ideal case. However, in our real world, there are many factors one has to take into account when discussing unitary evolution of quantum states. This will be the topic of this chapter where we introduce those viewpoints of quantum information science, which turn out to be relevant to real life.

The first concern is for a many-body system of N particles, in general the time evolution for a quantum state $|\psi\rangle$ should be given by an N-particle unitary U, i.e. $|\psi(t)\rangle = U|\psi(t_0)\rangle$. However, not all unitaries can be realized by real-world Hamiltonian t as $U = e^{-iH(t-t_0)}$. That is because a natural arising many-body Hamiltonian involves only few-body interactions, i.e. $H = \sum_i H_i$, where each H_i acting non-trivially on only a few number of particles. By a simple counting of parameters we know that this kind of natural Hamiltonians cannot result in all the unitary evolutions for the N-particle space.

The idea from quantum information science is to build any N-particle unitaries from those small-particle-number ones. In particular, it is known that two-qubit uni-

taries acting on any pair of particles suffice to produce any N-qubit unitary, and further more any single qubit unitary plus some fixed single two-qubit unitary suffice to produce any two-qubit unitary. This gives rise to the so called circuit model of quantum computing, where a diagram is introduced to illustrate how an N-qubit unitary is realized by single and two-particle unitaries.

However, one needs to be aware of that in general, the construction to realize an N-qubit unitary by single and two-particle unitaries is 'not efficient.' This means in general, exponentially many single and two-particle quantum unitaries are needed (in terms of number of qubits N). Nevertheless, those N-particle unitaries from naturally arising Hamiltonians can be realized with only polynomial number of single and two-particle quantum unitaries, which is the central idea of quantum simulation. This is also consistent with the previous discussion of parameter counting. When realizing an N-qubit unitary, the number of single and two-particle unitaries needed for a quantum circuit is called its circuit size, and polynomial size circuits (in terms of the system size N) are hence called efficient.

In practice, some of these single and two-particle unitaries on an N-particle system can be implemented in parallel. Therefore, the real time needed to realize a quantum circuit is the layer of unitaries where each layer contains parallel realizable single and two-particle unitaries. The number of layers is hence called the depth of the circuit. In general, a polynomial size circuit also needs to be realized by polynomial depth. In special cases it may be realized by a constant depth circuit, where the depth does not depend on the system size N (the number of particles). We will see in later chapters of this book that these constant depth circuits play an important role in characterizing gapped quantum phases.

Another issue for time evolution of a quantum system is due to decoherence. As already discussed in Chapter 1, the quantum state ρ_S of the system comes from a lager system $\mathscr{H}_S \otimes \mathscr{H}_E$, which is composed of both the system and its environment. The evolution of the total system, including both the system and its environment, is governed by the Schrödinger's equation and hence is unitary. However, when one only has access to the system but not the environment, the dynamics of the system only is in general non-unitary.

The question then becomes what the form of the general dynamics of the system could be. It should be of course a linear map as quantum mechanics is linear, but could this be enough? Quantum information theory developed a method of characterizing the general non-unitary dynamics of an open quantum system, called the completely positive trace-preserving map (TPCP). These maps can be characterized by a set of Kraus operators. The second half of this chapter will introduce this theory.

Physicists are likely more comfortable with dynamics governed by differential equations, and indeed theory of the differential equation for open quantum systems are substantially developed in quantum optics, which is the so called master equation. It is in general not possible to have such a differential equation, unless the evolution of the quantum system is 'Markovian,' in a sense that quantum state of a later time $\rho(t+dt)$ is completely determined by the quantum state of the previous time $\rho(t)$. Nevertheless, in many cases, the Markovian description is a very good

approximation. We will discuss the theory of master equation and use it to derive time evolution for a single qubit system corresponding to some general quantum noise, such as amplitude damping (i.e. spontaneous emission of a two-level atom), phase damping (dephasing), and depolarizing.

2.2 Unitary evolution

In the ideal case, the evolution of the wave function $|\psi_S\rangle \in \mathscr{H}_S$ of the system S is governed by the Schrödinger's equation

$$i\frac{\partial|\psi_S(t)\rangle}{\partial t} = H_S|\psi_S(t)\rangle, \tag{2.1}$$

where H_S is the Hamiltonian of the system $\mathscr{H}_S$, and we take $\hbar = 1$ for simplicity.

The solution of Eq. (2.1) is given by some unitary operator $U_S(t,t_0)$, that is,

$$|\psi_S(t)\rangle = U_S(t,t_0)|\psi_S(t_0)\rangle, \tag{2.2}$$

depending on the initial value of $|\psi_S(t_0)\rangle$. In case that the Hamiltonian H_S is time-independent, one has $U_S(t,t_0) = \exp[-iH_S(t-t_0)]$.

2.2.1 Single qubit unitary

Let us consider the unitary evolution of the simplest system - a two-level system (a qubit). Recall that the basis for a two-level quantum system is typically denoted by $|0\rangle$ and $|1\rangle$, and its two-dimensional Hilbert space is denoted by $\mathbb{C}_2$. Any quantum state $\alpha|0\rangle + \beta|1\rangle \in \mathbb{C}_2$ is called a qubit. Quantum evolution of a qubit is a 2×2 unitary matrix. The three Pauli matrices X,Y,Z are all unitary matrices, which together with I form a basis of 2×2 matrices.

Note that $X|0\rangle = |1\rangle$ and $X|1\rangle = |0\rangle$, i.e. the Pauli X operator flips the qubit basis states $|0\rangle \leftrightarrow |1\rangle$, therefore the Pauli X operator is also called 'bit flip'. The eigenvalues of X is ± 1 and the eigenvectors are

$$|\pm\rangle = \frac{1}{\sqrt{2}}(|0\rangle \pm |1\rangle). \tag{2.3}$$

We call the basis $\{|\pm\rangle\}$ the 'X basis'.

Also $Z|0\rangle = |0\rangle$ and $Z|1\rangle = -|1\rangle$, the Pauli Z operator flips the phase of the qubit basis state $|1\rangle$, therefore the Pauli Z is also called the 'phase flip'. Hence the eigenvalues of Z is ± 1 and the eigenvectors are $|0\rangle, |1\rangle$ respectively. We call the basis $\{|0\rangle, |1\rangle\}$ the 'Z basis' (or computational basis as discussed in Chapter 1).

The Hadamard operation R is given by

$$R = \frac{1}{\sqrt{2}}\begin{pmatrix} 1 & 1 \\ 1 & -1 \end{pmatrix}, \tag{2.4}$$

which is unitary. Note that $R^\dagger = R$, $R^2 = I$, and $RXR = Z$, $RZR = X$. That is, R is the transformation between the 'Z basis' and the 'X basis'.

And other important single-qubit unitaries are the X, Y, Z rotations given by

$$X_\theta = \exp(-i\theta X/2) = \cos\frac{\theta}{2}I - i\sin\frac{\theta}{2}X = \begin{pmatrix} \cos\frac{\theta}{2} & -i\sin\frac{\theta}{2} \\ -i\sin\frac{\theta}{2} & \cos\frac{\theta}{2} \end{pmatrix}, \tag{2.5}$$

and

$$Y_\theta = \exp(-i\theta Y/2) = \cos\frac{\theta}{2}I - i\sin\frac{\theta}{2}Y = \begin{pmatrix} \cos\frac{\theta}{2} & -\sin\frac{\theta}{2} \\ \sin\frac{\theta}{2} & \cos\frac{\theta}{2} \end{pmatrix}, \tag{2.6}$$

and

$$Z_\theta = \exp(-i\theta Z/2) = \cos\frac{\theta}{2}I - i\sin\frac{\theta}{2}Z = \begin{pmatrix} e^{-i\frac{\theta}{2}} & 0 \\ 0 & e^{i\frac{\theta}{2}} \end{pmatrix}. \tag{2.7}$$

Note that $X_\theta, Y_\theta, Z_\theta$ can be realized by the evolution of the Hamiltonian of the form X, Y, Z respectively, and the Hadamard operation R is actually $Z_\pi Y_{\pi/4} Z_\pi$. Actually we will show that Y, Z rotations together are enough to realize any single qubit unitary.

Box 2.1 Single-qubit unitary
For any unitary operation on a single qubit, there exist real numbers $\alpha, \beta, \gamma, \delta$ such that $U = e^{i\alpha} Z_\beta Y_\gamma Z_\delta$.

To show why this is the case, note that for any 2×2 unitary matrix U, the rows and columns of U are orthogonal plus that each row or column is a normalized vector. This then follows that there exist real numbers $\alpha, \beta, \gamma, \delta$ such that

$$U = \begin{pmatrix} e^{i(\alpha-\beta/2-\delta/2)}\cos\frac{\gamma}{2} & -e^{i(\alpha-\beta/2+\delta/2)}\sin\frac{\gamma}{2} \\ e^{i(\alpha+\beta/2-\delta/2)}\sin\frac{\gamma}{2} & e^{i(\alpha+\beta/2+\delta/2)}\cos\frac{\gamma}{2} \end{pmatrix}. \tag{2.8}$$

$U = e^{i\alpha} Z_\beta Y_\gamma Z_\delta$ then follows from Eq. (2.7) and Eq. (2.6).

2.2.2 *Two-qubit unitary*

Recall that a basis for an N-qubit system is chosen as the tensor products of $|0\rangle$s and $|1\rangle$s. For instance, for $N = 2$, the four basis states are $\{|00\rangle, |01\rangle, |10\rangle, |11\rangle\}$. As an example, here we discuss a two-qubit unitary operation which is the most-commonly used in quantum computing, called the controlled-NOT operation. It takes $|x\rangle \otimes |y\rangle$ to $|x\rangle \otimes |y \oplus x\rangle$, where $x, y \in \{0, 1\}$ and $\oplus$ is the addition mod 2.

Here the first qubit is called the control qubit, which remains unchanged, and the second qubit is called the target qubit, which is flipped if the control qubit is 1. In the basis of $\{|00\rangle,\ |01\rangle,\ |10\rangle,\ |11\rangle\}$ the matrix of a controlled-NOT gate is then given by

$$\begin{pmatrix} 1&0&0&0\\ 0&1&0&0\\ 0&0&0&1\\ 0&0&1&0 \end{pmatrix}. \tag{2.9}$$

Similarly, a controlled-NOT gate with the second qubit as the control qubit takes $|x\rangle\otimes|y\rangle$ to $|x\oplus y\rangle\otimes|y\rangle$.

Another important two-qubit unitary is called controlled-Z, which transforms the basis in the following way:

$$|00\rangle\to|00\rangle,\ |01\rangle\to|01\rangle,\ |10\rangle\to|10\rangle,\ |11\rangle\to-|11\rangle. \tag{2.10}$$

Given that the controlled-Z operation is symmetric between the two qubits, it is not necessary to specify which one is the control qubit and which one is the target qubit.

Now let us consider how to realize the controlled-NOT and the controlled-Z operations using some two-qubit Hamiltonian. Let us discuss a simple example where the interaction term H_{in} is Ising, i.e.

$$H_{in}=-JZ_1\otimes Z_2=-JZ_1Z_2. \tag{2.11}$$

Where Z_1,Z_2 are Pauli Z operations acting on the first and second qubits, respectively. We omit the tensor product symbol $\otimes$ when no confusion arises. Now observe that

$$\exp -i\frac{\pi}{4}(I-Z_1-Z_2+Z_1Z_2)=e^{-i\frac{\pi}{4}}e^{i\frac{Z_1\pi}{4}}e^{i\frac{Z_2\pi}{4}}e^{-i\frac{Z_1Z_2\pi}{4}}=\begin{pmatrix} 1&0&0&0\\ 0&1&0&0\\ 0&0&1&0\\ 0&0&0&-1 \end{pmatrix}, \tag{2.12}$$

which gives the controlled-Z operation. In other words, the single-qubit term Z together with the two-qubit Ising interaction term H_{in} can realize a controlled-Z operation.

For the controlled-NOT operation, note that

$$\begin{pmatrix} 1&0&0&0\\ 0&1&0&0\\ 0&0&0&1\\ 0&0&1&0 \end{pmatrix}=R_2\begin{pmatrix} 1&0&0&0\\ 0&1&0&0\\ 0&0&1&0\\ 0&0&0&-1 \end{pmatrix}R_2, \tag{2.13}$$

where R_2 is the Hadamard operation acting on the second qubit, i.e.

$$R_2 = I \otimes R = \begin{pmatrix} 1 & 0 \\ 0 & 1 \end{pmatrix} \otimes \frac{1}{\sqrt{2}} \begin{pmatrix} 1 & 1 \\ 1 & -1 \end{pmatrix} = \frac{1}{\sqrt{2}} \begin{pmatrix} 1 & 1 & 0 & 0 \\ 1 & -1 & 0 & 0 \\ 0 & 0 & 1 & 1 \\ 0 & 0 & 1 & -1 \end{pmatrix}. \tag{2.14}$$

Therefore, single qubit Hamiltonians of Y, Z terms together with the two-qubit Ising interaction term H_{in} can realize both the controlled-Z operation and the controlled-NOT operation.

Now let us look at another kind of two qubit unitary, called controlled-U, denoted by $\Lambda_{12}(U)$, where U is a single qubit unitary. Here qubit 1 is the control qubit, and qubit 2 is the target qubit. Similar as the controlled-NOT operation, $\Lambda_{12}(U)$ acts on any computational basis state as

$$\Lambda_{12}(U)|x\rangle \otimes |y\rangle = |x\rangle \otimes U^x|y\rangle, \tag{2.15}$$

where $x, y = 0, 1$. In this language, controlled-NOT is indeed $\Lambda_{12}(X)$ and controlled-Z is indeed $\Lambda_{12}(Z)$.

We are now ready to check that the following equation holds.

$$\Lambda_{12}(U) = (D \otimes A)\Lambda_{12}(X)(I \otimes B)\Lambda_{12}(X)(I \otimes C), \tag{2.16}$$

where

$$D = \begin{pmatrix} 1 & 0 \\ 0 & e^{i\alpha} \end{pmatrix}, \tag{2.17}$$

and U, α, A, B, C satisfy

$$\begin{aligned} U &= e^{i\alpha} AXBXC \\ I &= ABC. \end{aligned} \tag{2.18}$$

To see how this works, note that

$$\begin{aligned} &(D \otimes A)\Lambda_{12}(X)(I \otimes B)\Lambda_{12}(X)(I \otimes C)|x\rangle \otimes |y\rangle \\ =&(D \otimes A)\Lambda_{12}(X)(I \otimes B)\Lambda_{12}(X)|x\rangle \otimes C|y\rangle \\ =&(D \otimes A)\Lambda_{12}(X)(I \otimes B)|x\rangle \otimes X^x C|y\rangle \\ =&(D \otimes A)\Lambda_{12}(X)|x\rangle \otimes BX^x C|y\rangle \\ =&(D \otimes A)|x\rangle \otimes X^x BX^x C|y\rangle \\ =&D|x\rangle \otimes AX^x BX^x C|y\rangle \\ =&|x\rangle \otimes e^{i\alpha x} AX^x BX^x C|y\rangle. \end{aligned} \tag{2.19}$$

So for $x = 0$, the last line reads $|0\rangle \otimes |y\rangle$, and for $x = 1$, the last line reads $|1\rangle \otimes U|y\rangle$.

This then shows that any controlled-U unitary can be written as a product of single-qubit unitaries and controlled-NOT operations. Or in terms of Hamiltonians, single-qubit Hamiltonians of Y, Z terms together with the two-qubit Ising interaction

term H_{in} can realize any two-qubit controlled-U. In fact, these are enough to realize 'any' two-qubit unitary, as summarized below.

Box 2.2 Two-qubit unitary from single-qubit unitary and controlled-NOT

Any unitary operation on two qubits can be written as a product of single-qubit unitaries and controlled-NOT operations.

2.2.3 *N-qubit unitary*

Now consider a system of N qubits, whose Hilbert space $\mathbb{C}_2^{\otimes N}$ is the N-fold tensor product of $\mathbb{C}_2$. An N-qubit unitary is now a unitary operator U acting on N-qubits. In the general case, the corresponding Hamiltonian needed to implement this evolution U should contain interaction terms involving arbitrarily large number of qubits.

However, this is not the case of nature: the natural many-body Hamiltonians available usually contains only few-body interaction. That is, usually the Hamiltonian of the system can be written as the following form

$$H = \sum_j H_j, \tag{2.20}$$

where each term H_j involves only few-body interactions. Indeed, most of the time, H_js involve at most two-body interactions. For examples, the Ising model Hamiltonian H^{tIsing} in transverse magnetic field has the form

$$H^{\text{tIsing}} = -J\sum_{i,j} Z_i Z_j - B\sum_j X_j, \tag{2.21}$$

and the spin-$1/2$ Heisenberg Hamiltonian has the form

$$H_{\text{Heisenberg}} = -J\sum_{i,j} S_i \cdot S_j. \tag{2.22}$$

This then raises a question: can we realize an N-particle unitary U using two-body interactions only? This turns out to be possible, but one needs to pay some price. Before looking into more details, let us imagine a simpler scenario than those given by the many-body Hamiltonians (e.g Eq. (2.21) (2.22)), where one can indeed engineer the system Hamiltonian such that the two-body interaction between any of the two particles can be turned on or off (there are indeed those systems in lab, for instance in certain ion trap experiments and cavity QED experiments).

This simplified assumption then puts us in the scenario of the previous section. That is, suppose we have single qubit terms Y_i, Z_i available plus the Ising interaction $H_{ij} = -J_{ij} Z_i Z_j$, and can turn them on and off freely for any i, j. These then allow us

to perform any single qubit unitary operation and controlled-NOT between any two qubits.

In fact, as already mentioned, these are enough to realize any N-qubit unitary. In order not to get into too much technical details, we will discuss an example. We show how to implement a special kind of 3-qubit unitary, called controlled-controlled-U, denoted by $\Lambda^2_{123}(U)$, where U is a single qubit unitary. Here the qubits $1,2$ are the controlled qubits, and the qubit 3 is the target qubit. Similar as the controlled-U operation, $\Lambda^2_{123}(U)$ acts on any computational basis state as

$$\Lambda^2_{123}(U)|x\rangle \otimes |y\rangle \otimes |z\rangle = |x\rangle \otimes |y\rangle \otimes U^{xy}|z\rangle, \tag{2.23}$$

where $x, y, z \in \{0,1\}$.

For single qubit unitary U with the matrix form

$$U = \begin{pmatrix} a & b \\ c & d \end{pmatrix}, \tag{2.24}$$

$\Lambda^2_{123}(U)$ has the matrix form

$$\Lambda^2_{123}(U) = \begin{pmatrix} 1&0&0&0&0&0&0&0 \\ 0&1&0&0&0&0&0&0 \\ 0&0&1&0&0&0&0&0 \\ 0&0&0&1&0&0&0&0 \\ 0&0&0&0&1&0&0&0 \\ 0&0&0&0&0&1&0&0 \\ 0&0&0&0&0&0&a&b \\ 0&0&0&0&0&0&c&d \end{pmatrix}. \tag{2.25}$$

We are now ready to check the following equation holds.

$$\Lambda^2_{123}(U) = (\Lambda_{13}(V) \otimes I_2)(\Lambda_{12}(X) \otimes I_3)(I_1 \otimes \Lambda_{23}(V^\dagger))(\Lambda_{12}(X) \otimes I_3)(I_1 \otimes \Lambda_{23}(V)), \tag{2.26}$$

where $V^2 = U$.

To see why this is the case, recall that

$$\begin{aligned} \Lambda_{13}(V)|x\rangle \otimes |y\rangle \otimes |z\rangle &= |x\rangle \otimes |y\rangle \otimes V^x|z\rangle, \\ \Lambda_{12}(X)|x\rangle \otimes |y\rangle \otimes |z\rangle &= |x\rangle \otimes X^x|y\rangle \otimes |z\rangle, \\ \Lambda_{23}(V)|x\rangle \otimes |y\rangle \otimes |z\rangle &= |x\rangle \otimes |y\rangle \otimes V^y|z\rangle, \end{aligned} \tag{2.27}$$

hence

$$
\begin{aligned}
&(\Lambda_{13}(V)\otimes I_2)(\Lambda_{12}(X)\otimes I_3)(I_1\otimes\Lambda_{23}(V^\dagger))(\Lambda_{12}(X)\otimes I_3)(I_1\otimes\Lambda_{23}(V))|x\rangle\otimes|y\rangle\otimes|z\rangle\\
=&(\Lambda_{13}(V)\otimes I_2)(\Lambda_{12}(X)\otimes I_3)(I_1\otimes\Lambda_{23}(V^\dagger))(\Lambda_{12}(X)\otimes I_3)|x\rangle\otimes|y\rangle\otimes V^y|z\rangle,\\
=&(\Lambda_{13}(V)\otimes I_2)(\Lambda_{12}(X)\otimes I_3)(I_1\otimes\Lambda_{23}(V^\dagger))|x\rangle\otimes X^x|y\rangle\otimes V^y|z\rangle,\\
=&(\Lambda_{13}(V)\otimes I_2)(\Lambda_{12}(X)\otimes I_3)(I_1\otimes\Lambda_{23}(V^\dagger))|x\rangle\otimes|y\oplus x\rangle\otimes V^y|z\rangle,\\
=&(\Lambda_{13}(V)\otimes I_2)(\Lambda_{12}(X)\otimes I_3)|x\rangle\otimes|y\oplus x\rangle\otimes(V^\dagger)^{y\oplus x}V^y|z\rangle,\\
=&(\Lambda_{13}(V)\otimes I_2)|x\rangle\otimes X^x|y\oplus x\rangle\otimes(V^\dagger)^{y\oplus x}V^y|z\rangle,\\
=&(\Lambda_{13}(V)\otimes I_2)|x\rangle\otimes|y\rangle\otimes(V^\dagger)^{y\oplus x}V^y|z\rangle,\\
=&|x\rangle\otimes|y\rangle\otimes V^x(V^\dagger)^{y\oplus x}V^y|z\rangle. \qquad (2.28)
\end{aligned}
$$

Therefore, only when $x=y=1$, the last line $V^x(V^\dagger)^{y\oplus x}V^y=V^2=U$, otherwise $V^x(V^\dagger)^{y\oplus x}V^y=I$.

Note that although $\Lambda^2_{123}(U)$ acts on an 8-dimentional space, it is effectively a 'two-level unitary'. That is, it is a unitary on the subspace spanned by $|110\rangle,|111\rangle$. The observation is that two-level unitaries are enough to realize any N-qubit unitary, if one can implement two-level unitaries on any two-level of the system (i.e. any two-dimensional subspace of the 2^N-dimensional Hilbert space).

To illustrate the idea, consider an 3×3 unitary U. The claim is that it can be realized as $U=U_1U_2U_3$, where U_1,U_2,U_3 are of the form

$$
U_1=\begin{pmatrix} a_1 & b_1 & 0\\ c_1 & d_1 & 0\\ 0 & 0 & 1\end{pmatrix},\quad U_2=\begin{pmatrix} a_2 & 0 & b_2\\ 0 & 1 & 0\\ c_2 & 0 & d_2\end{pmatrix},\quad U_3=\begin{pmatrix} 1 & 0 & 0\\ 0 & a_3 & b_3\\ 0 & c_3 & d_3\end{pmatrix}. \qquad (2.29)
$$

The idea of decomposing an N-qubit unitary in terms of two-level unitaries is just similar.

Of course one still needs to show that single qubit unitaries and controlled-NOT between any two qubits can produce any two-level unitary. This is indeed possible and we omit the details. We then come to the result that is summarized below.

Box 2.2 ***N*-qubit unitary from single-qubit unitary and controlled-NOT**
Any unitary operation on N qubits can be written as a product of single-qubit unitaries and controlled-NOT operations.

In terms of Hamiltonians, we have shown that single-qubit Hamiltonians of Y,Z terms together with the two-qubit Ising interaction term H_{in} can realize any N-qubit unitary. In fact, there is nothing special about the Ising interaction $H_{ij}=-J_{ij}Z_iZ_j$. Any non-trivial two-qubit interaction, in a sense that it is able to produce entanglement when acting on some input pure state without entanglement (i.e. product state), is enough to realize any N-qubit unitary. We summarize this observation below.

Box 2.4 N-qubit unitary evolutions from single- and two-qubit ones
Single qubit terms and any non-trivial two-qubit interaction can generate an arbitrary N-qubit unitary evolution.

However, we need to emphasize the that the efficiency of this realization is in general poor. According to the steps we result in this realization, an arbitrary N-qubit unitary may be written as $\sim 4^N$ two-level unitary operations, and implementing a two-level operation needs $\sim N^2$ single particle and controlled-U operations, which gives $\sim N^2 4^N$ single particle and controlled-U operations to realize an arbitrary N-qubit unitary. We summarize this observation below.

Box 2.5 Inefficiency in realizing N-qubit unitaries from single- and two-qubit ones
In general, exponentially many single and two-qubit unitaries are needed for generating an N-qubit unitary evolution.

2.3 Quantum Circuits

In the previous section we have mentioned the name of 'quantum computing', but we do not even tell what a 'quantum computer' is. It is not our goal here to discuss the theory of computation, rather, we would like to tell that at least one model of quantum computing, called the circuit model, is based on the unitary evolution discussed in the previous section.

In this model, the initial N-qubit state $|\psi_i\rangle$ is usually chosen as the all $|0\rangle$ state $|0\rangle \otimes |0\rangle \cdots \otimes |0\rangle$, which is in short written as $|00\cdots0\rangle$ or $|0\rangle^{\otimes N}$. Then a sequence of single- and two-qubit quantum unitaries are applied on $|\psi_i\rangle$ to result in a final state $|\psi_f\rangle$. And finally single-qubit measurements are performed on each qubit, usually in the $\{|0\rangle, |1\rangle\}$ basis, to obtain the result of the computation. And we know that single and two-qubit quantum unitaries are enough to implement any N-qubit unitary, regardless it might be in an inefficient manner in general.

The sequence of single- and two-qubit unitaries then gives rise to a diagram called 'quantum circuit', and this model is then called the 'circuit model' of quantum computing. We discuss an example of the circuit diagram. Here each vertical line represents a qubit, and each box putting on a single line or across two lines are single and two-qubit uintaries, respectively. Time goes from bottom to top.

For a given circuit diagram, there are some important parameters to characterize its efficiency property.

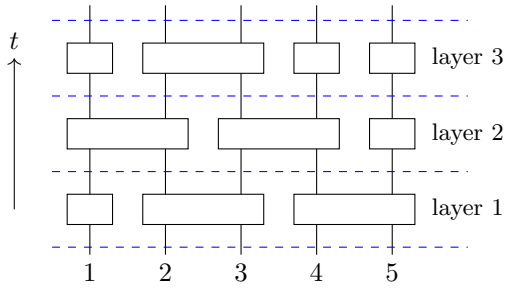

Fig. 2.1 Circuit diagram with the number of qubits $N = 5$ and the number of layers $M = 3$.

Box 2.6 Circuit size
The number of boxes in a circuit diagram is called its size. The circuit is efficient if when the number N of qubits grow, the circuit size does not grow exponentially with N, in other words, the size of the circuit is just some polynomial of N.

Also, as a box is only cross one or two lines, some of them can be implemented in one layer, i.e., in parallel. So the evolution time of the entire circuit will be the number of layers.

Box 2.7 Circuit depth
The number of layers in a circuit diagram is called its depth. A constant depth circuit is a circuit with depth which does not increase with N.

As we will discuss later in Chapter 7, constant depth circuits play an important role studying gapped quantum phases. Note that in general, an efficient circuit of size polynomial in N does not allow a constant depth circuit, so requiring 'constant depth' is a much stronger constraint than requiring 'efficiency'.

We now discuss an application of the quantum circuit model. We know that there are some N-qubit unitary evolutions which are hard to implement. However, we know that the natural occurring Hamiltonians usually involve only few-body interactions, such as the Ising Hamiltonian and the Heisenberg Hamiltonian. The good news is that the evolution of these natural Hamiltonians can be simulated efficiently by a quantum circuit model, meaning that it is possible to reproduce the evolution to certain precision using only $p(N)$ number of single and two-bit unitary operations, where $p(N)$ is any polynomial in N. In terms of Hamiltonians, we summarize this observation as following.

Box 2.8 Quantum simulation
The evolution of few-body Hamiltonians can be simulated efficiently by single qubit Y,Z terms and any non-trivial two-qubit interaction.

To see how this could be possible, recall that the solution to a Schrödinger's equation $i\frac{\partial|\psi(t)\rangle}{\partial t} = H|\psi(t)\rangle$ with a time independent Hamiltonian H is given by $|\psi(t)\rangle = \exp[-iH(t-t_0)]$. Now our task is to build an efficient quantum circuit with only polynomial number of single and two-qubit unitary operations, which reproduces the unitary evolution $\exp -iH(t-t_0)$ to certain precision. For simplicity we take $t_0 = 0$.

For a few body Hamiltonian H, we can write

$$H = \sum_{j=1}^{L} H_j, \tag{2.30}$$

where each H_i acting nontrivially only on a few number of particles, and L is a polynomial function of N.

In the simplest case, if $[H_j,H_k] = 0$ for all j,k, i.e. all the terms H_j commute, then the evolution $\exp -iHt$ is given by

$$\exp[-iHt] = \exp[-it\sum_{j=1}^{L} H_j] = \prod_{j=1}^{L} \exp[-iH_j t]. \tag{2.31}$$

This directly gives an efficient quantum circuit, as each $\exp[-iH_j t]$ is a unitary acting on only a few number of particles (which is independent of the number of particles N), hence can be realized by a constant number (i.e. independent of N) of single and two-particle unitary operations.

The real challenge is when those H_is do not commute. In this case we need the following Lie product formula.

Box 2.9 Lie product formula
$\lim_{s\to\infty}(e^{iAt/s}e^{iBt/s})^s = e^{i(A+B)t}$.

To prove this formula, note that the Taylor expansion for $e^{iAt/s}$ is given by

$$e^{iAt/s} = I + \frac{1}{s}(iAt) + O(\frac{1}{s^2}). \tag{2.32}$$

Here $O(\frac{1}{s^2})$ means the terms of the order $\frac{1}{s^2}$ or higher. Therefore,

$$e^{iAt/s}e^{iBt/s} = I + \frac{1}{s}i(A+B)t + O(\frac{1}{s^2}), \tag{2.33}$$

which gives

$$\left(e^{iAt/s}e^{iBt/s}\right)^s = \left(I + \frac{1}{s}i(A+B)t + O(\frac{1}{s^2})\right) = I + \sum_{k=1}^{s}\binom{s}{k}\frac{1}{s^k}\left[i(A+B)t\right]^k + O(\frac{1}{s^2}). \tag{2.34}$$

Since

$$\binom{s}{k}\frac{1}{s^k} = \frac{1}{k!}\left[1 + O(\frac{1}{s})\right], \tag{2.35}$$

taking the limit $s \to \infty$ gives

$$\lim_{s\to\infty}\left(e^{iAt/s}e^{iBt/s}\right)^s = \lim_{s\to\infty}\sum_{k=0}^{s}\frac{[i(A+B)t]^k}{k!}(1 + O(\frac{1}{s})) + O(\frac{1}{s^2}) = e^{i(A+B)t}. \tag{2.36}$$

The idea for quantum simulation is now to use a similar reasoning for proving the Lie product formula to approximate $\exp -iHt$ to certain precision. We look at some examples, and we consider a small time interval $\Delta t = \frac{t}{s}$. First note that

$$e^{i(A+B)\Delta t} = e^{iA\Delta t}e^{iB\Delta t} + O(\Delta t^2), \tag{2.37}$$

similarly

$$e^{i(A+B)\Delta t} = e^{iA\Delta t/2}e^{iB\Delta t}e^{iA\Delta t/2} + O(\Delta t^3). \tag{2.38}$$

For $H = \sum_{j=1}^{L} H_j$, one can further show that

$$e^{-2iH\Delta t} = \left[e^{-iH_1\Delta t}e^{-iH_2\Delta t}\ldots e^{-iH_L\Delta t}\right]\left[e^{-iH_L\Delta t}e^{-iH_{L-1}\Delta t}\ldots e^{-iH_1\Delta t}\right] + O(\Delta t^3), \tag{2.39}$$

Here each $\exp[-iH_j\Delta t]$ is a unitary operation on only a few number of particles, hence can be realized by a constant number (i.e. independent of N) of single and two-particle unitary operations.

A more detailed analysis will show that in order to achieve the precision ε for the simulation, in a sense that the output of the simulation is $|\psi'(t)\rangle$ such that

$$|\langle\psi'(t)|e^{-iHt}|\psi(0)\rangle|^2 \geq 1 - \varepsilon, \tag{2.40}$$

then one would need a quantum circuit with $\text{poly}(\frac{1}{\varepsilon})$ (i.e. polynomial in $\frac{1}{\varepsilon}$) number of single and two-particle unitary operations.

2.4 Open Quantum Systems

However, in the general case, the system S is coupled with the environment E, which results in non-unitary evolution of the system. In this case, the evolution of the wave function $|\psi_{SE}\rangle \in \mathscr{H}_S \otimes \mathscr{H}_E$ is governed by the Schrödinger's equation

$$i\frac{\partial|\psi_{SE}(t)\rangle}{\partial t} = H_{SE}|\psi_{SE}(t)\rangle, \tag{2.41}$$

where H_{SE} is the Hamiltonian of the total system $\mathscr{H}_S \otimes \mathscr{H}_E$, and the solution of Eq.(2.41) is given by some unitary operator $U_{SE}(t,t_0)$. That is,

$$|\psi_{SE}(t)\rangle = U_{SE}(t,t_0)|\psi_{SE}(t_0)\rangle, \tag{2.42}$$

depending on the initial value of $|\psi_{SE}(t_0)\rangle$.

For any density operator, ρ_{SE} acting on $\mathscr{H}_S \otimes \mathscr{H}_E$, its time evolution $\rho_{SE}(t)$ is then given by

$$\rho_{SE}(t) = U_{SE}(t,t_0)\rho_{SE}(t_0)U_{SE}^\dagger(t,t_0). \tag{2.43}$$

What we are interested in is the evolution of the system described by the density operator

$$\rho_S(t) = \mathrm{Tr}_E\,\rho_{SE}(t). \tag{2.44}$$

Suppose initially the system is in a product state with the environment and the environment is in some pure state, say $|0_E\rangle$, i.e. $\rho_{SE}(t_0) = \rho_S(t_0)\otimes|0_E\rangle\langle 0_E|$, then Eq.(2.44) becomes

$$\begin{aligned}\rho_S(t) &= \mathrm{Tr}_E\,\rho_{SE}(t)\\ &= \mathrm{Tr}_E\,U_{SE}(t,t_0)(\rho_S(t_0)\otimes|0_E\rangle\langle 0_E|)U_{SE}^\dagger(t,t_0)\\ &= \sum_k \langle k_E|U_{SE}(t,t_0)|0_E\rangle\rho_S(t_0)\langle 0_E|U_{SE}^\dagger(t,t_0)|k_E\rangle,\end{aligned} \tag{2.45}$$

where $\{|k_E\rangle\}$ is an orthonormal basis of H_E, and $\langle k_E|U_{SE}(t,t_0)|0_E\rangle$ is an operator acting on H_S, for each k. Let us write

$$E_k = \langle k_E|U_{SE}(t,t_0)|0_E\rangle, \tag{2.46}$$

then we have

$$\mathscr{E}(\rho_S(0)) = \rho_S(t) = \sum_k E_k\rho_S(t_0)E_k^\dagger. \tag{2.47}$$

Note that

$$\begin{aligned}\sum_k E_k^\dagger E_k &= \sum_k \langle 0_E|U_{SE}^\dagger(t,t_0)|k_E\rangle\langle k_E|U_{SE}(t,t_0)|0_E\rangle\\ &= \langle 0_E|U_{SE}^\dagger(t,t_0)U_{SE}(t,t_0)|0_E\rangle = I\end{aligned} \tag{2.48}$$

The map $\mathscr{E}$ defined by Eq.(2.47) is a linear map. One can write $\mathscr{E} = \{E_1, E_2, \ldots\}$, and when the property of Eq.(2.48) is satisfied, the map $\mathscr{E}$ is then called a superoperator. Eq.(2.47) is then called the operator sum representation of $\mathscr{E}$, or the Kraus representation where each E_k is a Kraus operator. We summarize this Kraus representation for non-unitary evolutions as below.

Box 2.10 Kraus representation for non-Unitary evolution
$\mathscr{E}(\rho_S(0)) = \rho_S(t) = \sum_k E_k \rho_S(t_0) E_k^\dagger$, where $\sum_k E_k^\dagger E_k = I$.

Note that for a given superoperator $\mathscr{E}$, the operator sum representation is not unique. This is because that in performing the partial trace as in Eq.(2.45). Say, if we instead use $\{\langle j_E| = \sum_k U_{jk}\langle k_E|\}$, then we get another representation

$$\mathscr{E}(\rho_S(0)) = \rho_S(t) = \sum_k F_k \rho_S(t_0) F_k^\dagger, \tag{2.49}$$

where $F_k = U_{jk}E_k$.

We now discuss some properties of the superoperator $\mathscr{E}$. From now on, we omit the superscript S for discussing the system evolution when no confusion arises. The most important property of $\mathscr{E}$ is that it maps density operators to density operators. This can be seen from Eq.(2.47) and Eq.(2.48):

1. $\rho(t)$ is Hermitian:

$$\rho(t)^\dagger = \left(\sum_k E_k \rho(t_0) E_k^\dagger\right)^\dagger = \sum_k E_k \rho^\dagger(t_0) E_k^\dagger = \rho(t) \tag{2.50}$$

2. $\rho(t)$ is with unit trace:

$$\mathrm{Tr}\,\rho(t) = \mathrm{Tr}\left(\sum_k E_k \rho(t_0) E_k^\dagger\right) = \mathrm{Tr}\left(\sum_k E_k^\dagger E_k \rho(t_0)\right) = \mathrm{Tr}(\rho(t_0)) = 1 \tag{2.51}$$

3. $\rho(t)$ is positive:

$$\langle\psi|\rho(t)|\psi\rangle = \sum_k (\langle\psi|E_k)\rho(t_0)(E_k^\dagger|\psi\rangle) \geq 0. \tag{2.52}$$

Finally, we remark that orthogonal measurements can also be 'interpreted' as in terms of the Kraus representation. In this case, take a set of operators $\{\Pi_k\}$ which are orthogonal projections in the Hilbert space $\mathscr{H}$, that is,

$$\Pi_k = \Pi_k^\dagger, \quad \Pi_j \Pi_k = \delta_{jk}\Pi_k, \quad \sum_k \Pi_k = I, \tag{2.53}$$

then the quantum operation $\mathscr{M}$ describing the measurement is

$$\mathscr{M}(\rho) = \sum_k \Pi_k \rho \Pi_k. \tag{2.54}$$

When ρ is a pure state $|\psi\rangle$, the measurement will take $|\psi\rangle\langle\psi|$ to

$$\frac{\Pi_k|\psi\rangle\langle\psi|\Pi_k}{\langle\psi|\Pi_k|\psi\rangle}, \tag{2.55}$$

with probability

$$p_k = \langle\psi|\Pi_k|\psi\rangle. \tag{2.56}$$

2.5 Master Equation

We know that the evolution of an open quantum system are given by superoperator on the density matrix of the system. For a closed system, the evolution is governed by the integrating the Schrödinger's equation Eq (2.41). A natural question is what is the differential equation governing the dynamics of an open system. This is the so-called master equation, which is extensively studied in the field of quantum optics. We will discuss master equation in this section.

2.5.1 The Lindblad Form

We start from rewriting the Schrödinger's equation Eq (2.41) in terms of density matrices.

$$\frac{d\rho_{SE}}{dt} = -i[H_{SE}, \rho_{SE}], \tag{2.57}$$

where $[H,\rho] = H\rho - \rho H$ is the commutator of H and ρ. Tracing out the environment will give us the time evolution of the density matrix of the system

$$\frac{d\rho_S}{dt} = \mathrm{Tr}_E(\frac{d\rho_{SE}}{dt}) = \mathrm{Tr}_E(-i[H_{SE}, \rho_{SE}]). \tag{2.58}$$

Now we consider the time evolution of the system density matrix $\rho(t)$, where we omit the subscript S. We know that in general Eq. (2.58) will give a time evolution governed by a superoperation in terms of Kraus operators, i.e.

$$\rho(t) = \mathscr{E}(\rho) = \sum_k E_k(t)\rho(t_0)E_k^\dagger(t). \tag{2.59}$$

To derive a differential equation for $\rho(t)$, let us consider the infinitesimal time interval dt, and write

$$\rho(t+dt) = \rho(t) + O(dt). \tag{2.60}$$

Note here an assumption is made: we assume that the evolution of the quantum system is 'Markovian,' in a sense that $\rho(t+dt)$ is completely determined by $\rho(t)$. This is not generally guaranteed by Eq. (2.59), as the environment, though inaccessible, may have some memory of the system. Nevertheless, in many situations, the Markovian description is a very good approximation.

Based on the Markovian approximation, we now further expand the Kraus operators in terms of dt, where we will have one of the operators E_0 with order one, that we write as

$$E_0 = I + (-iH + M)dt, \tag{2.61}$$

where both H, M are chosen to be Hermitian and are zeroth order in dt. And the other Kraus operators E_k with order $\sqrt{dt}$, which has the form

$$E_k = \sqrt{dt} L_k,\ k > 0, \tag{2.62}$$

where L_k are zeroth order in dt.

The condition $\sum_k E_k^\dagger E_k = I$ the gives

$$M = -\frac{1}{2}\sum_{k>0} L_k^\dagger L_k. \tag{2.63}$$

The first order of dt from Eq. (2.59) gives

Box 2.11 The Lindblad equation

$$\frac{d\rho}{dt} = -i[H,\rho] + \sum_{k>0}(L_k \rho L_k^\dagger - \frac{1}{2}L_k^\dagger L_k \rho - \frac{1}{2}\rho L_k^\dagger L_k). \tag{2.64}$$

The operators L_k are called Lindblad operators. The first term of Eq. (2.64) is usual Hamiltonian term which generates unitary evolutions. The other terms describe the dissipation of the system due to interaction with the environment.

To solve Eq. (2.64), it is helpful to look at the interaction picture. Let

$$\tilde{\rho}(t) = e^{iHt}\rho(t)e^{-iHt}, \tag{2.65}$$

which then gives

$$\frac{d\tilde{\rho}(t)}{dt} = \sum_{k>0}(\tilde{L}_k \tilde{\rho} \tilde{L}_k^\dagger - \frac{1}{2}\tilde{L}_k^\dagger \tilde{L}_k \tilde{\rho} - \frac{1}{2}\tilde{\rho}\tilde{L}_k^\dagger \tilde{L}_k), \tag{2.66}$$

where

$$\tilde{L}_k = e^{iHt} L_k e^{-iHt}. \tag{2.67}$$

2.5.2 Master equations for a single qubit

We now examine some examples of the non-unitary dynamics for a single quit. More precisely, we will discuss a qubit under amplitude damping, phase damping, and depolarizing respectively.

Amplitude Damping

By studying a typical example, we will show how to derive the master equation for a specified system. Here we consider a two-level atom interacting with an electromagnetic environment, which is modeled as

$$H = H_S + H_E + V, \tag{2.68}$$

where

$$H_S = \frac{\omega_a}{2}\sigma_z, \tag{2.69}$$

$$H_E = \sum_j \omega_j b_j^\dagger b_j, \tag{2.70}$$

$$V = \sum_j g_j(\sigma_+ b_j + \sigma_- b_j^\dagger). \tag{2.71}$$

Here H_S and H_E are the free Hamiltonians for the two-level atom and the electromagnetic environment respectively, and V describes the interactions between the atom and the environment. $\sigma_x, \sigma_y, \sigma_z$ are the Pauli matrices, $\sigma_\pm = \sigma_x \pm i\sigma_y$, and ω_a is the energy level splitting for the atom. b_j and $b_j^\dagger$ are the annihilation and creation operator for the j-th mode of the electromagnetic field with frequency ω_j, and g_j is the coupling strength between the atom and the j-th mode of the environment.

In the interaction picture, the dynamics of the global system is governed by

$$\frac{d\tilde{\rho}}{dt} = -i[\tilde{V}, \tilde{\rho}], \tag{2.72}$$

where

$$\begin{aligned}\tilde{V}(t) &= e^{i(H_S+H_E)t} V e^{-i(H_S+H_E)t} \\ &= \sum_j g_j(\sigma_+ b_j e^{-i(\omega_j-\omega_a)t} + \sigma_- b_j^\dagger e^{i(\omega_j-\omega_a)t}).\end{aligned} \tag{2.73}$$

First, we assume that the reservoir initially stays in a vacuum state, i.e., the photon number is zero. Furthermore, we assume that the condition for the Markov approximation is satisfied. Then the state of the global system at time t is approximated as

$$\tilde{\rho}(t) = \tilde{\rho}_S(t) \otimes \rho_E \tag{2.74}$$

with $\rho_E = \prod_j |0_i\rangle\langle 0_j|$.

To the second order approximation, the state evolution from time t to $t+\Delta t$ is

$$\tilde{\rho}(t+\Delta t) - \tilde{\rho}(t) = -i\int_t^{t+\Delta t} [\tilde{V}(t'), \tilde{\rho}(t)] + (-i)^2 \int_t^{t+\Delta t} dt' \int_t^{t'} dt'' [\tilde{V}(t'), [\tilde{V}(t''), \tilde{\rho}(t)]]. \tag{2.75}$$

Inserting Eq. (2.73) and Eq. (2.74) into Eq. (2.75), we have

$$\begin{aligned}
&\tilde{\rho}_S(t+\Delta t) - \tilde{\rho}_S(t) \\
&= -\int_t^{t+\Delta t} dt' \int_t^{t'} dt'' \\
&\left(\sum_j g_j^2 e^{-i(\omega_j - \omega_a)(t'-t'')} \mathrm{Tr}_E [\sigma_+ b_j, [\sigma_- b_j^\dagger, \tilde{\rho}_S(t) \otimes \rho_E]] + h.c. \right) \\
&= -\int_t^{t+\Delta t} dt' \int_t^{t'} dt'' \left(\sum_j g(t'-t'') [\sigma_+, \sigma_- \tilde{\rho}_S(t)] + h.c. \right)
\end{aligned}$$

where

$$g(\tau) = \sum_j g_j^2 e^{-i(\omega_j - \omega_a)\tau}. \tag{2.76}$$

Since $g(\tau)$ is a combination of many oscillation functions, then in many case it will decrease to zero in a characteristic time τ_c. We consider the case when $\Delta t \gg \tau_c$. Then

$$\tilde{\rho}_S(t+\Delta t) - \tilde{\rho}_S(t) \simeq -\int_0^\infty d\tau \int_t^{t+\Delta t} dt' \left(\sum_j g(\tau) [\sigma_+, \sigma_- \tilde{\rho}_S(t)] + h.c. \right) \tag{2.77}$$

Therefore we obatin

$$\begin{aligned}
\frac{d\tilde{\rho}_S(t)}{dt} &= -\int_0^\infty d\tau \left(g(\tau) [\sigma_+, \sigma_- \tilde{\rho}_S(t)] - g^*(\tau) [\sigma_-, \tilde{\rho}_S(t) \sigma_+] \right) \\
&= \frac{1}{2} \left((\Gamma + \Gamma^*) \sigma_- \tilde{\rho}_S \sigma_+ - \Gamma \sigma_+ \sigma_- \tilde{\rho}_S - \Gamma^* \tilde{\rho}_S \sigma_+ \sigma_- \right),
\end{aligned} \tag{2.78}$$

where

$$\Gamma = 2 \int_0^\infty d\tau g(\tau). \tag{2.79}$$

Since the imarginary part of Γ represents the energy shift due to the environment, we neglect its contribution here. Then

$$\begin{aligned}\Gamma &= \int_{-\infty}^{\infty} d\tau \int_0^{\infty} d\omega \rho(\omega) g^2(\omega) e^{-i(\omega-\omega_a)\tau} \\ &= 2\pi \int_0^{\infty} d\omega \rho(\omega) g^2(\omega) \delta(\omega-\omega_a) \\ &= 2\pi g(\omega_a)\rho(\omega_a), \end{aligned} \tag{2.80}$$

which is the decay rate of the excited level, consistent with the result from the Fermi golden rule.

Therefore, in the interaction picture, the master equation of amplitude damping is given by

$$\frac{d\rho}{dt} = \frac{\Gamma}{2}(2\sigma_-\rho\sigma_+ - \sigma_+\sigma_-\rho - \rho\sigma_+\sigma_-). \tag{2.81}$$

Recall that the bloch representation of the density matrix $\rho = \frac{1}{2}(I + \mathbf{r}\cdot\sigma)$. Solving this equation for $\mathbf{r}(t)$ then gives

$$\begin{aligned} r_x(t) &= r_x(0)e^{-\frac{\Gamma}{2}t} \\ r_y(t) &= r_y(0)e^{-\frac{\Gamma}{2}t} \\ r_z(t) &= r_z(0)e^{-\Gamma t} - 1 + e^{-\Gamma t}. \end{aligned} \tag{2.82}$$

Eq. (2.82) can be further written as

$$\rho_{00}(t) = \rho_{00}(0)e^{-\Gamma t}, \tag{2.83}$$

$$\rho_{01}(t) = \rho_{01}(0)e^{-\frac{\Gamma}{2}t}. \tag{2.84}$$

Eq. (2.83) implies that Γ is the decay rate of the excited state. It is worthy to note that in this case the decay rate of the non-diagonal term ρ_{01} is $\frac{\Gamma}{2}$.

Let $\gamma = 1 - e^{-\Gamma t}$, then one has

$$\rho(t) = E_0\rho E_0^\dagger + E_1\rho E_1^\dagger, \tag{2.85}$$

where the Kraus operators E_0, E_1 are given as the following.

Box 2.12 Kraus operators for amplitude damping

$$E_0 = \begin{pmatrix} 1 & 0 \\ 0 & \sqrt{1-\gamma} \end{pmatrix}, \quad E_1 = \begin{pmatrix} 0 & \sqrt{\gamma} \\ 0 & 0 \end{pmatrix}.$$

To give a physical explanation of the amplitude damping channel, let us imagine that the qubit is a two-level atom, and it is initially prepared in the excited state $|0\rangle$. Then the probability for the atom keeping in the excited state is

$$\langle 0|\rho|0\rangle(t) = \frac{1 + r_z(t)}{2} = e^{-\Gamma t}. \tag{2.86}$$

Eq. (2.86) implies that the atom spontaneously decays from the excited state to the ground state with the rate Γ. Therefore the amplitute damping channel physically corresponds to the spontaneous decay process in atomic physics.

Phase Damping

In this subsection, we consider another type of interaction between the two-level atom and the electromagnetic environment, which is described by

$$V = \sum_j g_j \sigma_z (b_j + b_j^\dagger). \tag{2.87}$$

Notice that this type of interaction does not change the system's energy, but labels different energy levels through the environment, which leads to the relative phase damping between the system's levels.

Similarly as the derivation for the case of amplitude damping, we get the master equation in the Lindblad form

$$\begin{aligned} \frac{d\rho}{dt} &= \frac{\Gamma}{4}[2\sigma_z\rho\sigma_z - \sigma_z^2\rho - \rho\sigma_z^2] \\ &= \frac{\Gamma}{2}[\sigma_z\rho\sigma_z - \rho], \end{aligned} \tag{2.88}$$

where Γ is a coefficent, whose meaning is explained as follows.

To have a physical understanding of the phase damping noise, we rewrite Eq. (2.88) as

$$\frac{d\langle 0|\rho|0\rangle}{dt} = 0, \tag{2.89}$$

$$\frac{d\langle 0|\rho|1\rangle}{dt} = -\Gamma\langle 0|\rho|1\rangle. \tag{2.90}$$

Thus we have

$$\langle 0|\rho(t)|0\rangle = \langle 0|\rho(0)|0\rangle, \tag{2.91}$$

$$\langle 0|\rho(t)|1\rangle = \langle 0|\rho(0)|1\rangle e^{-\Gamma t}. \tag{2.92}$$

Notice that the diagonal terms of the density matrix represent the populations in the ground and the excited states, and the non-diagonal terms describe the coherence between the ground state and the excited state. Thus the phase damping channel describe a decoherencing process without exchanging energy with the environment, and the coefficient Γ denotes the decay reate of coherence.

Let $\gamma = 1 - e^{-\Gamma t}$. Then the Kraus operators for the phase damping channel can be written as the following.

Box 2.13 Kraus operators for phase damping

$$E_0 = \sqrt{1-\gamma}I, \quad E_1 = \begin{pmatrix} \sqrt{\gamma} & 0 \\ 0 & 0 \end{pmatrix}, \quad E_2 = \begin{pmatrix} 0 & 0 \\ 0 & \sqrt{\gamma} \end{pmatrix}.$$

Depolarizing

In this subsection, we consider a two-level atom interacting with three independent reservoirs, whose Hamiltonian is

$$H = H_S + \sum_{j=1}^{3} H_{E_j} + V_j, \tag{2.93}$$

where

$$H_S = \frac{\omega_a}{2}\sigma_z, \tag{2.94}$$

$$H_{E_j} = \sum_k \omega_{jk} b_{jk}^\dagger b_{jk}, \tag{2.95}$$

$$V_j = \sum_k g_{jk}\sigma_j (b_{jk}^\dagger + b_{jk}). \tag{2.96}$$

Approximately, the system's evolution can be understood as the sum of the influences caused by the independent reservoirs.

Similarly we obtain the master equation of depolarizing in the Lindblad form

$$\frac{d\rho}{dt} = \frac{\Gamma}{6} \sum_{j=x,y,z} (2\sigma_j \rho \sigma_j - \sigma_j \sigma_j \rho - \rho \sigma_j \sigma_j). \tag{2.97}$$

Intuitively, the master equation of depolarizing can be understood as a combination of three different 'phase dampings'. Here Γ can be understood as the decay rate from any state to its orthogonal state.

Note that Eq. (2.97) can be simplified as

$$\frac{d\rho}{dt} = -\Gamma(\rho - \frac{I}{2}). \tag{2.98}$$

Eq.(2.98) gives

$$\rho(t) = \rho(0)e^{-\Gamma t} + (1 - e^{-\Gamma t})\frac{I}{2}. \tag{2.99}$$

Thus the depolarizing noise is the quantum operation that depolarizes the state into a completely mixed state. The depolarizing channel is so simple that it is often used in theoretical investigations related with the effect of quantum noise.

Let $\gamma = 1 - e^{-\Gamma t}$. Then the Kraus operators for the depolarizing channel as the following.

Box 2.14 Kraus operators for depolarizing

$$E_0 = \sqrt{1-\gamma}I, \quad E_1 = \sqrt{\frac{\gamma}{3}}\sigma_x, \quad E_2 = \sqrt{\frac{\gamma}{3}}\sigma_y, \quad E_3 = \sqrt{\frac{\gamma}{3}}\sigma_z.$$

2.6 Summary and further reading

In this chapter, we have discussed evolution for a quantum system S with Hilbert space $\mathscr{H}_S$, whose quantum state is described by a density matrix ρ_S. In the ideal case, the evolution of the wave function $|\psi_S\rangle \in \mathscr{H}_S$ is unitary, which is governed by the Schrödinger's equation. This unitary evolution gives rise to the circuit model of quantum computation, where the computational procedure is to 'apply' single- and two-bit unitary operations to the quantum state carrying information of the computation. This quantum circuit viewpoint is practical as usual Hamiltonians for an interacting systems involve only few-body interactions, and in the most cases two-body interactions, which can be use to carry out single- and two-qubit unitary operations.

It has been shown in quantum information theory that arbitrary single-qubit unitary operators and a non-trivial two-qubit unitary operator (e.g. the controlled-NOT) are enough to construct any N-qubit unitary operator. Historically, this was first shown in [5], which is extended and simplified in the follow-up paper [1].

Our treatment in Section 2.3 starting from two-level unitaries then controlled-NOTs is according to Chapter 4.5 of Nielsen and Chuang's book [11]. This approach is originally in [12]. It was shown in [4] and independently in [10] that almost any two-qubit unitary operation can be used to construct any N-qubit unitary.

The circuit model of quantum computing is originally due to Deutsch's 1989 work [3]. The circuit diagram we used in Fig. 2.1 is not a standard one used in quantum computation. In fact, circuit diagrams are draw with time evolution from left to right, and standard unitaries such as single-particle Pauli operators and controlled-NOT have their corresponding notation used for quantum circuits in quantum computing literatures. Readers interested in quantum circuits should refer to textbooks in quantum computing, for instance Chapter 4 in [11]. It is not the goal of this chapter to be involved too much with quantum circuit theory. Instead, we would introduce only the very basic concepts such as circuit size and depth, and in diagrams as Fig. 2.1, we adopt the tradition in theoretical physics to treat time evolution from down to up.

The idea for simulation of time evolution of many-body quantum systems by a quantum computer dates back to Feynman's famous 1982 paper [6]. The Lie product formula is due to [13]. Readers interested in quantum simulation may refer to Chapter 4 of [11], and references therein.

The theory of open quantum systems is extensively developed in the field of quantum theory and quantum optics, where many good textbooks are available for readers interested in this subject (e.g. [8, 7]).

The Kraus operators are due to Kraus [8]. The Lindblad form is due to Lindblad [9]. Our treatment on the master equations for amplitude damping noise is based on [2]. There are also many literatures in quantum information science discussing these noise and their Kraus operators. Interested reader may refer to Chapter 8 of [11] and references therein.

References

1. A. Barenco, C. H. Bennett, R. Cleve, D. P. Divincenzo, N. Margolus, P. Shor, T. Sleator, J. A. Smolin, and H. Weinfurter. Elementary gates for quantum computation. *Physical Review A*, 52:3457–3467, November 1995.
2. Claude Cohen-Tannoudji, Jacques Dupond-Roc, and Gilbert Grynberg. *Atom-photon interactions: Basic Processes and Applications*. John Wiley & Sons, 1998.
3. D. Deutsch. Quantum Computational Networks. *Royal Society of London Proceedings Series A*, 425:73–90, September 1989.
4. David Deutsch, Adriano Barenco, and Artur Ekert. Universality in quantum computation. *Proceedings: Mathematical and Physical Sciences*, 449(1937):pp. 669–677, 1995.
5. D. P. Divincenzo. Two-bit gates are universal for quantum computation. *Physical Review A*, 51:1015–1022, February 1995.
6. R. P. Feynman. Simulating Physics with Computers. *International Journal of Theoretical Physics*, 21:467–488, June 1982.
7. Crispin Gardiner and Peter Zoller. *Quantum Noise: A Handbook of Markovian and Non-Markovian Quantum Stochastic Methods with Applications to Quantum Optics*. Springer, 2004.
8. K. Kraus, A. Böhm, J. D. Dollard, and W. H. Wootters, editors. *States, Effects, and Operations Fundamental Notions of Quantum Theory*, volume 190 of *Lecture Notes in Physics, Berlin Springer Verlag*, 1983.
9. G. Lindblad. On the generators of quantum dynamical semigroups. *Communications in Mathematical Physics*, 48:119–130, June 1976.
10. S. Lloyd. Almost Any Quantum Logic Gate is Universal. *Physical Review Letters*, 75:346–349, July 1995.
11. M. Nielsen and I. Chuang. *Quantum computation and quantum information*. Cambridge University Press, 2000.
12. M. Reck, A. Zeilinger, H. J. Bernstein, and P. Bertani. Experimental realization of any discrete unitary operator. *Physical Review Letters*, 73:58–61, July 1994.
13. H. F. Trotter. On the product of semi-groups of operators. *Proceedings of the American Mathematical Society*, 10(4):pp. 545–551, 1959.

Chapter 3
Quantum Error-Correcting Codes

Abstract Any quantum system inevitably interacts with the environment which causes decoherence. While the environment is generally inaccessible, can we protect our system against noise to maintain its quantum coherence? One technique developed in quantum information science, called the quantum error-correcting codes, does the job. The main idea is to 'encode' the system into a subspace of the entire N-qubit space, called the 'code space', such that the errors caused by decoherence of the system can be 'corrected'.

3.1 Introduction

We have discussed in Chapter 2 that the evolution of a quantum system is in general non-unitary, which is caused by the inevitable interaction of the system with its environment. This is some bad news for quantum coherence, which is also the biggest obstacle for realizing large scale quantum computer in practice. It is not the goal of this book to discuss how to build a practical quantum computer. However, the techniques developed in quantum information theory for fighting against decoherence, turn out to have dramatic nice connection to modern condensed matter physics. The topic of this chapter is to introduce these techniques.

The central idea is to 'correct' the errors induced by non-unitary evolution. The idea of 'error correction' is actually borrowed from classical information theory that our modern life relies on every day. That is, when we communicate with each other, through either phones or internet, the communication channels between us are noisy. Therefore, information transmitted inevitably encounters errors that need to be corrected – the simplest idea is to send the same message multiple times. However, quantum information (carried by quantum states) is dramatically different from class information as they cannot be copied (no cloning theorem discussed in Chapter 1).

The breakthrough came in when it is realized that entanglement does help with maintaining coherence. Consider a case of two qubits, where the noise is to flip

the phase of either the first qubit or the second qubit, each with probability $\frac{1}{2}$. In other words, the Kraus operators are $\{\frac{1}{\sqrt{2}}Z_1, \frac{1}{\sqrt{2}}Z_2\}$. Now consider the state $\alpha|00\rangle + \beta|11\rangle$, then the evolution of this state under the noise is always unitary, which is in fact just Z_1 (or equivalently Z_2). This is to say, although the general evolution of states in the total four dimensional Hilbert space spanned by $\{|00\rangle, |01\rangle, |10\rangle, |11\rangle\}$ is non-unitary, the evolution of any state in the two dimensional subspace spanned by $|00\rangle, |11\rangle$ is unitary.

This simple example is indeed artificial. In general, one would like to know for the real physical noise, whether such a subspace with unitary evolution exists. Unfortunately, although such subspaces do exist for some cases, for many cases they do not exist. One can imagine another example of two qubits, where what the noise does, is to flip the phase of either the first qubit or the second qubit, or does nothing at all, which is a practical situation (phase flip) that the artificial one discussed above. In other words, the Kraus operators are $\{\frac{1}{\sqrt{3}}I, \frac{1}{\sqrt{3}}Z_1, \frac{1}{\sqrt{3}}Z_2\}$. Now one can check that the evolution of the states in the subspace spanned by $|00\rangle, |11\rangle$ is no longer unitary. In fact, there does not exist nontrivial subspace (i.e. dimension > 1) where the evolution under the noise could be unitary.

This is not the end of the story. Surprisingly, it turns out that measurements can help maintaining coherence. This is very counterintuitive, as general measurements project the quantum state to subspaces thus destroys coherence. We will explain in the next section how this could actually work out. The idea of measurements will then further leads to a general understanding how to 'error correct' for a known type of noise, called the 'quantum error correction criterion'. However, this elegant criterion does not directly provide practical ways of finding subspaces that correct the errors of given noise. There is indeed a practical method, called the stabilizer formalism, which finds those subspaces, that we will also introduce. Finally, we discuss the connection of stabilizer formalism to topology, using the example of the so called 'toric code'.

3.2 Basic idea of error correction

3.2.1 Bit flip code

Let us start to consider a simple example for a single qubit. Suppose the noise of the systems is to flip $|0\rangle$ to $|1\rangle$ and vice versa with probability p, i.e. the superoperator for this bit flip noise is given by

$$\mathscr{E}_{BF}(\rho) = (1-p)\rho + pX\rho X, \tag{3.1}$$

i.e. the Kraus operators are $\{\sqrt{1-p}I, \sqrt{p}X\}$.

Now suppose we have a single qubit pure state $|\phi\rangle = \alpha|0\rangle + \beta|1\rangle$ that we hope to maintain the coherence for unitary time evolution. However, due to the bit flip

noise, we will end up in a mixed state

$$\sigma = (1-p)|\phi\rangle\langle\phi| + pX|\phi\rangle\langle\phi|X. \tag{3.2}$$

Then the probability of failure is error due to noise is then reasonably given as

$$p_{err} = 1 - \langle\phi|\sigma|\phi\rangle = p(1-\langle\phi|X|\phi\rangle^2) = p(1-|\alpha^*\beta+\beta^*\alpha|^2), \tag{3.3}$$

which is of order p for general α, β.

Now in order to maintain the coherence, we wish to correct error and recover the original state $|\phi\rangle$. This is too much to hope for at the first place. As we already discussed, in general one can not find a subspace where the evolution could be unitary. Instead, let us try something more reasonable, that is, to reduce the error probability by one order of magnitude. In other words, we want to reduce the error probability from order t to the order of t^2. The simplest idea maybe that we copy the state for three times. However recall that due to the no cloning theorem, this cannot be done for unknown states. Instead of copying the state itself, we 'copy' the basis states three times.

$$|0\rangle \to |000\rangle, \quad |1\rangle \to |111\rangle. \tag{3.4}$$

In other words, instead of having a single qubit $|\phi\rangle = \alpha|0\rangle + \beta|1\rangle$, we now have three qubit which is in the state

$$|\psi\rangle = \alpha|000\rangle + \beta|111\rangle. \tag{3.5}$$

Then at the receiver's end, the output state is a mixed state ρ given by

$$\begin{aligned}\rho &= \mathscr{E}_{BF}^{\otimes 3}(|\psi\rangle\langle\psi|)\\ &= (1-p)^3|\psi\rangle\langle\psi|\\ &\quad + (1-p)^2 p\,(X_1|\psi\rangle\langle\psi|X_1 + X_2|\psi\rangle\langle\psi|X_2 + X_3|\psi\rangle\langle\psi|X_3)\\ &\quad + (1-p)p^2\,(X_1X_2|\psi\rangle\langle\psi|X_1X_2 + X_2X_3|\psi\rangle\langle\psi|X_2X_3 + X_1X_3|\psi\rangle\langle\psi|X_1X_3)\\ &\quad + p^3(X_1X_2X_3|\psi\rangle\langle\psi|X_1X_2X_3),\end{aligned} \tag{3.6}$$

where X_i is the Pauli operator acting on the ith qubit, for instance, $X_1 = X\otimes I\otimes I$ (and sometimes we write XII for short).

Our goal is to recover the transmitted state $\alpha|0\rangle + \beta|1\rangle$ as much as we can. Our strategy is that whenever we receive any of $000, 001, 010, 100$ we would like to interpret it as 0, and whenever we receive any of $111, 110, 101, 011$ we interpret it as 1. However, the difficulty in the quantum case is that we will need to keep the coherence between $|0\rangle$ and $|1\rangle$, that, to recover the superposition $\alpha|0\rangle + \beta|1\rangle$. In order to maintain the coherence, we perform an orthogonal measurement $\mathscr{M}$ with Kraus operators given as follows:

$$\begin{aligned}
\Pi_0 &= |000\rangle\langle 000| + |111\rangle\langle 111|, \\
\Pi_1 &= X_1(|000\rangle\langle 000| + |111\rangle\langle 111|)X_1, \\
\Pi_2 &= X_2(|000\rangle\langle 000| + |111\rangle\langle 111|)X_2, \\
\Pi_3 &= X_3(|000\rangle\langle 000| + |111\rangle\langle 111|)X_3.
\end{aligned} \tag{3.7}$$

Then we get either

$$\sigma_0 = (1-p)^3|\psi\rangle\langle\psi| + p^3 X_1X_2X_3|\psi\rangle\langle\psi|X_1X_2X_3, \tag{3.8}$$

or

$$\sigma_1 = (1-p)^2 pX_1|\psi\rangle\langle\psi|X_1 + (1-p)p^2X_2X_3|\psi\rangle\langle\psi|X_2X_3, \tag{3.9}$$

or

$$\sigma_2 = (1-p)^2 pX_2|\psi\rangle\langle\psi|X_2 + (1-p)p^2X_1X_3|\psi\rangle\langle\psi|X_1X_3, \tag{3.10}$$

or

$$\sigma_3 = (1-p)^2 pX_3|\psi\rangle\langle\psi|X_3 + (1-p)p^2X_1X_2|\psi\rangle\langle\psi|X_1X_2, \tag{3.11}$$

according to the measurement result. Note that σ_is are not normalized so that we can calculate the probability of getting each σ_i by its trace.

Now we interpret $000, 001, 010, 100$ as 0 and $111, 110, 101, 011$ as 1, so when we get σ_0, we do the inverse of Eq. (3.4); when we get σ_1, we perform X_1 and then the inverse of Eq. (3.4); when we get σ_2, we perform X_2 and then the inverse of Eq. (3.4); when we get σ_3, we perform X_3 and then the inverse of Eq. (3.4). Finally we get one of the following, respectively.

$$\begin{aligned}
\sigma_0' &= (1-p)^3|\psi\rangle\langle\psi| + p^3X_1X_2X_3|\psi\rangle\langle\psi|X_1X_2X_3, \\
\sigma_1' &= (1-p)^2 p|\psi\rangle\langle\psi| + (1-p)p^2X_1X_2X_3|\psi\rangle\langle\psi|X_1X_2X_3, \\
\sigma_2' &= (1-p)^2 p|\psi\rangle\langle\psi| + (1-p)p^2X_1X_2X_3|\psi\rangle\langle\psi|X_1X_2X_3, \\
\sigma_3' &= (1-p)^2 p|\psi\rangle\langle\psi| + (1-p)p^2X_1X_2X_3|\psi\rangle\langle\psi|X_1X_2X_3.
\end{aligned} \tag{3.12}$$

That is to say, the final state we receive is

$$\sigma' = \sum_{k=0}^{3} \sigma_i' \tag{3.13}$$

Then the probability of failure is given by

$$\begin{aligned}
p_{err}' &= 1 - \langle\psi|\sigma'|\psi\rangle \\
&= p^2(3-2p)(1 - \langle\psi|X_1X_2X_3|\psi\rangle^2) \\
&= p^2(3-2p)(1 - |\alpha^*\beta + \beta^*\alpha|^2),
\end{aligned} \tag{3.14}$$

which is of order p^2 for general α, β. For a given α, β and $p < \frac{1}{2}$, we have $p_{err}' < p_{err}$, meaning that we are able to reduce the error probability by adding redundancy.

Now let us ask the question of how we would be able to reduce the error probability from p to p^r for the bit flip noise. A simple method would be to 'copy' the

basis states $2r+1$ times. That is

$$|0\rangle \to |0\rangle^{\otimes(2r-1)}, \quad |1\rangle \to |1\rangle^{\otimes(2r-1)} \tag{3.15}$$

Now large enough r could get the error probability p^r arbitrarily small, so we can protect our qubits $\alpha|0\rangle+\beta|1\rangle$ almost perfectly against bit flip noise.

3.2.2 Shor's Code

However, as discussed in Chapter 2, quantum noise are in general much more complicated than just bit flip. For instance, the depolarizing noise $\mathscr{E}_{DP}$ models the qubit noise in a more general situation, where X, Y, Z errors are likely happen with equal probability. Is there any way that we can reduce the error probability by adding redundancy also for this kind of noise?

Before look into this question, let us look at what we could do for the phase flip noise $\mathscr{E}_{PF}$. In this case, we show that the code given by Eq. (3.15) does not correct even a single phase flip error.

In this case, one can simply use a similar idea as for the bit flip noise in Eq. (3.4). Recall that $HXH = Z$ and $HZH = X$, where H is the Hadamard gate, and define

$$\begin{aligned} |+\rangle &= H|0\rangle = \frac{1}{\sqrt{2}}(|0\rangle+|1\rangle) \\ |-\rangle &= H|1\rangle = \frac{1}{\sqrt{2}}(|0\rangle-|1\rangle), \end{aligned} \tag{3.16}$$

we can simply modify Eq. (3.4) as

$$|0\rangle \to |{+}{+}{+}\rangle, \quad |1\rangle \to |{-}{-}{-}\rangle. \tag{3.17}$$

In other words, instead of transmitting a qubit $\alpha|0\rangle+\beta|1\rangle$, we transmit $|\psi\rangle = \alpha|{+}{+}{+}\rangle + \beta|{-}{-}{-}\rangle$, then all the other analysis goes through by replacing all the Xs with Zs.

Now back to the depolarizing noise $\mathscr{E}_{DP}$,

$$\mathscr{E}_{DF}(\rho) = (1-p)\rho + \frac{p}{3}(X\rho X + Y\rho Y + Z\rho Z), \tag{3.18}$$

where the Kraus operators are $\{I, X_j, Y_j, Z_j\}$ (as discussed in Chapter 2.5.2, here we use the parameter p instead of Γ).

Note that $Y \propto XZ$, so if it is possible to tell that both X, Z happen, then it means an Y error happens. In other words, there might be a way to combine the idea of both Eq. (3.4) and Eq. (3.17) such that one can tell whether an X and a Z error happen. This indeed works as first observed by Shor, in the following way

$$|0\rangle \to \frac{1}{2\sqrt{2}}(|000\rangle + |111\rangle)^{\otimes 3} \equiv |0_L\rangle$$
$$|1\rangle \to \frac{1}{2\sqrt{2}}(|000\rangle - |111\rangle)^{\otimes 3} \equiv |1_L\rangle. \tag{3.19}$$

Then instead of transmitting a qubit $\alpha|0\rangle + \beta|1\rangle$, we transmit $|\psi_L\rangle = \alpha|0_L\rangle + \beta|1_L\rangle$. In other words, in order to reduce the error probability from order p to order p^2, we use 9 qubits to represent one qubit.

We leave the details of the calculation for $\mathscr{E}_{DP}^{\otimes 9}(|\psi_L\rangle\langle\psi_L|)$ to the reader. We remark that the orthogonal measurement $\mathscr{M}$ we perform will be given by projections of the form $R_i(|0_L\rangle\langle 0_L| + |1_L\rangle\langle 1_L|)R_i$, where $R \in \{I, X, Y, Z\}$ and $i \in [1, 2, \ldots 9]$. For each measurement result, we perform R_i and the reverse of Eq. (3.19). At the end of the day we will successfully reduce the error probability from order p to order p^2.

3.2.3 Other noise models

One would ask what happens in those more practical cases such as the phase damping noise and the amplitude damping noise as discussed in Chapter 2.5.2. Let us first discuss the phase damping noise

$$\mathscr{E}_{PD}(\rho) = \sum_{j=0}^{2} E_j \rho E_j^\dagger, \tag{3.20}$$

with the Kraus operators given in Chapter 2.5.2, which we rewrite as follows (we use the parameter p instead of γ)

$$E_0 = \sqrt{1-p}I, \quad E_1 = \frac{\sqrt{p}}{2}(I+Z), \quad E_2 = \frac{\sqrt{p}}{2}(I-Z). \tag{3.21}$$

We note that the Kraus operators are linear combinations of I and Z, which is in some sense similar to the Kraus operators of the phase flip noise with Kraus operators $\sqrt{1-p}I, \sqrt{p}Z$. So we would wonder whether it is possible to reduce the error probability for the phase damping noise using the same method as we have done for the phase flip noise?

Let us go ahead to examine what happens when we transmit $|\psi\rangle = \alpha|{+}{+}{+}\rangle + \beta|{-}{-}{-}\rangle$ instead of $\alpha|0\rangle + \beta|1\rangle$. And compute

$$\begin{aligned}\rho &= \mathscr{E}_{PD}^{\otimes 3}(|\psi\rangle\langle\psi|)\\ &= (1-\frac{3}{2}p+\frac{3}{4}p^2-\frac{1}{8}p^3)|\psi\rangle\langle\psi|\\ &+ (\frac{1}{2}p-\frac{1}{2}p^2+\frac{1}{8}p^3)\,(Z_1|\psi\rangle\langle\psi|Z_1+Z_2|\psi\rangle\langle\psi|Z_2+Z_3|\psi\rangle\langle\psi|Z_3)\\ &+ (\frac{1}{4}p^2-\frac{1}{8}p^3)\,(Z_1Z_2|\psi\rangle\langle\psi|Z_1Z_2+Z_2Z_3|\psi\rangle\langle\psi|Z_2Z_3+Z_1Z_3|\psi\rangle\langle\psi|Z_1Z_3)\\ &+ \frac{1}{8}p^3(Z_1Z_2Z_3|\psi\rangle\langle\psi|Z_1Z_2Z_3). \end{aligned} \tag{3.22}$$

It is then clear that the orthogonal measurement given by Eq. (3.7) (replacing all Xs by Zs) followed by the same procedure of correction as for the phase flip noise works to reduce the error probability from order p to p^2.

We remark here that in Eq. (3.22), the cross terms of the forms, for instance $Z_1|\psi\rangle\langle\psi|$ (or $|\psi\rangle\langle\psi|Z_1$) cancels in this special case. In general, there would be such terms. However, this will not be a problem as when we perform orthogonal measurements, these terms vanish. The above example then illustrate that, in general, *if we can deal with Kraus operators A and B, we can also deal with Kraus operators given by any kind of superposition of A and B*.

This then gives more meaning to the depolarizing noise with Kraus operators $\propto I,X,Y,Z$, as they form a basis for 2×2 matrices. That is to say, if we can able to reduce error probability for the depolarizing noise (indeed we do as using the Shor's method), then are able to reduce error probability for any qubit quantum noise using the same method. For instance, consider the amplitude damping noise discussed in Chapter 2.5.2, one can then rewrite the Kraus operators as (we use the parameter p instead of γ)

$$E_0 = \begin{pmatrix}1 & 0\\ 0 & \sqrt{1-p}\end{pmatrix} = \frac{1+\sqrt{1-p}}{2}I + \frac{1-\sqrt{1-p}}{2}Z, \tag{3.23}$$

$$E_1 = \begin{pmatrix}0 & \sqrt{p}\\ 0 & 0\end{pmatrix} = \frac{\sqrt{p}}{2}(X+iY), \tag{3.24}$$

then using Shor's method to reduce the error probability from order p to p^2.

3.3 Quantum error-correcting criteria, code distance

We have seen that how to reduce the error probability from order p to p^2 using Shor's code. From other point of view, if only one error happens, meaning $\mathscr{E}_{PD}\otimes I\otimes I$ (or $\mathscr{E}_{PD}$ could be on the second or third qubit), the Shor's code can maintain the coherence completely. Or in other words, we say that Shor's code is capable of correcting one error.

We now wonder what is the the general case for a quantum code capable of correcting certain types of errors. Before looking into that, let us consider what

really a quantum code is. From what we have done in the previous section, we know that by mapping the basis vectors and allowing all the superpositions, what we result in is a 'subspace' of the N-qubit Hilbert space.

Box 3.1 Quantum code
A quantum code is a subspace of the N-qubit Hilbert space.

For a given subspace, there are several ways to describe the space. First of all one can choose an orthonormal basis $\{|\psi_i\rangle\}$. Or, one can use the projection onto the code space

$$\Pi = \sum_i |\psi_i\rangle\langle\psi_i|. \tag{3.25}$$

Now suppose the error of the system is characterized by the quantum noise $\mathscr{E} = \{E_k\}$, where E_ks are the Kraus operators. In order to distinguish any basis state corrupted by an error, i.e. $E_k|\psi_i\rangle$ from any other basis state corrupted by another error, i.e. $E_l|\psi_j\rangle$, one must have $E_k|\psi_i\rangle \perp E_l|\psi_j\rangle$. Mathematically, this then means

$$\langle\psi_i|E_k^\dagger E_l|\psi_j\rangle = 0, \quad i \neq j. \tag{3.26}$$

Now let us see what could happen when $i = j$. In this case, in order to maintain coherence, imagine the case that each Kraus operator has every basis state $|\psi_i\rangle$ as its eigenvector with the same eigenvalue, i.e. $E_k|\psi_i\rangle = c_k|\psi_i\rangle$, which is independent of i. Therefore, for any state $|\psi\rangle = \sum_i \alpha_i|\psi_i\rangle$ which is in the code space, we have $E_k|\psi\rangle = c_k|\psi\rangle$, that is, up to an irrelevant constant, each Kraus operator E_k acts like identity on the code space, thus maintains coherence. To summarize, we then have the following

Box 3.2 Quantum error-correcting criteria
A quantum code with orthonormal basis $\{|\psi_i\rangle\}$ corrects the error set $\mathscr{E} = \{E_k\}$ if and only if

$$\langle\psi_i|E_k^\dagger E_l|\psi_j\rangle = c_{kl}\delta_{ij}.$$

One can equivalently formulate this criterion in terms of the projection Π onto the code space as given in Eq. (3.25). Let us look at the quantity

$$\Pi E_k^\dagger E_l \Pi = \sum_{i,j} |\psi_i\rangle\langle\psi_i|E_k^\dagger E_l|\psi_j\rangle\langle\psi_j|, \tag{3.27}$$

using Eq. (3.25) one then gets

$$\Pi E_k^\dagger E_l \Pi = c_{kl}\Pi. \tag{3.28}$$

As an example, now let us apply this criterion to check why Shor's code is capable of correcting an arbitrary single error. Here the correctable error set is

$$\mathscr{E} = \{I, X_i, Y_i, Z_i\}, \tag{3.29}$$

where $i = 1, 2, \ldots, 9$. And now our code basis can be chosen as $|\psi_j\rangle = |j_L\rangle$ $(j = 0, 1)$, as given in Eq. (3.19).

So first we need to check

$$\langle\psi_0|E_k^\dagger E_l|\psi_1\rangle = 0, \tag{3.30}$$

for any $E_k, E_l \in \mathscr{E}$, which is pretty straightforward.

Then we need to check

$$\langle\psi_0|E_k^\dagger E_l|\psi_0\rangle = \langle\psi_1|E_k^\dagger E_l|\psi_1\rangle, \tag{3.31}$$

for any $E_k, E_l \in \mathscr{E}$. Note that in general we no longer have $\langle\psi_0|E_k^\dagger E_l|\psi_0\rangle = \langle\psi_1|E_k^\dagger E_l|\psi_1\rangle = 0$. Rather, for instance, we have $\langle\psi_0|Z_1Z_2|\psi_0\rangle = \langle\psi_1|Z_1Z_2|\psi_1\rangle = 1$, since $Z_1Z_2|\psi_0\rangle = |\psi_0\rangle$ and $Z_1Z_2|\psi_1\rangle = |\psi_1\rangle$. One have similar results for

$$Z_2Z_3, Z_1Z_3, Z_4Z_5, Z_5Z_6, Z_4Z_6, Z_7Z_8, Z_8Z_9, Z_7Z_9. \tag{3.32}$$

And or other choices of $E_k, E_l \in \mathscr{E}$, $k \neq l$, one has $\langle\psi_0|E_k^\dagger E_l|\psi_0\rangle = \langle\psi_1|E_k^\dagger E_l|\psi_1\rangle = 0$.

In practice, the most common noise is uncorrelated ones. That is, those noise acting independently on each qubit. And in the most discussed cases, the single qubit noise is chosen as the depolarizing noise. Therefore, the quantum noise under consideration is $\mathscr{E}_{DP}^{\otimes N}$.

In this case one often measures the 'strength' of an error-correcting code by the number of errors the code is capable of correcting. In other words, if the code corrects t-errors, then it reduces the error probability from order p to p^{t+1}. This strength can be measured by a parameter called code distance. In order to understand code distance, let us first look at an N-qubit operator O of the form

$$O = O_1 \otimes O_2, \ldots, \otimes O_N, \tag{3.33}$$

where each O_k acting on the kth qubit. We are interested in those non-trivial O_ks, i.e. those O_ks which are different from identity. The number of those non-trivial O_ks is then called the weight of M, denoted by $\mathrm{wt}(O)$. Apparently $0 \leq \mathrm{wt}(O) \leq N$. When considering the depolarizing noise $\mathscr{E}_{DP}^{\otimes N}$, where we want a quantum code capable of correcting t-errors, it is enough to consider only Kraus operator O of weight $\leq t$ where each O_k are one of the Pauli operators $\{I, X_k, Y_k, Z_k\}$. In other words, a code is capable of correcting t errors for any O with weight $\leq 2t+1$, the following holds

$$\langle\psi_i|O|\psi_j\rangle = c_O\delta_{ij}, \tag{3.34}$$

where c_O is a constant that is independent of i, j. Now we are ready to introduce the concept of code distance.

Box 3.3 Quantum code distance

The distance for quantum code with orthonormal basis $\{|\psi_i\rangle\}$ is the largest possible weight d such that

$$\langle\psi_i|O|\psi_j\rangle = c_O\delta_{ij}$$

holds for all operators O with $\mathrm{wt}(O) < d$.

In other words, the distance of a quantum code is given by the smallest possible weight of O such that $\langle\psi_i|O|\psi_j\rangle = c_O\delta_{ij}$ violates. If we consider the situation where $i \neq j$, then code distance is the smallest possible weight of O such that $|\psi_i\rangle, |\psi_j\rangle$ are no longer distinguishable (i.e. orthogonal). Intuitively the code distance measures how far one basis state in the code space is 'away from' another basis state, hence the name 'distance'.

3.4 The stabilizer formalism

Quantum error correction criterion gives a 'standard' of finding quantum codes. Once the error set $\mathscr{E}$ is fixed, then the problem of finding the corresponding quantum code reduces to solve the equations for the unknown basis $|\psi_i\rangle$. This is in general not a practical way. The problem is that each N-qubit quantum state $|\psi_i\rangle$ is specified by $\sim 2^N$ complex parameters, which makes the equations almost impossible to solve.

Therefore one needs to find a better way such that the states $|\psi_i\rangle$ can be represented in a more efficient manner, i.e. by less parameters. We know that doing this will no longer allow $|\psi_i\rangle$s to be general N-qubit quantum state, but just a restricted sets of states. However, we will see that such restricted sets of states are with nice structure which makes things easy to understand. This set of states that we are going to discuss will then be so called 'stabilizer' state, and the corresponding quantum code is then called 'stabilizer' code.

3.4.1 Shor's code

To establish the idea of the stabilizer formalism, let us again look at the example of Shor's code. We have already noticed that $Z_1Z_2|0_L\rangle = |0_L\rangle$ and $Z_1Z_2|1_L\rangle = |1_L\rangle$. This means that for any state $|\phi\rangle = \alpha|0_L\rangle + \beta|1_L\rangle$, one has $Z_1Z_2|\phi\rangle = |\phi\rangle$. Or one can instead write $\Pi Z_1Z_2\Pi = \Pi$, where $\Pi = |0_L\rangle\langle 0_L| + |1_L\rangle\langle 1_L|$, is the projection onto the code space.

We will say that Z_1Z_2 'stabilizes' Shor's code, in a sense that the code is invariant under Z_1Z_2. Similarly, we know that $Z_2Z_3, Z_4Z_5, Z_5Z_6, Z_7Z_8, Z_8Z_9$ also stabilize the code. Furthermore, note that $X_1X_2X_3X_4X_5X_6, X_4X_5X_6X_7X_8X_9$ also stabilizes the code. To summarize, we have each row of

$$\begin{array}{ccccccccc} Z & Z & I & I & I & I & I & I & I \\ I & Z & Z & I & I & I & I & I & I \\ I & I & I & Z & Z & I & I & I & I \\ I & I & I & I & Z & Z & I & I & I \\ I & I & I & I & I & I & Z & Z & I \\ I & I & I & I & I & I & I & Z & Z \\ X & X & X & X & X & X & I & I & I \\ I & I & I & X & X & X & X & X & X \end{array} \tag{3.35}$$

stabilizes the code.

Now let us observe an important factor: every two rows, viewed as operators on nine qubits, commute with each other, and they hence have common eigenspace. What is more, the operator of each row squares to identity, which means it has only eigenvalues ± 1. The Shor code is nothing but the common eigenspace of these eight operators with eigenvalue 1 for each operators.

Let us denote each row of Eq. (3.35) by g_i, where $i = 1,2,\ldots,8$. Indeed, the product of any number of g_is also stabilizes Shor's code. Therefore, it is actually the group generated by g_is ($i = 1,2,\ldots,8$) that stabilizes the code. This group is indeed abelian, as any two elements commute. And it is also straightforward to check that the order of the group is 2^8. This group is called the stabilizer group (or in short, the stabilizer) of Shor's code, denoted by $\mathscr{S}$, and the g_is are the generators of $\mathscr{S}$. That is,

$$\mathscr{S} = \langle g_1, g_2, g_3, g_4, g_5, g_6, g_7, g_8 \rangle. \tag{3.36}$$

We know that $\mathscr{S}$ completely specifies Shor's code as the eigenspace of each group element with eigenvalue 1. Indeed, the projection on to the code space $|0_L\rangle\langle 0_L| + |1_L\rangle\langle 1_L|$ can be written in terms of stabilizers as

$$\Pi = \frac{1}{2^8} \prod_{i=1}^{8} (I + g_i). \tag{3.37}$$

To see why this is the case, let us first compute

$$\Pi^2 = \frac{1}{2^{16}} \prod_{i=1}^{8} (I + g_i)^2 = \Pi, \tag{3.38}$$

so Π is a projection. The second equality holds because $(I + g_i)^2 = 2(I + g_i)$ as $g_i^2 = I$. Then we further check that $\Pi(|0_L\rangle\langle 0_L| + |1_L\rangle\langle 1_L|)\Pi = |0_L\rangle\langle 0_L| + |1_L\rangle\langle 1_L|$. Moreover, because the stabilizer group contains 8 independent generators, the code space is at most two dimensional. Therefore $\Pi = |0_L\rangle\langle 0_L| + |1_L\rangle\langle 1_L|$.

The big advantage of specifying the code by stabilizers, is that one only needs in general order n generators instead of some basis states $|\psi_i\rangle$ each needs $\sim 2^n$ complex parameters. Another interesting thing of this stabilizer formalism is that one can write an Hamiltonian

$$H = -\sum_{i=1}^{8} g_i, \tag{3.39}$$

hence the code space is nothing but the ground state space of H.

Concerning the basis states $|0_L\rangle$ and $|1_L\rangle$, note that we have $X^{\otimes 9}|0_L\rangle = |0_L\rangle$, $X^{\otimes 9}|1_L\rangle = -|1_L\rangle$. In this sense, $X^{\otimes 9}$ acts like a 'logical Z' on the code basis, that let us write $Z_L = X^{\otimes 9}$. Or in other words, the basis state $|0_L\rangle$ is stabilized by

$$\mathscr{S}_0 = \langle g_1, g_2, g_3, g_4, g_5, g_6, g_7, g_8, Z_L\rangle. \tag{3.40}$$

As $g_7 = X_1X_2X_3X_4X_5X_6$, one can equivalently choose $Z_L = X_1X_2X_3$. Similarly, one can then choose $X_L = Z_1Z_4Z_6$, in a sense that $X_L|0_L\rangle = |1_L\rangle$, $X_L|1_L\rangle = |0_L\rangle$. And furthermore $X_LZ_L = -Z_LX_L$, which is the usual commutation relation for Pauli operators.

Similarly, the projection onto the the space $|0_L\rangle\langle 0_L|$ is

$$|0_L\rangle\langle 0_L| = \frac{1}{2^9}\prod_{i=1}^{8}(I + g_i)(I + Z_L). \tag{3.41}$$

One can also write the state $|0_L\rangle$ in terms of stabilizer elements in $\mathscr{S}_0$ as

$$|0_L\rangle = \frac{1}{2^{9/2}}\sum_{g\in\mathscr{S}_0} g|0\rangle^{\otimes 9}. \tag{3.42}$$

Indeed, it is enough to use only those elements in $\mathscr{S}_0$ which are products of Pauli X operators. That is,

$$|0_L\rangle = \frac{1}{2^{3/2}}(I + g_7)(I + g_8)(I + Z_L)|0\rangle^{\otimes 9}. \tag{3.43}$$

Now let us look at the quantum error correction criterion in terms of the stabilizer formalism. Let us look at $\Pi E_k^\dagger E_l \Pi$ with E_ks given by Eq. (3.29). Note that for any $E_k^\dagger E_l$, it either commute or anticommute with each g_i. Let us first consider the case that $E_k^\dagger E_l$ at least anticommute with one g_i, and let us assume it is g_r. In this case,

$$\Pi E_k^\dagger E_l \Pi = E_k^\dagger E_l \Pi' \Pi \tag{3.44}$$

where

$$\Pi' = \frac{1}{2^8}(I - g_r)\prod_{i=1, i\neq r}^{8}(I \pm g_i). \tag{3.45}$$

Here $\pm$ means it could be either $+$ or $-$, but not both.

Note that

$$(I-g_r)(I+g_r) = I+g_r-g_r-I = 0, \tag{3.46}$$

therefore

$$\Pi E_k^\dagger E_l \Pi = 0, \tag{3.47}$$

i.e. the quantum error correction criterion is satisfied with $c_{kl} = 0$.

Now we need to consider the case that $E_k^\dagger E_l$ commute with all g_is. Then one will have

$$\Pi E_k^\dagger E_l \Pi = E_k^\dagger E_l \Pi\Pi = E_k^\dagger E_l \Pi. \tag{3.48}$$

However this still not the quantum error correction condition unless $E_k^\dagger E_l \Pi = c_{kl}\Pi$. It is straightforward to check that this is indeed the case and either $c_{kl} = 1$ (e.g. $E_k^\dagger E_l = Z_1 Z_2$) or $c_{kl} = 0$ (e.g. $E_k^\dagger E_l = X_1 X_2$), so the quantum error correcting condition holds.

Let us now look at the case of two errors. We will show that Shor's code cannot correct two errors. In this case, the error set is

$$\mathscr{E} = \{I, X_k, Y_k, Z_k, X_l X_m, X_l Y_m, X_l Z_m, Y_l Y_m, Y_l Y_m, Y_l Z_m, Z_l X_m, Z_l Y_m, Z_l Z_m\}, \tag{3.49}$$

where $k,l,m = 1,2,\ldots,9$.

It is still true that for any $E_k, E_l \in \mathscr{E}$, if $E_k^\dagger E_l$ anticommute with at least one g_i, then $\Pi E_k^\dagger E_l \Pi = 0$. However, if $E_k^\dagger E_l$ commute with all g_is, then it is not longer true $E_k^\dagger E_l \Pi = c_{kl}\Pi$ for certain $E_k^\dagger E_l \Pi = c_{kl}\Pi$. For instance, choose $E_k = Z_1$, $E_l = Z_4 Z_7$, then $E_k^\dagger E_l = Z_1 Z_4 Z_7 = X_L$, which is the logical X of the code space. In this case,

$$E_k^\dagger E_l \Pi = X_L(|0_L\rangle\langle 0_L| + |1_L\rangle\langle 1_L|) = |1_L\rangle\langle 0_L| + |0_L\rangle\langle 1_L|, \tag{3.50}$$

which is no longer $c_{kl}\Pi$ for any constant c_{kl}. Therefore, quantum error correction criterion is no longer satisfied, hence Shor's code cannot correct two errors.

3.4.2 The stabilizer formalism

Let us now look at the general situation of the stabilizer formalism. We first recall N-qubit Pauli operators, which are operators of the form

$$O_1 \otimes O_2, \ldots, \otimes O_N, \tag{3.51}$$

where each $O_k \in \{I_k, X_k, Y_k, Z_k\}$, is a Pauli operator acting on the kth qubit.

Note that all such N-qubit Pauli operators together form a group that we denote by $\mathscr{P}_N$.

Box 3.4 Stabilizer code

Let $\mathscr{S} \subset \mathscr{P}_N$ be an abelian subgroup of the Pauli group that does not contain $-I$, and let

$$Q(\mathscr{S}) = \{|\psi\rangle \text{ s.t. } P|\psi\rangle = |\psi\rangle,\ \forall P \in \mathscr{S}\}.$$

Then $Q(\mathscr{S})$ is a stabilizer code and $\mathscr{S}$ is its stabilizer.

Let

$$\mathscr{S}^{\perp} = \{E \in \mathscr{P}_N,\ \text{s.t. } [E,S] = 0,\ \forall S \in \mathscr{S}\}. \tag{3.52}$$

The stabilizer code is the $+1$-eigenspace of all elements of the stabilizer $\mathscr{S}$. The dimension of this eigenspace is 2^M where $M = N - \#$ of generators of the stabilizer $\mathscr{S}$. The distance for a stabilizer code is given by the following

Box 3.5 Stabilizer code: dimension and distance
Let $\mathscr{S}$ be a stabilizer with $N-M$ generators. Then $\mathscr{S}$ encodes M qubits and has distance d, where d is the smallest weight of a Pauli operator in $\mathscr{S}^{\perp} \setminus \mathscr{S}$.

Let us consider an example where the code encodes more than one qubits, which the stabilizer $\mathscr{S}$ is generated by the following two Pauli operators.

$$\begin{array}{l} g_1 = X\ X\ X\ X \\ g_2 = Z\ Z\ Z\ Z \end{array} \tag{3.53}$$

There are total $n = 4$ qubits and 2 generators for the stabilizer, so this code encodes $4-2 = 2$ qubits. The logical $|0_L\rangle|0_L\rangle$ can be chosen as the state stabilized by the following four Pauli operators.

$$\begin{array}{l} g_1 = X\ X\ X\ X \\ g_2 = Z\ Z\ Z\ Z \\ \bar{Z}_1 = I\ \ Z\ Z\ I \\ \bar{Z}_2 = I\ \ I\ \ Z\ Z \end{array} \tag{3.54}$$

Here for convenience we use the notation $\bar{Z}_i$ to denote the logical Z operators (previously denoted as Z_L), where i refers to the ith encoded qubits, as there is more than one encode qubit.

Similarly, the logical $|0_L\rangle|1_L\rangle$ can be chosen as the state stabilized by $\{g_1,g_2,\bar{Z}_1, -\bar{Z}_2\}$, and $\{g_1,g_2,-\bar{Z}_1,\bar{Z}_2\}$ stabilizes the logical $|1_L\rangle|0_L\rangle$, $\{g_1,g_2,-\bar{Z}_1,-\bar{Z}_2\}$ stabilizes the logical $|1_L\rangle|1_L\rangle$.

The distance of this code is 2, meaning that the smallest weight Pauli operator which commute with g_1, g_2 is 2, for instance, $\bar{Z}_1$ is such an operator with weight 2.

3.4.3 Stabilizer states and graph states

If a stabilizer code of N-qubit has N generators, then the dimension of the common eigenspace of eigenvalue 1 will be of dimension $2^{N-N} = 1$. That is, the stabilizer code contains indeed only a unique state. Such kind of state is called stabilizer state.

For example, the 4-qubit version of the GHZ state (see Chapter 1.4.1 for the discussion of 3-qubit GHZ state)

$$|GHZ_4\rangle = \frac{1}{\sqrt{2}}(|0000\rangle + |1111\rangle) \tag{3.55}$$

is a stabilizer state. To see why, consider the following 4 stabilizer generators

$$\begin{aligned} g_1 &= Z\ Z\ I\ \ I \\ g_2 &= I\ \ Z\ Z\ I \\ g_3 &= I\ \ I\ \ Z\ Z \\ g_4 &= X\ X\ X\ X, \end{aligned} \tag{3.56}$$

and it is straightforward to check that $g_i|GHZ\rangle_4 = |GHZ\rangle_4$.

There is a special kind of stabilizer states called the graph states, whose stabilizer generators correspond to some given graphs. We start from a undirected graph G with n-vertices. For the ith vertex, we associate it with a stabilizer generator

$$g_i = X_i \bigotimes_{k \in \text{neighbor } i} Z_k, \tag{3.57}$$

where $k \in$ neighbor i means all the vertices which share an edge with i. It is straightforward to see that g_i, g_j commute for any i, j. g_is then gives a stabilizer group with N generators, whose common eigenspace of eigenvalue 1 is a single stabilizer state, which we call a graph state.

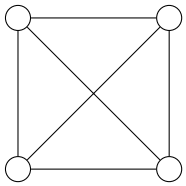

Fig. 3.1 A complete graph of 4 vertices

As an example, for the complete graph given in Fig. 3.1 with $N = 4$, the 4 stabilizer generators are given by

$$\begin{aligned} g_1 &= X\ Z\ Z\ Z \\ g_2 &= Z\ X\ Z\ Z \\ g_3 &= Z\ Z\ X\ Z \\ g_4 &= Z\ Z\ Z\ X \end{aligned} \tag{3.58}$$

The common eigenspace of eigenvalue 1 of these 4 stabilizer generators is a graph state, i.e. the graph state associated with the complete graph of 4 vertices.

3.5 Toric code

In this section, we discuss an interesting example of stabilizer code, namely the toric code. We will see later in this book that this is the simplest example of topologically ordered system. We will come back to talk about the physics of this model in later chapters of the book. Here we introduce the model and discuss from the viewpoint of quantum error-correcting code.

Consider a square lattice. The name *toric code* means 1) the square lattice is putting on a torus; 2) it is a stabilizer quantum code.

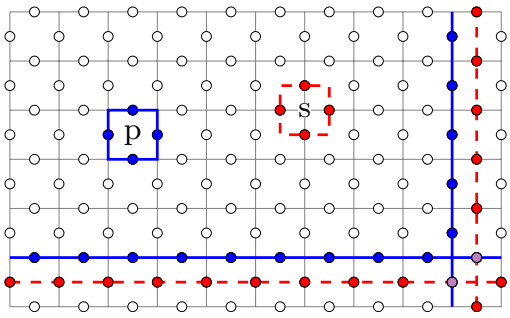

Fig. 3.2 Toric code. Each small circle represents a qubit, which are sitting on the link of the square lattice. The plaquette and star operators are illustrated with four blue and red dots. The logical operators for the two encoded qubits are illustrated with blue and red lines, respectively.

Fig. 3.2 illustrates the layout of the toric code on the square lattice of a torus. The solid lines gives the lattice, and on each edge of the lattice lies a green dot which represents a qubit. For an $r \times r$ lattice, we have $2r^2$ qubits.

There are two types of stabilizer generators.

Type I (Star type):

$$Q_s = \prod_{j \in star(s)} Z_j \tag{3.59}$$

Type II (Plaquette type):

$$B_p = \prod_{j \in plaquette(p)} X_j \tag{3.60}$$

It is straightforward to check that Q_s and B_p commute for any pair of s, p. Although there are total $r^2 + r^2 = 2r^2$ generators, there are indeed relations between them.

$$\prod_s Q_s = \prod_p B_p = I \tag{3.61}$$

It can be shown that these are the only relations therefore the code has dimension

$$2^{2r^2-(2r^2-2)} = 2^2, \tag{3.62}$$

in other words this code encodes two qubits into $2r^2$ qubits.

It seems that this code has a relative bad rate $\frac{2}{2r^2} = \frac{1}{r^2}$ (i.e. we use r^2 qubits to represent each logical qubit), which turns out to be small when r goes large. However, it turns out that the error correcting property of the code is good, as the minimum distance of the code is r. This is because that the logical operators are cycles on the torus, as shown in Fig. 3.2.

More precisely, the corresponding logical operators are given by

$$\begin{aligned} \bar{Z}_1 &= \prod_{j\in pink_v} Z_j, \quad & \bar{X}_1 &= \prod_{j\in pink_h} X_j, \\ \bar{Z}_2 &= \prod_{j\in green_h} Z_j, \quad & \bar{X}_2 &= \prod_{j\in green_v} X_j, \end{aligned} \tag{3.63}$$

where $pink_v$/$green_v$ refer to the vertical pink/green line and $pink_h$/$green_h$ refer to the vertical pink/green line in Fig. 3.2, respectively.

Similar to the case of Shor's code, we can write a logical state in the code space, or a ground state of H_{toric}, in terms of the stabilizer generators, i.e.

$$H_{\text{toric}} = -\sum_s Q_s - \sum_p B_p. \tag{3.64}$$

To do so, let $\mathscr{S}_Z = \langle Q_s \rangle$ and $\mathscr{S}_X = \langle B_p, \bar{X}_1, \bar{X}_2 \rangle$, i.e. the Z and X part of the stabilizers, respectively. Then one ground state can be given by the following

$$|\psi_{\text{toric}}\rangle = \sum_{g\in\mathscr{S}_X} g|0\rangle^{\otimes 2r^2}, \tag{3.65}$$

There is a nice geometrical viewpoint of this ground state. If we put a red line on the edge representing the qubit on the edge which is in state $|1\rangle$, then this ground state is the equal weight superposition of all closed loops, as demonstrated in Fig. 3.3.

We now summarize the property of toric code as follows.

Box 3.6 Properties of toric code

The toric code on a square lattice has the following properties.

1. Every stabilizer generator is local (i.e. each generator only involves interactions of nearby qubits).

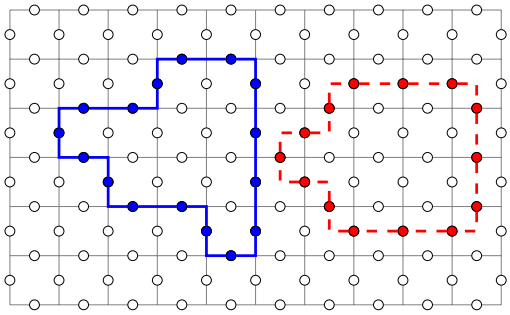

Fig. 3.3 Ground state of toric code on square lattice. The closed loops.

2. The code space encodes two qubits (i.e. four-dimensional subspace).
3. The code distance grows with r, as an order of $\sqrt{N}$ when N goes arbitrarily large.

3.6 Summary and further reading

In this chapter, we have discussed the idea for fighting again decoherence in open quantum systems. The ultimate goal is to maintain coherence (or unitary evolution) of the system. In practice, this cannot in general be done perfect, but in a manner of approximation to reduce the error caused by interaction with the environment by certain order of magnitude. The central idea to realize this reduction is the theory of quantum error correction.

Historically, the first quantum code was introduced by Shor in 1995 [22], which is the Shor's code we discussed in Sec. 3.2. It then followed by [5] and [23], which introduce a framework for constructing quantum error-correcting codes from classical linear codes, which is now called 'Calderbank-Shor-Steane (CSS) code'. The most well known CSS code is the 7-qubit Steane code, which is not discussed in this chapter. Interested readers may refer to [5] and [23] as mentioned above, or refer to some general textbooks such as the one by Nielsen and Chuang [17].

The quantum error-correcting criterion is first proposed in 1997 [14], which is now called the Knill-Laflamme condition. The stabilizer formalism is independently proposed in [9] and in [4]. It should be mentioned that the CSS codes are indeed a special case of the stabilizer codes, where the stabilizers of the CSS codes contain tensor product of only Pauli X operators, or tensor product of only Pauli Z operators.

The graph state is first proposed in [21]. Indeed they discussed not only graph states, but in a more general, case, graph codes. It was further showed in that any stabilizer code is equivalent to a graph code in some sense (i.e. 'local Clifford equivalence'), and similarly every stabilizer state is equivalent to a graph state [20].

The toric code is first proposed in [12]. More details can be found in the book by Kitaev, Sen, and Vyalyi [13]. A similar model, called the Wen-plaquette model is proposed in [25], whose physical properties with different lattice sizes (i.e. odd by odd, odd by even and even by even lattices) are further discussed in [15]. There are many literatures on topological quantum codes, we refer the reader to the survey [2] and references therein.

A special kind of graph state, called the cluster state, was first introduced in [3]. Cluster state correspond to graphs of lattices (e.g. a 1D chain or a 2D square lattice). One important application of cluster state is to be used as a resource state for one way quantum computing, which is proposed in [18]. More on cluster states, graph states and their application in one-way quantum computing can be found in a review article [11].

It is also realized that the cluster state can be viewed as a valence bond solid using the tenor product state (TPS) formalism [24], which will be discussed in part IV of this book. In 2007 it is further shown that the TPS formalism provides a powerful method to construct resource state for one-way quantum computing [10], which are better than cluster states in various circumstances, hence triggering lots of on-going related research ever since. Readers interested in these recent developments could refer to the review articles [16] and [19].

The most general framework for constructing quantum error-correcting codes known to date is the codeword stabilized (CWS) quantum code framework [8]. The CWS framework encompasses stabilizer codes, as well as all known examples of good codes beyond stabilizer codes. It also has a good connection with graph codes. Interested readers could refer to the original CWS code paper mentioned above, or the subsequent follow-up papers [7, 6, 1].

References

1. S. Beigi, I. Chuang, M. Grassl, P. Shor, and B. Zeng. Graph concatenation for quantum codes. *Journal of Mathematical Physics*, 52(2):022201, February 2011.
2. H. Bombin. An Introduction to Topological Quantum Codes. *ArXiv e-prints*, November 2013.
3. H. J. Briegel and R. Raussendorf. Persistent Entanglement in Arrays of Interacting Particles. *Physical Review Letters*, 86:910–913, January 2001.
4. Calderbank, Rains, Shor, and Sloane. Quantum error correction via codes over $GF(4)$. *IEEE Transactions on Information Theory*, 44(4):1369–1387, 1998.
5. A. R. Calderbank and P. W. Shor. Good quantum error-correcting codes exist. *Physical Review A*, 54:1098–1105, August 1996.
6. X. Chen, H. Chung, A. W. Cross, B. Zeng, and I. L. Chuang. Subsystem stabilizer codes cannot have a universal set of transversal gates for even one encoded qudit. *Physical Review A*, 78(1):012353, 2008. http://arxiv.org/abs/0801.2360.
7. I. L. Chuang, A. W. Cross, G. Smith, J. A. Smolin, and B. Zeng. Codeword stabilized quantum codes: algorithm and structure. *Journal of Mathematical Physics*, 50(4):042109, 2009. http://arxiv.org/abs/0803.3232.
8. Andrew Cross, Graeme Smith, John Smolin, and Bei Zeng. Codeword stabilized quantum codes. *IEEE Transactions on Information Theory*, 55(1):1369–1387, 2009.
9. D. Gottesman. *Stabilizer Codes and Quantum Error Correction*. PhD thesis, CalTech, 1997.

10. D. Gross and J. Eisert. Novel Schemes for Measurement-Based Quantum Computation. *Physical Review Letters*, 98(22):220503, June 2007.
11. M. Hein, W. Dür, J. Eisert, R. Raussendorf, M. Van den Nest, and H. . Briegel. Entanglement in Graph States and its Applications. *eprint arXiv:quant-ph/0602096*, February 2006.
12. A. Yu. Kitaev. Quantum computations: algorithms and error correction. *Russian Math. Surveys*, 52:1191–1249, 1997.
13. A. Yu. Kitaev, A.H. Shen, and M.N. Vyalyi. *Classical and Quantum Computation. Vol. 47 of Graduate Studies in Mathematics.* American Mathematical Society, Providence, RI, 2002.
14. E. Knill and R. Laflamme. Theory of quantum error-correcting codes. *Physical Review A*, 55:900–911, February 1997.
15. S.-P. Kou, M. Levin, and X.-G. Wen. Mutual Chern-Simons theory for Z_2 topological order. *Physical Review B*, 78(15):155134, October 2008.
16. L. C. Kwek, Z. Wei, and B. Zeng. Measurement-Based Quantum Computing with Valence-Bond-Solids. *International Journal of Modern Physics B*, 26:30002, 2012.
17. M. Nielsen and I. Chuang. *Quantum computation and quantum information*. Cambridge University Press, Cambridge, England, 2000.
18. R. Raussendorf and H. J. Briegel. A One-Way Quantum Computer. *Physical Review Letters*, 86:5188–5191, May 2001.
19. R. Raussendorf and T.-C. Wei. Quantum computation by local measurement. *ArXiv e-prints*, July 2012.
20. D. Schlingemann. Stabilizer codes can be realized as graph codes. *Quantum Information and Computation*, 2(4):307–323, 2002.
21. D. Schlingemann and R. F. Werner. Quantum error-correcting codes associated with graphs. *Physical Review A*, 65:012308, 2002.
22. P. W. Shor. Scheme for reducing decoherence in quantum computer memory. *Physical Review A*, 52(4):2493–2496, 1995.
23. A. Steane. Multiple-Particle Interference and Quantum Error Correction. *Royal Society of London Proceedings Series A*, 452:2551–2577, November 1996.
24. F. Verstraete and J. I. Cirac. Valence-bond states for quantum computation. *Physical Review A*, 70(6):060302, December 2004.
25. X.-G. Wen. Quantum Orders in an Exact Soluble Model. *Physical Review Letters*, 90(1):016803, January 2003.

Part II
Local Hamiltonians, Ground States, and Many-body Entanglement

Chapter 4
Local Hamiltonians and Ground States

Abstract We discuss many-body systems, where the Hamiltonian involves only few-body interactions. With the tensor product structure of the many-body Hilbert space in mind, we introduce the concept of locality. It is naturally associated with the spatial geometry of the system, where the most natural interaction between degrees of freedom are those 'local' ones, for instance nearest neighbor interactions. We discuss the effect of locality on the ground-state properties. We then discuss ways of determining the ground-state energy of local Hamiltonians, and their hardness. Theories have been developed in quantum information science to show that even with the existence of a quantum computer, there is no efficient way of finding the ground-state energy for a local Hamiltonian in general. However, for practical cases, special structures may lead to simpler method, such as Hartree's mean-field theory. We also discuss a special kind of local Hamiltonians, called the frustration-free Hamiltonians, where the ground state is also ground states of all the local interaction terms. However, to determine whether a Hamiltonian is frustration-free is in general hard.

4.1 Introduction

In Part I, we have introduced some basic concepts of quantum information theory that we will apply to study many-body systems. From this part on, we will focus on these systems. We will first revisit the Hilbert space of composite systems, discussing in detail the 'particle basis' representation and the 'occupation basis' representation of a many-body system. In many cases, the many-body Hilbert space is a tensor product of single body ones.

A many-body system is naturally associated with a many-body Hamiltonian. We have already seen some of these Hamiltonians in Part I, such as the Ising Hamiltonian, Heisenberg Hamiltonian and the Toric Code Hamiltonian. One important property of these Hamiltonians is that they usually involve only few-body interactions. What is more, for Hamiltonians living on some lattice, the few-body interactions usually only involve degrees of freedom 'near' each other on the lattice. This

naturally leads to a concept of locality, that the 'naturally-occurring' Hamiltonians are those 'local' with respect to some spatial lattice geometry. In other words, they involve only few-body interactions of nearby degrees of freedom. Hence we call these many-body Hamiltonians as 'local Hamiltonians'. Locality has an important consequence. That is, the ground states of these systems exhibit special correlation/entanglement properties compared to a 'generic' (i.e. randomly chosen) quantum state in the system Hilbert space. Exploring these properties is then a central topic of this part.

In condensed matter physics, one usually needs to consider infinitely large system (thermodynamic limit) for studying physical properties. However, in many cases, one can also read some important information from a finite system, and its 'scaling' properties with the system size N. Important basic things naturally include the ground-state properties, for instance their correlations and entanglement properties. We will start to look into these correlation properties for ground states of local Hamiltonians for finite systems. We will also discuss consequences of system size N getting large, in some places in this chapter, but mainly in the next chapter (Chapter 5).

We then move on to deal with more practical questions: given a local Hamiltonian of an N-body system, can we determine its ground state energy? Can we find its ground-state wave-functions, and other important properties such as degeneracy?

Anyone with some experience in quantum many-body physics knows that those questions should be very difficult in general. Although calculating ground-state properties for interacting system is so hard, we keep tackling them everyday by making good approximations and developing better algorithms. Quantum information science concurs with those hardness observations but at the same time raises a new interesting question: what if we have a quantum computer, can we compute ground-state energy for a given local Hamiltonian in an efficient way?

One seems to have some hope here because we have shown in Chapter 2 that quantum computer can efficiently simulate quantum evolution of a many-body system with local Hamiltonians. Unfortunately, it is no longer the case regarding computing ground state energy for local Hamiltonians. Quantum information science develops a theory, based on some computer science ideas to show that, even if there is a quantum computer, it is very unlikely that one can efficiently calculate the ground-state energy for local Hamiltonians in general.

This is on the one hand disappointing, which seems to reveal some limitations of quantum computing. On the other hand, this is acceptable as those 'general' local Hamiltonians might not be real (that it is unlikely for us to encounter them in practice). One may think that imposing a bit more structure might make things better, such as looking at a two-spatial dimensional (2D) systems with two-body nearest neighbor interactions only, or even just a one-spatial dimensional (1D) system. Unfortunately even under such restricted situations things do not get much better, which seems to reveal some intrinsic complexity of quantum many-body systems. Indeed, these system with 'hard to analyze' ground state properties are closely related to glassy systems, which needs exponential long cooling time to get to their ground states.

To further understand the local Hamiltonian problem, we discuss another approach, based on the reduced density matrix. This approach has been developed by the quantum chemistry community since 1960s, with recent progress obtained by the quantum information community. The basic idea is that for local Hamiltonians evolving only few-body interactions, the ground-state energy is completely determined by these few-body local reduced density matrices. Therefore, one only needs variations with local density matrices to find the ground-state energy, instead of variations with wave-functions on the entire Hilbert space, which saves exponentially number of variational parameters, in principle.

Unfortunately, it seems very hard to determine the conditions these few-body local density matrices have to satisfy, in order to be a 'part' of a larger quantum systems. In other words, to determine whether some given local density matrices are consistent with each other, i.e. whether they are the reduced density matrices of a state in a larger system, is a hard problem. And it is shown to be as hard as the local Hamiltonian problem.

Nevertheless, this gives an alternative approach for finding the ground-state energy of local Hamiltonians. Closely related, there is an interesting result on the structure of these local reduced density matrices, for bosonic systems, namely the quantum de Finetti's theorem. It states that any local reduced density matrix for bosonic systems in the $N \to \infty$ limit (N is the number of particles in the system) is always not entangled, i.e. it is a mixture of product states. This justifies the validity of Hatree's mean-field approximation, which always gives the exact ground-state energy for bosonic systems, although the ground-state itself may be genuinely entangled.

Another interesting topic we will discuss are the frustration-free systems. We have already known that frustration-free Hamiltonians are enough to produce interesting physics such as topological order, as discussed in Chapter 3.5 (toric code). And for frustration-free systems, the ground state energy can be easily determined as the ground state is just the ground state of each local term of the Hamiltonian. Now the question is, can we determine whether a given system is frustration-free or not. Unfortunately, again there is no efficient way of determining this even with the existence of a quantum computer.

There is one exception though. There is a way to determine whether a Hamiltonian of spin-$1/2$ system (e.g. qubits) involving only two-body interactions is frustration-free or not. And in case it is, one can further characterize the structure of the corresponding ground space structure. It turns out that there always exists a ground state for such a system which has no entanglement at all. This means that the ground state space 'lacks correlation' in a sense, so the ground-state energy as well as the ground state itself can be given by the mean-field theory. Therefore this kind of systems are relatively simple, which could not represent nontrivial strongly correlated phases in practice, whose ground states are expected to be highly entangled.

If one goes beyond spin-$1/2$ systems with two-body interactions, even frustration-free systems will have highly entangled ground states, for instance the toric code Hamiltonian. We will look at some other interesting frustration-free system and their ground state properties, such as the Affleck-Kennedy-Lieb-Tasaki (AKLT) model.

4.2 Many-body Hilbert space

Let's start by discussing carefully the basic concept of the Hilbert space of a many-body system. The Hilbert space of a many-body system is naturally obtained by putting together Hilbert spaces of single-body systems. While this may sound straight-forward, there are two different and both commonly used ways to do it, one from the point of view of particles, one from the point of view of 'modes'.

In the first approach, which we call the 'particle basis' representation, one starts from a single particle Hilbert space which contains all possible states $|\psi\rangle$ of this single particle (described by the position, momentum, angular momentum, etc. of the particle). A many-body system contains more than one, say N, particles, each being in a single particle state $|\psi_i\rangle$. The many-body Hilbert space is then the combination of the single particle Hilbert spaces, but usually with extra constraints.

The constraint comes from the quantum statistics of the particles, which can be either bosons, fermions or distinguishable particles. When the particles are distinguishable, there is no constraint. The many-body Hilbert space is the tensor product of the single-body Hilbert spaces. If a single particle can be in m orthogonal states, then the many-body Hilbert space is m^N dimensional. Particles are distinguishable when, for example, their locations are fixed and the only degrees of freedom in the system or those internal to the particles, like spin. Therefore, in what is called a 'spin system', the total Hilbert space $\mathscr{H}$ is a tensor product of the Hilbert space of individual spins $\mathbb{C}_m$

$$\mathscr{H} = \mathbb{C}_m^{\otimes N}. \tag{4.1}$$

where m is the dimension of a single spin Hilbert space.

When the particles are bosons, exchanging two of the particles should keep the total many-body wave function invariant. That is, if the many-body wave function contains a configuration $|\psi_1\rangle|\psi_2\rangle...|\psi_N\rangle$, it should also contain the configuration $|\psi_{S(1)}\rangle|\psi_{S(2)}\rangle...|\psi_{S(N)}\rangle$ with the same amplitude, where S is an arbitrary permutation on the N labels. When the particles are fermions, exchanging two of them should change the sign of the total wave function. That is, if the many-body wave function contains a configuration $|\psi_1\rangle|\psi_2\rangle...|\psi_N\rangle$, it should also contain the configuration $|\psi_{S(1)}\rangle|\psi_{S(2)}\rangle...|\psi_{S(N)}\rangle$ but with an extra sign factor $(-1)^{p(S)}$ where $p(S)$ is the parity of the permutation operation S. Therefore, the many-body wave functions for bosons or fermions are highly constrained and occupies a very small subspace in the m^N dimensional total Hilbert space.

A highly useful example of many-body wave function written in this form is Laughlin's wave function for quantum Hall states. Laughlin's wave function describes the motion of N bosons or fermions on a two dimensional plane. Each particle can be at different spatial locations labelled by $z = x + iy$. In the simplest Laughlin state, the amplitude for the N fermions to be at locations $z_1, z_2..., z_N$ is given by

$$\Psi(z_1, z_2, ..., z_N) = \prod_{N \geq i > j \geq 1} (z_i - z_j) \prod_{k=1}^{N} \exp(-|z_k|^2) \tag{4.2}$$

which obviously gets a minus sign if two particles are exchanged. In a simple Laughlin state for N bosons, the amplitude for them to be at location $z_1, z_2 ..., z_N$ is given by

$$\Psi(z_1, z_2, ..., z_N) = \prod_{N \geq i > j \geq 1} (z_i - z_j)^2 \prod_{k=1}^{N} \exp(-|z_k|^2) \tag{4.3}$$

which obviously remains invariant under any exchange.

This 'particle basis' representation is extremely useful, but it also has an important flaw: one cannot write wave functions for systems where the total particle number is fluctuating, like in a superfluid or superconductor. To have a more general way to write many-body wave functions, we can switch to an 'occupation basis' representation. The 'occupation basis' representation starts from individual 'modes' that single particles can occupy. A mode can be labeled by the position, momentum, angular momentum or other physical quantities of a single particle. A mode can be empty or occupied. If the system contains bosons, a single mode can be occupied by any number of particles; if the system contains fermions, a single mode can only be occupied by one (or zero) particle. The corresponding single mode Hilbert space is then ∞ dimensional or two dimensional. Usually we can assume that due to certain physical reason, it is not possible to put too many bosons in a single mode and there is an upper bound m. The single mode Hilbert space becomes m dimensional. The many-body Hilbert space is then obtained by putting N modes together and has a tensor product structure

$$\mathscr{H} = \mathbb{C}_m^{\otimes N}, \text{ or } \mathscr{H} = \mathbb{C}_2^{\otimes N} \tag{4.4}$$

There is no extra constraint on the many-body Hilbert space. Any wave function is in principle allowed. The difference between bosons and fermions not encoded in the structure of the many-body Hilbert space any more; instead it is encoded in the way operators act on states in the Hilbert space.

The 'particle basis' and 'occupation basis' representation of many-body Hilbert space and wave function are often also called the first and second quantization of many-body quantum systems. In our following discussion, in this chapter and for the rest of the book, we will be mainly focusing on the spin system, and boson, fermion systems in the 'occupation basis', so that the total Hilbert space has a tensor product structure. Occasionally, we will also use the 'particle basis' representation of boson fermion systems to discuss associated interesting problems. When we do so, we will explicitly state that we are using the 'particle basis' representation.

4.3 Local Hamiltonians

Consider an N-body system. For simplicity, we assume each degree of freedom is a qubit (i.e. a two-level spin degree of freedom), hence the single-body Hilbert space

has dimension 2, which is denoted by $\mathbb{C}_2$. Note that our discussion is readily applied to other systems with larger dimension of its single-body spaces.

The Hilbert space $\mathscr{H}$ of the N-body system is then the tensor product of the Hilbert space of all its subsystem, i.e.

$$\mathscr{H} = \mathbb{C}_2^{\otimes N}. \tag{4.5}$$

If for each single qubit subsystem, the Hilbert space is spanned by the orthonormal basis $\{|0\rangle, |1\rangle\}$, the orthonormal basis for $\mathscr{H} = \mathbb{C}_2^{\otimes N}$ can then be chosen as

$$\{|00\ldots0\rangle, |00\ldots1\rangle, \ldots |11\ldots1\rangle\}. \tag{4.6}$$

The Hamiltonian H of the system is usually given in terms of summation of many terms, i.e.

$$H = \sum_j H_j, \tag{4.7}$$

where each H_j involves only few-body interactions. We say H is a k-body Hamiltonian, if each H_i involves at most k-body interactions, where k is a constant that is independent of the system size N.

4.3.1 Examples

In general, for k-body interactions, there are total $\binom{N}{k}$ ways of choosing the k degrees of freedom involved. In practice, it is not always true that all of them has to show up in a k-body Hamiltonian H. For instance, for a lattice spin system, the interaction usually only involves the spins that are 'near each other'. As a concrete example, consider a 1D chain as shown in Fig. 4.1, the Ising model Hamiltonian in a transverse filed is given by

$$H^{\text{tIsing}} = -J\sum_j Z_j Z_{j+1} - B\sum_j X_j \tag{4.8}$$

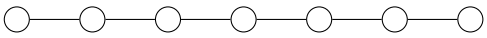

Fig. 4.1 A 1D lattice

H^{tIsing} involves only 2-body local interactions that in this sense we call H^{tIsing} a 2-local Hamiltonian.

For a 2D example, consider the following Hamiltonian on a 2D square lattice as shown in Fig. 4.2, which has the 2D cluster state (i.e. the graph state associated with the graph as a 2D square lattice, as discussed in Chapter 3.4.3) as its unique ground state, reads

$$H_{\text{clu}} = -\sum_{i,j} X_{i,j} Z_{i+1,j} Z_{i-1,j} Z_{i,j+1} Z_{i,j-1} \tag{4.9}$$

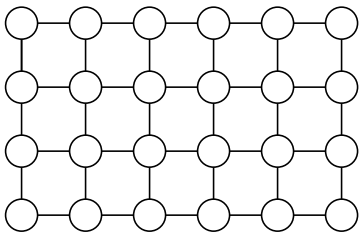

Fig. 4.2 A 2D square lattice

H_{clu} involves only 5-body local interactions, so we call H_{clu} a 5-local Hamiltonian.

In general, we will consider a D-spatial dimensional system, which in general refers to the usual Euclidean geometry in $\mathbb{R}^D$. We also discuss other manifolds such as torus, which we already encountered in Chapter 3.5 for toric code. We will further discuss dimensionality and locality from condensed-matter theory point of view, in Chapter 5.

4.3.2 The effect of locality

After talking about locality, which is associated with some spacial geometry, one natural question is that what is the effect of locality. Or putting in other words, what is the difference of a k-local Hamiltonian associated with some spacial geometry, compared with those 'non-local' k-body Hamiltonians. For simplicity, when we talk about locality of a D spatial dimensional system, we refer to the usual Euclidean geometry in $\mathbb{R}^D$.

Indeed, local Hamiltonians will be the main focus of this book, by studying the properties of their ground state space and beyond. In other words, most part of the book will deal with local Hamiltonians, which we have in mind the spatial locality for a D spatial dimensional system with respect to the Euclidean geometry in $\mathbb{R}^D$. Before we look further into these systems of spatially local Hamiltonians, we would like to understand a bit what is the difference between local Hamiltonians and those non-local k-body Hamiltonians.

Let us recall the toric code system on torus with a square lattice (as discussed in Chapter 3.5). Now our locality refers to the $D = 2$-dimensional Euclidean geometry. The system has $N = 2r^2$ spins, and the ground state space is four-fold degenerate, which is a stabilizer quantum error correcting code encoding 2 qubits. The code distance is d, which is of the order $\sqrt{N}$ for large N. It is natural to wonder whether

we can do better than this. For instance, does there exist a local Hamiltonian on the square lattice such that its degenerate ground state space has larger degeneracy, but meantime maintain the a code distance as good as $\sqrt{N}$.

Intuitively, this is not possible. If the degeneracy is too large, say, exponential in N, then local perturbation shall be enough to destroy such a degeneracy. This can be shown for a large class of local Hamiltonians.

For a k-local stabilizer Hamiltonian on a D-dimensional lattice, the ground state space degeneracy R and the code distance d satisfies a constraint

$$\log R \leq \frac{cN}{d^\alpha}, \ \alpha = \frac{2}{D-1}, \tag{4.10}$$

where c is some constant independent of the system size N. This means if $\log R/N$ is a constant, i.e. the degeneracy is exponential in N in a sense that $\log R/N$ is a constant, then the code distance d is upper bounded by a constant $\left(\frac{cN}{\log R}\right)^{\frac{1}{\alpha}}$. That is, the code distance cannot increase with N.

For $D = 2$, the code distance bound Eq.(4.10) becomes $\sqrt{\frac{cN}{\log R}}$. That is, d at most can scale as the square root of the system size N, which the toric code does.

However, a k-body but non-local Hamiltonian system can perform quite differently. There are indeed k-body but non-local Hamiltonians constructed on the $2D$ square lattice, such that the ground state space has dimension R which increases exponentially with N , i.e. $\log R/N$ is come constant. Meanwhile, the code distance d scales as the square root of N, similar to the toric code.

As to demonstrate the proof of the bound given by Eq.(4.10) as well as the construction of these highly nontrivial k-body but non-local Hamiltonians mentioned above is getting too much involved in the technical details of the theory quantum error-correcting code, which goes beyond the main scope of the book, so we omit those details. The main information to convey is that 'locality' does have strong restriction on how such physical systems could actually behave. Throughout the book, we will only look at 'local' Hamiltonians associated with Euclidean geometry on some (finite) D-spatial-dimensional lattice.

4.4 Ground-state energy of local Hamiltonians

Having built some general understanding for correlations in finite system, we now move into a more practical question: given a local Hamiltonian of an N-body system, can we determine its ground state energy? Can we find its ground state wave functions, and other important properties such as degeneracy?

Let us start from the first question to determine the ground- state energy of a k-local Hamiltonian. Our experience tells us to find the ground state energy of an interacting many-body system is a hard question. By 'hard' here we mean to deal with the task as computationally. Imagine to exact diagonalize a Hamiltonian of $N = 20$ qubits, which will be an $\sim 10^6 \times 10^6$ matrix. This is doable with today's personal

computers, but even supercomputers can hardly deal with $N = 30$, as the cost of computation, in terms of both memory use and computing time, grows exponentially with the number of degrees of freedom N.

On the other hand, we are talking about quantum computers, which can in principle exist. And we have already demonstrated its power for simulating evolution of quantum systems. Now the question is, if there were a quantum computer, could we determine the ground state energy of local systems efficiently. By efficient here we mean an algorithm running on a quantum computer whose computing time grows only polynomially with the number of degrees of freedom N. If this were the case, then we can easily compute a systems of hundreds or even thousands of qubits, whose behaviour could well approximate the practical condensed matter systems in the $N \to \infty$ limit.

Unfortunately, it turns out not the case. In other words, even a quantum computer is very unlikely to compute the ground state energy of a local Hamiltonian efficiently. In order to reach this definite conclusion, an important subfield of quantum information science, namely the theory of quantum computational complexity, has been extensively developed. It is beyond the scope of this book to go into the details of such a theory, but we would like to briefly review some important practical relevant results obtained from the theory.

4.4.1 The local Hamiltonian problem

We start to state the so called 'local Hamiltonian problem' explicitly.

Box 4.1 The local Hamiltonian problem

Given a local Hamiltonian $H = \sum_j H_j$, where each H_j acts non-trivially on at most k qubits. Denote E_0 the ground state energy of H. For given $(b-a) \propto 1/\text{poly}(N)$, determine which of the following is true.

1. $E_0 > b$.
2. $E_0 < a$.

Some points need to be clarified. Firstly, we have not only a single Hamiltonian H, but in fact, a family of Hamiltonians $\{H_N\}_{N=1}^{\infty}$. Here each H_N denotes the Hamiltonian for a systems of N degrees of freedom. When taking a limit N goes to infinity, we end up with the thermodynamic limit (an infinitely large system).

Secondly, $b-a$ gives the precision of this problem, i.e. the error we can actually tolerate for deciding the ground state energy. We know for numerical stability reasons, it makes no sense to take $b = a$. For technical reasons, for all the problems studied, the precision $b-a$ is set to be scale as an inverse polynomial of the system's size N, i.e. $b-a \propto 1/\text{poly}(N)$, where poly is some polynomial function, and $\propto$ means up to some constant factor.

Under these setups, the quantum computational complexity theorem provides the following rather surprising assertion.

Box 4.2 The hardness of the local Hamiltonian problem
The local Hamiltonian problem is very unlikely to be efficiently solvable, even with the existence of a quantum computer.

As mentioned we are not digging into the details of how this result is technically shown. Rather, we would try to explain some aspects as a consequence of this result which are of more practical interest.

First of all, we would say something regarding what we meant by 'very unlikely to be efficiently solvable'. We know that efficiently solvable means that there exists a polynomial size quantum circuit (i.e. circuits with poly(N) gates), which answers the problem for H_N. So by saying 'unlikely to be efficiently solvable', we mean that it is very unlikely to have such kind of quantum circuits. The underline reason is that if such a circuit exists, then it will contradict some common belief in the fundamental theory of computer science. That is, the class of problems whose solutions can efficiently verified (the so-called '**NP**' class), is in fact different from the class of problem whose solutions can be efficiently found (the so-called '**P**' class). This $\mathbf{P} \neq \mathbf{NP}$ conjecture is widely believed to be true among computer scientists, yet no rigorous proof ever found. Note that what is directly relevant to discussions in Box 4.6 is the 'quantum analogy' of this $\mathbf{P} \neq \mathbf{NP}$ conjecture, which for technical reasons we omit the details.

We then discuss the structure of the Hamiltonian H. In the assertion it is only roughly said that H is a local Hamiltonian, but has not yet specified its local structure (i.e. spatial dimension, nearest-neighbor etc.). One might think that the local structure which leads to the asserted result might be quite non-physical, in a sense that it might involve $k \geq 3$-body interactions, or interactions between degrees of freedom which are geometrically not nearest neighbors. Quite counter-intuitively, the local structure could be surprisingly simple: it can only be associated with nearest-neighbor interactions on a $2D$ square lattice, or even nearest neighbor interactions on a $1D$ chain. It worth mentioning that $1D$ result is with a designed Hamiltonian not for qubit (i.e spin $1/2$) systems, but for a spin system with spin-$23/2$ (i.e. single-spin Hilbert space dimension 12), which does not seems quite realistic. However, this is still very surprising given the usually impression that a $1D$ systems should be relatively simple. We will discuss more about $1D$ many-body systems in later chapters.

It is interesting to note that there is another way of looking at the local Hamiltonian problem, from the viewpoint of quantum simulation. Recall that the quantum simulation problem is to find the quantum state $\rho(t)$, where the evolution is governed by the Schrödinger's equation, i.e.

$$\rho(t) = \frac{(e^{-iHt})^\dagger \rho(0) e^{-iHt}}{\mathrm{Tr}\left[(e^{-iHt})^\dagger \rho(0) e^{-iHt}\right]}, \tag{4.11}$$

where t is a real number indicates the 'real' time.

Now imagine that t to be purely imaginary, i.e. $t = -i\beta$, where $\beta = \frac{1}{\kappa T}$. Choose $\rho_0 = \frac{I}{\mathrm{Tr}I}$, then Eq.(4.11) becomes $\rho(\beta) = \frac{e^{-2\beta H}}{\mathrm{Tr}e^{-2\beta H}}$. The ground state ρ_g of the Hamiltonian can then be given by

$$\rho_g = \lim_{\beta\to\infty} \frac{e^{-2\beta H}}{\mathrm{Tr}e^{-2\beta H}}. \tag{4.12}$$

This then indicates that to find the ground state of the Hamiltonian H is equivalently to 'simulate' the imaginary time evolution for β large, or alternatively, to simulate the 'cooling' of the system to its zero temperature (i.e $T = 0$) ground state. The local Hamiltonian problem with a given local Hamiltonian H is hard then means that in the worst case, the time taken to cool the system to its ground state is 'exponentially long' (here 'exponential' is again, in terms of the system size N). In practice, there are indeed physical systems which are 'hard' to cool to its ground state, for instance, the spin glasses. These systems have access to a large number of metastable states such that they are much easier ending up in some metastable states than their ground states. In other words, for those physical systems whose ground states are hard to compute with a quantum computer may be just those systems whose ground states are 'not real', i.e. they never end up in their ground states in real world.

Finally we remark a bit more on the $b - a \propto 1/\mathrm{poly}(N)$ in the local Hamiltonian problem. It is not yet known how much this condition can be relaxed, e.g. say, can we set $b - a \propto$, the number of the local interaction terms in local Hamiltonian, i.e. the number of terms in summation of $H = \sum_j H_j$, but the local Hamiltonian problem remains hard? Quite surprisingly, in the classical case, the answer is affirmative, which is given by the so-called probabilistically checkable proof (PCP) theorem. However, the quantum case remains open, while it is stated as the 'quantum PCP conjecture', which means the answer is indicated to be true by some evidences. This problem has raised considerably attention in the quantum information community in recent years, as its solution will need the development of many new tools, while provide a fundamental understanding of what many-body quantum systems are the true 'hard' ones.

4.4.2 The quantum marginal problem

We now would like to look at the local Hamiltonian problem from another point of view, namely the variational approach. For the local Hamiltonian $H = \sum_j H_j$, the ground state energy E_0 can be given by

$$E_0 = \min_{|\psi\rangle} \langle\psi|H|\psi\rangle, \tag{4.13}$$

where the minimization is over all wave functions $|\psi\rangle$.

Now because H is local, so for any $|\psi\rangle$, we can write

$$\langle\psi|H|\psi\rangle = \sum_j \mathrm{Tr}(H_j\rho_j), \tag{4.14}$$

where ρ_j is the reduced density matrix for particles sets that H_j acting non-trivially on.

Now in order to find the ground-state energy, we can do minimization over the set of $\{\rho_j\}$ instead. This at first glance seems to be much simpler than the minimization over the n-particle wave function $|\psi\rangle$, as the set of $\{\rho_j\}$ has much less parameters. However, there is a problem: the minimization is not over the set of all density matrices for particles sets that H_j acting non-trivially on, but over the set of all *reduced* density matrices or particles sets that H_j acting non-trivially on. Therefore, one has to first determine the condition such that the density matrices are indeed reduced density matrices. This is the so called quantum marginal problem.

Box 4.3 The quantum marginal problem
Given a set of local density matrices $\{\rho_j\}$, determine whether there exists an n-particle state ρ, such that $\{\rho_j\}$ are reduced density matrices of ρ.

To understand this marginal problem better, let us look at a simple example. Suppose we have a system with three qubits A,B,C. Now given a density matrices ρ_{AB} of qubits A,B and ρ_{AC} of qubits A,C. We ask whether these exists a three-qubit states ρ_{ABC}, such that $\rho_{AB} = \mathrm{Tr}_C\,\rho_{ABC}$ and $\rho_{AC} = \mathrm{Tr}_B\,\rho_{ABC}$.

Unfortunately, even in this simple case, no analytical condition is known to tell the answer easily. Let us then try to further simplify the problem a bit. Let us assume $\rho_{AB} = \rho_{AC}$, in other words, we assume a symmetry when interchanging qubit B with qubit C. Now we would like to explore the conditions that ρ_{AB} has to satisfy to guarantee the existence of some ρ_{ABC}, which is also assumed to be symmtric when interchanging qubit B with qubit C. In this sense, ρ_{ABC} is also called the symmetric extension of ρ_{AB}.

This symmetric extension problem happen to have an elegant analytical solution. That is, a two-qubit state ρ_{AB} has symmetric extension if and only if

$$\mathrm{Tr}(\rho_B^2) \geq \mathrm{Tr}(\rho_{AB}^2) - 4\sqrt{\det(\rho_{AB})}, \tag{4.15}$$

where $\rho_B = \mathrm{Tr}_A(\rho_{AB})$.

To demonstrate that Eq. (4.15) makes sense, let us first consider the case where ρ_{ABC} could be a pure state. That is, ρ_{AB} is 'pure symmetric extendable', and $\rho_{ABC} = |\psi_{ABC}\rangle\langle\psi_{ABC}|$. Using Schmidit decomposition between qubits A,B and qubit C, we can write $|\psi_{ABC}\rangle$ as

$$|\psi_{ABC}\rangle = \sum_\alpha \lambda_\alpha |\alpha_{AB}\rangle|\alpha_C\rangle. \tag{4.16}$$

This means that the non-zero eigenvalues of $\rho_{AB} = \mathrm{Tr}_C |\psi_{ABC}\rangle\langle\psi_{ABC}|$ is the same as those of $\rho_B = \rho_C = \mathrm{Tr}_{AB} |\psi_{ABC}\rangle\langle\psi_{ABC}|$, where $\rho_B = \rho_C$ comes from the symmetry assumption between qubits B and C. Therefore we have $\mathrm{Tr}(\rho_B^2) = \mathrm{Tr}(\rho_{AB}^2)$. And because ρ_{AB} is at most rank 2, so $\det(\rho_{AB}) = 0$. Therefore the equality of Eq.(4.15) holds.

It is interesting to mention that the validity of Eq. (4.15) is to explicitly construct a corresponding local Hamiltonian

$$H = H_{AB} + H_{AC}, \tag{4.17}$$

such that

$$\mathrm{Tr}(H_{AB}\rho_{AB}) \geq 0 \tag{4.18}$$

for any ρ_{AB} satisfying Eq. (4.15). Here H_{AB} acts on the qubits A, B and H_{AC} acts on the qubits A, C. Due to symmetry between qubits B, C, H_{AB} and H_{AC} are in fact the same operator.

To further understand the meaning of Eq (4.18), notice that for any ρ_{AB} that satisfies the equality of Eq (4.18), the corresponding ρ_{ABC} is in fact the ground state of H. It turns out that for any rank 4 σ_{AB} that satisfies the equality of Eq. (4.15), the corresponding H_{AB} that has ρ_{AB} as a ground state has an explicit form given by

$$H_{AB}(\sigma_{AB}) = \sqrt{\det \sigma_{AB}}\,\sigma_{AB}^{-1} - \sigma_{AB} + \sigma_B. \tag{4.19}$$

Let us consider an example of the two-qubit state

$$\rho_W(p) = (1-p)\frac{I}{4} + p|\phi\rangle\langle\phi|, \tag{4.20}$$

where $|\phi\rangle = \frac{1}{\sqrt{2}}(|00\rangle + |11\rangle)$, and $p \in [0,1]$.

The equality of Eq. (4.15) gives

$$\mathrm{Tr}\left(\rho_W^2(p)\right) = \mathrm{Tr}\left(\left(\mathrm{Tr}_A\,\rho_W(p)\right)^2\right) + 4\sqrt{\det \rho_W(p)}, \tag{4.21}$$

providing a unique solution of $p = \frac{2}{3}$.

Then Eq. (4.19) gives

$$H_{AB}\left(\rho_W\left(\frac{2}{3}\right)\right) = \begin{pmatrix} \frac{2}{9} & 0 & 0 & -\frac{4}{9} \\ 0 & \frac{2}{3} & 0 & 0 \\ 0 & 0 & \frac{2}{3} & 0 \\ -\frac{4}{9} & 0 & 0 & \frac{2}{9} \end{pmatrix} \tag{4.22}$$

The ground-state space of the Hamiltonian $H = H_{AB} + H_{AC}$ is two-fold degenerate and spanned by

$$|\psi_0\rangle = \frac{1}{\sqrt{6}}(2|000\rangle + |101\rangle + |110\rangle),$$
$$|\psi_1\rangle = \frac{1}{\sqrt{6}}(2|111\rangle + |010\rangle + |001\rangle). \tag{4.23}$$

And it it straightforward to check that

$$\rho_W(\frac{2}{3}) = \frac{1}{2}\mathrm{Tr}_C(|\psi_0\rangle\langle\psi_0| + |\psi_1\rangle\langle\psi_1|). \tag{4.24}$$

This means that the symmetric extension of $\rho_W(\frac{2}{3})$ is in fact the maximally mixed state of the ground-state space of $H\left(\rho_W(\frac{2}{3})\right)$.

We remark that the validity of Eq (4.18) does not mean that the operator H_{AB} is non-negative, which one can easily observe from the example of Eq. (4.22). What Eq (4.18) says is that the operator $H = H_{AB} + H_{AC}$ is non-negative, for example the ground states $|\psi_0\rangle, |\psi_1\rangle$ have zero energy. This illustrate the concept of 'frustration,' where the ground state of the 3-qubit system with the Hamiltonian $H = H_{AB} + H_{AC}$ does not need to be also the ground state of each interaction term H_{AB}, H_{AC}. Generally local Hamiltonians are frustrated, but the special case of frustration-free Hamiltonians are also of importance that we will discuss more in Chapter 4.5.

Although Eq.(4.15) is valid for two-qubit case, it is known to be not generalizable to almost any other case, even for two-qubit marginals ρ_{AB}, ρ_{AC} without symmetry between B, C. In fact, the real trouble is that spectra of the marginal ρ_{AB} is in almost all cases, not enough to fully solve the quantum marginal problem. In other words Eq.(4.15) is just a lucky situation for two qubits, and in general there is not much hope to have a simple condition which answers the question raised by the quantum marginal problem. Therefore, we now turn our hope to computers: can we design an algorithm that approximate the answer to the question, and could such an algorithm be efficient, possibly on a quantum computer.

The answer to the first question is no doubt affirmative. One can simply parametrize ρ_{ABC} in a general operator basis, and then check the condition that $\mathrm{Tr}_C \rho_{ABC} = \rho_{AB}$, $\mathrm{Tr}_B \rho_{ABC} = \rho_{AC}$, and $\rho_{ABC} \geq 0$ to see whether such a ρ_{ABC} exists. However, we know that an general n-qubit density matrix has exponentially many parameters in terms of n, so this procedure cannot efficiently deal with large n cases. Worse, even with a quantum computer, there is not much hope for an efficient algorithm, as given by the following fact shown in quantum computational complexity theory.

Box 4.4 The hardness of the quantum marginal problem
The quantum marginal problem is as hard as the local Hamiltonian problem.

This fact, however, is very natural. Because the local Hamiltonian problem and the quantum marginal problem, both used to determine the ground state energy of local Hamiltonians, are in fact to look at the same problem from different perspectives. Therefore their computational complexities should be essentially the same.

4.4.3 The N-representability problem

The quantum marginal problem has also been extensively studied in the field of quantum chemistry, for bosonic/fermionic systems, which correspond to states supported on the symmetric/antisymmetric subspace of the N-particle Hilbert space. Due to symmetry, all the two-particle reduced density matrices (2-RDMs) are the same, which we simply denote by ρ_2. Also, the single-particle Hilbert space is no longer a qubit, but in general with a large dimension in order to have non-vanishing fermionic wave function (in the first quantization picture). The corresponding quantum marginal problem, also called the N-representability problem, is formulated in the following way.

Box 4.5 The N-representability problem
Given a two-particle bosonic/fermionic density matrices $\{\rho_2\}$, determine whether there exists an N-particle bosonic/fermionic state ρ, such that $\{\rho_2\}$ is the two-particle reduced density matrices of ρ.

The symmetry requirement seem to simplify the problem a bit. As an example, for the bosonic case, the conjecture given by Eq.(4.15) holds, which leads to a simple condition. That is, a 2-matrix ρ_2 of a two-mode bosonic system is 3-representable if and only if

$$\mathrm{Tr}\,\rho_1^2 \geq \mathrm{Tr}\,\rho_2^2, \tag{4.25}$$

where ρ_1 is the single-particle reduced density matrix of ρ_2. Note that in terms of Eq.(4.15), the bosonic 2-matrix is only supported on the symmetric subspace of the two-qubit Hilbert space, thus the determinant term vanishes.

In general, the condition given in Eq.(4.25) is also necessary for 3-fermion or 3-boson systems with arbitrary single particle dimension. That is, if a bosonic/fermionic 2-matrix ρ_2 satisfies $\mathrm{Tr}\,\rho_1^2 \geq \mathrm{Tr}\,\rho_2^2$, where ρ_1 is the single-particle reduced density matrix of ρ_2, then ρ_2 is 3-representable.

However, Eq.(4.25) is not sufficient for higher dimensional single particle space, where the equality in Eq.(4.25) does not even imply that the spectra of ρ_2 and ρ_1 are equal. This shows that the dimension m of the single particle space is a crucial parameter which may determine the hardness of the N-representability problem. When m is small, the dimension of the N-particle Hilbert space is also relatively small. However, in the cases where m is relatively large, we have

Box 4.6 The hardness of the N-representability problem
The N-representability Problem for either bosonic/fermionic system with large enough dimension of the single particle space, is as hard as the Local Hamiltonian Problem.

Here by large we mean that the dimension m of the single particle space is at least twice the particle number, i.e. $m \geq 2N$, and in general m grows with N. This condition makes perfect sense for fermions as the Pauli principle and particle-hole duality tells us that the system of m single-particle states is the same as that of $m-N$ single-particle states. In fact, the validity of the results in Box 4.6 for fermions are shown by a mapping between N-fermion system with $2N$ single particle states and an N-qubit system. The bosonic case is a bit more complicated but essentially the dimension of single particle space plays the key role in the hardness conclusion. The result in Box 4.6 matches our general sense that the interacting bosonic/fermonic systems are hard to understand.

4.4.4 de Finetti theorem and mean-field bosonic systems

When considering an N-particle bosonic system, the single-particle space dimension m could be just a constant that is independent of N (m can in fact even be infinite, as long as it does not grow with N, see the discussion below). It is natural to expect in this case that the corresponding N-representability should not be as hard as the case when m grows with N. Now the question is, can we say anything about the set of 2-RDMs?

To examine this question, we would like to go back to the discussion of the symmetric extension problem discussed in Chapter 4.4.2. We want to know a little bit more regarding what kind of states could have symmetric extension. Let us start from the simplest possible case of a bipartite separable state, as given in Box 1.19 of Chapter 1.3.6, i.e.

$$\rho_{AB} = \sum_i p_i |\varphi_{i_A}\rangle\langle\varphi_{i_A}| \otimes |\phi_{i_B}\rangle\langle\phi_{i_B}|. \tag{4.26}$$

This separable ρ_{AB} obviously has symmetric extension. In fact, then only thing one needs to do is to 'copy' qubit B, which results in

$$\rho_{ABB'} = \sum_i p_i |\varphi_{i_A}\rangle\langle\varphi_{i_A}| \otimes |\phi_{i_B}\rangle\langle\phi_{i_B}| \otimes |\phi_{i_{B'}}\rangle\langle\phi_{i_{B'}}|. \tag{4.27}$$

Now let us further extend ρ_{AB} to a state $\rho_{ABB_1B_2}$, where B_1, B_2 are another two qubits, by 'copying' the qubit B twice, which has full symmetry between the qubits B, B_1, B_2. We can continue to make more s copies of qubit B to produce a state $\rho_{ABB_1B_2\ldots B_s}$, which has full symmetry between the qubits $B, B_1, B_2 \ldots B_s$.

We may ask the question for a given s, what kind of bipartite state ρ_{AB} admits an s-copy symmetric extension. That is, there exists a state $\rho_{ABB_1B_2\ldots B_s}$, which has full symmetry between the qubits $B, B_1, B_2 \ldots B_s$, such that ρ_{AB} is the reduced density matrix after tracing out the qubits $B_1, B_2 \ldots B_s$. Notice that if ρ_{AB} admits an s-copy symmetric extension, then it naturally admits an $s-1$-copy symmetric extension (by tracing out B_s). Therefore, the set of bipartite states that admit s-copy symmetric

extensions is a subset of those admit $s-1$ symmetric extensions. And for any s, this set contains the separable states as a subset.

A more interesting question is what happens if we take the limit $s \to \infty$. That is, what kind of ρ_{AB} admit s-copy symmetric extension for any s. It turns out that only separable ρ_{AB} could admit all s-copy symmetric extension. In other words, the $s \to \infty$ limit of s-copy symmetric extendible states is the set of all separable states.

This is pretty much the situation for an N two-mode boson system, where all the particles are fully symmetrized. In other words, the set of 2-RDMs for this N-boson system contains only states that are very close to separable states when N goes large. This observation can also be generalized to the situation of m modes (i.e. m single particle states) and for k-RDMs, whenever m and k are fixed.

This is given by the following finite quantum de Finetti's theorem.

Box 4.7 The finite quantum de Finetti's theorem

The k-RDM ρ_k of an N-particle bosonic state can be approximated with an error at most $O(m^2k/N)$ by a mixture of product states of the form $|\alpha\rangle^{\otimes k}$, where $|\alpha\rangle$ is some single-particle bosonic state.

One immediately sees that if m is a fixed constant that is independent of N, and if one takes the limit $N \to \infty$, then the error $m^2k/N \to 0$ for any fixed k. This is to say, any k-RDM of a bosonic system of infinite size with finite modes can only be a mixture of product states (i.e. separable states). This is the very content of the quantum de Finetti's theorem.

In fact, the validity of quantum de Finetti's is much more general. It applies to the situation beyond that the single-particle Hilbert space with finite dimension m. It is true even when the single-particle Hilbert space is 'separable', which is a mathematical term meaning that the single-particle Hilbert space has countable number of basis states. That is, the single-particle Hilbert space can have infinite dimension with basis labeled by some integer m. This is a very general case for quantum mechanics, where observables (energy, angular momentum etc.) are with quantized eigenvalues, and the corresponding eigenvectors form a basis of the Hilbert space.

We now present the quantum de Finetti's theorem as below.

Box 4.8 The quantum de Finetti's theorem

Consider an N-boson system with a separable single-particle Hilbert space $\mathscr{H}$. For any N-boson wave function $|\Psi_N\rangle$ that lies in the symmetric subspace of $\mathscr{H}^{\otimes N}$, and for any constant integer $k > 0$ that is independent of N, the k-RDM ρ_k of $|\Psi_N\rangle$ is a mixture of product states of the form $|\alpha\rangle^{\otimes k}$, in the $N \to \infty$ limit.

The de Finetti's theorem has an immediate physical consequence – it justifies the validity of Hartree's mean-field theory to calculate the ground-state energy of a

large class of interacting bosonic systems. To be more concrete, let us consider an n-particle bosonic system with an interaction of the following (generic) form

$$H_N = \sum_{j=1}^{N} T_j + \frac{1}{N-1} \sum_{1\le k<l\le N} \omega_{kl}, \tag{4.28}$$

where T_j is a single-particle operator on the jth boson, and ω_{kl} is a symmetric operator on the two-particle space $\mathscr{H}^{\otimes 2}$.

The Hartree's mean-field theory assumes that the (variational) ground state is a product state with the form $|\Psi_\alpha\rangle = |\alpha\rangle^{\otimes N}$, so the the ground-state energy (per particle), denoted by E_0^h, is given by

$$\varepsilon_0^h = \min_{\Psi_\alpha} \frac{\langle\Psi_\alpha|H_N|\Psi_\alpha\rangle}{N} = \frac{1}{2} \min_{|\alpha\rangle} \{\langle\alpha|^{\otimes 2} H_2 |\alpha\rangle^{\otimes 2}\}. \tag{4.29}$$

Now for any wavefunction $|\Psi\rangle$ of the system, the corresponding energy per particle is given by

$$\frac{\langle\Psi|H_N|\Psi\rangle}{N} = \mathrm{Tr}(\rho_1 T) + \frac{1}{2}\mathrm{Tr}(\rho_2 \omega) = \frac{1}{2}\mathrm{Tr}(\rho_2 H_2). \tag{4.30}$$

Therefore, in the thermodynamic limit, the ground-state energy (per particle) is given by

$$\varepsilon_0 = \lim_{N\to\infty} \frac{\langle\Psi|H_N|\Psi\rangle}{N} = \frac{1}{2} \min_{\rho_2} \{\mathrm{Tr}(\rho_2 H_2)\}. \tag{4.31}$$

According to the quantum de Finetti's theorem, ρ_2 is a mixture of product states of the form $|\alpha\rangle^{\otimes 2}$, therefore, we only need to take minimization over all $|\alpha\rangle^{\otimes 2}$, i.e.

$$\varepsilon_0 = \frac{1}{2} \min_{|\alpha\rangle} \{\langle\alpha|^{\otimes 2} H_2 |\alpha\rangle^{\otimes 2}\}. \tag{4.32}$$

which is exactly the same as the mean-field ground state energy ε_0^h as given by Eq. (4.29). In other words, the mean-field ground-state energy, although comes from a trivial wave-function, is in fact exact. We summarize this fact below.

Box 4.9 The validity of the mean-field approximation

For a generic interacting bosonic system, the ground-state energy given by the Hartree's mean-field approximation is exact. This is a consequence of the special structure of the bosonic reduced density matrices in the thermodynamic limit (the quantum de Finetti's theorem), which does not depend on any specific properties of the Hamiltonian.

We remark that this result does not contradict the hardness of the N-presentability problem as discussed in Box 4.6. The key difference is that here the dimension of single-particle system (i.e. m), once chosen, is fixed, which does not grow with N.

In other words, in the $N \to \infty$ limit, the number of particle per mode is in fact $\gg 1$, which corresponds to the so called 'high density' limit in physics.

Also, although the mean-field theory gives the exactly ground-state energy ε_0, the ground-state wave-function $|\Psi_0\rangle$ may not be anywhere near a product state $|\alpha\rangle^{\otimes N}$. In other words, despite that the k-RDMs are mixture of product states, the ground-state wave-function may be genuinely entangled.

Let us consider a concrete example. Consider a two-body Hamiltonian

$$H_{ij} = |1_i 1_j\rangle\langle 1_i 1_j| + |\phi^s_{ij}\rangle\langle\phi^s_{ij}|, \tag{4.33}$$

where $|\phi^s_{ij}\rangle = \frac{1}{\sqrt{2}}(|0_i 1_j\rangle - |1_i 0_j\rangle)$ is the singlet state, and i (j) corresponds to the ith (jth) particle.

For the Hamiltonian

$$H_0 = \sum_{1\le i<j\le N} H_{ij}, \tag{4.34}$$

the ground state is two-fold degenerate, and is spanned by $|0\rangle^{\otimes N}$ and

$$|W_N\rangle = \frac{1}{\sqrt{N}}(|10\ldots00\rangle + |01\ldots00\rangle\cdots + |00\ldots01\rangle). \tag{4.35}$$

Now further consider the Hamiltonian

$$H = \sum_{1\le i<j\le N} H_{ij} + B\sum_{j=1}^{N} Z_j. \tag{4.36}$$

For small $B < 0$ (as a perturbation to H_0), the ground state of H is then $|W_N\rangle$.

Notice that $|W_N\rangle$ is genuinely entangled. And it is not anywhere near a product state $|\alpha\rangle^{\otimes N}$. This can be seen from its maximal overlap with $|\alpha\rangle^{\otimes N}$, which is given by

$$\Lambda_{\max}(|W_N\rangle) = \left(\frac{N-1}{N}\right)^{\frac{N-1}{2}}. \tag{4.37}$$

This means that the geometric measure of entanglement, as discussed in Chapter 1, increases with N.

On the other hand, the 2-RDM ρ_2 of $|W_N\rangle$ is given by

$$\rho_2(|W_N\rangle) = \frac{N-2}{N}|00\rangle\langle 00| + \frac{1}{2N}(|01\rangle + |10\rangle)(\langle 01| + \langle 10|), \tag{4.38}$$

which is not separable but approaches $|00\rangle\langle 00|$ when $N \to \infty$. This is consistent with the prediction of the quantum de Finetti's theorem.

4.5 Frustration-free Hamiltonians

In this subsection, we discuss a special kind of local Hamiltonian, namely, the frustration-free Hamiltonians, which will be extensively used later in this book. We have already seen an example demonstrating the concept of 'frustration' in Sec. 4.4.2. We now start from stating more formally what a frustration-fee Hamiltonian is.

Box 4.8 The frustration-free Hamiltonians
A k-local Hamiltonian $H = \sum_j H_j$ is frustration-free, if the ground state state $|\psi_0\rangle$ of H is also the ground states of each H_j.

4.5.1 Examples of frustration-free Hamiltonians

Frustration-free Hamiltonians are widely found in practical many-body spin models. One simple example is the ferromagnetic Ising chain with an interacting Hamiltonian

$$H_{FIC} = -\sum_i J_i Z_i Z_{i+1}, \tag{4.39}$$

where $J_i > 0$. The two-fold degenerate ground state space of H_{FIC} is spanned by

$$|0\rangle^{\otimes N} = |00\ldots0\rangle, \quad |1\rangle^{\otimes N} = |11\ldots1\rangle, \tag{4.40}$$

i.e. all spin up or all spin down. It is then easy to observe that both $|0\rangle^{\otimes N}$ and $|1\rangle^{\otimes N}$ are ground states of each interaction term $-J_i Z_i Z_{i+1}$.

The Hamiltonian H_0 given by Eq. (4.34) is also frustration-free, since both $|0\rangle^{\otimes N}$ and $|W_N\rangle$ are ground states of each term H_{ij} as given by Eq. (4.33).

The toric code Hamiltonian given by the Hamiltonian H_{toric} in Eq.(3.64) is also a frustration-free one. The ground state $|\psi_g\rangle$ given in Eq. (3.65) is the ground state of each operators $-Q_s$ and $-B_p$ for any s, p. This is straightforward to see. For Q_s, as B_p commutes with any $g \in \mathscr{S}_X$, and $Q_s|0\rangle^{\otimes 2r^2} = |0\rangle^{\otimes 2r^2}$, we have $Q_s|\psi_g\rangle = |\psi_g\rangle$. For B_p, because $|\psi_g\rangle$ sums over all $g \in \mathscr{S}_X$ where $\mathscr{S}_X$ is a group, we have $B_p|\psi_g\rangle = |\psi_g\rangle$. This agrees with our previous discuss in Chapter 3.5 that $|\psi_g\rangle$ is the stabilizer state stabilized by the stabilizer group generated by Q_s and B_p. In fact, any stabilizer state, with its stabilizer group generated by local Pauli operators, is the unique ground state corresponding to the local Hamiltonian given by the minus sum of all the local stabilizer generators.

Another famous frustration-free systems, namely, the Affleck-Kennedy-Lieb-Tasaki (AKLT) system, considers a spin-1 chain. The AKLT Hamiltonian is given by

$$H_{AKLT} = \sum_j \mathbf{S}_j \cdot \mathbf{S}_{j+1} + \frac{1}{3}(\mathbf{S}_j \cdot \mathbf{S}_{j+1})^2 = \sum_j 2P_{j,j+1}^{(J=2)} - \frac{2}{3}. \tag{4.41}$$

Here $\mathbf{S}_j$ is the spin operator of the j-th spin, and $P_{j,j+1}^{(J=2)}$ is the projection onto the total spin $J = 2$ subspace of each neighboring pair of particles.

Fig. 4.3 A Valence-bond Solid. Each blue dot denotes a spin-1/2 particle. Each solid line connecting two particles are called a 'bond', which represents a singlet state. Each oval contains two particles, which represents the projection of those two particles onto the spin triples subspace

The AKLT Hamiltonian H_{AKLT} is known to be frustration-free, by explicitly constructing the ground state. The idea is to use the picture of the valence-bond solid, which is illustrated in Fig. 4.3, where each bond denotes the singlet state

$$|\text{singlet}\rangle = \frac{1}{\sqrt{2}}(|01\rangle - |10\rangle), \tag{4.42}$$

and each oval represents the projection onto the triplet subspace, i.e.

$$\Pi_{triplet} = |+1\rangle\langle 00| + |0\rangle\frac{1}{\sqrt{2}}(\langle 01| + \langle 10|) + |-1\rangle\langle 11|, \tag{4.43}$$

where $|\pm 1\rangle$ and $|0\rangle$ are the eigenstates of spin S_z operator, corresponding to the eigenvalues $\pm 1, 0$, respectively.

This then gives us a state of a spin-1 chain, called the AKLT state denoted by $|\psi_{AKLT}\rangle$, when periodic boundary condition is considered. $|\psi_{AKLT}\rangle$ is a ground state of H_{AKLT}, because it is the ground state of each projection $P_{j,j+1}^{(J=2)}$. This is because, among the four spin-1/2s making up a pair of neighboring spin-1s, the two in the middle form a spin singlet. Therefore, the total spin of the four spin-1/2s, and correspondingly the total spin of the pair of neighboring spin-1s, can only be 0 and 1 but not 2. Therefore, the Hamiltonian H_{AKLT} is frustration-free.

$\Pi_{triplet}$ given in Eq. (4.43) in fact gives a matrix product state (MPS) representation for $|\psi_{AKLT}\rangle$, which will be discussed in more detail in Chapter 8. Also, H_{AKLT} can be viewed as the parent Hamiltonian of the MPS state $|\psi_{AKLT}\rangle$, see Chapter 8.2.10. In fact, all the MPS parent Hamiltonians discussed in Chapter 8.2.10 are frustration-free, with the corresponding MPS state as a ground state.

We would like to mention here that the AKLT state is an example of the symmetry-protected topologically ordered (SPT) phase, where the nontrivial order of the state is protected by the symmetry of the Hamiltonian H_{AKLT}. That is to say, when breaking the corresponding symmetry, there is no intrinsic long range entanglement in the AKLT state, so there exists a constant depth quantum circuit to transform $|\psi_{AKLT}\rangle$ to the product state $|0\rangle^{\otimes N}$. We will examine these symmetry and transformation in more detail in Chapter 10.

4.5.2 The frustration-free Hamiltonians problem

If we know that a local Hamiltonian $H = \sum_j H_j$ is frustration-free, then its ground state energy is $E_0 = \sum_j E_{0j}$, where E_{0j} is the ground state energy of H_j, which is easy to find given that each H_j acts nontrivially only on a few particles. However, for a given local Hamiltonian H, one first needs to determine whether it is frustration-free. In the theory of quantum computational complexity, this problem is formulated as follows.

Box 4.9 The frustration-free Hamiltonian problem
Given a local Hamiltonian $H = \sum_j H_j$, where each H_j acts non-trivially on at most k qubits whose ground state energy is 0.
For a given $b > c/\text{poly}(N)$, where $c > 0$ is a constant, denote E_0 the ground state energy of H. Determine which of the following is true.
1. H is frustration free, i.e. $E_0 = 0$.
2. $E_0 > b$.

When formulated in this form, it hints that the frustration-free Hamiltonian problem is quite similar to the local Hamiltonian problem except that E_0 is exactly zero, while in the latter E_0 is upper-bounded by some constant $a < b$. It is quite the case as given by the following result as reached in the quantum computational complexity theory.

Box 4.10 The hardness of the frustration-free Hamiltonian problem
Given a local Hamiltonian $H = \sum_j H_j$ of an N-qubit system, with each H_j acting nontrivially on at most k particles, the problem of determining whether H is frustration-free or not, is as hard as the local Hamiltonian problem for $k \geq 3$.

This observation indicates that frustration-free Hamiltonians may be already enough to characterize many kind of interesting physics. For instance, the toric code Hamiltonian gives a simple example of the so-called 'topologically ordered system', which exhibit quantum phases beyond the explanation of the Landau symmetry-breaking theory. These topologically ordered systems will be the major topic in the rest chapters of this book.

4.5.3 The 2-local frustration-free Hamiltonians

The problem can be significantly simplified when restricting to special cases. It turns out that it is easy to determine whether a 2-local qubit-Hamiltonian H is frustration-

free or not. By easy we mean that for an N-qubit systems, there is an algorithm with running time polynomial in N, which determines whether H is frustration-free or not. However, we know that for the local Hamiltonian problem, even the $k = 2$ case is hard. In other words, although to determine whether a 2-local qubit-Hamiltonian H is frustration-free or not is easy; on the other hand, if we know H is not frustration-free, then determining the ground state energy of H to some precision is still hard.

To see how to determine whether a 2-local qubit-Hamiltonian H is frustration-free or not, we give a procedure which finds a special kind of ground state for H. To do so, we start from a simple fact that if a local Hamiltonian $H = \sum_j H_j$ is frustration-free, then for $L = \bigotimes_{i=1}^N L_i$, where each L_i is a invertible operator acting on a single qubit i, the Hamiltonian

$$H' = L^\dagger H L = \sum_j L^\dagger H_j L \tag{4.44}$$

is also frustration-free, because $L^{-1}|\psi\rangle$ is a ground state of $L^\dagger H_j L$ if and only if $|\psi\rangle$ is a ground state of H_j. Note that H' does not have the same spectra as those of H, just that the frustration-free property of H remains after the transformation L.

To understand more about the effect of L, let us start from the two-particle case, i.e. $N = 2$. Due to Schmidt decomposition, any 2-qubit state can be written as, in some basis

$$|\psi_{AB}\rangle = \sum_{\alpha=0}^{1} \sqrt{\lambda_\alpha}|\alpha_A\rangle|\alpha_B\rangle. \tag{4.45}$$

There are then two nontrivial cases: 1. if one of λ_α is zero, then up to the transformation L, $|\psi_{AB}\rangle$ is essentially a product state $|00\rangle$; 2. none of λ_α is zero, then up to the transformation L $|\psi_{AB}\rangle$ is essentially a singlet state $\frac{1}{\sqrt{2}}(|01\rangle - |10\rangle)$.

Now let us move to the case of $n = 3$. After some mathematics, which we omit here, one can show that up to L, there are essentially four possibilities to write a general three-qubit state $|\psi_{ABC}\rangle$:

1. a product state, i.e. $|000\rangle$.
2. a tensor product of $|0\rangle$ and a singlet state $\frac{1}{\sqrt{2}}(|01\rangle - |10\rangle)$.
3. a GHZ state $|GHZ\rangle = \frac{1}{\sqrt{2}}(|000\rangle + |111\rangle)$.
4. a W state $|W_3\rangle = \frac{1}{\sqrt{3}}(|001\rangle + |010\rangle + |100\rangle$.

For case 3, suppose $|GHZ\rangle$ is a ground state of some 2-local frustration-free qubit Hamiltonian H_{GHZ}, then $|GHZ'\rangle = \frac{1}{\sqrt{2}}(|000\rangle - |111\rangle)$ is also the ground state of the same H_{GHZ}, because the 2-RDMs of $|GHZ\rangle$ and $|GHZ'\rangle$ are exactly the same. In other words, $|000\rangle$ must be the ground state of H_{GHZ}.

For case 4, suppose $|W\rangle$ is a ground state of some 2-local frustration-free qubit Hamiltonian H_W, then $|000\rangle$ must also be the ground state of H_W. In fact, any of the 2-RDMs of $|W\rangle$ is supported on the two-dimensional subspace spanned by $|1\rangle\sqrt{2}(|01\rangle + |10\rangle)$ and $|00\rangle$, which contains the subspace that any of the 2-RDMs of $|000\rangle$ is supported on (which is nothing but $|00\rangle$). Or in another viewpoint, a 2-local frustration-free Hamiltonian only 'sees' the information of the range of the

2-RDMs of its ground states, i.e. independent on any details of the 2-RDMs beyond just its range.

As a result, in all the four possible cases of $N = 3$, there always exists a ground state for any 2-local frustration-free qubit Hamiltonian, which is either a product state, or a tensor product of a single qubit state $|0\rangle$ and a singlet state $\frac{1}{\sqrt{2}}(|01\rangle - |10\rangle)$, up to certain transformation L. This result generalizes to the case $N > 3$ by some induction argument, whose technical details are omitted here. We summarize this result as follows.

Box 4.11 A ground state for 2-local frustration-free qubit Hamiltonian
for any 2-local frustration-free qubit Hamiltonian H, there always exits a ground state which is either a product state, or a tensor product of some single qubit states and some singlet states, up to certain transformation L.

A possible pattern of a ground state for a 2-local frustration-free qubit Hamiltonian is illustrated in Fig. 4.4. Here each dot black denotes a single qubit state, and each solid line linking two black dots denote any two-qubit entangled state. This is not translational invariant though. In practice, if translational invariance is taken into account, we will end up with tensor product of only single qubit states, or only two-qubit entangled states, but not both. Physically, that result is pretty much saying that some kind of mean-field method always works perfect, if a 2-local qubit Hamiltonian is frustration-free. The existence of such a single solutions provides an algorithm to efficiently determine whether a 2-local qubit Hamiltonian is frustration-free or not.

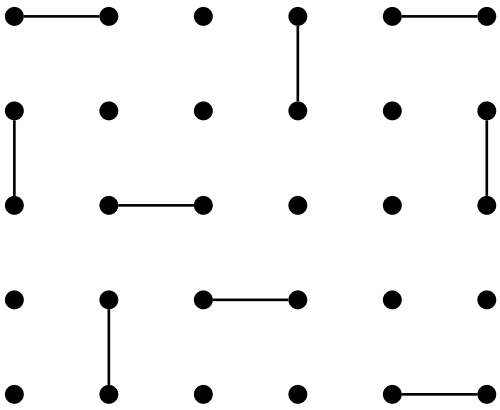

Fig. 4.4 A possible pattern of a ground state for a 2-local frustration-free qubit Hamiltonian

In fact, it is not only that one can determine whether a 2-local qubit-Hamiltonian H is frustration-free or not within a reasonable amount of computational cost, but also the structure of the entire ground space can be characterized. That is, the ground

state space of any 2-local frustration-free qubit Hamiltonian can be spanned by some (maybe nonorthogonal) basis $\{|\psi_i\rangle\}$ where each basis state is is either a product state, or a tensor product of some single qubit states and some singlet states, up to certain transformation L. Furthermore, these basis state share similar tensor product structures, for example, if $|\psi_1\rangle$ is a tensor product of a singlet state of the first and second qubit, and single-qubit states of all the remaining qubits, up to some transformation L_1, then if $|\psi_2\rangle$ is a tensor product of a singlet state of the first and second qubit, and single-qubit states of all the remaining qubits, up to some transformation L_2, etc.

Finally, it needs to be mentioned that the results on 2-local qubit-Hamiltonians are not extendable for 2-local non-qubit Hamiltonians. In other words, one no longer hopes to always find a ground state whose structure is pretty much a product state (i.e. a tensor product of single-particle states and some two-particle states). On example is that the AKLT state, which is in fact the unique ground state of H_{AKLT}, possesses a quite complicated entanglement structure. Note that the AKLT states does not hint anything about the hardness of the 2-local frustration-free Hamiltonian problem in the case of systems with single-particle dimension $m = 3$, where its ground state is easy to construct.

What is known to date in quantum computational complexity theory, for how hard a the frustration-free Hamiltonian problem is, for 2-local Hamiltonians, is the following result.

Box 4.12 The hardness of the frustration-free Hamiltonian problem for 2-local Hamiltonians

Given a 2-local Hamiltonian $H = \sum_j H_j$ of an N-particle system with single-particle dimension m, the problem of determining whether H is frustration-free or not, is as hard as the Local Hamiltonian Problem for $m \geq 5$. For $m \geq 3$, the problem is hard to solve on a classical computer.

However, the hardness with quantum computers for the cases of $m = 3, 4$ remains unknown. That is, there might exist some other 2-local Hamiltonian for spin-1 systems, such that whether it is frustration-free or not is hard to determine even with a quantum computer.

4.6 Summary and further reading

In this chapter, we introduced the concept of local Hamiltonians, and discussed related problems studied in the quantum information theory. We started with 're-emphasizing' the tensor product structure which is already discussed in Chapter 1. Traditionally many-body physics has this tensor product structure in mind, however is not emphasized. Quantum information science, however, systematically studies

this structure and naturally extends this structure as a tool to study correlation and entanglement in many-body systems.

Equipped with the tensor product structure of the Hilbert space, it is then natural to discuss locality of a Hamiltonian. Usually a local Hamiltonian is associated with some spatial geometry. It turns out that this spatial locality does play a crucial role in the study of properties for local Hamiltonians. For Hamiltonians involving only k-body interactions, the ground-state property is quite differently for those with interactions 'localized' with respect to some D-dimensional lattice. In viewing the ground state space as a quantum error-correcting code, a k-local stabilizer Hamiltonian on a D-dimensional lattice, the ground state space degeneracy R and the code distance d satisfies a constraint as given in Eq.(4.10), that is, if $\log R \propto N$, then the distance d can only be some constant independent of N. This result is obtained in [5], which is further extended to more general cases beyond stabilizer quantum code in [6]. In contrast, a general Hamiltonian involving only k-body interactions could have $d \propto \sqrt{N}$, even if $\log R \propto N$. This result is obtained in [33], and further studied in more detail with different systems in [22].

Given a k-local Hamiltonian H, the local Hamiltonian problem concerns determining the ground-state energy to certain precision. It is one of the most extended studied problems in quantum computational complexity theory, with a general assertion that the local Hamiltonian problem is hard even with the existence of a quantum computer. This observation is first proposed in [20], which shows that the local Hamiltonian problem is hard for some 5-local Hamiltonian. Following the original work [20], considerable progress has been made. It is shown that the 3-local Hamiltonian problem is hard [19], followed by [18] showing that the 2-local Hamiltonian problem is hard.

Further taking into account of spatial geometry, it is shown that the local Hamiltonian problem is hard for a Hamiltonian involving only nearest-neighbour interaction on a $2D$ square lattice [29]. A surprising fact was discovered in [2] that the local Hamiltonian problem remains hard even for a Hamiltonian associated with a $1D$ chian, involving only nearest-neighbour interactions. Review articles on quantum computational complexity includes [3] and [30].

The N-representability problem has been studied in quantum chemistry for several decades, see e.g. [9]. For the history and of the quantum marginal problem, we refer to [21]. It is shown that the quantum marginal problem is hard, even with the existence of a quantum computer [25]. The hardness of the N-representability problem is shown in [26]. The hardness of the N-representability problem is also looked at in [34].

The notion of symmetric extendibility for a bipartite quantum state was introduced in [11] as a test for entanglement, as a state without symmetric extension is evidently entangled. The condition of symmetric extension for two-qubit state as given in Eq. (4.15) is conjectured in [27] and proved in [8].

The original de Finetti's theorem is a theorem in probability theory, which is named in honour of Italian statistician Bruno de Finetti. The theorem states that an infinite exchangeable sequence of Bernoullli random variable is a mixture of independent and identically distributed Bermoulli random variables. The finite version

of de Finetti's theorem is due to [10]. The quantum version of de Finetti's theorem dates back to 1960s paper [32, 16]. The development of quantum information theorem raises great attention of the quantum de Finetti's theorem and its finite version, due to its applications in many aspects. For a recent review we direct the readers to [15] and references therein. For the validity of Hartree's mean-field theory for bosonic systems, we refer to [24] and references therein.

The ALKT Hamiltonian is originally discussed by Affleck, Kennedy, Lieb and Tasaki in 1987 [1]. The computational complexity of frustration-free Hamiltonians was first studies in [4], which showed that for qubit Hamiltonians, the frustration-free Hamiltonian problem is easy for the 2-local case, and is hard for the 4-local case.

It is further shown in [7] that for any 2-local frustration-free qubit Hamiltonian H, there always exits a ground state which is either a product state, or a tensor product of some single qubit states and some singlet states, up to certain transformation L. The ground-state space structure for any 2-local frustration-free qubit Hamiltonian is characterized in [17]. Recently it is shown that the frustration-free Hamiltonian problem is hard for the 3-local case [14].

For the 2-local case of the frustration-free Hamiltonian problem, it is shown that the $m = 5$ care is hard with the existence of a quantum computer [12]. It is known in 1979 already that the $m = 3$ case is hard with a classical computer [13]. However, whether this case (and $m = 4$) is also hard with a quantum computer remains unknown. It is worth mentioning that the 2-local Hamiltonian constructed in [2] is in fact frustration-free.

For review articles on frustration-free Hamiltonians, we refer to [28]. Frustration-free Hamiltonians also play important role in the area of the so-called 'measurement-based quantum computing'. Related review particles include [31] and [23].

References

1. Ian Affleck, Tom Kennedy, Elliott H. Lieb, and Hal Tasaki. Rigorous results on valence-bond ground states in antiferromagnets. *Physical Review Letters*, 59(7):799–802, 1987.
2. D. Aharonov, D. Gottesman, S. Irani, and J. Kempe. The Power of Quantum Systems on a Line. *Communications in Mathematical Physics*, 287:41–65, April 2009.
3. D. Aharonov and T. Naveh. Quantum NP - A Survey. *eprint arXiv:quant-ph/0210077*, October 2002.
4. S. Bravyi. Efficient algorithm for a quantum analogue of 2-SAT. *arXiv:quant-ph/0602108*, February 2006.
5. S. Bravyi and B. Terhal. A no-go theorem for a two-dimensional self-correcting quantum memory based on stabilizer codes. *New Journal of Physics*, 11(4):043029, April 2009.
6. Sergey Bravyi. Subsystem codes with spatially local generators. *Phys. Rev. A*, 83:012320, Jan 2011.
7. J. Chen, X. Chen, R. Duan, Z. Ji, and B. Zeng. No-go theorem for one-way quantum computing on naturally occurring two-level systems. *Physical Review A*, 83(5):050301, May 2011.
8. Jianxin Chen, Zhengfeng Ji, David Kribs, Norbert Lütkenhaus, and Bei Zeng. Symmetric extension of two-qubit states. *Physical Review A*, 90(3):032318, 2014.
9. A. J. Coleman. Structure of fermion density matrices. *Rev. Mod. Phys.*, 35:668–686, Jul 1963.

10. Persi Diaconis and David Freedman. Finite exchangeable sequences. *The Annals of Probability*, pages 745–764, 1980.
11. Andrew C Doherty, Pablo A Parrilo, and Federico M Spedalieri. Distinguishing separable and entangled states. *Physical Review Letters*, 88(18):187904, 2002.
12. Lior Eldar and Oded Regev. Quantum sat for a qutrit-cinquit pair is qma1-complete. In *ICALP '08 Proceedings of the 35th international colloquium on Automata, Languages and Programming, Part I*, pages 881–892, 2008.
13. Michael R. Garey and David S. Johnson. *Computers and Intractability. A Guide to the Theory of NP-Completeness.* W. H. Freeman and Company, San Francisco, CA, 1979.
14. D. Gosset and D. Nagaj. Quantum 3-SAT is QMA1-complete. *ArXiv e-prints*, February 2013.
15. Aram W Harrow. The church of the symmetric subspace. *arXiv preprint arXiv:1308.6595*, 2013.
16. RL Hudson and GR Moody. Locally normal symmetric states and an analogue of de finetti's theorem. *Probability Theory and Related Fields*, 33(4):343–351, 1976.
17. Z. Ji, Z. Wei, and B. Zeng. Complete Characterization of the Ground Space Structure of Two-Body Frustration-Free Hamiltonians for Qubits. *Physical Review A*, 84(4):042338, October 2011.
18. J. Kempe, A. Kitaev, and O. Regev. The complexity of the local hamiltonian problem. In *FSTTCS 2004: Foundations of Software Technology and Theoretical Computer Science (Lecture Notes in Computer Science vol 3328)*, pages 372–83. Chennai, India, Berlin: Springer, 2004. arXiv:quant-ph/0406180.
19. J. Kempe and O. Regev. 3-Local Hamiltonian is QMA-complete. *Quantum Inform. Comput*, 3:258–64, February 2003.
20. A. Yu. Kitaev, A.H. Shen, and M.N. Vyalyi. *Classical and Quantum Computation. Vol. 47 of Graduate Studies in Mathematics.* American Mathematical Society, Providence, RI, 2002.
21. A. A. Klyachko. Quantum marginal problem and N-representability. *Journal of Physics Conference Series*, 36:72–86, April 2006.
22. Alexey A. Kovalev and Leonid P. Pryadko. Improved quantum hypergraph-product ldpc codes. In *Proceedings of the 2012 IEEE International Symposium on Information Theory*, pages 348–352, 2012. arXiv:1202.0928.
23. L. C. Kwek, Z. Wei, and B. Zeng. Measurement-Based Quantum Computing with Valence-Bond. *International Journal of Modern Physics B*, 26:30002, 2012.
24. Mathieu Lewin, Phan Thành Nam, and Nicolas Rougerie. Derivation of hartrees theory for generic mean-field bose systems. *Advances in Mathematics*, 254:570–621, 2014.
25. Y.-K. Liu. Consistency of Local Density Matrices is QMA-complete. *eprint arXiv:quant-ph/0604166*, April 2006.
26. Yi-Kai Liu, Matthias Christandl, and F. Verstraete. Quantum computational complexity of the n-representability problem: Qma complete. *Phys. Rev. Lett.*, 98:110503, Mar 2007.
27. Geir Ove Myhr and Norbert Lütkenhaus. Spectrum conditions for symmetric extendible states. *Physical Review A*, 79(6):062307, 2009.
28. D. Nagaj. Local Hamiltonians in Quantum Computation. *ArXiv e-prints*, August 2008.
29. R. Oliveira and B. M. Terhal. The complexity of quantum spin systems on a two-dimensional square lattice. *Quantum Inform. Comput*, 8:900–24, April 2008.
30. T. J. Osborne. Hamiltonian complexity. *Reports on Progress in Physics*, 75(2):022001, February 2012.
31. R. Raussendorf and T.-C. Wei. Quantum computation by local measurement. *Annual Review of Condensed Matter Physics*, 26:239–261, July 2012.
32. Erling Størmer. Symmetric states of infinite tensor products of c-algebras. *Journal of Functional Analysis*, 3(1):48–68, 1969.
33. Jean-Pierre Tillich and Gilles Zémor. Quantum ldpc codes with positive rate and minimum distance proportional to $n^{1/2}$. In *Proceedings of the 2009 IEEE International Symposium on Information Theory*, pages 799–803, 2009. arXiv:0903.0566.
34. Tzu-Chieh Wei, Michele Mosca, and Ashwin Nayak. Interacting boson problems can be qma hard. *Phys. Rev. Lett.*, 104:040501, Jan 2010.

Chapter 5
Gapped Quantum Systems and Entanglement Area Law

Abstract We discuss quantum systems of large system size N, in particular the $N \to \infty$ limit (thermodynamic limit). We call them the quantum many-body systems. We ask about the physical properties of these quantum many-body systems in the thermodynamic limit. Our main focus in this chapter will be many-body systems with an energy gap and the entanglement properties of their ground states. We introduce the entanglement area law and its constant correction – the topological entanglement entropy. We discuss the information-theoretic meaning of topological entanglement entropy, and generalize it to construct a 'universal entanglement detector', whose values on the gapped ground states provide non-trivial information of the system.

5.1 Introduction

The solid or liquid materials we encounter everyday are macroscopic systems comprised of a large number of quantum particles, like bosons, fermions or spins. The number of particles in the systems are so large that amazing macroscopic quantum phenomena emerge, like superfluidity, superconductivity and topological order, which are not possible with a small number of quantum particles. These are the systems of interest in the study of quantum condensed matter physics.

From our experience in the last chapter, it seems impossible to theoretically study quantum systems of this size, as solving quantum systems of a few tens of particles are already extremely hard. However, the quantum materials we are interested in comprise a special set of all quantum system where the notion of dimensionality, locality, and thermodynamic limit play an important role and allow generic features of such quantum systems to be attainable. We will start to look at these concepts in section 5.2 and discuss how they determine important properties like the correlation, gap and entanglement in the system.

We will then focus on studying gapped systems, in particular the entanglement properties of their ground states. We will demonstrate with examples that different

gapped systems may exhibit different features in their ground-state entanglement pattern, such that they belong to different 'order'. Although the readers may be familiar with the term 'symmetry breaking order', the terms of 'topological order' and even 'symmetry-protected topological (SPT) order' may not sound familiar. We will formally define the concept of 'quantum phase' in Chap 7 and discuss a general theory based on local transformations. Here in this chapter, we will just use those terms together with the corresponding examples, hoping to give the readers some feelings about their meaning through looking at concrete examples.

In section 5.3, we discuss a general structure of ground-state entanglement for gapped systems, namely the entanglement area law, which states that the entropy of the reduced density matrix of some connected area of the system is proportional to the boundary length of the area. If the system is 'topologically ordered', then there will be also a subleading constant term of the entropy apart from the area law, which is the so called 'topological entanglement entropy', denoted by S_{topo}. The existence of such an topological entanglement entropy for some gapped ground states then indicates that the system is topologically ordered. In other words, a non-zero S_{topo} detects topological order.

In section 5.4, we develop an information-theoretic viewpoint for the topological entanglement entropy S_{topo}. We show that S_{topo} essentially captures the 'irreducible tripartite correlation' $C_{tri}(\rho_{ABC})$ (as discussed in Chapter 1.4.2) for gapped systems for the areas A,B,C. The relevant general quantity in quantum information theory is the conditional mutual information $I(A{:}C|B)$, which is the quantum mutual information of the parts A and C, conditioned on the existence of the part B. When choosing large enough areas A,B,C of the system, and A,C are far from each other, a non-zero $I(A{:}C|B)$ hence indicates a non-trivial kind of many-body entanglement. This then generalizes the topological entanglement entropy, which can be also used to detect other orders (e.g. symmetry breaking orders, SPT orders) of the system (even without knowing the symmetry of the system).

In section 5.5, we discuss the property of the degenerate ground-state space of a gapped system from the viewpoint of quantum error-correcting codes (QECC), which has been discussed in Chapter 3. We know that toric code is a QECC with a macroscopic distance. We show that, for systems with symmetry constraints and 'symmetry breaking orders' and even 'SPT orders', if we only consider the errors that respect the symmetry of the system, then the corresponding degenerate ground-state spaces are also QECCs with macroscopic distances.

We briefly discuss gapless systems in Sec. 5.6, where the area law is violated. We show that the conditional mutual information $I(A{:}C|B)$ depends on the shapes of the areas A,B,C, which can also provide information for critical systems (e.g. central charge), if one calculates $I(A{:}C|B)$ for different area shapes. In this sense, $I(A{:}C|B)$ is a 'universal entanglement detector' for both gapped and gapless systems, which contains non-trivial information of the orders of the systems.

5.2 Quantum many-body systems

In this section, we discuss the concepts of dimensionality, locality, and thermodynamic limit and how they determine important properties like the correlation, gap and entanglement in the system.

5.2.1 Dimensionality and locality

Condensed matter systems usually live in a space of fixed dimension. For example, a sodium crystal is composed of ions forming a three dimensional lattice, a graphene sheet is made of carbon atoms in a two-dimensional (2D) lattice and nanowires are effectively one-dimensional (1D). The electrons in these systems are confined to move within their dimensions.

Systems in the same dimension can have different geometry or topology. For example, in one dimension, the system can be in an open chain with two end points or a closed ring with no boundary; in two dimension, the system can be in a disc with a one dimensional boundary or in a sphere or torus with no boundary but different topology; similarly in three dimension system can be on a cube with a two dimensional boundary or we can imagine hyperthetically putting the system in a closed three dimensional manifold by closing the boundary. Closed three dimensional manifold can also have different topology.

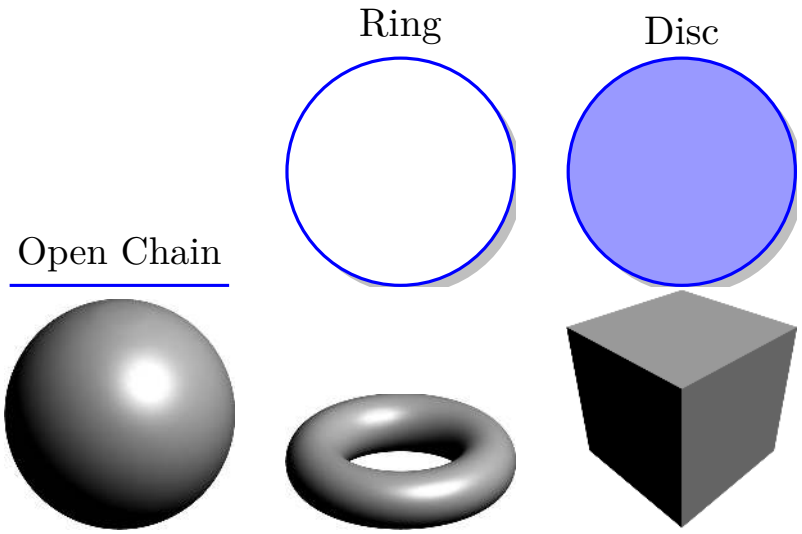

Fig. 5.1 Manifolds with geometry or topologies in one, two and three dimensions.

The dimensionality not only confines the motion of the quantum particles within the system, it also puts restrictions on how particles interact with each other. In condensed matter systems, particles can only interact with one another if they are within certain distance. The strength of interaction decays to zero if the particles are sufficiently far apart. Therefore, the notion of locality is more strict than in the quantum systems we considered in the last chapter. Besides the request that only a few (for example 2 or 3) quantum particles can be involved in an interaction, the particles also have to be close enough. Exactly how close the particles have to be to interact depends on the physical details of the system. In general, we consider systems with a finite interaction range. That is the interaction strength decay to zero beyond a fixed length scale while the total system size N can be taken to be infinity. Therefore, in the following discussion, by local interaction, we refer to interactions involving not only a finite number of particles but also within a finite range. The total Hamiltonian H of the system is a sum of such local interaction terms

$$H = \sum_j H_j. \tag{5.1}$$

5.2.2 Thermodynamic limit and universality

For quantum systems of the size of 10^{23} (or even much smaller), it is impossible to know all the details of the system. However, in most cases, we are not interested in most details. What we care most about are some global generic features like whether the material is conducting, whether it is a superfluid, etc. Such properties are observed on the macroscopic scale of the system and does not depend on a lot of details at the microscopic scale. Therefore, in the study of quantum condensed matter systems we are generally interested only in what happens when the system size N goes to infinity, the so-called thermodynamic limit, and how the system respond to external probes on a macroscopic length and time scale. In particular, we will be investigating the physical properties such as their gap Δ, correlation ξ, and entanglement S, which determine the electronic, magnetic, or optical properties of the system. In the thermodynamic limit, generic features appear for these quantities in a quantum many-body systems. Such generic features are said to be 'universal' for the quantum many-body systems, which do not depend on much of the details of the system.

5.2.3 Gap

In the limit of the system size $N \to \infty$, one important property of the Hamiltonian H is the gap Δ. Denote H_N the system Hamiltonian with system size N. The system is called gapped if one of the following case is true.

(1) As $N \to \infty$, the ground state degeneracy m_N of H_N is upper bounded by a finite integer m, and the gap Δ_N between the ground states and the first excited states of H_N is lower bounded by a finite positive number Δ.
(2) As $N \to \infty$, there are a finite number m of lowest energy states which have energy separations ε among themselves, which is exponentially small in N, and the energy separation of these lowest energy states to all the other states is lower bounded by a finite number Δ for arbitrary N.

The energy levels in these two cases are illustrated in Fig.5.2 (notice that case (1) is in fact case (2) with $\varepsilon = 0$). In both cases (1) and (2), m is said to be the ground state degeneracy of the system in thermodynamic limit, even though in case (2), the ground states are not exactly degenerate for any finite system size N. A more formal definition of gap will be discussed in Chapter 7.

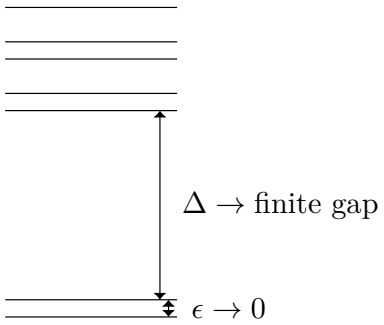

Fig. 5.2 The energy spectrum of a gapped system: ε vanishes as system size increases, while Δ approaches a finite non-zero value (which is called the energy gap).

The transverse Ising model on a 1D chain, with Ising coupling between nearest neighbor pairs, is described by the Hamiltonian

$$H^{\text{tIsing}} = -J\sum_j Z_j Z_{j+1} - B\sum_j X_j \tag{5.2}$$

is gapped as long as $J \neq B$. When $|J| > |B|$, the ground state degeneracy is $m = 2$ (see Fig. 5.3(a,b); when $|J| < |B|$, the ground state is nondegenerate with $m = 1$. In particular, when $B = 0$, the ground space is spanned by

$$|0\rangle^{\otimes N} = |00...0\rangle,\ |1\rangle^{\otimes N} = |11...1\rangle \tag{5.3}$$

and when $J = 0$, the ground state is

$$|+\rangle^{\otimes N} = \left(\frac{1}{\sqrt{2}}|0\rangle + \frac{1}{\sqrt{2}}|1\rangle\right)^{\otimes N} \tag{5.4}$$

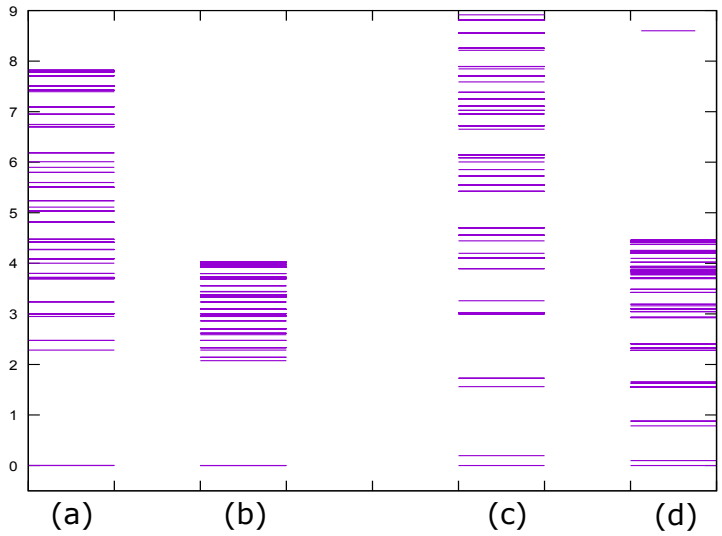

Fig. 5.3 Change in energy level spacings with system size in gapped (a and b) and gapless (c and d) systems. (a) The first 100 energy levels of transverse Ising model with $J = 1, B = 0.5$ on a ring of 8 sites. (b) The first 100 energy levels with $J = 1, B = 0.5$ on a ring of 16 sites. (c) The first 100 energy levels with $J = 1, B = 1$ on a ring of 8 sites. (d) The first 100 energy levels with $J = 1, B = 1$ on a ring of 16 sites. In (a) and (b) the ground states are nearly two-fold degenerate (within the thickness of the line).

Sometimes we say a state is a gapped quantum state without explicitly identifying the interactions in the Hamiltonian of the system. In such cases we are implying that a Hamiltonian with local interactions can be constructed which has the state as a gapped ground state.

If we cannot find a finite set of exponentially close lowest energy states which are finitely separated from all excited states, then the system is called gapless. The most generic energy spectrum of a gapless system has a continuum of energy levels above the ground states with energy spacing between them being polynomially small in system size N. Simple examples of gapless system include the Ising model at critical point, i.e. when $|J| = |B|$ (see Fig. 5.3(c,d)). Also, the spin-$1/2$ Heisenberg model

$$H_{\text{Heisenberg}} = -J \sum_j \mathbf{S}_j \cdot \mathbf{S}_{j+1} \tag{5.5}$$

on a one dimensional chain with nearest neighbor coupling is gapless, where $\mathbf{S}_j = (X_j, Y_j, Z_j)$ is the spin operator acting on the jth spin.

5.2.4 Correlation

Correlation in a quantum many body system is usually measured between local operators. Suppose that O_1 and O_2 are operators acting on finite regions R_1 and R_2 separated by a distance r, then the (connected) correlation function between O_1 and O_2 is defined as

$$C^{O_1,O_2}(r) = \langle O_1 O_2 \rangle - \langle O_1 \rangle \langle O_2 \rangle \tag{5.6}$$

where $\langle \cdot \rangle$ denotes taking average in the ground state (at zero temperature) or the thermal state (at finite temperature) of the system.

The behavior of the correlation function as r goes to infinity is an important indicator of the physical properties of the system.

If a gapped system at zero temperature has a unique ground state, then all correlation functions of the ground state decay exponentially with r.

$$C(r) \sim e^{-r/\xi} \tag{5.7}$$

where ξ is called the correlation length of the system. Therefore, a gapped quantum system with non-degenerate ground state has a finite correlation length at zero temperature. For example, in the Ising model with $|J| < |B|$, the unique ground state has a finite correlation length. In particular at the point of $J = 0$, the ground state is a total product state of all spins pointing in the x direction and has correlation length $\xi = 0$. States with finite correlation length ξ (i.e. a constant $\xi > 0$ that is independent of the system size N) for all local operators are called short range correlated states.

On the other hand, if the system is gapless, for example a system with a fermi surface, the correlation function in the ground state decays polynomially with r

$$C(r) \sim \frac{1}{r^\alpha} \tag{5.8}$$

with $\alpha > 0$. As inverse polynomial functions decay slower than any inverse exponential functions, such systems are said to have infinite correlation lengths ξ. For example the correlation functions all decay polynomially in the ground state of the Heisenberg model. Correlation functions for different operators decay with different coefficient α.

In the case where the system is gapped but has ground state degeneracy, the behavior of correlation functions depends on the origin of the ground state degeneracy. Let us consider the examples in two different cases: the Ising model and the toric code model. In the Ising model with $|J| > |B|$, the ground state is two fold degenerate. There is a set of basis states, for example the $|0\rangle^{\otimes N}$ and the $|1\rangle^{\otimes N}$ state at $B = 0$, which individually have finite correlation length for all operators O. However, if we measure correlation length in the full ground space of operators Z, we find that

$$C^{Z,Z}(r) = \langle Z_i Z_{i+r} \rangle_2 - \langle Z_i \rangle_2 \langle Z_i \rangle_2 \overset{r\to\infty}{\to} \text{constant} \tag{5.9}$$

where $\langle\cdot\rangle_2$ denotes taking average in the two dimensional ground space. In particular, when $B=0$, $C^{Z,Z}(r) \overset{r\to\infty}{\to} 1$.

Such constant correlation functions are closely related to the face that the Hamiltonian of the system is invariant under the symmetry of spin flipping $|0\rangle \leftrightarrow |1\rangle$ while the two short range correlated ground states are not. In fact, the two short range correlated ground states are mapped into each other under this symmetry transformation. This phenomena is called symmetry breaking and is going to be explained further in detail in Chapter 7. Here we just want to mention that constant correlation functions for operators (operator Z in this example) which break the symmetry of the system (spin flip in this example) is the most important indicator of symmetry breaking.

However, in the case of the toric code model as discussed in Chapter 3.5, the situation is very different. The ground space of the toric code Hamiltonian

$$H_{\text{toric}} = -\sum_s \prod_{j\in \text{star}(s)} Z_j - \sum_p \prod_{j\in \text{plaquette}(p)} X_j. \tag{5.10}$$

as given in Eq.(3.64) is four-fold degenerate. The correlation length of any state in this four dimensional space is 0. This is very different from the Ising model and is closely related to the fact that the ground state degeneracy in the toric code model has a topological original. The notion of topological order is going to be discussed in more detail in Chapter 7.

5.2.5 Entanglement

As we have seen from Chapter 1, the entanglement property of systems with 3 or 4 quantum degrees of freedom has already become extremely complicated. For condensed matter systems with 10^{23} degrees of freedom, it is impossible and in most cases not necessary to understand the entanglement structure of the many-body system exactly. The philosophy in studying many-body entanglement in condensed matter systems is to again focus on the scaling behavior of certain entanglement quantities of the system in the thermodynamic limit.

Entanglement quantities which has been extensively used in such studies include: (1) entanglement entropy (mutual information or other entanglement measures) with respect to a bipartition of the system in the limit of the size of both regions going to infinity (2) entanglement entropy (geometric entanglement, negativity or other entanglement measures) of two local regions in the system as the distance of the two regions going to infinity.

In the following discussion, we are going to focus on entanglement quantities of the first type, which has been shown to be able to reveal much of the universal properties of the system. In particular, in a large class of physically interesting systems, the bipartite entanglement is found to be proportional to the area of the boundary between the two parts of the system, satisfying the so-called area law. On top of

that, we discuss the sub-leading correction term to this area law behavior – the topological entanglement entropy S_{topo}. Unlike the two types of entanglement entropy mentioned above, S_{topo} is essentially the quantum conditional mutual information $I(A{:}C|B)$ for three large regions of the system. We will further explore the meaning of $I(A{:}C|B)$, based on which we design entanglement detectors to detect different orders in the system.

Just like correlation functions, the behavior of many-body entanglement quantities in the thermodynamic limit are closely related to the physical properties of the system. For example, they behave differently in systems with or without a gap. Moreover, many-body entanglement quantities measures the 'quantum correlation' in the system that is not detected by the classical correlation function and play an important role in the study of topological orders, which will be the main focus of later chapters.

Let us summarize some basic properties of many-body entanglement in different types of systems. The fact that degrees of freedom can interact only locally with each other in condensed matter systems puts a strong constraint on the amount and form of entanglement that can be present in many-body systems.

5.3 Entanglement area law in gapped systems

5.3.1 Entanglement area law

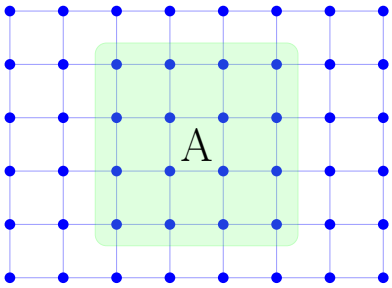

Fig. 5.4 2D square lattice with subregion A

Consider, for example, a system on a two dimensional square lattice as shown in Fig. 5.4 with local interactions. If the system is gapped (i.e. $\Delta > 0$), then the many-body entanglement in the ground state satisfies a surprising property called the 'entanglement area law'. More specifically, suppose we take a subregion A (as shown in Fig. 5.4) of size L^2 from the whole system and calculate the entanglement entropy $S = Tr(\rho_A \ln \rho_A)$ for this region. This calculation is done in the limit of total system size going to infinity. The number of degrees of freedom in this region is

proportional to L^2, so the maximum entanglement entropy we can get (and actually will get for a generic many-body entangled state) scales as L^2. However, the calculation for a gapped ground state always gives an entanglement entropy S which is proportional to the length of the boundary of the region, which grows as L.

Box 5.1 Entanglement area law for gapped systems

For a gapped system in 2D, we have

$$S_A \sim \alpha L \tag{5.11}$$

Therefore, a gapped ground state in a locally interacting system always contains much less entanglement than a generic quantum many-body entangled state.

The term 'area law' is better suited to describe three dimensional system where the entanglement entropy of a subregion in a gapped ground state scales as the surface area of the region rather than the volume of the region. The basic idea applies to systems in any dimension though, which says that the entanglement entropy of a subregion scales as the size of the boundary rather than the size the bulk of the system. In particular, in one dimension, the boundary of a subregion – a segment of the chain – contains only two points. Therefore, entanglement entropy of a segment is bounded by a constant $S_A \leq$ constant in a one dimensional gapped system. In two dimension, the entanglement entropy scales as the linear size of the subregion $S_A \sim \alpha L$ while in three dimension, the entanglement entropy scales as the linear size squared $S_A \sim \alpha L^2$.

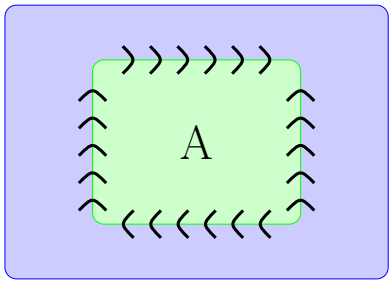

Fig. 5.5 In a local gapped quantum system, entanglement between a subregion A and the rest of the system is due to local entanglement along the boundary and hence scales as the size of the boundary.

The existence of such an 'area law' in many-body entanglement depends crucially on the locality of the interactions and the existence of a gap in the system. An intuitive way to understand why the 'area law' holds for gapped quantum systems is to realize that quantum correlation is generated by interactions. If the local degrees of freedom in different regions of the system do not interact at all, the ground state

would be a total product state and hence no entanglement exists. If the local degrees of freedom interact locally in the system, then between the subregion A and the rest of the system, only degrees of freedom close to the boundary can be interacting with each other. Moreover, in a gapped system, correlations exist in the system only under a finite length scale. Intuitively, this means that degrees of freedom in the system can only 'feel' those within a finite region around it. Therefore, the entanglement between a subregion A and the rest of the system is only due to the entanglement between degrees of freedom along the boundary. Pictorially, we can imagine the subregion A and the rest of the system being 'sewed' together by entangled pairs along the boundary as shown in Fig.5.5. The number of degrees of freedom along the boundary scales as the size of the boundary, hence the entanglement satisfies the 'area law'. Of course, if the locality condition is removed, the area law no longer holds. If the system is not gapped, the 'area law' will also be violated, but only mildly, as we discuss in the next section.

While the scaling of entanglement entropy with boundary size is a universal feature for gapped systems, the coefficient of the area law scaling α is not universal and depends strongly on the details of the interactions in the system. In one dimension, the constant bound on the entanglement entropy of a segment is also not universal. For example, in the one dimensional Ising model, when $J = 0$, the ground state is a total product state and $S_A = 0$ for any subregion. When $|J| \ll |s|$, the ground state is still unique and gapped. However, a segment in the chain would in general be entangled with with rest of the system and S_A attains a larger value as $|J|$ increases.

The existence of such an 'area law' also makes it possible to have an efficient description of many-body entangled states in gapped quantum systems, as discussed in Chapter 9 in terms of tensor product states.

5.3.2 Topological entanglement entropy

Other than revealing the gapped/gapless nature of the system, entanglement entropy can provide more detailed information about the order in the quantum state if we look at it more carefully. In particular for a gapped quantum system, if the system has nontrivial topological order, then the entanglement entropy of a region contains a sub-leading constant term apart from the leading area law term.

Box 5.2 Entanglement area law for topologically ordered systems

For a topologically ordered system in 2D

$$S_A \sim \alpha L - \gamma \tag{5.12}$$

with $\gamma > 0$.

Such a term indicates the existence of certain long-range entanglement structure that originates from the topological nature of the system (see Chapter 7 for a detailed discussion on long/short-range entanglement). γ is called the topological entanglement entropy of the system.

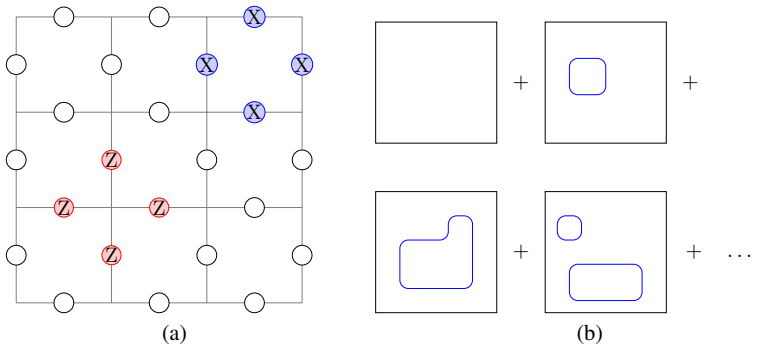

Fig. 5.6 Hamiltonian (a) and ground state wave function (b) of the toric code model.

While we have not defined what a topological order is, we are going to illustrate the topological entanglement entropy with the simple example of the toric code model. The value of γ can be easily derived from a simple understanding of the ground state wave function of the system. The Hamiltonian of the toric code reads,

$$H_{\text{toric}} = -\sum_{s} \prod_{j \in \text{star}(s)} Z_j - \sum_{p} \prod_{j \in \text{plaquette}(p)} X_j \tag{5.13}$$

where Z_j and X_j are Pauli operators acting on the qubits living on the links of, for example, a square lattice as shown in Fig.5.6. If we interpret the $|0\rangle$ state as a link with no string and the $|1\rangle$ as a link with a string, then the first term in the Hamiltonian $\prod_{j \in \text{star}(s)} Z_j$ requires that there is always an even number of strings going through a vertex. In othe words, the strings always form closed loops. The second term $\prod_{j \in \text{plaquette}(p)} X_j$ creates, annhilates, or moves closed loops around each plaquette. Therefore, the ground state wave function is an equal weight superposition of all closed loop configurations $\mathscr{C}$,

$$|\psi_{\text{toric}}\rangle = \sum_{\mathscr{C}} |\mathscr{C}\rangle \tag{5.14}$$

$\mathscr{C}$ includes the vacuum configuration, small loop configurations, large loop configurations and multiple loop configurations, as shown in Fig.5.6 (b).

From such a string-net picture of the ground state wave function, we can easily calculate the entanglement entropy of a subregion in the system. To make the boundary more symmetric, we split the sites on the boundary links into two sites (see Fig.5.7). The wave function $|\psi_{\text{toric}}\rangle$ generalizes to the new lattice in the natural

way (by identifying the $|0\rangle$ and $|1\rangle$ state on sites on the same link). The new wave function (still denoted by $|\psi_{\text{toric}}\rangle$) has the same entanglement entropy.

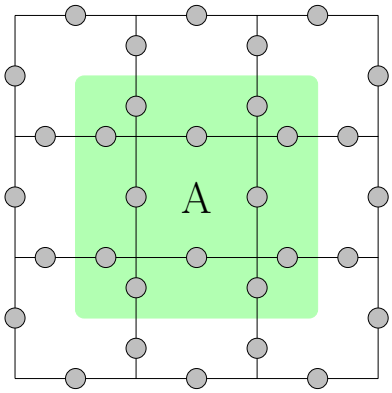

Fig. 5.7 When taking out a subregion A from the lattice to calculate the entanglement entropy, we split the sites on the boundary links into two. The total wave function $|\psi_{\text{toric}}\rangle$ generalizes to the new lattice in the natural way.

When the total system is divided into regions in A and out of A (denoted by $\bar{A}$), we can effectively view the system as a bipartite system with two parts A and $\bar{A}$. According to the Schmidt decomposition as discussed in Chapter 1.3.3, with respect to the bipartition A and $\bar{A}$, we can decompose the ground state wave function as $|\psi_{\text{toric}}\rangle = \sum_q |\psi_q^{\text{in}}\rangle|\psi_q^{\text{out}}\rangle$, where $|\psi_q^{\text{in}}\rangle$ are wave functions of spins inside A and $|\psi_q^{\text{out}}\rangle$ are wave functions of spins outside A (i.e. in $\bar{A}$). They are connected by spins on the boundary $q_1, \ldots q_L$. A simple decomposition can be obtained using the string picture. For any $q_1, \ldots, q_L$, with $q_m = 0, 1$, and $\sum_m q_m$ even, we can define a wave function $\psi^{\text{in}}_{q_1,\ldots,q_L}$ on the spins inside of A: Let X denote a particular spin configuration inside A, $\psi^{\text{in}}_{q_1,\ldots,q_L}(X) = 1$ if (a) the strings in X form closed loops and (b) X satisfies the boundary condition that there is a string on i_m if $q_m = 1$, and no string if $q_m = 0$. Similarly, we can define a set of wave functions $\psi^{\text{out}}_{r_1,\ldots,r_L}$ on the spins outside of A.

If we glue ψ^{in} and ψ^{out} together - setting $q_m = r_m$ for all m - the result is ψ. Formally, this means that

$$|\psi_{\text{toric}}\rangle = \sum_{q_1+\ldots+q_L \text{even}} |\psi^{\text{in}}_{q_1,\ldots q_L}\rangle|\psi^{\text{out}}_{q_1,\ldots q_L}\rangle \tag{5.15}$$

It is not hard to see that the functions $\{|\psi^{\text{in}}_{q_1,\ldots q_L}\rangle : \sum_m q_m \text{even}\}$, and $\{|\psi^{\text{out}}_{r_1,\ldots r_L}\rangle : \sum_m r_m \text{even}\}$ are orthonormal up to an irrelevant normalization factor. Therefore, the density matrix for the region A is an equal weight mixture of all the $\{|\psi^{\text{in}}_{q_1,\ldots q_L}\rangle : \sum_m q_m \text{even}\}$. There are 2^{L-1} such states. The entropy is therefore

$$S_{A,\text{toric}} = (L-1)\log 2 \tag{5.16}$$

That is, the topological entanglement entropy for toric code model $\gamma = \log 2$.

The value of γ is closely related to the kind of topological order in the system and is the same for quantum systems having the same topological order, independent of all other details of the system. Therefore, it provides a universal quantum number to characterize the topological order in a system, a concept which we are going to explain in much more detail in later chapters.

In a generic quantum system with non-zero correlation length, the calculation of topological entanglement entropy may not be as straight forward as in the case for the toric code model. This is because the topological entanglement entropy γ is only a subleading term in the entanglement entropy of a subregion S_A. It can be hard to separate this term from the leading 'area law' term and various other non-universal contributions to S_A from finite size effects in actual calculations. To properly extract this universal value, the following two schemes can be used for calculation.

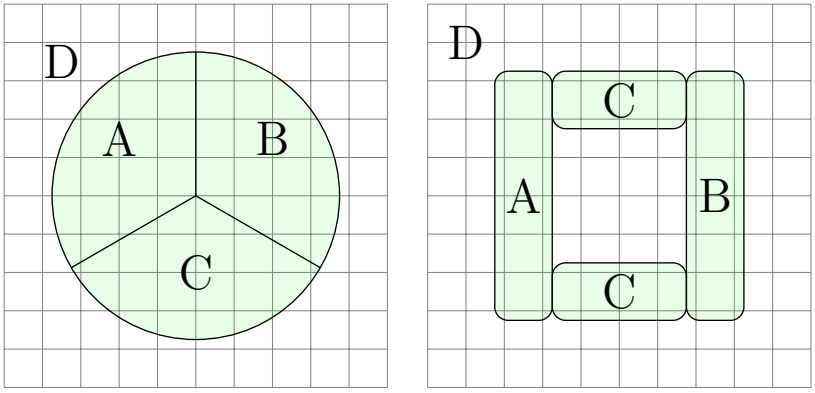

Fig. 5.8 Schemes for calculating topological entanglement entropy from a wave function.

In the first scheme, the subregion $\bar{D}$ is divided into three parts A, B and C, as shown in Fig. 5.8(a). The topological entanglement entropy γ can be calculated in the limit of both total system size and the size of A, B, C going to infinity as

$$\gamma = S_{AB} + S_{BC} + S_{AC} - S_A - S_B - S_C - S_{ABC} \tag{5.17}$$

In the second scheme, a ring shape region $\bar{D}$ is taken which is divided into three parts A, B, and C, as shown in Fig. 5.8(b). The topological entanglement entropy γ can be calculated in the limit of both total system size and the size of A, B, C going to infinity as

$$2\gamma = S_{AB} + S_{BC} - S_B - S_{ABC} \tag{5.18}$$

It can be checked that with this linear combination of entanglement entropy of different regions, the contributions from the 'area law' part and other non-universal

part which depends on the details of the shape of the regions are all cancelled out. Only the universal γ value is retained in the thermodynamic limit. The factor of 2 in Eq. (5.18) compared to Eq. (5.17) is due to the fact that the region $\bar{D}$ in Fig.5.8 (b) in fact has two boundaries (one inner boundary and one outer boundary).

In the following, we will mainly focus on the meaning and generalizations of the quantity given in the r.h.s. of Eq. (5.18), and denote it by S_{topo}. And without confusion, we will just call S_{topo} the 'topological entanglement entropy'.

Box 5.3 Topological entanglement entropy

The topological entanglement entropy S_{topo} is given by

$$S_{\text{topo}} = S_{AB} + S_{BC} - S_B - S_{ABC}, \tag{5.19}$$

where A, B, C are parts of the ring shape region $\bar{D}$, as shown in Fig. 5.8(b).

5.4 Generalizations of topological entanglement entropy

We have learned that the topological entanglement entropy γ is a universal quantity for many-body ground states of gapped systems. If the system is topologically ordered, then it ground state has a nonzero γ. The other direction is also true, that is, if a ground state of a gapped system has a nonzero γ, the system is topologically ordered. Here we further examine the meaning of γ, which essentially characterizes 'irreducible many-body correlation' (a concept introduced in Chapter 1.4.2) in the system. We start to look at γ from an information-theoretic viewpoint, which will lead to generalizations of the concept of γ to also study gapped systems without topological order. To do so, instead of only considering a quantum system with topological order, we will consider general many-body quantum systems, with local Hamiltonians.

5.4.1 Quantum conditional mutual information

Notice that Eq. (5.17) looks familiar - it is in fact the 'trial' version of tripartite entanglement as given in Eq.(1.77). This suggests an information-theoretic meaning of Eq. (5.17), which captures the 'true' tripartite correlation between the parts ABC that is not contained in bipartite systems AB, BC and AC.

As discussed in Chapter 1.4.2, the trouble of using the r.h.s. of Eq. (5.17) as a measure of the 'true' tripartite correlation is that it could be negative. For instance, if the wave function is the N-qubit GHZ state $\frac{1}{\sqrt{2}}(|0\rangle^{\otimes N} + |1\rangle^{\otimes N})$ (a direct generalization of the 3-qubit GHZ state as discussed in Chapter 1.4.2), then r.h.s. of Eq. (5.17)

is -1. However, for topologically ordered systems, γ is always positive. Therefore, the r.h.s. of Eq. (5.17) is a good measure of the 'true' tripartite correlation in topologically ordered systems.

For Eq. (5.18), if the mutual information between the parts A and C vanishes, i.e.

$$I(A{:}C) = S_A + S_C - S_{AC} = 0, \tag{5.20}$$

then the r.h.s. of Eq. (5.18) is identical to the r.h.s. Eq. (5.17). Notice that however, the area ABC has different geometry in Fig.5.8 (a) and Fig.5.8 (b).

For the geometry of Fig.5.8 (b), the areas A and C are geometrically 'far from' each other. Therefore, there will be not much correlation between them when the total system size and the size of A, B, C go to infinity. Consequently, similarly to Eq. (5.17), Eq. (5.18) also gives a good measure of the 'true' tripartite correlation of the parts A,B,C for topologically ordered system.

Different from Eq. (5.17), the r.h.s. of Eq. (5.18) is always non-negative, for any tripartite quantum state ρ_{ABC}. It in fact measures the correlation of the parts A,C conditioned on the existence of the part B. This quantity is in fact the conditional mutual information of the parts A,C and denoted by $I(A{:}C|B)$.

Box 5.4 Quantum conditional mutual information

For any tripartite state ρ_{ABC}, the quantum conditional mutual information $I(A{:}C|B)$ (i.e. the quantum mutual information between the parts A,C, conditioned on the existence of the part B), is given by

$$I(A{:}C|B) = S_{AB} + S_{BC} - S_B - S_{ABC}. \tag{5.21}$$

It is known that $I(A{:}C|B)$ is always non-negative, given by the strong subaddtivity in quantum information theory.

Box 5.5 Strong subadditivity

The inequality $I(A{:}C|B) \geq 0$ is valid for any tripartite state ρ_{ABC}.

Recall that as discussed in Chapter 1, in the most general case, the 'true' tripartite correlation of ρ_{ABC} is measured by

$$C_{tri}(\rho_{ABC}) = S(\rho^*_{ABC}) - S(\rho_{ABC}), \tag{5.22}$$

where ρ^*_{ABC} is the maximum entropy state among all the tripartite states σ_{ABC} that satisfy the reduced density matrix constraint $\sigma_{AB} = \rho_{AB}$, $\sigma_{BC} = \rho_{BC}$, $\sigma_{AC} = \rho_{AC}$.

If we consider the case when the parts A and C are geometrically 'far from' each other, hence there is not much correlation between them, then ρ_{AB} and ρ_{AC} may be enough to determine ρ^*_{ABC} without the information of ρ_{AC}, and in fact it is generically the case. In this case, we can redefine

$$\rho^*_{ABC} = \text{argmax}(S(\sigma_{ABC})|\sigma_{AB} = \rho_{AB}, \sigma_{BC} = \rho_{BC}). \tag{5.23}$$

Now we apply the strong subadditivity inequality to

$$S(\rho_{AB}) + S(\rho_{AC}) - S(\rho_B) - S(\rho^*_{ABC}) \geq 0 \tag{5.24}$$

This reduces to

$$S(\rho^*_{ABC}) - S(\rho_{ABC}) \leq S(\rho_{AB}) + S(\rho_{AC}) - S(\rho_B) - S(\rho_{ABC}). \tag{5.25}$$

Box 5.6 Inequality for quantum conditional mutual information

The following inequality holds

$$C_{tri}(\rho_{ABC}) \leq I(A{:}C|B), \tag{5.26}$$

where the equality holds when ρ^*_{ABC} is a quantum Markov state, i.e.

$$\rho^*_{ABC} = (I_A \otimes \mathcal{N}_{B\to BC})\rho_{AB}. \tag{5.27}$$

Here $\mathcal{N}_{B\to BC}$ is a quantum operation acting on the part B only. Eq. (5.27) means that the state of part BC comes from a quantum operation acting on part B which does not depend on part A. In this sense the parts A, C are only correlated conditionally on the existence of part B. More explicitly, ρ_{ABC} has the form

$$\rho_{ABC} = (I_A \otimes \rho_{BC}^{1/2})[(I_A \otimes \rho_B^{-1/2})\rho_{AB}(I_A \otimes \rho_B^{-1/2}) \otimes I_C](I_A \otimes \rho_{BC}^{1/2}). \tag{5.28}$$

When we consider a many-body system where each of the parts ABC has the size going to infinity, the correlation between two far-apart parts AC should be independent of some local factors such as the shape of the parts ABC. In this sense, the correlation between AC (conditioned on the existence of B) is a universal quantity that does not depend much on the details of the system. It is believed that this is indeed the case for gapped systems. Or in other words, $I(A{:}C|B)$ captures the true tripartite correlation $C_{tri}(\rho_{ABC})$ for gapped systems.

We believe that the following is true for any gapped system.

Box 5.7 $C_{tri}(\rho_{ABC})$ vs. $I(A{:}C|B)$ for gapped systems

$$C_{tri}(\rho_{ABC}) = I(A{:}C|B)$$

for gapped quantum systems in thermodynamic limit, where the parts A, B, C are large, and A, C are far from each other.

We then propose to use $I(A{:}C|B)$ to detect non-trivial many-body entanglement in quantum systems. Here 'non-trivial' intuitively means some 'long-range' correlation that is contained in the parts A,C conditioned on the existence of B. We will later clarify the precise meaning of 'non-trivial' in Chapter 7 using the language of local transformations.

Box 5.8 $I(A{:}C|B)$ as a detector for non-trivial many-body entanglement
A nonzero $I(A{:}C|B)$ for certain large areas A,B,C (larger than the correlation length of the system) with A,C far from each other, is a good detector for non-trivial many-body entanglement.

For a topologically ordered system, if one chooses A,B,C as parts of the ring shape region $\bar{D}$, as shown in Fig. 5.8(b), then we know that $I(A{:}C|B)$ is nothing but the topological entanglement entropy S_{topo}, which detects non-trivial topological order when it is nonzero. In this sense, we say that $I(A{:}C|B)$ is a generalization of S_{topo}, that can be also used to study quantum systems without topological order. A related theory based on local transformations will be discussed in Chapter 7.

To see that $I(A{:}C|B)$ detects phases of different kinds in gapped systems, we will discuss some simple examples. We will start from a system with topological order, then move on to systems without topological order.

5.4.2 *Toric code in a magnetic field*

We start from a system with topological order. We consider the toric code system in an external magnetic field along the direction $\mathbf{h}$, with the Hamiltonian

$$H_{\text{toric}}(\mathbf{h}) = -H_{\text{toric}} - \sum_i (h_x X_i + h_y Y_i + h_z Z_i), \tag{5.29}$$

where H_{toric} is the toric code Hamiltonian as given in Eq. (3.64) and $\mathbf{h} = (h_x, h_y, h_z)$.

In this concrete example, to illustrate the relationship between $C_{tri}(\rho_{ABC})$ and $I(A{:}C|B)$ (in this case S_{topo}), we will calculate them for a small system on an $L_1 \times L_2$ square lattice. Calculations of S_{topo} with the tensor network method will be discussed in Chapter 9.4.4.

An example of a 3×4 square lattice is given in Fig. 5.9. Qubits sit on each link, and with periodic boundary condition there are a total of 24 qubits.

We take the qubit 1 as our part A, qubit 4 as our part C, qubits $2,3,5,6$ as our part B, and the rest of qubits as part D. For $h_y = 0$, we calculate $C_{tri}(\rho_{ABC})$ for different values of h_x, h_z. The results are shown in Fig. 5.10.

From Fig. 5.10, we clearly see that there are two different phases: the red region corresponding to the 'topological phase' (for small values of h_x, h_z), and the blue region corresponding to the 'trivial phase' (i.e. $C_{tri}(\rho_{ABC}) = 0$, for large values of

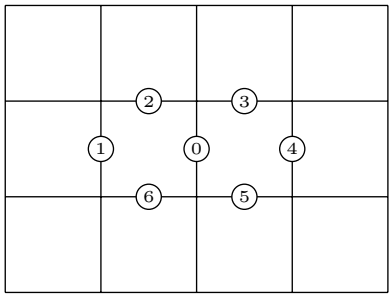

Fig. 5.9 A 3×4 square lattice. Qubits sit on each link.

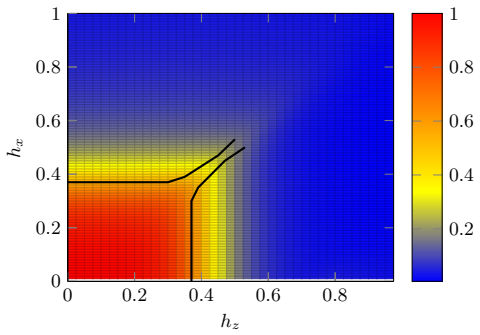

Fig. 5.10 For the 3×4 square lattice with periodic boundary condition, the calculation of $C_{tri}(\rho_{ABC})$ for different values of h_x, h_z.

h_x, h_y). In other words, a crucial feature of topological order is the non-vanishing irreducible tripatite correlation contained in the state ρ_{ABC}.

To compare with S_{topo}, we calculate both $C_{tri}(\rho_{ABC})$ and S_{topo} for different lattice size. For $h_y = h_z = 0$, the results are shown in Fig. 5.11 for $C_{tri}(\rho_{ABC})$ and in Fig. 5.12 for S_{topo}, for different values of h_x.

From Fig. 5.11 $C_{tri}(\rho_{ABC})$ and Fig. 5.12, it is clear that for any value of h_x, S_{topo} is an upper bound of $C_{tri}(\rho_{ABC})$ (i.e. $C_{tri}(\rho_{ABC}) \leq S_{\text{topo}}$). For system this small (with at most 24 qubits and the part ABC contain only 6 qubits), the result of $C_{tri}(\rho_{ABC})$ (compared to S_{topo}) does seem to give a better prediction of the behavior of the system. In Fig. 5.11, all the four line intersect at a point that corresponding to approximately $h_x = 0.34$ as the phase transition point, while the system is known to have a second order phase transition at approximately $h_x = 0.328$.

However, once the system gets large, with both the total number of particles and the number of particles in ABC going to infinity, we expect $C_{tri}(\rho_{ABC}) = S_{\text{topo}} = 2$ for $0 \leq h_x < 0.328$ (as discussed in Section 5.3.2 for $h_x = 0$) and $C_{tri}(\rho_{ABC}) = S_{\text{topo}} = 0$ for $h_x > 0.328$. The reason we get $C_{tri}(\rho_{ABC})$ or S_{topo} equal to 1, not 2, for the small system discussed above, is that the system is too small that can only capture the irreducible correlation contributed by the X loop, but not the Z loop.

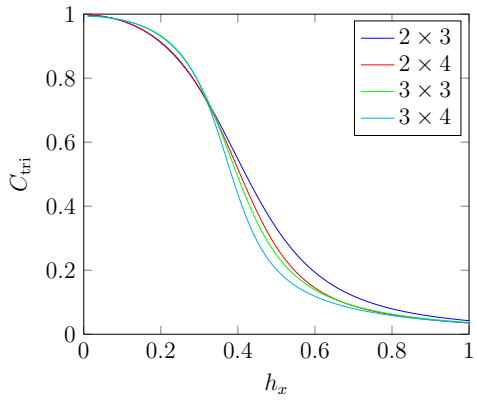

Fig. 5.11 $C_{tri}(\rho_{ABC})$ for different values of h_x, and with different lattice size. The horizontal axis is the magnetic field h_x. The vertical axis is $C_{tri}(\rho_{ABC})$ for the ground state of $H^{\text{toric}}(\mathbf{h})$.

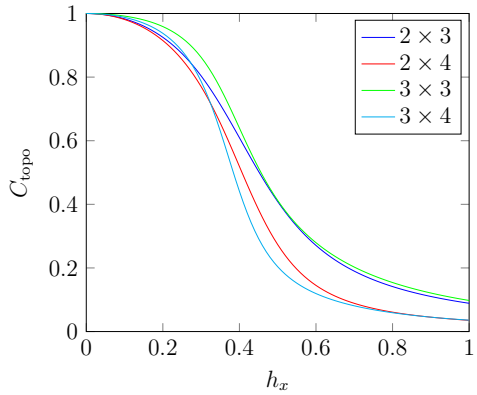

Fig. 5.12 S_{topo} for different values of h_x. The horizontal axis is the magnetic field h_x. The vertical axis is S_{topo} for the ground state of $H^{\text{toric}}(\mathbf{h})$.

For $h_x = h_z = 0$, the results are shown in Fig. 5.13 for $C_{tri}(\rho_{ABC})$ and in Fig. 5.14 for S_{topo}, for different values of h_y. Again, these results demonstrate that $C_{tri}(\rho_{ABC}) \leq S_{\text{topo}}$. And this system is known to have a first order phase transition at approximately $h_y = 1$. This transition can be clearly seen from both $C_{tri}(\rho_{ABC})$ and S_{topo}, even for such a small system.

For both the case of $h_y = h_z = 0$ and $h_x = h_z = 0$, we see that when the system size increases, the behaviors of $C_{tri}(\rho_{ABC})$ and S_{topo} become more similar. In large systems, $C_{tri}(\rho_{ABC})$ is very hard to calculate while S_{topo} is easier to get. Therefore, we proposed in Section 5.4.1 to use $I(A{:}C|B)$ (instead of $C_{tri}(\rho_{ABC})$) to detect non-trivial many-body entanglement in quantum systems.

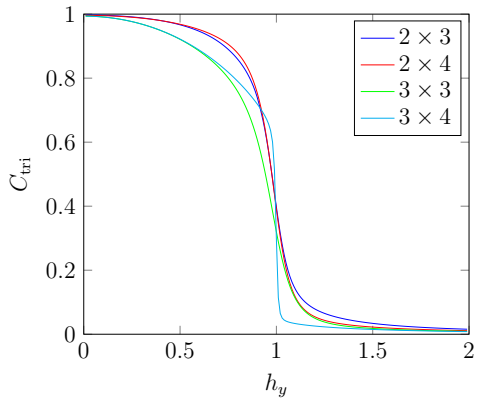

Fig. 5.13 $C_{tri}(\rho_{ABC})$ for different values of h_y. The horizontal axis is the magnetic field h_y. The vertical axis is $C_{tri}(\rho_{ABC})$ for the ground state of $H^{\text{toric}}(\mathbf{h})$.

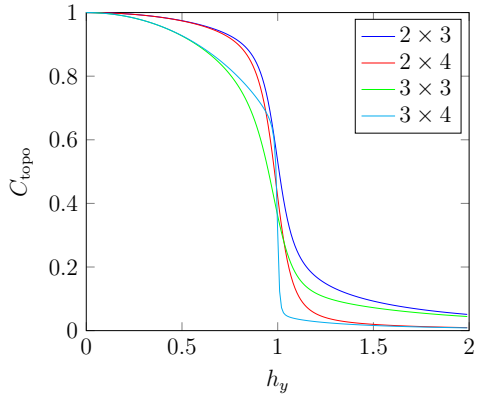

Fig. 5.14 S_{topo} for different values of h_y. The horizontal axis is the magnetic field h_y. The vertical axis is S_{topo} for the ground state of $H^{\text{toric}}(\mathbf{h})$.

5.4.3 The transverse-field Ising model

We will then considers systems without topological order. Our first such example is the 1D transverse-field Ising model, with the Hamiltonian

$$H^{\text{tIsing}}(B) = -\sum_i Z_i Z_{i+1} - B\sum_i X_i \tag{5.30}$$

for $B > 0$ (we choose $J = 1$). This system has no topological order for any value of B.

For $B = 0$, the ground-state space is two-fold degenerate (even for a finite system with n particles) and is spanned by $\{|0\rangle^{\otimes N}, |1\rangle^{\otimes N}\}$. For $B < 1$, the ground-state space

is still two-fold degenerate but only in the thermodynamic limit. It is well-known that the system encounters a quantum phase transition at $B = 1$.

Notice that the Hamiltonian H^{tIsing} has a $\mathbb{Z}_2$ symmetry that is given by $\bar{X} = \prod_i X_i$. That is, $[H^{\text{tIsing}}(B), \bar{X}] = 0$. Therefore, the ground-state space must also have the same $\mathbb{Z}_2$ symmetry. That is, for the projection onto the ground-state space $P_g(B)$, $[P_g(B), \bar{X}] = 0$.

For $B < 1$, the system is said to be in a 'symmetry breaking' phase with symmetry breaking order, in a sense that although $P_g(B)$ is symmetric, the short range correlated states within $P_g(B)$ are not.

When the system size is finite and generically when $B \neq 0$, the two ground states splits in energy. The symmetry principle of the system dictates that the lowest energy state must be symmetric. The special feature of the 'symmetry breaking' order is then encoded in a rich many-body entanglement structure of the lowest energy state. To probe such kind of entanglement, we can use $I(A{:}C|B)$ as a probe, with a proper choice of the parts A, B, C. For a 1D system with a periodic boundary condition (i.e. a ring), we can choose the parts A, B, C as illustrated in Fig. 5.15(a). Similarly, for a 2D system on a sphere, we can choose the parts A, B, C as illustrated in Fig. 5.15(b).

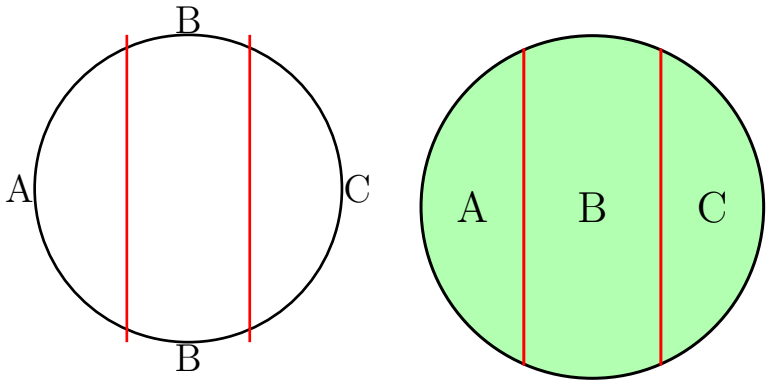

Fig. 5.15 (a) Cutting of a 1D Chain (b) Cutting of a 2D sphere

The key point here is to cut the entire system into only three parts, with parts A, C far from each other. With respect to this cutting, we name the corresponding $I(A{:}C|B)$ the 'tri-topological entanglement entropy' and denote it $S^{\text{t}}_{\text{topo}}$, which is given by

$$S^{\text{t}}_{\text{topo}} = S_{AB} + S_{BC} - S_B - S_{ABC}. \tag{5.31}$$

We choose the area A, C and each connected component of the area B to have $1, 2, 3, 4, 5$ qubits, respectively. So we compute $S^{\text{t}}_{\text{topo}}$ for a total of $n = 4, 8, 12, 16, 20$ qubits, for the corresponding ground state of the Hamiltonian $H^{\text{tIsing}}(B)$. The results are shown in Fig. 5.16. The five curves intersect at the well-known phase transition

point $B = 1$. In the limit of $N \to \infty$, we will expect $S^{t}_{topo} = 1$ for $0 \leq B < 1$, and $S^{t}_{topo} = 0$ for $B > 1$.

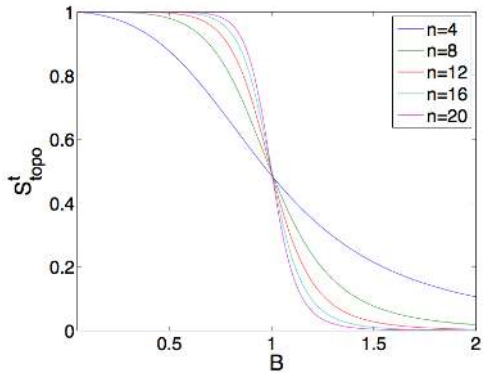

Fig. 5.16 S^{t}_{topo} for the transverse-field Ising model. The horizontal axis is the magnetic field B. The vertical axis is S^{t}_{topo} for the ground state of $H^{tIsing}(B)$.

This example shows us that S^{t}_{topo} nicely signals the two different quantum phases and the phase transitions for the transverse Ising model. The system has no topological order, but for the symmetry breaking phase, the exact symmetric ground state of a finite system exhibits the feature of non-trivial many-body entanglement with $S^{t}_{topo} = 1$. This feature is similar to the one contained in the symmetry ground state for $B = 0$, which is nothing but a GHZ state for the N-qubit system:

$$|GHZ\rangle = \frac{1}{\sqrt{2}}(|0\rangle^{\otimes N} + |1\rangle^{\otimes N}). \tag{5.32}$$

And it is straightforward to see that $S^{t}_{topo} = 1$ for $|GHZ\rangle$. This then provides an example that $I(A{:}C|B)$ is used to detect symmetry breaking order.

It is important to note that the choice of the regions A, B, C should respect the locality of the system. If we consider one-dimensional systems with open boundary condition, we can choose the A, B, C regions as shown in Fig. 5.20(a). For the transverse-field Ising model with open boundary condition, this choice will give a similar diagram of S^{t}_{topo} as in Fig. 5.16, which is given in Fig. 5.17.

However, if the partition in Fig. 5.20(a) is used for the Ising model with periodical boundary condition, as given in Fig 5.18, the behaviour of S^{t}_{topo} will be very different. In fact, in this case S^{t}_{topo} reflects nothing but the 1D area law of entanglement, which will diverge at the critical point $B = 1$ in the thermodynamic limit. For a finite system as illustrated in Fig. 5.19, S^{t}_{topo} does not clearly signal the two different quantum phases and the phase transition.

Notice that, we do not need to know the symmetry of the system or the associated symmetry breaking order parameter to calculate S^{t}_{topo}. Still, a non-zero S^{t}_{topo} indicates the existence of symmetry breaking order in the system. In fact, S^{t}_{topo} probes

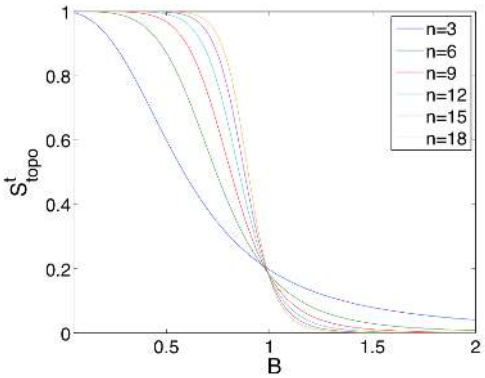

Fig. 5.17 S^t_{topo} of the transverse-field Ising model with open boundary condition and the A,B,C regions as chosen in Fig. 5.20(a). The horizontal axis is the magnetic field B. The vertical axis is S^t_{topo} for the ground state of $H^{\text{tIsing}}(B)$.

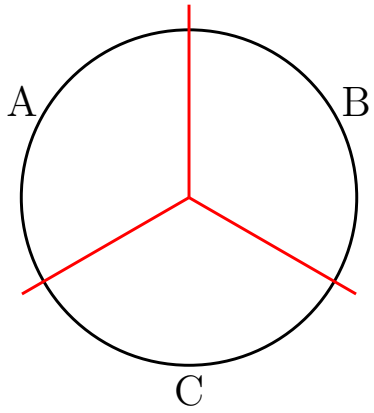

Fig. 5.18 A,B,C cutting on a 1D ring.

the symmetry breaking property hidden in the exact ground state of a finite system, which does not break any symmetry, in a form of many-body entanglement that the symmetric ground state exhibits.

5.4.4 The transverse-field cluster model

Our next example is another 1D system. We consider a 1D graph, which corresponds to a graph state as discussed in Chapter 3. The generators of the stabilizer group is given by $\{Z_{j-1}X_jZ_{j+1}\}$. The corresponding stabilizer state is called the '1D' cluster state, which is the unique ground state of the Hamiltonian

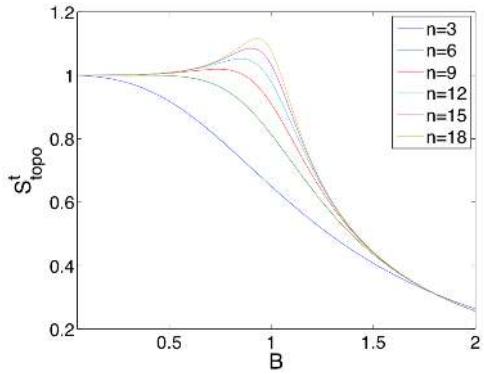

Fig. 5.19 $S^{\mathrm{t}}_{\mathrm{topo}}$ of the transverse-field Ising model with periodical boundary condition and the A,B,C regions as chosen in Fig. 5.18. The horizontal axis is the magnetic field B. The vertical axis is $S^{\mathrm{t}}_{\mathrm{topo}}$ for the ground state of $H^{\mathrm{tIsing}}(B)$.

$$H_{clu} = -\sum_j Z_{j-1}X_jZ_{j+1}. \tag{5.33}$$

For a 1D ring without boundary, the ground state of H_{clu} is the unique graph state stabilized by $\{Z_{j-1}X_jZ_{j+1}\}$. For a chain with boundary, where the summation index j runs from 2 to $N-1$, the ground state is then 4-fold degenerate. There is a slight difference between even and odd N, but the details do not matter to our discussion. For convenience, we will just assume N is even.

It is straightforward to see that the two commuting logical operators of this code can be all chosen as the form of tensor products of X_js, which are given by

$$\bar{X}_1 = \prod_k X_{2k-1}, \quad \bar{X}_2 = \prod_k X_{2k}, \tag{5.34}$$

with k runs from 1 to $N/2$.

Another way to view $\bar{X}_1$ and $\bar{X}_2$ is that they generate the group $\mathbb{D}_2 = \mathbb{Z}_2 \times \mathbb{Z}_2$ that preserves the 'topological order' of the system. Any local perturbation respecting the symmetry cannot lift the ground state degeneracy (in the thermodynamic limit). In this sense, the system is said to have 'symmetry-protected topological (SPT) order' (we will have more detailed discussions of SPT orders in Chapter 10, and we will also see this cluster state model again in Chapter 10.2).

One way to view this symmetry protection is to add a magnetic field along the X direction to the system, which does not break the $\mathbb{D}_2$ symmetry. That is, X_j commutes with $\bar{X}_1$ and $\bar{X}_2$. The corresponding Hamiltonian then reads

$$H_{clu}(B) = -\sum_j Z_{j-1}X_jZ_{j+1} - B\sum_j X_j. \tag{5.35}$$

It is known that there is a phase transition at $B = 1$ (for periodic boundary condition).

It is interesting to compare the system $H_{clu}(B)$ with a symmetry breaking ordered Hamiltonian

$$H_{syb}(B) = -\sum_j Z_{j-1}Z_{j+1} - B\sum_j X_j, \tag{5.36}$$

with the same symmetry $\mathbb{D}_2$ given by $\bar{X}_1, \bar{X}_2$.

As B goes from 0 to ∞, both $H_{clu}(B)$ and $H_{syb}(B)$ go through phase transitions, indicating nontrivial order in both the cluster state Hamiltonian $H_{clu}(0)$ and the Ising Hamiltonian $H_{syb}(0)$. However, $H_{clu}(0)$ and $H_{syb}(0)$ have different orders, one with symmetry protected topological order and one with symmetry breaking order. While we have not explained the exact meaning of these orders, let's see their difference with entanglement measures first.

Denote the symmetric ground state of $H_{syb}(B)$ by $|\psi_{syb}(B)\rangle$. Then $|\psi_{syb}(0)\rangle$ is a stabilizer state stabilized by $Z_{j-1}Z_{j+1}$ $(j = 2,\ldots,N-2)$ and $\bar{X}_1$, $\bar{X}_2$. Similarly, we denote the symmetric ground state of $H_{clu}(B)$ by $|\psi_{clu}(B)\rangle$. Then $|\psi_{clu}(0)\rangle$ is a stabilizer state stabilized by $Z_{j-1}X_jZ_{j+1}$ $(j = 2,\ldots,N-2)$ and $\bar{X}_1$, $\bar{X}_2$.

However, the two systems $H_{clu}(B)$ to $H_{syb}(B)$ are very different. One may see this from the fact that the ground-state space of $H_{syb}(B)$ remains to be four-fold degenerate even if closing the boundary. However, the ground state of $H_{clu}(B)$ is non-degenerate with a periodic boundary condition. That is, as already mentioned, $|\psi_{clu}(0)\rangle$ is in fact stabilized by $Z_{j-1}X_jZ_{j+1}$ with a periodic boundary condition.

In order to detect the non-trivial quantum order in the system of $H_{clu}(B)$, which should be different from the symmetry breaking order of $H_{syb}(B)$, we will again use $I(A{:}C|B)$ with some properly chosen cuttings. There are two kinds of cuttings introduced in Fig. 5.20. Fig. 5.20(a) cuts the system into three parts, and we denote the corresponding topological entanglement entropy by $S^{\mathrm{t}}_{\mathrm{topo}}$. Fig. 5.20$(b)$ cuts the system into four parts, and we denote the corresponding quantum mutual information $I(A{:}C|B)$ by $S^{\mathrm{q}}_{\mathrm{topo}}$.

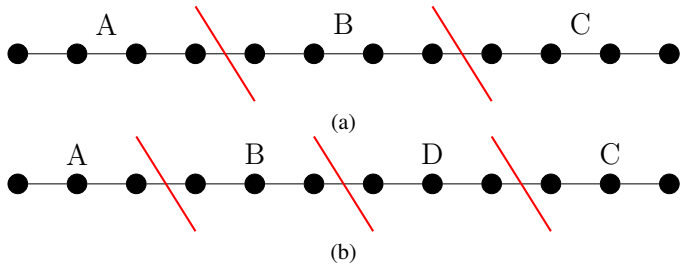

Fig. 5.20 (a) Cutting a 1D chain into A,B,C parts; (b) Cutting a 1D chain into A,B,C,D parts.

We first examine $S^{\mathrm{t}}_{\mathrm{topo}}$. For the ideal state of $B = 0$, $S^{\mathrm{t}}_{\mathrm{topo}} = 2$ for both $|\psi_{clu}(0)\rangle$ and $|\psi_{syb}(0)\rangle$. When B increases, for $|\psi_{clu}(B)\rangle$, $S^{\mathrm{t}}_{\mathrm{topo}}$ signals a phase transition. To demonstrate this, we perform an exact diagonalization of the Hamiltonian $H_{clu}(B)$, and calculate S^{t}_{topo} for the corresponding ground state. We do the calculation with

$6,12,18,24$ qubits, where each part of A,B,C contains $2,4,6,8$ qubits respectively. The results are shown in Fig. 5.21. In the limit of $N \to \infty$, we will expect $S^{\mathrm{t}}_{\mathrm{topo}} = 2$ for $0 \leq B < 1$, and $S^{\mathrm{t}}_{\mathrm{topo}} = 0$ for $B > 1$.

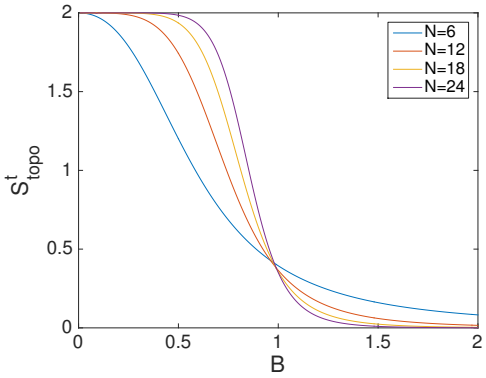

Fig. 5.21 $S^{\mathrm{t}}_{\mathrm{topo}}$ for the ground state of H_{clu}. The horizontal axis is the magnetic field B. The vertical axis is $S^{\mathrm{t}}_{\mathrm{topo}}$ for the ground state of $H_{clu}(B)$.

However, the symmetry breaking order hidden in the exact symmetric ground state $|\psi_{syb}(B)\rangle$ can also be detected by $S^{\mathrm{t}}_{\mathrm{topo}}$. In fact, for the same calculation with $6,12,18,24$ qubits, one gets a very similar figure, as shown in Fig. 5.22. Again, in the limit of $N \to \infty$, we will expect $S^{\mathrm{t}}_{\mathrm{topo}} = 2$ for $0 \leq B < 1$, and $S^{\mathrm{t}}_{\mathrm{topo}} = 0$ for $B > 1$.

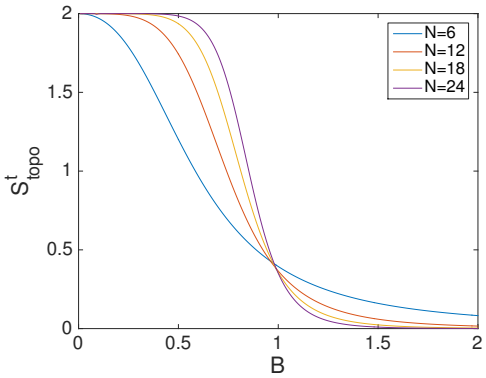

Fig. 5.22 $S^{\mathrm{t}}_{\mathrm{topo}}$ for the ground state of H_{syb}. The horizontal axis is the magnetic field B. The vertical axis is $S^{\mathrm{t}}_{\mathrm{topo}}$ for the ground state of $H_{syb}(B)$.

To distinguish SPT orders from a symmetry breaking one, we can instead use $S^{\mathrm{q}}_{\mathrm{topo}}$. Since the topological entanglement entropy is only carried in the entire wave function of the exact symmetric ground state for symmetry breaking orders, computing $S^{\mathrm{q}}_{\mathrm{topo}}$ on its reduced density matrix of parts ABC returns nearly zero value (due

to finite size effect) that do not signal any topological phase, as shown in Fig. 5.23. Here we do the calculation with $12, 16, 20, 24$ qubits, where each part of A, B, C, D contains $3, 4, 5, 6$ qubits respectively.

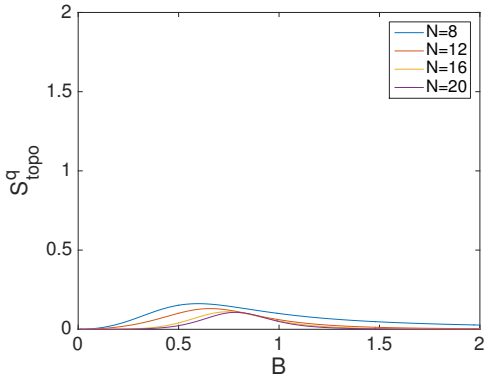

Fig. 5.23 S^q_{topo} for the ground state of H_{syb}. The horizontal axis is the magnetic field B. The vertical axis is S^q_{topo} for the ground state of $H_{syb}(B)$.

However, $S^q_{topo} = 2$ for $|\psi_{clu}(0)\rangle$, because the 'topology' of the SPT states is essentially carried on the boundary, tracing out part of the bulk has no effect on detecting the topological order. For $|\psi_{clu}(B)\rangle$, S^q_{topo} signals the topological phase transition, as shown in Fig. 5.24. Again, in the limit of $N \to \infty$, we will expect $S^q_{topo} = 2$ for $0 \leq B < 1$, and $S^q_{topo} = 0$ for $B > 1$.

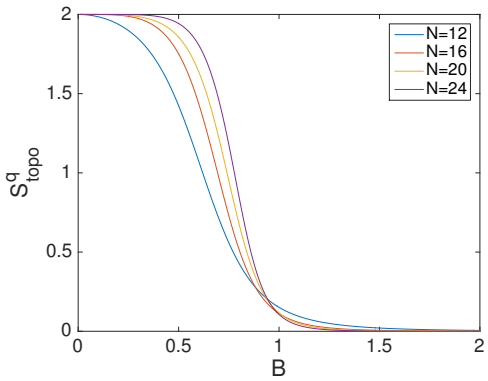

Fig. 5.24 S^q_{topo} for the ground state of H_{clu}. The horizontal axis is the magnetic field B. The vertical axis is S^q_{topo} for the ground state of $H_{clu}(B)$.

Notice that, similar to the symmetry breaking case, we do not need to know the symmetry of the system to calculate S^t_{topo} and S^q_{topo}. Still, non-zero S^t_{topo} and S^q_{topo}

indicate the existence of SPT order in the system. In this sense, $S^{\mathrm{t}}_{\mathrm{topo}}$ and $S^{\mathrm{q}}_{\mathrm{topo}}$ probe the SPT property hidden in the exact ground state of a finite system, which does not break any symmetry, in a form of many-body entanglement that the symmetric ground state exhibits.

5.4.5 Systems with mixed orders

There could also be systems containing mixed orders of symmetry breaking, SPT and topological orders. Our third example will be such a system with mixed orders. We consider a stabilizer group generated by $Z_{j-1}X_jX_{j+1}Z_{j+2}$ with j running from 2 to $N-2$. On a 1D chain with boundary, i.e. for $j = 2,3,\ldots,N-2$, the Hamiltonian $-\sum_j Z_{j-1}X_jX_{j+1}Z_{j+2}$ has 8-fold ground-state degeneracy.

The ground-state as an error-correcting code has logical operators $\bar{X}_1 = \prod_k X_{3k-2}$, $\bar{X}_2 = \prod_k X_{3k-2}$, $\bar{X}_3 = \prod_k X_{3k}$. Therefore, if one adds a magnetic field along the X direction, i.e.

$$H_{ZXXZ}(B) = -\sum_j Z_{j-1}X_jX_{j+1}Z_{j+2} - B\sum_j X_j, \tag{5.37}$$

the orders of the system (either SPT or symmetry breaking) will be protected when B is small.

It turns out that the system combines a $\mathbb{Z}_2$ symmetry breaking order and a $\mathbb{D}_2$ SPT-order. This can be seen from the fact that for $B = 0$, the symmetric ground state has $S^{\mathrm{t}}_{\mathrm{topo}} = 3$ and $S^{\mathrm{q}}_{\mathrm{topo}} = 2$. $S^{\mathrm{t}}_{\mathrm{topo}}$ probes both the symmetry breaking order and the SPT order, as illustrated in Fig. 5.25. $S^{\mathrm{q}}_{\mathrm{topo}}$ probes only the SPT order, as illustrated in Fig. 5.26. In the limit of $N \to \infty$, we will expect $S^{\mathrm{t}}_{\mathrm{topo}} = 3$ and $S^{\mathrm{q}}_{\mathrm{topo}} = 2$ for $0 \le B < 1$, and $S^{\mathrm{t}}_{\mathrm{topo}} = S^{\mathrm{q}}_{\mathrm{topo}} = 0$ for $B > 1$.

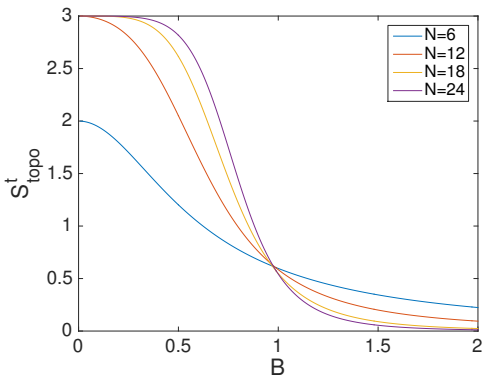

Fig. 5.25 $S^{\mathrm{t}}_{\mathrm{topo}}$ the ground state of $H_{ZXXZ}(B)$. The horizontal axis is the magnetic field B. The vertical axis is $S^{\mathrm{t}}_{\mathrm{topo}}$ for the ground state of $H_{ZXXZ}(B)$. For $N = 6$, the maximum value of $S^{\mathrm{t}}_{\mathrm{topo}}$ is 2 due to that the system size is too small.

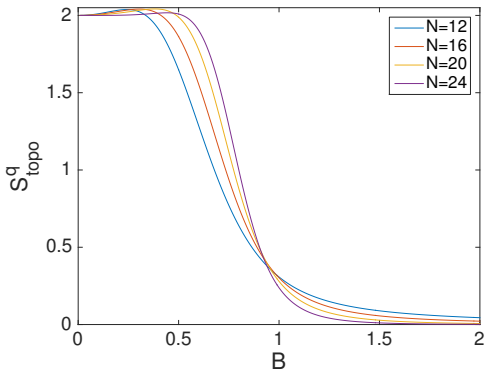

Fig. 5.26 S^{q}_{topo} for the ground state of $H_{ZXXZ}(B)$. The horizontal axis is the magnetic field B. The vertical axis is S^{q}_{topo} for the ground state of $H_{ZXXZ}(B)$.

Again, we do not need to know the symmetry of the system to calculate S^{t}_{topo} and S^{q}_{topo}. S^{t}_{topo} and S^{q}_{topo} probe the symmetry breaking and/or SPT property hidden in the exact ground state of a finite system, which does not break any symmetry, in a form of many-body entanglement that the symmetric ground state exhibits.

5.4.6 $I(A{:}C|B)$ as a detector of non-trivial many-body entanglement

From our previous discussions, we observe that to use $I(A{:}C|B)$ to detect quantum phase and phase transitions, it is crucial to choose the areas A,C that are *far from each other*. Here 'far' is determined by the locality of the system. For instance, on an 1D chain, the areas A,C in Fig. 5.15(a) and Fig. 5.20 are far from each other, but in Fig. 5.18 are not.

One may also generalize the idea of different types of topological entanglement entropy to higher spatial dimensions. For instance, in 2D, a straightforward way is to replace the chain by a cylinder with boundary, then use the similar cuttings as in Fig. 5.20.

One may also consider a disk with boundary. For any gapped ground state (one may need to avoid the situation of a gapless boundary by adding symmetric local terms to the Hamiltonian), still using $I(A{:}C|B)$, one can consider two kinds of cuttings, as given in Fig. 5.27. Similar to the 1D case, the cutting of Fig. 5.27(a) probes both the symmetry breaking orders and the SPT orders, and the cutting of Fig. 5.27(a) probes only SPT orders.

To summarize, we have shown that a nonzero $I(A{:}C|B)$ for certain large areas A,B,C (larger than the correlation length of the system) with A,C far from each other, is a good detector for non-trivial many-body entanglement. With different choices of the cuttings for A,B,C, $I(A{:}C|B)$ can detect different quantum orders and signal different kinds of quantum phase transitions.

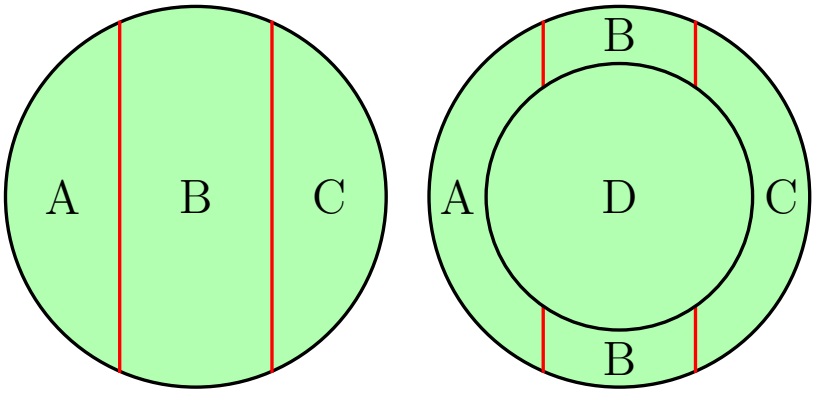

(a) (b)

Fig. 5.27 Cuttings of a 2D disk: (a) into three parts A,B,C (b) into four parts A,B,C,D

We have discussed three kinds of different cuttings that leads to different (generalized) topological entanglement entropy based on $I(A{:}C|B)$, i.e. S_{topo}, $S^{\text{t}}_{\text{topo}}$ and $S^{\text{q}}_{\text{topo}}$. For a product state (trivial order), all three of S_{topo}, $S^{\text{t}}_{\text{topo}}$ and $S^{\text{q}}_{\text{topo}}$ are zero. A nonzero of any one of the three indicates some non-trivial order in the system. And for probing symmetry breaking and/or SPT orders, we do not need to know the symmetry of the system to calculate these quantities (for the exact ground state that does not break any symmetry, for any finite system). We summarize their use to detect different kinds of orders in the table below.

Box 5.9 Detecting quantum orders by $I(A{:}C|B)$

Order of the quantum system	Nonzero $I(A{:}C\|B)$	Zero $I(A{:}C\|B)$
Trivial Order		S_{topo}, $S^{\text{t}}_{\text{topo}}$, $S^{\text{q}}_{\text{topo}}$
Topological Order	S_{topo}, $S^{\text{q}}_{\text{topo}}$	$S^{\text{t}}_{\text{topo}}$
Symmetry-Breaking Order	$S^{\text{t}}_{\text{topo}}$	S_{topo}, $S^{\text{q}}_{\text{topo}}$
Symmetry-Protected Topological Order	$S^{\text{t}}_{\text{topo}}$, $S^{\text{q}}_{\text{topo}}$	S_{topo}

5.5 Gapped ground states as quantum-error-correcting codes

In Chap.3, we have discussed the properties of the toric code. We know that the distance of the toric code grow as $\sqrt{N}$, where N is the number of qubits in the system.

In this section, we also discuss the properties of the ground- state space of other systems, from the viewpoint of quantum error-correcting code.

Let us first consider the transverse Ising model $H^{\text{tIsing}}(B)$. For $B=0$, the ground-state space is two-fold degenerate and is spanned by $\{|0\rangle^{\otimes N},\{|1\rangle^{\otimes N}\}$. Denote this space by V_{tIsing}.

Notice that the quantum error-correcting code V_{tIsing} spanned by $\{|0\rangle^{\otimes N},\{|1\rangle^{\otimes N}\}$ has only distance 1, since one can choose another orthonormal basis

$$|GHZ_{\pm}\rangle = \frac{1}{\sqrt{2}}(|0\rangle^{\otimes N} \pm |1\rangle^{\otimes N}), \tag{5.38}$$

and we have

$$\langle GHZ_{+}|Z_i|GHZ_{-}\rangle = 1, \tag{5.39}$$

for any qubit i.

However, if we only consider the code's ability to correct bit flip errors (i.e. X_i), the code actually has a 'large distance'. That, for any orthonamal basis $|\psi_0\rangle, |\psi_1\rangle$ of V_{tIsing}, if

$$\langle\psi_0|O_X|\psi_1\rangle \neq 0 \tag{5.40}$$

holds for any operator O_X that is a tensor product of X_is, one must have $O_X = X^{\otimes N}$ (e.g. $X^{\otimes N}|0\rangle^{\otimes N} = |1\rangle^{\otimes N}$).

Or, one can view V_{tIsing} as a stabilizer code, whose stabilizer group is generated by Z_iZ_{i+1} for $i = 1,2,\ldots,N-1$. And the logical operator which is a tensor product of X_is is given by $X^{\otimes N}$. This means that this stabilizer code has 'X-distance' N.

In this sense, V_{tIsing} for correcting the X-only errors, is an analogy of the classical repetition code of N bits with codewords $\{00\ldots0, 11\ldots1\}$ for correcting bit flip error that sends $0 \leftrightarrow 1$. And the distance of the classical repetition code of N bits is N, which is the minimal number of bit flips needed to transform $00\ldots0$ to $11\ldots1$. In this sense, we say that V_{tIsing} has a large 'classical' distance, which is 'macroscopic' that grows with the system size N.

In fact, the error-correcting properties of V_{tIsing} goes much beyond of just the 'classical code with large distance', given its quantum nature. Recall that the system has a $\mathbb{Z}_2$ symmetry that is given by $X^{\otimes N}$. In fact, with respect to any local operator L that does not break this $\mathbb{Z}_2$ symmetry, i.e. $[L, X^{\otimes N}] = 0$, the code V_{tIsing} has a 'macroscopic' distance. That is, we will need to apply L to number of local sites that grows the system size, to transform any orthonamal basis state $|\psi_0\rangle$ to the other state $|\psi_1\rangle$.

For $0 < B < 1$, the ground-state space of $H^{\text{tIsing}}(B)$ is also two-fold degenerate, and with an error-correcting property that is very similar to the case of $B = 0$. We summarize the property as below.

Box 5.10 The ground-state space of symmetry breaking orders
For errors that do not break the symmetry, the degenerate ground-state space of a symmetry breaking ordered system is a quantum error-correcting code with a macroscopic distance.

We now consider the transverse field cluster mode $H_{clu}(B)$. For $B = 0$ and with open boundary condition, the ground-state space is 4-fold degenerate. Denote this space by V_{clu}. As a stabilizer code, the stabilizer group of V_{clu} is generated by $Z_{i-1}X_iZ_{i+1}$ for $i = 2,\ldots,N-1$. The code only has distance 1, as Z_1 (Z_N) is a logical operator that commutes with all the $Z_{i-1}X_iZ_{i+1}$.

However, if we only consider the code's ability to correct bit flip errors (i.e. X_i), the code actually has a 'large distance'. In fact, the logical operators that are tensor products of X_is are given by $\bar{X}_1$ and $\bar{X}_2$, therefore it has 'X-distance' $N/2$, which is a macroscopic distance that is half of the system size. In this sense, we say that V_{clu} is quantum error-correcting code with 'classical' distance $N/2$.

Similar to the symmetry breaking case, the error-correcting property V_{clu} goes beyond just a quantum code with large 'classical' distance. Since the system has a $\mathbb{Z}_2 \times \mathbb{Z}_2$ symmetry that is given by $\bar{X}_1, \bar{X}_2$, for any local operator L that does not break this $\mathbb{D}_2$ symmetry, i.e. $[L, X_1] = 0$ and $[L, X_2] = 0$, the code V_{tIsing} has a 'macroscopic' distance. We summarize this property as below.

Box 5.11 The ground-state space of SPT orders
For errors that do not break the symmetry, the degenerate ground-state space of a SPT ordered system is a quantum error-correcting code with a macroscopic distance.

We now summarize the error-correcting property of different gapped systems as below. Here by 'classical code', we mean that the quantum code has an orthonormal basis that can be chosen as product states (e.g. V_{tIsing}). And by 'classical' distance, we actually mean that the distance is with respect to certain symmetry, which is an analogy as the distance for classical codes.

Box 5.11 Gapped ground states as quantum-error-correcting codes

	Degenerate Ground-State Space	Code Distance
Topological Order	Quantum Code	Macroscopic Quantum Distance
Symmetry-Breaking Order	'Classical' Code	Macroscopic 'Classical' Distance
Symmetry-Protected Topological Order	Quantum Code	Macroscopic 'Classical' Distance

5.6 Entanglement in gapless systems

In a critical or gapless system, the area law can be violated, but usually only mildly by a term that scales as the logarithm of the size of the subregion. For example, at one dimensional critical points described by conformal field theory, the entanglement entropy of a segment of length L in the chain scales as

$$S_A \sim \frac{c+\bar{c}}{6} \log L \tag{5.41}$$

where c and $\bar{c}$ are the central charges of the conformal field theory. As before, the entanglement entropy is calculated as the total system size goes to infinity. Compared to 1D gapped systems where S_A is bounded by a constant, S_A for 1D conformal critical points is unbounded, but only grows very slowly with the segment size.

Also for gapless free fermion system in D spatial dimensions with a Fermi surface, the entanglement entropy of a region of linear size L scales as

$$S_A \sim \alpha L^{D-1} \log L \tag{5.42}$$

Apart from the 'area law' scaling part αL^{D-1}, the entanglement entropy also contains a logarithmic part $\log(L)$. The violation of area law comes from the existence of low energy excitations which carries correlations as it propagates. The correlation length is infinite in the system which generates more entanglement across the boundary than in the gapped case. However, the locality constraint still exists and and keeps the entanglement content in the state far from maximum ($\sim L^D$).

The change in entanglement content from an 'area law' to beyond as one moves from gapped phases to phase transitions has become a useful tool in detecting phase transitions. In fact, not only entanglement entropy, but also many other different entanglement measures have been found to exhibit diverging behavior as a phase transition point is approached and therefore can be used as a probe for detecting phase transitions. While numerical and experimental challenges remain to calculate or measure entanglement in a system, one special advantage of such a probe is that it works for both symmetry breaking and topological systems. Some conventional probes of phase transitions, like order parameter, apply only to symmetry breaking phases and fail for topological phases. Entanglement measures, however, are generic probes independent of the nature of the phase transition.

In fact, we can also use the quantum conditional mutual information $I(A{:}C|B)$ to detect non-trivial entanglement structures in gapless systems. Once we choose the large enough areas A,B,C with A,C far from each other, a nonzero $I(A{:}C|B)$ also provides information for gapless systems. Unlike the area law, $I(A{:}C|B)$ does not

diverge for critical systems. And due to the dependence with L, the area ratio of the A,B,C parts will give different values of $I(A{:}C|B)$.

As an example, at the transition point $B=1$ for the transverse-field Ising model H_{tIsing}, where the system is gapless, the five curves in Fig. 5.16 intersect at $S^{\text{t}}_{\text{topo}} \sim 0.5$. However, this value of $S^{\text{t}}_{\text{topo}}$ is not a constant, which depends on the shape of the areas A,B,C. Define the ratio

$$r = \frac{\#\text{ in each of the area A,C}}{\#\text{ in each connected component of } B} \tag{5.43}$$

where # means the number of qubits.

If we choose the ratio $r=2:1$, and to have $1,2,3$ qubits for each connected component of the area B, then we can compute $S^{\text{t}}_{\text{topo}}$ for total $N=6,12,18$ qubits, as shown in Fig. 5.28.

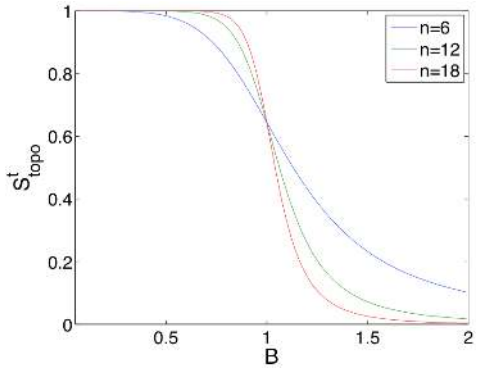

Fig. 5.28 $S^{\text{t}}_{\text{topo}}$ for the transverse-field Ising model. The ratio $r=2:1$, and the system sizes are $N=6,12,18$ qubits. The horizontal axis is the magnetic field B. The vertical axis is $S^{\text{t}}_{\text{topo}}$ for the ground state of $H^{\text{tIsing}}(B)$.

And if we choose $r=1:2$, and to have $2,4,6$ qubits for each connected component of the area B, then we can compute $S^{\text{t}}_{\text{topo}}$ for total $N=6,12,18$ qubits, as shown in Fig. 5.29.

This ratio dependence is typical in critical systems. And the results for $I(A{:}C|B)$ with various ratios of the areas of A,B,C are consistent with the conformal field theory (CFT) calculation. In other words, by varying the ratio of the areas of A,B,C, $I(A{:}C|B)$ can provide information for gapless/critical systems, for instance the value of the central charge.

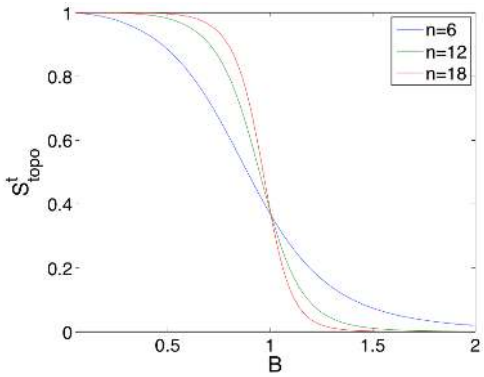

Fig. 5.29 $S^{\mathrm{t}}_{\mathrm{topo}}$ for the transverse-field Ising model. The ratio $r = 1:2$, and the system sizes are $N = 6, 12, 18$ qubits. The horizontal axis is the magnetic field B. The vertical axis is $S^{\mathrm{t}}_{\mathrm{topo}}$ for the ground state of $H^{\mathrm{tIsing}}(B)$.

5.7 Summary and further reading

In this chapter, we consider quantum systems in the limit of system size $N \to \infty$, which effectively describe macroscopic condensed matter systems containing $\sim 10^{23}$ degrees of freedom. New ideas and notions need to be introduced to study such many-body quantum systems. In particular, we introduce the concept of dimensionality, locality, thermodynamic limit, universality, gap, correlation, and many-body entanglement to characterize properties of quantum many-body systems.

The behavior of quantum many-body entanglement is of special importance which we discuss in detail in different cases. For gapped quantum many-body systems, their many-body entanglement is found to satisfy an 'area law', which imposes a strong constraint on the amount and form of many-body entanglement contained in the system. Gapless systems can violate this 'area law', but usually only mildly with a logarithmic correction term. Moreover, in gapped quantum systems a constant subleading term exists in the entanglement entropy which is closely related to the topological order in the system.

We study the meaning of topological entanglement entropy from an information-theoretic viewpoint. This allows us to build a link between the topological entanglement entropy, the quantum conditional mutual information $I(A{:}C|B)$, and the irreducible three-party correlation discussed in Chapter 1. The proof of the strong subadditivity inequality $I(A{:}C|B) \geq 0$ is given in [17]. The structure of states that satisfy the equality is discussed in [10], which are quantum Markov states with the form given in Eq. (5.27).

We show that for large enough areas A, B, C and A, C far from each other, nonzero $I(A{:}C|B)$ indicates non-trivial orders of the system. Calculating $I(A{:}C|B)$ for different choices of the areas A, B, C could then detect different orders for gapped system (e.g. symmetry breaking, SPT, topological orders). And for probing symmetry breaking and/or SPT orders, we do not need to know the symmetry of the system

to calculate $I(A{:}C|B)$ (for the exact ground state that does not break any symmetry, for any finite system). For gapless systems, the value of $I(A{:}C|B)$ depends on the shapes of A, B, C, which also contains information of the critical system (e.g. central charge). In this sense, $I(A{:}C|B)$ is a 'universal entanglement detector' for both gapped and gapless system, which contains non-trivial information of the orders for the systems.

In one dimensional systems, the existence of an area law in gapped quantum systems has been established as a rigorous mathematical theorem first by Hastings in [9]. The constant bound on the entanglement entropy of a segment of the chain scales exponentially with the correlation length in Hastings proof, which has been subsequently tightened to a polynomial scaling in the work by Arad, Landau and Vazirani[2]. In two or higher dimensions, a full proof of the 'area law' does not exist yet but it has been supported by a large amount of numerical evidence. For a more detailed review of the subject, see [7].

In gapless systems, the entanglement 'area law' is violated. Such a violation is particularly well understood at one dimensional critical points described by conformal field theory (CFT). In [11], it was proposed that the scaling of entanglement entropy in one dimensional critical systems is logrithmic and the scaling coefficient is related to the central charge of the CFT. In [20], numerical calculation for some one dimensional critical points was carried out which clearly demonstrated such a relation. For a more systematic discussion about entanglement entropy in CFT, see [3]. The scaling of entanglement entropy in higher dimensional gapless/critical systems is less well understood. [7] also reviews what we currently know about such systems.

Various entanglement measures have become popular tools in studying quantum phase transitions. For summary of how to use entanglement measures to detect quantum phase transitions, see [1].

The idea of topological entanglement entropy was proposed in [14, 15] and two different schemes for calculation were provided. It has been used in numerical calculations to successfully identify nontrivial topological orders in physical systems. For example, see [12, 13].

The information-theoretic aspects of topological entanglement entropy and its relationship to irreducible many-body correlation are discussed in [18, 4]. The generalizations of topological entanglement entropy to study symmetry breaking orders are discussed in [4, 21] and to study SPT orders and mixed orders are discussed in [22]. The error-correcting properties of the SPT ground-states are discussed in [6, 22]. The generalized topological entanglement entropy of critical systems are discussed in [21], where the results for the transverse-field Ising model is shown to be consistent with the CFT calculation given in [8, 5].

Recently, it has been realized that more detailed information about topological order can be extracted from the entanglement structure of the system than just a single number of entanglement entropy. It has been proposed in [16, 19] that, the entanglement spectrum, i.e. the eigenvalue spectrum of the reduced density matrix, has meaning of its own. In fact for a gapped topologically ordered system, the 'low energy' sector of the entanglement spectrum should reflect the nature of the low

energy excitations on the edge of the system. Moreover, it was realized that entanglement entropy of systems on nontrivial manifolds, like cylinder or torus, can provide more information about the quasiparticle content of the topological system than that calculated on a plane [23].

References

1. Luigi Amico, Rosario Fazio, Andreas Osterloh, and Vlatko Vedral. Entanglement in many-body systems. *Rev. Mod. Phys.*, 80:517–576, May 2008.
2. Itai Arad, Zeph Landau, and Umesh Vazirani. Improved one-dimensional area law for frustration-free systems. *Phys. Rev. B*, 85:195145, May 2012.
3. Pasquale Calabrese and John Cardy. Entanglement entropy and conformal field theory. *Journal of Physics A: Mathematical and Theoretical*, 42(50):504005, 2009.
4. Jianxin Chen, Zhengfeng Ji, Chi-Kwong Li, Yiu-Tung Poon, Yi Shen, Nengkun Yu, Bei Zeng, and Duanlu Zhou. Discontinuity of maximum entropy inference and quantum phase transitions. *New Journal of Physics*, 17(8):083019, 2015.
5. Cristiano De Nobili, Andrea Coser, and Erik Tonni. Entanglement entropy and negativity of disjoint intervals in cft: Some numerical extrapolations. *arXiv preprint arXiv:1501.04311*, 2015.
6. Andrew C. Doherty and Stephen D. Bartlett. Identifying phases of quantum many-body systems that are universal for quantum computation. *Phys. Rev. Lett.*, 103:020506, Jul 2009.
7. Jens Eisert, Marcus Cramer, and Martin B. Plenio. *Colloquium* : Area laws for the entanglement entropy. *Rev. Mod. Phys.*, 82:277–306, Feb 2010.
8. Shunsuke Furukawa, Vincent Pasquier, and Jun'ichi Shiraishi. Mutual information and boson radius in a $c = 1$ critical system in one dimension. *Phys. Rev. Lett.*, 102:170602, Apr 2009.
9. Matthew B. Hastings. An area law for one-dimensional quantum systems. *Journal of Statistical Mechanics: Theory and Experiment*, 2007(08):P08024, 2007.
10. Patrick Hayden, Richard Jozsa, Dénes Petz, and Andreas Winter. Structure of states which satisfy strong subadditivity of quantum entropy with equality. *Communications in mathematical physics*, 246(2):359–374, 2004.
11. Christoph Holzhey, Finn Larsen, and Frank Wilczek. Geometric and renormalized entropy in conformal field theory. *Nuclear Physics B*, 424(3):443 – 467, 1994.
12. Sergei V. Isakov, Matthew B. Hastings, and Roger G. Melko. Topological entanglement entropy of a bose-hubbard spin liquid. *Nat Phys*, 7(10):772–775, October 2011.
13. Hong-Chen Jiang, Zhenghan Wang, and Leon Balents. Identifying topological order by entanglement entropy. *Nat Phys*, 8(12):902–905, December 2012.
14. Alexei Kitaev and John Preskill. Topological entanglement entropy. *Phys. Rev. Lett.*, 96(11):110404, Mar 2006.
15. Michael Levin and Xiao-Gang Wen. Detecting topological order in a ground state wave function. *Phys. Rev. Lett.*, 96(11):110405, Mar 2006.
16. Hui Li and F. Duncan M. Haldane. Entanglement spectrum as a generalization of entanglement entropy: Identification of topological order in non-abelian fractional quantum hall effect states. *Phys. Rev. Lett.*, 101:010504, Jul 2008.
17. Elliott H Lieb and Mary Beth Ruskai. Proof of the strong subadditivity of quantum-mechanical entropy. In *Inequalities*, pages 63–66. Springer, 2002.
18. Yang Liu, Bei Zeng, and D L Zhou. Irreducible many-body correlations in topologically ordered systems. *New Journal of Physics*, 18(2):023024, 2016.
19. Frank Pollmann, Ari M. Turner, Erez Berg, and Masaki Oshikawa. Entanglement spectrum of a topological phase in one dimension. *Phys. Rev. B*, 81:064439, Feb 2010.
20. Guifré Vidal, José I. Latorre, E. Rico, and A. Kitaev. Entanglement in quantum critical phenomena. *Phys. Rev. Lett.*, 90:227902, Jun 2003.

21. Bei Zeng and Xiao-Gang Wen. Gapped quantum liquids and topological order, stochastic local transformations and emergence of unitarity. *Physical Review B*, 91(12):125121, 2015.
22. Bei Zeng and D. L. Zhou. Topological and error-correcting properties for symmetry-protected topological order. *EPL (Europhysics Letters)*, 113(5):56001, 2016.
23. Yi Zhang, Tarun Grover, Ari Turner, Masaki Oshikawa, and Ashvin Vishwanath. Quasiparticle statistics and braiding from ground-state entanglement. *Phys. Rev. B*, 85:235151, Jun 2012.

Part III
Topological Order and Long-Range Entanglement

Chapter 6
Introduction to Topological Order

Abstract In primary school, we were told that there are four states of matter: solid, liquid, gas, and plasma. In college, we learned that there are much more than four states of matter. For example, there are ferromagnetic states as revealed by the phenomenon of magnetization and superfluid states as defined by the phenomenon of zero-viscosity. The various phases in our colorful world are extremely rich. So it is amazing that they can be understood systematically by the symmetry breaking theory of Landau. However, in last 20 – 30 years, we discovered that there are even more interesting phases that are beyond Landau symmetry breaking theory. In this chapter, we discuss new 'topological' phenomena, such as topological degeneracy, that reveal the existence of those new phases – topologically ordered phases. Just like zero-viscosity defines the superfluid order, the new 'topological' phenomena define the topological order at macroscopic level.

6.1 Introduction

6.1.1 Phases of matter and Landau's symmetry breaking theory

Although all matter is formed by only three kinds of particles: electrons, protons and neutrons, matter can have many different properties and appear in many different forms, such as solid, liquid, conductor, insulator, superfluid, magnet, etc. According to the principle of emergence in condensed matter physics, the rich properties of materials originate from the rich ways in which the particles are organized in the materials. Those different organizations of the particles are formally called 'orders'.

For example, particles have a random distribution in a liquid (see Fig. 11.18a), so a liquid remains the same as we displace it by an arbitrary distance. We say that a liquid has a 'continuous translation symmetry'. After a phase transition, a liquid can turn into a crystal. In a crystal, particles organize into a regular array (a lattice) (see Fig. 11.18b). A lattice remains unchanged only when we displace it by a par-

(a) (b)

Fig. 6.1 (a) Particles in liquids do not have fixed relative positions. They fluctuate freely and have a random but uniform distribution. (b) Particles in solids form a fixed regular lattice.

ticular set of distances (integer times of the lattice constant), so a crystal has only 'discrete translation symmetry'. The phase transition between a liquid and a crystal is a transition that reduces the continuous translation symmetry of the liquid to the discrete symmetry of the crystal. Such a change in symmetry is called 'spontaneous symmetry breaking'. We note that the equation of motions that govern the dynamics of the particles respects the continuous translation symmetry for both cases of liquid and crystal. However, in the case of crystal, the stronger interaction makes the particles to prefer being separated by a fixed distance and a fixed angle. This makes particles to break the continuous translation symmetry down to discrete translation symmetry 'spontaneously' in order to choose a low energy configuration (see Fig. 6.2). Therefore, the essence of the difference between liquids and crystals is that the organizations of particles have different *symmetries* in the two phases.

Liquid and crystal are just two examples. In fact, particles can organize in many ways which lead to many different orders and many different types of materials. Landau's symmetry breaking theory [37, 19, 38] provides a general and a systematic understanding of these different orders. It points out that different orders actually correspond to different symmetries in the organizations of the constituent particles. As a material changes from one order to another order (*i.e.* , as the material undergoes a phase transition), what happens is that the symmetry of the organization of the particles changes.

Box 6.1 Landau's symmetry breaking theory (classical)
If a classical system with a symmetry is in a symmetry breaking phase, then its degenerate minimal-free-energy states (or minimal-energy states at zero temperature) break the symmetry. Two systems with the same symmetry belong to different phases if their minimal-free-energy states have different symmetries.

Landau's symmetry breaking theory is a very successful theory. For a long time, physicists believed that Landau's symmetry breaking theory describes all possible phases in materials, and all possible (continuous) phase transitions.

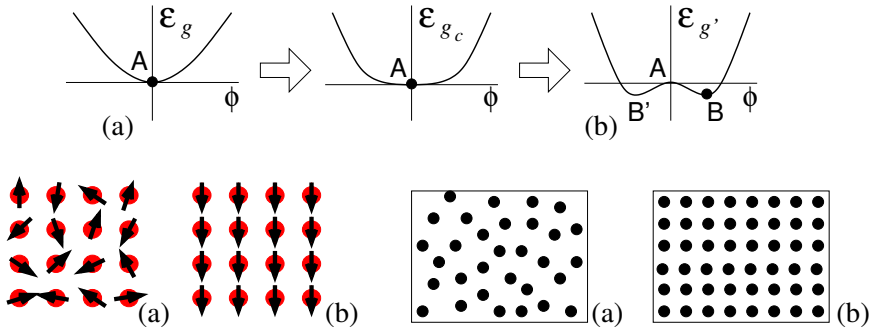

Fig. 6.2 (a) Disordered states that do not break the symmetry. (b) Ordered states that spontaneously break the symmetry. The energy function $\varepsilon_g(\phi)$ has a symmetry $\phi \to -\phi$: $\varepsilon_g(\phi) = \varepsilon_g(-\phi)$. However, as we change the parameter g, the minimal energy state (the ground state) may respect the symmetry (a), or may not respect the symmetry (b). This is the essence of spontaneous symmetry breaking.

6.1.2 Quantum phases of matter and transverse-field Ising model

Quantum phases of matter are phases of matter at zero temperature. So quantum phases correspond to the ground states of the quantum Hamiltonians that govern the systems. In this book, we mainly discuss those quantum phases of matter. Crystal, conductor, insulator, superfluid, and magnets can exist at zero temperature and are examples of quantum phases of matter.

Again, physicists used to believe that Landau symmetry breaking theory also describes all possible quantum phases of matter, and all possible (continuous) quantum phase transitions. (Quantum phase transitions, by definition, are zero temperature phase transitions.) For example, the superfluid is described by a $U(1)$ symmetry breaking.

The simplest example to demonstrate the Landau symmetry breaking theory for quantum phases is the transverse-field Ising model on a 1-dimensional chain. The total Hilbert space of the transverse-field Ising model is formed by 1/2 spins (qubits) on each site. The Hamiltonian is given by

$$H^{\text{tIsing}} = -\sum_i (Z_i Z_{i+1} + B X_i), \tag{6.1}$$

where X_i, Y_i, Z_i are the Pauli matrices acting on the i^{th} spin. The Hamiltonian has a spin-flip symmetry, $\uparrow \leftrightarrow \downarrow$, generated by $\otimes_i X_i$: $[H, \otimes_i X_i] = 0$.

One way to obtain the ground state of the transverse-field Ising model is to use the variational approach. To design the variational trial wave function, we note that when $B = 0$ the ground states are two-fold degenerate and are given by $\otimes_i |\uparrow\rangle_i$ and $\otimes_i |\downarrow\rangle_i$. When $B >> 1$ the ground states is given by $\otimes_i (|\uparrow\rangle_i + |\downarrow\rangle_i)/\sqrt{2}$. Thus we choose our trial wave function as

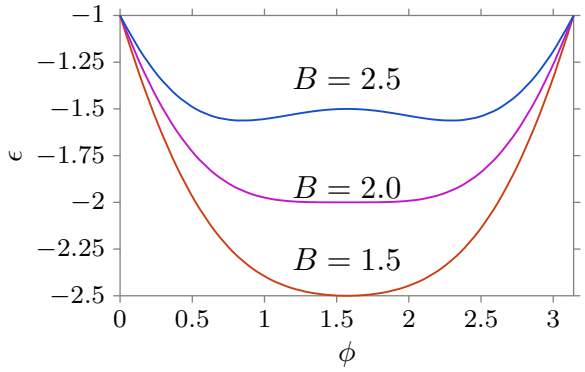

Fig. 6.3 The variational energies $\varepsilon(\phi)$ for $B = 1.5, 2, 2.5$.

$$|\Psi_\phi\rangle = \otimes_i \Big[\cos(\phi/2)|\uparrow\rangle_i + \sin(\phi/2)|\downarrow\rangle_i \Big], \tag{6.2}$$

where ϕ is the variational parameter. The average energy per site is given by

$$\varepsilon(\phi) = \frac{\langle\Psi_\phi|H|\Psi_\phi\rangle}{N_{\text{site}}} = -[\cos^2(\phi/2) - \sin^2(\phi/2)]^2 - 2B\cos(\phi/2)\sin(\phi/2). \tag{6.3}$$

We note that the spin-flip transformation $\otimes_i X_i$ changes $|\Psi_\phi\rangle \to |\Psi_{\pi-\phi}\rangle = \otimes_i X_i|\Psi_\phi\rangle$. So $\varepsilon(\phi)$ satisfies $\varepsilon(\phi) = \varepsilon(\pi - \phi)$ due to the spin-flip symmetry.

In Fig. 6.3, we plot the variational energy $\varepsilon(\phi)$ for $B = 1.5, 2, 2.5$. We see that there is a symmetry breaking transition at $B = 2$. For $B > 2$, the energy is minimized at $\phi = \pi/2$ and the trial ground state does not break the spin-flip symmetry $\phi \to \pi - \phi$. For $B < 2$, the energy is minimized at two places $\phi = \pi/2 \pm \Delta\phi$, which give rise to two degenerate ground states $|\Psi_{\pi-\Delta\phi}\rangle$ and $|\Psi_{\pi+\Delta\phi}\rangle$. Each of the ground state breaks the spin-flip symmetry.

6.1.3 Physical ways to understand symmetry breaking in quantum theory

The above understanding of symmetry breaking in quantum system is not satisfactory. It is based on a calculational trick – the variational approach, rather than physical measurements in real or numerical experiments. So what is the physical ways to understand symmetry breaking in quantum theory?

Here, we will concentrate on numerical experiments. One of a numerical experiment is the energy spectrum of transverse Ising model for $J = 1$, $B = 0.5$ (see Fig. 5.3(a,b)). The ground states have a near two-fold degeneracy, with exponentially small energy splitting in large system size limit. The appearance of such a near two-fold degeneracy is a very remarkable phenomenon.

The transverse-field Ising model has a $\mathbb{Z}_2$ spin-flip symmetry $|\uparrow\rangle \leftrightarrow |\downarrow\rangle$. But such a $\mathbb{Z}_2$ symmetry has only one dimensional representations and cannot give rise to two-fold degeneracy. So, the near two-fold degeneracy is not the exact degeneracy protected by symmetry, because they do not belong to a single irreducible representation of the $\mathbb{Z}_2$ symmetry group. One may wonder, the near two-fold degeneracy has nothing to do with the $\mathbb{Z}_2$ spin-flip symmetry. However, this is not true. If we explicitly break the the $\mathbb{Z}_2$ symmetry by adding a term $B_z \sum_i Z_i$ to the Hamiltonian of transverse Ising model, then the near two-fold degeneracy will be destroyed. Therefore, the near two-fold degeneracy is protected by the symmetry despite they do not belong to a single irreducible representation of the symmetry group (*i.e.* they are not the exact degeneracy protected by symmetry). We note that the above emergence of ground state degeneracy happens on spaces with any shape, such as a ring S^1 or a segment I. This way, we find that

Box 6.2 Symmetry breaking in quantum theory I

A quantum system with a finite symmetry group is in a symmetry breaking phase at zero-temperature, iff it has robust emergent nearly degenerate ground states that belong to atleast two different irreducible representations of the symmetry group, on any shapes of space. Here, the term "robust" means that emergent ground state degeneracy is robust against any perturbations that preserve the symmetry.

We also note that, in quantum theory, $|\Psi_+\rangle = (|\Psi_{\pi-\Delta\phi}\rangle + |\Psi_{\pi+\Delta\phi}\rangle)/2$ is also a ground state which does not break the spin-flip symmetry. In fact, for finite systems, $|\Psi_+\rangle$ represents the true ground state of the system. Such a true ground state $|\Psi_+\rangle$ does not break any symmetry. Thus, the symmetry breaking state of a system is not characterized by the symmetry breaking breaking properties of its true ground state. On the other hand, we note that $|\Psi_+\rangle$ has a GHZ-type of quantum entanglement. Therefore the symmetry breaking state of a system is characterized by the GHZ-type of quantum entanglement in this true ground state:

Box 6.3 Symmetry breaking in quantum theory II

If a quantum system with a finite symmetry group is in a symmetry breaking phase at zero-temperature, then its true ground state has a GHZ-type of quantum entanglement.

6.1.4 Compare a finite-temperature phase with a zero-temperature phase

It is interesting to compare a finite-temperature phase, *liquid*, with a zero-temperature phase, *superfluid*. A liquid is described by a random *probability* distributions of particles (such as atoms), while a superfluid is described by a quantum wave function which is the *superposition* of a set of random particle configurations:

$$|\Phi_{\text{superfluid}}\rangle = \sum_{\text{random configurations}} \left| \quad \right\rangle \tag{6.4}$$

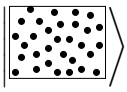

The superposition of many different particle positions are called quantum fluctuations in particle positions.

Since Landau's symmetry breaking theory suggests that all quantum phases are described by symmetry breaking, thus we can use group theory to classify all those symmetry breaking phases: All symmetry breaking quantum phases are classified by a pair of mathematical objects (G_H, G_Φ), where G_H is the symmetry group of the Hamiltonian and G_Φ is the symmetry group of the ground state. For example, the symmetry breaking phase of the transverse-field Ising model is labeled by $(\mathbb{Z}_2, \{1\})$, where $\mathbb{Z}_2$ is the symmetry group of the Hamiltonian, and $\{1\}$ is the trivial group that describe the symmetry of the ground state.

6.2 Topological order

6.2.1 The discovery of topological order

However, in late 1980s, it became clear that Landau symmetry breaking theory did not describe all possible phases. In an attempt to explain high temperature superconductivity, the chiral spin state was introduced [32, 79]. At first, physicists still wanted to use Landau symmetry breaking theory to describe the chiral spin state. They identified the chiral spin state as a state that breaks the time reversal and parity symmetries, but not the spin rotation symmetry [79]. This should be the end of story according to Landau symmetry breaking description of orders.

But, it was quickly realized that there are many different chiral spin states that have exactly the same symmetry [65]. So symmetry alone was not enough to characterize and distinguish different chiral spin states. This means that the chiral spin states must contain a new kind of order that is beyond the usual symmetry description. The proposed new kind of order was named 'topological order' [66]. (The name 'topological order' was motivated by the low energy effective theory of the chiral spin states which is a Chern-Simons theory [79] – a topological quantum field theory (TQFT) [82]). New quantum numbers (or new topological probes), such as ground state degeneracy [65, 76] and the non-Abelian geometric phase of degen-

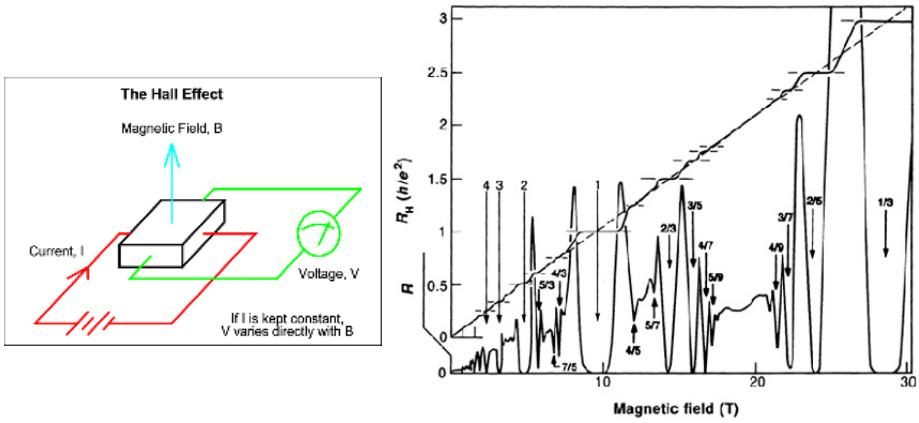

Fig. 6.4 2D electrons in strong magnetic field may form FQH states. Each FQH state has a quantized Hall coefficient R_H.

erate ground states [66, 33], were introduced to characterize/define the different topological orders in chiral spin states.

But experiments soon indicated that chiral spin states do not describe high-temperature superconductors, and the theory of topological order became a theory with no experimental realization. However, the similarity [32] between chiral spin states and fractional quantum Hall (FQH) states [59, 39] allows one to use the theory of topological order to describe different FQH states.

FQH states are gapped ground states of 2D electrons under strong magnetic field. FQH states have a property that a current density will induce an electric field in the transverse direction: $E_y = R_H j_x$ (see Fig. 6.4). It is an amazing discovery that the Hall coefficient R_H of a FQH state is precisely quantized as a rational number $\frac{p}{q}$ if we measure the Hall coefficient R_H in unit of $\frac{h}{e^2}$: $R_H = \frac{p}{q}\frac{h}{e^2}$ (see Fig. 6.4) [59]. Different quantized R_H correspond to different FQH states. Just like the chiral spin states, different FQH states all have the same symmetry and cannot be distinguished by symmetry breaking. So there is no way to use different symmetry breaking to describe different FQH states, and FQH states must contain *new* orders. One finds that the new orders in quantum Hall states can indeed be described by topological orders [76]. So the theory of topological order does have experimental realizations.

We would like to point out that before the topological-order understanding of FQH states, people have tried to use the notions of off-diagonal long-range order and order parameter from Ginzburg-Landau theory to describe FQH states [20, 51, 86, 14]. Such an effort leads to a Ginzburg-Landau Chern-Simons effective theory for FQH states [86, 14]. At same time, it was also realized that the order parameter in the Ginzburg-Landau Chern-Simons is not gauge invariant and is not physical. This is consistent with the topological-order understanding of FQH states which suggests that FQH has no off-diagonal long-range order and cannot be described by local order parameters. So we can use effective theories without order parameters

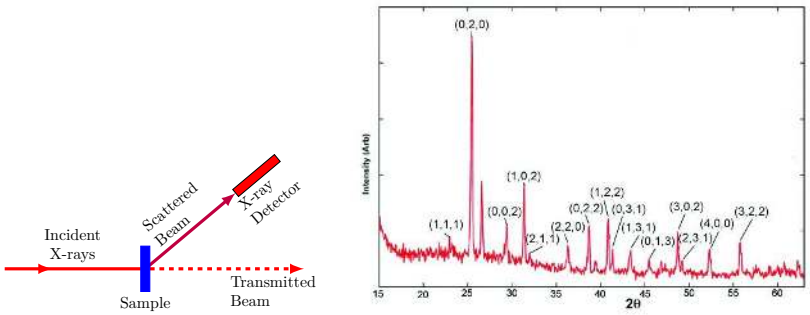

Fig. 6.5 A X-ray diffraction pattern defines/probes the crystal order.

to describe FQH states, and such effective theories are pure Chern-Simons effective theories [76, 9, 18, 16, 80, 17]. The deeper understanding gained from pure Chern-Simons effective theories leads to a K-matrix classification [80, 6] of all Abelian topologically ordered states (which include all Abelian FQH states).

FQH states were discovered in 1982 [59] before the introduction of the concept of topological order. But FQH states are not the first experimentally discovered topologically ordered states. The real-life superconductors, having a $\mathbb{Z}_2$ topological order [71, 68, 24], were first experimentally discovered topologically ordered states.[1] (Ironically, the Ginzburg-Landau symmetry breaking theory was developed to describe superconductors, despite the real-life superconductors are not symmetry breaking states, but topologically ordered states.)

6.3 A macroscopic definition of topological order

In the above, we have described topological order as a new order which is not a symmetry breaking order. But what *is* topological order? Here, we would like to point out that *to define a physical concept (such as symmetry breaking order or topological order) is to design experiments or numerical calculations that allow us to probe and characterize the concept*. For example, the concept of superfluid order, is defined by zero viscosity and the quantization of vorticity, and the concept of crystal order is defined by X-ray diffraction experiment (see Fig. 6.5).

The experiments that we use to define/characterize superfluid order and crystal order are linear responses, such as viscosity and X-ray diffraction. Linear re-

[1] Note that real-life superconductivity can be described by the Ginzburg-Landau theory with a *dynamical* $U(1)$ gauge field. The condensation of charge $2e$ electron pair break the $U(1)$ gauge theory into a $\mathbb{Z}_2$ gauge theory at low energies. A $\mathbb{Z}_2$ gauge theory is an effective theory of $\mathbb{Z}_2$ topological order. Thus a real-life superconductor has a $\mathbb{Z}_2$ topological order. In many textbook, superconductivity is described by the Ginzburg-Landau theory without the dynamical $U(1)$ gauge field, which fails to describe the real-life superconductors with dynamical electromagnetic interaction. Such a textbook superconductivity is described by a $U(1)$ symmetry breaking.

Order	Experimental probes
Crystal order	X-ray diffraction
Ferromagnetic order	Magnetization
Anti-ferromagnetic order	Neutron scattering
Superfluid order	Zero-viscosity & vorticity quantization
Topological order (Global dancing pattern)	Topological degeneracy, non-Abelian geometric phase

Table 6.1 Symmetry breaking orders can be probed/defined through linear responses. But topological order cannot be probed/defined through linear responses. We need topological probes to define topological orders.

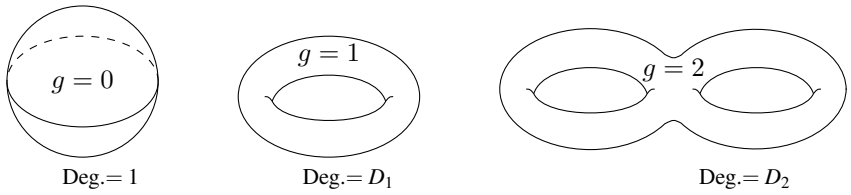

Fig. 6.6 The topological ground state degeneracies of topologically ordered states depend on the topology of the space, such as the genus g of two dimensional closed surfaces.

sponses are easily accessible in experiments and the symmetry breaking order that they define are easy to understand (see Table 6.1). However, topological order is such a new and elusive order that it cannot be probed/defined by any linear responses. To probe/define topological order we need to use very unusual 'topological' probes. In 1989, it was conjectured that topological order can be completely defined/characterized by using only two topological properties (at least in 2+1 dimensions) [66]:
(1) *Topological ground state degeneracies* on closed spaces of various topologies. (see Fig. 6.6) [65].
(2) *Non-Abelian geometric phases*[81] of those degenerate ground states from deforming the spaces (see Fig. 6.7) [66, 33].
It was through such topological probes that we introduce the concept of topological order. Just like zero viscosity and the quantization of vorticity define the concept of superfluid order, the topological degeneracy and the non-Abelian geometric phases of the degenerate ground states define the concept of topological order.

Box 6.4 Topological order
Topological order can be probed/defined by topological degeneracy and non-Abelian geometric phases of the ground states.

6.3.1 What is 'topological ground state degeneracy'

Topological ground state degeneracy, or simply, topological degeneracy is a phenomenon of quantum many-body systems, that the ground state of a gapped many-body system become degenerate in the large system size limit. The topological degeneracy has the following characters:

1. For a finite system, the topological degeneracy is not exact. The low energy ground states have a small energy splitting.
2. The topological degeneracy becomes exact when the system size becomes infinite.
3. The above property is robust against any local perturbations. In other words, the topological degeneracy *cannot be lifted by any local perturbations* as long as the system size is large [65, 76, 64, 25].
4. The topological degeneracy for a given system usually is different for different topologies of space [21]. For example, for a $\mathbb{Z}_2$ topologically ordered state in two dimensions [52, 69], the topological degeneracy is $D_g = 4^g$ on genus g Riemann surface (see Fig. 6.6).

People usually attribute the ground state degeneracy to symmetry. But topological degeneracy, being robust against any local perturbations that can break all the symmetries, is not due to symmetry. So the very existence of topological degeneracy is a surprising and amazing phenomenon. Such an amazing phenomenon defines the notion of topological order. As a comparison, we know that the existence of zero-viscosity is also an amazing phenomenon, and such an amazing phenomenon defines the notion of superfluid order. So topological degeneracy, playing the role of zero-viscosity in superfluid order, implies the existence of a new kind of quantum phase – topologically ordered phases.

6.3.2 What is 'non-Abelian geometric phase of topologically degenerate states'

However, the ground state degeneracy is not enough to completely characterize/define topological order. Two different topological orders may have exactly the same topological degeneracy on space of any topology. We would like to find, as many as possible, quantum numbers associated with the degenerate ground states, so that by measuring these quantum numbers we can completely characterize/define topological order. The non-Abelian geometric phases of topologically degenerate states are such quantum numbers [66, 33].

The non-Abelian geometric phase is a unitary matrix U that can be calculated from an one parameter family of gapped Hamiltonians H_g, $g \in [0,1]$, provided that $H_0 = H_1$ [81]. U is a one by one matrix if there is only one ground state below the gap. U is n dimensional if the ground state degeneracy is n for all $g \in [0,1]$.

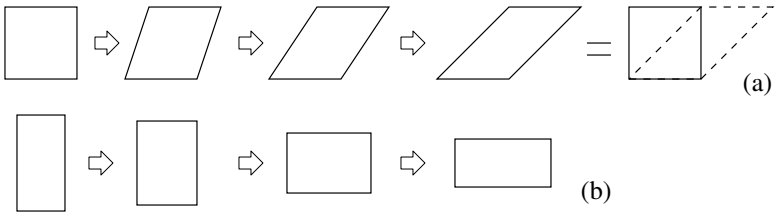

Fig. 6.7 (a) The shear deformation of a torus generate a (projective) non-Abelian geometric phase T, which is a generator of a projective representation modular transformation. The last shear-deformed torus is the same as the original torus after a coordinate transformation: $x \to x + y$, $y \to y$. (b) The squeezing deformation of a torus generate a (projective) non-Abelian geometric phase S, which is the other generator of a projective representation modular transformation. The last squeeze-deformed torus is the same as the original torus after a coordinate transformation: $x \to y$, $y \to -x$.

To use non-Abelian geometric phases to characterize/define topological order, let us put the many-body state on a torus [66, 33, 87, 88], and perform a 'shear' deformation of the torus to obtain a one parameter family of gapped Hamiltonians that form a loop (*i.e.* $H_0 = H_1$) (see Fig. 6.7a). The non-Abelian geometric phase obtained this way is denoted as T. Similarly, a 'squeezing' deformation of the torus gives rise to another non-Abelian geometric phase S. Both S and T are D_1 dimensional unitary matrices where D_1 is the topological degeneracy on torus. For different deformation paths that realize the loops in Fig. 6.7, S and T may be different. However, because the ground state degeneracy is robust, the difference is *only* in the total phase factors. Since the two deformations in Fig. 6.7 generate the modular transformations, thus S and T generate a projective representation of the modular transformations. S and T contain information about the topological properties of the topologically ordered states, such as fractional statistics [66, 33, 60, 85, 12]. It was conjectured that

Box 6.5 A complete characterization of topological order
S and T (plus the path dependent total phase factor) provides a complete characterization and definition of topological orders in 2+1 dimensions [66, 33].

6.4 A microscopic picture of topological orders

6.4.1 The essence of fractional quantum Hall states

C. N. Yang once asked: the microscopic theory of fermionic superfluid and superconductor, BCS theory, capture the essence of the superfluid and superconductor,

but what is this essence? This question led him to develop the theory of off-diagonal long range order [83] which reveal the essence of superfluid and superconductor. In fact long range order is the essence of any symmetry breaking order.

Similarly, we may ask: Laughlin's theory [39] for FQH effect capture the essence of the FQH effect, but what is this essence? Our answer is that the topological order (defined by the topological ground state degeneracy and the non-Abelian geometric phases of those degenerate ground states) is the essence of FQH effect.

One may disagree with the above statement by pointing out that the essence of FQH effect should be the quantized Hall conductance. However, such an opinion is incorrect, since even after we break the particle number conservation (which breaks the quantized Hall conductance), a FQH state is still a non-trivial state with topological degeneracy and non-Abelian geometric phases. The non-trivialness of FQH state does not rely on any symmetry (except the conservation of energy). In fact, the topological degeneracy and the non-Abelian geometric phases discussed above are the essence of FQH states which can be defined even without any symmetry. They provide a characterization and definition of topological order that does not rely on any symmetry. We would like to point out that the topological entanglement entropy is another way to characterize the topological order without any symmetry (see Chapter 5.3.2) [36, 43].

6.4.2 Intuitive pictures of topological order

Topological order is a very new concept that describes quantum entanglement in many-body systems. Such a concept is very remote from our daily experiences and it is hard to have an intuition about it. So before we define topological order in general terms (which can be abstract), let us first introduce and explain the concept through some intuitive pictures.

We can use dancing to gain an intuitive picture of topological order. But before we do that, let us use dancing picture to describe the old symmetry breaking orders (see Fig. 6.8). In the symmetry breaking orders, every particle/spin (or every pair of particles/spins) dance by itself, and they all dance in the same way. (The 'same way' of dancing represents a long-range order.) For example, in a ferromagnet, every electron has a fixed position and the same spin direction. We can describe an anti-ferromagnet by saying every pair of electrons has a fixed position and the two electrons in a pair have opposite spin directions. In a boson superfluid, each boson is moving around by itself and doing the same dance, while in a fermion superfluid, fermions dance around in pairs and each pair is doing the same dance.

We can also understand topological orders through such dancing pictures. Unlike fermion superfluid where fermions dance in pairs, a topological order is described by a global dance, where every particle (or spin) is dancing with every other particle (or spin) in a very organized way: (a) all spins/particles dance following a set of *local* dancing 'rules' trying to lower the energy of a *local* Hamiltonian. (b) If all the spins/particles follow the local dancing 'rules', then they will form a global dancing

Ferromagnet Anti-ferromagnet

Superfluid of bosons Superfluid of fermions

Fig. 6.8 The dancing patterns for the symmetry breaking orders.

FQH state String liquid (spin liquid)

Fig. 6.9 The dancing patterns for the topological orders.

pattern, which correspond to the topological order. (c) Such a global pattern of collective dancing is a pattern of quantum fluctuation which corresponds to a pattern of *long-range entanglement*. (A more rigorous definition of long-range entanglement will be given in Chapter 7.)

For example in FQH liquid, the electrons dance following the following local dancing rules:
(a) electron always dances anti-clockwise which implies that the electron wave function only depend on the electron coordinates (x,y) via $z = x + \mathrm{i}y$.
(b) each electron always takes exact three steps to dance around any other electron, which implies that the phase of the wave function changes by 6π as we move an electron around any other electron.
The above two local dancing rules fix a global dance pattern which correspond to the Laughlin wave function $\Phi_{\text{FQH}} = \prod_{i<j}(z_i - z_j)^3$ [39]. Such an collective dancing gives rise to the topological order (or long-range entanglement) in the FQH state.

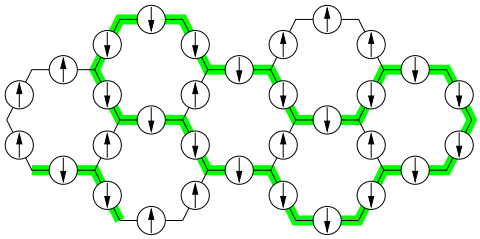

Fig. 6.10 The strings in a spin-1/2 model. In the background of up-spins, the down-spins form closed strings.

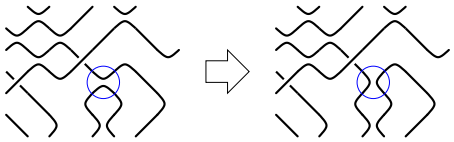

Fig. 6.11 In string liquid, strings can move freely, including reconnecting the strings.

In additional to FQH states, some spin liquids also contain topological orders [79, 52, 68, 47, 48]. (Spin liquids refer to ground states of quantum spin systems that do not *spontaneously* break the spin rotation and the translation symmetries in the spin Hamiltonians.) In those spin liquids, the spins 'dance' following the follow local dancing rules:
(a) Down spins form closed strings with no open ends, in the background of up-spins (see Fig. 6.10).
(b) Strings can otherwise move freely, including reconnect freely (see Fig. 6.11).
The global dance formed by the spins following the above dancing rules gives us a quantum spin liquid which is a superposition of all closed-string configurations [35]: $|\Phi_{\text{string}}\rangle = \sum_{\text{closed string pattern}} \left|\quad\right\rangle$. Such a state is called a string or string-net condensed state [41]. The collective dancing gives rise to a non-trivial topological order and a pattern of long range entanglement in the spin liquid state.

Box 6.6 Microscopic picture of topological order
Topological orders correspond to global correlated dances which are produced by various local dancing rules. The global correlated dances produce patterns of long-range entanglement, which is the microscopic origin of topological order.

6.5 What is the significance of topological order?

The above descriptions of topological order is intuitive and not concrete. It is not clear if the topological order (the global dancing pattern or the long-range entanglement) has any experimental significance. In order for the topological order to be a useful concept, it must have new experimental properties that are different from any symmetry breaking states. Those new experimental properties should indicate the non-trivialness of the topological order. In fact, the concept of topological order should be defined by the collection of those new experimental properties.

Indeed, topological order does have new characteristic properties. Those properties of topological orders reflect the significance of topological order:

1. The finite-energy defects of topological order (*i.e.* the quasiparticles) can carry fractional statistics [23, 2] (including non-Abelian statistics[70, 50]) and fractional charges [31, 39] (if there is a symmetry). Such a property allows us to use topologically ordered states as a medium for topological quantum memory [13] and topological quantum computations [35]. Fractional statistics and fractional charges also provide us ways to experimentally detect topological orders.
2. Some topological orders have gapless boundary excitations [22, 67, 46]. Such gapless boundary excitations are topologically protected, which cannot be gapped/localized by any impurities on the boundary. Those topologically protected gapless modes lead to perfect conducting boundary channels even with magnetic impurities [61]. This property may lead to device applications.
3. Topologically ordered states and their gapless generalization, quantum ordered states [73], can produce emergent gauge theory. Those states can gives rise to new kind of waves (*i.e.* the gapless collective excitations above the ground states)[72, 58, 74, 75, 49, 26, 45, 44, 10] that satisfy the Maxwell equations or the Yang-Mills equations [84]. The new kind of waves can be probed/studied in practical experiments, such as neutron scattering experiments [49]. (For details, see Chapter 11.)

Box 6.7 The significance of topological order
Topological order can produce quasiparticles with fraction quantum numbers and fractional statistics, robust gapless boundary states, and emergent gauge excitations.

In the following, we will study some examples of topological orders and reveal their amazing topological properties.

6.6 Quantum liquids of unoriented strings

Our first example of topological order is a quantum liquid of qubits, where qubits organize into unoriented strings. Quantum liquids of unoriented strings are simplest topologically ordered states. The strings in quantum liquids of unoriented strings can be realized in a spin-1/2 model. We can view up-spins as background and lines of down-spins as the strings (see Fig. 6.10). Clearly, such string is unoriented. The simplest topologically ordered state in such spin-1/2 system is given by the equal-weight superposition of all closed strings [35]: $|\Phi_{\mathbb{Z}_2}\rangle = \sum_{\text{all closed strings}}$  . Such a wave function represents a global dancing pattern that correspond to a non-trivial topological order.

As we have mentioned before, the global dancing pattern is determined by local dancing rules. What are those local rules that give rise to the global dancing pattern $|\Phi_{\mathbb{Z}_2}\rangle = \sum_{\text{all closed strings}}$ 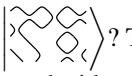 ? The first rule is that, in the ground state, the down-spins are always connected with no open ends. To describe the second rule, we need to introduce the amplitudes of close strings in the ground state: Φ  . The ground state is given by

$$\sum_{\text{all closed strings}} \Phi \left(\right) \left| \right\rangle . \tag{6.5}$$

Then the second rule relates the amplitudes of close strings in the ground state as we change the strings locally:

$$\Phi \left(\right) = \Phi \left(\right), \qquad \Phi \left(\right) = \Phi \left(\right), \tag{6.6}$$

In other words, if we locally deform/reconnect the strings as in Fig. 6.11, the amplitude (or the ground state wave function) does not change.

The first rule tells us that the amplitude of a string configuration only depend on the topology of the string configuration. Starting from a single loop, using the local deformation and the local reconnection in Fig. 6.11, we can generate all closed string configurations with any number of loops. So all those closed string configurations have the same amplitude. Therefore, the local dancing rule fixes the wave function to be the equal-weight superposition of all closed strings: $|\Phi_{\mathbb{Z}_2}\rangle = \sum_{\text{all closed strings}}$ 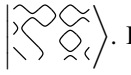 . In other words, the local dancing rule fixes the global dancing pattern.

If we choose another local dancing rule, then we will get a different global dancing pattern that corresponds to a different topological order. One of the new choices is obtained by just modifying the sign in eqn. (6.6):

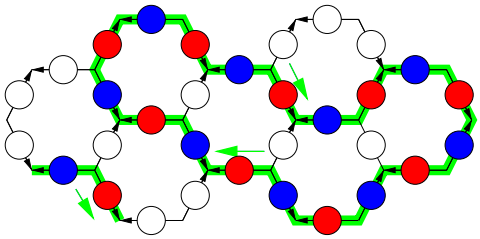

Fig. 6.12 The oriented strings in a spin-1 model. In the background of $S_z = 0$ spins (the white dots), the $S_z = 1$ spins (the red dots) and the $S_z = -1$ spins (the blue dots) form closed strings.

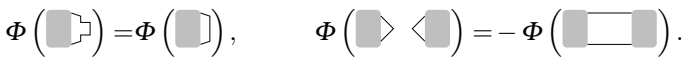

(6.7)

We note that each local reconnection operation changes the number of loops by 1. Thus the new local dancing rules gives rise to a wave function which has a form $|\Phi_{\text{Sem}}\rangle = \sum_{\text{all closed strings}} (-)^{N_{\text{loops}}}$  , where N_{loops} is the number of loops. The wave function $|\Phi_{\text{Sem}}\rangle$ corresponds to a different global dance and a different topological order.

In the above, we constructed two quantum liquids of unoriented strings in a spin-1/2 model. Using a similar construction, we can also obtain a quantum liquid of oriented strings which gives rise to waves satisfying Maxwell equation as discussed before (see Chapter 11). To obtain quantum liquid of oriented strings, we need to start with a spin-1 model, where spins live on the links of honeycomb lattice (see Fig. 6.12). Since the honeycomb lattice is bipartite, each link has an orientation from the A-sublattice to the B-sublattice (see Fig. 6.12). The oriented strings is formed by alternating $S_z = \pm 1$ spins on the background of $S_z = 0$ spins. The string orientation is given be the orientation of the links under the $S_z = 1$ spins (see Fig. 6.12). The superposition of the oriented strings gives rise to quantum liquid of oriented strings.

6.7 The emergence of fractional quantum numbers and Fermi/fractional statistics

Why the two wave functions of unoriented strings, $|\Phi_{\mathbb{Z}_2}\rangle$ and $|\Phi_{\text{Sem}}\rangle$, have non-trivial topological orders? This is because the two wave functions give rise to non-trivial topological properties. The two wave functions correspond to different topological orders since they give rise to different topological properties. In this section, we will discuss two topological properties: emergence of fractional statistics and topological degeneracy on compact spaces.

6.7.1 Emergence of fractional angular momenta

The two topological states in two dimensions contain only closed strings, which represent the ground states. If the wave functions contain open strings (*i.e.* have non-zero amplitudes for open string states), then the ends of the open strings will correspond to point-like topological excitations above the ground states. Although an open string is an extended object, its middle part merge with the strings already in the ground states and is unobservable. Only its two ends carry energies and correspond to two point-like particles.

We note that such a point-like particle from an end of string cannot be created alone. Thus an end of string correspond to a topological point defect, which may carry fractional quantum numbers. This is because an open string as a whole always carry non-fractionalized quantum numbers. But an open string corresponds to *two* topological point defects from the two ends. So we cannot say that each end of string carries non-fractionalized quantum numbers. Some times, they do carry fractionalized quantum numbers.

Let us first consider the defects in the $|\Phi_{\mathbb{Z}_2}\rangle$ state. To understand the fractionalization, let us first consider the spin of such a defect to see if the spin is fractionalized or not [15, 63]. An end of string can be represented by

$$|\,\vert\,\rangle_{\text{def}} = |\,\vert\,\rangle + |\,\circlearrowright\,\rangle + |\,0\,\rangle + \ldots. \tag{6.8}$$

which is an equal-weight superposition of all string states obtained from the deformations and the reconnections of $\vert$.

Under a 360° rotation, the end of string is changed to $|\,\text{◉}\,\rangle_{\text{def}}$, which is an equal weight superposition of all string states obtained from the deformations and the reconnections of ◉. Since $|\,\vert\,\rangle_{\text{def}}$ and $|\,\text{◉}\,\rangle_{\text{def}}$ are alway different, $|\,\vert\,\rangle_{\text{def}}$ is not an eigenstate of 360° rotation and does not carry a definite spin.

To construct the eigenstates of 360° rotation, let us make a 360° rotation to $|\,\text{◉}\,\rangle_{\text{def}}$. To do that, we first use the string reconnection move in Fig. 6.11, to show that $|\,\text{◉}\,\rangle_{\text{def}} = |\,\text{◉}\,\rangle_{\text{def}}$. A 360° rotation on $|\,\text{◉}\,\rangle_{\text{def}}$ gives us $|\,\vert\,\rangle_{\text{def}}$.

We see that the 360° rotation exchanges $|\,\vert\,\rangle_{\text{def}}$ and $|\,\text{◉}\,\rangle_{\text{def}}$. Thus the eigenstates of 360° rotation are given by $|\,\vert\,\rangle_{\text{def}} + |\,\text{◉}\,\rangle_{\text{def}}$ with eigenvalue 1, and by $|\,\vert\,\rangle_{\text{def}} - |\,\text{◉}\,\rangle_{\text{def}}$ with eigenvalue -1. So the particle $|\,\vert\,\rangle_{\text{def}} + |\,\text{◉}\,\rangle_{\text{def}}$ has a spin 0 (mod 1), and the particle $|\,\vert\,\rangle_{\text{def}} - |\,\text{◉}\,\rangle_{\text{def}}$ has a spin 1/2 (mod 1).

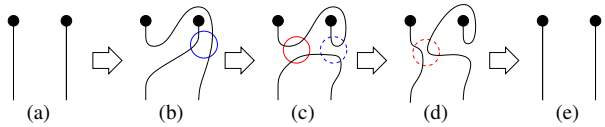

Fig. 6.13 Deformation of strings and two reconnection moves, plus an exchange of two ends of strings and a 360° rotation of one of the end of string, change the configuration (a) back to itself. Note that from (a) to (b) we exchange the two ends of strings, and from (d) to (e) we rotate of one of the end of string by 360°. The combination of those moves do not generate any phase.

6.7.2 Emergence of Fermi and fractional statistics

If one believes in the spin-statistics theorem, one may guess that the particle $|\uparrow\rangle_{\text{def}} + |\circlearrowleft\rangle_{\text{def}}$ is a boson and the particle $|\uparrow\rangle_{\text{def}} - |\circlearrowleft\rangle_{\text{def}}$ is a fermion. This guess is indeed correct. Form Fig. 6.13, we see that we can use deformation of strings and two reconnection moves to generate an exchange of two ends of strings and a 360° rotation of one of the end of string. Such operations allow us to show that Fig. 6.13a and Fig. 6.13e have the same amplitude, which means that an exchange of two ends of strings followed by a 360° rotation of one of the end of string do not generate any phase. This is nothing but the spin-statistics theorem.

The emergence of Fermi statistics in the $|\Phi_{\mathbb{Z}_2}\rangle$ state of a purely bosonic spin-1/2 model indicates that the state is a topologically ordered state. We also see that the $|\Phi_{\mathbb{Z}_2}\rangle$ state has a bosonic quasi-particle $|\uparrow\rangle_{\text{def}} + |\circlearrowleft\rangle_{\text{def}}$, and a fermionic quasi-particle $|\uparrow\rangle_{\text{def}} - |\circlearrowleft\rangle_{\text{def}}$. The bound state of the above two particles is a boson (not a fermion) due to their mutual semion statistics. Such quasi-particle content agrees exactly with the $\mathbb{Z}_2$ gauge theory which also has three type of non-trivial quasi-particles excitations, two bosons and one fermion. In fact, the low energy effective theory of the topologically ordered state $|\Phi_{\mathbb{Z}_2}\rangle$ is the $\mathbb{Z}_2$ gauge theory and we will call $|\Phi_{\mathbb{Z}_2}\rangle$ a $\mathbb{Z}_2$ topologically ordered state.

Next, let us consider the defects in the $|\Phi_{\text{Sem}}\rangle$ state. Now

$$|\uparrow\rangle_{\text{def}} = |\uparrow\rangle + |\uparrow\circlearrowleft\rangle - |\uparrow 0\rangle + ... \tag{6.9}$$

and a similar expression for $|\circlearrowleft\rangle_{\text{def}}$, due to a change of the local dancing rule for reconnecting the strings (see eqn. (6.7)). Using the string reconnection move in Fig. 6.11, we find that $|\circlearrowleft\rangle_{\text{def}} = -|\circlearrowleft\rangle_{\text{def}}$. So a 360° rotation, changes $(|\uparrow\rangle_{\text{def}}, |\circlearrowleft\rangle_{\text{def}})$ to $(|\circlearrowleft\rangle_{\text{def}}, -|\uparrow\rangle_{\text{def}})$. We find that $|\uparrow\rangle_{\text{def}} + \mathrm{i}|\circlearrowleft\rangle_{\text{def}}$ is the eigenstate of the 360° rotation with eigenvalue $-\mathrm{i}$, and $|\uparrow\rangle_{\text{def}} - \mathrm{i}|\circlearrowleft\rangle_{\text{def}}$ is the other eigenstate of the 360° rotation with eigenvalue i. So the particle $|\uparrow\rangle_{\text{def}} + \mathrm{i}|\circlearrowleft\rangle_{\text{def}}$ has a spin $-1/4$, and the particle

$|\uparrow\rangle_{\text{def}} - \mathrm{i}\,|\circlearrowleft\rangle_{\text{def}}$ has a spin $1/4$. The spin-statistics theorem is still valid for $|\Phi_{\text{Sem}}\rangle_{\text{def}}$ state, as one can see form Fig. 6.13. So, the particle $|\uparrow\rangle_{\text{def}} + \mathrm{i}\,|\circlearrowleft\rangle_{\text{def}}$ and particle $|\uparrow\rangle_{\text{def}} - \mathrm{i}\,|\circlearrowleft\rangle_{\text{def}}$ have fractional statistics with statistical angles of semion: $\pm\pi/2$. Thus the $|\Phi_{\text{Sem}}\rangle$ state contains a non-trivial topological order. We will call such a topological order a double-semion topological order.

It is amazing to see that the long-range quantum entanglement in string liquid can gives rise to fractional spin and fractional statistics, even from a purely bosonic model. Fractional spin and Fermi statistics are two of most mysterious phenomena in natural. Now, we can understand them as merely a phenomenon of long-range quantum entanglement. They are no longer mysterious.

Box 6.8 Fractional quantum numbers and fractional statistics
Fractional quantum numbers and fractional statistics can be determined from the global dancing pattern (*i.e.* the pattern of long-range entanglement) in the ground state.

6.8 Topological degeneracy of unoriented string liquid

The $\mathbb{Z}_2$ and the double-semion topological states (as well as many other topological states) have another important topological property: topological degeneracy [65, 66]. Topological degeneracy is the ground state degeneracy of a gapped many-body system that is robust against any local perturbations as long as the system size is large. We like to make a few remarks.

1. Topological degeneracy can be used as protected qubits which allows us to perform topological quantum computation [35].
2. It is believed that the appearance of topological degeneracy implies the topological order (or long-range entanglement) in the ground state [65, 66].
3. Many-body states with topological degeneracy are described by topological quantum field theory at low energies [82].

The simplest topological degeneracy appears when we put topologically ordered states on compact spaces with no boundary. We can use the global dancing pattern to understand the topological degeneracy. We know that the local dancing rules determine the global dancing pattern. On a sphere, the local dancing rules determine a unique global dancing pattern. So the ground state is non-degenerate. However on other compact spaces, there can be several global dancing patterns that all satisfy the local dancing rules. In this case, the ground state is degenerate.

For the $\mathbb{Z}_2$ topological state on torus, the local dancing rule relate the amplitudes of the string configurations that differ by a string reconnection operation in Fig. 6.11.

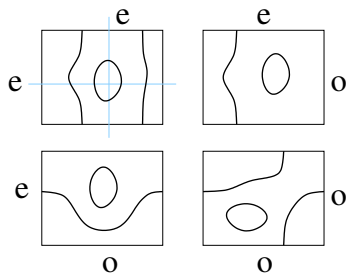

Fig. 6.14 On a torus, the closed string configurations can be divided into four sectors, depending on even or odd number of strings crossing the x- or y-axises.

On a torus, the closed string configurations can be divided into four sectors (see Fig. 6.14), depending on even or odd number of strings crossing the x- or y-axises. The string reconnection move only connect the string configurations within each sector. So the superposition of the string configurations in each sector represents a different global dancing pattern. Most importantly, we cannot distinguish the four global dancing patterns locally by examine a local region of the system, since they all follow the same local dancing rule. As a result, the four global dancing patterns degenerate ground states. Therefore, the local dancing rule for the $\mathbb{Z}_2$ topological order gives rise to four fold degenerate ground state on torus [68]. Similarly, the double-semion topological order also gives rise to four fold degenerate ground state on torus.

Box 6.9 Topological degeneracy
The topological degeneracy is determined from the global dancing pattern (*i.e.* the pattern of long-range entanglement) in the ground state.

6.9 Topological excitations and string operators

In the last a few sections, we have used simple intuitive pictures to explain several important properties of topologically ordered states. We stress that those topological properties are results of long-range entanglement in the ground state. In this section, we will use more rigorous approach to obtain those topological properties

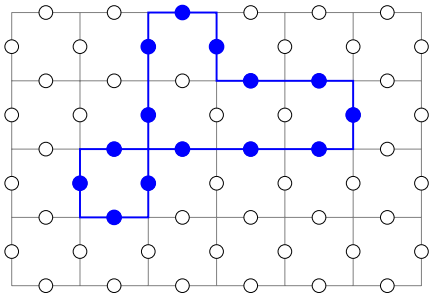

Fig. 6.15 The toric code model with spin-1/2 spins on the links. A light dot represents a up-spin and a dark dot a down-spin. A closed string state is shown.

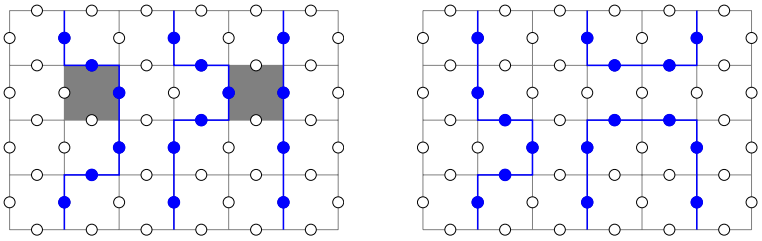

Fig. 6.16 Applying the $\prod_{j\in \text{plaquette}(p)} X_j$ operator to the shaded squares will change the shape of the string, or reconnect the strings.

6.9.1 Toric code model and string condensation

The $\mathbb{Z}_2$ topological order from the condensation of unoriented strings can be realized by the toric code model (see Chapter 3.5) [35], which is formed by spin-1/2 spins on links of square lattice. The Hamiltonian is given by

$$H_{\mathbb{Z}_2} = -U\sum_s Q_s - g\sum_p B_p, \quad B_p \equiv \prod_{j\in \text{plaquette}(p)} X_j, \quad Q_s \equiv \prod_{j\in \text{star}(s)} Z_j. \tag{6.10}$$

Here p labels the plaquettes and $\prod_{j\in \text{plaquette}(p)} X_j$ is the product of the four Pauli operators X_j on the four edges of the plaquette p. s labels the vertices and $\prod_{j\in \text{star}(s)} Z_j$ is the product of the four Pauli operators Z_j on the four legs of the vertex s.

If we view an up-spin as a state with no string and string as line of down-spins, we find that the U-terms enforce the first dancing rule to make spins to form closed strings in the ground state. Since $\prod_{j\in \text{star}(s)} Z_j = 1$ for all closed string states (including the no string state), all closed string states have the same low energy. Every end of open string will cost an energy $+2U$.

If we only have the U-terms, the ground states will be highly degenerate which include all the closed string states. The g-term enforce the second dancing rule where only a particular 'dance' (*i.e.* superposition) of closed string corresponds to the ground state. We note that the operator $\prod_{j\in \text{plaquette}(p)} X_j$ creates/annhilates

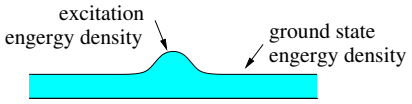

Fig. 6.17 The energy density distribution of a particle-like excitation.

a small loop of string around a square. So the operator will change the shape of the strings or reconnect the strings (see Fig. 6.16). Due to the minus sign in the g-term, The change of the shapes and the reconnection of the strings will not change the amplitude. Thus, the different shapes and different connections of closed strings in the ground state will have the same amplitude. Therefore, the ground state of $H_{\mathbb{Z}_2}$ satisfies the two dancing rules and describe the $\mathbb{Z}_2$ topological order.

In fact since $[Q_s, B_p] = 0$, $H_{\mathbb{Z}_2}$ is exactly soluble. The exact eigenstates of $H_{\mathbb{Z}_2}$ are the common eigenstates of Q_s and B_p where the eigenvalues of Q_s is $q_s = \pm 1$ and the eigenvalues of B_p is $b_p = \pm 1$. The energy of an eigenstate is given by $-U\sum_s q_s - g\sum_p b_p$. The ground state is given by $|\Psi_{\text{grnd}}\rangle = |q_s = b_p = 1\rangle$. We can show that the state $|q_s = b_p = 1\rangle$ is an equal weight superposition of all closed string states: $|q_s = b_p = 1\rangle = \sum |\text{all closed-strings}\rangle$.

Using the arguments in Section 6.8, we see that the ground states of $H_{\mathbb{Z}_2}$ have a four-fold degeneracy on torus. The four-fold degeneracy can also be understood through the following argument. We note that there are operator identities $\prod_s Q_s = 1$ and $\prod_p F_p = 1$ if the square lattice form a torus. Therefore, the number of independent quantum numbers $b_p = \pm 1$, $q_s = \pm 1$ on torus is $2^N_{\text{site}} 2^N_{\text{site}}/4$ where N_{site} is the number of sites. The number of states on torus $2^N_{\text{site}} 2^N_{\text{site}}$. So the number of independent labels $b_p = \pm 1$, $q_s = \pm 1$ is 1/4 of the number of states. Each label correspond to 4 states. Since, the energy is a function of b_p, q_s. The degeneracy of each energy eigenvalue (including the ground states) is 4. Such a four-fold degeneracy is a topological degeneracy, which implies that the ground states of $H_{\mathbb{Z}_2}$ have a nontrivial topological order.

Next, we will discuss the quasiparticle excitations in the $\mathbb{Z}_2$ topologically ordered state described by $H_{\mathbb{Z}_2}$. In particular, we will discuss their nontrivial statistics. But before we do that, we would like to have a general discussion of topological excitations. Only topological excitations can have nontrivial statistics and fractional quantum numbers.

6.9.2 Local and topological excitations

Topological orders (or patterns of long range entanglement) can be characterized by the appearance of the 'topological excitations'. In this section, we will discuss/define the notion of topological excitations.

First we define the notion of 'particle-like' excitations. Consider a system with translation symmetry. The ground state has a uniform energy density. If we have a

state with an excitation, we can measure the energy distribution of the state over the space. If for a local area, the energy density is higher than ground state, while for the rest area the energy density is the same as ground state, one may say that there is a 'particle-like' excitation, or a quasiparticle, in this area (see Fig. 6.17). Quasiparticles defined like this can be further divided into two classes. The first class can be created or annihilated by local operators, such as a spin flip. So the first class of the particle-like excitations is called local quasiparticle excitations. The second class cannot be created or annihilated by any finite number of local operators (in the infinite system size limit). In other words, the higher local energy density cannot be created or removed by *any* local operators in that area. The second class of the particle-like excitations is called topological quasiparticle excitations.

From the notions of local quasiparticles and topological quasiparticles, we can also introduce a notion of topological quasiparticle types, or simply, quasiparticle types. We say that local quasiparticles belong to the trivial type, while topological quasiparticles belong to nontrivial types. Also two topological quasiparticles are of the same type if and only if they differ by local quasiparticles. In other words, we can turn one topological quasiparticle into the other one of the same type by applying some local operators.

Box 6.10 Topological excitation

A topological excitation is a particle-like excitation with localized energy, that cannot be created/annihlate by any local operators near the excitation.

The $\mathbb{Z}_2$ topologically ordered state described by $H_{\mathbb{Z}_2}$ have nontrivial topological excitations. In fact, it has three types of nontrivial topological excitations. In the following, we will discuss those topological excitations.

6.9.3 Three types of quasiparticles

The first type of topological excitations, denoted as e, corresponds to ends of strings which we have discussed before. In the $\mathbb{Z}_2$ model $H_{\mathbb{Z}_2}$, the ground state is described by $|\Psi_{\text{grnd}}\rangle = |q_s = b_p = 1\rangle$. If we change one q_s from 1 to -1, we will create a topological excitation of the first type. We see that, to create a topological excitation of the first type, we break the first dancing rule – the closed string condition.

In contrast, to create a topological excitation of the second type, denoted as m, we keep the first dancing rule, but break the second dancing rule – the equal amplitude condition. If there is a topological excitation of the second type at x, it wave function given by

$$\Phi(X_{\text{open}}) = 0, \quad \Phi(X_{\text{closed}}) = (-)^{W_x(X_{\text{closed}})}, \tag{6.11}$$

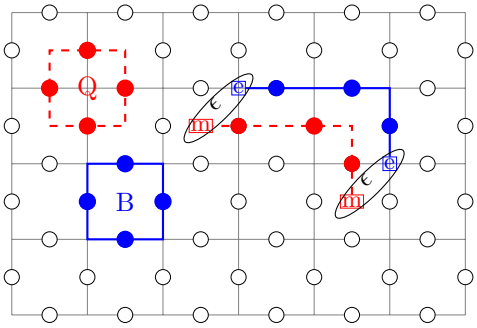

Fig. 6.18 The black lines are the type-I strings and the shaded lines are the type-II strings. Here, the open type-I string and the open type-II string are related by a displacement $(1/2, 1/2)$. A type-I string operator is a product of X_i's on a type-I string. A type-II string operator is a product of Z_i's on a type-II string.

where X_{open} represents string configurations with open ends, and X_{closed} represents closed string configurations. Here $W_x(X_{\text{closed}})$ is the number of times that the closed strings wind around x. In the $\mathbb{Z}_2$ model $H_{\mathbb{Z}_2}$, if we change one b_p from 1 to -1, we will create a topological excitation of the second type.

The third type of topological excitations, denoted as ε, corresponds to the bond states of one e and one m. The above three nontrivial topological excitations plus the trivial one are the four types of topological excitations in the $\mathbb{Z}_2$ topologically ordered state.

6.9.4 Three types of string operators

As we have stressed that, although the excitations e, m, and ε have local energy distributions, they cannot be created by local operators. However, we can create a pair of e via a non-local string operator. Similarly, we can also create a pair of m or ε via other non-local string operators.

First let us introduce a notion of type-I string. A type-I string is a string formed by the links of the square lattice which connects the vertices of the square lattice (see Fig. 6.18). A type-I string operator $W_{\text{type-I}}$ is a product of X_i's on a type-I string (see Fig. 6.18):

$$W_{\text{type-I}} = \prod_{i \in \text{type-I string}} X_i. \tag{6.12}$$

A type-I string operator creates an open string, and creates two e's at its two ends (see Fig. 6.18).

A type-II string is a string formed by the lines that connects the squares of the square lattice (see Fig. 6.18). A type-II string operator $W_{\text{type-II}}$ is a product of Z_i's on a type-II string (see Fig. 6.18):

$$W_{\text{type-II}} = \prod_{i\in\text{type-II string}} Z_i. \tag{6.13}$$

A type-II string operator creates two m's at its two ends (see Fig. 6.18). This is because the type-II string operator anti-commutes with the two B_p operators at its two ends and commute with other B_p operators. So a type-II string operator flips the sign of b_p at its two ends and hence creates to m excitations. It is interesting to note that B_p is a small loop of type-I string operator and Q_I is a small loop of type-II string operator (see Fig. 6.18).

A type-III string operator $W_{\text{type-III}}$ is a product of a type-I string operator $W_{\text{type-I}}$ and a type-II string operator $W_{\text{type-II}}$:

$$W_{\text{type-III}} = \prod_{i\in\text{type-I string}} X_i \prod_{i\in\text{type-II string}} Z_i, \tag{6.14}$$

where the type-II string is obtained by displacing the type-I string by $(1/2, 1/2)$ (see Fig. 6.18). A type-III string operator creates two ε's at its two ends (see Fig. 6.18).

Box 6.11 String operator and topological excitation
A pair of topological excitation can be created by an open string operator at the two ends of the open string.

Although the string operator is non-local, it creates a two point-like energy distribution (*i.e.* two quasiparticles) at its two ends. In other words, the closed string operators without ends commute with the Hamiltonian and leave the ground state unchanged:

$$\begin{aligned}
&[W^{\text{closed}}_{\text{type-I}}, H_{\mathbb{Z}_2}] = [W^{\text{closed}}_{\text{type-II}}, H_{\mathbb{Z}_2}] = [W^{\text{closed}}_{\text{type-III}}, H_{\mathbb{Z}_2}] = 0,\\
&W^{\text{closed}}_{\text{type-I}}|\Psi_{\text{grnd}}\rangle = W^{\text{closed}}_{\text{type-II}}|\Psi_{\text{grnd}}\rangle = W^{\text{closed}}_{\text{type-III}}|\Psi_{\text{grnd}}\rangle = |\Psi_{\text{grnd}}\rangle.
\end{aligned} \tag{6.15}$$

We also note that, on a torus, a closed string operator (such as $W^{\text{closed}}_{\text{type-I}}$) can map a degenerate ground state of $H_{\mathbb{Z}_2}$ to another ground state if the closed string operator winds all the way around the torus. This is because $W^{\text{closed}}_{\text{type-I}}$ can change the number of closed strings going around the torus by an odd number. Since the closed string operator that winds all the way around the torus contains L local operators where L is the linear size of the system, therefore, we can use a product of L local operators to mix the different degenerate ground states. But we cannot use a product of any finite numbers of local operators to mix the different degenerate ground states in the $L \to \infty$ limit. So the 'code distance' (see Section 3.3) for the degenerate ground states is large (of order L). This large 'code distance' is why the ground state degeneracy is robust against any local perturbations, since a local perturbation always contains a finite number of local operators which cannot mix the degenerate ground states.

Let $W^{\text{closed}}_{\text{type-I;x}}$ be the type-I closed string operator that winds around the torus once in x-direction. Let $W^{\text{closed}}_{\text{type-I;y}}$ be the type-I closed string operator that winds around the

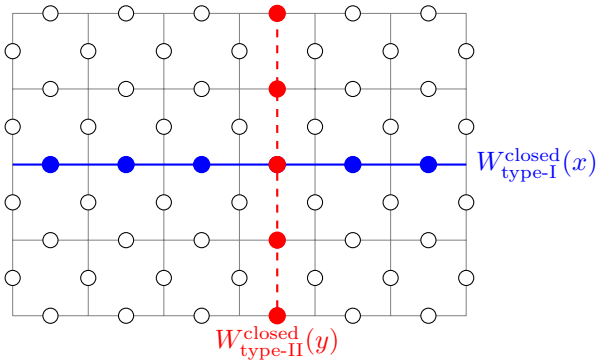

Fig. 6.19 The type-I and type-II closed string operators.

torus once in y-direction. Similarly, we can also define $W^{\text{closed}}_{\text{type-II;x}}$ and $W^{\text{closed}}_{\text{type-II;y}}$. We find that

$$\begin{aligned} W^{\text{closed}}_{\text{type-I;x}} W^{\text{closed}}_{\text{type-II;y}} &= -W^{\text{closed}}_{\text{type-II;y}} W^{\text{closed}}_{\text{type-I;x}}, \\ W^{\text{closed}}_{\text{type-I;y}} W^{\text{closed}}_{\text{type-II;x}} &= -W^{\text{closed}}_{\text{type-II;x}} W^{\text{closed}}_{\text{type-I;y}}. \end{aligned} \tag{6.16}$$

So the closed string operators form two independent algebra $\hat{A}\hat{B} = -\hat{B}\hat{A}$. Since the algebra $\hat{A}\hat{B} = -\hat{B}\hat{A}$ has only one two-dimensional irreducible representation, the algebra of the closed string operators eqn. (6.16) has only one four-dimensional irreducible representation. Since all closed string operators commute with $H_{\mathbb{Z}_2}$, all the eigenvalues of $H_{\mathbb{Z}_2}$ are four-fold degenerate.

6.9.5 Statistics of ends of strings

We have seen that a pair of topological excitations e can be created by a type-I open string operator $W_{\text{type-I}}$. Since $W_{\text{type-I}}$ is a product of bosonic spin operators, It can only create bosonic excitations. So a pair of e must be bosonic. But what is the statistics of a single e. Since the bound state of two e's is a boson, the statistics of a single e can be bosonic, fermionic, or semionic. To go further, we need a new way to calculate the statistics of a single e.

To obtain a new way to calculate the statistics of a particle-like excitation, we note that the statistics of a particle is determined by hopping operators of the particle [40]. Let $|i\cdots\rangle$ be a state with the particle at site i, where $\cdots$ describes the location of other particles. The hopping operator $\hat{t}_{ji}$ moves the particle at site-i to site-j:

$$|j\cdots\rangle = \hat{t}_{ji}|i\cdots\rangle. \tag{6.17}$$

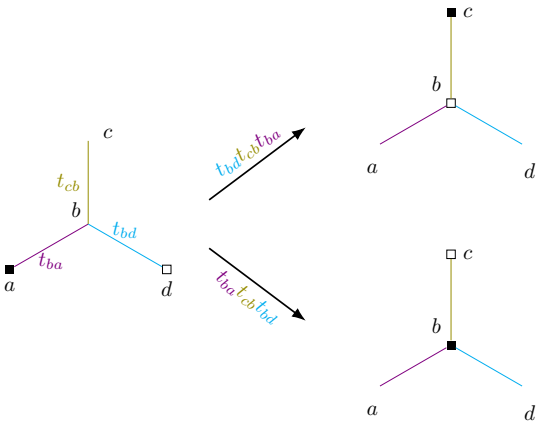

Fig. 6.20 There are two ways to move a two-particle state (with the two particles at site-a and site-d) to another two-particle state (with the two particles at site-b and site-c). The ways differ by an exchange of the two particles.

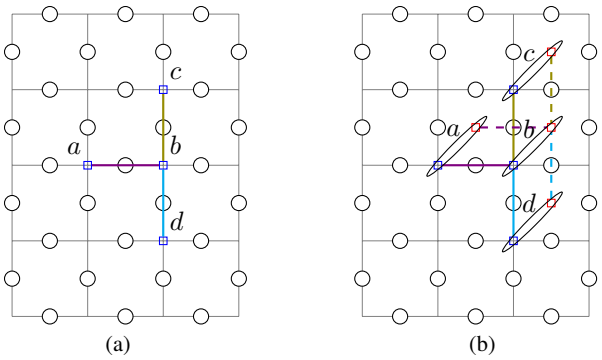

Fig. 6.21 (a) Type-e particles hoping among the four sites a, b, c, d. (b) Type-ε particles hoping among the four sites a, b, c, d.

From Fig. 6.20, we see that, starting from a two-particle state with the two particle at site-a and site-d, there are two ways to move the two particles to site-b and site-c. The two ways of hopping differ by an exchange of the two particles. Therefore, the statistics of the particle can be determined by the algebra of the hopping operators. If the hopping operator satisfies

$$\hat{t}_{bd}\hat{t}_{cb}\hat{t}_{ba} = \mathrm{e}^{\mathrm{i}\theta}\hat{t}_{ba}\hat{t}_{cb}\hat{t}_{bd}, \tag{6.18}$$

then the statistics of the particle is given by $\mathrm{e}^{\mathrm{i}\theta}$.

So, to calculate the statistics of e, we need to know the algebra of the hopping operator for e. This can be easily done since the hopping operator $\hat{t}_{ji}$ for e is nothing but the type-I open string operator $W_{\text{type-I}}$ that connect the site-i and site-j. There-

fore, the algebra of the open string operator determine the statistics of the string ends.

For type-e particles, hoping among the four sites a, b, c, d in Fig. 6.21a, their hopping operators are given by $\hat{t}_{ba} = \sigma_1^x$, $\hat{t}_{cb} = \sigma_2^x$, $\hat{t}_{bd} = \sigma_3^x$. We note that the sites for the type-e particles are vertices of the lattice. We find $\hat{t}_{bd}\hat{t}_{cb}\hat{t}_{ba} = \hat{t}_{ba}\hat{t}_{cb}\hat{t}_{bd}$. Thus the type-$e$ particles (*i.e.* the ends of type-I string) are a boson.'

Similarly, we can calculate the statistics of type-ε particles. For type-ε particles, hoping among the four sites a, b, c, d in Fig. 6.21b, their hopping operators are given by $\hat{t}_{ba} = \sigma_1^x\sigma_2^z$, $\hat{t}_{cb} = \sigma_2^x\sigma_4^z$, $\hat{t}_{bd} = \sigma_3^x\sigma_5^z$. We note that the sites for the type-e particles are represented by the ellipses in Fig. 6.21b. We find $\hat{t}_{bd}\hat{t}_{cb}\hat{t}_{ba} = -\hat{t}_{ba}\hat{t}_{cb}\hat{t}_{bd}$. The type-$\varepsilon$ particles (*i.e.* the ends of type-III strings) are fermions.

Using the same method, we can show that the type-m particles are bosons. We note that the sites for the type-m particles are at the center of squares.

Box 6.12 Hopping algebra and statistics of the ends of string

An open string operator can be viewed as a hopping operator for its ends. The statistics of the ends of string is determined by the hopping algebra of the open string operators.

6.10 Summary and further reading

In this chapter, we introduced a macroscopic definition of topological order in terms of the topological degeneracy and the non-Abelian geometric phases of the ground states. We also discussed some microscopic pictures of topological orders, the global dance, that lead to simple microscopic many-body wave functions, realizing the topologically ordered states. Through those wave functions, we calculate some physical properties, such as fraction quantum number and fractional statistics, of topological order.

The simple local dancing rules eqn. (6.6) and eqn. (6.7) can be generalized, which allow strings to have different types and allow three strings to join at a point. The generalized local dancing rules can be quantitatively described by a complex tensor $F^{ijm,\alpha}_{kln,\beta}$. Not all the tensors $F^{ijm,\alpha}_{kln,\beta}$ can lead to a global dancing pattern. Only the tensors that satisfy certain conditions can lead to valid global dancing patterns (*i.e.* well defined many-body wave functions). By find all those valid tensors, we can obtain a systematic theory for a class of topological order in 2+1 dimensions with gapped boundary. We can even calculate the topological properties of the topological order, such as the ground state degeneracy and the fractional statistics, from the valid tensors $F^{ijm,\alpha}_{kln,\beta}$. For more details, see Refs. [42, 27, 11, 28, 62, 34, 30, 29].

We can also use sequences of integers $\{S_a\}$, $a = 2, 3, \cdots$ (the pattern of zeros), to quantitatively describe local dancing rules in FQH wave functions. Again, not all the sequences $\{S_a\}$ give rise to valid global dances. Only the sequences that

satisfy certain conditions can lead to valid global dancing patterns (*i.e.* well defined many-body wave functions). By find all those valid sequences, we obtain a quite systematic theory for a class of FQH states. We can even calculate the topological properties of the FQH states, such as the ground state degeneracy and the fractional charges, from the valid sequences. For more details, see Refs. [55, 7, 56, 77, 78, 1, 53, 57, 8, 3, 54, 4, 5].

References

1. Eddy Ardonne, Emil J Bergholtz, Janik Kailasvuori, and Emma Wikberg. Degeneracy of non-abelian quantum hall states on the torus: domain walls and conformal field theory. *Journal of Statistical Mechanics: Theory and Experiment*, 2008(04):P04016, 2008.
2. D. Arovas, J. R. Schrieffer, and F. Wilczek. Fractional statistics and the quantum hall effect. *Phys. Rev. Lett.*, 53:722–723, 1984.
3. Maissam Barkeshli and Xiao-Gang Wen. Structure of quasiparticles and their fusion algebra in fractional quantum hall states. *Phys. Rev. B*, 79:195132, 2009.
4. Maissam Barkeshli and Xiao-Gang Wen. Classification of abelian and non-abelian multilayer fractional quantum hall states through the pattern of zeros. *Phys. Rev. B*, 82:245301, 2010.
5. Maissam Barkeshli and Xiao-Gang Wen. Non-abelian two-component fractional quantum hall states. *Phys. Rev. B*, 82:233301, 2010.
6. D. Belov and G. W. Moore. Classification of abelian spin Chern-Simons theories. 2005.
7. E. J. Bergholtz, J. Kailasvuori, E. Wikberg, T. H. Hansson, and A. Karlhede. The pfaffian quantum hall state made simple–multiple vacua and domain walls on a thin torus. *Phys. Rev. B*, 74:081308, 2006.
8. B. Andrei Bernevig and F. D. M. Haldane. Fractional quantum hall states and jack polynomials. *Phys. Rev. Lett.*, 100:246802, 2008.
9. B. Blok and Xiao-Gang Wen. Effective theories of fractional quantum hall effect: Hierarchical construction. *Phys. Rev. B*, 42:8145, 1990.
10. C. Castelnovo, R. Moessner, and S. L. Sondhi. Spin Ice, Fractionalization and Topological Order. *Annual Review of Condensed Matter Physics*, 3:35, 2012.
11. Xie Chen, Zheng-Cheng Gu, and Xiao-Gang Wen. Local unitary transformation, long-range quantum entanglement, wave function renormalization, and topological order. *Phys. Rev. B*, 82:155138, 2010.
12. L. Cincio and G. Vidal. Characterizing topological order by studying the ground states of an infinite cylinder. *Phys. Rev. Lett.*, 110:067208, 2013.
13. Eric Dennis, Alexei Kitaev, Andrew Landahl, and John Preskill. Topological quantum memory. *J. Math. Phys.*, 43:4452–4505, 2002.
14. Z. F. Ezawa and A. Iwazaki. *Phys. Rev. B*, 43:2637, 1991.
15. L. Fidkowski, M. Freedman, C. Nayak, K. Walker, and Z. Wang. From String Nets to Non-abelions. 2006.
16. J. Fröhlich and T. Kerler. *Nucl. Phys. B*, 354:369, 1991.
17. J. Fröhlich and U. M. Studer. *Rev. of Mod. Phys.*, 65:733, 1993.
18. J. Fröhlich and A. Zee. *Nucl. Phys. B*, 364:517, 1991.
19. V. L. Ginzburg and L. D. Landau. On the theory of superconductivity. *Zh. Eksp. Teor. Fiz.*, 20:1064–1082, 1950.
20. S. M. Girvin and A. H. MacDonald. Off-diagonal long-range order, oblique confinement, and the fractional quantum hall effect. *Phys. Rev. Lett.*, 58:1252, 1987.
21. F. D. M. Haldane and E. H. Rezayi. Periodic laughlin-jastrow wave functions for the fractional quantized hall effect. *Phys. Rev. B*, 31:2529–2531, 1985.
22. B. I. Halperin. Quantized hall conductance, current-carrying edge states, and the existence of extended states in a two-dimensional disordered potential. *Phys. Rev. B*, 25:2185–2190, 1982.

23. B. I. Halperin. Statistics of quasiparticles and the hierarchy of fractional quantized hall states. *Phys. Rev. Lett.*, 52:1583, 1984.
24. T. H. Hansson, Vadim Oganesyan, and S. L. Sondhi. Superconductors are topologically ordered. *Annals of Physics*, 313:497, 2004.
25. M. B. Hastings and Xiao-Gang Wen. Quasi-adiabatic continuation of quantum states: The stability of topological ground state degeneracy and emergent gauge invariance. *Phys. Rev. B*, 72:045141, 2005.
26. Michael Hermele, Matthew P. A. Fisher, and Leon Balents. Pyrochlore photons: The U(1) spin liquid in a S=1/2 three-dimensional frustrated magnet. *Phys. Rev. B*, 69:064404, 2004.
27. S.-M. Hong. On symmetrization of 6j-symbols and Levin-Wen Hamiltonian. 2009.
28. Y. Hu, S. D. Stirling, and Y.-S. Wu. Ground State Degeneracy in the Levin-Wen Model for Topological Phases. 2011.
29. Y. Hu, Y. Wan, and Y.-S. Wu. Twisted Quantum Double Model of Topological Phases in Two–Dimension. *Phys. Rev. B*, 87:125114, 2013.
30. L.-Y. Hung and Y. Wan. String-Net Models with Z_N Fusion Algebra. *Phys. Rev.*, 86:235132, 2012.
31. R. Jackiw and C. Rebbi. Solitons with fermion number 1/2. *Phys. Rev.*, 13:3398 – 3409, 1976.
32. V. Kalmeyer and R. B. Laughlin. Equivalence of the resonating-valence-bond and fractional quantum hall states. *Phys. Rev. Lett.*, 59:2095–2098, 1987.
33. E. Keski-Vakkuri and Xiao-Gang Wen. Ground state structure of hierarchical QH states on torus and modular transformation. *Int. J. Mod. Phys. B*, 7:4227, 1993.
34. A. Kitaev and L. Kong. Models for gapped boundaries and domain walls. *Commun. Math. Phys.*, 313:351 – 373, 2012.
35. A. Yu. Kitaev. Fault-tolerant quantum computation by anyons. *Ann. Phys. (N.Y.)*, 303:2–30, 2003.
36. Alexei Kitaev and John Preskill. Topological entanglement entropy. *Phys. Rev. Lett.*, 96:110404, 2006.
37. L. D. Landau. Theory of phase transformations i. *Phys. Z. Sowjetunion*, 11:26, 1937.
38. L. D. Landau and E. M. Lifschitz. *Statistical Physics - Course of Theoretical Physics Vol 5*. Pergamon, London, 1958.
39. R. B. Laughlin. Anomalous quantum hall effect: An incompressible quantum fluid with fractionally charged excitations. *Phys. Rev. Lett.*, 50:1395–1398, 1983.
40. Michael Levin and Xiao-Gang Wen. Fermions, strings, and gauge fields in lattice spin models. *Phys. Rev. B*, 67:245316, 2003.
41. Michael Levin and Xiao-Gang Wen. String-net condensation: A physical mechanism for topological phases. In *Phys. Rev. B* [42], page 045110.
42. Michael Levin and Xiao-Gang Wen. String-net condensation: A physical mechanism for topological phases. *Phys. Rev. B*, 71:045110, 2005.
43. Michael Levin and Xiao-Gang Wen. Detecting topological order in a ground state wave function. *Phys. Rev. Lett.*, 96:110405, 2006.
44. Michael Levin and Xiao-Gang Wen. Quantum ether: photons and electrons from a rotor model. *Phys. Rev. B*, 73:035122, 2006.
45. Michael A. Levin and Xiao-Gang Wen. Photons and electrons as emergent phenomena. *Rev. Mod. Phys.*, 77:871, 2005.
46. A. H. MacDonald. *Phys. Rev. Lett.*, 64:220, 1990.
47. G. Misguich, C. Lhuillier, B. Bernu, and C. Waldtmann. Spin-liquid phase of the multiple-spin exchange hamiltonian on the triangular lattice. *Phys. Rev. B*, 60:1064, 1999.
48. R. Moessner and S. L. Sondhi. Resonating valence bond phase in the triangular lattice quantum dimer model. *Phys. Rev. Lett.*, 86:1881, 2001.
49. R. Moessner and S. L. Sondhi. Three-dimensional resonating-valence-bond liquids and their excitations. *Phys. Rev. B*, 68:184512, 2003.
50. G. Moore and N. Read. *Nucl. Phys. B*, 360:362, 1991.
51. N. Read. *Phys. Rev. Lett.*, 62:86, 1989.
52. N. Read and Subir Sachdev. Large-N expansion for frustrated quantum antiferromagnets. *Phys. Rev. Lett.*, 66:1773, 1991.

53. A. Seidel. Pfaffian statistics through adiabatic transport in the 1D coherent state. *Phys. Rev. Lett.*, 101:196802, 2008.
54. A. Seidel. S-duality constraints on 1D patterns associated with fractional quantum Hall states. *Phys. Rev. Lett.*, 105:026802, 2010.
55. Alexander Seidel and Dung-Hai Lee. Abelian and non-abelian hall liquids and charge density wave: Quantum number fractionalization in one and two dimensions. *Phys. Rev. Lett.*, 97:056804, 2006.
56. Alexander Seidel and Dung-Hai Lee. Domain wall type defects as anyons in phase space. *Phys. Rev. B*, 76:155101, 2007.
57. Alexander Seidel and Kun Yang. Halperin (m, m',n) bilayer quantum hall states on thin cylinders. 2008.
58. T. Senthil and O. Motrunich. Microscopic models for fractionalized phases in strongly correlated systems. *Phys. Rev. B*, 66:205104–205113, 2002.
59. D. C. Tsui, H. L. Stormer, and A. C. Gossard. Two-dimensional magnetotransport in the extreme quantum limit. *Phys. Rev. Lett.*, 48:1559–1562, 1982.
60. Hong-Hao Tu, Yi Zhang, and Xiao-Liang Qi. Momentum polarization: an entanglement measure of topological spin and chiral central charge. *arXiv preprint arXiv:1212.6951*, 2012.
61. K. von Klitzing, G. Dorda, and M. Pepper. New method for high-accuracy determination of the fine-structure constant based on quantized hall resistance. *Phys. Rev. Lett.*, 45:494–497, 1980.
62. K. Walker and Z. Wang. (3+1)-TQFTs and Topological Insulators. 2011.
63. Zhenghan Wang. *Topological Quantum Computation*. CBMS Regional Conference Series in Mathematics, 2010.
64. X.-G. Wen and A. Zee. Topological degeneracy of quantum hall fluids. *Phys. Rev. B*, 58:15717, 1998.
65. Xiao-Gang Wen. Vacuum degeneracy of chiral spin state in compactified spaces. *Phys. Rev. B*, 40:7387, 1989.
66. Xiao-Gang Wen. Topological orders in rigid states. *Int. J. Mod. Phys. B*, 4:239, 1990.
67. Xiao-Gang Wen. Gapless boundary excitations in the FQH states and in the chiral spin states. *Phys. Rev. B*, 43:11025, 1991.
68. Xiao-Gang Wen. Mean field theory of spin liquid states with finite energy gaps. In *Phys. Rev. B* [69], page 2664.
69. Xiao-Gang Wen. Mean field theory of spin liquid states with finite energy gaps. *Phys. Rev. B*, 44:2664, 1991.
70. Xiao-Gang Wen. Non-abelian statistics in the FQH states. *Phys. Rev. Lett.*, 66:802, 1991.
71. Xiao-Gang Wen. Topological orders and chern-simons theory in strongly correlated quantum liquid. *Int. J. Mod. Phys. B*, 5:1641, 1991.
72. Xiao-Gang Wen. Origin of gauge bosons from strong quantum correlations (origin of light). *Phys. Rev. Lett.*, 88:11602, 2002.
73. Xiao-Gang Wen. Quantum order: a quantum entanglement of many particles. *Physics Letters A*, 300:175, 2002.
74. Xiao-Gang Wen. Artificial light and quantum order in systems of screened dipoles. *Phys. Rev. B*, 68:115413, 2003.
75. Xiao-Gang Wen. Quantum order from string-net condensations and origin of light and massless fermions. *Phys. Rev. D*, 68:065003, 2003.
76. Xiao-Gang Wen and Q. Niu. Ground state degeneracy of the FQH states in presence of random potentials and on high genus riemann surfaces. *Phys. Rev. B*, 41:9377, 1990.
77. Xiao-Gang Wen and Zhenghan Wang. Classification of symmetric polynomials of infinite variables: Construction of abelian and non-abelian quantum hall states. *Phys. Rev. B*, 77:235108, 2008.
78. Xiao-Gang Wen and Zhenghan Wang. Topological properties of abelian and non-abelian quantum hall states from the pattern of zeros. *Phys. Rev. B*, 78:155109, 2008.
79. Xiao-Gang Wen, F. Wilczek, and A. Zee. Chiral spin states and superconductivity. *Phys. Rev. B*, 39:11413, 1989.

80. Xiao-Gang Wen and A. Zee. A classification and matrix formulation of the abelian FQH states. *Phys. Rev. B*, 46:2290, 1992.
81. Frank Wilczek and A. Zee. Appearance of gauge structure in simple dynamical systems. *Phys. Rev. Lett.*, 52:2111, 1984.
82. E. Witten. Quantum field theory and the jones polynomial. *Comm. Math. Phys.*, 121:351–399, 1989.
83. C. N. Yang. Concept of Off-Diagonal Long-Range Order and the Quantum Phases of Liquid He and of Superconductors. *Rev. Mod. Phys.*, 34:694 – 704, 1962.
84. C. N. Yang and R. L. Mills. Conservation of isotopic spin and isotopic gauge invariance. *Phys. Rev.*, 96:191, 1954.
85. M. P. Zaletel, R. S. K. Mong, and F. Pollmann. Topological characterization of fractional quantum Hall ground states from microscopic Hamiltonians. 2012.
86. S. C. Zhang, T. H. Hansson, and S. Kivelson. Effective-field-theory model for the fractional quantum hall effect. *Phys. Rev. Lett.*, 62:82, 1989.
87. Y. Zhang, T. Grover, A. Turner, M. Oshikawa, and A. Vishwanath. Quasi-particle Statistics and Braiding from Ground State Entanglement. *Phys. Rev. B*, 85:235151, 2012.
88. Y. Zhang and A. Vishwanath. Establishing non-Abelian topological order in Gutzwiller projected Chern insulators via Entanglement Entropy and Modular S-matrix. 2012.

Chapter 7
Local Transformations and Long-Range Entanglement

Abstract To understand the origin of the topological phenomena discussed in the previous chapters, we need a microscopic theory for topological order. It was realized that the key microscopic feature of topologically ordered systems is the existence of long-range many-body entanglement in the ground-state wave function. Useful tools from quantum information theory to characterize many-body entanglement are local transformations, including local unitary (LU) transformation and stochastic local (SL) transformation. In this chapter, we apply these tools to the study of gapped quantum phases and phase transitions and establish the connection between topological order and long/short range entanglement. This allows us to obtain a general theory to study topological order and symmetry breaking order within the same framework. This leads to a basic understanding of the structure of the full quantum phase diagram.

7.1 Introduction

After the experimental discovery of superconducting order via zero-resistance and Meissner effect, it took 40 years to obtain the microscopic understanding of superconducting order through the condensation of fermion pairs. However, we are luckier for topological orders. After the theoretical discovery of topological order via the topological degeneracy and the non-Abelian geometric phases of the degenerate ground states, it took us only 20 years to obtain the microscopic understanding of topological order: topological order is due to long-range entanglement and different topological orders come from different patterns of long-range entanglement. In this section, we will explain such a microscopic understanding.

This chapter is structured as follows. In section 7.2, we review the general idea of a quantum phase. We start from an intuitive picture of systems with very different physical properties being in different phases and arrive at a definition of phase based on phase transitions. In section 7.3, we introduce the concept of local unitary (LU) transformation. Based on the idea of defining quantum phase in terms of phase

transitions, we show that quantum states are in the same phase if and only if they are connected through LU transformations. We present two equivalent forms of LU transformation: the LU time evolution and the LU quantum circuit, which are useful in different circumstances. In section 7.4, we develop a general framework to study topological order, in the thermodynamic limit. We introduce the concept of 'gapped quantum liquid', and show that topological orders are in fact stable gapped quantum liquids. Classifying topological order hence corresponds to classifying stable gapped quantum liquids. In section 7.5.2, we show that symmetry breaking orders for on-site symmetry are also gapped quantum liquids, but with unstable ground-state degeneracy. The universality classes of generalized local unitary (gLU) transformations contain both topologically ordered states and symmetry breaking states. In section 7.5.3, we introduce the concept of stochastic local (SL) transformations. We show that the universality classes of topological orders and symmetry breaking orders can be distinguished by SL transformations: small SL transformations can convert the symmetry breaking classes to the trivial class of product states with finite probability of success, while the topological-order classes are stable against any small SL transformations, demonstrating a phenomenon of emergence of unitarity. This allows us to give a definition of long-range entanglement based on SL transformations, under which only topologically ordered states are long-range entangled. In section 7.6, we discuss the situations where the system has certain symmetries and we obtain a generic structure of the possible phase diagram when symmetries are taken into account.

7.2 Quantum phases and phase transitions

Generally speaking, a phase is a collection of condensed matter systems with qualitatively the same but possibly quantitatively different properties, like density, magnetization, conductance, etc. As a system evolves within a phase, for example by changing temperature or external magnetic field, its property changes smoothly. However, when we reach a critical temperature or magnetic field, something dramatic could happen in the system and its property changes qualitatively as the system transits into a different phase. This is the point of phase transition. Different phases are hence separated by singular phase transition points where some physical observables of the system diverges.

Therefore, two systems are in the same phase if and only if they can evolve into each other smoothly without inducing singularity in any local physical observable. In this sense, liquid water and water vapor belong to the same phase because the two can change into each other smoothly by following, for example, the dashed line past the critical point in the phase diagram, as shown in 7.1. Note that in order to show two systems are in different phases, we need to explore all possible paths of evolution and show there is no smooth way to connect the two phases.

A similar definition holds for quantum systems as well. One special aspect of quantum many-body systems is that even at zero temperature, there can be different

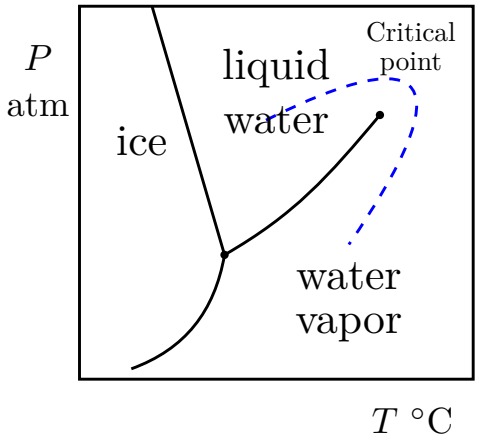

Fig. 7.1 Phase diagram of water.

phases and phase transitions can happen without adding heat to the system. In our following discussions, we will focus mostly on quantum systems at zero temperature with a finite energy gap between the ground state and all the excited states.

For gapped quantum systems, quantum phase transition at zero temperature is closely related to gap closing in the system. Consider a local Hamiltonian $H(0)$, with ground state $|\psi(0)\rangle$ and a finite gap $\Delta(0)$ above the ground state. Expectation value of any physical observable O is given by $\langle O\rangle(0) = \langle\psi(0)|O|\psi(0)\rangle$. Suppose that we smoothly change certain parameter g in the Hamiltonian so that the system follows a path $H(g)$. The ground state $|\psi(g)\rangle$ and the expectation value of the physical observable $\langle O\rangle(g) = \langle\psi(g)|O|\psi(g)\rangle$ will change accordingly. It is generally believed that, as long as the gap of the system $\Delta(g)$ remains finite, $\langle O\rangle(g)$ will change smoothly. Roughly speaking, when $\Delta(g) > 0$, we can use perturbation theory to calculate the change in $\langle O\rangle(g)$ as we change g by a small amount, which will give rise to a smooth dependence. Only when the gap $\Delta(g)$ closes can there be singularity in any physical quantity. The possible and impossible situations are depicted in Fig. 7.2. Therefore, for gapped quantum systems at zero temperature, two systems $H(0)$ and $H(1)$ are within the same phase if and only if there exists a smooth path $H(g), 0 \le g \le 1$ connecting the two and has a finite gap for all g.

A question which is of general interest in condensed matter physics and which we will try to address is: what quantum phases could possibly exist at zero temperature in local gapped quantum systems? That is, for the class of local gapped quantum systems, how many sets can we group them into such that systems within a set can be smoothly connected and systems in different sets can not? Here we are considering quantum systems with arbitrary local degrees of freedom: bosons, fermions, spins... (spin and bosonic degrees of freedom have no intrinsic difference from each other, as in both cases operators on degrees of freedom at different spatial locations commute with each other. In our following discussion, we may use the words inter-

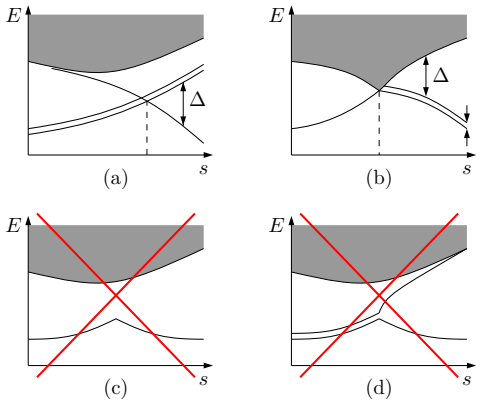

Fig. 7.2 Energy spectrum of a gapped system as a function of a parameter s in the Hamiltonian. (a,b) For gapped system, a quantum phase transition can happen only when energy gap closes. (a) describes a first order quantum phase transition (caused by level crossing). (b) describes a continuous quantum phase transition which has a continuum of gapless excitations at the transition point. (c) and (d) cannot happen for generic states. A gapped system may have ground state degeneracy, where the energy splitting ε between the ground states vanishes when system size $L \to \infty$: $\lim_{L\to\infty} \varepsilon = 0$. The energy gap Δ between ground and excited states on the other hand remains finite as $L \to \infty$.

changably.) We also allow arbitrary form of local interaction between them, as long as the interaction involves a finite number of parties and affects a finite region in the lattice.

We want to emphasize that quantum phase is a property of a class of Hamiltonians, not of a single Hamiltonian. We call such a class of Hamiltonian an H-class. Usually we are considering an H-class of fermionic or bosonic degrees of freedom, of a certain dimension and with possible symmetry constraints. For example we can consider two dimensional fermionic systems with charge conservation symmetry or three dimensional bosonic systems with no special symmetry. For a specific H-class, we can ask whether the Hamiltonians in it are separated into different groups by phase transition and hence form different phases. Two Hamiltonians in an H-class are in the same/different phase if they can/cannot be connected *within the H-class* without going through phase transition. We see that without identifying the class of Hamiltonians under consideration, it is not meaningful to ask which phase a Hamiltonian belongs to. Two Hamiltonians can belong to the same/different phases if we embed them in different H-classes. We will see examples of this kind below.

For an H-class with certain symmetry constraints, one mechanism leading to distinct phases is symmetry breaking. Starting from Hamiltonians with the same symmetry, the ground states of them can have different symmetries, hence resulting in different phases. This symmetry breaking mechanism for phases and phase transitions is well understood with Landau' symmetry breaking theory.

However, it has been realized that quantum systems at zero temperature can be in different phases even without breaking any symmetry. Such phases are often said to be 'topological'. Fractional quantum Hall is one of the first and most important systems found to have topological order. It was realized that, different fractional quantum Hall systems at different filling fractions all have the same symmetry in the ground state, yet there must be a phase transition if the system is to go from one to another. In one dimension, the spin-1 chain $H = \sum S_i \cdot S_{i+1}$ is another example of gapped topological phase, which does not break any symmetry of the system and is separated from a trivial phase. More recently, the exciting discovery of topological insulators and superconductors offers another class of topological phases with interesting topological features.

So we would like to have a theory beyond Landau's symmetry breaking theory for a more complete understanding of the quantum phase diagram at zero temperature.

7.3 Quantum phases and local unitary transformations

Quantum phase and phase transitions are usually discussed in terms of the Hamiltonian of the system. For example for gapped quantum systems at zero temperature, two systems are in the same phase if and only if their Hamiltonians can be connected smoothly without closing gap. On the other hand, gapped quantum phases at zero temperature can be equally well studied in terms of their ground states. In this section, we describe how to determine the phase relation between two systems from their ground states.

In the following we may say that a quantum state $|\psi\rangle$ is gapped. Note that when we say so, we are always assuming that there exists a gapped Hamiltonian which has the state as its ground state. There can be multiple Hamiltonians satisfying this requirement, but their difference is not important, as their zero temperature property is completely determined by $|\psi\rangle$.

7.3.1 Quantum phases and local unitary evolutions in ground states

Suppose that we have two gapped quantum systems with Hamiltonians $H(0)$ and $H(1)$ and ground states $|\Phi(0)\rangle$ and $|\Phi(1)\rangle$ respectively. We want to determine from the ground states when the two systems are in the same phase. In order to have a well defined problem, we need to specify the H-class containing both $H(0)$ and $H(1)$. In this section, we will be considering H-classes with either bosonic or fermionic degrees of freedom, of a specific dimension and with no particular symmetry constraint. The symmetry constrained case is considered later. Note that systems in the same H-class can have different local Hilbert spaces, e.g. spin $1/2$ or spin $3/2$ on

each site. In general, we are allowed to change the local Hilbert space by adding or removing local bosonic (fermionic) degrees of freedom in a bosonic (fermionic) system in the process of evolution.

From the Hamiltonians, we know that they are in the same phase iff there exists a gapped smooth path $H(g), 0 \leq g \leq 1$ connecting them in the H-class. Such a smooth connection in Hamiltonians induces an adiabatic evolution connecting the ground states. That is, if we change the Hamiltonian $H(g)$ very slowly (compared to the inverse gap of the system), then the ground state follows an adiabatic evolution which begins with $|\Phi(0)\rangle$ and ends with $|\Phi(1)\rangle$. Therefore, we see that: if two gapped quantum states are in the same phase $|\Phi(0)\rangle \sim |\Phi(1)\rangle$ then they can be connected by an adiabatic evolution that does not close the energy gap.

Given two states, $|\Phi(0)\rangle$ and $|\Phi(1)\rangle$, determining the existence of such a gapped adiabatic connection can be hard. We would like to have a more operationally practical equivalence relation between states in the same phase. Here we would like to show that

Box 7.1 The same quantum phase
Two gapped states $|\Phi(0)\rangle$ and $|\Phi(1)\rangle$ are in the same phase, if and only if they are related by a local unitary (LU) evolution.

We define a local unitary(LU) evolution as an unitary operation generated by time evolution of a local Hamiltonian for a finite time. That is,

$$|\Phi(1)\rangle \sim |\Phi(0)\rangle \text{ iff } |\Phi(1)\rangle = \mathscr{T}[e^{-i\int_0^1 dg\tilde{H}(g)}]|\Phi(0)\rangle \tag{7.1}$$

where $\mathscr{T}$ is the path-ordering operator and $\tilde{H}(g) = \sum_i O_i(g)$ is a sum of local Hermitian operators. Note that $\tilde{H}(g)$ is in general different from the adiabatic path $H(g)$ that connects the two states.

First, we have shown in the above that if two states $|\Phi(0)\rangle$ and $|\Phi(1)\rangle$ are in the same phase, then we can find an adiabatic path $H(g)$ between the states. It has been shown that, the existence of a gap prevents the system to be excited to higher energy levels and leads to a local unitary evolution, the Quasi-adiabatic Continuation, that maps from one state to the other. That is,

$$|\Phi(1)\rangle = U|\Phi(0)\rangle, \quad U = \mathscr{T}[e^{-i\int_0^1 dg\tilde{H}(g)}] \tag{7.2}$$

The exact form of $\tilde{H}(g)$ can be found from $H(g)$. For details see "summary and further reading" section at the end of this chapter.

On the other hand, the reverse is also true: *if two gapped states* $|\Phi(0)\rangle$ *and* $|\Phi(1)\rangle$ *are related by a local unitary evolution, then they are in the same phase.* Since $|\Phi(0)\rangle$ and $|\Phi(1)\rangle$ are related by a local unitary evolution, we have $|\Phi(1)\rangle = \mathscr{T}[e^{-i\int_0^1 dg\tilde{H}(g)}]|\Phi(0)\rangle$. Let us introduce the partial evolution operator

$$|\Phi(s)\rangle = U(s)|\Phi(0)\rangle, \quad U(s) = \mathscr{T}[e^{-i\int_0^s dg\tilde{H}(g)}]. \tag{7.3}$$

Assume that $|\Phi(0)\rangle$ is a ground state of $H(0)$, then $|\Phi(s)\rangle$ is a ground state of $H(s) = U(s)HU^{\dagger}(s)$. If $H(s)$ remains local and gapped for all $s \in [0,1]$, then we have found an adiabatic connection between $|\Phi(0)\rangle$ and $|\Phi(1)\rangle$.

To see this, first let us show that $H(s)$ is a local Hamiltonian. Since H is a local Hamiltonian, it has a form $H = \sum_i O_i$ where O_i only acts on a cluster whose size is ξ. ξ is called the range of interaction of H. We see that $H(s)$ has a form $H(s) = \sum_i O_i(s)$, where $O_i(s) = U(s)O_iU^{\dagger}(s)$. To show that $O_i(s)$ only acts on a cluster of a finite size, we note that for a local system described by $\tilde{H}(g)$, the propagation velocities of its excitations have a maximum value v_{max}. Since $O_i(s)$ can be viewed as the time evolution of O_i by $\tilde{H}(t)$ from $t = 0$ to $t = s$, we find that $O_i(s)$ only acts on a cluster of size $\xi + \tilde{\xi} + sv_{max}$, where $\tilde{\xi}$ is the range of interaction of $\tilde{H}$. Thus $H(s)$ is indeed a local Hamiltonian. Secondly, if H has a finite energy gap, then it is easy to see that $H(s)$ also have a finite energy gap for any s because $H(s)$ is obtained from H by a unitary transformation.

Therefore, $H(0)$ and $H(1)$ are connected by a smooth local gapped path $H(s)$. As s goes for 0 to 1, the ground state of the local Hamiltonians, $H(s)$, goes from $|\Phi(0)\rangle$ to $|\Phi(1)\rangle$. Thus the two states $|\Phi(0)\rangle$ and $|\Phi(1)\rangle$ belong to the same phase. This completes our argument that states related by a local unitary evolution belong to the same phase.

The finiteness of the evolution time is very important in the above discussion. Here 'finite' means the evolution time does not grow with system size, and in the thermodynamic limit, phases remain separate under such evolutions. On the other hand, if the system size under consideration is finite, there is a critical time limit above which phase separation could be destroyed. The time limit depends on the propagation speed of interactions in the Hamiltonian.

Thus through the above discussion, we show that: Two gapped ground states, $|\Phi(0)\rangle$ and $|\Phi(1)\rangle$, belong to the same phase if and only if they are related by a local unitary evolution Eqn. (7.1).

The relation Eqn. (7.1) defines an equivalence relation between $|\Phi(0)\rangle$ and $|\Phi(1)\rangle$. The equivalence classes of such an equivalence relation represent different quantum phases. So the above result implies that the equivalence classes of the LU evolutions are the universality classes of quantum phases for gapped states.

7.3.2 Local unitary evolutions and local unitary quantum circuits

The LU evolutions introduced here is closely related to *quantum circuits with finite depth*. To define quantum circuits, let us introduce piece-wise local unitary operators. A piece-wise local unitary operator has a form $U_{pwl} = \prod_i U_i$ where $\{U_i\}$ is a set of unitary operators that act on non overlapping regions. The size of each region is less than some finite number l. The unitary operator U_{pwl} defined in this way is called a piece-wise local unitary operator with range l. A quantum circuit with depth M is given by the product of M piece-wise local unitary operators.

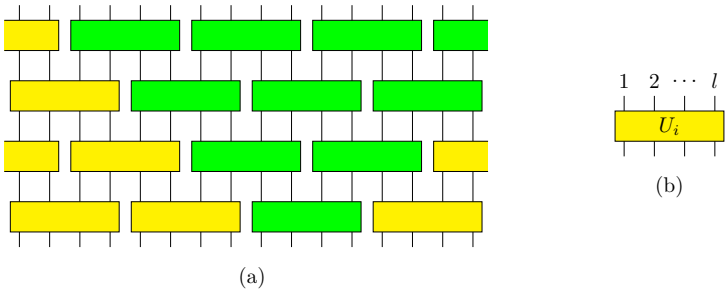

Fig. 7.3 (a) A graphic representation of a quantum circuit, which is formed by (b) unitary operations on patches of finite size l. The green shading represents a causal structure.

Box 7.2 Local unitary (LU) transformation

An LU transformation, as shown in Fig. 7.3, is given by a finite number of layers (i.e. the number of layers is a constant that is independent of the system size) of piecewise local unitary transformations

$$U^M_{circ} = U^{(1)}_{pwl} U^{(2)}_{pwl} \cdots U^{(M)}_{pwl}$$

where each layer has a form

$$U_{pwl} = \prod_i U^i.$$

.

Here $\{U^i\}$ is a set of unitary operators that act on non-overlapping regions. The size of each region is less than a finite number l.

In quantum information theory, it is known that finite time unitary evolution with local Hamiltonian (LU evolution defined before) can be simulated with constant depth quantum circuit and vice-verse. The simulation of LU evolution by a LU quantum circuit proceeds as follows.

Consider the LU evolution generated by a local Hamiltonian $\mathscr{T}[e^{-i\int_0^1 dg \tilde{H}(g)}]$. First group local terms in $\tilde{H}(g)$ into m sets $\tilde{H}^i(g)$, $i = 1, ..., m$, such that local terms in each set $\tilde{h}^i_k(g)$ commute with each other.

$$\tilde{H}(g) = \tilde{H}^1(g) + \tilde{H}^2(g) + ...\tilde{H}^m(g) = \sum_k \tilde{h}^1_k(g) + \sum_k \tilde{h}^2_k(g) + ... + \sum_k \tilde{h}^m_k(g) \quad (7.4)$$

Because all terms in $\tilde{H}(g)$ are local, such a grouping can always be achieved with a finite number of groups. For example, if $\tilde{H}(g)$ is composed of nearest neighbor two-body interaction terms $h_{i,i+1}$ on a one dimensional chain, $h_{2i,2i+1}$ commute with each other and $h_{2i-1,2i}$ commute with each other. Therefore, $m = 2$ is enough.

Although $\tilde{H}^i(g)$ in general does not commute with $\tilde{H}^{i'}(g)$, we can simulate the unitary evolution generated by $\tilde{H}(g)$ with Trotter decomposition. In particular, divide the evolution time into N small intervals δt. Evolve with each $\tilde{H}^i(0)$ separately for time δt. Then evolve with each $\tilde{H}^i(\delta t)$ separately for time δt... Repeat the process for N times. That is, we simulate the LU evolution generated by $\tilde{H}(g)$ as

$$\mathcal{T}[e^{-i\int_0^1 dg\tilde{H}(g)}] \approx \left(\prod_{i=1}^{m} e^{i\tilde{H}^i(0)\delta t}\right)\left(\prod_{i=1}^{m} e^{i\tilde{H}^i(\delta t)\delta t}\right)\ldots\left(\prod_{i=1}^{m} e^{i\tilde{H}^i(1)\delta t}\right) \tag{7.5}$$

As shown in Chapter 2, the approximation becomes more and more accurate with larger and larger N.

In this way, we have decomposed the LU evolution into Nm layers of unitary transformations. While N is a large number, it remains finite for infinite system size. Therefore, the number of layers Nm is also finite. Each layer can be further decomposed into local pieces. This step is exact as local terms in each $\tilde{H}^i(g)$ commute with each other.

$$e^{i\tilde{H}^i(g)\delta t} = \prod_k e^{i\tilde{h}^i_k(g)\delta t} \tag{7.6}$$

Therefore, the LU evolution can be simulated with a piece-wise local quantum unitary circuit, as shown in Fig. 7.3. Further more, the quantum circuit has only a constant number of layers, i.e. a constant depth.

The equivalence relation defined using LU evolution eqn. (7.1) can therefore be equivalently stated in terms of constant depth quantum circuits:

$$|\Phi(1)\rangle \sim |\Phi(0)\rangle \text{ iff } |\Phi(1)\rangle = U^M_{circ}|\Phi(0)\rangle \tag{7.7}$$

where M is a constant independent of system size. Because of their equivalence, we will use the term 'Local Unitary (LU) Transformation' to refer to both local unitary evolution and constant depth quantum circuit in general. Similar to LU evolution, we are allowed to add or remove local degrees of freedom in an LU quantum circuit, although this step is not explicitly shown in Fig. 7.3.

The idea of using LU transformation to study gapped phases can be easily generalized to study topological orders and quantum phases with symmetries (see section 7.6). One difference between the LU evolution and the LU quantum circuit is that the quantum circuit breaks translation symmetry explicitly while the LU evolution does not. Therefore, the LU transformation defined through LU evolution Eqn. (7.1) is more general and can be used to study systems with translation symmetry. The LU quantum circuit has a more clear and simple causal structure. Although it cannot be used to study systems with translation symmetry, it can be applied to study topological orders and quantum phases with other (e.g. internal) symmetries.

7.3.3 *Local unitary quantum circuits and wave function renormalization*

As an application of the notion of LU quantum circuits, we would like to describe a wave function renormalization group flow. The idea of wave function renormalization group flow is to use LU operators to remove entanglement at small length scales, simplify the wave function and reach a fixed point form of wave function at a large enough length scale. As LU transformations map between states within the same phase, the wave function renormalization group flow is expected to flow every gapped quantum states to the fixed point wave function in the phase it belongs to.

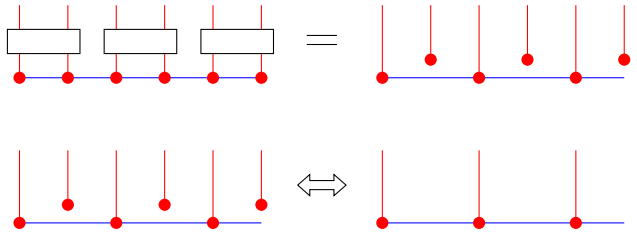

Fig. 7.4 A piece-wise local unitary transformation can transform some degrees of freedom in a state $|\Phi\rangle$ into a direct product. Removing/adding the degrees of freedom in the form of direct product defines an additional equivalence relation between quantum states.

To implement such a renormalization flow on wave functions, first we can use a LU transformation U to transform some degrees of freedom in a state into direct product (see Fig. 7.4). We can then remove those degrees of freedom in the form of direct product. Such a procedure does not change the phase the state belongs to. The reverse process of adding degrees of freedom in the form of direct product states also does not change the phase. We call the local transformation in Fig. 7.4 which involves changing the degrees of freedom a generalized local unitary (gLU) transformation. It is clear that a generalized local unitary transformation inside a region A does not change the reduced density matrix ρ_A for the region A. This is the reason why we say that (generalized) local unitary transformations cannot change entanglement structure at large length scale and the quantum phase of the system.

Let us define the gLU transformation U more carefully and in a more general setting. Consider a state $|\Phi\rangle$. Let ρ_A be the reduced density matrix of $|\Phi\rangle$ in region A. Let $|\psi_i\rangle, i = 1,...,D_A$ be a basis of the total Hilbert space V_A in region A, where D_A is the dimension of V_A. ρ_A may act in a subspace of V_A, which is called the support space V_A^{sp} of region A. The dimension D_A^{sp} of V_A^{sp} is called the support dimension of region A. Now the Hilbert space V_A in region A can be written as $V_A = V_A^{sp} \oplus \bar{V}_A^{sp}$. Let $|\tilde{\psi}_i\rangle$, $i = 1,...,D_A^{sp}$ be a basis of this support space V_A^{sp}, $|\tilde{\psi}_i\rangle$, $i = D_A^{sp} + 1,...,D_A$ be a basis of $\bar{V}_A^{sp}$. We can introduce a LU transformation U^{full} on the full D_A dimensional Hilbert space which rotates the basis $|\psi_i\rangle$ to $|\tilde{\psi}_i\rangle$. We note that in the new basis, the wave function only has non-zero amplitudes on the first D_A^{sp} basis

vectors. Thus, in the new basis $|\tilde{\psi}_i\rangle$, we can reduce the range of the label i from $[1,D_A]$ to $[1,D_A^{sp}]$ without losing any information. This motivates us to introduce the gLU transformation U as composed of two parts: 1. a rotation from the basis of the full Hilbert space $|\psi_i\rangle$, $i=1,...,D_A$ to the basis of the support space $|\tilde{\psi}_i\rangle$, $i=1,...,D_A^{sp}$ with a rectangular matrix U' is given by $U'_{ij}=\langle\tilde{\psi}_i|\psi_j\rangle$. 2. a unitary transformation restricted to the support space alone. We also regard the inverse of U, $U^\dagger$, as a gLU transformation. A LU transformation is viewed as a special case of gLU transformation where the degrees of freedom are not changed. Clearly $U^\dagger U = P$ and $UU^\dagger = P'$ are two projectors. The action of P does not change the state $|\Phi\rangle$ (see Fig. 7.5(b)).

We note that despite the reduction of degrees of freedom, a gLU transformation defines an equivalent relation. Two states related by a gLU transformation belong to the same phase. The renormalization flow induced by the gLU transformations always flows within the same phase. Therefore, in general, we are allowed to use such gLU transformations in the wave function renormalization scheme as long as they are unitary on the support space of a local region in the wave function.

After applying several rounds of the wave function renormalization procedure, nonuniversal local entanglement structures at larger and larger length scales are removed and the wave function is expected to flow to a simplified fixed point form which remains invariant under the renormalization transformation. Note that under the renormalization flow, the degrees of freedom in the system can change and so does the lattice structure of the system. Therefore, the fixed point wave function is not a single wave function, but rather a set of wave functions having the same form on lattice structures of different length scales.

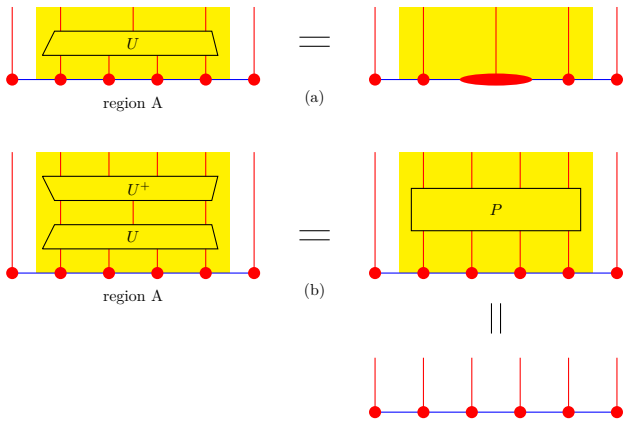

Fig. 7.5 (a) A gLU transformation U acts in region A of a state $|\Phi\rangle$, which reduces the degree freedom in region A to those contained only in the support space of $|\Phi\rangle$ in region A. (b) $U^\dagger U = P$ is a projector that does not change the state $|\Phi\rangle$.

Let us consider some simple examples of model wave functions which are fixed points under a wave function renormalization group flow.

The simplest example is a total product state, for example the Ising paramagnet where all the spins point to the $+x$ direction.

$$|\Phi^+\rangle = \otimes_i(|\uparrow\rangle_i + |\downarrow\rangle_i) \tag{7.8}$$

As all the spins are already disentangled from each other, to renormalize the state to a doubled length scale, we simply remove the redundant degrees of freedom, as shown in Fig.7.6. After the renormalization step, the wave function is still a total product state of spins in the $+x$ direction. Therefore, the product state is a fixed point under the wave function renormalization group flow.

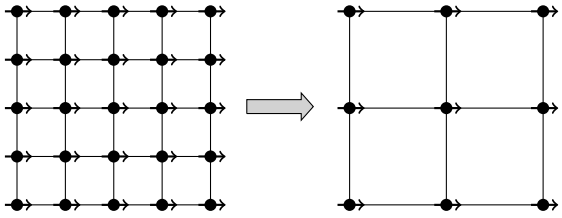

Fig. 7.6 Wave function renormalization group transformation on a product state. The form of the product state remains invariant under this transformation.

A nontrivial example of fixed point wave function is given by the toric code model. Remember that for a toric code model defined on a squre lattice with spins on the links, the ground state wave function is an equal weight superposition of all closed loop configurations, where spin 0 corresponds to no string and spin 1 corresponds to having string on a link. The toric code wave function is the fixed point of the following renormalization flow.

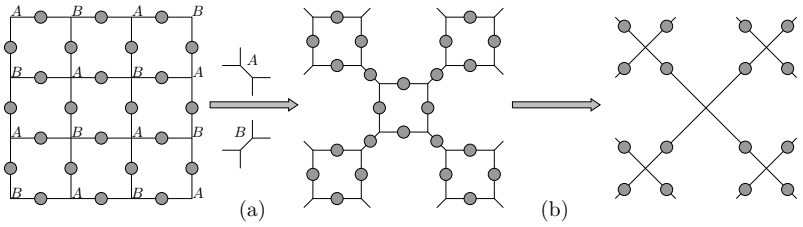

Fig. 7.7 Wave function renormalization group transformation on the toric code wave function. The form of the wave function remains invariant under this transformation.

First we divide the lattice into A and B sublattices and add an extra spin at each vertex in the state $|0\rangle$. Then apply a unitary transformation U_1 to the spins around

each vertex. For vertices in sublattice A, apply a σ_x operator to the added spin if the up and left links carry an odd number of strings and do nothing otherwise. For vertices in sublattice B, apply a σ_x operator to the added spin if the up and right links carry an odd number of strings and do nothing otherwise. From Fig.7.7 we can see that such an operation splits the degree four vertex into two degree three ones and the added spin is on the link between the two vertices. The unitary transformation is applied such that the number of strings going through each vertex is still even and the ground state wave function is still an equal weight superposition of all closed loop configurations, now on the modified lattice as shown in the middle of Fig.7.7. Now apply a unitary transformation U_2 on the eight spins around each square (four on the diagonal links *abcd* and four on the square boundaries *ijkl*). From the previous discussion we know that we only need to describe the action of this transformation on the support space of the eight spins. In the support space, the four diagonal spins *abcd* always carry an even number of strings. For each fixed configuration of *abcd*, *ijkl* is in a superposition of two configurations, both satisfying the constraint at the four vertices and differing by a loop around the square. For example if *abcd* are all 0, then *ijkl* is in a superposition of 0000 and 1111. Now for each fixed configuration of *abcd*, apply a transformation to *ijkl* and map the state to 0000. Because *abcd* remain invariant during this process, the resulting states are still orthogonal to each other, even though the state of *ijkl* become the same. From this we can see that $U_2^\dagger U_2$ is identity on the support space of the eight spins and U_2 a gLU as defined before. After this step, the *ijkl* spins are totally decoupled from everything else and can be removed. In this way, we have shrunk the square bubbles to a point. The resulting state (with the diagonal spins) live on a renormalized lattice and is still an equal weight superposition of all closed loop configurations as in the whole renormalization process we did not break the closed loop constraint and did not change the amplitude of any loop configuration. Therefore, the toric code wave function is a fixed point under this renormalization scheme .

7.4 Gapped Hamiltonians and topological order

In this section, we will discuss the relationship between gapped Hamiltonians and topological order. We first point out that the topologically ordered systems are not arbitrary gapped systems, but belong to a special kind of gapped quantum systems, called *gapped quantum liquids*. We will discuss the concept of gapped quantum liquids.

We remark that the notion of gapped quantum liquids can also be applied to solve the problem of taking the thermodynamic limit for systems without translation symmetry. In general, in the presence of strong randomness, the thermodynamic limit is not well defined (without impurity average). We show that for gapped quantum liquids, the thermodynamic limit is well defined even without impurity average. Consequently, the notions of quantum phases and quantum phase transitions are well defined for gapped quantum liquids.

7.4.1 Gapped quantum systems and gapped quantum phases

Topologically ordered systems are gapped quantum systems. We have discussed the idea of gapped quantum systems in Chapter 5. Here we would like to clarify the concepts of gapped quantum systems in a more formal manner.

Since a gapped system may have gapless excitations on the boundary (such as quantum Hall systems), so to discuss gapped Hamiltonians, we put the Hamiltonian on a space with no boundary. Also, system with certain sizes may contain non-trivial excitations (such as a spin liquid state of spin-1/2 spins on a lattice with an odd number of sites), so we need to specify that the system has a certain sequence of sizes when we take the thermodynamic limit. These observations lead to the following notion.

Box 7.3 Gapped quantum system

Consider a local Hamiltonian of a qubit system on a graph with no boundary, with finite spatial dimension D. If there is a sequence of sizes of the system N_k, $N_k \to \infty$, as $k \to \infty$, such that the size-N_k system has the following 'gap property' (as given in Box 7.4), then the system, defined by the Hamiltonian sequence $\{H_{N_k}\}$, is said to be gapped. Here N_k can be viewed as the number of qubits in the system.

The notion of 'gap property' is given below.

Box 7.4 Gap property

There is a fixed Δ (i.e. independent of N_k) such that (1) the size-N_k Hamiltonian has no eigenvalue in an energy window of size Δ; (2) the number of eigenstates below the energy window does not depend on N_k; (3) the energy splitting of those eigenstates below the energy window approaches zero as $N_k \to \infty$.

Note that the notion of 'gapped quantum system' is not for a single Hamiltonian. It is a property of a sequence of Hamiltonians, $\{H_{N_k}\}$, in the large size limit $N_k \to \infty$ (i.e. an 'H-class' as discussed previously). In the rest of this chapter, the term 'a gapped quantum system' refers to a sequence of Hamiltonians $\{H_{N_k}\}$, which satisfy the gap property.

Now we introduce the notion of ground-state degeneracy and ground-state space.

Box 7.5 Ground-state degeneracy and ground-state space

The number of eigenstates below the energy window is the ground-state degeneracy of the gapped system $\{H_{N_k}\}$. The states below the energy window span the *ground-state space*, which is denoted as $\mathcal{V}_{N_k}$.

Now we discuss the concept of gapped quantum phase. Recall that as discussed in Sec. 7.3, two gapped systems connected by an LU transformation can deform into each other smoothly without closing the energy gap, and thus belong to the same phase. We summarize this observation in a more formal manner as below.

Box 7.6 Gapped quantum phase

Two gapped quantum systems $\{H_{N_k}\}$ and $\{H'_{N_k}\}$ are equivalent if the *ground-state spaces* of H_{N_k} and H'_{N_k} are connected by LU transformations for all N_k. The equivalence classes of the above equivalence relation are the gapped quantum phases (see Fig. 7.8).

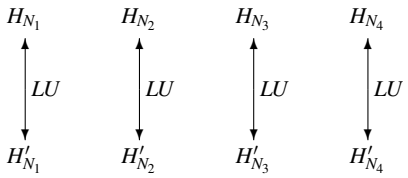

Fig. 7.8 The two rows of Hamiltonians describe two gapped quantum systems. The two rows connected by LU transformations represent the equivalence relation between the two gapped quantum systems, whose equivalence classes are gapped quantum phases.

It is highly desired to identify topological orders as gapped quantum phases, since both concepts do not involve symmetry. In the following, we will show that gapped quantum phases, sometimes, are not well behaved in the thermodynamic limit. As a result, it is not proper to associate topological orders with all gapped quantum phases. To fix this problem, we will introduce the concept of gapped quantum liquid phase.

7.4.2 Gapped quantum liquid system and gapped quantum liquid phase

We start by examining the question of why gapped quantum systems may not be well-behaved in the thermodynamic limit. This is because the Hamiltonians with different sizes may not be related in a way based on our notion of gapped quantum systems (i.e. the way as shown in Fig. 7.8). As a result, we are allowed to choose totally different H_{N_k} and $H_{N_{k+1}}$ as long as the Hamiltonians have the same ground-state degeneracy. For example, one can be topologically ordered and the other can be symmetry breaking.

To overcome this problem, we choose a subclass of gapped quantum systems which are well-behaved in the thermodynamic limit. Those gapped quantum systems are 'shapeless' and can 'dissolve' any product states on additional sites to increase its size. Such gapped quantum systems are called *gapped quantum liquid systems*.

Box 7.7 Gapped quantum liquid system

A gapped quantum liquid system is a gapped quantum system, described by the sequence $\{H_{N_k}\}$, with two additional properties: (1) $0 < c_1 < (N_{k+1} - N_k)/N_k < c_2$ where c_1 and c_2 are constants that do not depend on the system size; (2) the ground-state spaces of H_{N_k} and $H_{N_{k+1}}$ are connected by a generalized local unitary (gLU) transformation (see Fig. 7.9).

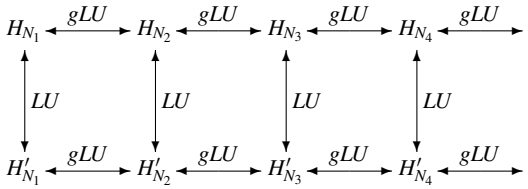

Fig. 7.9 The two rows define two gapped quantum liquid systems via gLU transformations. The two rows connected by LU transformations represent the equivalence relation between two gapped quantum liquid systems, whose equivalence classes are gapped quantum liquid phases.

We need to explain the concept of gLU transformation. For the system H_{N_k}, we first need to add $N_{k+1} - N_k$ qubits. We would like to do this addition 'locally'. That is, the distribution of the added qubits may not be uniform in space but maintains a finite density (number of qubits per unit volume). We call this 'local addition' (LA) transformation. We then discuss how to write Hamiltonians after adding particles to the system, as given below.

Box 7.8 Local addition (LA) transformation

For adding $N_{k+1} - N_k$ qubits to the system H_{N_k} locally, we consider the Hamiltonian $H_{N_k} + \sum_{i=1}^{N_{k+1}-N_k} Z_i$ for the combined system (see Fig. 7.10b), where Z_i is the Pauli Z operator acting on the i^{th} qubit. This defines an LA transformation from H_{N_k} to $H_{N_k} + \sum_{i=1}^{N_{k+1}-N_k} Z_i$.

Now we are ready to discuss the notion of gLU transformation.

Box 7.9 gLU transformation

If for any LA transformation from H_{N_k} to $H_{N_k} + \sum_{i=1}^{N_{k+1}-N_k} Z_i$, the ground-state space of $H_{N_k} + \sum_{i=1}^{N_{k+1}-N_k} Z_i$ can be transformed into the ground-state space of $H_{N_{k+1}}$ via an LU transformation, then we say H_{N_k} and $H_{N_{k+1}}$ are connected by a gLU transformation.

Fig. 7.10 illustrates how we transform H_{N_k} to $H_{N_{k+1}}$ via a gLU transformation.

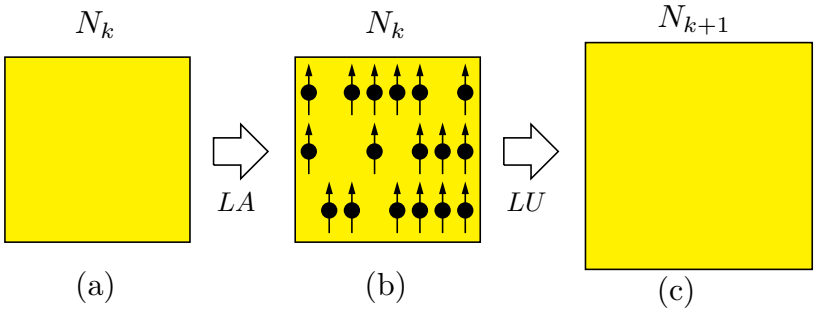

Fig. 7.10 Two systems (a) and (c), with size N_k and N_{k+1}, are described by H_{N_k} and $H_{N_{k+1}}$ respectively. (a) $\to$ (b) is an LA transformation where we add $N_{k+1} - N_k$ qubits to the system H_{N_k} to obtain the Hamiltonian $H_{N_k} + \sum_i Z_i$ for the combined system (b). Under the LA transformation, the ground states of H_{N_k} is tensored with a product state to obtain the ground states of $H_{N_k} + \sum_i Z_i$. In (b) $\to$ (c), we transform the ground-state space of $H_{N_k} + \sum_i Z_i$ to the ground-state space of $H_{N_{k+1}}$ via an LU transformation.

According to our notion, the sequence of following Hamiltonians

$$H_{N_k}^{\text{trivial-liquid}} = -\sum_{i=1}^{N_k} Z_i, \tag{7.9}$$

gives rise to a gapped quantum liquid system. The topologically-ordered toric code Hamiltonian $H_{N_k}^{\text{toric}}$ is also a gapped quantum liquid, as illustrated in Fig. 7.11. This reveals one important feature of a gapped quantum liquid – the corresponding lattice in general does not have a 'shape' (i.e. the system can be defined on an arbitrary lattice with a meaningful thermodynamic limit).

To have an example of a gapped quantum system that is not a gapped quantum liquid, consider another sequence of Hamiltonians

$$H_{N_k}^{\text{non-liquid}} = -\sum_{i=1}^{N_k-1} Z_i. \tag{7.10}$$

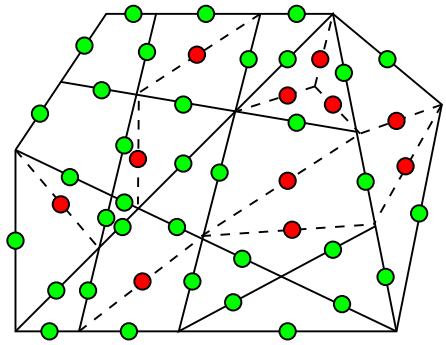

Fig. 7.11 Toric code as a gapped quantum liquid: toric code of N_k qubits on an arbitrary 2D lattice, where the green dots represent qubits sitting on the link of the lattice (given by solid lines). By adding $N_{k+1} - N_k$ qubits (red dots), the gLU transformation $H_{N_k} \to H_{N_{k+1}}$ 'dissolves' the red qubits in the new lattice (with both the solid lines and dashed lines).

It describes a gapped quantum system with two-fold degenerate ground states (coming from the N_k^{th} qubit which carries no energy). However, such a gapped quantum system is not a gapped quantum liquid system. Because the labelling of the N_{k+1} qubit is essentially arbitrary, for some LA transformations, the map from $H_{N_k} + \sum_{i=1}^{N_{k+1}-N_k} Z_i$ to $H_{N_{k+1}}$ cannot be local.

Through the above example, we see that a gapped quantum system may not have a well defined thermodynamic limit (because the low energy property – the degenerate ground states, is given by an isolated qubit which is not a thermodynamic property). Similarly, gapped quantum phase (as given in Box 7.6) is not a good concept, since it is not always a thermodynamic property. In contrast, gapped quantum liquid system and gapped quantum liquid phase (given below in Box 7.10) are good concepts, because they are always related to thermodynamic properties.

Box 7.10 Gapped quantum liquid phase

Two gapped quantum liquid systems $\{H_{N_k}\}$ and $\{H'_{N_k}\}$ are equivalent if the ground-state spaces of H_{N_k} and H'_{N_k} are connected by LU transformations for all N_k. The equivalence classes of this relation are the gapped quantum liquid phases (see Fig. 7.9).

7.4.3 Topological order

Using the notion of gapped quantum liquid phase, we can discuss the concept of topological order in a more formal way. First, we introduce the concept of 'stable gapped quantum system'.

Box 7.11 Stable gapped quantum system
If the ground-state degeneracy of a gapped quantum system is stable against any local perturbation (in the large N_k limit), then the gapped quantum system is stable.

An intimately related fact to this concept is that the ground-state space of a stable gapped quantum system (in the large N_k limit) is a quantum error-correcting code with macroscopic distance. This is to say, for any orthonormal basis $\{|\Phi_i\rangle\}$ of the ground-state space, for any local operator M, we have

$$\langle\Phi_i|M|\Phi_j\rangle = C_M\delta_{ij}, \tag{7.11}$$

where C_M is a constant which only depends on M (see the discussions in Chapter 3 and 5).

Note that a gapped quantum liquid system may not be a stable gapped quantum system. A symmetry breaking system is an example, which is a gapped quantum liquid system but not a stable gapped quantum system (the ground-state degeneracy can be lifted by symmetry breaking perturbations). Also a stable gapped quantum system may not be a gapped quantum liquid system. A non-Abelian quantum Hall states with traps that trap non-Abelian quasiparticles is an example. Since the ground state with traps contain non-Abelian quasiparticles, the resulting degeneracy is robust against any local perturbations. So the system is a stable gapped quantum system. However, for such a system, H_{N_k} and $H_{N_{k+1}}$ are not connected via gLU transformations, hence it is not a gapped quantum liquid system.

Now we can introduce the notion of topological order (or different phases of topologically ordered states):

Box 7.12 Topological order
Topological orders are stable gapped quantum liquid phases.

We remark that we in fact associate different topological orders as different equivalence classes. One of these equivalence classes represents the trivial (topological) order. Here we put trivial and non-trivial topological orders together to have a simple definition. This is similar to symmetry transformations, which usually include both trivial and non-trivial transformations, so that we can say symmetry transformations form a group. Similarly, if we include the trivial one, then we can say that topological orders form a monoid under the stacking operation.

The first order phase-transition point is also an unstable gapped quantum liquid system, which is with accidental degenerate ground states.

Box 7.13 First-order phase transition for gapped quantum liquid systems

A deformation of a gapped quantum liquid system experiences a first order phase transition if the Hamiltonian remains gapped along the deformation path and if the ground-state degeneracy at a point on the deformation path is different from its neighbours. That point is the transition point of the first order phase transition.

From the above discussions, we see that topological orders are the universality classes of stable gapped quantum liquid systems that are separated by gapless quantum systems or unstable gapped quantum systems. Moving from one universality class to another universality class by passing through a gapless system corresponds to a continuous phase transition. Moving from one universality class to another universality class by passing through an unstable gapped system corresponds to a first order phase transition.

We summarize the different kinds of gapped quantum systems in Fig. 7.12.

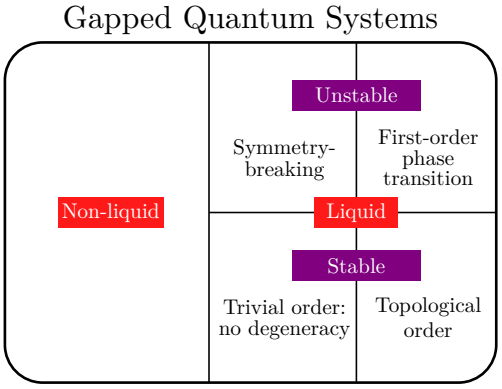

Fig. 7.12 Summary of gapped quantum systems: gapped quantum systems include gapped quantum liquid systems, and systems that are not liquid (nonliquid). For gapped quantum liquids, there are stable systems (including the trivial systems given by e.g. the Hamiltonian $H_{N_k}^{\text{non-liquid}}$ and the topologically ordered systems) and unstable systems (including symmetry breaking systems and first-order phase transitions).

7.5 Universality classes of many-body wave functions

We would like to emphasize that the topological order is a notion of universality classes of local Hamiltonians (or more precisely, gapped quantum systems). In the following, we will introduce the universality classes of many-body wave functions. We can also use the universality classes of many-body wave functions to understand topological orders.

7.5.1 Gapped quantum liquid

Box 7.14 Gapped quantum state
A gapped quantum system is given by a sequence of Hamiltonians $\{H_{N_k}\}$. Let $\mathcal{V}_{N_k}$ be the ground-state space of H_{N_k}. The sequence of ground-state spaces $\{\mathcal{V}_{N_k}\}$ is referred to as a gapped quantum state.

Note that a gapped quantum state is not described by a single wave function, but by a sequence of ground-state spaces $\{\mathcal{V}_{N_k}\}$. Similarly,

Box 7.15 Gapped quantum liquid
The sequence of ground-state spaces $\{\mathcal{V}_{N_k}\}$ of a gapped quantum liquid system given by $\{H_{N_k}\}$ is referred to as a gapped quantum liquid.

Now we are ready to introduce the concept of gapped quantum liquid phase in terms of ground-state subspaces, which is indeed the same as the notion of gapped quantum liquid phase given in Box 7.10 in terms of Hamiltonians.

Box 7.16 Gapped quantum liquid phase and topologically ordered phase
Two gapped quantum liquids, given by two sequences of ground-state spaces $\{\mathcal{V}_{N_k}\}$ and $\{\mathcal{V}'_{N_k}\}$ (on graphs with no boundary), are equivalent if they can be connected via LU transformations. The equivalence classes of gapped quantum liquids are gapped quantum liquid phases (See Fig. 7.13).

To study the universality classes of many-body wave functions, a natural idea is from the LU transformations as discussed in Sections 7.3 and 7.4. We will analyze the classes of wave functions under LU transformations, or more generally, gLU transformations.

As discussed above, the gLU transformations define an equivalence relation among many-body ground-state spaces. The equivalence classes defined by such

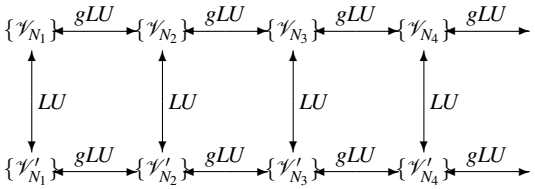

Fig. 7.13 The two rows define two gapped quantum liquids via gLU transformations. The two rows connected by LU transformations represent the equivalence relation between two gapped quantum liquids, whose equivalence classes are gapped quantum liquid phases. The ground-state spaces $\mathcal{V}_{N_k}$ and $\mathcal{V}'_{N_k}$ of two equivalent quantum liquids are connected by the LU transformations.

an equivalence relation will be called the gLU classes. The gLU classes of gapped quantum liquids correspond to gapped quantum liquid phases.

We now ask the following question.

Box 7.17 gLU classes

Since the notion of the gLU classes does not require symmetry, do the gLU classes of gapped quantum liquid have a one-to-one correspondence with topological orders (as given in Box 7.12)?

We will show that the answer is no, i.e. there are *unstable* gapped quantum liquids. Only the gLU classes for *stable* gapped quantum liquids have a one-to-one correspondence with topological orders.

7.5.2 Symmetry breaking order

Example of unstable gapped quantum liquids are given by symmetry breaking states. These unstable gapped quantum liquids are in a different gLU class from the trivial phase, and thus are non-trivial gapped quantum liquid phases.

Let us consider an example of the unstable gapped quantum liquids, the 1D transverse Ising model with the Hamiltonian (with periodic boundary condition)

$$H^{\text{tIsing}}_{N_k}(B) = -\sum_{i=1}^{N_k} Z_i Z_{i+1} - B\sum_{i=1}^{N_k} X_i, \tag{7.12}$$

where Z_i and X_i are the Pauli Z/X operators acting on the ith qubit. The Hamiltonian $H^{\text{tIsing}}_{N_k}(B)$ has a $\mathbb{Z}_2$ symmetry, which is given by $\prod_{i=1}^{N_k} X_i$. The gapped ground states are non-degenerate for $B > 1$. For $0 \le B < 1$, the gapped ground states are two-fold degenerate. The degeneracy is unstable against perturbation that breaks the $\mathbb{Z}_2$ symmetry.

The phase for $B > 1$ is a trivial gapped liquid phase. The phase for $0 < B < 1$ is a non-trivial gapped liquid phase. This is due to a very simple reason: the two phases have different group state degeneracy, and the ground-state degeneracy is an gLU invariant. Gapped quantum liquids with different ground-state degeneracy always belong to different gapped liquid phases.

Now, let us make a more non-trivial comparison. Here we view $H_{N_k}^{\text{tIsing}}(B)$ (with $0 < B < 1$) as a gapped quantum system (rather than a gapped quantum liquid system). We compare it with another gapped quantum system $H_{N_k}^{\text{non-liquid}}$ (see eqn. (7.10)) discussed before. Both gapped systems have two-fold degenerate ground states. Do the two systems belong to the same gapped quantum phase (as given in Box 7.6)?

Consider $H_{N_k}^{\text{tIsing}}(B)$ for any $0 < B < 1$ and any size $N_k < \infty$. The (symmetric) exact ground state $|\Psi_{N_k}^+(B)\rangle$ is an adiabatic continuation of the GHZ state

$$|GHZ_{N_k}^+\rangle = \frac{1}{\sqrt{2}}(|0\rangle^{\otimes N_k} + |1\rangle^{\otimes N_k}), \tag{7.13}$$

i.e. $|\Psi_{N_k}^+(B)\rangle$ is in the same gLU class of $|GHZ_{N_k}^+\rangle$. There is another state $|\Psi_-(B)\rangle$ below the energy window Δ which is an adiabatic continuation of the state

$$|GHZ_{N_k}^-\rangle = \frac{1}{\sqrt{2}}(|0\rangle^{\otimes N_k} - |1\rangle^{\otimes N_k}). \tag{7.14}$$

The energy splitting of $|\Psi_{N_k}^+(B)\rangle$ and $|\Psi_{N_k}^-(B)\rangle$ approaches zero as $N_k \to \infty$.

However, we know that the GHZ state $|GHZ_{N_k}^+\rangle$ (hence $|\Psi_{N_k}^+(B)\rangle$) and the product state $|0\rangle^{\otimes N_k}$ belong to two different gLU classes. Both states are regarded to have the same trivial topological order. So gLU transformations assign GHZ states, or symmetry breaking many-body wave functions, to non-trivial classes. Therefore by studying the gLU classes of gapped quantum liquids, we can study both the topologically ordered states and the symmetry breaking states.

To be more precise, the ground-state space of $H_{N_k}^{\text{tIsing}}(B)$ $(0 < B < 1)$ contain non-trivial GHZ states. On the other hand, the ground-state space of $H_{N_k}^{\text{non-liquid}}$ contain only product states. There is no GHZ states. That make the two systems $H_{N_k}^{\text{tIsing}}(B)$ and $H_{N_k}^{\text{non-liquid}}$ to belong to two different gapped quantum phases, even though the two systems have the same ground-state degeneracy.

We now discuss the concept of 'gapped symmetry breaking quantum system'.

Box 7.18 Gapped symmetry breaking quantum system

A gapped symmetry breaking system is a gapped quantum liquid system with certain symmetry and degenerate ground states, where the symmetric ground states have the GHZ-form of entanglement.

We recall that as discussed in Chapter 5.5, the ground-state space of a gapped symmetry breaking quantum system is a 'classical' error-correcting code with macroscopic distance, correcting errors that do not break the symmetry. This is to say, for any orthonormal basis $\{|\Phi_i\rangle\}$ of the ground-state space, for any local operator M_s that does not break symmetry, we have

$$\langle\Phi_i|M_s|\Phi_j\rangle = C_{M_s}\delta_{ij}, \tag{7.15}$$

where M_s is a constant that only depends on M_s.

Here by 'classical' we mean the following. For the ground-state space, there exists a basis $\{|\Phi_i\rangle\}$ that is connected by symmetry. In this basis, the ground-state space is a classical error-correcting code of macroscopic distance, in the sense that for any local operator M, we have

$$\langle\Phi_i|M|\Phi_j\rangle = 0,\ i \neq j. \tag{7.16}$$

Notice that Eq (7.16) does not contain the coherence condition for $i = j$, which is the requirement to make the space a 'quantum' code.

The transverse Ising mode is an example of such a special case with $\mathbb{Z}_2$ symmetry. The basis that is connected by the $\mathbb{Z}_2$ symmetry are $|\Psi^{\pm}_{N_k}(B)\rangle$. And it is obvious that $\langle\Psi^{+}_{N_k}(B)|M|\Psi^{-}_{N_k}(B)\rangle = 0,\ i \neq j$, for $N_k \to \infty$.

We have now shown that gapped liquid phases also contain symmetry breaking phases. We summarize the LU classes for ground states of local Hamiltonians in Fig. 7.14.

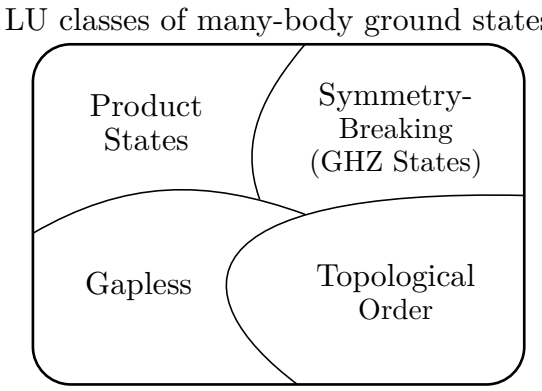

Fig. 7.14 LU classes for ground states (many-body wave functions) of local Hamiltonians.

7.5.3 Stochastic local transformations and long-range entanglement

We have seen that the non-trivial equivalence classes of many-body wave functions under the gLU transformations contain both topologically ordered phases and symmetry breaking phases (described by the symmetric many-body wave functions with GHZ-form of entanglement). In this section, we will introduce the generalized stochastic local (gSL) transformations, which are local invertible transformations that are not necessarily unitary. The term 'stochastic' means that these transformations can be realized by generalized local measurements with finite probability of success.

We show that the many-body wave functions for symmetry breaking phases (i.e. the states of GHZ-form of entanglement) are convertible to the product states under the gSL transformations with a finite probability, while the topological ordered states are not. This allows discuss the notion of long-range entanglement under which only topologically ordered states are long-range entangled. We further show that the topological orders are stable against small stochastic local transformations, while the symmetry breaking orders are not.

The idea for using gSL transformations is simple. The topologically *stable* degenerate ground states for a topologically ordered system is not only stable under real-time evolutions (which are described by gLU transformations), they are also stable and are the fixed points under imaginary-time evolutions. The imaginary-time evolutions of the ground states are given by the gSL transformations (or local non-unitary transformations), therefore the topological orders are robust under (small) gSL transformations.

On the other hand, the states of GHZ-form of entanglement are not robust under small gSL transformations, and can be converted into product states with a finite probability. Thus, there is no emergence of unitarity for symmetry- breaking states.

To discuss gSL transformations, we recall from Chapter 2.4 that the most general form of quantum operations are completely-positive trace-preserving maps. A quantum operation $\mathscr{E}$ acting on any density matrix ρ has the form

$$\mathscr{E}(\rho) = \sum_{k=1}^{r} A_k \rho A_k^\dagger, \tag{7.17}$$

with

$$\sum_{k=1}^{r} A_k^\dagger A_k = I, \tag{7.18}$$

where I is the identity operator.

The operators A_k are called Kraus operators of ρ and satisfies

$$A_k^\dagger A_k \leq I. \tag{7.19}$$

This means that the operation $A_k \rho A_k^\dagger$ can be realized with probability $\mathrm{Tr}(A_k \rho A_k^\dagger)$ for a normalized state $\mathrm{Tr}\rho = 1$. In the following we will drop the label k for the measurement outcome.

We will now definite gSL transformations along a similar line as the definition of gLU transformations. Let us first define a layer of SL transformation that has a form

$$W_{pwl} = \prod_i W^i$$

where $\{W^i\}$ is a set of invertible operators that act on non-overlapping regions, and each W^i satisfies

$$W^{i\dagger} W^i \leq I. \tag{7.20}$$

The size of each region is less than a finite number l. The invertible operator W_{pwl} defined in this way is called a layer of piecewise local stochastic transformation with a range l.

A stochastic local (SL) transformation is then given by a finite layers of piecewise local invertible transformation:

$$W_{circ}^M = W_{pwl}^{(1)} W_{pwl}^{(2)} \cdots W_{pwl}^{(M)}$$

We note that such a transformation does not change the degree of freedom of the state.

Similarly to the gLU transformations, we can also have a transformation that can change the degree of freedom of the state, by a tensor product of the state with another product state $|\Psi\rangle \to \left(\otimes_i |\psi_i\rangle\right) \otimes |\Psi\rangle$, where $|\psi_i\rangle$ is the wave function for the i^{th} qubit. A finite combination of the above two types of transformations is then a generalized stochastic local (gSL) transformation. Here we use the notion $|\Psi\rangle$ to represent a sequence of states $\{|\Psi\rangle_{N_k}\}$.

We remark that, although it is similar to the gLU transformations, gSL transformations are more subtle to deal with. First of all, notice that gSL transformations do not preserve the norm of quantum states (i.e. not trace-preserving, as given by Eq. (7.20)). Furthermore, as we are dealing with thermodynamic limit ($N_k \to \infty$), we are applying gSL transformations on a system of infinite dimensional Hilbert space. In this case, even if each W^i is invertible, $W_{pwl} = \prod_i W^i$ may be non-invertible due to the thermodynamic limit. We will discuss these issues in more detail in the next subsection.

It is known in fact that the SL convertibility in infinite dimensional systems is subtle, and to avoid technical difficulties dealing with the infinite dimensional Hilbert space, we would instead use ε-convertibility instead to talk about the exact convertibility of states under gSL. For simplicity we will omit the notation 'ε' and still name it 'gSL convertibility'.

Box 7.19 Convertibility by gSL transformation

We say that $|\Psi\rangle$ is convertible to $|\Phi\rangle$ by a gSL transformation, if for any $\varepsilon > 0$, there exists an integer N, a probability $0 < p < 1$, and gSL transformations W_{N_k}, such that for any $N_k > N$, W_{N_k} satisfy the condition

$$\left\| \frac{W_{N_k}(|\Psi_{N_k}\rangle\langle\Psi_{N_k}|)W_{N_k}^\dagger}{\mathrm{Tr}\left(W_{N_k}(|\Psi_{N_k}\rangle\langle\Psi_{N_k}|)W_{N_k}^\dagger\right)} - \frac{|\Phi\rangle\langle\Phi_{N_k}|}{\mathrm{Tr}(|\Phi_{N_k}\rangle\langle\Phi_{N_k}|)} \right\|_{\mathrm{tr}} < \varepsilon, \tag{7.21}$$

where $\|\cdot\|_{\mathrm{tr}}$ is the trace norm and

$$\frac{\mathrm{Tr}(W_{N_k}|\Psi_{N_k}\rangle\langle\Psi_{N_k}|W_{N_k}^\dagger)}{\mathrm{Tr}(|\Psi_{N_k}\rangle\langle\Psi_{N_k}|)} > p. \tag{7.22}$$

The idea underlying the definition in Box 7.19 is that $|\Psi\rangle$ can be transformed to any neighbourhood of $|\Phi\rangle$, though not $|\Phi\rangle$ itself, and these neighbourhood states become indistinguishable from $|\Phi\rangle$ in the thermodynamic limit.

Using the idea of gSL transformations, we can have a definition for short-range and long-range entanglement.

Box 7.20 Short/long-range entanglement

A state is short-range entangled (SRE) if it is convertible to a product state by a gSL transformation. Otherwise the state is long-range entangled (LRE).

Under this definition, the states which can be transformed to product states by gLU transformations are SRE. However, the SRE states under gSL transformations will also include some of the states that cannot be transformed to product states by gLU transformations.

As an example, the state

$$|GHZ_{N_k}^+(a)\rangle = a|0\rangle^{\otimes N_k} + b|1\rangle^{\otimes N_k} \tag{7.23}$$

with $|a|^2 + |b|^2 = 1$ cannot be transformed to product states under gLU transformations. However if one allows gSL transformations, then all the $|GHZ_{N_k}^+(a)\rangle$ are convertible to $|GHZ_{N_k}^+(1)\rangle$, i.e. the product state $|0\rangle^{\otimes N_k}$. To see this, one only needs to apply the gSL transformation

$$W_{N_k} = \prod_{i=1}^{N_k} O_i, \tag{7.24}$$

where O_i is the invertible operator

$$\begin{pmatrix} 1 & 0 \\ 0 & \gamma \end{pmatrix} \tag{7.25}$$

acting on the i the qubit, and $0 < \gamma < 1$. And we have

$$\begin{pmatrix} 1 & 0 \\ 0 & \gamma \end{pmatrix}^{\dagger} \begin{pmatrix} 1 & 0 \\ 0 & \gamma \end{pmatrix} \leq \begin{pmatrix} 1 & 0 \\ 0 & 1 \end{pmatrix} = I. \tag{7.26}$$

That is

$$W_{N_k}|GHZ_{N_k}^{+}(a)\rangle = a|0\rangle^{\otimes N_k} + b\gamma^{N_k}|1\rangle^{\otimes N_k} = |\Gamma_{N_k}(a)\rangle. \tag{7.27}$$

Obviously, the right hand side of Eq. (7.27) can be arbitrarily close to the product state $|0\rangle^{\otimes N_k}$ as long as N_k is large enough. Furthermore, $\mathrm{Tr}(|\Gamma_{N_k}(a)\rangle\langle\Gamma_{N_k}(a)|) > |a|^2$ for any N_k. Therefore, according to Box 7.19, $|GHZ_{N_K}^{+}(a)\rangle$ is convertible to the product state $|0\rangle^{\otimes N_k}$ by the gSL transformation W_{N_k}.

If $|\Psi\rangle$ is convertible to $|\Phi\rangle$ by a gSL transformation, we write

$$|\Psi\rangle \xrightarrow{\text{gSL}} |\Phi\rangle. \tag{7.28}$$

Notice that $|\Psi\rangle \xrightarrow{\text{gSL}} |\Phi\rangle$ does not mean $|\Phi\rangle \xrightarrow{\text{gSL}} |\Psi\rangle$. For example, while we have

$$|GHZ_{N_k}^{+}(a)\rangle \xrightarrow{\text{gSL}} |0\rangle^{\otimes N_k}, \tag{7.29}$$

$|0\rangle^{\otimes N_k}$ is not gSL convertible to $|GHZ_{N_k}^{+}(a)\rangle$.

That is, the gSL convertibility is not an equivalence relation. It instead defines a partial order (in terms of set theory) on all the quantum states. That is, if $|\Psi\rangle \xrightarrow{\text{gSL}} |\Phi\rangle$ and $|\Phi\rangle \xrightarrow{\text{gSL}} |\Omega\rangle$, then $|\Psi\rangle \xrightarrow{\text{gSL}} |\Omega\rangle$. And there exists $|\Psi\rangle$ and $|\Phi\rangle$ that is not comparable under gSL, i.e. neither $|\Psi\rangle$ is gSL convertible to $|\Phi\rangle$, nor is $|\Phi\rangle$ gSL convertible to $|\Psi\rangle$. Based on this partial order we can further define equivalent classes.

Box 7.21 gSL equivalent states

We say that two states $|\Psi\rangle$ and $|\Phi\rangle$ are equivalent under gSL transformations if they are convertible to each other by gSL transformations. That is,

$$|\Psi\rangle \xrightarrow{\text{gSL}} |\Phi\rangle \text{ and } |\Phi\rangle \xrightarrow{\text{gSL}} |\Psi\rangle.$$

Under this notion, all the states $|GHZ_{N_k}^{+}(a)\rangle$ are in the same gSL class unless $a = 0, 1$. The product states with $a = 0, 1$ are not in the same gSL class, but any $|GHZ_{N_k}^{+}(a)\rangle$ is convertible to the product states by gSL transformations. The converse is not true, that a product state is not convertible to $|GHZ_{N_k}^{+}(a)\rangle$ with $a \neq 0, 1$ by gSL transformations.

That is to say, the states with GHZ-form of entanglement are indeed 'more entangled' than product states, but they are 'close enough' to produce states under gSL transformations. Furthermore, the topological entanglement entropy $S^{\mathrm{t}}_{\mathrm{topo}}$ for these types of states are unstable under small gSL transformations. In this sense, we can still treat the GHZ-form of entanglement as product states, i.e. states with no long-range entanglement.

We can now define topologically ordered states based on gSL transformations (notice that Box 7.12 defines topological order through properties of the Hamiltonian).

Box 7.22 Topologically ordered states
Topologically ordered states are LRE gapped quantum liquids. In other words, a ground state $|\Psi\rangle$ of a gapped Hamiltonian has a nontrivial topological order if it is not convertible to a product state by any gSL transformation.

Not all LRE states can be transformed into each other via gSL transformations. Thus LRE states can belong to different phases: i.e. the LRE states that are not connected by gSL transformations belong to different phases. When we restrict ourselves to LRE gapped quantum liquids, those different phases are nothing but the topologically ordered phases.

Box 7.23 Topologically ordered phases
Topologically ordered phases are equivalence classes of LRE gapped quantum liquids under the gSL transformations.

We now consider the property of the topological entanglement entropy S_{topo} (discussed in Chapter 5.4) under the local transformations. It is known that S_{topo} an LU invariant. And it is also believed that in general the quantum conditional mutual information $I(A{:}C|B)$ (hence the generalized topological entanglement entropy $S^{\mathrm{t}}_{\mathrm{topo}}$ or $S^{\mathrm{q}}_{\mathrm{topo}}$ as discussed in Chapter 5) is also an LU invariant. We summarize this observation as below.

Box 7.24 (Generalized) topological entanglement entropy under gLU transformations
For large enough areas A,B,C and A,C far from each other, the quantum conditional mutual information $I(A{:}C|B)$ is invariant under gLU transformations. Consequently, the topological entanglement entropy S_{topo} and the generalized topological entanglement entropy $S^{\mathrm{t}}_{\mathrm{topo}}$ are $S^{\mathrm{q}}_{\mathrm{topo}}$ are all gLU invariants.

However, in general $I(A:C|B)$ is not an gSL invariant. However, for small gSL transformations, the topological entanglement entropy S_{topo} stands out, which will remain unchanged. We believe the following observation is true, which provides a support to the above picture and notion of topologically ordered phases.

Box 7.25 S_{topo} under small gSL transformations
The topological entanglement entropy S_{topo} for topological order is stable under small gSL transformations. Furthermore, S_{topo} is an invariant for any gSL equivalence class of topological orders.

Similarly, for symmetry breaking orders, we have

Box 7.26 $S^{\text{t}}_{\text{topo}}$ under small gSL transformations
The generalized entanglement entropy $S^{\text{t}}_{\text{topo}}$ for symmetry breaking orders is stable under small gSL transformations that do not break symmetry, but unstable under small gSL transformations that break the symmetry. Furthermore, $S^{\text{t}}_{\text{topo}}$ is not an invariant for any gSL equivalence class of symmetry breaking orders.

As an example, in the transverse Ising model, the gSL transformation which transforms $|GHZ^{+}_{N_k}(a)\rangle$ of different a breaks the $\mathbb{Z}_2$ symmetry. However, $|GHZ^{+}_{N_k}(a)\rangle$ of different a are in the same gSL equivalent class, yet with different topological entanglement entropy.

The second sentence of Box 7.26 is more subtle, as the topological entanglement entropy S_{topo} for topological order is not an invariant of gSL transformations (as a finite probability p as given in Eq. (7.22) may not exist). This is because that unlike gLU transformations, gSL transformations can be taken arbitrarily close to a non-invertible transformation. For instance, take the gSL transformation W_{N_k} as given in Eq. (7.24). If we allow γ to be arbitrarily close to zero, then for any wave function, applying W_{N_k} is 'as if' we are just projecting everything to $|0\rangle^{N_k}$, which should not protect any topological order.

On the other hand, the option to choose γ arbitrarily small does not mean any quantum state is gSL convertible to a product state. The key point here is the existence of a finite probably p that is independent of system size N_k, as given in Box 7.19. For states with GHZ-form of entanglement, we know that we can always find such a finite probability p.

However, for topological ordered states, there does not exist such a finite probability p. In fact, we have $p \to 0$ when $N_k \to \infty$, and furthermore the speed of p approaching 0 may be exponentially fast in terms of the growth of N_k. Therefore $S^{\text{tri}}_{\text{topo}}$ shall remain invariant within any gSL equivalent class.

The above idea is further supported by the results known for the geometric measure of entanglement for topological ordered states. More precisely, let us divide

the system to m non-overlapping local parts, as illustrated in Fig. 7.3 for one layer. Label each part by i and write the Hilbert space of the system by $\mathscr{H} = \bigotimes_{i=1}^{M} \mathscr{H}_i$. Now for any normalized wave function $|\Psi\rangle \in \mathscr{H}$, the goal is to determine how far $|\Psi\rangle$ is from a normalized product state

$$|\Phi\rangle = \otimes_{i=1}^{M} |\phi_i\rangle \tag{7.30}$$

with $|\phi_i\rangle \in \mathscr{H}_i$.

Recall that, as discussed in Chapter 1, the geometric measure of entanglement $E_G(|\Psi\rangle)$ is then revealed by the maximal overlap

$$\Lambda_{\max}(|\Psi\rangle) = \max_{|\Phi\rangle} |\langle\Phi|\Psi\rangle|, \tag{7.31}$$

and is given by

$$E_G(|\Psi\rangle) = -\log \Lambda^2_{\max}(|\Psi\rangle). \tag{7.32}$$

Notice that for $\Lambda_{\max}(|\Psi\rangle)$, the maximum is also taken for all the partition of the system into local parts.

For a topologically ordered state $|\Psi\rangle$, $E_G(|\Psi\rangle)$ is proportional to the number of qubits in the system. This means that the probability to project $|\Psi\rangle$ to any product state is exponentially small in terms of the system size N_k. Therefore one shall not expect $|\Psi\rangle$ to be convertible to any product state with a finite probability p.

In contract, the geometric entanglement for states with GHZ-form of entanglement is a constant independent of the system size N_k. As an example, for the state $|GHZ^+_{N_k}\rangle$, the maximal overlap $\Lambda_{\max}(|GHZ_+\rangle) = \frac{1}{2}$, with the maximum at either $|0\rangle^{\otimes N_k}$ or $|1\rangle^{\otimes N_k}$, hence the geometric measure of entanglement is $E_G(|GHZ^+_{N_k}\rangle) = 1$. And it remains to be the case for the entire symmetric-breaking phase, which indicates that these GHZ-form states are convertible to product states with some finite probability p.

7.6 Symmetry-protected topological order

In the above discussions, we have defined phases without any symmetry consideration. The $\tilde{H}(g)$ or U_{pwl} in the LU transformation does not need to have any symmetry and can be the sum / product of any local operators. In this case, two Hamiltonians with an adiabatic connection are in the same phase even if they may have different symmetries. Also, all states with short-range entanglement belong to the same phase (under the LU transformations that do not have any symmetry).

On the other hand, we can consider only Hamiltonians H with certain symmetries and define phases as the equivalent classes of symmetric local unitary transformations:

$$|\Psi\rangle \sim \mathscr{T}\left(e^{-i\int_0^1 dg\, \tilde{H}(g)}\right)|\Psi\rangle \;\text{ or }\; |\Psi\rangle \sim U^M_{circ}|\Psi\rangle \tag{7.33}$$

where $\tilde{H}(g)$ or U^M_{circ} has the same symmetries as H. [1]

The equivalence classes of the symmetric LU transformations have very different structures compared to those of LU transformations without symmetry. Each equivalence class of the symmetric LU transformations is smaller and there are more kinds of classes, in general.

In particular, states with short range entanglement can belong to different equivalence classes of the symmetric LU transformations even if they do not spontaneously break any symmetry of the system. (In this case, the ground states have the same symmetry.) We say those states have Symmetry Protected Topological orders. Haldane phase in spin-1 chains and the spin-0 chains are examples of states with the same symmetry which belong to two different equivalence classes of symmetric LU transformations (with spin rotation symmetry). Band and topological insulators are other examples of states that have the same symmetry and at the same time belong to two different equivalence classes of symmetric LU transformations (with time reversal symmetry). Systems with symmetry protected topological order cannot have ground state degeneracy, fractional charge and statistics, nor nonzero topological entanglement entropy. They can, however, have gapless edge excitations which are protected by symmetry.

We are now ready to summarize what we have learned and obtain a general structure of the quantum phase diagram of gapped systems at zero temperature.

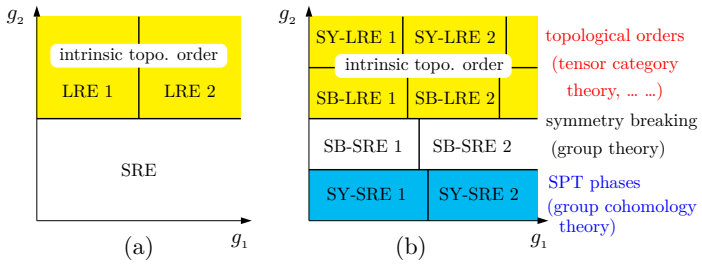

Fig. 7.15 (a) The possible phases for a Hamiltonian $H(g_1, g_2)$ without any symmetry. (b) The possible phases for a Hamiltonian $H_{\text{symm}}(g_1, g_2)$ with some symmetries. The shaded regions in (a) and (b) represent the phases with short range entanglement (i.e. those ground states can be transformed into a direct product state via a generic LU transformations that do not have any symmetry.)

Fig. 7.15 compares the structure of phases for systems without any symmetry and systems with some symmetry in more detail.

For a system without any symmetry, all the short-range-entangled (SRE) states (i.e. those ground states can be transformed into a direct product state via a generic

[1] We note that the symmetric local unitary transformation in the form $\mathcal{T}\left(e^{-i\int_0^1 dg\, \tilde{H}(g)}\right)$ always connect to the identity transformation continuously. This may not be the case for the transformation in the form U^M_{circ}. To rule out that possibility, we define symmetric local unitary transformations as those that connect to the identity transformation continuously.

LU transformations that do not have any symmetry) are in the same phase (SRE in Fig. 7.15(a)). On the other hand, long range entanglement (LRE) can have many different patterns that give rise to different 'intrinsic' topological phases (LRE 1 and LRE 2 in Fig. 7.15(a)). The different 'intrinsic' topological orders usually give rise to quasi particles with different fractional statistics.

For a system with some symmetries, the phase structure can be much more complicated. The short-range-entangled states no longer belong to the same phase, since the equivalence relation is described by more special symmetric LU transformations:
(A) States with short range entanglement belong to different equivalence classes of the symmetric LU transformations if they break symmetry in different ways. They correspond to the symmetry breaking (SB) short-range-entangled phases SB-SRE 1 and SB-SRE 2 in Fig. 7.15(b). They are Landau's symmetry breaking states.
(B) States with short range entanglement can belong to different symmetry protected topological phases if they do not break any symmetry of the system. They correspond to the symmetric (SY) short-range-entangled phases SY-SRE 1 and SY-SRE 2 in Fig. 7.15(b).

Also, for a system with some symmetries, the long-range-entangled states are divided into more classes (more phases):
(C) Symmetry breaking and long range entanglement can appear together in a state, such as SB-LRE 1, SB-LRE 2, etc. in Fig. 7.15(b). The topological superconducting states are examples of such phases.
(D) Long-range-entangled states that do not break any symmetry can also belong to different phases such as the symmetric long-range-entangled phases SY-LRE 1, SY-LRE 2, etc. in Fig. 7.15(b). They are called the Symmetry Enriched Topological Phases. The many different $\mathbb{Z}_2$ symmetric spin liquids with spin rotation, translation, and time-reversal symmetries are examples of those phases. Some time-reversal symmetric topological orders, called topological Mott-insulators or fractionalized topological insulators, also belong to this case.

Having obtained the general structure of the phase diagram, our next goal is to find out all the entries in the diagram, or in other words, to classify all possible phases in strongly correlated systems, especially the topological ones. In the next two chapter, we will study topological phases in one and two dimensions, with the help of tensor network representations.

7.7 A new chapter in physics

Our world is rich and complex. When we discover the inner working of our world and try to describe it, we ofter find that we need to invent new mathematical language describe our understanding and insight. For example, when Newton discovered his law of mechanics, the proper mathematical language was not invented yet. Newton (and Leibniz) had to develop calculus in order to formulate the law of me-

chanics. For a long time, we tried to use theory of mechanics and calculus to understand everything in our world.

As another example, when Einstein discovered the general equivalence principle to describe gravity, he needed a mathematical language to describe his theory. In this case, the needed mathematics, Riemannian geometry, had been developed, which leaded to the theory of general relativity. Following the idea of general relativity, we developed the gauge theory. Both general relativity and gauge theory can be described by the mathematics of fiber bundles. Those advances led to a beautiful geometric understanding of our world based on quantum field theory, and we tried to understand everything in our world in term of quantum field theory.

It appears that we are at another turning point. In a study of quantum matter, we find that long-range entanglement can give rise to many new quantum phases. So long-range entanglement is a natural phenomenon that can happen in our world. This greatly expand our understanding of possible quantum phases, and bring the research of quantum matter to a whole new level. To gain a systematic understanding of new quantum phases and long-range entanglement, we like to know what mathematical language should we use to describe long-range entanglement? The answer is not totally clear. But early studies suggest that tensor category and group cohomology should be a part of the mathematical frame work that describes long-range entanglement. The further progresses in this direction will lead to a comprehensive understanding of long-range entanglement and topological quantum matter.

However, what is really exciting in the study of quantum matter is that it might lead to a whole new point of view of our world. This is because long-range entanglement can give rise to both gauge interactions and Fermi statistics. In contrast, the geometric point of view can only lead to gauge interactions. So maybe we should not use geometric pictures, based on fields and fiber bundles, to understand our world. Maybe we should use entanglement pictures to understand our world. This way, we can get both gauge interactions and fermions from a single origin – qubits. We may live in a truly quantum world. So, quantum entanglement represents a new chapter in physics.

7.8 Summary and further reading

In this chapter, we start to establish a microscopic theory for topological order. We use tools from quantum information theory to characterize many-body entanglement. We begin from the fundamental notion of gapped quantum phase and phase transition and explore its implication on the structure of the ground-state wave function. We find that an equivalence relation can be established between ground states of gapped quantum systems in the same phase in terms of a local unitary (LU) transformation which takes the form of either a finite time unitary evolution with a local Hamiltonian or a finite depth quantum circuit. Such a LU transformation gives rise to a renormalization group flow on gapped quantum states which can be used to simplify the wave functions and flow the states to fixed points.

We develop a general framework to study topological order, in thermodynamic limit. We introduce the concept of 'gapped quantum liquid', and show that topological orders are stable gapped quantum liquids. Classifying topological order hence corresponds to classifying stable gapped quantum liquids. We show that symmetry breaking orders for on-site symmetry are also gapped quantum liquids, but with unstable ground-stable degeneracy. The universality classes of generalized local unitary (gLU) transformations contains both topologically ordered states and symmetry breaking states.

We introduce the concept of stochastic local (SL) transformations, and show that the universality classes of topological orders and symmetry breaking orders can be distinguished by SL: small SL transformations can convert the symmetry breaking classes to the trivial class of product states with finite probability of success, while the topological-order classes are stable against any small SL transformations, demonstrating a phenomenon of emergence of unitarity. Based on the small SL transformations, we give a definition of long-range entanglement (LRE), under which only topologically ordered states are long-range entangled. This then implies that the key to topological order is the existence of LRE in the ground-state wave function which cannot be changed under LU and small SL transformation. This allows us to obtain a general theory to study topological order and symmetry breaking order within a same framework. Based on such an understanding, a general structure of the quantum phase diagram is obtained which contains much more possibilities than that given by the conventional symmetry- breaking theory on phase and phase transitions.

The idea of local unitary transformation and wave funcion renormalization has been used in various studies of quantum states. In [26], the wave function renormalization for string-net states is discussed, which can reduce the string-net wave functions to very simple forms [25]. In [46], the local unitary transformations described by quantum circuits was used to define a renormalization group transformations for states and establish an equivalence relation in which states are equivalent if they are connected by a local unitary transformation. Such an approach was used to classify 1D matrix product states. In [47], the local unitary transformations with disentanglers was used to perform a renormalization group transformations for states, which give rise to the multi-scale entanglement renormalization ansatz (MERA) in one and higher dimensions. The disentanglers and the isometries in MERA can be used to study quantum phases and quantum phase transitions in one and higher dimensions. For a class of exactly solvable Hamiltonians which come from the stabilizer codes in quantum computation, topological order has also been classified using local unitary circuits [58].

In establishing the equivalence relation in terms of local unitary transformations, the quasi-adiabatic continuation plays an important role and was proved in [14]. It proves that any local observable changes smoothly when one gapped Hamiltonian is changed into another without closing gap and provides an explicit local unitary transformation between their ground states. An important idea used in the proof is the existence of an upper bound on the interaction propagation velocity in a gapped quantum system, which was derived in [27]. An improved version of the local uni-

tary transformation can be found in [3]. In [5] it was further shown that in order to connecte different topological phases, the quantum circuit needs to have a depth which scales at least linearly with system size. On the other hand, the simulability of local unitary evolution by a local unitary quantum circuit was shown in [28]. [6] gives a general discussion of the local unitary equivalence condition, the relation between topological order and long/short range entanglement, and wave function renormalization.

The concept of gapped quantum liquid is introduced in [59]. The discussions in Chap.7.4-7.5 are mainly based on (with some parts taken from) [59]. The cubic code of the Haah model provides an example of gapped quantum system that is not a gapped quantum liquid system [11]. Denote $H_{N_k}^{\text{Haah}}$ the Hamiltonian of the cubit code of size N_k. There exists a sequence of the linear sizes of the cube: $L_k \to \infty$, where the ground-state degeneracy is two, provided that $L_k = 2^k - 1$ (or $L_k = 2^{2k+1} - 1$) for any integer k, and correspondingly $N_k = L_k^3$. However, $H_{N_{k+1}}^{\text{Haah}}$ cannot be connected by a gLU transformation [12, 45]. Topological quantum liquid is also discussed in therms of the s source framework [45], which is shown to obey area law and have $s \leq 1$. The cubic code can be described by the generalized s-source framework [12, 45]. Also a stable gapped quantum system may not be a gapped quantum liquid system. A non-Abelian quantum Hall states [31, 50] with traps as discussed in [24] that trap non-Abelian quasiparticles is an example.

The definition of topological order given in Box 7.11 also include the trivial order. Under this definition we can say that topological orders form a monoid under the stacking operation [21]. And when we restrict ourselves to LRE gapped quantum liquids, the different phases are nothing but the topologically ordered phases [49, 51, 52, 18, 8, 9, 33, 42]. The relationship between topological order and quantum error-correcting codes is discussed in [4].

The term 'stochastic' means that these transformations can be realized by generalized local measurements with finite probability of success, which is introduced in [1]. The 'convertibility by gSL transformation' given in Box 7.19 borrows the idea of [35] to use ε-convertibility instead to talk about the exact convertibility of states under gSL.

As another example, we can see how to convert a ground state of any 1D gapped quantum liquid to a product state by gSL transformations. Hence there is no long-range entangled states (i.e. no topological order) in 1D systems (for details, see Chapter 8.4). We may use the isometric form of the matrix product state representation [43]

$$\sum_{\alpha} |\alpha, \ldots, \alpha\rangle \otimes |\omega_{D_\alpha}\rangle^{\otimes N_k} \tag{7.34}$$

(for more details, see Chapter 8). This state is the convertible to a product state by gSL transformations via two steps: the first step is an gLU transformation to convert the $|\omega_{D_\alpha}\rangle^{\otimes N_k}$ part to a product state and end up with a GHZ state. The the next step is to apply the gSL transformation W_{N_k} as given in Eq. (7.27), which transforms the GHZ state to a product state with a finite probability.

The geometrical entanglement for topological ordered states is discussed in [34], which shows that for a topologically ordered state $|\Psi\rangle$, $E_G(|\Psi\rangle)$ is proportional to

the number of qubits in the system. And the geometrical entanglement case for the symmetric-breaking phase is discussed in [48], which indicates that these GHZ-form states are convertible to product states with some finite probability p.

Examples of 'intrinsic' topologically ordered systems include quantum Hall systems[55], chiral spin liquids,[15, 56] $\mathbb{Z}_2$ spin liquids,[41, 53, 30] quantum double model[19] and string-net model[26]. Examples of symmetry protected topological phases include the Haldane phase[13] of spin-1 chain[10, 37] and topological insulators[16, 2, 17, 32, 7, 38]. The topological superconducting states are examples of topologically ordered phases with symmetry breaking.[40, 20] Examples of symmetry enriched topological phases include various $\mathbb{Z}_2$ spin liquids with spin rotation, translation, and time-reversal symmetries[54, 22, 23] and topological Mott-insulators or fractionalized topological insulators with time reversal symmetry[39, 60, 36, 57, 29, 44].

References

1. Charles H. Bennett, Sandu Popescu, Daniel Rohrlich, John A. Smolin, and Ashish V. Thapliyal. Exact and asymptotic measures of multipartite pure-state entanglement. *Phys. Rev. A*, 63:012307, Dec 2000.
2. B. Andrei Bernevig and Shou-Cheng Zhang. Quantum spin hall effect. *Phys. Rev. Lett.*, 96:106802, Mar 2006.
3. Sergey Bravyi, Matthew B. Hastings, and Spyridon Michalakis. Topological quantum order: Stability under local perturbations. *Journal of Mathematical Physics*, 51(9):093512, 2010.
4. Sergey Bravyi, Matthew B Hastings, and Spyridon Michalakis. Topological quantum order: stability under local perturbations. *Journal of Mathematical Physics*, 51(9):093512, 2010.
5. Sergey Bravyi, Matthew B. Hastings, and Frank Verstraete. Lieb-robinson bounds and the generation of correlations and topological quantum order. *Phys. Rev. Lett.*, 97:050401, Jul 2006.
6. Xie Chen, Zheng-Cheng Gu, and Xiao-Gang Wen. Local unitary transformation, long-range quantum entanglement, wave function renormalization, and topological order. *Phys. Rev. B*, 82(15):155138, Oct 2010.
7. Liang Fu, Charles L. Kane, and Eugene J. Mele. Topological insulators in three dimensions. *Phys. Rev. Lett.*, 98:106803, 2007.
8. Shunsuke Furukawa, Grégoire Misguich, and Masaki Oshikawa. Systematic derivation of order parameters through reduced density matrices. *Physical review letters*, 96(4):047211, 2006.
9. Shunsuke Furukawa, Grégoire Misguich, and Masaki Oshikawa. Reduced density matrices and topological order in a quantum dimer model. *Journal of Physics: Condensed Matter*, 19(14):145212, 2007.
10. Zheng-Cheng Gu and Xiao-Gang Wen. Tensor-entanglement-filtering renormalization approach and symmetry-protected topological order. *Phys. Rev. B*, 80(15):155131, Oct 2009.
11. Jeongwan Haah. Local stabilizer codes in three dimensions without string logical operators. *Phys. Rev. A*, 83:042330, Apr 2011.
12. Jeongwan Haah. Bifurcation in entanglement renormalization group flow of a gapped spin model. *Physical Review B*, 89(7):075119, 2014.
13. F. Duncan M. Haldane. Continuum dynamics of the 1-D heisenberg antiferromagnet: Identification with the O(3) nonlinear sigma model. *Physics Letters A*, 93:464, 1983.
14. M. B. Hastings and Xiao-Gang Wen. Quasiadiabatic continuation of quantum states: The stability of topological ground-state degeneracy and emergent gauge invariance. *Phys. Rev. B*, 72:045141, Jul 2005.

15. Vadim Kalmeyer and Robert B. Laughlin. Equivalence of the resonating-valence-bond and fractional quantum hall states. *Phys. Rev. Lett.*, 59:2095–2098, 1987.
16. Charles L. Kane and Eugene J. Mele. Quantum spin hall effect in graphene. *Phys. Rev. Lett.*, 95:226801, Nov 2005.
17. Charles L. Kane and Eugene J. Mele. Z_2 topological order and the quantum spin hall effect. *Phys. Rev. Lett.*, 95:146802, Sep 2005.
18. Esko Keski-Vakkuri and Xiao-Gang Wen. The ground state structure and modular transformations of fractional quantum hall states on a torus. *International Journal of Modern Physics B*, 7(25):4227–4259, 1993.
19. Alexei Yu Kitaev. Fault-tolerant quantum computation by anyons. *Annals of Physics*, 303(1):2 – 30, 2003.
20. Wing-Ho Ko, Patrick A. Lee, and Xiao-Gang Wen. Doped kagome system as exotic superconductor. *Phys. Rev. B*, 79(21):214502, Jun 2009.
21. Liang Kong and Xiao-Gang Wen. Braided fusion categories, gravitational anomalies, and the mathematical framework for topological orders in any dimensions. *arXiv preprint arXiv:1405.5858*, 2014.
22. Su-Peng Kou, Michael Levin, and Xiao-Gang Wen. Mutual chern-simons theory for z_2 topological order. *Phys. Rev. B*, 78(15):155134, Oct 2008.
23. Su-Peng Kou and Xiao-Gang Wen. Translation-symmetry-protected topological orders in quantum spin systems. *Phys. Rev. B*, 80(22):224406, Dec 2009.
24. T. Lan and X.-G. Wen. Topological quasiparticles and the holographic bulk-edge relation in 2+1D string-net models. 2013.
25. Michael Levin and Xiao-Gang Wen. Detecting topological order in a ground state wave function. *Phys. Rev. Lett.*, 96(11):110405–, March 2006.
26. Michael A. Levin and Xiao-Gang Wen. String-net condensation: A physical mechanism for topological phases. *Phys. Rev. B*, 71(4):045110–, January 2005.
27. Elliott H. Lieb and Derek W. Robinson. The finite group velocity of quantum spin systems. *Communications in Mathematical Physics*, 28:251–257, 1972. 10.1007/BF01645779.
28. Seth Lloyd. Universal quantum simulators. *Science*, 273(5278):1073–1078, 1996.
29. Joseph Maciejko, Xiao-Liang Qi, Andreas Karch, and Shou-Cheng Zhang. Fractional topological insulators in three dimensions. *Phys. Rev. Lett.*, 105:246809, Dec 2010.
30. Roderich Moessner and Shivaji L. Sondhi. Resonating valence bond phase in the triangular lattice quantum dimer model. *Phys. Rev. Lett.*, 86:1881–1884, Feb 2001.
31. Gregory Moore and Nicholas Read. Nonabelions in the fractional quantum hall effect. *Nuclear Physics B*, 360(2):362–396, 1991.
32. Joel E. Moore and Leon Balents. Topological invariants of time-reversal-invariant band structures. *Phys. Rev. B*, 75:121306, Mar 2007.
33. Zohar Nussinov and Gerardo Ortiz. A symmetry principle for topological quantum order. *Annals of Physics*, 324(5):977–1057, 2009.
34. Román Orús, Tzu-Chieh Wei, Oliver Buerschaper, and Maarten Van den Nest. Geometric entanglement in topologically ordered states. *New Journal of Physics*, 16(1):013015, 2014.
35. Masaki Owari, Samuel L Braunstein, Kae Nemoto, and Mio Murao. ε-convertibility of entangled states and extension of schmidt rank in infinite-dimensional systems. *Quantum Information & Computation*, 8(1):30–52, 2008.
36. Dmytro Pesin and Leon Balents. Mott physics and band topology in materials with strong spin-orbit interaction. *Nature Phys*, 6(5):376–381, May 2010.
37. Frank Pollmann, Erez Berg, Ari M. Turner, and Masaki Oshikawa. Symmetry protection of topological phases in one-dimensional quantum spin systems. *Phys. Rev. B*, 85:075125, Feb 2012.
38. Xiao-Liang Qi, Taylor L. Hughes, and Shou-Cheng Zhang. Topological field theory of time-reversal invariant insulators. *Phys. Rev. B*, 78(19):195424, Nov 2008.
39. Sri Raghu, Xiao-Liang Qi, Carsten Honerkamp, and Shou-Cheng Zhang. Topological mott insulators. *Phys. Rev. Lett.*, 100:156401, Apr 2008.

40. Nicholas Read and Dmitry Green. Paired states of fermions in two dimensions with breaking of parity and time-reversal symmetries and the fractional quantum hall effect. *Phys. Rev. B*, 61:10267–10297, Apr 2000.
41. Nicholas Read and Subir Sachdev. Large- N expansion for frustrated quantum antiferromagnets. *Phys. Rev. Lett.*, 66:1773–1776, Apr 1991.
42. Norbert Schuch, Ignacio Cirac, and David Pérez-García. Peps as ground states: Degeneracy and topology. *Annals of Physics*, 325(10):2153–2192, 2010.
43. Norbert Schuch, David Perez-Garcia, and Ignacio Cirac. Classifying quantum phases using matrix product states and projected entangled pair states. *Phys. Rev. B*, 84:165139, Oct 2011.
44. Brian Swingle, Maissam Barkeshli, John McGreevy, and Todadri Senthil. Correlated topological insulators and the fractional magnetoelectric effect. *Phys. Rev. B*, 83(19):195139–+, May 2011.
45. Brian Swingle and John McGreevy. Renormalization group constructions of topological quantum liquids and beyond. *arXiv preprint arXiv:1407.8203*, 2014.
46. F. Verstraete, J. I. Cirac, J. I. Latorre, E. Rico, and M. M. Wolf. Renormalization-group transformations on quantum states. *Phys. Rev. Lett.*, 94:140601, Apr 2005.
47. G. Vidal. Entanglement renormalization. *Phys. Rev. Lett.*, 99:220405, Nov 2007.
48. Tzu-Chieh Wei, Dyutiman Das, Swagatam Mukhopadyay, Smitha Vishveshwara, and Paul M Goldbart. Global entanglement and quantum criticality in spin chains. *Physical Review A*, 71(6):060305, 2005.
49. X. G. Wen. Vacuum degeneracy of chiral spin states in compactified space. *Phys. Rev. B*, 40:7387–7390, Oct 1989.
50. X. G. Wen. Non-abelian statistics in the fractional quantum hall states. *Phys. Rev. Lett.*, 66:802–805, Feb 1991.
51. X. G. Wen and Q. Niu. Ground-state degeneracy of the fractional quantum hall states in the presence of a random potential and on high-genus riemann surfaces. *Phys. Rev. B*, 41:9377–9396, May 1990.
52. Xiao-Gang Wen. Topological orders in rigid states. *International Journal of Modern Physics B*, 4(02):239–271, 1990.
53. Xiao-Gang Wen. Mean-field theory of spin-liquid states with finite energy gap and topological orders. *Phys. Rev. B*, 44(6):2664–2672, Aug 1991.
54. Xiao-Gang Wen. Quantum orders and symmetric spin liquids. *Phys. Rev. B*, 65(16):165113, Apr 2002.
55. Xiao-Gang Wen and Qian Niu. Ground-state degeneracy of the fractional quantum hall states in the presence of a random potential and on high-genus riemann surfaces. *Phys. Rev. B*, 41(13):9377–9396, May 1990.
56. Xiao-Gang Wen, Frank Wilczek, and Anthony Zee. Chiral spin states and superconductivity. *Phys. Rev. B*, 39(16):11413–11423, Jun 1989.
57. Bohm-Jung Yang and Yong Baek Kim. Topological insulators and metal-insulator transition in the pyrochlore iridates. *Phys. Rev. B*, 82:085111, Aug 2010.
58. Beni Yoshida. Classification of quantum phases and topology of logical operators in an exactly solved model of quantum codes. *Annals of Physics*, 326(1):15 – 95, 2011. ¡ce:title¿January 2011 Special Issue¡/ce:title¿.
59. Bei Zeng and Xiao-Gang Wen. Gapped quantum liquids and topological order, stochastic local transformations and emergence of unitarity. *Physical Review B*, 91(12):125121, 2015.
60. Yi Zhang, Ying Ran, and Ashvin Vishwanath. Topological insulators in three dimensions from spontaneous symmetry breaking. *Phys. Rev. B*, 79:245331, Jun 2009.

Part IV
Gapped Topological Phases and Tensor Networks

Chapter 8
Matrix Product State and 1D Gapped Phases

Abstract Based on the general notions introduced in the previous chapters, including local unitary transformations and short / long range entanglement, we study gapped phases in one spatial dimension in this chapter. Our goal is to understand what short / long range entangled phases exist in 1D and for this purpose, a useful tool is the matrix product state representation. The matrix product state representation provides an efficient description of the ground state wave function of 1D gapped systems. We introduce this formalism in this chapter and discuss its various properties. By mapping matrix product states to their fixed point form through renormalization group transformations, we show that there is actually no long range entangled phase, hence no intrinsic topological order, in one dimensional spin systems.

8.1 Introduction

Having established the general structure of the quantum phase diagram and the criteria for classifying gapped quantum phases, we would like to apply it to condensed matter systems of interest. In this chapter, we consider one dimensional gapped boson / spin systems, and try to find all possible short / long range entangled phases. Completely classifying strongly correlated boson / spin systems seems to be a hard task as in general strongly interacting quantum many-body systems are very hard to solve. Instead of starting from the Hamiltonian, we focus on the ground state wave function of the system which encodes all the important low energy property of the phase. It was realized that the many body entanglement pattern in 1D gapped ground states has very nice structural properties, allowing a complete understanding of the quantum phases they correspond to.

In particular, it has been shown that 1D gapped ground states can be well represented using the Matrix Product State representation. On the one hand, matrix product states capture the essential features of 1D gapped ground states, like an entanglement area law and a finite correlation length, and provide an efficient de-

scription of the wave function. On the other hand, generic matrix product states satisfying a condition called 'injectivity' are all gapped ground states of local 1D Hamiltonians. Therefore, studying this class of matrix product states will enable us to give a full classification of 1D gapped systems.

Now the question of what gapped phases exist in 1D boson / spin systems can be restated as what equivalence classes of matrix product states exist under local unitary transformations. To answer this question, we first introduce the definition and basic properties of matrix product states in section 8.2, including their entanglement property, gauge degree of freedom, parent Hamiltonian, etc. Next, in section 8.3, we describe a way to perform wave function renormalization group transformation on matrix product states and obtain a simple fixed point form. Using such a procedure, we are able to show in section 8.4 that there are no long range entangled phases in 1D boson / spin systems and all short range entangled states belong to the same phase. In other words, there is no intrinsic topological order in 1D. Note that there is no fundamental difference between spin and boson systems in our discussion, as they are both composed of local degrees of freedom which commute with each other.

In this chapter we focus only on boson / spin systems without special symmetry constraint. In systems with symmetry, the phase diagram is more interesting as there are various symmetry protected topological phases, which we will discuss in Chapter 10. Also, the discussion about 1D gapped phases in fermion systems is deferred to Chapter 10, as 1D fermion systems can be mapped to 1D boson / spin systems with an extra $\mathbb{Z}_2$ symmetry through Jordan Wigner transformation.

8.2 Matrix product states

8.2.1 Definition and examples

Matrix product states describe many-body entangled states of spins living on a one dimensional chain.

Box 8.1 Matrix Product State

A matrix product state (MPS) of a chain of N spins is described as

$$|\psi\rangle = \sum_{i_1,i_2,\ldots,i_N} \mathrm{Tr}(A^{[1]}_{i_1} A^{[2]}_{i_2} \ldots A^{[N]}_{i_N}) |i_1 i_2 \ldots i_N\rangle \tag{8.1}$$

$i_k = 1 \ldots d$, $A^{[k]}_{i_k}$'s are $D \times D$ matrices on site k with D being the dimension of the MPS. d is the dimension of the physical Hilbert space at each site and is called the physical dimension. D is the dimension of the matrices used in the matrix product representation which does not correspond to physical Hilbert spaces. D is called the

inner dimension of the MPS. We suppress the normalization of the wave functions here. The representation is efficient as with fixed D for a state of N spins, the number of parameters involved is at most ND^2 as compared to d^N in the generic case. If the set of matrices does not depend on site label k, then the state represented is translation invariant.

Taking the trace of all matrices $A^{[k]}$ corresponds to periodic boundary condition on the one dimensional chain. If the chain has open boundary condition, it may be more convenient to use a slightly different form of MPS.

$$|\psi\rangle = \sum_{i_1,i_2,\ldots,i_N} \langle l|A^{[1]}_{i_1}A^{[2]}_{i_2}\ldots A^{[N]}_{i_N}|r\rangle |i_1 i_2 \ldots i_N\rangle \tag{8.2}$$

where $|l\rangle$ and $|r\rangle$ are two D dimensional vectors giving the left and right boundary conditions in the state.

If $D = 1$, i.e. if A are numbers, then $|\psi\rangle$ is a product state. For example, if $d = 2$ and $A^{[i]}_1 = \frac{1}{\sqrt{2}}$ and $A^{[i]}_2 = \frac{1}{\sqrt{2}}$, then $|\psi\rangle$ describes a product state of two level spins of the form

$$|\psi\rangle = \left[\frac{1}{\sqrt{2}}(|1\rangle + |2\rangle)\right]\left[\frac{1}{\sqrt{2}}(|1\rangle + |2\rangle)\right]\ldots\left[\frac{1}{\sqrt{2}}(|1\rangle + |2\rangle)\right] \tag{8.3}$$

However, if $D \geq 2$, then $|\psi\rangle$ would in general be an entangled state of many spins. As the simplest example, consider matrices

$$A_0 = \begin{pmatrix} 1 & 0 \\ 0 & 0 \end{pmatrix}, A_1 = \begin{pmatrix} 0 & 0 \\ 0 & 1 \end{pmatrix} \tag{8.4}$$

which are independent of site. Then the matrix product state they produce is the many-body entangled GHZ state introduced in Eq. (5.32) (unnormalized),

$$|GHZ\rangle = |0\rangle^{\otimes N} + |1\rangle^{\otimes N} \tag{8.5}$$

One of the most important examples of matrix product states is the AKLT state describing an anti-ferromagnetic ground state of spin 1 chains, introduced in section 4.5.1. For spin 1 chains, $d = 3$ and the three basis states can be chosen as the eigenstate of spin in the z direction with $S_z = -1, 0$ and 1. The matrices defining the (unnormalized) AKLT state $|\psi\rangle_{AKLT}$ (as discussed in Chapter 4.5) are site independent and are given by

$$A_{-1} = -(X - iY)/\sqrt{2},\ A_0 = -Z,\ A_1 = (X + iY)/\sqrt{2} \tag{8.6}$$

We can also choose a different set of basis states for spin 1 as

$$|x\rangle = \frac{1}{\sqrt{2}}(-|-1\rangle + |1\rangle),\ |y\rangle = \frac{-i}{\sqrt{2}}(|-1\rangle + |1\rangle),\ |z\rangle = -|0\rangle \tag{8.7}$$

where $|x\rangle$, $|y\rangle$ and $|z\rangle$ are eigenvalue 0 eigenstates of the spin in the x, y and z directions respectively. In this basis, the matrices for the AKLT state take the nice form

$$A_x = X,\ A_y = Y,\ A_z = Z \tag{8.8}$$

Graphically, the set of matrices are represented as shown in Fig.8.1 (a) where the vertical bond denotes the physical index and the two horizontal bonds denote the inner indices. An MPS is then represented as in Fig.8.1 (b), with all the inner indices contracted between neighboring sites.

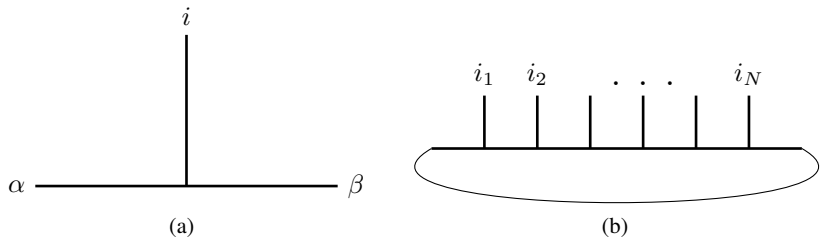

Fig. 8.1 Graphical representation of (a) the set of matrices (b) a matrix product state.

8.2.2 Double tensor

An important mathematical construction in the MPS description is the double tensor.

Box 8.2 The double tensor

The double tensor of a matrix product state is defined as

$$\mathbb{E}_{\alpha\gamma,\beta\chi} = \sum_i A_{i,\alpha\beta} \times (A_{i,\gamma\chi})^* \tag{8.9}$$

If we combine α with γ and β with χ and treat $\mathbb{E}$ as a matrix, then we can write

$$\mathbb{E} = \sum_i A_i \otimes A_i^* \tag{8.10}$$

Graphically, it is represented as in Fig.8.2 (a) where the phyiscal indices of the lower and upper set of matrices are contacted.

On the other hand, if we combine α with β and γ with χ, $\mathbb{E}$ can be thought of as a different matrix, rotated 90 degrees. In this perspective, $\mathbb{E}$ is a Hermitian matrix with non-negative eigenvalues. If α, β, γ, χ are of dimension D, then the eigenvalue

decomposition of $\mathbb{E}$ with respect to indices $\alpha\beta$ and $\gamma\chi$ yields at most D^2 positive eigenvalues. If we think of α and β as the input indices and γ and χ as the output indices, $\mathbb{E}$ actually describes the non-unitary evolution of an open quantum systems with Kraus operators A_i, as introduced in section 2.4.

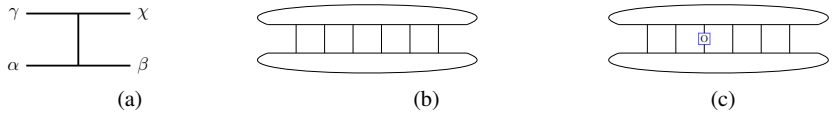

(a) (b) (c)

Fig. 8.2 Graphical representation of (a) the double tensor (b) the norm (c) expectation value of local observable (un-normalized by norm) in a matrix product state.

If two set of matrices A_i and B_i are related by a a unitary transformation U on the physical index i:

$$B_{i,\alpha\beta} = \sum_j U_{ij} A_{j,\alpha\beta}. \tag{8.11}$$

Then they give rise to the same double tensor, which can be seen from

$$\mathbb{E}_B = \sum_j B_{j,\alpha\beta} \times (B_{j,\gamma\chi})^* = \sum_{ii'j} U_{ij} U^*_{i'j} A_{i,\alpha\beta} \times (A_{i',\gamma\chi})^* = \sum_i A_{i,\alpha\beta} \times (A_{i,\gamma\chi})^* = \mathbb{E}_A \tag{8.12}$$

The reverse is also true and is the most important property of the double tensor: A double tensor $\mathbb{E}$ uniquely determines the matrices A_i up to some unitary transformation on the physical index i. That is, if

$$\mathbb{E}_{\alpha\gamma,\beta\chi} = \sum_i A_{i,\alpha\beta} \times (A_{i,\gamma\chi})^* = \sum_i B_{i,\alpha\beta} \times (B_{i,\gamma\chi})^* \tag{8.13}$$

then $A_{i,\alpha\beta}$ and $B_{i,\alpha\beta}$ are related by a unitary transformation U on the physical index i:

$$B_{i,\alpha\beta} = \sum_j U_{ij} A_{j,\alpha\beta}. \tag{8.14}$$

Therefore, states described by A_i and B_i can be related by unitary transformations on each physical index which only change basis for each spin without affecting the entanglement structure in the sate.

Box 8.3 Unitary equivalence of MPS with the same double tensor
If two matrix product states have the same double tensor, then the two states can be mapped to each other by unitary transformations on each physical index.

This property is useful for applying renormalization transformation on the state, as discussed in section 8.3.

A straight-forward way to obtain one possible form of A_i from $\mathbb{E}$ is to think of $\mathbb{E}$ as a matrix with left index $\alpha\beta$ and right index $\gamma\chi$. As discussed before, in this perspective, $\mathbb{E}$ is a Hermitian matrix with non-negative eigenvalues. Find the eigenvalues η_i of $\mathbb{E}$ and the corresponding eigenvectors v_i. That is

$$\mathbb{E}_{\alpha\beta,\gamma\chi} = \sum_i \eta_i v_{i,\alpha\beta} \times v^*_{i,\gamma\chi} \tag{8.15}$$

Then define $A_{i,\alpha\beta} = \sqrt{\eta_i} v_{i,\alpha\beta}$, which are exactly the matrices we are looking for with physical index i and inner indices $\alpha\beta$ and satisfies

$$\mathbb{E}_{\alpha\gamma,\beta\chi} = \sum_i A_{i,\alpha\beta} \times (A_{i,\gamma\chi})^* \tag{8.16}$$

All other possible forms of matrices giving rise to the same $\mathbb{E}$ are related to this particular form of A_i by a unitary transformation on the physical index i.

8.2.3 Calculation of norm and physical observables

The double tensor is useful for the calculation of the norm and physical observables of the matrix product state.

The norm of an MPS is given by

$$\langle\psi|\psi\rangle = \mathrm{Tr}(\mathbb{E} \times \mathbb{E} \ldots \times \mathbb{E}) = \mathrm{Tr}(\mathbb{E}^N) \tag{8.17}$$

as shown graphically in Fig.8.2 (b).

The expectation value of measuring any local observable O (on the kth spin for example) on the state is equal to

$$\langle O\rangle = \frac{\mathrm{Tr}(\mathbb{E}^{k-1}\mathbb{E}[O]\mathbb{E}^{N-k})}{\langle\psi|\psi\rangle}, \text{ where } \mathbb{E}[O] = \sum_{i,j} O_{i,j} A_i \otimes A^*_j \tag{8.18}$$

The numerator is graphically shown as in Fig.8.2 (c). Note that as matrix multiplication takes time $\sim D^3$, the calculation of any physical observable is efficient (polynomial in inner dimension D and linear in system size N) for MPS.

8.2.4 Correlation length

From this we can see that the double tensor is directly related to an important quantity for many-body systems, the correlation length. In fact, an MPS has a finite

correlation length if the largest eigenvalue of $\mathbb{E}$ is nondegenerate. This is shown as follows:

WLOG, we can set the largest eigenvalue of $\mathbb{E}$ to be 1 and hence the norm goes to a finite value (dimension of the eigenspace) as N goes to infinity. The correlation function between two operators O_1 and O_2 becomes

$$\langle O_1 O_2\rangle - \langle O_1\rangle\langle O_2\rangle = \frac{\mathrm{Tr}(\mathbb{E}^{N-L-2}\mathbb{E}[O_1]\mathbb{E}^L\mathbb{E}[O_2])}{\mathrm{Tr}(\mathbb{E}^N)} - \frac{\mathrm{Tr}(\mathbb{E}^{N-1}\mathbb{E}[O_1])\,\mathrm{Tr}(\mathbb{E}^{N-1}\mathbb{E}[O_2])}{\mathrm{Tr}^2(\mathbb{E}^N)} \tag{8.19}$$

Denote the projection onto the eigenspace of eigenvalue λ as P_λ. At large system size N, the correlation function becomes

$$\frac{\mathrm{Tr}(P_1\mathbb{E}[O_1](\sum_\lambda \lambda P_\lambda)^L\mathbb{E}[O_2])}{\mathrm{Tr}(P_1)} - \frac{\mathrm{Tr}(P_1\mathbb{E}[O_1])\,\mathrm{Tr}(P_1\mathbb{E}[O_2])}{\mathrm{Tr}^2(P_1)} \tag{8.20}$$

When L is large, we keep only the first order term in $(\sum_\lambda \lambda P_\lambda)^L$ and the correlation function goes to

$$\frac{\mathrm{Tr}(P_1\mathbb{E}[O_1]P_1\mathbb{E}[O_2])}{\mathrm{Tr}(P_1)} - \frac{\mathrm{Tr}(P_1\mathbb{E}[O_1])\,\mathrm{Tr}(P_1\mathbb{E}[O_2])}{\mathrm{Tr}^2(P_1)} \tag{8.21}$$

If $P_1 = |v_1\rangle\langle v_1|$ is one dimensional, the two terms both become

$$\langle v_1|\mathbb{E}[O_1]|v_1\rangle\langle v_1|\mathbb{E}[O_2]|v_1\rangle \tag{8.22}$$

and cancel each other for any O_1, O_2 and the second order term in $(\sum_\lambda \lambda P_\lambda)^L$ dominates which decays as λ^L. For $\lambda < 1$, the correlator goes to zero exponentially and the matrix product state as finite correlation length. On the other hand, if P_1 is more than one dimensional, the first order term has a finite contribution independent of L:

$$\frac{\sum_{i,j}\langle v_i|\mathbb{E}[O_1]|_j\rangle\langle v_j|\mathbb{E}[O_2]|v_i\rangle}{\mathrm{Tr}(P_1)} - \frac{\langle v_i|\mathbb{E}[O_1]|v_i\rangle\langle v_j|\mathbb{E}[O_2]|v_j\rangle}{\mathrm{Tr}^2(P_1)} \tag{8.23}$$

where v_i, v_j are eigenbasis for P_1. Therefore, degeneracy of the largest eigenvalue of the double tensor implies non-decaying correlation. To describe quantum states with finite correlation length, the double tensor must have a largest eigenvalue which is non-degenerate and the correlation length ξ is given by

$$\xi = -1/\ln\lambda_2 \tag{8.24}$$

where λ_2 is the second largest eigenvalue and $\lambda_2 < 1$. Here ξ is measured in units of lattice spacing.

Box 8.4 MPS with finite correlation length

A matrix product state has finite correlation length if and only if the largest eigenvalue of its double tensor is non-degenerate.

8.2.5 Entanglement area law

Double tensor is important in studying not only the correlation length but also the many-body entanglement structure of an MPS. In fact, $\mathbb{E}$ uniquely determines the state up to a local change of basis on each site and hence contains all the entanglement information of the state. First, we will show with the help of double tensor that many-body entanglement in a matrix product state satisfies an exact area law. Actually, if we take a continuous segment out of the chain, the reduced density matrix has rank at most D^2.

Suppose that we cut the chain into the left half with site 1 to k and the right half with site $k+1$ to N. If we think of the doulbe tensors on each site as matrices with left index α, γ and right index β, χ, then the double tensor of the left half of the chain is the product of all double tensors from sites 1 to k. Similarly, the double tensor of the right half of the chain is the product of all double tensors from sites $k+1$ to N.

$$\mathbb{E}_l = \prod_{i=1}^{k} \mathbb{E}_i,\ \mathbb{E}_r = \prod_{i=k+1}^{N} \mathbb{E}_i \tag{8.25}$$

The entanglement between the left and right half of the chain is faithfully captured by $\mathbb{E}_l$ and $\mathbb{E}_r$. Now we can decompose double tensors $\mathbb{E}_l$ and $\mathbb{E}_r$ back into matrices and find an upper bound on entanglement. In order to do this, we rotate the double tensors 90 degrees and think of them as matrices with left index α, β and right index γ, χ. $\mathbb{E}_l$ and $\mathbb{E}_r$ are both $D^2 \times D^2$ Hermitian matrices in this perspective with non-negative eigenvalues. When we perform the eigenvalue decomposition and obtain the matrices A_i^l and A_i^r as described previously, we find that there are at most D^2 nonzero eigenvalues hence D^2 nonzero A_i^l and A_i^r. This is saying that under separate unitary transformations on the left and right half of the chain, the number of phyiscal degrees of freedom can be reduced to $\leq D^2$ on both sides.

Box 8.5 Entanglement area law in matrix product states

The entanglement entropy between the left and right half of the chain (in fact between any segment and the rest of the chain) is upper bounded by $2\ln D$.

$$S \leq 2\ln(D) \tag{8.26}$$

With D being constant, the MPS satisfies an exact entanglement 'area law' in one dimension.

On the other hand, it is not true that every one-dimensional state satisfying an exact area law can be written exactly as a matrix product state with finite inner dimension D. For example, consider a 1D chain of boson modes where each mode can host any integer number i of bosons. Consider the state that is composed of nearest-neighbor dimers between boson modes $2k-1$ and $2k$ of the form

$$|\psi\rangle = \sum_i \alpha_i |ii\rangle \tag{8.27}$$

This state satisfies area law as long as $\sum_i \alpha_i \ln \alpha_i$ is finite. But this does not necessarily mean that there is a finite number of i's. As long as α_i decays fast enough with i, the entanglement of a segment will be bounded. However, if i is unbounded, the reduced density matrix of a segment will have an infinite rank and therefore not possible to represent with a finite dimensional MPS.

The situation is not too bad though. It has been shown that for any 1D state satisfying an area law, the necessary inner dimension to approximately describe the state scales only polynomially with system size. Therefore the matrix product state representation is still efficient. Moreover it has been proven that all gapped ground states of 1D local Hamiltonians satisfy an area law, therefore the matrix product representation for such states is always efficient. The power of matrix product states is limited to one spatial dimension though. To represent a gapped two-dimensional quantum state satisfying an area law using matrix product formalism would require in general matrices of exponential size. Therefore, we need more general constructions – the tensor product states – to deal with higher dimensional systems.

8.2.6 Gauge degree of freedom

The matrix product state representation is not unique.

Box 8.6 Gauge degree of freedom of MPS representation
An MPS represented by a set of matrices $\{A_i\}$ is equally well represented by $\{B_i = MA_iM^{-1}\}$, for any invertible matrix M.

This is true because

$$\mathrm{Tr}(B_{i_1}B_{i_2}...B_{i_N}) = \mathrm{Tr}(MA_{i_1}M^{-1}MA_{i_2}M^{-1}...MA_{i_N}M^{-1}) = \mathrm{Tr}(A_{i_1}A_{i_2}...A_{i_N}) \tag{8.28}$$

This property can be generalized to site-dependent M and A's as well.

This gauge degree of freedom will play an important role in our understanding of symmetry protected topological orders in one dimension.

8.2.7 Projected entangled pair picture

Matrix product states have another name – the Projected Entangled Pair State (PEPS). It comes from the following construction. (The construction applies to higher dimensional tensor product states as well.)

Consider a chain of maximally entangled pairs as shown in Fig. 8.3. Suppose that they connect into a ring, Each pair of connected dots represents a maximally

Fig. 8.3 Projected Entangled Pair State(PEPS)

entangled pair of spins in state

$$|\psi\rangle = \frac{1}{\sqrt{D}} \sum_{\alpha=1}^{D} |\alpha\alpha\rangle \tag{8.29}$$

where D is the dimension of each spin. Each shaded big circle represents a projection P (a mapping) from two spins of dimension D to a physical degree of freedom of dimension d (a physical spin)

$$P = \sum_{i,\alpha,\beta} A_{i,\alpha,\beta} |i\rangle\langle\alpha\beta| \tag{8.30}$$

where the summation is over $i = 1...d$, and $\alpha, \beta = 1..D$. Direct calculation shows that after the projection, we obtain a many-body entangled state of physical spins which can be written as

$$|\psi\rangle = \sum_{i_1,i_2...i_N} \mathrm{Tr}(A_{i_1} A_{i_2} ... A_{i_N}) |i_1 i_2 ... i_N\rangle \tag{8.31}$$

which is exactly the matrix product states given in Eqn. (8.45). Here A_i is treated as a matrix with row index α and column index β. In this projected entangled pair construction of matrix product states, the spins in maximally entangled pairs are said to be virtual and the spins obtained after projection are physical.

The PEPS and MPS (or more generally tensor product states (TPS)) formalisms are totally equivalent. But sometimes, one picture is more convenient and intuitive than the other.

8.2.8 Canonical form

A canonical form exists for the matrices in an MPS representation, which provides much insight into the structure of the many-body state. We are not going to prove but only state the result in this section. We focus on the case where the matrices are not site dependent and hence the state is translational invariant.

The matrices A_i's in an MPS representation can be put into a 'canonical' form which is block diagonal

$$A_i = \begin{bmatrix} A_i^{(0)} & & \\ & A_i^{(1)} & \\ & & \ddots \end{bmatrix} \tag{8.32}$$

where the double tensor for each block $\mathbb{E}^{(k)} = \sum_i A_i^{(k)} \otimes (A_i^{(k)})^*$ has a positive non-degenerate largest eigenvalue $\lambda_k > 0$. Note that each $\mathbb{E}^{(k)}$ can have eigenvalues with the same magnitude as λ_k, in the form $\lambda_i e^{i2\pi/p}$, $p \in \mathbb{Z}_{q_k}$.

There are several implications that can be directly read from this 'canonical form'. First the matrix product state $|\psi\rangle$ represented by A_i can be written as a superposition of $|\psi^{(k)}\rangle$'s, represented by matrices $A_i^{(k)}$.

$$|\psi\rangle = \sum_k |\psi^{(k)}\rangle \tag{8.33}$$

If $\mathbb{E}^{(k)}$ has only one eigenvalue with magnitude λ_k, then $|\psi^{(k)}\rangle$ is short range correlated (with finite correlation length). If $\mathbb{E}^{(k)}$ has other eigenvalues with the same magnitude as λ_k, then $|\psi^{(k)}\rangle$ can be further decomposed into states $|\psi_p^{(k)}\rangle$ with block translation symmetry of block size q_k and finite correlation length. $|\psi_p^{(k)}\rangle$ is related to $|\psi_1^{(k)}\rangle$ by translation of p sites.

$$|\psi\rangle = \sum_k \sum_{p=1}^{q_k} |\psi_p^{(k)}\rangle \tag{8.34}$$

Therefore, the canonical form directly yields a decomposition of the MPS into a finite (and minimum) number of short range correlated states.

8.2.9 Injectivity

If the canonical form of an MPS contains only one block and the double tensor has only one eigenvalue with largest magnitutde, then the MPS is said to be 'injective'. Otherwise, the MPS is said to be 'noninjective'. Injective MPS hence has only one component in the canonical decomposition and is short range correlated.

For example, the matrices for the GHZ state $|00...0\rangle + |11...1\rangle$ contain only one block and the double tensor is

$$\mathbb{E}_{GHZ} = \begin{pmatrix} 1 & 0 \\ 0 & 0 \end{pmatrix} \otimes \begin{pmatrix} 1 & 0 \\ 0 & 0 \end{pmatrix} + \begin{pmatrix} 0 & 0 \\ 0 & 1 \end{pmatrix} \otimes \begin{pmatrix} 0 & 0 \\ 0 & 1 \end{pmatrix} = \begin{pmatrix} 1 & 0 & 0 & 0 \\ 0 & 0 & 0 & 0 \\ 0 & 0 & 0 & 0 \\ 0 & 0 & 0 & 1 \end{pmatrix} \tag{8.35}$$

which has two-fold degenerate largest eigenvalue 1. Therefore, the matrix product representation of the GHZ state is 'noninjective'.

On the other hand, the matrices for the AKLT state contain only one block as well but the double tensor is

$$\mathbb{E}_{GHZ} = X \otimes X^* + Y \otimes Y^* + Z \otimes Z^* = \begin{pmatrix} 1 & 0 & 0 & 2 \\ 0 & -1 & 0 & 0 \\ 0 & 0 & -1 & 0 \\ 2 & 0 & 0 & 1 \end{pmatrix} \tag{8.36}$$

which has a single eigenvalue with the largest magnitude 3. The eigenvalue with the second largest magnitude is -1. Therefore, the matrix product representation of the AKLT state is 'injective'.

Here the terminology is related to the injectiveness of the following map

$$\Gamma_L : W \mapsto \sum_{i_1,...i_L=1}^{d} \mathrm{Tr}(WA_{i_1}...A_{i_L})|i_1...i_L\rangle \tag{8.37}$$

Γ_L being injective means that for different W, $\sum_{i_1,...i_L=1}^{d} \mathrm{Tr}(WA_{i_1}...A_{i_L})|i_1...i_L\rangle$ are always different. An MPS is injective if there exists a finite L_0 such that Γ_L is an injective map for $L \leq L_0$. Therefore, the previous definition of injectivity in terms of canonical form is equivalent to the following.

Box 8.7 Injective matrix product states

A matrix product state described by matrices A_i is injective if there exists a finite L_0 such that the set of matrices

$$\tilde{A}_{I_{L_0}} = A_{i_1}...A_{i_{L_0}} \tag{8.38}$$

spans the the whole space of $D \times D$ matrices.

If this condition is satisfied for L_0, then obviously it is satisfied for all $L > L_0$.

In the case of GHZ state, no matter how big a segment we take, the set of matrices for a segment of length L always contain only two matrices

$$A_{0...0} = \begin{pmatrix} 1 & 0 \\ 0 & 0 \end{pmatrix}, A_{1...1} = \begin{pmatrix} 0 & 0 \\ 0 & 1 \end{pmatrix} \tag{8.39}$$

These two matrices cannot span the whole space of 2×2 matrices, therefore the MPS representation of the GHZ state is noninjective.

For AKLT state, there are three matrices on a single site

$$A_x = X,\ A_y = Y,\ A_z = Z \tag{8.40}$$

which do not span the 4 dimensional space of 2×2 matrices. However, on two sites there are nine matrices

$$A_{xx} = A_{yy} = A_{zz} = I, A_{xy} = -A_{yx} = iZ, A_{yz} = -A_{zy} = iX, A_{zx} = -A_{xz} = iY \tag{8.41}$$

which do span the whole space of 2×2 matrices. Obviously, on segments of length larger than 2, the set of matrices also span the whole space of 2×2 matrices. Therefore, the MPS representation of the AKLT state is injective, which is consistent with the conclusion obtained by examining the canonical form of the MPS.

Actually, the 'injectivity' property is generically true for random matrix product states. The number of matrices on a segment of length L is d^L, which grows exponentially with L. Generically, for a fixed inner dimension D, it is always possible to span the whole space of $D \times D$ matrices with d^L matrices for a large enough L, unless the matrices are designed to have special structures like in the GHZ state. If we pick an MPS randomly, then it always satisfies the injective condition.

Therefore, 'injectivity' plays an important role in our study of matrix product state. First, a random matrix product state is always injective; secondly, any MPS has a canonical decomposition into a finite number of injective components; moreover, injective MPS enjoys very nice properties like finite correlation length. In the next section, we discuss another nice property of injective MPS: the existence of a local gapped Hamiltonian which has the MPS has its unique ground state.

8.2.10 Parent Hamiltonian

We set out to study MPS because it describes gapped ground states of 1D local Hamiltonians. However, up to now, it is unclear what the Hamiltonian is for a given MPS and what kind of gapped ground state is the MPS. We address this question in this section.

From the decomposition obtained from the 'canonical form', a 'parent Hamiltonian' can be constructed which has the MPS as a gapped ground state, thus making contact with usual condensed matter studies.

In particular, if the MPS is injective, that is if there is only one component in the decomposition of $|\psi\rangle$, then the parent Hamiltonian has $|\psi\rangle$ as a unique gapped ground state. As a single block MPS has finite correlation length, we find

Box 8.8 Parent Hamiltonian for MPS with finite correlation length
A parent Hamiltonian can be constructed for a finite dimensional matrix product state with finite correlation length, such that the matrix product state is the unique gapped ground state of the parent Hamiltonian.

The procedure for constructing the parent Hamiltonian is as follows:

1. take a large enough but finite segment of length l of the chain
2. calculate the reduced density matrix ρ_l of this segment
3. write the projection operator P_l onto the support space of ρ_l

The parent Hamiltonian is the MPS is then the sum of all such local projectors

$$H = \sum_i (1 - P_l^i) \tag{8.42}$$

where P_l^i is the projector applied to the segment centered around site i.

Obviously, each term in the Hamiltonian has energy 0 on the matrix product state. Therefore, the MPS is a frustration free ground state of the parent Hamiltonian (as discussed in Chapter 4.5). Is the MPS a unique and gapped ground state of the parent Hamiltonian? The answer is yes and this is guaranteed by the injectivity of the MPS. It can be shown that if the MPS is injective, then as long as l is large enough, the projectors P_l^i impose strong enough constraints such that H has a unique ground state and a finite energy gap.

The parent Hamiltonian for the AKLT state can be obtained in this way. Written in terms of spin variables, the Hamiltonian reads

$$H = \sum_i \mathbf{S}_i \mathbf{S}_{i+1} + \frac{1}{3}(\mathbf{S}_i \mathbf{S}_{i+1})^2 \tag{8.43}$$

which takes the same form as that given in Eq. 4.41 in Chapter 4.5.1. Note that because the ground state is unique and gapped, if the Hamiltonian has certain symmetry, then the ground state also has it.

On the other hand, if $|\psi\rangle$ can be decomposed into a set of short range correlated $|\psi^{(k)}\rangle$'s, then it cannot be the unique gapped ground state of a local Hamiltonian. A parent Hamiltonian can be constructed which is still gapped but has a degenerate ground space spanned by all $|\psi^{(k)}\rangle$'s. To construct such a parent Hamiltonian, first notice that on large enough segments, the support space of the reduced density matrices $\rho_l^{(k)}$ and $\rho_l^{(k')}$ are orthogonal to each other. The parent Hamiltonian can then be written as

$$H = \sum_i \sum_k (1 - (P_l^i)^{(k)}) \tag{8.44}$$

where $(P_l^i)^{(k)}$ are projectors onto the support space of $\rho_l^{(k)}$ centered around site i. Obviously, $|\psi\rangle$ is a frustration-free ground state of H but not the unique one. Actually, all superpositions of $|\psi^{(k)}\rangle$'s are ground states of H. It can still be proved

that H has a finite energy gap above this ground subspace. Therefore, noninjective MPS is one of the degenerate ground states of a local gapped Hamiltonian. One important consequence of ground state degeneracy is that if the Hamiltonian has a certain symmetry, each of the $|\psi^{(k)}\rangle$'s does not have to. They can be related to each other by the symmetry transformation.

8.3 Renormalization group transformation on MPS

The wave function renormalization group transformation, as discussed in the last chapter, aims to remove short range entanglement structures from a quantum state and extract the universal properties of the phase from the fixed point of the renormalization flow. The key to a successful renormalization procedure is in choosing the right local unitary operators which removes short range entanglement in an optimal way. The matrix product representation provides us with an efficient way to find such local unitaries and implement the renormalization procedures.

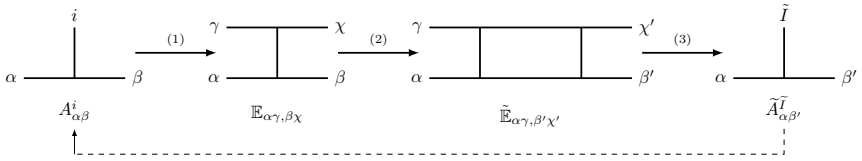

Fig. 8.4 Quantum state renormalization group transformation on matrix product state.

Consider matrix product state

$$|\psi\rangle = \sum_{i_1,i_2,\ldots,i_N} \mathrm{Tr}(A^{i_1}A^{i_2}\ldots A^{i_N})|i_1 i_2 \ldots i_N\rangle \tag{8.45}$$

where $i_k = 1\ldots d$ with d being the physical dimension of a spin at each site, A^{i_k}'s are $\chi\times\chi$ matrices related to the physical state $|i_k\rangle$ with χ being the inner dimension of the MPS.

To implement the wave function renormalization group transformation on the matrix product state, first construct the double tensor

$$\mathbb{E}_{\alpha\gamma,\beta\chi} = \sum_i A^i_{\alpha\beta} \times (A^i_{\gamma\chi})^* \tag{8.46}$$

as shown in Fig.8.4 step (1). Treat $\mathbb{E}$ as a $\chi^2\times\chi^2$ matrix with row index $\alpha\gamma$ and column index $\beta\chi$. Combine the double tensor of the two sites together into

$$\tilde{\mathbb{E}}_{\alpha\gamma,\beta'\chi'} = \sum_{\beta\chi} \mathbb{E}_{\alpha\gamma,\beta\chi}\mathbb{E}_{\beta\chi,\beta'\chi'} \tag{8.47}$$

as shown in Fig.8.4 step (2). Then think of $\tilde{\mathbb{E}}_{\alpha\gamma,\beta'\chi'}$ as a matrix with row index $\alpha\beta'$ and column index $\gamma\chi'$. It is easy to see that with such a recombination, $\tilde{\mathbb{E}}$ is a positive matrix and can be diagonalized

$$\tilde{\mathbb{E}}_{\alpha\gamma,\beta'\chi'} = \sum_{\tilde{i}} \lambda_{\tilde{i}} V_{\tilde{i},\alpha\beta'} V^*_{\tilde{i},\gamma\chi'}, \tag{8.48}$$

where we have kept only the non-zero eigenvalues $\lambda_{\tilde{i}} (> 0)$ and the corresponding eigenvectors $V_{\tilde{i},\alpha\beta'}$. $\tilde{A}$ is then given by

$$\tilde{A}^{\tilde{i}}_{\alpha\beta'} = \sqrt{\lambda_{\tilde{i}}} V_{\tilde{i},\alpha\beta'} \tag{8.49}$$

which are the matrices representing the renormalized state, which form the basis for the next round of renormalization transformation.

These steps apply one round of renormalization procedure on the matrix product state by applying local unitaries to each pair of neighboring sites, removing local entanglement between them and combining the remaining degrees of freedom of the two sites into one. To see how this is achieved, notice that an important property of $\mathbb{E}$ is that it uniquely determines the matrices, and hence the state, up to a local change of basis on each site, as discussed in section 8.2.2. That is, if

$$\mathbb{E}_{\alpha\gamma,\beta\chi} = \sum_i A^i_{\alpha\beta} \times (A^i_{\gamma\chi})^* = \sum_i B^j_{\alpha\beta} \times (B^j_{\gamma\chi})^* \tag{8.50}$$

then $A^i_{\alpha\beta}$ and $B^j_{\alpha\beta}$ are related by a unitary transformation U:

$$B^j_{\alpha\beta} = \sum_i U_{ji} A^i_{\alpha\beta} \tag{8.51}$$

Therefore, in decomposing $\tilde{\mathbb{E}}$ into $\tilde{A}$, we have implemented a unitary on every two sites and the wave function has been transformed as

$$|\psi\rangle \to |\tilde{\psi}\rangle = U_{1,2} \otimes U_{3,4} \otimes \ldots \otimes U_{2i-1,2i} \otimes \ldots |\psi\rangle. \tag{8.52}$$

$\tilde{\mathbb{E}}$ contains all the information about the entanglement of the two sites with the rest of the system but not any detail of entanglement structure among the two sites. By setting the range of $\tilde{i}$ to be over only the nonzero λ's, we have reduced the physical dimension of the two sites to only those necessary for describing the entanglement between them and the rest of the system. Local entanglement among the two sites has been optimally removed. Repeating this procedure several times correspond to a (generalized) local unitary transformation on the quantum state as shown in Fig.8.5 and the matrices flow from $A^{(0)}$ to $A^{(1)}$,..., until the fixed point form of $A^{(\infty)}$ from which the universal properties of the state can be determined.

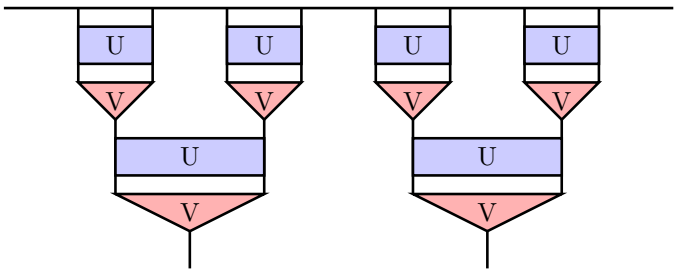

Fig. 8.5 Quantum state renormalization group transformation on 1D quantum states.

8.4 No intrinsic topological order in 1D bosonic systems

Let's apply this wave function renormalization group transformation to gapped, short range correlated matrix product states and determine what quantum phases exist in bosonic systems. First when no symmetry is required for the class of system, we want to know what kind of long range entanglement exists and thereby classify intrinsic topological orders in 1D gapped boson systems. We will show that:

Box 8.9 Classification of gapped 1D bosonic systems without symmetry
All gapped 1D bosonic systems belong to the same phase if no symmetry is required.

In other words, there is no intrinsic topological order in 1D bosonic systems and all gapped quantum states are short range entangled.

To obtain such a result, we use the fact that gapped 1D bosonic states are described by short-range correlated matrix product states. Then one can show that all short-range correlated matrix product states can be mapped to product states with LU transformations. Therefore there is no intrinsic topological order in 1D.

Consider a generic system without any symmetry whose gapped ground state is described as an MPS with matrices A^i. In general, the system may not have translation symmetry and A^i can vary from site to site. For simplicity of notation, we will not write the site label for the matrices explicitly. As we are interested in matrix product states with a finite correlation length and as the gapped ground state of a local Hamiltonian, we only need to consider the so-called 'injective' matrix product states. That is, the canonical form of the MPS contains only one block and the double tensor $\mathbb{E}_{\alpha\gamma,\beta\chi}$ has only one eigenvalue with the largest magnitutde (set to be 1) when treated as a matrix with row index $\alpha\gamma$ and colomn index $\beta\chi$. The corresponding left eigenvector is $\Lambda^l_{\alpha\gamma}$ and the right eigenvector is $\Lambda^r_{\beta\chi}$

$$\mathbb{E}_{\alpha\gamma,\beta\chi} = \Lambda^l_{\alpha\gamma}(\Lambda^r_{\beta\chi})^* + ... \tag{8.53}$$

where all the other terms in this decomposition has norm smaller than 1. Let's label this starting point of renormalization group transformation as $\mathbb{E}^{(0)}$.

Apply the renormliazation group transformation to this matrix product state and we can see that the fixed point has a very simple form. Note that in each step of the renormalization group transformation, the double tensor changes as

$$\mathbb{E}^{(n+1)} = \mathbb{E}^{(n)}\mathbb{E}^{(n)} \tag{8.54}$$

Therefore,

$$\mathbb{E}^{(N)} = \left(\mathbb{E}^{(0)}\right)^{2^N} \tag{8.55}$$

In this procedure, the terms in $\mathbb{E}$ with < 1 eigenvalues all decay exponentially. After repeating the renormalization process a finite number of times, $\mathbb{E}^{(N)}$ will be arbitrarily close to a fixed point form $\mathbb{E}^{(\infty)}$ with only one nonzero eigenvalue 1 and

$$\mathbb{E}^{(\infty)}_{\alpha\gamma,\beta\chi} = \Lambda^l_{\alpha\gamma}(\Lambda^r_{\beta\chi})^* \tag{8.56}$$

This process is shown in Fig.8.6 step (1).

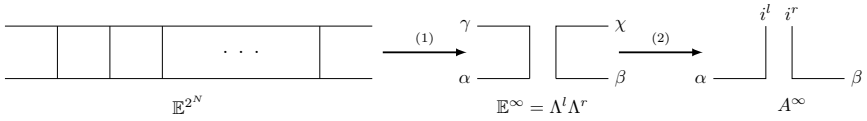

Fig. 8.6 Renormalization fixed point for injective matrix product states.

Now we can decompose $\mathbb{E}^{(\infty)}$ into matrices to find the fixed point wave function as shown in Fig.8.6 step (2). Because $\mathbb{E}^{\infty}$ is positive when treated as a matrix with row index $\alpha\beta$ and colomn index $\gamma\chi$, Λ^l (Λ^r) is also positive when treated as a matrix with row index α (β) and column index γ (χ). Λ_l and Λ_r can be decomposed as

$$\Lambda^l_{\alpha\gamma} = \sum_i \lambda_i v^i_\alpha (v^i_\gamma)^*, \Lambda^r_{\beta\chi} = \sum_j \eta_j u^j_\beta (u^j_\chi)^* \tag{8.57}$$

where $i, j = 1, ..., D$, $\lambda_i, \eta_j > 0$ and $\{v^i\}$, $\{u^j\}$ are two sets of orthonormal vectors.

It then follows that fixed point matrices $A^{(\infty)}$ of the following form can give rise to the fixed point double tensor $\mathbb{E}^{(\infty)}$

$$\left(A^{(\infty)}\right)^{i^l,i^r}_{\alpha\beta} = \sqrt{\lambda_{i^l}\eta_{i^r}}\, v^{i^l}_\alpha u^{i^r}_\beta \tag{8.58}$$

From this structure of $A^{(\infty)}$, we can see that at fixed point the physical degrees of freedom on each site splits into two parts labeled by i^l and i^r. Moreover, i^l is only entangled with degrees of freedom to the left of the site and i^r is only entangled with those to the right of the site. This can be seen more clearly when we put the

fixed point matrices $A^{(\infty)}$ together and find the ground state wave function, as shown in Fig.8.7. The total wave function takes a valence bond structure and is the tensor product of entangled pairs between neighboring sites

$$|\psi^{(\infty)}\rangle = \prod_k |EP_{k_r,k+1_l}\rangle = \prod_k \left(\sum_{i^r,i^l} \sqrt{\lambda_{i^l}\eta_{i^r}} \left(\sum_\alpha v_\alpha^{i^l} u_\alpha^{i^r} \right) |i^r i^l\rangle \right)_{k,k+1} \tag{8.59}$$

The form of the entangled pair $|EP_{k_r,k+1_l}\rangle$ between site k and $k+1$ looks rather complicated. But this is of no importance as we are free to apply a local unitary transformation and change it to any other state between the right spin on site k and the left spin on site $k+1$.

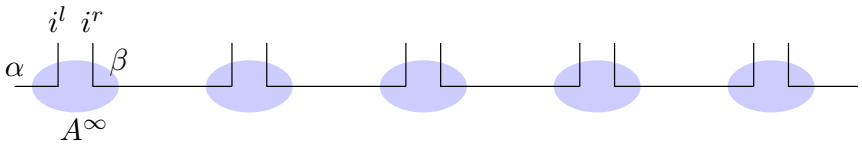

Fig. 8.7 Valence bond structure of fixed point wave function for short range correlated 1D quantum states.

In particular, we can disentangle these pairs by applying one layer of local unitary transformations between every neighboring sites and map the state to a product state (Fig. 8.8).

Through these steps we have shown that all SRC matrix product states can be mapped to product states with LU transformations and have only short range entanglement. Therefore, there is no topological order in 1D gapped bosonic system.

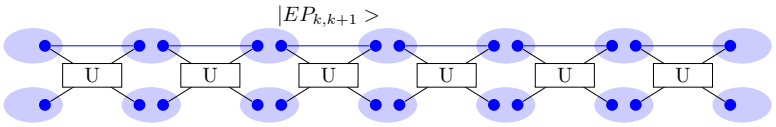

Fig. 8.8 Disentangling fixed point wave function (upper layer, product of entangled pairs) into direct product state (lower layer) with LU transformations.

8.5 Summary and further reading

In this chapter, we introduce the matrix product state representation of 1D states and use it to classify 1D gapped phases in boson / spin systems without symmetry

constraint. First, we discuss in detail the definition and basic properties of matrix product states, including their entanglement property, gauge degree of freedom and parent Hamiltonian. In particular, matrix product states satisfying the 'injectivity' condition have a finite correlation length and is the unique gapped ground state of a local parent Hamiltonian. This set of matrix product states form the basis for our classification of 1D gapped phases. We describe a renormalization group transformation based on local unitary circuits and apply it to flow any 'injective' matrix product state to a simple fixed point form. By analyzing the structure of all possible fixed point states, we show that all gapped phases in 1D are short range entangled and there is no intrinsic topological order in 1D boson / spin systems. We leave the discussion of fermion phases and phases with symmetry constraint to Chapter 10.

The one-dimensional AKLT state is the earliest example of matrix product states studied[1]. Generalizations of this model were discussed in terms of 'Finitely Correlated States'[4, 5] where it was shown that matrix product states with a finite correlation length are all gapped ground states of local Hamiltonians. A more detailed study of matrix product states, including its canonical form, is given in [11]. It was later realized that, the powerful numerical method of Density Matrix Renormalization Group (DMRG)[15] can be interpreted as a variational calculation with matrix product state ansatz[10, 7]. Recent efforts have put the efficiency of the DMRG algorithm on more rigorous footing. It has been shown that all gapped ground states of one dimensional local Hamiltonians satisfy an entanglement area law[6, 2] and that the necessary inner dimension to approximately describe these state scales only polynomially with system size[13]. Therefore, the matrix product representation for such states is always efficient. Moreover, it has been rigorously proven that a polynomial time algorithm exist to find the matrix product state representation of 1D gapped states, although the algorithm differs from DMRG[8].

The fact that the double tensor of a matrix product state (or a tensor product state in general) uniquely determines the state up to a local change of basis was proved in [9] in the form of the unitary degree of freedom in the operator sum representation of quantum channels $\mathscr{E}$ which is defined in terms the matrices as $\mathscr{E}(X) = \sum_i A_i X A_i^\dagger$.

The renormalization group transformation on matrix product states described in this chapter was proposed in [14], where a partial classification of 1D matrix product states were obtained. It was shown in [3, 12] using matrix product states that no intrinsic topological order exist in 1D boson / spin systems.

References

1. Ian Affleck, Tom Kennedy, Elliott H. Lieb, and Hal Tasaki. Rigorous results on valence-bond ground states in antiferromagnets. *Phys. Rev. Lett.*, 59:799–802, Aug 1987.
2. Itai Arad, Alexei Kitaev, Zeph Landau, and Umesh Vazirani. An area law and sub-exponential algorithm for 1d systems. January 2013.
3. Xie Chen, Zheng-Cheng Gu, and Xiao-Gang Wen. Complete classification of one-dimensional gapped quantum phases in interacting spin systems. *Phys. Rev. B*, 84:235128, Dec 2011.

4. Mark Fannes, Bruno Nachtergaele, and Reinhard F. Werner. Finitely correlated states on quantum spin chains. *Communications in Mathematical Physics*, 144:443–490, 1992. 10.1007/BF02099178.
5. Mark Fannes, Bruno Nachtergaele, and Reinhard F. Werner. Finitely correlated pure states. *Journal of Functional Analysis*, 120(2):511 – 534, 1994.
6. Matthew B. Hastings. An area law for one-dimensional quantum systems. *Journal of Statistical Mechanics: Theory and Experiment*, 2007(08):P08024, 2007.
7. J. Dukelsky, M.A. Martín-Delgado, T. Nishino, and G. Sierra. Equivalence of the variational matrix product method and the density matrix renormalization group applied to spin chains. *Europhys. Lett.*, 43(4):457–462, 1998.
8. Zeph Landau, Umesh Vazirani, and Thomas Vidick. A polynomial-time algorithm for the ground state of 1d gapped local hamiltonians. July 2013.
9. Michael A. Nielsen and Isaac L. Chuang. *Quantum Computation and Quantum Information*. Cambridge University Press, 1 edition, October 2000.
10. Stellan Östlund and Stefan Rommer. Thermodynamic limit of density matrix renormalization. *Phys. Rev. Lett.*, 75:3537–3540, Nov 1995.
11. David Pérez-García, Frank Verstraete, Michael M. Wolf, and J. Ignacio Cirac. Matrix Product State Representations. *Quant. Inf. Comput.*, 7:401, May 2007.
12. Norbert Schuch, David Pérez-García, and Ignacio Cirac. Classifying quantum phases using matrix product states and projected entangled pair states. *Phys. Rev. B*, 84:165139, Oct 2011.
13. Norbert Schuch, Michael M. Wolf, Frank Verstraete, and J. Ignacio Cirac. Entropy scaling and simulability by matrix product states. *Phys. Rev. Lett.*, 100(3):030504, Jan 2008.
14. Frank Verstraete, J. Ignacio Cirac, José I. Latorre, Enrique Rico, and Michael M. Wolf. Renormalization-group transformations on quantum states. *Phys. Rev. Lett.*, 94:140601, Apr 2005.
15. Steven R. White. Density matrix formulation for quantum renormalization groups. *Phys. Rev. Lett.*, 69:2863–2866, Nov 1992.

Chapter 9
Tensor Product States and 2D Gapped Phases

Abstract Tensor product state is a natural generalization of matrix product state to two and higher dimensions. It is similar to matrix product states in many ways, like satisfying the entanglement area law and having a projected entangled pair interpretation. However, it is also different from matrix product states in that it represents not only states with short-range entanglement but topologically ordered states with long-range entanglement as well. In this chapter, we first introduce the basic properties of tensor product states and then proceed to discuss how it represents symmetry breaking phases and topological phases with explicit examples. In particular, we are going to focus on the general structural properties of the local tensors which are responsible for the corresponding symmetry breaking or topological order. Other forms of tensor network state, including the tree tensor network state and MERA (multiscale entanglement renormalization ansatz), are also discussed.

9.1 Introduction

The matrix product state representation had a great success in 1D both analytically and numerically. Can we achieve the same kind of success in two and higher dimension? Tensor product states (TPS) provide a natural generalization of matrix product states to higher dimensions by placing higher rank tensors, instead of matrices, on each lattice site. The representation hence obtained is similar to matrix product states in many ways. For example, TPS satisfies the entanglement area law. As ground states in general dimensions are found to obey the area law, TPS is expected to provide a good representation of them.

On the other hand, it is much harder to achieve analytical rigorousness and numerical efficiency with TPS. It has not been proven that the TPS representation of gapped ground states is always efficient. Also it is not easy to identify which subset of TPS correspond to gapped ground states and which subset to gapless ones. On the numerical side, variational simulation using TPS requires the contraction of a two

dimensional tensor network, which is in general computationally hard. Computation accuracy needs to be sacrificed in order to achieve efficiency.

Despite all this, tensor product state is also more interesting than matrix product state because it can describe long-range entangled states, apart from short ranged ones. Simple tensor product representation exists for a large class of topologically ordered states. A better understanding of how topological order, as a global feature, can emerge out of local tensors provides a deeper understanding of the special entanglement structure in such phases.

In this chapter, we start by introducing the definition and basic properties of tensor product states in section 9.2. In particular, we compare and contrast it to what we already know about matrix product states. We then move on to discuss how to represent different 2D phases using tensor product states. In section 9.3 symmetry breaking phases are discussed with the example of Ising model, and in section 9.4 topological phases is discussed with the example of toric code. We focus in particular on the structural properties of the local tensors which is responsible for the corresponding symmetry breaking or topological order. Matrix product states and tensor product states are special examples of tensor network representations. In section 9.5, we briefly introduce other forms of tensor network states, including the tree tensor network state and MERA (the multiscale entanglement renormalization ansatz).

9.2 Tensor product states

The idea of introducing extra inner indices to efficiently represent many-body entangled states can be generalized to higher dimensions. In describing one dimensional many-body entangled states, a set of matrices were used whose left and right indices encode the entanglement to the left and right part of the chain. To describe two and higher dimensional many-body entangled states, we need tensors with three or more inner indices to represent entanglement in a higher dimensional space. Such higher dimensional generalizations of matrix product states are in general called the 'Tensor Product States'. Tensor product states share many properties with their matrix product counterparts, like an entanglement area law and a projected entangled pair picture. However, some properties of matrix product states do not generalize to tensor product states and in general we know much less about tensor product states than matrix product states. In this section, we summarize what we know and what we do not know about tensor product states.

9.2.1 Definition and examples

Box 9.1 Tensor product state

A tensor product state in a many-body spin system is represented as

$$|\psi\rangle = \sum_{i_1,i_2,\ldots i_m\ldots} \mathrm{tTr}(T^{i_1}T^{i_2}\ldots T^{i_m}\ldots)|i_1 i_2\ldots i_m\ldots\rangle \tag{9.1}$$

Here $i_k = 1\ldots d$, with d being the physical dimension of each spin in the system. T_i's are tensors living on each site of a lattice with three or more inner indices. They are usually connected according to the underlying lattice structure of the system and tTr represents tensor contraction. Here by tensor we mean in general a set of numbers labeled by several indices. A vector is a tensor with one index and a matrix is a tensor with two indices. WLOG, the word 'tensor' is usually used when there are three or more indices. Two tensors can be contracted if we match their corresponding indices, multiply their values and sum over the matched indices. For vectors or matrices, such an operation corresponds to vector or matrix multiplication.

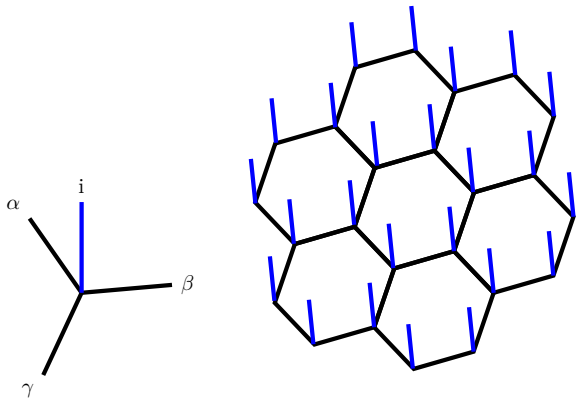

Fig. 9.1 Left: tensor T representing a 2D quantum state on hexagonal lattice. i is the physical index, α,β,γ are inner indices. Right: a tensor product state where each vertex is associated with a tensor. The inner indices of the neighboring tensors connect according to the underlying hexagonal lattice.

For example, consider a two-dimensional spin model on a hexagonal lattice with one spin (or one qudit) living at each vertex. The state can be represented by assigning to every vertex a set of tensors $T^i_{\alpha\beta\gamma}$, where i labels the local physical dimension and takes value from 1 to d. α,β,γ are inner indices along the three directions in the hexagonal lattice respectively. The dimension of the inner indices is D. Fig. 9.1

gives a side view of a local tensor and a tensor product state with inner indices in the horizontal plane and the physical indices pointing in the vertical direction.

Note that a 'Tensor Product State' is different from a 'Product State'. By 'Product State', we mean that the wave function is a product of wave functions on each individual spin

$$|\psi_{\text{product state}}\rangle = |\psi_1\rangle \otimes ... \otimes |\psi_N\rangle \tag{9.2}$$

However, a 'Tensor Product State' is in general an entangled state. By 'Tensor Product State', we mean that the wave function is written as in Eq. 9.1 in terms of local tensors. When a product state is written in terms of the tensor product formalism, we only need trivial local tensors with all inner indices being one dimensional.

Nontrivial tensor product states are many-body entangled. For example, the GHZ state

$$|\psi_{\text{GHZ}}\rangle = \frac{1}{\sqrt{2}}(|00...0\rangle + |11...1\rangle) \tag{9.3}$$

can be represented with tensors (ignore normalization of the wave function)

$$T^0_{0...0} = 1,\ T^1_{1...1} = 1,\ \text{all other terms are 0} \tag{9.4}$$

More interestingly, some highly nontrivial topological states can also be represented in a very simple way using tensors. Toric code is an example. Consider a toric code model defined on a two dimensional square lattice with one spin $1/2$ per each link. The Hamiltonian of the toric cdoe is a sum of vertex and plaquette term (as introduced in chapter 3 and chapter 5)

$$H_{\text{toric code}} = -\sum_s \prod_{j\in \text{star}(s)} Z_j - \sum_p \prod_{j\in \text{plaquette}(p)} X_j \tag{9.5}$$

and the ground state wave function is an equal weight superposition of all closed loop configurations

$$|\psi\rangle_{\text{toric code}} = \sum_C |C\rangle \tag{9.6}$$

This wave function can be represented as a tensor product state with two sets of tensors, one at each vertex and one on each link. The one at the vertex T has four two-dimensional inner indices but no physical index

$$\begin{aligned} T_{ijkl} &= 1,\ \text{ if } i+j+k+l = 0 \bmod 2; \\ T_{ijkl} &= 0,\ \text{ if } i+j+k+l = 1 \bmod 2; \end{aligned}$$

The one on each link t has two two-dimensional inner indices and one two-dimensional physical index

$$t^0_{00} = t^1_{11} = 1,\ \text{all other terms are 0} \tag{9.7}$$

The tensors connect according to the underlying square lattice as shown in Fig. 9.7.

It is easy to see why these tensors give rise to the wave function in Eq. 9.6 by interpreting the 0 inner index as no string and the 1 inner index as with a string. t

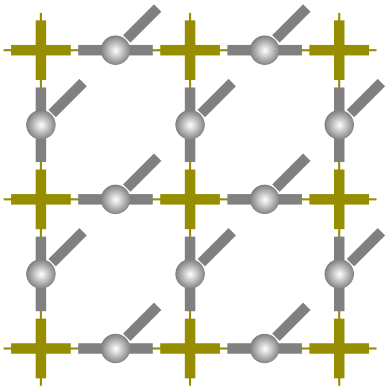

Fig. 9.2 Tensor product representation of the toric code state.

then connects the physical spin state with the string and T enforces the constraint that all strings form closed loops. All closed loop configurations enter the wave function with an equal amplitude.

9.2.2 Properties

9.2.2.1 Properties similar to matrix product state

Tensor product states are similar to matrix product states in terms of the formulation of double tensor, entanglement area law, gauge degree of freedom, and PEPS description although it is not clear when it describes a short range correlated gapped state and when it does not.

For tensor product states, we can similarly define a double tensor which can be used for the calculation of the norm and local observables on the state.

$$\mathbb{T}_{\alpha\ldots\gamma,\tilde{\alpha}\ldots\tilde{\gamma}} = \sum_i T^i_{\alpha\ldots\gamma} \left(T^i_{\tilde{\alpha}\ldots\tilde{\gamma}}\right)^* \tag{9.8}$$

The norm of the tensor product state can be calculated by contracting all the double tensors according to the tensor network structure of the tensor product state

$$\langle\psi|\psi\rangle = \mathrm{tTr}(\mathbb{T}[1]\mathbb{T}[2]\ldots\mathbb{T}[m]\ldots) \tag{9.9}$$

where $\mathbb{T}[m]$ is the double tensor at the mth lattice site.

The expectation value of a local observable O at site n is given by

$$\langle O\rangle = \frac{\mathrm{tTr}(\mathbb{T}[1]\mathbb{T}[2]\ldots\mathbb{T}_O[n]\ldots\mathbb{T}[m]\ldots)}{\mathrm{tTr}(\mathbb{T}[1]\mathbb{T}[2]\ldots\mathbb{T}[n]\ldots\mathbb{T}[m]\ldots)} \tag{9.10}$$

where

$$(\mathbb{T}_O)_{\alpha\ldots\gamma,\tilde{\alpha}\ldots\tilde{\gamma}} = \sum_{i,j} O_{ij} T^i_{\alpha\ldots\gamma} \left(T^j_{\tilde{\alpha}\ldots\tilde{\gamma}}\right)^* \tag{9.11}$$

Tensor product states also enjoy the nice property of having an entanglement area law. In fact, for a tensor product state with inner dimension D, the rank of the reduced density matrix of a subregion is bounded by D^n, where n is the number of indices connecting the subregion with the rest of the system. As n scales linearly with the boundary L of the subregion, the entanglement entropy of a subregion also scales linearly with with L.

Box 9.2 Entanglement area law for tensor product states

In a finite dimensional tensor product state, the entanglement entropy of a subregion scales linearly with the length L of the boundary of the subregion

$$S \sim \alpha L \tag{9.12}$$

Therefore, tensor product states could provide a nice description of gapped quantum systems in two and higher dimensions.

Similar to the matrix product state representation, the tensor product state representation also has a gauge degree of freedom. In particular,

$$T'_{\alpha'\beta'\gamma'} = \sum_{\alpha,\beta,\gamma} M_{\alpha'\alpha} N_{\beta'\beta} O_{\gamma'\gamma} T_{\alpha\beta\gamma} \tag{9.13}$$

represents the same state as T if the invertible matrices M,N,O cancel out for each pair of connected indices.

The projected entangled pair state (PEPS) representation of tensor product states can be constructed analogously as for matrix product states. Starting from a two or higher dimensional lattice with maximally entangled virtual pairs $|\psi\rangle = \frac{1}{\sqrt{D}} \sum_{\alpha=1}^{D} |\alpha\alpha\rangle$ between nearest neighbor sites, apply a mapping P from virtual spins at each site to the physical Hilbert space

$$P = \sum_{i,\alpha,\ldots,\gamma} T^i_{\alpha,\ldots,\gamma} |i\rangle\langle\alpha\ldots\gamma| \tag{9.14}$$

The wave function obtained in this procedure is the tensor product state represented by tensors $T^i_{\alpha,\ldots,\gamma}$. Equivalently, we are start from other maximally entangled state which are all local unitary equivalent to each other.

An interesting many-body entangled state that can be understood in the PEPS representation is the AKLT state (in two or higher dimensions). For a lattice with degree n vertices, put singlet pairs $|\psi\rangle = \frac{1}{\sqrt{2}}(|01\rangle - |10\rangle)$ onto each link. Then project the n spin $1/2$'s at each vertex to the spin $n/2$ space. The wave function obtained in this way is called the spin $n/2$ AKLT state. From this construction we can see that it is naturally invariant under global spin rotation symmetry.

9.2.2.2 Properties different from matrix product states

On the other hand, tensor product states are also different from matrix product states in many ways.

First of all, there is no known efficient way to extract the correlation length of the state from the tensors. Therefore it is not easy to identify tensor product states which are gapped ground states of local Hamiltonians. An analogous notion of injectivity can be defined for tensor product states. An injective tensor product state satisfies that for a large enough region with L sites inside, the following map is injective

$$\Gamma_L : W \mapsto \sum_{i_1,\ldots i_L=1}^{d} \mathrm{tTr}(WT^{i_1}\ldots T^{i_L})|i_1\ldots i_L\rangle \tag{9.15}$$

where W is a tensor which contracts to all the open inner indices around the boundary of the region. Injectivity is still a generic property for tensor product states on two and three dimensional (or any finite dimensional) lattice, however, they are no longer directly related to finite correlation length. In fact, it is known that there are injective tensor product states whose correlation functions only decay polynomially. Therefore, it is not clear which subset of tensor product states describe short range correlated, gapped quantum states.

Moreover, one major difficulty with using tensor product states for numerical simulation is that the contraction of tensor networks in two and higher dimensions is in general not efficient. Usually an approximate renormalization algorithm is used, but the error is not always well bounded.

9.2.2.3 Approximate calculation of local observables

In order to calculate expectation value of local observables in a tensor product state, we need to contract two-dimensional tensor networks. Unlike in the one-dimensional case, the contraction of a two-dimensional tensor network is not efficient in general. Approximate methods have been developed to efficiently evaluate the tensor contraction for physical tensor networks of interest and can be implemented as follows.

Consider, for example, a tensor network on a honeycomb lattice with one three-indexed tensor T_{ijk} per each site. First, combine each pair of tensors in dashed circles in Fig. 9.3(a). Apply a singular value decomposition in the perpendicular direction and obtain tensors S^1 and S^2 which satisfy

$$\sum_m T^1_{ijm} T^2_{mkl} = \sum_n S^1_{iln} S^2_{njk} \tag{9.16}$$

In order to keep the computation efficient, we need to keep an upper bound D_{cut} on the dimension of the indices. In this decomposition step, we may need to cut off on the dimension of n if the number of nonzero singular values exceeds D_{cut}. The most natural way to do this cut-off is to throw away dimensions with singular values of

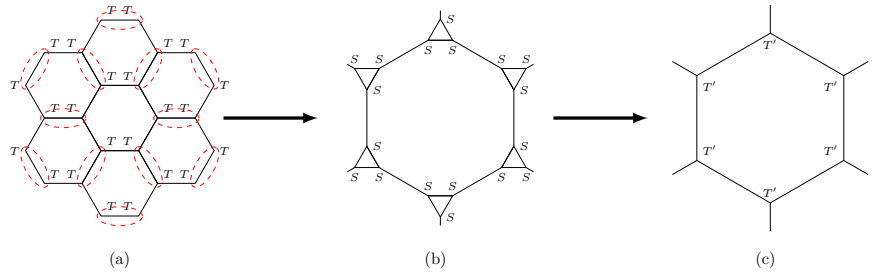

Fig. 9.3 Tensor renormalization on hexagonal lattice.

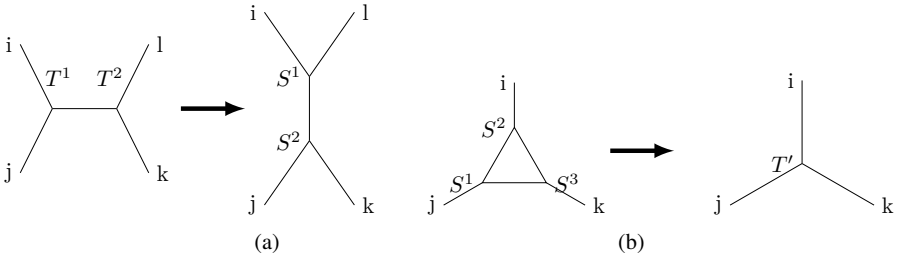

Fig. 9.4 Individual steps of tensor renormalization on hexagonal lattice.

smallest weights. This also guarantees the best approximation of the original tensor network by the transformed one.

After such a step, the hexagonal lattice changes into a structure depicted in Fig.9.3(b). Then combine the three S tensors around a triangle into a T' tensor

$$\sum_{lmn} S^1_{iln} S^2_{ljm} S^3_{mnk} = T'_{ijk} \tag{9.17}$$

No approximation is necessary in this step. After this combination, the lattice is transformed back into a regular hexagonal structure as shown in Fig.9.3(c), but with lattice constant $\sqrt{3}$ times that of the original lattice in (a) and only one third the number of tensors. With these steps, we have finished one round of tensor renormalization group transformation and the resultant T' tensor can be used as the starting point for the next round of RG. After N rounds of RG transformaiton, we can reduce a tensor network with, for example, 3^{N+1} tensors to one with only 3 tensors, which is then trivial to evaluate. Therefore, this RG scheme provides us with an efficient, although approximate way to contract big tensor networks.

A similar RG procedure can also be devised for a square lattice tensor network.

As shown in Fig.9.6(a), first take a local tensor T_{ijkl} and do a singular value decomposition into two tensors S^1 and S^2. The two ways of decomposition are applied to the two sublattice (red and green) in the square lattice as shown in Fig.9.5(a).

$$T_{ijkl} = \sum_m S^1_{jkm} S^2_{mil} \text{ or } T_{ijkl} = \sum_m S^1_{ijm} S^2_{mkl} \tag{9.18}$$

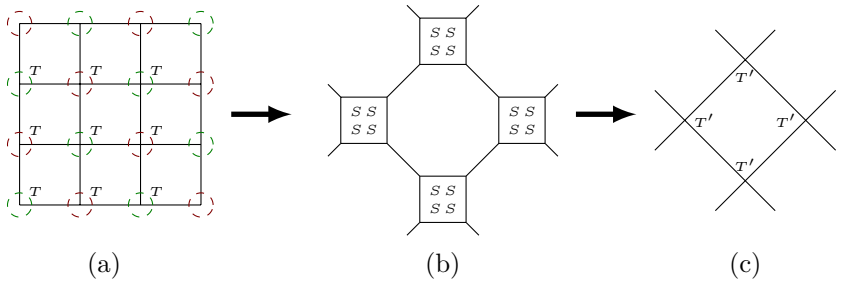

Fig. 9.5 Tensor renormalization on square lattice.

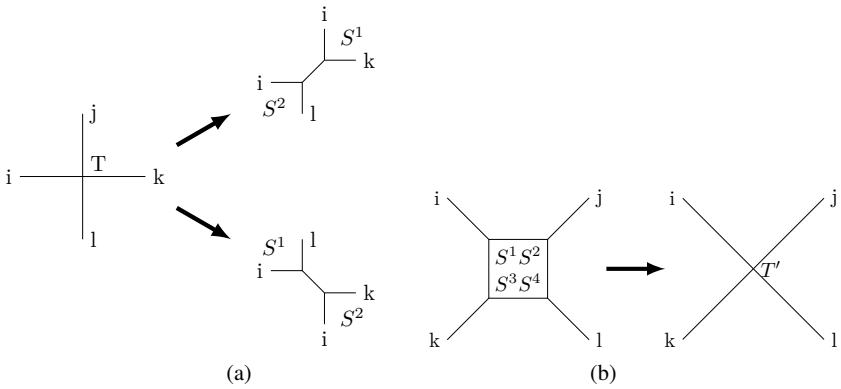

Fig. 9.6 Individual steps of tensor renormalization on square lattice.

After the decomposition, the lattice structure is transformed into Fig.9.5(b). Similarly, we may need to cut-off the dimension of m at D_{cut} to keep the computation efficient.

Then combine four S tensors around a square into a T' tensor, as shown in Fig.9.6(b)

$$\sum_{mnpq} S^1_{iqm} S^2_{jmn} S^3_{knp} S^4_{lpq} = T'_{ijkl} \tag{9.19}$$

No cut-off is necessary in this step. After the combination, the lattice is transformed back into a square lattice structure (Fig.9.5(c)), with $\sqrt{2}$ times the lattice constant and half the number of tensors as the original lattice (Fig.9.5(a)). The resultant tensor T' serves as the input of the next round of RG process. Similar to the hexagonal case, this provides us with a way to efficiently approximately contract a 2D tensor network on a square lattice.

9.3 Tensor network for symmetry breaking phases

The transverse field Ising model is a prototypical example of a gapped symmetry breaking phase and we are going to use it for the study of the tensor network representation of symmetry breaking phases. We are going to see how symmetry breaking is encoded in the structure of the local tensors representing the ground states. As a simple and interesting example of short range entangled states, it will be compared to later when we discuss the long range entangled cases.

9.3.1 Ising model

On a 2D lattice of two-level spins, the Hamiltonian of the transverse field Ising model takes the form

$$H^{\text{tIsing}} = -J \sum_{<ij>} Z_i Z_j - B \sum_i X_i \tag{9.20}$$

where $< ij >$ are nearest neighbor pairs of spins on the lattice. The system has a $\mathbb{Z}_2$ symmetry of

$$U = \prod_i X_i \tag{9.21}$$

which flips the spins between $|\uparrow\rangle$ and $|\downarrow\rangle$.

When $J = 1$ and $B = 0$, the system is in a symmetry breaking phase with two degenerate ground states $|\uparrow\uparrow ... \uparrow\rangle$ and $|\downarrow\downarrow ... \downarrow\rangle$. Each state breaks the $\mathbb{Z}_2$ symmetry and maps into each other under the symmetry transformation. Their superposition, $|\uparrow\uparrow ... \uparrow\rangle + |\downarrow\downarrow ... \downarrow\rangle$, is however symmetric under $\mathbb{Z}_2$ and has a tensor network representation as

$$T^{\uparrow}_{000} = 1,\ T^{\downarrow}_{111} = 1, \quad \text{all other terms being 0} \tag{9.22}$$

on a hexagonal lattice and

$$T^{\uparrow}_{0000} = 1,\ T^{\downarrow}_{1111} = 1, \quad \text{all other terms being 0} \tag{9.23}$$

on a square lattice. Here in $T^{i}_{\alpha\beta...}$, i is the physical index and $\alpha\beta...$ are the inner indices.

When $J = 0$ and $B = 1$, the system is in a simple symmetric phase with a unique ground state $|\rightarrow\rightarrow ... \rightarrow\rangle$ where $|\rightarrow\rangle = (|\uparrow\rangle + |\downarrow\rangle)/\sqrt{2}$. The tensor product representation for this state is simply $T^{\uparrow} = 1$, $T^{\downarrow} = 1$.

9.3.2 Structural properties

The tensor for the symmetric ground state in the symmetry breaking phase has some interesting structural properties.

First of all, we can see that it is not injective. The notion of injectivity was defined in chapter 6. The tensor on any local region is supported on only two dimensions of the inner indices $|00...0\rangle$ and $|11...1\rangle$. All other dimensions are 0. In fact, the tensor can be decomposed into two blocks T_a and T_b

$$T^{\uparrow}_{a,00...0} = 1, \text{ all other terms being } 0 \tag{9.24}$$

and

$$T^{\downarrow}_{b,11...1} = 1, \text{ all other terms being } 0 \tag{9.25}$$

T_a and T_b are each supported on orthogonal inner dimensions and there are no cross terms in the tensor.

Moreover, the tensor has a $\mathbb{Z}_2$ symmetry which acts as X on the physical index and X on the inner indices. The two blocks map into each other under the symmetry and the whole tensor is invariant. When the tensor network is contracted togehter, the X transformation on the inner indices cancel in pairs and the full state is invariant under $\prod_i X_i$ on all the physical indices, as expected.

9.3.3 Symmetry breaking and the block structure of tensors

While the meaning of symmetry breaking is straight-forward in classical system, this concept is more subtle in the quantum setting. The tensor network representation provides better insight into the notion of quantum symmetry breaking.

A classical system is in a symmetry breaking phase if each possible ground state has lower symmetry than the total system. For example, the classical Ising model with Hamiltonian

$$H_c = \sum_{<ij>} n^i n^j \tag{9.26}$$

has a spin flip symmetry between spin up $\uparrow$ and spin down $\downarrow$. Here $n = 1$ for spin up $\uparrow$ and $n = -1$ for spin down $\downarrow$. However neither of its ground states $\uparrow\uparrow ... \uparrow$ and $\downarrow\downarrow ... \downarrow$ has this symmetry. Therefore, the meaning of symmetry breaking in classical systems is obvious.

However, in the quantum Ising model discussed above, at $J = 1$ and $B = 0$, the ground space contains not only the two states of $|\uparrow\uparrow ... \uparrow\rangle$ and $|\downarrow\downarrow ... \downarrow\rangle$, but also any superposition of them. While each of $|\uparrow\uparrow ... \uparrow\rangle$ and $|\downarrow\downarrow ... \downarrow\rangle$ breaks the $\mathbb{Z}_2$ symmetry, their superposition $|\uparrow\uparrow ... \uparrow\rangle + |\downarrow\downarrow ... \downarrow\rangle$ is invariant under this symmetry. This is the GHZ state as we discussed before. In fact, if we move away from the exactly solvable point by adding symmetry preserving perturbations (such as transverse field $B\sum_i X_i$) and solve for the ground state with finite system size, we will

always get a state symmetric under this spin flip symmetry. Only in the thermodynamic limit does the ground space become two dimensional. How do we tell then whether the ground states of the system spontaneously break the symmetry?

With the tensor network representation (including the matrix product state representation), the symmetry breaking pattern can be easily seen from the tensors (matrices). Suppose that we solved the ground state of a system with certain symmetry at finite size and found a unique minimum energy state which has the same symmetry. To see whether the system is in the symmetry breaking phase, we can write this minimum energy state in the tensor product state representation. The tensors in the representation can be put into a block form

$$T^i_{\alpha\beta\ldots} = T^i_{a,\alpha_a\beta_a\ldots} \oplus T^i_{b,\alpha_b\beta_b\ldots} \oplus \ldots \tag{9.27}$$

where α_a, α_b, etc. span orthogonal sub-dimensions of α, β_a, and β_b, etc. span orthogonal sub-dimensions of β. When the tensor network is contracted, only tensors of the same block contract with each other. Tensors of different blocks are supported on orthogonal dimensions and their contraction is 0. This decomposition of T^i is such that T^i_a, T^i_b etc. each represents a short range correlated state. Then if in the thermodynamic limit, the block form of the tensor contains only one block, this minimum energy state is short range correlated and the system is in a symmetric phase. However, if the block form splits into more than one block with equal amplitude, then we say the symmetry of the system is spontaneously broken in the ground states.

We can see that the tensors for the $J = 1, B = 0$ ground states contain two blocks while the tensors for the $J = 0, B = 1$ ground state contain only one block. Therefore, we say the symmetry is spontaneously broken in the former and not broken in the latter.

The symmetry breaking interpretation of the block form can be understood as follows. Each block T_k represents a short range correlated state $|\psi_k\rangle$. Note that here by correlation we always mean connected correlation $< O_1 O_2 > - < O_1 >< O_2 >$. Therefore, the symmetry breaking states like $|\uparrow\uparrow \ldots \uparrow\rangle$ and $|\downarrow\downarrow \ldots \downarrow\rangle$ both have short range correlation. Two different short range correlated state $|\psi_k\rangle$ and $|\psi_{k'}\rangle$ have zero overlap $\langle\psi_k|\psi_{k'}\rangle = 0$ and any local observable has zero matrix element between them $\langle\psi_k|O|\psi_{k'}\rangle = 0$. The ground state represented by T^i is an equal weight superposition of them $|\psi\rangle = \sum_k |\psi_k\rangle$. Actually the totally mixed state $\rho = \sum_k |\psi_k\rangle\langle\psi_k|$ has the same energy as $|\psi\rangle$ as $\langle\psi_k|H|\psi_{k'}\rangle = 0$ for $k \neq k'$. Therefore, the ground space is spanned by all $|\psi_k\rangle$'s. Consider the operation which permutes the $|\psi_k\rangle$'s. This operation keeps ground space invariant and can be a symmetry of the system. However, each short range correlated ground state is changed under this operation. Therefore, we say that the ground states spontaneously break the symmetry of the system.

Box 9.3 Symmetry breaking and block structure of tensors

Tensors representing the Ising symmetry breaking ground state have multiple blocks with each block representing different short range correlated spin configurations.

9.4 Tensor network for topological phases

While the quantum symmetry breaking phases have their classical counterparts and can be understood at least qualitatively using a classical picture, the topological phases are intrinsically quantum and demand an inherently quantum approach of study. Tensor networks can be used to represent a large class of topological states and provide a promising tool for both analytical and numerical study of topological phases. The fact that states with long range entanglement can be represented with local tensors is very surprising and in this section we are going to discuss, with the example of the toric code model, how the topological property of the state is manifested in the tensors.

9.4.1 Toric code model

Recall the toric code tensor network introduced in section 9.2.1. The Hamiltonian reads

$$H_{\text{toric code}} = -\sum_s \prod_{j\in \text{star}(s)} Z_j - \sum_p \prod_{j\in \text{plaquette}(p)} X_j \tag{9.28}$$

and the ground state wave function can be represented as a tensor product state with T tensors at the vertex and t tensors on the links

$$T_{ijkl} = 1, \text{ if } i+j+k+l = 0 \text{ mod } 2;$$
$$T_{ijkl} = 0, \text{ if } i+j+k+l = 1 \text{ mod } 2;$$

The one on each link t has two two-dimensional inner indices and one two-dimensional physical index

$$t^0_{00} = t^1_{11} = 1, \text{ all other terms are } 0 \tag{9.29}$$

The tensors connect according to the underlying square lattice as shown in Fig. 9.7.

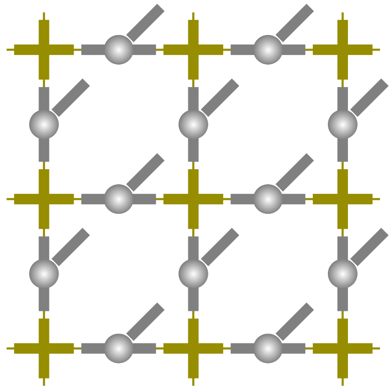

Fig. 9.7 Tensor product representation of the toric code state.

9.4.2 Structural properties

The most important property of the above tensor is that it has certain inner symmetry, that is, the tensor is invariant under some non-trivial operations on the inner indices, as shown in Fig. 9.8 (a).

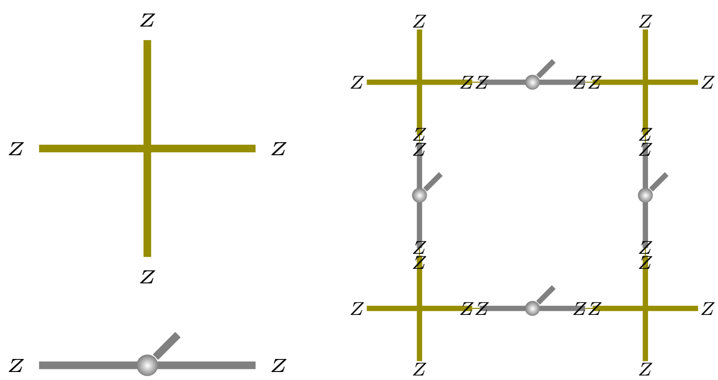

(a) (b)

Fig. 9.8 Symmetry of the toric code tensor. (a) Each local tensor remains invariant under the action of $Z \otimes Z \otimes Z$ on its inner indices. (b) A region of tensor network is invariant under $\prod_i Z_i$ on its open inner indices.

Z does nothing to the tensor when the index is 0 and changes the sign of the tensor when the index is 1. In the T tensor of the ideal toric code (Eq.9.29), only even configurations of the inner indices are non-zero. Hence applying Z at the same time to all four inner indices doesn't change the tensor. That is, $Z \otimes Z \otimes Z \otimes Z$ is a symmetry of the tensor. Similarly, in the t tensor (Eq.9.29), the two inner indices are

either both 0 or both 1. Therefore, applying Z at the same time to both inner indices does not change the tensor. That is, $Z \times Z$ is a symmetry of the tensor. Note that this symmetry operation does not act on the physical indices at all and is purely an inner property of the tensor.

As Z squares to identity, we will say that the tensor has a $\mathbb{Z}_2$ symmetry. Note that we can insert a set of unitary operators $U, U^\dagger$ between any connected links in a tensor network without affecting the result of tensor contraction and hence the quantity represented by the tensor network. Therefore, the $\mathbb{Z}_2$ symmetry could take any form which is local unitary equivalent to $Z \otimes Z \otimes Z \otimes Z$.

This symmetry property is true not only for each local tensor but for any region in the tensor network as well. As shown in Fig.9.8 (b), when the local tensors are put together, the symmetry transformation on the contracted inner indices cancel in pairs and the symmetry transformation on the outer un-contracted inner indices are left behind. Therefore, this piece of tensor network has also a $\mathbb{Z}_2$ symmetry given by $\prod_i Z_i$ over all its outer inner indices.

This $\mathbb{Z}_2$ symmetry is closely related to the closed loop constraint of the state. Due to this symmetry, the tensor network cannot be 'injective', because only even configurations can be nonzero on each any piece of tensor network. But the tensor does span the full space which is even under this $\mathbb{Z}_2$ transformation.

Box 9.4 $\mathbb{Z}_2$ injectivity of toric code tensor

The tensor representing the toric code ground state has an inner $\mathbb{Z}_2$ symmetry and it spans the full space which is $\mathbb{Z}_2$ invariant. The tensor is hence said to be $\mathbb{Z}_2$ injective.

9.4.3 Topological property from local tensors

Encoded in this $\mathbb{Z}_2$ symmetry of the tensor are some interesting topological properties of the toric code wave function.

Consider a tensor network as shown in Fig.9.9. For clarity, we are not drawing the physical indices unless they are acted upon. Insert Z operators on the inner indices around a region, as shown in Fig.9.9 (a). As discussed above, as long as the Z operators act on all the outer inner indices of a region, the tensors are invariant and the state represented remains the same. Due to the one-to-one correspondence between the inner configurations and the physical configurations, such an action on the inner indices translates into a physical action on the spin-$1/2$'s in the wave function, as shown in Fig.9.9 (b). Therefore, the toric code wave function is invariant under a loop operator of Z's around a region. This is the so-called 'Wilson-loop' operator and is a hall-mark for topological phases.

If we insert Z operators not around a full loop but only along a defect line (solid line in Fig.9.10), then the tensor network does change, but only near the two end

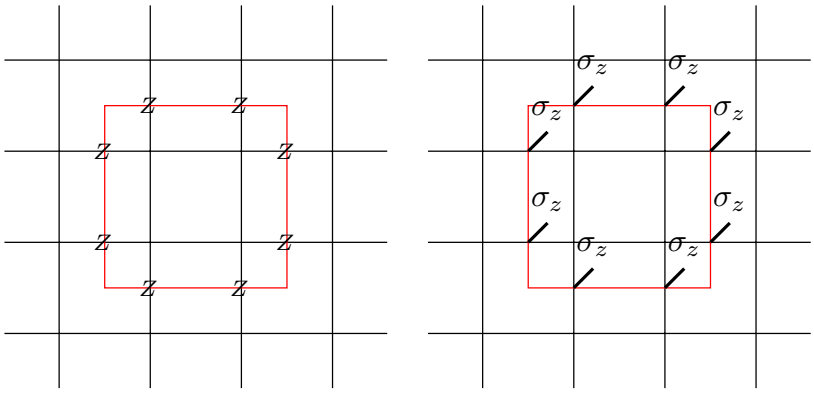

Fig. 9.9 The tensor network is invariant under (a) acting Z on all inner indices surrounding a region (b) acting Z on all the spin-$1/2$'s in a loop. Physical indices are not shown unless they are acted upon.

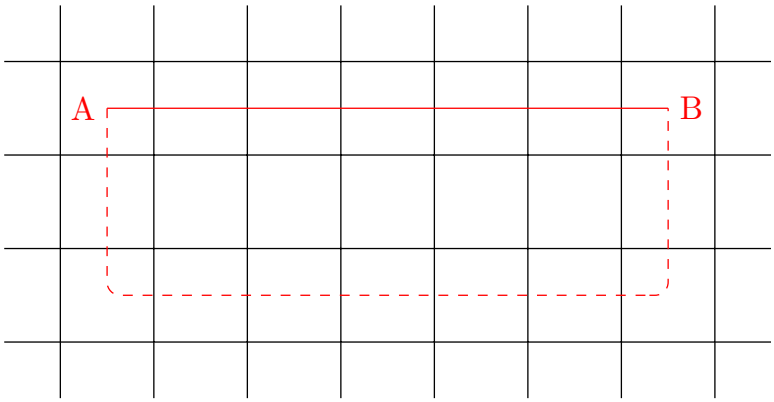

Fig. 9.10 Acting Z operators along a defect line changes the state only near the two end points, which does not depend on the exact path of the defect line.

points (A and B). This is easy to understand by noting that if we complete the circle by inserting Z's along another defect line connecting the same end points (dashed line in Fig.9.10), the tensor network goes back to itself. As the two lines can be very far away from each other except at the end points, their effects cannot cancel anywhere else. Therefore, in the middle part of the defect line, the state represented remains the same. Such a string operator hence creates two local excitations in the system near the end points, which are actually the 'charge' particle of the corresponding $\mathbb{Z}_2$ gauge theory. We are free to move the defect line around and the excitations remain the same as long as we keep the end points fixed. From the string operator it is easy to see that when the 'charge' particles braid with each other, the resulting statistics is trivial.

Now imagine putting the tensor network onto a torus. The ground space of the toric code model is four fold degenerate and the state represented with tensors in Eq.9.29 and 9.29 is one of them. Insert the Z operators long a nontrivial loop of the torus. As the nontrivial loop does not enclose any region, the tensor network does change. However, as discussed above, we can move the location of the loop around without effecting the resulting state. This is because two nontrivial loops in the same direction on the torus always enclose a region and keeps the original tensor network invariant. Therefore, the effect of a single nontrivial loop is the same no matter where the loop is.

Because of this, the resulting state must have the same energy or any local observable as the original state because in calculating them we can always move the inserted loop to be very far away from the location of the operator. That is, the loop operator maps between degenerate ground states of the toric code model which cannot be distinguished from each other with any local operator. Translated to the physical spin-$1/2$, this corresponds to a nontrivial loop of Z operators which is one of the logical operators that rotates the degenerate ground space on the torus.

9.4.4 Stability under symmetry constraint

The inner $\mathbb{Z}_2$ symmetry is essential for keeping the stability of the topological order represented by the tensor network state. A slight violation of the symmetry at each local tensor can immediately destroy the topological order of the state, as shown in the example below.

Let us break the $\mathbb{Z}_2$ symmetry by assigning a small and equal weight ε to all odd configurations in the T tensor, which now reads,

$$\begin{aligned} T_{ijkl} &= 1, \ \text{ if } i+j+k+l = 0 \bmod 2; \\ T_{ijkl} &= \varepsilon, \ \text{ if } i+j+k+l = 1 \bmod 2; \end{aligned}$$

We keep the t tensor invariant.

$$t^0_{00} = t^1_{11} = 1, \text{ all other terms are } 0 \tag{9.30}$$

Note that even though each t tensor is still $\mathbb{Z}_2$ symmetric, a piece of tensor network involving both T and t tensors will in general break the symmetry.

When $\varepsilon = 0$, this is reduced to the tensors in the ideal toric code TPS. When ε is non-zero, odd configurations are allowed at each vertex, which correspond to end of strings. The wave function with nonzero ε then contains all possible string configurations, closed loop or open string. The weight of each string configuration is exponentially small in the number of end of strings contained.

$$|\psi^{\varepsilon}_{\text{toric code}}\rangle = \sum_{C'} \varepsilon^{N(C')} |C'\rangle \tag{9.31}$$

where the summation is over all possible string configurations C' (both closed and open) and $N(C')$ is the number of end of strings in a particular configuration C'.

To see how topological order of the state changes as ε varies from 0, we can calculate the topological entanglement entropy γ of the state as defined in Eq. 5.17 in section 5.3.2. As is shown below for any finite value of ε, γ goes to zero when system size goes to infinity. Hence topological order is unstable under this kind of variation. Let us first go through the process of the calculation and then discuss the implication of the result.

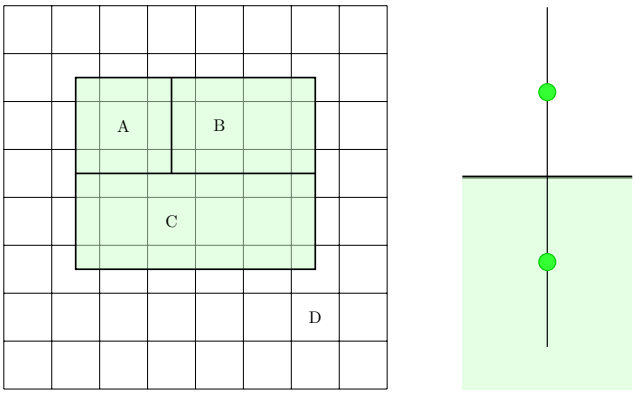

Fig. 9.11 (a) Dividing the system into four regions for the calculation of topological entanglement entropy; (b) for simplicity of calculation, we double the number of spins per link and cut between them when dividing regions.

To calculate topological entanglement entropy, we first divide the lattice into four regions as shown in Fig.9.11 (a) and use the formula

$$\gamma = S_{AB} + S_{BC} + S_{CA} - S_A - S_B - S_C - S_{ABC} \tag{9.32}$$

Let us calculate the entanglement entropy to each region. For simplicity of calculation, when dividing the lattice, we double the number of spins per each link and cut between them, as shown in Fig.9.11 (b). We require that the two spins per each link are either both in the $|0\rangle$ state or both in the $|1\rangle$ state, therefore, they represent a continuous string configuration on each link. Correspondingly, in the tensor network representation, we double the t tensor per each link.

Without the closed loop constraint, a region with m boundary links has 2^m different boundary configurations. Rewriting the wave function according different boundary configuration b_i as

$$|\psi^{\varepsilon}_{\text{toric code}}\rangle = \sum_b \beta_b |\phi_b^{out}\rangle |\phi_b^{in}\rangle \tag{9.33}$$

Because different b's are orthogonal to each other, we have obtained the Schmidt-decomposed form of the wave function and all we need to know to calculate entanglement entropy are the β_b's and the norm.

To calculate the norm, form the double tensor $\mathbb{T}$ and $\mathbb{S}$ as

$$\mathbb{T}_{ijkl,i'j'k'l'} = T_{ijkl} \times T^*_{i'j'k'l'},\ \mathbb{S}_{ij,i'j'} = \sum_n t^n_{ij} (t^n_{i'j'})^* \tag{9.34}$$

Combine each $\mathbb{T}$ with the four $\mathbb{S}$ around it, we obtain the double tensor $\mathbb{T}'$

$$\begin{aligned} \mathbb{T}'_{ijkl,i'=i\ j'=j\ k'=k\ l'=l} &= 1, \quad \text{if } i+j+k+l = 0 \bmod 2; \\ \mathbb{T}'_{ijkl,i'=i\ j'=j\ k'=k\ l'=l} &= \varepsilon^2, \ \text{if } i+j+k+l = 1 \bmod 2 \end{aligned}$$

Contracting the $\mathbb{T}'$ tensors on each site gives us the norm of the wave function. It happens that such a contraction can be done easily with a change of basis for the inner indices. For each pair of inner indices ii', jj', kk', ll', apply transformation

$$|00\rangle + |11\rangle \to |\tilde{0}\rangle,\ |00\rangle - |11\rangle \to |\tilde{1}\rangle \tag{9.35}$$

$\mathbb{T}'$ is transformed into

$$\mathbb{T}'_{\tilde{0}\tilde{0}\tilde{0}\tilde{0}} = \frac{1+\varepsilon^2}{2}, \mathbb{T}'_{\tilde{1}\tilde{1}\tilde{1}\tilde{1}} = \frac{1-\varepsilon^2}{2}, \text{ all other terms are zero} \tag{9.36}$$

Obviously, this tensor network can be contracted easily and gives the norm of the wave function

$$norm = \langle \psi^{\varepsilon}_{\text{toric code}} | \psi^{\varepsilon}_{\text{toric code}} \rangle = 2^N (1+\varepsilon^2)^N + 2^N (1-\varepsilon^2)^N \tag{9.37}$$

where N is the total systems size.

In a similar way, we can calculate $|\beta_b|^2$. To do so, we fix the boundary configuration and replace the double tensor $\mathbb{T}'$ on the boundary with

$$\begin{aligned} \mathbb{T}'_{ijkl,i'=i\ j'=j\ k'=k\ l'=l} &= 1, \quad \text{if } i+j+k+l = 0 \bmod 2,\ i = 0 \text{ or } 1; \\ \mathbb{T}'_{ijkl,i'=i\ j'=j\ k'=k\ l'=l} &= \varepsilon^2, \ \text{if } i+j+k+l = 1 \bmod 2,\ i = 0 \text{ or } 1 \end{aligned}$$

where i corresponds to the link divided by the boundary. Then apply the same transformation as given in Eq.9.35 and contract the tensor network, we find

$$|\beta_b|^2 = \frac{2^N}{2^m} \left((1+\varepsilon^2)^N + (1-\varepsilon^2)^N + (1+\varepsilon^2)^{N_i} (1-\varepsilon^2)^{N_o} + (1-\varepsilon^2)^{N_i} (1+\varepsilon^2)^{N_o} \right) \tag{9.38}$$

where N_i is the number of vertices inside a region and N_o is the number of vertices outside the region. Taking the limit of large system size $N_i \to \infty$, $N \to \infty$

$$|\beta_b|^2 / norm = \frac{1}{2^m} \tag{9.39}$$

The entanglement entropy of a region is

$$S = m \tag{9.40}$$

which satisfy the area law. Therefore, topological entanglement entropy is 0.

At first sight this may be a surprising result, as we are only changing the tensors locally and we are not expected to change the global entanglement pattern of the state. However, when we write out the wave function explicitly we will see that we have actually induced global changes to the state. The wave function in Eq.9.33 can be expanded in powers of ε as

$$|\psi^{\varepsilon}_{\text{toric code}}\rangle = |\psi_{\text{toric code}}\rangle + \varepsilon^2 \sum_{v_i,v_j} |\psi^{v_i,v_j}_{\text{toric code}}\rangle + \ldots \tag{9.41}$$

where the v's are any vertices in the lattice. $|\psi^{v_i,v_j}_{\text{toric code}}\rangle$ is an excited eigenstate of the toric code Hamiltonian (Eq. 9.28) which minimizes energy of all local terms except the vertex terms at v_i, v_j and is hence an equal weight superposition of all configurations with end of strings at v_i and v_j. Note that end of strings always appear in pairs. v_i, v_j can be separated by any distance and the number of local operations needed to take $|\psi_{\text{toric code}}\rangle$ to $|\psi^{v_i,v_j}_{\text{toric code}}\rangle$ scales with this distance.

On the other hand, with arbitrary local perturbation to the dynamics, the Hamiltonian reads

$$H' = H_{TC} + \eta \sum_u h_u \tag{9.42}$$

where h_u's are any local operator and η is small. The perturbed ground state wave function will contain terms like $|\psi^{v_i,v_j}_{\text{toric code}}\rangle$ but only with weight $\eta^{distance(v_i,v_j)}$. When v_i, v_j are separated by a global distance, the weight will be exponentially small. Hence a constant, finite weight ε^2 for all $|\psi^{v_i,v_j}_{\text{toric code}}\rangle$ as required in Eq. 9.41 is not possible. Therefore, while we are only modifying the tensors locally, we introduce global 'defects' to the state, which cannot be the result of any local perturbation to the Hamiltonian. We can, of course, design a Hamiltonian H_ε which has $|\Phi^{\varepsilon}_{TC}\rangle$ as its exact ground state. However, H_ε will not be able to smoothly connect to H_{TC} as $\varepsilon \to 0$.

Therefore, the $\mathbb{Z}_2$ inner symmetry is essential in maintaining the topological order represented by the tensor network. As soon as such a symmetry is broken, the topological order is lost. On the other hand, if only variations preserving the symmetry is allowed to be added to the tensor, the topological order is always stable. That is, the tensor network state has topological entanglement entropy $\gamma = 1$ as long as the variation is small enough. This is because all such variation can be generated with local *physical* operations and topological order is always stable against such *physical* actions.

Box 9.5 Stability of topological order in TPS

In the tensor product representation of the toric code wave function, the $\mathbb{Z}_2$ symmetry is essential for the stability of topological order. Any variation in

the tensor that breaks the $\mathbb{Z}_2$ symmetry can destroy the topological order immediately.

9.5 Other forms of tensor network representation

Beside matrix product states and tensor product states, other forms of tensor network representations have also been deviced and applied to study many-body systems with different forms of many-body entanglement. We discuss two examples in this section: the Multiscale Entanglement Renormalization Ansatz (MERA) and the Tree Tensor Network State.

9.5.1 Multiscale entanglement renormalization ansatz

The Multiscale Entanglement Renormalization Ansatz (MERA) provides a tensor network approach to study gapless systems in one spatial dimension. As discussed previously, matrix product states all satisfy an entanglement area law, hence incapable of describing gapless systems which contain a logrithmic violation of the area law. MERA utilizes a multi-layer structure to properly represent the entanglement in a gapless system and therefore has become a useful tool in the analytical and numerical study of such systems.

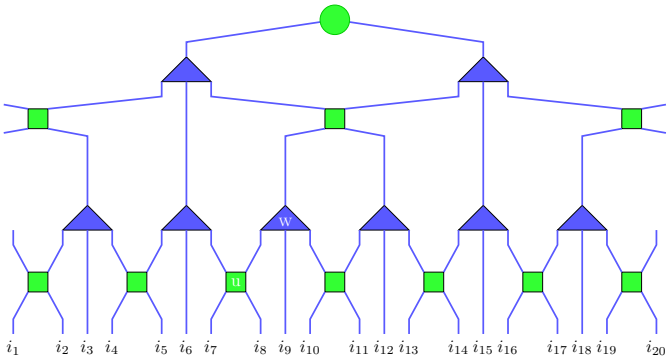

Fig. 9.12 The Multiscale Entanglement Renormalization Ansatz (MERA).

The tensors in a typical MERA are organized as shown in Fig.9.12. The physical indices of the tensor network $i_1, ..., i_N$ are at the lowest layer and all the other indices are inner indices. The u tensors are called disentanglers while the w tensors

are called the isometries. They are organized in a way to mimic the renormalization group (RG) transformation process of the gapless state. As we go from the kth layer to the $k+1$th layer, the number of lattice sites are reduced by a fixed fraction ($2/3$ as shown in Fig.9.12). The gapless state is an RG fixed point and the tensor network contains an infinite number of layers, which scales logrithmically with the system size. The amount of entanglement contained in such a tensor network may go beyond an area law and can adequately describe a gapless state.

The disentangler u is chosen to satisfy

$$\sum_{\gamma\delta} u_{\alpha\beta,\gamma\lambda} \times \left(u_{\alpha'\beta',\gamma\lambda}\right)^* = \delta_{\alpha\alpha'}\delta_{\beta\beta'} \tag{9.43}$$

and the isometry w satisfies

$$\sum_{\beta\gamma\lambda} w_{\alpha,\beta\gamma\lambda} \times \left(w_{\alpha',\beta\gamma\lambda}\right)^* = \delta_{\alpha\alpha'} \tag{9.44}$$

as illustrated in Fig.9.13.

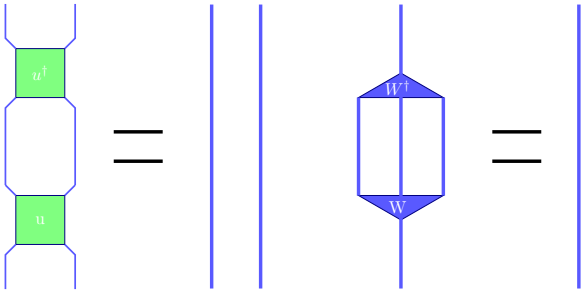

Fig. 9.13 Property of disentanglers and isometries in MERA.

Using this property, the tensor network for calculating the norm and local observables of a MERA can be reduced and efficiently contracted as illustrated in Fig.9.14.

9.5.2 Tree tensor network state

Another important tensor network state has a tree structure as shown in Fig.9.15 and is called the Tree Tensor Network. The tree tensor network is made up of local tensors with three indices and they are connected in such a way that there are no loops in the tensor network.

The open indices $i_1, \ldots, i_N$ on the outer edge of the graph are the physical indices of the state it represents. A simple counting shows that in order to represent an N spin state, we need $N-2$ tensors. When a link in this tensor network is broken,

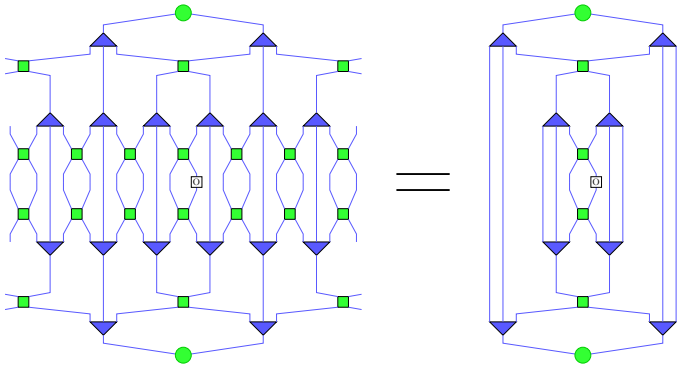

Fig. 9.14 Property of disentanglers and isometries in MERA.

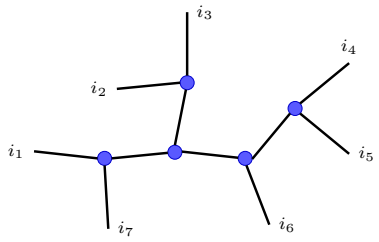

Fig. 9.15 The Tree Tensor Network.

the graph breaks into two parts. Therefore, the Schmidt rank of such a bipartition is bounded by the dimension χ of the indices.

A nice property of the tree tensor network state is that several manipulations of the network can be implemented in an efficient way. For example, the calculation of reduced density matrix and the simulation of time evolution on the state. The required computation time for these tasks scales at most linearly in the number N of spins and as a small polynomial in the dimension χ of the inner indices.

9.6 Summary and further reading

In this chapter, we introduce the tensor product state representation and study how it can be used to represent different phases in two dimension. First, we discuss the definition and basic properties of tensor product states. While tensor product states share many nice properties with matrix product states, including an entanglement area law, the correspondence between 'injectivity' and finite correlation length breaks down, making it much less clear which tensor product states are gapped and which ones not. Numerically, it is also much harder to contract two dimensional tensors. An approximate algorithm is introduced to do the computation efficiently. The tensor

product representation of the Ising model and the toric code model is discussed in detail as examples of symmetry breaking phases and topologically ordered phases. In particular, the block structure of the local tensor is found to be closely related to the symmetry breaking order while some internal symmetry of the local tensor is found to be essential for the existence of topological order.

The extension of the DMRG (matrix product) formalism to higher dimensions was used for the calculation of classical partition functions in e.g. [11, 10]. On the quantum side, the representation of two dimensional AKLT state in a tensor product form was discussed in [1] and variational parameters were introduced into the tensors in [9, 16, 7] to simulate more general spin systems. A renormalization algorithm based on tensor product state (also called the 'projected entangled pair state') was proposed in [18], with various properties of the tensor product representation discussed in [21]. The fact that injective tensor product states are unique but not necessarily gapped ground states is pointed out in [12]. The approximate method for the contraction of 2D tensor networks was proposed in [8].

A review of the matrix product states and tensor product states formalism, including various numerical algorithms based on them, is given in [20].

The tensor network representation of the toric code wave function was discussed first in [19]. Later it was found that a much larger class of topological wave functions – the string-net states – can all be represented with tensor networks.[6, 3]. The gauge symmetry in tensors for topologically ordered states was emphasized in [17, 14, 2, 13], where various topological properties was derived simply from the local tensors.

The stability of the topological order under variation of the toric code tensor was studied in [5], where the necessary symmetry condition is demonstrated. Our discussion in section 9.4.4 follows closely this paper and details of the computation can be found therein.

A wave function renormalization algorithm for tensor product states was discussed in [4], where it is shown that the algorithm can flow a tensor to its fixed point form from which the symmetry breaking or topological order contained in the state can be identified.

The idea of Multiscale Entanglement Renormalization Ansatz was proposed in [22]. The Tree Tensor Network was first studied in [15].

References

1. Ian Affleck, Tom Kennedy, ElliottH. Lieb, and Hal Tasaki. Valence bond ground states in isotropic quantum antiferromagnets. *Communications in Mathematical Physics*, 115(3):477–528, 1988.
2. Oliver Buerschaper. Twisted injectivity in projected entangled pair states and the classification of quantum phases. *Annals of Physics*, 351:447 – 476, 2014.
3. Oliver Buerschaper, Miguel Aguado, and Guifré Vidal. Explicit tensor network representation for the ground states of string-net models. *Phys. Rev. B*, 79:085119, Feb 2009.
4. Xie Chen, Zheng-Cheng Gu, and Xiao-Gang Wen. Local unitary transformation, long-range quantum entanglement, wave function renormalization, and topological order. *Phys. Rev. B*, 82(15):155138, Oct 2010.

5. Xie Chen, Bei Zeng, Zheng-Cheng Gu, Isaac L. Chuang, and Xiao-Gang Wen. Tensor product representation of a topological ordered phase: Necessary symmetry conditions. *Phys. Rev. B*, 82(16):165119, Oct 2010.
6. Zheng-Cheng Gu, Michael Levin, Brian Swingle, and Xiao-Gang Wen. Tensor-product representations for string-net condensed states. *Phys. Rev. B*, 79:085118, Feb 2009.
7. Yasuhiro Hieida, Kouichi Okunishi, and Yasuhiro Akutsu. Numerical renormalization approach to two-dimensional quantum antiferromagnets with valence-bond-solid type ground state. *New Journal of Physics*, 1(1):7, 1999.
8. Michael Levin and Cody P. Nave. Tensor renormalization group approach to two-dimensional classical lattice models. *Phys. Rev. Lett.*, 99:120601, Sep 2007.
9. H. Niggemann, A. Klümper, and J. Zittartz. Quantum phase transition in spin-3/2 systems on the hexagonal lattice — optimum ground state approach. *Zeitschrift für Physik B Condensed Matter*, 104(1):103–110, 1997.
10. Tomotoshi Nishino, Yasuhiro Hieida, Kouichi Okunishi, Nobuya Maeshima, Yasuhiro Akutsu, and Andrej Gendiar. Two-dimensional tensor product variational formulation. *Progress of Theoretical Physics*, 105(3):409–417, 2001.
11. Tomotoshi Nishino and Kouichi Okunishi. A density matrix algorithm for 3d classical models. *Journal of the Physical Society of Japan*, 67(9):3066–3072, 1998.
12. David Pérez-García, Frank Verstraete, J. Ignacio Cirac, and Michael M. Wolf. Peps as unique ground states of local hamiltonians. *Quant.Inf.Comp.*, 8:0650, 2008.
13. Mehmet Burak Şahinoğlu, Dominic Williamson, Nick Bultinck, Michael Mariën, Jutho Haegeman, Norbert Schuch, and Frank Verstraete. Characterizing topological order with matrix product operators. September 2014.
14. Norbert Schuch, J. Ignacio Cirac, and David Pérez-García. Peps as ground states: Degeneracy and topology. *Annals of Physics*, 325(10):2153 – 2192, 2010.
15. Y.-Y. Shi, L.-M. Duan, and G. Vidal. Classical simulation of quantum many-body systems with a tree tensor network. *Phys. Rev. A*, 74:022320, Aug 2006.
16. G. Sierra and M.A. Martin-Delgado. The density matrix renormalization group, quantum groups and conformal field theory. November 1998.
17. Brian Swingle and Xiao-Gang Wen. Topological properties of tensor network states from their local gauge and local symmetry structures. *ArXiv e-prints*, January 2010.
18. F. Verstraete and J. I. Cirac. Renormalization algorithms for Quantum-Many Body Systems in two and higher dimensions. July 2004.
19. F. Verstraete, M. M. Wolf, D. Perez-Garcia, and J. I. Cirac. Criticality, the area law, and the computational power of projected entangled pair states. *Phys. Rev. Lett.*, 96:220601, Jun 2006.
20. Frank Verstraete, Valentin Murg, and J.Ignacio Cirac. Matrix product states, projected entangled pair states, and variational renormalization group methods for quantum spin systems. *Advances in Physics*, 57(2):143–224, 2008.
21. Frank Verstraete, Michael M. Wolf, David Pérez-García, and J. Ignacio Cirac. Criticality, the area law, and the computational power of projected entangled pair states. *Phys. Rev. Lett.*, 96:220601, Jun 2006.
22. Guifré Vidal. Entanglement renormalization. *Phys. Rev. Lett.*, 99:220405, Nov 2007.

Chapter 10
Symmetry Protected Topological Phases

Abstract Short range entangled states can all be connected to each other through local unitary transformations and hence belong to the same phase. However, if certain symmetry is required, they break into different phases. First of all, the symmetry can be spontaneously broken in the ground state leading to symmetry breaking phases. Even when the ground state remains symmetric, there can be different Symmetry Protected Topological (SPT) phases, whose nontrivial nature is reflected in their symmetry protected degenerate or gapless edge states. In this chapter, we discuss these phases in detail. Using the matrix product state formalism, we completely classify SPT phases in 1D boson / spin systems. By mapping 1D fermion systems to spins through Jordan Wigner transformation, we obtain a classification for fermionic SPT phases as well. In 2D, the tensor product representation falls short of firmly establishing a complete classification. But we present a exactly solvable construction of SPT phase with $\mathbb{Z}_2$ symmetry, which can be generalized to any internal symmetry and in any dimension.

10.1 Introduction

Symmetry protected topological (SPT) phases are gapped quantum phases with topological properties protected by symmetry. The ground states of SPT phases contain only short-range entanglement and can be smoothly deformed into a totally trivial product state if the symmetry requirement is not enforced in the system. However, with symmetry, the nontrivial SPT order is manifested in the existence of gapless edge states on the boundary of the system which cannot be removed as long as symmetry is not broken. What symmetry protected topological phases exist and what nontrivial properties do they have? This is the question that we are going to address in this chapter.

First we focus on one dimensional SPT phases in section10.2. We start by introducing some simple examples of nontrivial SPT orders in 1D. To have a more complete understanding of 1D bosonic SPT phases, the matrix product state repre-

sentation provides us with a powerful tool. In fact, we can obtain a complete classification of boson / spin SPT phases systems by studying the form of symmetric fixed point states using the matrix product formalism. A one to one correspondence is found between bosonic SPT phases and the projective representations of group G. Note that there is no fundamental difference between spin and boson systems in our discussion, as they are both composed of local degrees of freedom which commute with each other.

By mapping 1D fermion system to 1D spin systems through Jordan Wigner transformation, we obtain a classification of 1D fermionic SPT phases as well. An important difference of fermion systems compared to bosonic ones is that fermion system has an intrinsic $\mathbb{Z}_2$ symmetry related to fermion parity conservation. Such a symmetry cannot be broken, not even spontaneously. The bosonic $\mathbb{Z}_2$ symmetry breaking phase when mapped back to fermion chains through inverse Jordan Wigner transformation results in a topological phase with nontrivial edge state, as we explain in section 10.3.

With a good understanding of SPT phases in 1D, we move on to construct SPT phases in 2D interacting boson / spin systems in section 10.4. We generalize the short range entanglement structure in 1D SPT phases to 2D and design the symmetry action per each site such that the system always has gapless excitations on the edge unless symmetry is explicitly or spontaneously broken. Such a construction actually generalize to any dimension and any internal symmetry, as we discuss in section 10.5, providing a systematic understanding of SPT phases in interacting boson and spin systems.

10.2 Symmetry protected topological order in 1D bosonic systems

10.2.1 Examples

Let's start by introducing some simple models with nontrivial SPT order in 1D.

The AKLT model on a spin 1 chain discussed in Chap. 8 is a prototypical example. The Hamiltonian of the AKLT model is

$$H_{AKLT} = \sum_i \mathbf{S}_i \cdot \mathbf{S}_{i+1} + \frac{1}{3} (\mathbf{S}_i \cdot \mathbf{S}_{i+1})^2 \tag{10.1}$$

where $\mathbf{S}$ is the spin 1 spin operator. This Hamiltonian is obviously invariant under the $SO(3)$ spin rotation symmetry generated by S^x, S^y and S^z. The ground state wave function of this Hamiltonian can be explicitly constructed using a simple projected entangled pair picture. As shown in Fig. 10.1.

Each lattice site (big oval) contains two spin $1/2$s (small circle), which form singlet pairs (connected bonds) $|\uparrow\downarrow\rangle - |\downarrow\uparrow\rangle$ with another spin $1/2$ on a neighboring

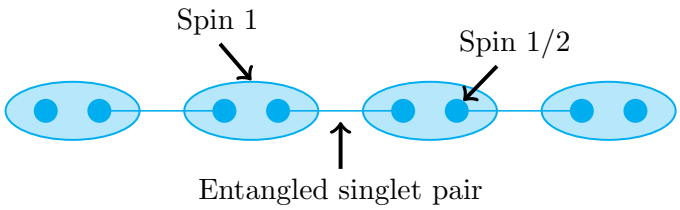

Fig. 10.1 Projected entangled pair structure of the AKLT wave function.

site. By projecting the two spin $1/2$s on each lattice site to a spin 1, we obtain the ground state wave function H_{AKLT}.

On a ring with periodic boundary condition, the ground state preserves spin rotation symmetry and is unique and gapped. On a chain with boundary, on the other hand, there are isolated spin $1/2$s at each end of the chain which are not coupled with anything and give rise to a two fold degenerate edge state. The full ground state on an open chain is hence four fold degenerate. The degenerate edge state is stable as long as spin rotation symmetry is preserved. In particular, spin $1/2$s transform under spin rotation in a very special way with a 2π rotation around any axis giving rise to a -1 phase factor. Because of this, the edge state cannot be smoothly connected to a trivial spin 0, which gets a phase factor of 1 under 2π rotation, without closing the bulk gap. With a gapped symmetric bulk and degenerate edge states protected by spin rotation symmetry, the AKLT model is hence in a nontrivial SPT phase.

Box 10.1 SPT order of the AKLT model

The 1D AKLT model has nontrivial symmetry protected topological order protected by $SO(3)$ spin rotation symmetry, as indicated by its degenerate spin $1/2$ edge state.

The 1D cluster state on a spin $1/2$ chain discussed in Chap. 5 provides another example of nontrivial SPT order. The Hamiltonian of the 1D cluster state is

$$H_{clu} = -\sum_j Z_{j-1}X_jZ_{j+1}. \tag{10.2}$$

Here, Z and X are Pauli operators for the spin $1/2$s. As explained in Chap. 5, for a 1D ring without boundary, the ground state of H_{clu} is the unique graph state stabilized by $\{Z_{j-1}X_jZ_{j+1}\}$. For a chain with boundary, where the summation index j runs from 2 to $N-1$, the ground state is then 4-fold degenerate.

This 4-fold degeneracy is a result of two edge states, each being 2-fold degenerate protected by a $\mathbb{Z}_2 \times \mathbb{Z}_2$ symmetry. The $\mathbb{Z}_2 \times \mathbb{Z}_2$ symmetry is generated by

$$\bar{X}_1 = \prod_k X_{2k-1}, \quad \bar{X}_2 = \prod_k X_{2k}, \tag{10.3}$$

Any local perturbation to the system cannot lift the degeneracy as long as this $\mathbb{Z}_2 \times \mathbb{Z}_2$ symmetry is preserved. To see this, first we notice that the effective Pauli $\tilde{X}$ and $\tilde{Z}$ operators on the 2-fold degenerate edge states (at the left end of the chain for example) can be chosen as $\tilde{X} = X_1 Z_2$ and $\tilde{Z} = Z_1$, which commute with all the bulk Hamiltonian terms and anti-commute with each other. Next, we find that the effective action of $\bar{X}_1$ and $\bar{X}_2$ on the edge state is the same as $\tilde{X}$ and $\tilde{Z}$ because

$$\bar{X}_1 \prod_{k=2}^{\infty} Z_{2k-2} X_{2k-1} Z_{2k} = X_1 Z_2 = \tilde{X}, \;\; \bar{X}_2 \prod_{k=1}^{\infty} Z_{2k-1} X_{2k} Z_{2k+1} = Z_1 = \tilde{Z} \tag{10.4}$$

From this we can see that the $\mathbb{Z}_2 \times \mathbb{Z}_2$ symmetry acts on the edge state in a very special way: the two $\mathbb{Z}_2$'s anti-commute with each other! Because of this, the edge state must be at least two fold degenerate and the degeneracy cannot be removed without breaking the symmetry or going through a bulk phase transition. This demonstrates the nontrivial-ness of the SPT order in the cluster state.

Box 10.2 SPT order of the cluster state model

The 1D cluster state model has nontrivial symmetry protected topological order protected by a $\mathbb{Z}_2 \times \mathbb{Z}_2$ symmetry, as indicated by its two fold degenerate edge state.

Through the AKLT model and the cluster state model, we see some common features of SPT order in 1D: the bulk wave function is gapped and symmetric while the edge state must be degenerate because it transforms in a nontrivial way under the symmetry. This picture can be generalized to all kinds of symmetries and we want to understand what 1D SPT phases exist in general with any given symmetry. The matrix product formalism again provides a powerful tool in addressing this question. In the following, we are going to follow a procedure similar to Chap. 8 and completely classify SPT phases in 1D interacting boson / spin systems using a renormalization group transformation on matrix product states.

When the class of systems under consideration has certain symmetry, the equivalence classes of states are defined in terms of LU transformations that do not break the symmetry. Therefore, when applying the renormalization procedure, we should carefully keep track of the symmetry and make sure that the resulting state has the same symmetry at each step. Due to such a constrain on local unitary equivalence, we will see that gapped ground states which do not break the symmetry of the system divide into different universality classes corresponding to different symmetry protected topological orders. We will first study in detail the case of on-site unitary symmetries. Then we will also discuss systems with time reversal (anti-unitary) symmetry. Finally, we shall study translational invariant (TI) systems, with the possibility of having on-site symmetry or parity symmetry.

10.2.2 On-site unitary symmetry

A large class of systems are invariant under on-site symmetry transformations. For example, the Ising model is symmetric under the $\mathbb{Z}_2$ spin flip transformation and the Heisenberg model is symmetric under $SO(3)$ spin rotation transformations. In this section, we will consider the general case where the system is symmetric under $u(g)\otimes ...\otimes u(g)$ with $u(g)$ being a unitary representation of a symmetry group G on each site and satisfy

$$u(g_1)u(g_2) = u(g_1g_2) \tag{10.5}$$

We will focus on the case where the on-site symmetry is the only symmetry required for the class of system. In particular, we do not require translational symmetry for the systems. We will classify possible phases for different G when the ground state is invariant (up to a total phase) under such on-site symmetry operations and is gapped (i.e. short-range correlated). Specifically, the ground state $|\phi\rangle$ satisfies

$$u(g)\otimes ...\otimes u(g)|\psi\rangle = \alpha^L(g)|\psi\rangle \tag{10.6}$$

where $|\alpha(g)| = 1$ is a one-dimensional representation of G and L is the system size.

Now we will try to classify these symmetric ground states using symmetric LU transformations and we find that:

Box 10.3 Classification of bosonic symmetry protected topological phases
For 1D bosonic systems with ONLY an on-site symmetry of group G, the gapped phases that do not break the symmetry are labeled by the projective representations of the group G.

This result applies when the 1D representations $\alpha(G)$ form a finite group, when $G = U(1)$, further classification according to different $\alpha(U(1))$ exist.

10.2.2.1 Symmetric RG transformation and fixed point

We will again use the fact that all gapped states can be represented as short range correlated matrix product states and use the renormalization flow discussed in section 8.3 to simplify the matrix product states. We find that

1. With symmetric LU transformations, all gapped bosonic states with on-site symmetry can be mapped to the fixed point form shown in Fig.8.7.
2. In the fixed point wave function, each of the two degrees of freedom on a site carries a projective representation of the symmetry.

In order to compare different equivalent classes under *symmetric* LU transformations, it is important to keep track of the symmetry while doing renormalization.

First, in the renormalization procedure we group two sites together into a new site. The on-site symmetry transformation becomes $u(g)\otimes u(g)$, which is again a linear representation of G. The next step in RG procesure applies a unitary transformation w_1 to the support space of new site. This is actually itself composed of two steps. First we project onto the support space of the new site, which is the combination of two sites in the original chain. This is an allowed operation compatible with symmetry G as the reduced density matrix ρ_2 is invariant under $u(g)\otimes u(g)$, so the support space form a linear representation for G. The projection of $u(g)\otimes u(g)$ onto the support space $P_2(u(g)\otimes u(g))P_2$ hence remains a linear representation of G. In the next step, we do some unitary transformation w_1 within this support space which relabels different states in the space. The symmetry property of the state should not change under this relabeling. In order to keep track of the symmetry of the state, the symmetry operation needs to be redefined as

$$u^{(1)}(g) = w_1 P_2(u(g)\otimes u(g))P_2(w_1)^\dagger \tag{10.7}$$

After this redefinition, the symmetry operations $u^{(1)}(g)$ on each new site form a new linear representation of G. By redefining $u^{(N)}(g)$ at each step of the RG transformation, we keep track of the symmetry of the system. Finally at the fixed point (i.e. at a large RG step N), we obtain a state described by $\left(A^{(\infty)}\right)_{i^l,i^r}$ which is again given by the fixed point form eqn. (8.58). The symmetry transformation on each site is given by $u^{(\infty)}(g)$.

One may want to proceed to disentangle each pair in the fixed point state and map the state to a total product state. However, it is not always possible to do so without breaking symmetry. Consider the case where the entangled pairs in the fixed point state are spin $1/2$ singlets. The total state is invariant under $SO(3)$ symmetry, but there does not seem to be a way to disentangle the singlet without breaking symmetry. Actually, all product states of two spin $1/2$'s necessarily break spin rotation symmetry! As we show in the following, this is a very general observation and is related inherently to the nontrivial SPT order in the state.

But first, let's look more closely at the fixed point matrices we obtained. In fact, the form of the fixed point is already simple enough that we can extract useful information about the universal properties of the phase from it. The fact that the fixed point state is invariant under $u^{(\infty)}(g)$ requires special transformation property of $\left(A^{(\infty)}\right)_{i^l,i^r}$ under the symmetry. We are going to derive this transformation property in the following and see that how projective representations of the symmetry group emerge in the MPS representation.

Because $\left(A^{(\infty)}\right)_{i^l,i^r}$ is injective, the transformed matrices must be equivalent to the original ones by a gauge transformation on the inner indices. That is (we are omitting the fixed point label ∞ in the following)

$$\sum_{j^l j^r} u_{i^l i^r, j^l j^r}(g) A_{j^l j^r} = \alpha(g) M^{-1}(g) A_{i^l i^r} M(g) \tag{10.8}$$

with invertible matrices $M(g)$ and $\alpha(g)$ is a 1D representation of G. Since $\frac{u(g)}{\alpha(g)}$ is also a linear unitary representation of G, we can absorb $\alpha(g)$ into $u(g)$ and rewrite eqn. (10.8) as

$$\sum_{j^l j^r} u_{i^l i^r, j^l j^r}(g) A_{j^l j^r} = M^{-1}(g) A_{i^l i^r} M(g) \tag{10.9}$$

We note that matrix elements $A_{i^l i^r, \alpha\beta}$ is non-zero only when $\alpha = i^l$, $\beta = i^r$ and the full set of $\{A_{i^l i^r}\}$ form a complete basis in the space of $D \times D$ dimensional matrices. Such a symmetry transformation property of the fixed point matrices can be represented graphically as in Fig.10.2.

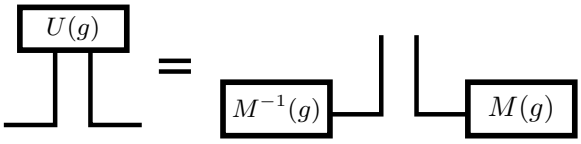

Fig. 10.2 Symmetry transformation of fixed point matrices under on-site symmetry G.

$M(g)$ does not necessarily form a linear representation of G. But the fixed point form of the matrices requires that $M(g)$ be a so-called 'projective' representation, as on the one hand

$$\begin{aligned} &\sum_{j^l j^r} u_{i^l i^r, j^l j^r}(g_1 g_2) A_{j^l j^r} \\ =&\sum_{j^l j^r k^l k^r} u_{i^l i^r, k^l k^r}(g_1) u_{k^l k^r, j^l j^r}(g_2) A_{j^l j^r} \\ =&\sum_{k^l k^r} u_{i^l i^r, k^l k^r}(g_1) M^{-1}(g_2) A_{k^l k^r} M(g_2) \\ =&M^{-1}(g_2) M^{-1}(g_1) A_{i^l i^r} M(g_1) M(g_2) \end{aligned} \tag{10.10}$$

and on the other hand

$$\sum_{j^l j^r} u_{i^l i^r, j^l j^r}(g_1 g_2) A_{j^l j^r} = M^{-1}(g_1 g_2) A_{i^l i^r} M(g_1 g_2) \tag{10.11}$$

Therefore

$$M^{-1}(g_2) M^{-1}(g_1) A_{i^l i^r} M(g_1) M(g_2) = M^{-1}(g_1 g_2) A_{i^l i^r} M(g_1 g_2) \tag{10.12}$$

for all $i^l i^r$. However, the set of matrices $\{A_{i^l i^r}\}$ form a complete basis in the space of $D \times D$ dimensional matrices. Therefore, $M(g_1)M(g_2)$ can differ from $M(g_1 g_2)$ by at most a phase factor

$$M(gh) = \omega(g,h)M(g)M(h), \tag{10.13}$$

with $|\omega(g_1,g_2)| = 1$. Therefore, $M(g)$ are a set of matrices labeled by group elements and satisfy the group multiplication rule up to a phase factor. That is, $M(g)$ form a projective representation of the symmetry group G.

The transformation law of the fixed point matrices is related to the transformation law of the degrees of freedom in the fixed point wave function.

Let us rewrite eqn. (10.9) as

$$M(g)(\sum_{j^l j^r} u_{i^l i^r, j^l j^r}(g) A_{j^l j^r}) M^{-1}(g) = A_{i^l i^r} \tag{10.14}$$

We note that

$$M(g)(\sum_{j^l j^r} (Nl^{-1})_{j^l, i^l} Nr_{i^r, j^r} A_{j^l j^r}) M^{-1}(g) = A_{i^l i^r} \tag{10.15}$$

where the matrices Nl and Nr are given by

$$Nl_{\alpha\beta} = M_{\alpha\beta} \frac{\sqrt{\lambda_\alpha}}{\sqrt{\lambda_\beta}}, \quad Nr_{\alpha\beta} = M_{\alpha\beta} \frac{\sqrt{\eta_\beta}}{\sqrt{\eta_\alpha}}. \tag{10.16}$$

Since the set of matrices $\{A_{i^l i^r}\}$ form a complete basis in the space of $D \times D$ dimensional matrices, we find

$$u_{i^l i^r, j^l j^r}(g) = Nl^{-1}_{j^l, i^l}(g) Nr_{i^r, j^r}(g). \tag{10.17}$$

That is, the symmetry transformation acts on the two degrees of freedom on each site separately and in a projective way similar to $M(g)$.

$$\begin{aligned} Nl^{-1}(g_1)Nl^{-1}(g_2) &= \omega^{-1}_{g_1,g_2} Nl^{-1}(g_1 g_2) \\ Nr(g_1)Nr(g_2) &= \omega_{g_1,g_2} Nr(g_1 g_2) \end{aligned}$$

Therefore, in the fixed point wave function as shown in Fig.10.3, the two degrees of freedom on a site each carry a projective representation of the symmetry and form a singlet state with another degree of freedom on a neighboring site. Note that the symmetry representation on each full site is still linear and the total wave function is invariant under the symmetry.

10.2.2.2 Example

Let's look at some examples of gapped states with on-site symmetry and find their corresponding fixed point structure.

The symmetric phase of the Ising model provides a trivial example. At the exactly solvable limit, the Hamiltonian is $H = -\sum_i X_i$ and the ground state wave function is a total product state of spins pointing in the $+x$ direction

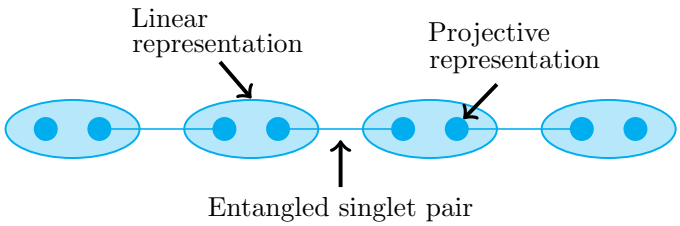

Fig. 10.3 Fixed point wave function with on-site symmetry.

$$|\psi\rangle = |+\rangle \otimes |+\rangle \otimes ... \otimes |+\rangle \tag{10.18}$$

which is invariant under the $\mathbb{Z}_2$ symmetry of $X \otimes X \otimes ... \otimes X$. This wave function is already in the fixed point form where each site contains two spins in state $|+\rangle$ and each spin forms a linear representation of the $\mathbb{Z}_2$ symmetry – a trivial projective representation with $\omega(g,h) = 1$. Also there is no entanglement between neighboring sites.

Let's see how the nontrivial SPT order is manifested in the AKLT model

$$H_{AKLT} = \sum_i \mathbf{S}_i \cdot \mathbf{S}_{i+1} + \frac{1}{3}(\mathbf{S}_i \cdot \mathbf{S}_{i+1})^2 \tag{10.19}$$

which is invariant under the $SO(3)$ spin rotation symmetry generated by S^x, S^y and S^z. Its unique gapped ground state is given by the matrix product representation

$$A_x = X,\ A_y = Y, A_z = Z \tag{10.20}$$

where the basis states $|x\rangle$, $|y\rangle$ and $|z\rangle$ written in the S_z basis are

$$|x\rangle = \frac{1}{\sqrt{2}}(|1\rangle - |-1\rangle),\ |y\rangle = \frac{-i}{\sqrt{2}}(|1\rangle + |-1\rangle),\ |z\rangle = -|0\rangle \tag{10.21}$$

The AKLT state is $SO(3)$ symmetric and, as we will see, in a nontrivial way with nontrivial projective representations in its fixed point. To see this, first we construct its double tensor

$$\mathbb{E} = \frac{1}{3}[X \otimes X^* + Y \otimes Y^* + Z \otimes Z^*] = \frac{1}{3}\begin{pmatrix} 1 & 0 & 0 & 2 \\ 0 & -1 & 0 & 0 \\ 0 & 0 & -1 & 0 \\ 2 & 0 & 0 & 1 \end{pmatrix} \tag{10.22}$$

Normalization factor is added to ensure that the largest eigenvalue is 1. The fixed point double tensor is then

$$\mathbb{E}^{(\infty)} = \lim_{N\to\infty} \mathbb{E}^N = \frac{1}{2}\begin{pmatrix} 1&0&0&1\\ 0&0&0&0\\ 0&0&0&0\\ 1&0&0&1 \end{pmatrix} \tag{10.23}$$

which can be decomposed as

$$A_s^{(\infty)} = I_2,\ A_x^{(\infty)} = X,\ A_y^{(\infty)} = Y,\ A_z^{(\infty)} = Z \tag{10.24}$$

Here among the four fixed point basis states, $|s\rangle$ is a spin 0 state and $|x\rangle$, $|y\rangle$, $|z\rangle$ form a spin 1. I_2 is the 2×2 identity matrix. We can then compute the symmetry transformation matrices $M(g)$ on the inner indices by rotating the physical spins. For example, under the rotation around z axis for an angle θ, the matrices change into

$$\tilde{A}_s^{(\infty)} = I_2,\ \tilde{A}_x^{(\infty)} = \cos\theta X - \sin\theta Y,\ \tilde{A}_y^{(\infty)} = \cos\theta Y + \sin\theta X,\ \tilde{A}_z^{(\infty)} = Z \tag{10.25}$$

from which we can see that $M(R_z(\theta)) = e^{i\theta Z/2}$. Similar calculation for all the other rotations show that

$$M(R_{\mathbf{n}}(\theta)) = e^{i\frac{\theta}{2}(n_x X + n_y Y + n_z Z)} \tag{10.26}$$

That is, the symmetry transformation on the inner indices is generated by an effective spin $1/2$. Correspondingly, in the fixed point wave function, the two degrees of freedom on each site are spin $1/2$'s and they form spin singlets between neighboring sites. This is similar to the structure shown in Fig.10.1, except that at fixed point we do not need to project the two spin $1/2$ per each site to a spin 1 any more.

The most important property of $M(g)$ is that, it forms a projective rather than linear representation of the $SO(3)$ group which can be seen from 2π rotations

$$M(R_{\mathbf{n}}(2\pi)) = e^{i\frac{2\pi}{2}(n_x X + n_y Y + n_z Z)} = -I \tag{10.27}$$

Rotation by 2π is equivalent to the identity operation while the matrix representation $M(R_{\mathbf{n}}(2\pi))$ is only equivalent to the identity matrix up to a minus sign. Therefore, nontrivial sign factors $\omega(g,h)$ occur in composing $M(g)$ and $M(h)$. For example

$$M(R_{\mathbf{n}}(\pi))M(R_{\mathbf{n}}(\pi)) = -M(R_{\mathbf{n}}(0)) \tag{10.28}$$

And $M(R_{\mathbf{n}}(\theta))$ generated by spin $1/2$ spin operators form a projective representation of the $SO(3)$ rotation symmetry.

In the ground state, such a projective representation is most clearly seen when we cut the system open and put it on an open chain. On an open chain, there are isolated spin $1/2$'s at either end of the chain which do not form singlets with other spin $1/2$'s. They give rise to a total of four fold ground state degeneracy on an open chain as long as spin rotation symmetry is preserved. That is, the projective representation leads to degenerate edge states on an open chain protected by the symmetry. Of course, if the symmetry is broken, by for exmaple adding a magnetic field, the degeneracy will be removed.

This is a generic feature of one dimensional bosonic systems with on-site symmetry protected topological orders, as we discuss for an arbitrary group G in the next section.

10.2.2.3 Projective representation and edge state

Let's first define projective representation for a general group G more carefully. Operators $u(g)$ form a projective representation of symmetry group G if

$$u(g_1)u(g_2) = \omega(g_1,g_2)u(g_1g_2), \quad g_1,g_2 \in G. \tag{10.29}$$

Here $\omega(g_1,g_2) \in U(1)$, the factor system of the projective representation, satisfies

$$\omega(g_2,g_3)\omega(g_1,g_2g_3) = \omega(g_1,g_2)\omega(g_1g_2,g_3), \tag{10.30}$$

for all $g_1,g_2,g_3 \in G$, which comes from the associativity condition of the representation $[u(g_1)u(g_2)]u(g_3) = u(g_1)[u(g_2)u(g_3)]$ If $\omega(g_1,g_2) = 1$, this reduces to the usual linear representation of G.

On the other hand, not all projective representations with $\omega(g_1,g_2) \neq 1$ are nontrivial. Notice that a different choice of pre-factor for the representation matrices $u'(g) = \beta(g)u(g)$ will lead to a different factor system $\omega'(g_1,g_2)$:

$$\omega'(g_1,g_2) = \frac{\beta(g_1g_2)}{\beta(g_1)\beta(g_2)}\omega(g_1,g_2). \tag{10.31}$$

Therefore, if a factor system satisfies $\omega(g_1,g_2) = \frac{\beta(g_1)\beta(g_2)}{\beta(g_1g_2)}$, then by redefining the pre-factor of the matrices, we can reduce the factor system to 1 and hence the projective representation to a linear one. Only $\omega(g_1,g_2)$'s which cannot be reduced to 1 in this way are nontrivial. Moreover, if two factor systems $\omega'(g_1,g_2)$ and $\omega(g_1,g_2)$ can be related as in eqn. (10.31), then their corresponding representation matirces $u'(g)$ and $u(g)$ differ only by a pre-factor and belong to the same class of projective representation.

Suppose that we have one projective representation $u_1(g)$ with factor system $\omega_1(g_1,g_2)$ of class ω_1 and another $u_2(g)$ with factor system $\omega_2(g_1,g_2)$ of class ω_2, obviously $u_1(g) \otimes u_2(g)$ is a projective presentation with factor system $\omega_1(g_1,g_2)\omega_2(g_1,g_2)$. The corresponding class ω can be written as a sum $\omega_1 + \omega_2$. Under such an addition rule, the equivalence classes of factor systems form an Abelian group, which is called the second cohomology group of G and denoted as $H^2(G,U(1))$. The identity element ω_0 of the group is the class that contains the linear representation of the group.

Here are some simple examples:

1. cyclic groups $\mathbb{Z}_n$ do not have non-trivial projective representation. Hence for $G = \mathbb{Z}_n$, $H^2(G,U(1))$ contains only the identity element.

2. a simple group with non-trivial projective representation is the Abelian dihedral group $D_2 = \mathbb{Z}_2 \times \mathbb{Z}_2$. For the four elements of the group $(0/1,0/1)$, consider representation with Pauli matrices $g(0,0) = \begin{bmatrix} 1 & 0 \\ 0 & 1 \end{bmatrix}$, $g(0,1) = \begin{bmatrix} 0 & 1 \\ 1 & 0 \end{bmatrix}$, $g(1,0) = \begin{bmatrix} 1 & 0 \\ 0 & -1 \end{bmatrix}$, $g(1,1) = \begin{bmatrix} 0 & -i \\ i & 0 \end{bmatrix}$. It can be check that this gives a non-trivial projective representation of D_2.
3. when $G = SO(3)$, $H^2(G,U(1)) = \mathbb{Z}_2$. The two elements correspond to integer and half-integer representations of $SO(3)$ respectively.
4. when $G = U(1)$, $H^2(G,U(1))$ is trivial: $H^2(U(1),U(1)) = Z_1$. We note that $\{e^{im\theta}\}$ form a representation of $U(1) = \{e^{i\theta}\}$ when m is an integer. But $\{e^{im\theta}\}$ will form a projective representation of $U(1)$ when m is not an integer. But under the equivalence relation Eqn. (10.31), $\{e^{im\theta}\}$ correspond to the trivial projective representation, if we choose $\beta(g) = e^{-im\theta}$. Note that $\beta(g)$ can be a discontinuous function over the group manifold.

An important property of nontrivial projective representations is that the representation space must be at least two dimensional. That is, there are no one-dimensional nontrivial projective representations. This has direct physical consequence for nontrivial SPT states. When the nontrivial SPT states are put on an open chain, there are isolated spins carrying projective representations at each end of the chain. These spins are always of dimension larger than 1, hence giving rise to a ground state degeneracy at each end of the chain. This degeneracy is stable as long as the symmetry of the system is not broken. This property holds not only at the fixed point, but at any point in the symmetry protected topological phase. Therefore, we see that the most distinctive property of 1D SPT phases with on-site symmetry is the existence of nontrivial edge state around a gapped and nondegenerate bulk, which is protected by the symmetry of the system.

10.2.2.4 Equivalence between symmetric fixed point states

In section 10.2.2.1 we have shown that all gapped bosonic states with on-site symmetry G can be mapped to a fixed point form with symmetric LU transformations. If we can further determine the equivalence relation between different symmetric fixed points under symmetric LU transformation, we would be able to obtain a complete classification of SPT phases. This is what we are going to do in this section.

From the discussion in section 10.2.2.1, we know that the fixed point state symmetric under on-site symmetry of group G takes the form

$$|\psi\rangle^{(\infty)} = |EP_{1,2}\rangle|EP_{2,3}\rangle...|EP_{k,k+1}\rangle... \tag{10.32}$$

where $|EP_{k,k+1}\rangle$ is an entangled pair between the right spin on site k and the left spin on site $k+1$(see Fig. 8.7). Each entangled pair is invariant under a linear symmetry transformation of the form $u^{[k],r}(g) \otimes u^{[k+1],l}(g)$

$$u^{[k],r}(g)\otimes u^{[k+1],l}(g)|EP_{k,k+1}\rangle = |EP_{k,k+1}\rangle \tag{10.33}$$

But $u^{[k],r}(g)$ or $u^{[k+1],l}(g)$ alone might not form a linear representation of G. They could in general be a projective representation of G. If $u^{[k],r}(g)$ is a projective representation corresponding to class ω in $H^2(G,U(1))$, then $u^{[k+1],l}$ must correspond to class $-\omega$. ω does not vary from site to site and labels a particular symmetric fixed point state.

Now we want to show that symmetric fixed point states with the same ω can be connected through symmetric LU transformations and hence belong to the same phase while those with different ω cannot and belong to different phases.

First, suppose that two symmetric fixed point states $|\phi_1\rangle$ and $|\phi_2\rangle$ are related with the same ω, i.e.

$$\begin{aligned} u_1^{[k],r}(g)\otimes u_1^{[k+1],l}(g)|EP_{k,k+1}\rangle_1 &= |EP_{k,k+1}\rangle_1 \\ u_2^{[k],r}(g)\otimes u_2^{[k+1],l}(g)|EP_{k,k+1}\rangle_2 &= |EP_{k,k+1}\rangle_2 \end{aligned} \tag{10.34}$$

where $|EP_{k,k+1}\rangle_{1(2)}$ is an entangled pair of spins on Hilbert space $\mathscr{H}_{1(2)}^{[k],r}\otimes\mathscr{H}_{1(2)}^{[k+1],l}$. $u_{1(2)}^{[k],r}(g)$ is a projective representation of G corresponding to ω on $\mathscr{H}_{1(2)}^{[k],r}$ and $u_{1(2)}^{[k+1],l}(g)$ a projective representation corresponding to $-\omega$ on $\mathscr{H}_{1(2)}^{[k+1],l}$. As $u_1^{[k],r}(g)$ and $u_2^{[k],r}(g)$ ($u_1^{[k+1],l}(g)$ and $u_2^{[k+1],l}(g)$) belong to the same ω, we can choose their pre-factor such that they have the same factor system. In the following discussion, we will assume WLOG that this is true.

We can think of $|EP_{k,k+1}\rangle_1$ and $|EP_{k,k+1}\rangle_2$ as living together in a joint Hilbert space $(\mathscr{H}_1^{[k],r}\oplus\mathscr{H}_2^{[k],r})\otimes(\mathscr{H}_1^{[k+1],l}\oplus\mathscr{H}_2^{[k+1],l})$. The symmetry representation on this joint Hilbert space can be defined as

$$u^{[k],r}(g)\otimes u^{[k+1],l}(g) = (u_1^{[k],r}(g)\oplus u_2^{[k],r}(g))\otimes(u_1^{[k+1],l}(g)\oplus u_2^{[k+1],l}(g)) \tag{10.35}$$

As $u_1^{[k],r}(g)$ and $u_2^{[k],r}(g)$ (also $u_1^{[k+1],l}(g)$ and $u_2^{[k+1],l}(g)$) both correspond to ω ($-\omega$), their direct sum $u^{[k],r}(g)(u^{[k+1],l}(g))$ is also a projective representation corresponding to $\omega(-\omega)$. Therefore, we have a linear representation of G on each site k, $u^{[k],l}(g)\otimes u^{[k],r}(g)$ and both $|EP_{k,k+1}\rangle_1$ and $|EP_{k,k+1}\rangle_2$ are symmetric under $u^{[k],r}(g)\otimes u^{[k+1],l}(g)$.

Now we can perform a LU transformation on the joint Hilbert space and rotate continuously between $|EP_{k,k+1}\rangle_1$ and $|EP_{k,k+1}\rangle_2$. That is,

$$U(\theta) = \cos(\frac{\theta}{2})I - i\sin(\frac{\theta}{2})(|a\rangle\langle b| + |b\rangle\langle a|) \tag{10.36}$$

where $|a\rangle = |EP_{k,k+1}\rangle_1$, $|b\rangle = |EP_{k,k+1}\rangle_2$ and θ goes from 0 to π. By doing this locally to each pair, we can map $|\phi_1\rangle$ to $|\phi_2\rangle$ (and vice verse) with LU transformations without breaking the on-site symmetry of group G. Therefore, $|\phi_1\rangle$ and $|\phi_2\rangle$ belong to the same phase if they are related with the same ω.

On the other hand, if $|\phi_1\rangle$ and $|\phi_2\rangle$ are related to different ω_1 and ω_2 respectively, they cannot be connected by any LU transformation that does not break the symmetry. In fact, no matter what symmetric LU transformation we apply on the state, as long as the system remains gapped and short range correlated, we can always perform an RG transformation to the resulting state and find the projective representation on the edge state. Because the classes of projective representations are discrete, they cannot jump from one to another under symmetric LU transformation. Therefore, $|\phi_1\rangle$ and $|\phi_2\rangle$ cannot be related through symmetric LU transformation and hence belong to different SPT phases.

In this way, we are able to classify one dimensional gapped bosonic phases with on-site symmetry and find that:

Box 10.4 1D bosonic SPT with on-site symmetry

Symmetry protected topological phases in one-dimensional bosonic systems with on-site symmetry of group G have a one to one correspondence with the classes of projective representations of G, labeled by group elements of $H^2(G,U(1))$.

This result applies when the 1D representations $\alpha(G)$ form a finite group, when $G = U(1)$, further classification according to different $\alpha(U(1))$ exist.

10.2.3 Time reversal symmetry

Time reversal, unlike other symmetries, is represented by anti-unitary operator T, which is equivalent to the complex conjugate operator K followed by a unitary operator u. The classification of gapped 1D time reversal invariant phases follows closely the cases discusses before. In this section, we will highlight the differences and give our conclusion.

First, a state $|\psi\rangle$ is called time reversal invariant if

$$u \otimes u ... \otimes uK|\psi\rangle = \beta|\psi\rangle \tag{10.37}$$

where $|\beta| = 1$. But for anti-unitary T, the global phase β is arbitrary and in particular we can redefine $|\psi'\rangle = \sqrt{\beta}|\psi\rangle$, such that $u \otimes u ... \otimes uK|\psi'\rangle = |\psi'\rangle$. Therefore, in the following discussion, we will assume WLOG that $\beta = 1$.

Time reversal symmetry action on each site can belong to two different types with $T^2 = uu^* = I$ or $-I$ respectively. For example, on a spin $1/2$, time reversal acts as $T = iYK$ and hence $T^2 = -I$, while on a spin 1, $T = ie^{i\pi S_y}K$ and $T^2 = I$. However, as long as we are considering systems without translational symmetry, $T^2 = I$ or $-I$ does not make any difference as we can always take block size 2 so that on the renormalized site, T^2 is always equal to I. WLOG, we will consider only the case with $T^2 = I$ on each site.

Using argument similar to the case of on-site unitary symmetry, we can keep track and redefine symmetry operations as we do renormalization. Finally, at the fixed point we have a state described by matrices $A^{(\infty)}_{i^l i^r}$ which is invariant under time reversal operation $T^{(\infty)} = u^{(\infty)}K$, that is,

$$\sum_{j^l j^r} u_{i^l i^r, j^l j^r} A^*_{j^l j^r} = M^{-1} A_{i^l i^r} M \tag{10.38}$$

where the fixed-point label ∞ has been omitted.

Solving this equation we find,
(a)$MM^* = e^{i\theta} I$. As M is invertible, $e^{i\theta} = m = \pm 1$.
(b)$u = u^l \otimes u^r$. where u^l and u^r acts on i^l and i^r respectively, $u^l (u^l)^* = mI$ and $u^r (u^r)^* = mI$, $m = \pm 1$. In the fixed point wave function, each entangled pair is time reversal invariant

$$(u^{[k],r} \otimes u^{[k+1],l}) K |EP_{k,k+1}\rangle = |EP_{k,k+1}\rangle \tag{10.39}$$

The definition of projective representation can be generalized to the anti-unitary case, from which we can see that the two cases with $m = \pm 1$ correspond to two different projective representations and hence two SPT phases with time reversal symmetry. Suppose that we have a group of symmetry actions $\tau(g)$, $g \in G$, some of which can be anti-unitary. We give a label to each symmetry operator $s(g)$, where $s(g) = 1$ if $\tau(g)$ is unitary and $s(g) = -1$ if $\tau(g)$ is anti-unitary. $s(g)$ satisfies $s(g_1)s(g_2) = s(g_1 g_2)$. Factor system of this representation $\omega(g_1, g_2)$ is again given by

$$\tau(g_1)\tau(g_2) = \omega(g_1, g_2)\tau(g_1 g_2) \tag{10.40}$$

but satisfies a modified consistency condition due to associativity

$$\omega(g_1, g_2)\omega(g_1 g_2, g_3) = \omega^{s(g_1)}(g_2, g_3)\omega(g_1, g_2 g_3) \tag{10.41}$$

By changing the pre-factor of $\tau(g)$ by $\beta(g)$, we find that two factor systems are equivalent up to

$$\omega(g_1, g_2) \sim \omega'(g_1, g_2) = \omega(g_1, g_2) \frac{\beta(g_1 g_2)}{\beta(g_1)\beta^{s(g_1)}(g_2)} \tag{10.42}$$

According to this definition, $MM^* = -1$ corresponds to a nontrivial projective representation of time reversal while $MM^* = 1$ corresponds to a trivial one. Similar to the unitary case, nontrivial projective representations of time reversal cannot be one-dimensional, givigin rise to a nontrivial edge degeneracy in the fixed point state with the protection of time reversal symmetry. Moreover, we can show that the time reversal invariant fixed point states can be mapped into each other if and only if they are related to the same m value. Therefore, our classification result for time reversal symmetry is:

Box 10.5 1D bosonic SPT with time reversal symmetry
For 1D gapped boson / spin systems with ONLY time reversal symmetry, there are two phases that do not break the symmetry.

10.2.4 Translation invariance

In this section, we would like to discuss translational invariant (TI) systems whose ground states are gapped and also translational invariant. The renormalization procedure discussed in section 8.3 breaks translation symmetry and hence can not be used to study topological phases with translation symmetry. In this section, we will use the time evolution formulation of LU transformation and find a smooth path of gapped TI Hamiltonian whose adiabatic evolution connects two states within the same TI phase.

10.2.4.1 Translation invariance only

First, as an example, we consider the case of TI only and show that there is only one gapped TI phase. Each translational invariant MPS is described(up to local change of basis) by a double tensor $\mathbb{E}$

$$\mathbb{E}_{\alpha\gamma,\beta\chi} = \sum_i A_{i,\alpha\beta} \otimes A^*_{i,\gamma\chi} \tag{10.43}$$

Note that here the matrices and the double tensor are site independent. The MPS is short-range correlated if $\mathbb{E}$ has a non-degenerate largest eigenvalue 1. $\mathbb{E}$ can be written as

$$\mathbb{E}_{\alpha\gamma,\beta\chi} = \mathbb{E}^0_{\alpha\gamma,\beta\chi} + \mathbb{E}'_{\alpha\gamma,\beta\chi} = \Lambda^l_{\alpha\gamma}\Lambda^r_{\beta\chi} + \mathbb{E}'_{\alpha\gamma,\beta\chi} \tag{10.44}$$

where Λ^l (Λ^r) is the left (right) eigenvector of eigenvalue 1 and $\mathbb{E}'$ is of eigenvalue less than 1. As we have discussed previously, with a suitable choice of basis,

$$\Lambda^l_{\alpha\gamma} = \lambda_\alpha \delta_{\alpha\gamma},\ \lambda_\alpha > 0$$
$$\Lambda^r_{\beta\chi} = \eta_\beta \delta_{\beta\chi},\ \eta_\beta > 0$$

Obviously, $\mathbb{E}^0$ is a valid double tensor and represents a state in the fixed point form.

Next we show that we can smoothly change $\mathbb{E}$ to $\mathbb{E}^0$ by turning down the $\mathbb{E}'$ term to 0 from $t = 0$ to $t = T$ as

$$\mathbb{E}(t) = \mathbb{E}^0 + (1 - \frac{t}{T})\mathbb{E}' \tag{10.45}$$

We will demonstrate that this process corresponds to an LU time evolution preserving translation symmetry.

Every $\mathbb{E}(t)$ represents a TI SRC MPS state. To see this, note that if we recombine the indices $\alpha\beta$ as row index and $\gamma\chi$ as column index and denote the new matrix as $\hat{\mathbb{E}}$, then both $\hat{\mathbb{E}}$ and $\hat{\mathbb{E}}^0$ are positive semidefinite matrices. But then every $\hat{\mathbb{E}}(t)$ is also positive semidefinite, as for any vector $|v\rangle$

$$\begin{aligned}\langle v|\hat{\mathbb{E}}(t)|v\rangle &= \langle v|\hat{\mathbb{E}}^0|v\rangle + (1-\tfrac{t}{T})\langle v|\hat{\mathbb{E}}'|v\rangle \\ &= (1-\tfrac{t}{T})\langle v|\hat{\mathbb{E}}|v\rangle + \tfrac{t}{T}\langle v|\hat{\mathbb{E}}^0|v\rangle > 0\end{aligned}$$

$\mathbb{E}(t)$ is hence a valid double tensor and the state represented can be determined by decomposing $\mathbb{E}(t)$ back into matrices $A_i(t)$. Such a decomposition is not unique. $A_i(t)$ at different time is determined only up to a local unitary on the physical index i. But WLOG, we can choose the local unitary to be continuous in time, so that $A_i(t)$ vary continuously with time and reach the fixed point form at $t = T$(up to local change of basis). The state represented $|\psi(t)\rangle$ hence also changes smoothly with t and is a pure state with a finite correlation length as all eigenvalues of $\mathbb{E}(t)$ expect for 1 are diminishing with t. Therefore, $\mathbb{E}(t)$ represents a smooth path in TI SRC MPS that connects any state to a fixed point state(up to local change of basis).

How do we know that no phase transition happens along the path? This is because for every state $|\psi(t)\rangle$, we can find a parent Hamiltonian which changes smoothly with t and has the state as a unique gapped ground state. Following the discussion in chapter 6, we choose a sufficiently large but finite l and set the parent Hamiltonian to be

$$H(t) = -\sum_k h(t)_{k,k+l} \tag{10.46}$$

where $h(t)_{k,k+l}$ is the projection onto the support space of the reduced density matrix on site k to $k+l$ at time t. Note that this Hamiltonian is translation invariant. For large enough l, $h(t)_{k,k+l}$ will always be $D \times D$ dimensional. As the state changes continuously, its reduced density matrices of site k to $k+l$ changes smoothly. Because the dimension of the space does not change, $h(t)_{k,k+l}$ also changes smoothly with time. Moreover, it can be shown that $H(t)$ is always gapped as the second largest eigenvalue of $\mathbb{E}(t)$ never approaches 1. Therefore, by evolving the Hamiltonian adiabatically from $t = 0$ to $t = T$, we obtain a local unitary transformation connecting any state to the fixed point form, and in particular without breaking the translation symmetry.

Because any TI fixed point state can be disentangled into product state in a TI way, we find that

Box 10.6 1D bosonic SPT with translation symmetry

All translation invariant 1D gapped ground states are in the same phase, if no other symmetries are required

10.2.4.2 Translation invariance and on-site symmetry

If the system is TI and has on-site symmetry, we need to maintain the on-site symmetry while doing the smooth deformation. We will not present the detailed derivation here but only summarize what we have learned.

First we can show that:

Box 10.7 Nonexistence of short range correlated ground states
For a 1D spin system with translation and an on-site projective symmetry $u(g)$, the symmetric ground state cannot be short-range correlated, if the projective symmetry $u(g)$ corresponds to a non-trivial element in $H^2(G,U(1))$.

The reason is as follows. If a 1D state with translation symmetry is short-range correlated, it can be represented by a TI MPS. Suppose that we perform the RG transformation described in section 8.3 and flow the state to a fixed point form with on-site symmetry $\tilde{u}(g)$. With a proper choice of block size n in each RG step, we can make $u(g)$ and $\tilde{u}(g)$ to be the same type of projective representation described by $\omega_{sym} \in H^2(G,U(1))$. The fixed point matrices then transform as

$$\sum_{j^l j^r} \tilde{u}_{i^l i^r, j^l j^r}(g) A_{j^l j^r} = M^{-1}(g) A_{i^l i^r} M(g) \tag{10.47}$$

Because $M^{-1}(g)$ and $M(g)$ form projective representations of class ω and $-\omega$, ω_{sym} has to be 0, that is, the trivial element in $H^2(G,U(1))$. So, if $\omega_{sym} \neq 0$, the 1D TI state cannot be short-range correlated. In other words, 1D spin systems with translation and an on-site projective symmetry are always gapless or have degenerate ground states that break the symmetries.

If the ground state of the 1D spin system does not break the on-site symmetry and the translation symmetry, then ground state is not short-range correlated and is gapless. If the ground state of the 1D spin system breaks the on-site symmetry or the translation symmetry, then the ground state is degenerate.

As an application of the above result, we find that:

Box 10.8 Nonexistence of short range correlated half integer spin chain
1D half-integer-spin systems with translation and the $SO(3)$ spin rotation symmetry are always gapless or have degenerate ground states.

Note that this condition is not necessary in systems without translation symmetry. Indeed, without TI, $A^{[k]}_{j^l j^r}$ may depend on site label k and when transformed under symmetry as

$$\sum_{j^l j^r} \tilde{u}^{[k]}_{i^l i^r, j^l j^r}(g) A^{[k]}_{j^l j^r} = (M^{[k]}(g))^{-1} A_{i^l i^r} M^{[k+1]}(g) \tag{10.48}$$

$M^{[k]}(g)$ and $M^{[k+1]}(g)$ may form projective representations of different types. Therefore, it is possible to have SRC non-translation invariant state with projective symmetry action per site. In particular, 1D half-integer spin chains with $SO(3)$ spin rotation symmetry can be gapped and SRC if the spins are dimerized (form singlets between site $2i-1$ and $2i$) and break translation symmetry explicitly.

On the other hand, to have a gapped TI 1D state with an on-site symmetry, the symmetry must act linearly (i.e. not projectively). In this case, new labels are needed for SPT states besides the projective representation class. In particular, for 1D bosonic systems of L sites with translation and an on-site linear symmetry of group G, a gapped state that does not break the two symmetries must transform as

$$u(g)\otimes ...\otimes u(g)|\psi_L\rangle = [\alpha(g)]^L|\psi_L\rangle \tag{10.49}$$

for all values of L that is large enough. Here $u(g)$ is the linear representation of G acting on the physical states in each site and $\alpha(g)$ is a one-dimensional linear representation of G. Due to translation symmetry, the symmetric LU transformations cannot change 1D representation $\alpha(g)$. So the different SPT phases are also distinguished by the 1D representations α of G.

Similar to the derivation in the previous section, we find that SRC MPS with translation and on-site linear symmetry can be mapped to a fixed point form which transform under the on-site symmetry as

$$\sum_{j^l j^r} \tilde{u}_{i^l i^r, j^l j^r}(g) A_{j^l j^r} = \alpha(g) M^{-1}(g) A_{i^l i^r} M(g) \tag{10.50}$$

where $\tilde{u}_{i^l i^r, j^l j^r}(g)$ is the on-site linear symmetry at fixed point, $\alpha(g)$ is the 1D representation of G and $M(g)$ is a projective representation of G. Both $\alpha(g)$ and the class of $M(g)$ have to be the same for two SPT states to be connectable through symmetric LU transformations.

Box 10.9 1D bosonic SPT with translation and on-site symmetry

For 1D boson / spin systems with only translation and an on-site linear symmetry G, all the phases of gapped states that do not break the two symmetries are classified by a pair (ω,α) where $\omega \in H^2(G,U(1))$ label different types of projective representations of G and α label different 1D representations of G.

Here are a few concrete examples:

If we choose the symmetry group to be $G=\mathbb{Z}_n$, we find: For 1D spin systems with only translation and on-site $\mathbb{Z}_n$ symmetry, there are n phases for gapped states that do not break the two symmetries.

This is because $\mathbb{Z}_n$ has no projective representations and has n different 1D representations. As an example, consider the following model

$$H = \sum_i [-h\sigma_i^z - \sigma_{i-1}^x \sigma_i^y \sigma_{i+1}^z], \tag{10.51}$$

where $\sigma^{x,y,z}$ are the Pauli matrices. The model has a $\mathbb{Z}_2$ symmetry generated by σ^z. The two different $\mathbb{Z}_2$ symmetric phases correspond the $h \to \infty$ phase and the $h \to -\infty$ phase of the model.

If we choose the symmetry group to be $G = SO(3)$, we find: For 1D integer-spin systems with only translation and $SO(3)$ spin rotation symmetry, there are two phases for gapped states that do not break the two symmetries.

This is because $SO(3)$ has only one 1D representation and $H^2(SO(3), U(1)) = \mathbb{Z}_2$. A nontrivial example in this classification is given by the AKLT state in spin-1 chains and a trivial example is given by the direct product state with spin-0 on each site.

On the other hand, if $\alpha(g)$ does not form a 1D representation of G, then the state cannot be both symmetric and short range correlated.

Let us apply the above result to a boson system with p/q bosons per site. Here the bosons number is conserved and there is an $U(1)$ symmetry. Certainly, the system is well defined only when the number of sites L has a form $L = Jq$ (assuming p and q have no common factors). For such an L, we find that $\alpha_L(g) = \alpha_0(g)^J = \alpha_0(g)^{L/q}$, where $\alpha_0(g)$ is the generating 1D representation of the $U(1)$ symmetry group. So eqn. (10.49) is *not* satisfied for some large L. Therefore

Box 10.10 Nonexistence of gapped boson state at fractional filling
A 1D state of conserved bosons with fractional bosons per site must be gapless, if the state does not break the $U(1)$ and the translation symmetry.

In higher dimensions, the situation is very different. A 2D state of conserved bosons with fractional bosons per site can be gapped, and, at same time, does not break the $U(1)$ and the translation symmetry. 2D fractional quantum Hall states of bosons on lattice provide examples for such kind of states.

Results discussed in this section apply not only to unitary on-site symmetry, but to anti-unitary time reversal symmetry as well.

10.2.4.3 Translation invariance and parity symmetry

In this section, we will consider the case of parity symmetry for translational invariant system. The parity operation P for a spin (boson) chain is in general composed of two parts: P_1, exchange of sites n and $-n$; P_2, on-site unitary operation u where $u^2 = I$. [1]

[1] The $\mathbb{Z}_2$ operation u is necessary in the definition of parity if we want to consider for example, fixed point state with $|EP\rangle = |00\rangle + |11\rangle$ be to parity symmetric. The state is not invariant after exchange of sites, and only maps back to itself if in addition the two spins on each site are also exchanged with u.

Following previous discussions, it is possible to show that the matrices describing the SRC state with translation and parity symmetry can be deformed to a fixed point form, which satisfies:

$$\sum_{j^l j^r} u_{i^l i^r, j^l j^r} A^T_{j^l j^r} = \pm M^{-1} A_{i^l i^r} M \tag{10.52}$$

for some invertible matrix M and $u^2 = I$, where we have used that the 1D representation of parity is either $(1,1)$ or $(1,-1)$. We label the two 1D representations with $\alpha(P) = \pm 1$. Here M satisfies $M^{-1}M^T = e^{i\theta}$. But $M = (M^T)^T = e^{2i\theta}M$, therefore, $e^{i\theta} = \pm 1$ and correspondingly M is either symmetric $M = M^T$ or antisymmetric $M = -M^T$. We will label this sign factor as $\beta(P) = \pm 1$.

Solving this equation gives that $u = \alpha(P)v(u^l \otimes u^r)$, where v is the exchange operation of the two spins i^l and i^r and u^l,u^r act on i^l,i^r respectively. $(u^l)^T = \beta(P)u^l$ and $(u^r)^T = \beta(P)u^r$. It can then be shown that each entangled pair $|EP_{k,k+1}\rangle$ must be symmetric under parity operations and satisfies $u^r_k \otimes u^l_{k+1}|EP_{k+1,k}\rangle = \alpha(P)|EP_{k,k+1}\rangle$. There are hence four different symmetric phases corresponding to $\alpha(P) = \pm 1$ and $\beta(P) = \pm 1$. We can show similarly as before that fixed points within each class can be mapped from one to the other with TI LU transformation preserving the parity symmetry. On the other hand, fixed points in different classes can not be connected without breaking the symmetries. Therefore, there are four parity symmetric TI phases.

Box 10.11 1D bosonic SPT with translation and parity symmetry

For 1D boson / spin systems with only translation and parity symmetry, there are four phases for gapped states that do not break the two symmetries.

As an example, consider the following model

$$H = \sum_i [-BS^z_i + S_i \cdot S_{i+1}], \tag{10.53}$$

where S_i are the spin-1 operators. The model has a parity symmetry. The $B = 0$ phase and the $B \to +\infty$ phase of the model correspond to two of the four phases discussed above. The $B = 0$ state is in the same phase as the AKLT state. In the fixed-point state for such a phase, $|EP_{k,k+1}\rangle = |\uparrow\downarrow\rangle - |\downarrow\uparrow\rangle$. The parity transformation exchange the first and the second spin, and induces a minus sign: $P : |EP_{k,k+1}\rangle \to -|EP_{k,k+1}\rangle$. The $B \to +\infty$ state is the $S^z = 1$ state. Its entangled pairs are $|EP_{k,k+1}\rangle = |\uparrow\uparrow\rangle$ which do not change sign under the parity transformation. Thus the stability of the Haldane/AKLT state is also protected by the parity symmetry.

To understand why there are four parity symmetric phases instead of two (parity even/parity odd), we give four representative states in Fig. 10.4, one for each phase. Connected pair of black dots denotes an entangled pair. $+$ stands for a parity even pair, for example $|00\rangle + |11\rangle$, and $-$ stands for a parity odd pair, for example $|01\rangle - |10\rangle$. Each rectangle corresponds to one site, with four spin degrees of freedom on

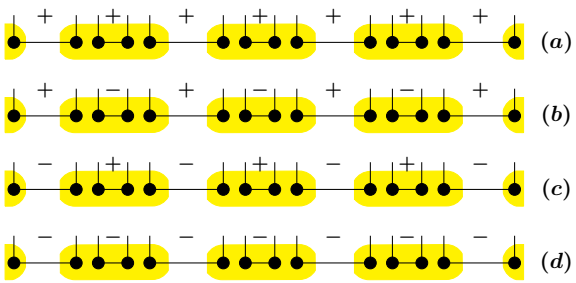

Fig. 10.4 Representative states of the four parity symmetric phases, each corresponding to (a) $\alpha(P)=1, \beta(P)=1$ (b) $\alpha(P)=-1, \beta(P)=1$ (c) $\alpha(P)=-1, \beta(P)=-1$ (d) $\alpha(P)=1, \beta(P)=-1$. $+$ stands for a parity even entangled pair (e.g. $|00\rangle+|11\rangle$), $-$ stands for a parity odd entangled pair (e.g. $|01\rangle-|10\rangle$). Each site contains four virtual spins.

each site. The four states are all translational invariant. If the parity operation is defined to be exchange of sites together with exchange of spins 1 and 4, 2 and 3 on each site, then states (a) and (d) are parity even while (b) and (c) are parity odd. But (a) and (d) (or (b) and (c)) are different parity even (odd) states and cannot be mapped to each other through local unitary transformations without breaking parity symmetry. Written in the matrix product representation, the matrices of the four states will transform with $\alpha(P)=\pm 1$ and $\beta(P)=\pm 1$ respectively. Therefore, the parity even/odd phase breaks into two smaller phases and there are in all four phases for parity symmetric systems.

10.2.5 Summary of results for bosonic systems

Here we summarize the classification of topological phases in 1D bosonic systems with different symmetries in Table 10.1.

10.3 Topological phases in 1D fermion systems

Although our previous discussions have been focused on boson/spin systems, it actually also applies to fermion systems. Because in 1D fermion systems and spin systems can be mapped to each other through Jordan Wigner transformation, we can classify fermionic phases by classifying the corresponding spin phases, as we discuss in this section. We are not going to study the fermionic topological phases in detail and related references are given in Summary and Further Reading.

Specifically, for a class of fermion systems with certain symmetry we are going to do the following

Symmetry	No. or Label of Different Phases	Example System
None	1	
On-site Symmetry of Group G (*)	$\omega \in H^2(G,U(1))$	On-site $\mathbb{Z}_n$ or $SU(2)$: 1 phase On-site $SO(3)/D_2$ on integer spin: 2 phases
Time Reversal(TR)	2	
Translational Invariance(TI)	1	
TI+On-site Linear Symmetry of Group G	$\omega \in H^2(G,U(1))$ and $\alpha(G)$	TI+On-site $\mathbb{Z}_n$: n phases TI+On-site $SO(3)$ on integer spin: 2 phases
TI+ On-site Projective Symmetry of Group G	0	TI+On-site $SO(3)$ or D_2 on half-integer spin: no gapped phase
TI+Parity	4	
TI+TR	2 if $T^2 = I$ 0 if $T^2 = -I$	TI+TR on integer spin: 2 phases on half-integer spin: no gapped phase

Table 10.1 Summary of classification result for 1D gapped spin system with symmetric ground states. TI stands for translational invariance. TR stands for time reversal symmetry. $H^2(G,U(1))$ is the second cohomology group of group G over complex number $U(1)$. $\alpha(G)$ is a 1D representation of G. (*): this result applies when $\alpha(G)$ form a finite group, when $G = U(1)$, further classification according to different $\alpha(U(1))$ exist.

1. identify the corresponding class of spin systems by mapping the symmetry to spin

2. classify possible spin phases with this symmetry, including symmetry breaking and symmetry protected topological phases

3. map the spin phases back to fermions and identify the fermionic order

In the following we are going to apply this strategy to 1D fermion systems in four cases: no symmetry(other than fermion parity), time reversal symmetry for spinless fermions, time reversal symmetry for spin half integer fermions, and $U(1)$ symmetry for fermion number conservation. One special property of fermionic systems is that it always has a fermionic parity symmetry. That is, the Hamiltonian is a sum of terms composed of even number of fermionic creation and annihilation operators. Therefore, the corresponding spin systems we classify always have an on-site $\mathbb{Z}_2$ symmetry. Note that this approach can only be applied to systems defined on an open chain. For system with translation symmetry and periodic boundary condition, Jordan Wigner transformation could lead to non-local interactions in the spin system.

10.3.1 Jordan Wigner transformation

First, let us briefly summarize the procedure of Jordan Wigner transformation for mapping 1D fermion systems to 1D spin systems.

Consider the simplest case where each site k in the fermion system contains one fermion mode with creation and annhilation operator $a_k^\dagger$ and a_k. The local Hilbert space is two dimensional and can be mapped to a spin $1/2$ degree of freedom

$$|\Omega_k\rangle \to |0_k\rangle,\ a_i^\dagger|\Omega_k\rangle \to |1_k\rangle \tag{10.54}$$

where $|\Omega_k\rangle$ is the unoccupied fermionic state on site k, $|0_k\rangle$ and $|1_k\rangle$ are spin states with $\pm\frac{1}{2}$ spin in z direction.

The mapping between operators, however, has to be non-local to preserve the anti-commutation relation between fermionic operators on different sites. In particular,

$$a_k \to \frac{1}{2}\prod_{j<k} Z_j(X_k + iY_k),\ a_k^\dagger \to \frac{1}{2}\prod_{j<k} Z_j(X_k - iY_k) \tag{10.55}$$

It can be checked explicitly that the operator algebra is preserved under this mapping. The fermion occupation number on site k is mapped to

$$a_k^\dagger a_k \to \frac{1}{2}(I_k - Z_k) \tag{10.56}$$

and the total fermion parity operator is mapped to

$$P_f = \prod_k (1 - 2a_k^\dagger a_k) \to \prod_k Z_k \tag{10.57}$$

Local Hamiltonian terms in the middle of the 1D fermionic chain are mapped to local Hamiltonian terms in the spin system. For example, fermion hopping terms are mapped as

$$a_k^\dagger a_{k+1} + a_{k+1}^\dagger a_k \to \frac{1}{2}X_k X_{k+1} + Y_k Y_{k+1} \tag{10.58}$$

Terms across the boundary however may become nonlocal. For example

$$a_N^\dagger a_1 + a_1^\dagger a_N = -\frac{1}{2}\prod_k Z_k (X_N X_1 + Y_N Y_1) \tag{10.59}$$

Therefore, with periodic boundary condition, local fermion models do not exactly map into local spin models. However, if the total fermion parity ($\prod_k Z_k$) is fixed, the boundary term becomes local, as can be seen from the previous example. Therefore, if we are considering gapped fermion systems with nondegenerate ground state, which has a fixed fermion parity, the Jordan-Wigner transformation is effectively local.

If the local Hilbert space on site i is larger than two dimensional, we can always embed it into a larger (finite dimensional) Hilbert space of the form $H_f \otimes H_b$, where H_f is the two dimensional Hilbert space corresponding to a fermion mode and H_b is a bosonic Hilbert space. Note that the classification we are considering is stable with respect to addition of local degrees of freedom. Therefore, embedding into a larger local Hilbert space is allowed. After this embedding, Jordan Wigner transformation proceeds as described above on the H_f sector only.

10.3.2 Fermion parity symmetry only

For a 1D fermion system with only fermion parity symmetry, how many gapped phases exist?

To answer this question, first we do a Jordan-Wigner transformation and map the fermion system to a spin chain. The fermion parity operator $P_f = \prod(1-2a_i^\dagger a_i)$ is mapped to an on-site $\mathbb{Z}_2$ operation. On the other hand, any 1D spin system with an on-site $\mathbb{Z}_2$ symmetry can always be mapped back to a fermion system with fermion parity symmetry(expansion of local Hilbert space maybe necessary). As the spin Hamiltonian commute with the $\mathbb{Z}_2$ symmetry, it can be mapped back to a proper physical fermion Hamiltonian. Therefore, the problem of classifying fermion chains with fermion parity is equivalent to the problem of classifying spin chains with $\mathbb{Z}_2$ symmetry.

There are two possibilities in spin chains with $\mathbb{Z}_2$ symmetry: (1) the ground state is symmetric under $\mathbb{Z}_2$. As $\mathbb{Z}_2$ does not have non-trivial projective representation, there is one symmetric phase. (If translational symmetry is required, systems with even number of fermions per site are in a different phase from those with odd number of fermions per site. This difference is somewhat trivial and we will ignore it.) (2) the ground state breaks the $\mathbb{Z}_2$ symmetry. The ground state will be two-fold degenerate. Each short-range correlated ground state has no particular symmetry and they are mapped to each other by the $\mathbb{Z}_2$ operation. There is one such symmetry breaking phases. These are the two different phases in spin chains with $\mathbb{Z}_2$ symmetry.

This tells us that there are two different phases in fermion chains with only fermion parity symmetry. But what are they? First of all, fermion states cannot break the fermion parity symmetry. All fermion states must have a well-defined parity. Does the spin symmetry breaking phase correspond to a real fermion phase?

The answer is yes and actually the spin symmetry breaking phase corresponds to a $\mathbb{Z}_2$ symmetric fermion phase. Suppose that the spin system has two short-range correlated ground states $|\psi_0\rangle$ and $|\psi_1\rangle$. All connected correlations between spin operators decay exponentially on these two states. Mapped to fermion systems, $|\psi_0^f\rangle$ and $|\psi_1^f\rangle$ are not legitimate states because they don't have fixed fermion parity but $|\tilde{\psi}_0^f\rangle = |\psi_0^f\rangle + |\psi_1^f\rangle$ and $|\tilde{\psi}_1^f\rangle = |\psi_0^f\rangle - |\psi_1^f\rangle$ are. They have even/odd fermion parity respectively. In spin system, $|\tilde{\psi}_0\rangle$ and $|\tilde{\psi}_1\rangle$ are not short range correlated states but mapped to fermion system they are. To see this, note that any correlator between bosonic operators on the $|\tilde{\psi}_0^f\rangle$ and $|\tilde{\psi}_1^f\rangle$are the same as that on $|\psi_0\rangle$ and $|\psi_1\rangle$ and hence decay exponentially. Any correlator between fermionic operators on the $|\tilde{\psi}_0^f\rangle$ and $|\tilde{\psi}_1^f\rangle$ gets mapped to a string operator on the spin state, for example $a_i^\dagger a_j$ is mapped to $(X-iY))_i Z_{i+1}...Z_{j-1}(X-iY)_j$, which also decays with separation between i and j. Therefore, the symmetry breaking phase in spin chain corresponds to a fermionic phase with symmetric short range correlated ground states.

This phase can be realized in Kitaev's Majorana chain model. Consider a 1D fermionic chain with one fermion mode per site. Denote the creation and annihilation operator of the fermion mode on site k as $a_k^\dagger$ and a_k. To understand the special

property of the Majorana chain model, it is helpful to represent each fermion mode as two Majorana fermion modes

$$\gamma_{2k-1} = a_k^\dagger + a_k, \quad \gamma_{2k} = i(a_k^\dagger - a_k) \tag{10.60}$$

such that the γ's are all Hermitian and $\gamma^2 = I$. Now suppose that each Majorana mode couples to another Majorana mode on a neighboring site as shown in Fig.10.5. The Hamiltonian of this system reads

$$H = \sum_k i\gamma_{2k}\gamma_{2k+1} \tag{10.61}$$

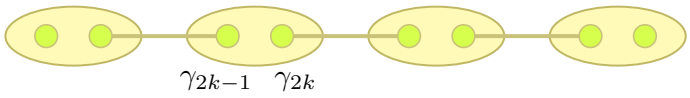

Fig. 10.5 Majorana chain model.

If we recombine the Majorana modes into fermion modes as

$$b_k^\dagger = \frac{1}{2}(\gamma_{2k} - i\gamma_{2k+1}), b_k = \frac{1}{2}(\gamma_{2k} + i\gamma_{2k+1}) \tag{10.62}$$

then we can map the Hamiltonian into the form

$$H = 2b_k^\dagger b_k - 1 \tag{10.63}$$

The Hamiltonian decouples into individual terms for each b_k mode and it is easy to see that the ground state is the vacuum state for all such modes.

Now we are ready to see the most interesting feature of this model: with periodic boundary condition, all the Majorana modes are coupled in pairs and the system has a unique ground state (the vacuum state for all b_k modes); with open boundary condition however, the two modes on the boundary are not coupled to anything, as shown in Fig.10.5 and leaves a two fold degeneracy in the ground state. The degenerate ground states are $|\tilde{\psi}_0^f\rangle = |\psi_0^f\rangle + |\psi_1^f\rangle$ and $|\tilde{\psi}_1^f\rangle = |\psi_0^f\rangle - |\psi_1^f\rangle$ discussed above.

Note that while Fig.10.5 has a similar structure to Fig.10.3 for bosonic SPT states, they have one important difference: each dot in Fig.10.3 represents a well defined Hilbert space but each dot in Fig.10.5 does not. The dots in Fig.10.5 represent Majorana modes and only by combining pairs of them do we have a well define Hilbert space of dimension two.

To summarize, the symmetry breaking phase of the spin chain corresponds to a topological phase in the fermion chain with Majorana edge modes. On the other hand, the symmetric phase in the spin chain corresponds to a topologically trivia phase for the fermions. A representative Hamiltonian in this phase can be written as

$$H = \sum_k 2a_k^\dagger a_k - 1 = \sum_k i\gamma_{2k-1}\gamma_{2k} \tag{10.64}$$

The ground state of this Hamiltonian is the vacuum state for all a_k modes which is unique and gapped with both closed and open boundary conditions. As the two fermion phases have different edge states, they cannot be connected under any physical fermionic perturbation without closing gap and going through phase transition.

Box 10.12 1D fermionic gapped phases with fermion parity symmetry
For 1D fermion system with only fermion parity symmetry, there are two gapped phases, one with Majorana edge mode and one without.

10.3.3 Fermion parity and $T^2 = 1$ time reversal

Now consider the more complicated situation where aside from fermion parity, there is also a time reversal symmetry. Time reversal acts as an anti-unitary $T = UK$ on each site. In this section we consider the case where $T^2 = 1$(spinless fermion).

So now the total symmetry for the fermion system is the $\mathbb{Z}_2$ fermion parity symmetry P_f and $T^2 = 1$ time reversal symmetry. T commutes with P_f. The on-site symmetry group is a $\mathbb{Z}_2 \times \mathbb{Z}_2$ group and has four elements $G = \{I, T, P_f, TP_f\}$. Mapped to spin system, the symmetry group structure is kept.

The possible gapped phases for a spin system with on-site symmetry $G = \{I, T, P_f, TP_f\}$ include both symmetry breaking and symmetric phases. If we use G' to label the unbroken symmetry subgroup on the SRC ground state, then the possibilities are:

(1) $G' = G$. Following discussion in previous sections we find that it has four different projective representations. Examples of the four representations are a.$\{I, K, Z, KZ\}$, b. $\{I, iYK, Z, iYKZ\}$, c. $\{I, iYKZ \otimes I, I \otimes Z, iYKZ \otimes Z\}$ d. $\{I, K, Y, KY\}$. There are hence four different symmetric phases. (If translational symmetry is required, the number is multiplied by 2 due to $\alpha(\mathbb{Z}_2)$)

(2) $G' = \{I, P_f\}$ with no non-trivial projective representation, the time reversal symmetry is broken. There is one such phase. (If translational symmetry is required, there are two phases)

(3) $G' = \{I, T\}$, with two different projective representations(time reversal squares to $\pm I$ on boundary spin). The $\mathbb{Z}_2$ fermion parity is broken. There are two phases in this case.

(4) $G' = \{I, TP_f\}$, with two different projective representations. The fermion parity symmetry is again broken. Two different phases.

(5) $G' = I$, no projective representation, all symmetries are broken.

Mapped back to fermion systems, fermion parity symmetry is never broken. Instead, the P_f symmetry breaking spin phases are mapped to fermion phases with

Majorana boundary mode on the edge as discussed in the previous section. Therefore the above spin phases correspond in the fermion system to:

(1) Four different symmetric phases

(2) One time reversal symmetry breaking phase.

(3) Two symmetric phases with Majorana boundary mode

(4) Another two symmetric phases with Majorana boundary mode.

(5) One time reversal symmetry breaking phase.

Among all these cases, (1)(3)(4) contains the eight symmetric phases for time reversal invariant fermion chain with $T^2 = 1$.

Box 10.13 1D fermionic gapped phases with $T^2 = 1$ time reversal

For 1D fermion system with $T^2 = 1$ time reversal symmetry and fermion parity symmetry, there are eight different gapped phases.

10.3.4 Fermion parity and $T^2 \neq 1$ time reversal

When $T^2 \neq I$, the situation is different. This happens when we take the fermion spin into consideration and for a single particle, time reversal is defined as $e^{i\pi S_y}K$. With half integer spin, $\left(e^{i\pi S_y}K\right)^2 = -I$. Note that for every particle the square of time reversal is $-I$, however when we write the system in second quantization as creation and annihilation operator on each site, the time reversal operation defined on each site satisfies $T^2 = P_f$. Therefore, the symmetry group on each site is a Z_4 group $G = \{I, T, P_f, TP_f\}$. To classify possible phases, we first map everything to spin.

The corresponding spin system has on-site symmetry $G = \{I, T, P_f, TP_f\}$. $T^2 = P_f$, $P_f^2 = I$. The possible phases are:

(1) $G' = G$, with two possible projective representations, one with $T^4 = I$, the other with $T^4 = -I$. Example for the latter includes $T = (1/\sqrt{2})(X + Y)K$. Therefore, there are two possible symmetric phases. (If translational symmetry is required, there are four phases.)

(2) $G' = \{I, P_f\}$, the time reversal symmetry is broken. One phase. (If translational symmetry is required, there are two phases.)

(3) $G' = I$, all symmetries are broken. One phase.

Therefore, the fermion system has the following phases:

(1) Two symmetric phases

(2) One time reversal symmetry breaking phase

(3) One time reversal symmetry breaking phase with Majorana boundary mode.

Among all these cases, (1) contains the time reversal symmetry protected topological phase.

Box 10.14 1D fermionic gapped phases with $T^2 = P_f$ time reversal
For 1D fermion system with $T^2 = P_f$ time reversal symmetry and fermion parity symmetry (P_f), there are two different gapped phases.

10.3.5 Fermion number conservation

Consider the case of a gapped fermion system with fixed fermion number. This corresponds to an on-site $U(1)$ symmetry, $e^{i\theta N}$. Mapped to spins, the spin chain will have an on-site $U(1)$ symmetry. This symmetry cannot be broken and $U(1)$ does not have a non-trivial projective representation. One thing special about $U(1)$ symmetry though, is that it has an infinite family of 1D representations. The fermion number per site is a good quantum number and labels different phases. Therefore, mapped back to fermions, there is an infinite number of phases with different average number of fermions per site.

Box 10.15 1D fermionic gapped phases with $U(1)$ symmetry
For 1D fermion system with $U(1)$ charge conservation symmetry, there is an infinite number of phases with different average number of fermions per site.

10.4 2D symmetry protected topological order

Having understood symmetry protected topological order in 1D, we can ask are there similar phases in two and higher dimensions? That is, we want to know if there exist gapped phases in two and higher dimension with short range entanglement in the bulk and symmetry protected nontrivial edge state on the boundary. From the study of free fermion system, we know that there are indeed such phases such as topological insulators and superconductors. These phases are gapped in the bulk and have gapless edge states as along as certain symmetries are preserved. However, it is not clear from the study of such free fermion system what SPT phases exist in general interacting system. In particular, it is not even clear whether SPT order can exist in bosonic system where without interaction no nontrivial topological order can emerge. In this section, we describe two strongly interaction bosonic models with nontrivial SPT order. The first one – the 2D AKLT model – is a straight forward generalization of the 1D AKLT model to 2D. Similar to the 1D version, the 2D AKLT state has spin rotation symmetry. However, its gapless edge state is protected only when translation symmetry is also preserved. The second model – the CZX model – demonstrates that translation symmetry is not always necessary

for nontrivial SPT order to exist in 2D bosonic systems. That is, the gapless edge state of the CZX model is robust even in the presence of disorder, as long as certain internal symmetry is preserved. This is similar to what happens in topological insulators and superconductors in free fermion systems.

10.4.1 2D AKLT model

10.4.1.1 Bulk definition and boundary state

This simple picture of 1D SPT phases, in particular the 1D AKLT state, can be generalized to two dimension to give the 2D AKLT model. Consider the 2D state in Fig. 10.6.

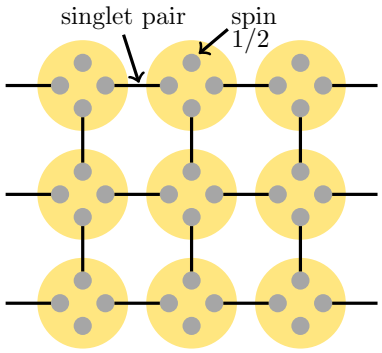

Fig. 10.6 The 2D AKLT model which is short range entangled and symmetric under spin rotation symmetry. Each site contains four spin $1/2$s. Two spin $1/2$s connected by a bond form a singlet under spin rotation symmetry. On a lattice with boundary, the boundary degrees of freedom are a chain of spin $1/2$s.

Every site contains four spin $1/2$s. Each spin $1/2$ forms a projective representation of the spin rotation symmetry $SO(3)$, but the four spins on each site together form a linear representation of $SO(3)$. Two spins on neighboring sites which are connected by a bond form a singlet pair $|01\rangle - |10\rangle$. Similar to the 1D case, the total state is invariant under spin rotation. The state is short range entangled and can be the gapped ground state of a simple Hamiltonian

$$H = \sum_{<ab>} X_a X_b + Y_a Y_b + Z_a Z_b \tag{10.65}$$

where $< ab >$ labels the pairs of spins connected by a bond.

If the system is defined on a disk with boundary, there will be free spin $1/2$s at each site on the boundary, as shown in Fig. 10.6. These boundary spins can couple

to each other, for example through nearest neighbor Heisenberg interaction,

$$H = \sum_i X_i X_{i+1} + Y_i Y_{i+1} + Z_i Z_{i+1} \tag{10.66}$$

With such a coupling the boundary is in a gapless state. Of course, other types of coupling terms can also exist. The question is then, is the gapless edge state protected? Correspondingly, does the 2D AKLT state possess nontrivial SPT order.

If only spin rotation symmetry is considered, then the answer is no. Indeed, if we introduce modulation to the coupling strength of the Heisenberg interaction on the boundary

$$H = \sum_i J_1 (X_{2i} X_{2i+1} + Y_{2i} Y_{2i+1} + Z_{2i} Z_{2i+1}) + J_2 (X_{2i+1} X_{2i+2} + Y_{2i+1} Y_{2i+2} + Z_{2i+1} Z_{2i+2}) \tag{10.67}$$

the spin $1/2$s on the boundary would become 'dimerized' and gapped, without breaking spin rotation symmetry. This is easiest to understand in the limit of $J_1 > 0$, $J_2 = 0$. Then every pair of $2i$th spin and $2i+1$th spin couple into a singlet pair. The $2i+1$th spin and the $2i+2$th spin are decoupled from each other. The total state is hence gapped and preserves spin rotation symmetry. Therefore, the 2D AKLT state does not have nontrivial SPT order protected by spin rotation symmetry alone.

However, the story changes once translation symmetry is added to the picture. If translation symmetry is also preserved, the boundary as a spin $1/2$ chain with translation symmetry is always gapless. Therefore, the 2D AKLT state has translation symmetry and spin rotation symmetry preserved gapless edge state and hence nontrivial SPT order under these symmetries.

Box 10.16 SPT order of 2D AKLT state

2D AKLT state has nontrivial symmetry protected topological order protected by translation and spin rotation symmetry.

Such a construction can be generalized to all kinds of internal symmetries. Consider an on-site symmetry of group G. On each site, instead of spin $1/2$s, we would have four degrees of freedom which carry projective representations of G. A pair of degree of freedom connected by a bond have projective representation ω and $-\omega$ respectively. Together they form an entangled state which is a linear representation of G. Therefore, the bulk of the system is gapped and symmetric. On the boundary, each site contains one projective representation. If translation symmetry is preserved, each boundary degree of freedom is well defined and the projective representation they carry do label different SPT phases. If each site forms a nontrivial projective representation of G, then translation symmetry requires that the boundary be gapless, indicating nontrivial SPT order in the bulk. On the other hand, in the absence of translation symmetry, the boundary degrees of freedom can be combined. As projective representations form an additive group (the second cohomology group $\mathscr{H}^2(G,U(1))$ of G), combining boundary spins would change the

projective representations from one class to another and in particular, to the trivial class. Therefore, without translation symmetry, all 2D states with a bond form as shown in Fig. 10.6 belong to the same phase.

10.4.1.2 Tensor network representation

Such a bond state has a simple tensor network representation. More interestingly, the way the tensor transforms under symmetry contains important information about the SPT order of the state. This is what we are going to discuss in this section.

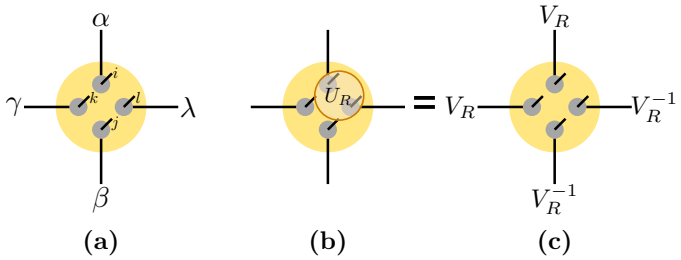

Fig. 10.7 The tensor network representation of the 2D AKLT state.

Consider the 2D AKLT example. The tensor on each site is composed of four parts $(t^i_\alpha)_u$, $(t^j_\beta)_d$, $(t^k_\gamma)_l$, $(t^l_\lambda)_r$, as shown in Fig. 10.7 (a). Each part contains one two-dimensional physical index i, j, k or l, and one two-dimensional inner index α, β, γ, or λ. The nonzero terms are

$$(t^0_0)_u = 1,\ (t^1_1)_u = 1;\ (t^0_1)_d = -1,\ (t^1_0)_d = 1$$
$$(t^0_0)_l = 1,\ (t^1_1)_l = 1;\ (t^0_1)_r = -1,\ (t^1_0)_r = 1$$

All other terms in the tensor are zero. With such a tensor, it is straight forward to check that two spin $1/2$'s connected by a bond are in the singlet state $|01\rangle - |10\rangle$.

Now let's see how the tensor transform under spin rotation symmetry. Apply a spin rotation transformation to the physical spins

$$U_R = \prod_i e^{i\frac{\theta}{2}(n_x X_i + n_y Y_i + n_z Z_i)} \tag{10.68}$$

as shown in Fig.10.7 (b). If such a transformation is applied to all spins in the system, the wave function remains invariant. On the other hand, if we consider the action of the transformation on each individual tensor, the tensor may not remain invariant. They can change by some gauge transformation under the symmetry operation, similar to the 1D case we discussed previously. In particular, the tensor

given in Eq. 10.68 change by unitary transformations V_R, V_R, V_R^{-1}, V_R^{-1} on the up, left, down, right inner indices respectively

$$V_R = e^{-i\frac{\theta}{2}(n_x X^* + n_y Y^* + n_z Z^*)} \tag{10.69}$$

V_R corresponds to the rotation of a spin $1/2$, which forms a projective representation of the $SO(3)$ symmetry group.

Of course, this tensor only represents a very special point in the SPT phase with zero correlation length. In general, wave functions in the same SPT phase can have a finite correlation length and the tensors representing them maybe more complicated and have larger bond dimension. However, for any tensor in the same SPT phase as the 2D AKLT model, we expect them to transform under symmetry in a similar way. In particular, if we apply symmetry operator U_R to the physical indices, the tensors would transform by a gauge transformation $\tilde{V}_R$ (or $\tilde{V}_R^{-1}$) on each inner index and $\tilde{V}_R$ (or $\tilde{V}_R^{-1}$) forms a projective representation of the $SO(3)$ symmetry group. That is, $\tilde{V}_R$ (or $\tilde{V}_R^{-1}$) represents spin rotation on half integer spins and satisfies

$$\tilde{V}_R(2\pi) = -1 \tag{10.70}$$

In general, if we take not just one tensor, but a piece of tensor network on a connected region and apply symmetry transformation, this would induce gauge transformation $\tilde{V}_R$ (or $\tilde{V}_R^{-1}$) on each of the inner index on the boundary of this region. Such a gauge transformation on the tensors corresponds to the symmetry transformation on the boundary degrees of freedom if we physically open a boundary to the system.

10.4.2 2D CZX model

On the other hand, SPT phases are known to exist in two and higher dimensions without the protection of translation symmetry, for example in topological insulators. The simple bond picture above therefore cannot account for their SPT order. In order to have nontrivial SPT order, we need to generalize the 2D AKLT state in two ways: (1) the local entanglement structure is not bonds between two spins, but rather plaquettes among four spins on sites around a square. This alone is not enough to construct new SPT order. We also need (2) symmetry transformation on each site does not factorize into separate operations on each of the four spins. That is, the total linear symmetry operation on each site is not a tensor product of four projective representations as otherwise the state can be reduced to a bond state.

Following this line of thought, we construct the CZX model in this section. The CZX model has an on-site $\mathbb{Z}_2$ symmetry that does not factorize into projective representations and the symmetry protected topological order of the state is robust against disorder. The boundary effective degrees of freedom in CZX model has an effective $\mathbb{Z}_2$ symmetry which cannot be written in an on-site form. Moreover, the boundary

cannot be in a gapped symmetric state under the effective symmetry. In other words, the boundary must either break the $\mathbb{Z}_2$ symmetry or have gapless excitations. This is different from the 2D AKLT state discussed above(Fig.10.6). In the 2D AKLT state, the boundary degrees of freedom are the boundary spins with projective representations. The effective symmetry is still on-site. Several boundary spins can form a singlet if their projective representations add up to a linear representation. Therefore, in the 2D AKLT state, the boundary can be in a gapped symmetric state under on-site symmetry simply by breaking translation symmetry. However, in the CZX model, this is not possible.

10.4.2.1 Bulk definition

In this section, we construct the CZX model explicitly which turns out to have non-trivial SPT order protected only by on-site $\mathbb{Z}_2$ symmetry.

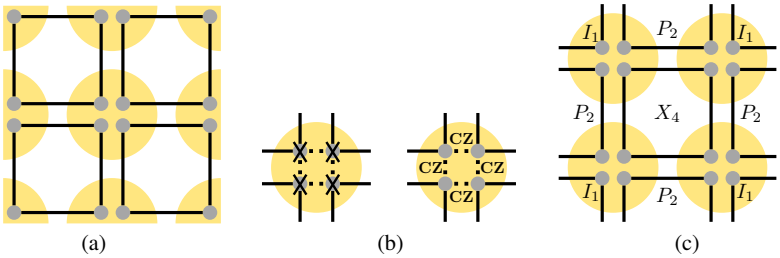

Fig. 10.8 CZX model (a) each site (circle) contains four spins (dots) and the spins in the same plaquette (square) are entangled. (b) on-site $\mathbb{Z}_2$ symmetry is generated by $U_{CZX} = X_1X_2X_3X_4CZ_{12}CZ_{23}CZ_{34}CZ_{41}$ (c) a local term in the Hamiltonian, which is a tensor product of one X_4 term and four P_2 terms as defined in the main text.

Consider a square lattice with four two-level spins per site, as shown in Fig. 10.8(a) where sites are represented by circles and spins are represented by dots. We denote the two levels as $|0\rangle$ and $|1\rangle$. The system has an on-site $\mathbb{Z}_2$ symmetry as given in Fig. 10.8(b). It is generated by

$$U_{CZX} = U_X U_{CZ} \tag{10.71}$$

where

$$U_X = X_1 \otimes X_2 \otimes X_3 \otimes X_4 \tag{10.72}$$

X_i is Pauli X operator on the ith spin and

$$U_{CZ} = CZ_{12}CZ_{23}CZ_{34}CZ_{41} \tag{10.73}$$

where CZ is the controlled-Z operator on two spins defined as

$$CZ = |00\rangle\langle 00| + |01\rangle\langle 01| + |10\rangle\langle 10| - |11\rangle\langle 11| \tag{10.74}$$

As defined, CZ does nothing if at least one of the spins is in state $|0\rangle$ and it adds a minus sign if both spins are in state $|1\rangle$. Different CZ operators overlap with each other. But because they commute, U_{CZ} is well defined. Note that U_{CZ} cannot be decomposed into separate operations on the four spins and the same is true for U_{CZX}. U_X and U_{CZ} both square to I and they commute with each other. Therefore, U_{CZX} generates a $\mathbb{Z}_2$ group.

The Hamiltonian of the system is defined as a sum of local terms around each plaquette. Plaquettes are represented by squares in Fig. 10.8. $H = \sum H_{p_i}$, where the term around the ith plaquette H_{p_i} acts not only on the four spins in the plaquette but also on the eight spins in the four neighboring half plaquettes as shown in Fig. 10.8(c)

$$H_{p_i} = -X_4 \otimes P_2^u \otimes P_2^d \otimes P_2^l \otimes P_2^r \tag{10.75}$$

where X_4 acts on the four spins in the middle plaquette as

$$X_4 = |0000\rangle\langle 1111| + |1111\rangle\langle 0000| \tag{10.76}$$

and P_2 acts on the two spins in every neighboring half plaquette as

$$P_2 = |00\rangle\langle 00| + |11\rangle\langle 11| \tag{10.77}$$

$P_2^u, P_2^d, P_2^l, P_2^r$ acts on the up, down, left and right neighboring half plaquettes respectively. For the remaining four spins at the corner, H_{p_i} acts as identity on them. The P_2 factors ensure that each term in the Hamiltonian satisfies the on-site $\mathbb{Z}_2$ symmetry defined before.

All the local terms in the Hamiltonian commute with each other, therefore it is easy to solve for the ground state. If the system is defined on a closed surface, it has a unique ground state which is gapped. In the ground state, every four spins around a plaquette are entangled in the state

$$|\psi_{p_i}\rangle = |0000\rangle + |1111\rangle \tag{10.78}$$

and the total wavefunction is a product of all plaquette wavefunction. If we allow any local unitary transformation, it is easy to see that the ground state can be disentangled into a product state, just by disentangling each plaquette separately into individual spin states. Therefore, the ground state is short range entangled. However, no matter what local unitary transformations we apply to disentangle the plaquettes, they necessarily violate the on-site symmetry and in fact, the plaquettes cannot be disentangled if the $\mathbb{Z}_2$ symmetry is preserved, due to the nontrivial SPT order of this model which we will show in the next sections.

It can be checked that this ground state is indeed invariant under the on-site $\mathbb{Z}_2$ symmetry. Obviously this state is invariant under U_X applied to every site. It is also invariant under U_{CZ} applied to every site. To see this note that between every two neighboring plaquettes, CZ is applied twice, at the two ends of the link along which they meet. Because the spins within each plaquette are perfectly correlated (they are

all $|0\rangle$ or all $|1\rangle$), the effect of the two CZ's cancel each other, leaving the total state invariant.

Therefore, we have introduced a 2D model with on-site $\mathbb{Z}_2$ symmetry whose ground state does not break the symmetry and is short-range entangled. In particular, this on-site symmetry is inseparable as discussed in the introduction and therefore cannot be characterized by projective representation as in the 2D AKLT state. We can add small perturbation to the system which satisfies the symmetry and the system is going to remain gapped and the ground state short range entangled and symmetric. It seems that the system is quite trivial and boring. However, we are going to show that surprising things happen if the system has a boundary and because of these special features the system cannot be smoothly connected to a trivial phase even if translation symmetry is not required.

10.4.2.2 Boundary description

The non-trivialness of this model shows up on the boundary. Suppose that we take a simply connected disk from the lattice, as shown in Fig.10.9(a).

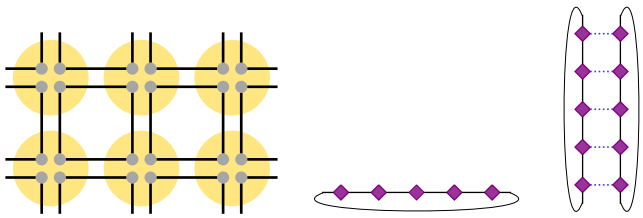

Fig. 10.9 (a)CZX model on a disk with boundary (b) boundary effective degrees of freedom form a 1D chain which cannot have a SRE symmetric state (c) two boundaries together can have a SRE symmetric state which is a product of entangled pairs between effective spins connected by a dashed line.

The reduced density matrix of spins in this region is invariant under on-site symmetry in this region. The reduced density matrix is a tensor product of individual terms on each full plaquette, half plaquette and corner of plaquette respectively. On a full plaquette

$$\rho_4 = (|0000\rangle + |1111\rangle)(\langle 0000| + \langle 1111|) \tag{10.79}$$

On a half plaquette

$$\rho_2 = |00\rangle\langle 00| + |11\rangle\langle 11| \tag{10.80}$$

On a corner of a plaquette

$$\rho_1 = |0\rangle\langle 0| + |1\rangle\langle 1| \tag{10.81}$$

The state of spins on the plaquettes totally inside this region is completely fixed. But on the boundary there are free degrees of freedom. However, unlike in the 2D AKLT state, only part of the total Hilbert space of the spins on the boundary is free. In particular, two spins in a half plaquette on the boundary are constrained to the two-dimensional subspace $|00\rangle\langle 00| + |11\rangle\langle 11|$ and form an effective spin degree of freedom if we map $|00\rangle$ to $|\tilde{0}\rangle$ and $|11\rangle$ to $|\tilde{1}\rangle$.

In Fig. 10.9(b), we show the effective degrees of freedom on the boundary as diamonds on a line. Projecting the total symmetry operation on the disk to the space supporting reduced density matrix, we find that the effective symmetry operation on the boundary effective spins is

$$\tilde{U}_{CZX} = \prod_{i=1}^{N} \tilde{X}_i \prod_{i=1}^{N} \tilde{CZ}_{i,i+1} \tag{10.82}$$

with Pauli $\tilde{X}$ on each effect spin and $\tilde{CZ}$ operation between neighboring effective spins. The boundary is periodic and $\tilde{CZ}_{N,N+1}$ acts on effective spin N and 1. This operator generates a $\mathbb{Z}_2$ symmetry group.

This is a very special symmetry on a 1D system. First it is not an on-site symmetry. In fact, no matter how we locally group sites and take projections, the symmetry operations are not going to break down into an on-site form. Moreover, no matter what interactions we add to the boundary, as long as it preserves the symmetry, the boundary cannot have a gapped symmetric ground state.

We can start by considering some simple cases. The simplest interaction term preserving this symmetry is Z_iZ_{i+1}. This is an Ising interaction term and we know that the ground state of

$$H = \sum_i Z_iZ_{i+1} \tag{10.83}$$

breaks the $\mathbb{Z}_2$ symmetry. In the transverse Ising model, the system goes to a symmetric phase if magnetic field in the x direction is increased. However, X_i breaks the $\mathbb{Z}_2$ symmetry $\tilde{U}_{CZX}$ on the boundary and therefore cannot be added to the Hamiltonian. Because X_i is mapped into $Z_{i-1}X_iZ_{i+1}$ under the $\mathbb{Z}_2$ transformation, a possible symmetric Hamiltonian reads

$$H = \sum_i X_i + Z_{i-1}X_iZ_{i+1} \tag{10.84}$$

Direct calculation shows that this Hamiltonian has a gapless spectrum. This is actually the transverse field cluster model discussed in Eq. 5.35 in section 5.4.4. $B = 1$ in order to satisfy the $\mathbb{Z}_2$ symmetry and the Hamiltonian is known to be gapless.

In fact, we are going to prove that, as long as the $\mathbb{Z}_2$ symmetry is preserved, the boundary cannot have SRE symmetric ground state (actually a more generalized version of it) in the next section. This is one special property that differs the CZX model from the 2D AKLT in Fig.10.6. In the 2D AKLT state, the symmetry operations on the boundary are just projective representations on each site. Without translational invariance, there can always be a SRE symmetric state with this symmetry.

The special property on the boundary only shows up when there is an isolated single boundary. If we put two such boundaries together and allow interactions between them, everything is back to normal. As shown in Fig.10.9(c), if we have two boundaries together, there is indeed a SRE symmetric state on the two boundaries. The state is a product of entangled pairs of effective spins connected by a dashed line. The entangled pair can be chosen as $|\tilde{0}\tilde{0}\rangle + |\tilde{1}\tilde{1}\rangle$. In contrast to the single boundary case, we can locally project the two effective spins connected by a dashed line to the subspace $|\tilde{0}\tilde{0}\rangle\langle\tilde{0}\tilde{0}| + |\tilde{1}\tilde{1}\rangle\langle\tilde{1}\tilde{1}|$ and on this subspace, the symmetry acts in an on-site fashion.

This result should be expected because if we have two pieces of sheet with boundary and glue them back into a surface without boundary, we should have the original SRE 2D state back. Indeed if we map the effective spins back to the original degrees of freedom $|\tilde{0}\rangle \to |00\rangle$ and $|\tilde{1}\rangle \to |11\rangle$, we see that the SRE state between two boundaries is just the a chain of plaquettes $|0000\rangle + |1111\rangle$ in the original state.

This model serves as an example of non-trivial SPT order in 2D SRE states that only needs to be protected by on-site symmetry. In order to prove the special property on the boundary of CZX model and have a more complete understanding of possible SPT orders in 2D SRE states with on-site symmetry, we are going to introduce a mathematical tool called Matrix Product Unitary Operator. We will show that 2D SPT phases are related to elements in $\mathscr{H}^3(G,U(1))$ which emerge in the transformation structure of the matrix product unitary operators. The discussion in the next section is general, but we will work out the CZX example explicitly for illustration.

10.4.2.3 Boundary property

10.4.2.4 Matrix product unitary operators and its relation to 3 cocycle

In this section, we discuss the matrix product unitary operator (MPUO) formalism and show how the effective symmetry operation on the boundary of CZX model can be expressed as MPUO. Moreover, we are going to relate MPUO of a symmetry group to the 3-cocycle of the group and in particular, we are going to show that the CZX model corresponds to a nontrivial 3-cocycle of the $\mathbb{Z}_2$ group.

A matrix product operator acting on a 1D system is given by,

$$O = \sum_{\{i_k\},\{i'_k\}} Tr(T^{i_1,i'_1} T^{i_2,i'_2} ... T^{i_N,i'_N}) |i'_1 i'_2 ... i'_N\rangle\langle i_1 i_2 ... i_N| \tag{10.85}$$

where for fixed i and i', $T^{i,i'}$ is a matrix with index α and β. Here we want to use this formalism to study symmetry transformations, therefore we restrict O to be a unitary operator U. Using matrix product representation, U does not have to be an on-site symmetry. U is represented by a rank-four tensor $T^{i,i'}_{\alpha,\beta}$ on each site, where i and i' are input and output physical indices and α, β are inner indices. The matrix

product unitary operators also have a canonical form, similar to matrix product states discussed in Chap. 8.

In particular, the symmetry operator U_{CZX} (we omit the $\sim$ label for effective spins in following discussions) on the boundary of the CZX model can be represented by tensors

$$\begin{aligned} &T^{0,1}(CZX) = |0\rangle\langle +|, \\ &T^{1,0}(CZX) = |1\rangle\langle -|, \\ &\text{other terms are zero} \end{aligned} \tag{10.86}$$

where $|+\rangle = |0\rangle + |1\rangle$ and $|-\rangle = |0\rangle - |1\rangle$. It is easy to check that this tensor indeed gives $U_{CZX} = CZ_{12}...CZ_{N1}X_1...X_N$.

The other element in the $\mathbb{Z}_2$ group–the identity operation–can also be represented as MPUO with tensors

$$\begin{aligned} &T^{0,0}(I) = |0\rangle\langle 0|, \\ &T^{1,1}(I) = |0\rangle\langle 0|, \\ &\text{other terms are zero} \end{aligned} \tag{10.87}$$

These two tensors are both in the canonical form, following a similar definition as in Chap.8.

If two MPUO $T(g_2)$ and $T(g_1)$ are applied subsequently, their combined action should be equivalent to $T(g_1g_2)$. However, the tensor $T(g_1,g_2)$ obtained by contracting the output physical index of $T(g_2)$ with the input physical index of $T(g_1)$, see Fig. 10.10, is usually more redundant than $T(g_1g_2)$ and might not be in the canonical form. It can only be reduced to $T(g_1g_2)$ if certain projection P_{g_1,g_2} is applied to the inner indices (see Fig. 10.10).

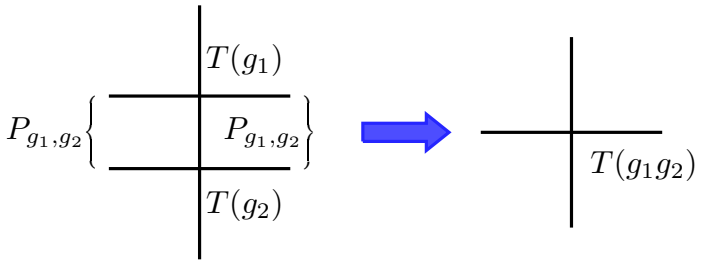

Fig. 10.10 Reduce combination of $T(g_2)$ and $T(g_1)$ into $T(g_1g_2)$.

P_{g_1,g_2} is only defined up to an arbitrary phase factor $e^{i\theta(g_1,g_2)}$. If the projection operator on the right side P_{g_1,g_2} is changed by the phase factor $e^{i\theta(g_1,g_2)}$, the projection operator $P^\dagger_{g_1,g_2}$ on the left side is changed by phase factor $e^{-i\theta(g_1,g_2)}$. Therefore the total action of P_{g_1,g_2} and $P^\dagger_{g_1,g_2}$ on $T(g_1,g_2)$ does not change and the reduction procedure illustrated in Fig.10.10 still works. In fact, P_{g_1,g_2} is unique up to a phase factor (on the unique block in the canonical form of $T(g_1,g_2)$).

Let us illustrate how the reduction is done for the symmetry group (I,U_{CZX}). For example, if we apply $U_{CZX}U_{CZX}$ the totally action should be equivalent to I.

However the tensor $T(CZX,CZX)$ is given by

$$\begin{array}{l} T^{0,0}(CZX,CZX) = |01\rangle\langle +-|, \\ T^{1,1}(CZX,CZX) = |10\rangle\langle -+|, \\ \text{other terms are zero} \end{array} \tag{10.88}$$

This tensor is reduced to $T(I)$ if projection

$$P_{CZX,CZX} = (|01\rangle - |10\rangle)\langle 0| \tag{10.89}$$

and its Hermitian conjugate are applied to the right and left of $T(CZX,CZX)$ respectively.[2] Adding an arbitrary phase factor $e^{i\theta(CZX,CZX)}$ to $P_{CZX,CZX}$ does not affect the reduction at all. By writing $P_{CZX,CZX}$ in the above form, we have made a particular choice of phase.

Below we list the (right) projection operators for all possible combinations of g_1 and g_2 of this $\mathbb{Z}_2$ group.

$$\begin{array}{ll} P_{I,I} & = |00\rangle\langle 0| \\ P_{CZX,I} & = |00\rangle\langle 0| + |10\rangle\langle 1| \\ P_{I,CZX} & = |00\rangle\langle 0| + |10\rangle\langle 1| \\ P_{CZX,CZX} & = (|01\rangle - |10\rangle)\langle 0| \end{array} \tag{10.90}$$

Note that in giving P_{g_1,g_2} we have picked a particular choice of phase factor $e^{i\theta(g_1,g_2)}$. In general, any phase factor is allowed.

Nontrivial phase factors appear when we consider the combination of three MPUO's. See Fig. 10.11.

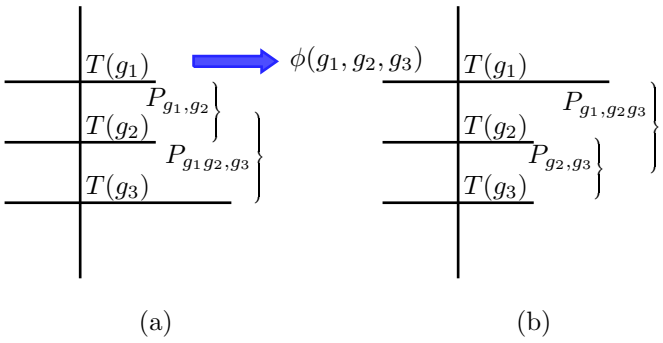

Fig. 10.11 Different ways to reduce combination of $T(g_3)$, $T(g_2)$ and $T(g_1)$ into $T(g_1g_2g_3)$. Only the right projection operators are shown. Their combined actions differ by a phase factor $\phi(g_1,g_2,g_3)$.

[2] The mapping actually reduces $T(CZX,CZX)$ to $-T(I)$. But this is not a problem as we can redefine $\tilde{T}(CZX) = iT(CZX)$ and the extra minus sign would disappear.

There are two different ways to reduce the tensors. We can either first reduce the combination of $T(g_1)$, $T(g_2)$ and then combine $T(g_3)$ or first reduce the combination of $T(g_2)$,$T(g_3)$ and then combine $T(g_1)$. The two different ways should be equivalent. More specifically, they should be the same up to phase on the unique block of Tg_1,g_2,g_3. Denote the projection onto the unique block of $T(g_1,g_2,g_3)$ as Q_{g_1,g_2,g_3}. We find that

$$\begin{aligned} &Q_{g_1,g_2,g_3}(I_3 \otimes P_{g_1,g_2})P_{g_1g_2,g_3} = \\ &\phi(g_1,g_2,g_3)Q_{g_1,g_2,g_3}(P_{g_2,g_3} \otimes I_1)P_{g_1,g_2g_3} \end{aligned} \tag{10.91}$$

From this we see that the reduction procedure is associative up to a phase factor $\phi(g_1,g_2,g_3)$ which satisfies

$$\frac{\phi(g_2,g_3,g_4)\phi(g_1,g_2g_3,g_4)\phi(g_1,g_2,g_3)}{\phi(g_1g_2,g_3,g_4)\phi(g_1,g_2,g_3g_4)} = 1 \tag{10.92}$$

From the definition of cocycles given in section 10.5.1, we see that $\phi(g_1,g_2,g_3)$ forms a 3-cocycle of group G.

Let's calculate $\phi(g_1,g_2,g_3)$ explicitly for the group generated by U_{CZX}.

$$\begin{aligned} &\phi(I,I,I) = 1 && \phi(I,I,CZX) = 1 \\ &\phi(I,CZX,I) = 1 && \phi(CZX,I,I) = 1 \\ &\phi(I,CZX,CZX) = 1 && \phi(CZX,CZX,I) = 1 \\ &\phi(CZX,I,CZX) = 1 && \phi(CZX,CZX,CZX) = -1 \end{aligned} \tag{10.93}$$

We can check that ϕ is indeed a 3-cocycle. The last term shows a nontrivial -1. This minus one cannot be removed by redefining the phase of P_{g_1,g_2} in any way. Therefore ϕ corresponds to a nontrivial 3-cocycle for the $\mathbb{Z}_2$ group.

What does this nontrivial mathematical structure imply about the physics of the CZX model? In the next section we are going to answer this question by proving that MPUO related to a nontrivial 3-cocycle cannot have a short range entangled symmetric state. That is, the boundary of the CZX model cannot have a gapped symmetric ground state. It either breaks the symmetry or is gapless.

10.4.2.5 Nontrivial 3-cocycle of MPUO and nonexistence of SRE symmetric state

In this section we will show that a symmetry defined by a MPUO on a 1D chain can have a SRE symmetric state only if the MPUO corresponds to a trivial 3-cocycle. Therefore, the boundary of the CZX model must be gapless or have symmetry breaking. For this proof, we will be using the matrix product state representation of SRE states.

Suppose that the symmetry on a 1D chain is represented by tensors $T^{i,i'}_{\alpha,\beta}(g)$. Assume that it has a SRE symmetric state represented by matrices $A^i_{\lambda,\eta}$ which is also single-blocked and in the canonical form.

Because the state represented by A^i is symmetric under $T^{i,i'}$, the set of matrices obtained by acting $T^{i,i'}$ on A_i can be related to A_i through a gauge transformation.

$$A^i = V^\dagger(\sum_{i'} T^{i,i'}(g)A^{i'})V \tag{10.94}$$

where $V^\dagger V = I$ and V is unique on the single block of $\sum_{i'} T^{i,i'}(g)A^{i'}$ up to phase. This is saying that we can reduce the MPS obtained from $\sum_{i'} T^{i,i'}(g)A^{i'}$ back to the original form A^i by applying $V^\dagger$ and V to the left and right of the matrices respectively. See Fig. 10.12.

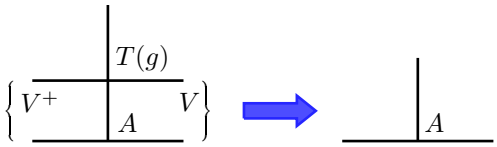

Fig. 10.12 Reduction of the combination of $T(g)$ and A into A. Here $T^{i,i'}(g)$ is a MPUO, A^i is a matrix product state symmetric under $T^{i,i'}(g)$.

For a fixed representation of the SRE state A^i and fixed representation of the MPUO symmetry $T(g)$, V is fixed up to phase. We can pick a particular choice of phase for V.

Now we consider the combined operation of $T(g_1)$ and $T(g_2)$ on A. See Fig.10.13.

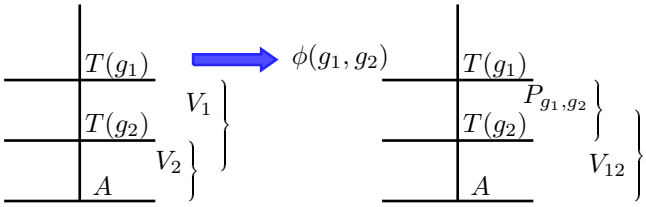

Fig. 10.13 Two ways of reducing the combination of $T(g_2)$, $T(g_1)$ and A into A. Only the right projection operators are shown. Their combined actions differ by a phase factor $\varphi(g_1,g_2)$.

We can either first combine $T(g_2)$ and A and then combine $T(g_1)$ and A or first combine $T(g_1)$ and $T(g_2)$ and then combine $T(g_1g_2)$ and A. The right projection operator for these two methods differ by a phase factor $\varphi(g_1,g_2)$. This phase factor can be arbitrarily changed by changing the phase of P_{g_1,g_2}. For following discussions, we fix the phase of P_{g_1,g_2} and hence $\varphi(g_1,g_2)$.

This is all the freedom we can have. If we are to combine three or more T's with A, different reduction methods differ by a phase factor but the phase factor are

all determined by $\varphi(g_1,g_2)$. Consider the situation in Fig. 10.14, where we are to combine $T(g_3)$, $T(g_2)$ and $T(g_1)$ with A.

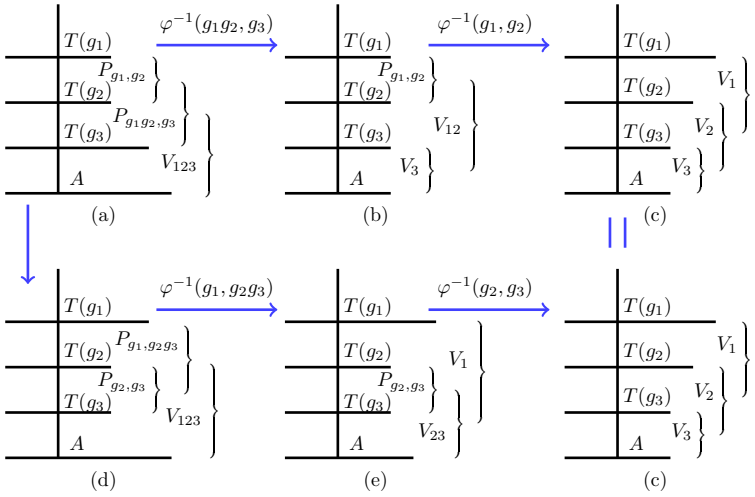

Fig. 10.14 Different ways of reducing the combination of $T(g_3)$, $T(g_2)$, $T(g_1)$ and A into A. Only the right projection operators are shown. Their combined actions differ by a phase factor written on the arrow.

To change the reduction procedure in Fig.10.14(a) to that in Fig.10.14(c), we can either go through step (b) or steps (d) and (e). If we go through step (b), the phase difference in the right projection operators is

$$\varphi^{-1}(g_1g_2,g_3)\varphi^{-1}(g_1,g_2) \tag{10.95}$$

On the other hand, if we go through steps (d) and (e), the phase difference in the right projection operators is

$$\phi(g_1,g_2,g_3)\varphi^{-1}(g_1,g_2g_3)\varphi^{-1}(g_2,g_3) \tag{10.96}$$

But these two procedures should be equivalent as the initial and final configurations are the same whose phases have been fixed previously. Therefore, we find that

$$\phi(g_1,g_2,g_3)=\frac{\varphi(g_1,g_2g_3)\varphi(g_2,g_3)}{\varphi(g_1g_2,g_3)\varphi(g_1,g_2)} \tag{10.97}$$

For the $\phi(g_1,g_2,g_3)$ given in Eq.10.93, we can check explicitly that such a equation cannot be satisfied for any φ. Therefore we found a contradiction. This shows that the boundary of the CZX model must be either gapless or breaks symmetry. Therefore,

Box 10.17 SPT order of 2D CZX model
2D CZX model has nontrivial symmetry protected topological order protected by a on-site unitary $\mathbb{Z}_2$ symmetry.

as we promised in section 10.4.2.

10.4.2.6 Tensor network representation

Finally we want to discuss the tensor network representation of the CZX wave function. As we will see, the tensors representing the state have a very simple form and its transformation under the $\mathbb{Z}_2$ symmetry encodes important information about the nontrivial SPT order.

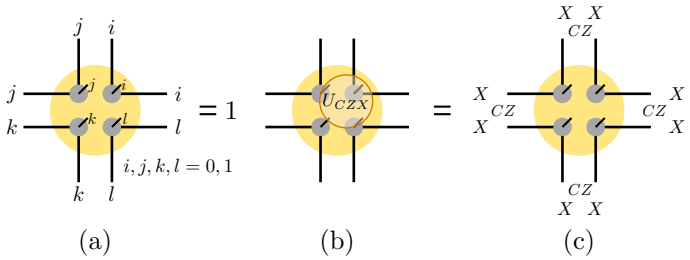

Fig. 10.15 The tensor network representation of the 2D CZX state.

The tensor shown in Fig. 10.15 represents the ground state of the CZX model, which is the tensor product of entangled plaquettes in the state $|0000\rangle + |1111\rangle$. The tensor is composed of four parts, as shown in Fig. 10.15 (a), each containing one two-dimensional physical index (slanted) and two two-dimensional inner indices (horizontal and vertical). Each part of the tensor is nonzero and equal to 1 if and only if the physical index and two inner indices take on the same value (0 or 1). Otherwise, the tensor is zero.

It is interesting to see how the tensor transform under the $\mathbb{Z}_2$ symmetry. As shown in Fig. 10.15 (b) and (c), applying the $\mathbb{Z}_2$ symmetry to the physical index on each site induces gauge transformation on the inner indices. The gauge transformation is

$$V = (X \otimes X)CZ \tag{10.98}$$

It looks similar to the transformation of the AKLT tensor. However, one important difference for the gauge transformation in the CZX tensor is that V does not form a representation of the $\mathbb{Z}_2$ symmetry group, not even projectively. In fact,

$$V^2 = -Z \otimes Z \tag{10.99}$$

On the whole tensor, the action of V^2 is trivial, due to the identification of pairs of inner indices connected to the same physical index. Therefore the tensor remains invariant if we apply the $\mathbb{Z}_2$ symmetry twice, as expected. However, the action of V^2 is not identify on inner indices in each direction alone.

More interestingly, we notice a close relation between V and the boundary symmetry action $\tilde{U}_{CZX}$ given in Eq. 10.82. In general, for any state in the same SPT phase, we expect the same relation to apply. That is, the gauge transformation of the tensor network in a region under the $\mathbb{Z}_2$ symmetry operation corresponds to the effective symmetry action on the boundary degrees of freedom when the system has an edge.

10.5 General construction of SPT phases

The above discussion regarding CZX model can be generalized to arbitrary symmetry groups and to arbitrary dimensions. In order to do this, let us define group cohomology in more generality.

10.5.1 Group cohomology

For a group G, Let $\omega_n(g_1,...,g_n)$ be a function from n group elements to a $U(1)$ phase factor. Group elements $g \in G$ can act on ω. In particular, if g is a unitary operation, the action is trivial

$$g \cdot \omega = \omega \tag{10.100}$$

If g is an anti-unitary operation, like time reversal, the action is nontrivial

$$g \cdot \omega = \omega^* \tag{10.101}$$

Let $\mathscr{C}^n(G,M) = \{\omega_n\}$ be the space of all such functions. Note that $\mathscr{C}^n(G,M)$ is an Abelian group under the function multiplication

$$\omega_n''(g_1,...,g_n) = \omega_n(g_1,...,g_n)\omega_n'(g_1,...,g_n) \tag{10.102}$$

We define a map d_n from $\mathscr{C}^n[G,U(1)]$ to $\mathscr{C}^{n+1}[G,U(1)]$:

$$\begin{aligned}(d_n\omega_n)(g_1,...,g_{n+1}) = {} & g_1 \cdot \omega_n(g_2,...,g_{n+1})\omega_n^{(-1)^{n+1}}(g_1,...,g_n) \\ & \times \prod_{i=1}^{n} \omega_n^{(-1)^i}(g_1,...,g_{i-1},g_ig_{i+1},g_{i+2},...g_{n+1})\end{aligned} \tag{10.103}$$

Let

$$\mathscr{B}^n(G,M) = \{\omega_n | \omega_n = d_{n-1}\omega_{n-1} | \omega_{n-1} \in \mathscr{C}^{n-1}(G,M)\} \tag{10.104}$$

and

$$\mathscr{Z}^n(G,M) = \{\omega_n | d_n\omega_n = 1, \omega_n \in \mathscr{C}^n(G,M)\} \tag{10.105}$$

$\mathscr{B}^n(G,M)$ and $\mathscr{Z}^n(G,M)$ are also Abelian groups which satisfy $\mathscr{B}^n(G,M) \subset \mathscr{Z}^n(G,M)$ where $\mathscr{B}^1(G,M) \equiv \{1\}$. The n-cocycle of G is defined as

$$\mathscr{H}^n(G,M) = \mathscr{Z}^n(G,M)/\mathscr{B}^n(G,M) \tag{10.106}$$

Let us discuss some examples. When $n = 1$, Eq.10.103 reads

$$(d_1\omega_1)(g_1,g_2) = \omega_1^{s_1}(g_2)\omega_1(g_1)/\omega_1(g_1g_2) \tag{10.107}$$

where $s_1 = 1$ if g_1 is unitary and $s_1 = -1$ if g_1 is anti-unitary. We see that

$$\mathscr{Z}^1(G,U(1)) = \{\omega_1 | \omega_1^{s_1}(g_2)\omega_1(g_1) = \omega_1(g_1g_2)\}. \tag{10.108}$$

In other words, $\mathscr{Z}^1(G,U(1))$ is the set formed by all the 1D representations of G. Since $\mathscr{B}^1(G,U(1)) \equiv \{1\}$ is trival. $\mathscr{H}^1(G,U(1)) = \mathscr{Z}^1(G,U(1))$ is also the set of all the 1D representations of G.

When $n = 2$, Eq.10.103 reads

$$(d_2\omega_2)(g_1,g_2,g_3) = \omega_2^{s_1}(g_2,g_3)\omega_2(g_1,g_2g_3)/\omega_2(g_1g_2,g_3)\omega_2(g_1,g_2) \tag{10.109}$$

we see that

$$\mathscr{Z}^2(G,U(1)) = \{\omega_2 | \omega_2^{s_1}(g_2,g_3)\omega_2(g_1,g_2g_3) = \omega_2(g_1g_2,g_3)\omega_2(g_1,g_2)\} \tag{10.110}$$

and

$$\mathscr{B}^2(G,U(1)) = \{\omega_2 | \omega_2(g_1,g_2) = \omega_1^{s_1}(g_2)\omega_1(g_1)/\omega_1(g_1g_2)\} \tag{10.111}$$

The 2-cocycle $\mathscr{H}^2(G,U(1)) = \mathscr{Z}^2(G,U(1))/\mathscr{B}^2(G,U(1))$ classify the projective representations discussed in section 10.2.2.3.

When $n = 2$, Eq.10.103 reads

$$(d_3\omega_3)(g_1,g_2,g_3,g_4) = \frac{\omega_3 s_1(g_2,g_3,g_4)\omega_3(g_1,g_2g_3,g_4)\omega_3(g_1,g_2,g_3)}{\omega_3(g_1g_2,g_3,g_4)\omega_3(g_1,g_2,g_3g_4)} \tag{10.112}$$

we see that

$$\mathscr{Z}^3(G,U(1)) = \{\omega_3 | \frac{\omega_3^{s_1}(g_2,g_3,g_4)\omega_3(g_1,g_2g_3,g_4)\omega_3(g_1,g_2,g_3)}{\omega_3(g_1g_2,g_3,g_4)\omega_3(g_1,g_2,g_3g_4)} = 1\} \tag{10.113}$$

and

$$\mathscr{B}^3(G,U(1)) = \{\omega_3 | \omega_3(g_1,g_2,g_3) = \frac{\omega_2^{s_1}(g_2,g_3)\omega_2(g_1,g_2g_3)}{\omega_2(g_1g_2,g_3)\omega_2(g_1,g_2)}\} \tag{10.114}$$

which give us the 3-cocycle $\mathscr{H}^3(G,U(1)) = \mathscr{Z}^3(G,U(1))/\mathscr{B}^3(G,U(1))$.

10.5.2 SPT model from group cohomology

Now we can discuss the general construction of SPT phases in n dimension with $\mathscr{H}^{n+1}$ group cocycle.

When $n = 0$, we have a quantum mechanical system with symmetry G. We cannot talk about quantum phases in 0 dimension, but the system can have a unique symmetric ground state $|\psi\rangle$. It transforms under symmetry operator U_g as

$$U_g|\psi\rangle = \omega_1(g)|\psi\rangle \tag{10.115}$$

where $\omega_1(g)$ is a 1D representation of G. Therefore, a symmetric 0 dimensional quantum state is labeled by $\omega_1(g) \in \mathscr{H}^1(G,U(1))$. When moving between states labeled by different ω_1, there must a level crossing – the 0 dimensional analogue of phase transition.

When $n = 1$, as we discussed in section 10.2, different SPT phases are labeled by projective representations with inequivalent factor system $\omega_2(g_1,g_2) \in \mathscr{H}^2(G,U(1))$. Given a ω_2, we can construct a state in the corresponding SPT phase as follows.

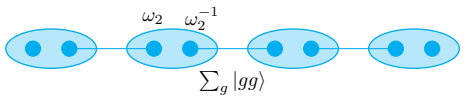

Fig. 10.16 Model 1D state with SPT order corresponding to 2-cocycle $\omega_2 \in \mathscr{H}^2(G,U(1))$.

Every lattice site (big oval) contains two spins (small circle), each with basis state $|g\rangle$, $g \in G$. Symmetry operation on the left and right spin is given by

$$U_h^l|g\rangle = \omega_2(g^{-1}h^{-1},h)|hg\rangle,\ U_h^r|g\rangle = \omega_2^{-1}(g^{-1}h^{-1},h)|hg\rangle \tag{10.116}$$

Each pair of connected spins are in the maximally entangled state

$$|\psi\rangle = \sum_g |gg\rangle \tag{10.117}$$

It is straight-forward to check that U_g^l and U_g^r form projective representations with factor systems ω and ω^{-1} respectively. Therefore, each lattice site contains a linear representation of the symmetry and the total wave function as a product of $|\psi\rangle =$

$\sum_g |gg\rangle$ is invariant under the global symmetry. When the system has a boundary, the edge state carries projective representations of the symmetry with factor systems ω and ω^{-1}, as expected for an SPT phase.

Similarly, when $n = 2$, the construction of the CZX model can be generalized to arbitrary symmetry groups. Given a 3-cocycle $\omega_3 in \mathscr{H}^3(G,U(1))$, we can construct a state in the corresponding SPT phase as follows.

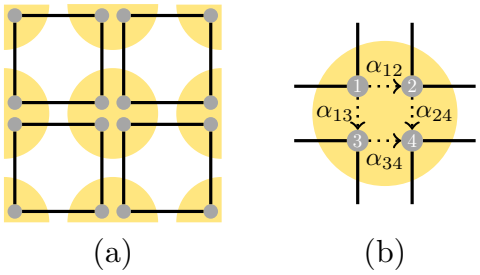

Fig. 10.17 Model 2D state with SPT order corresponding to 3-cocycle $\omega_3 \in \mathscr{H}^3(G,U(1))$.

Every lattice site (big oval) contains four spins (small circle), each with basis state $|g\rangle$, $g \in G$. Symmetry operation on the four spins of each site is given by

$$U_h|g_1,g_2,g_3,g_4\rangle = \frac{\omega_3(g_1^{-1}g_2,g_2^{-1}h^{-1},h)\omega_3(g_2^{-1}g_4,g_4^{-1}h^{-1},h)}{\omega_3(g_1^{-1}g_3,g_3^{-1}h^{-1},h)\omega_3(g_3^{-1}g_4,g_4^{-1}h^{-1},h)}|hg_1,hg_2,hg_3,hg_4\rangle \tag{10.118}$$

Note that this symmetry operation on four spins does not decompose into a tensor product of operators on the four spins individually.

Each four spins connected in a square are in the maximally entangled state

$$|\psi\rangle = \sum_g |gggg\rangle \tag{10.119}$$

It is straight-forward to check using the property of ω_3 that 1. each lattice site contains a linear representation of the symmetry; 2. the total wave function as a product of $|\psi\rangle = \sum_g |gggg\rangle$ is invariant under the global symmetry; 3. when the system has a boundary, the symmetry transformation on the boundary is described by a MPUO whose local transformation as given in Fig.10.11 is related to $\omega_3 g_1,g_2,g_3$. Reference for the proof of these facts can be found in summary and further reading.

The proof outline in section10.4.2.5 regarding the nonexistence of SRE edge states with nontrivial 3-cocycle applies to the general case. Therefore, the above construction gives a trivial / nontrivial SPT phase if we started from a trivial / nontrivial 3-cocycle.

Note that the CZX model is not written in this 'canonical' form, but gives rise to the same SPT phase and the same edge physics as the MPUO on the boundary transform with the same $\omega_3 \in \mathscr{H}^3(\mathbb{Z}_2,U(1))$.

Box 10.18 General construction of SPT models from group cocycle
Using different group cocycles from $\mathscr{H}^{n+1}$, n-dimensional boson / spin models with symmetry protected topological orders of internal (on-site unitary or time reversal) symmetry can be constructed.

10.6 Summary and further reading

In this chapter, we study symmetry protected topological phases in strongly interacting boson / spin systems. In one dimension, a complete classification can be obtained. In particular, for SPT order with internal symmetry, it was found that the edge of a nontrivial SPT phase is always degenerate, carrying a nontrivial projective representation of the symmetry. As 1D fermion system can be mapped to 1D boson system through Jordan Wigner transformation, we get the classification for 1D fermion system as a bonus. Generalizing our understanding of 1D SPT to higher dimension, a systematic construction of SPT phases is presented where symmetry action is related to group cocycles. In particular, we prove that, in the 2D SPT phases we constructed, their edge state is always gapless unless the symmetry is broken, establishing the nontrivial SPT order in the model.

The first and most well understood 1D SPT phase is the spin 1 chain with antiferromagnetic Heisenberg interaction. It was first proposed by Haldane that, unlike spin $1/2$ Heisenberg chains, the spin 1 chain is gapped[19]. Moreover, it was found to have degenerate edge spin-1/2 states[18, 14, 31] and non-trivial string order parameter[10, 25], indicating its nontrivial order. These properties of the 'Haldane phase' were established rigorously by the exactly solvable AKLT point in the phase[2], whose ground state has a simple projected entangled pair structure.

Following the example of the AKLT state, the idea of symmetry protected topological order was generalized to other symmetries[15, 33]. It was realized that the SPT order is closely related to the entanglement structure of the system and projective representations of the edge state[35, 15], based on which order parameters for detecting SPT order were found in [34, 17]. The classification discussed in this chapter follows the work in [6] and was also derived in [38].

A full classification of 1D bosonic phases with symmetry, including both the symmetry breaking and the symmetric phases, can be found in [7, 38]. It was observed that 1D gapped spin phases with on-site symmetry of group G are basically labeled by (1) the unbroken symmetry subgroup G', (2) the projective representations of G'. Also the gaplessness of 1D translational invariant spin $1/2$ chains was proved in [29] and was generalized to higher dimensions in [20].

For 1D fermion systems, the existence of the so-called 'Majorana chain' with Majorana edge modes at the end of the chain was proposed by Kitaev [27]. The classification of 1D fermionic topological phases (with various symmetries) was

obtained in [11, 12, 39] and is consistent with the result obtained in this chapter using Jordan Wigner transformation.

The matrix product operator, used in section 10.4, was introduced in [32].

The 2D AKLT model was first introduced in [1]. In section 10.4.1 we used a slightly different version of this model. In [1], all the spins on a single lattice site are projected onto their symmetric subspace. For example, on a square lattice model, the four spin $1/2$'s are projected onto the total spin 2 subspace. In the version in section 10.4.1, no projection is done.The model with and without this projection are supposed to be in the same phase and have the same SPT order.

The CZX model was introduced in [8] and the general construction of SPT phases using group cocycle was discussed in [4, 5].

We focused mostly on interacting boson / spin systems in our discuss. On the other hand, SPT phases have been extensively studied in fermion systems. In particular, topological insulators in 2D and 3D free fermion systems have not only been theoretically predicted[23, 3, 13, 30, 36], but also experimentally realized[28, 21, 22, 9]. Moreover, SPT phases in free fermion systems have been completely classified[37, 26]. However, a complete understanding of SPT phases in interacting fermion systems is much harder. For recent progress see for example [16, 24].

References

1. I. Affleck, T. Kennedy, E.H. Lieb, and H. Tasaki. Valence bond ground states in isotropic quantum antiferromagnets. *Communications in Mathematical Physics*, 115:477–528, September 1988.
2. Ian Affleck, Tom Kennedy, Elliott H. Lieb, and Hal Tasaki. Rigorous results on valence-bond ground states in antiferromagnets. *Phys. Rev. Lett.*, 59:799–802, Aug 1987.
3. B. Andrei Bernevig, Taylor L. Hughes, and Shou-Cheng Zhang. Quantum Spin Hall Effect and Topological Phase Transition in HgTe Quantum Wells. *Science*, 314(5806):1757–1761, 2006.
4. Xie Chen, Zheng-Cheng Gu, Zheng-Xin Liu, and Xiao-Gang Wen. Symmetry-protected topological orders in interacting bosonic systems. *Science*, 338(6114):1604–1606, 2012.
5. Xie Chen, Zheng-Cheng Gu, Zheng-Xin Liu, and Xiao-Gang Wen. Symmetry protected topological orders and the group cohomology of their symmetry group. *Phys. Rev. B*, 87:155114, Apr 2013.
6. Xie Chen, Zheng-Cheng Gu, and Xiao-Gang Wen. Classification of gapped symmetric phases in one-dimensional spin systems. *Phys. Rev. B*, 83(3):035107, Jan 2011.
7. Xie Chen, Zheng-Cheng Gu, and Xiao-Gang Wen. Complete classification of one-dimensional gapped quantum phases in interacting spin systems. *Phys. Rev. B*, 84:235128, Dec 2011.
8. Xie Chen, Zheng-Xin Liu, and Xiao-Gang Wen. Two-dimensional symmetry-protected topological orders and their protected gapless edge excitations. *Phys. Rev. B*, 84(23):235141–, December 2011.
9. Y. L. Chen, J. G. Analytis, J.-H. Chu, Z. K. Liu, S.-K. Mo, X. L. Qi, H. J. Zhang, D. H. Lu, X. Dai, Z. Fang, S. C. Zhang, I. R. Fisher, Z. Hussain, and Z.-X. Shen. Experimental realization of a three-dimensional topological insulator, bi2te3. *Science*, 325(5937):178–181, 2009.
10. Marcel den Nijs and Koos Rommelse. Preroughening transitions in crystal surfaces and valence-bond phases in quantum spin chains. *Phys. Rev. B*, 40:4709–4734, Sep 1989.

11. Lukasz Fidkowski and Alexei Kitaev. Effects of interactions on the topological classification of free fermion systems. *Phys. Rev. B*, 81(13):134509, Apr 2010.
12. Lukasz Fidkowski and Alexei Kitaev. Topological phases of fermions in one dimension. *Phys. Rev. B*, 83(7):075103, Feb 2011.
13. Liang Fu, C. L. Kane, and E. J. Mele. Topological insulators in three dimensions. *Phys. Rev. Lett.*, 98:106803, 2007.
14. Sivert H. Glarum, Stanley Geschwind, K. M. Lee, M. L. Kaplan, and J. Michel. Observation of fractional spin S =1/2 on open ends of S =1 linear antiferromagnetic chains: Nonmagnetic doping. *Phys. Rev. Lett.*, 67:1614–1617, Sep 1991.
15. Zheng-Cheng Gu and Xiao-Gang Wen. Tensor-entanglement-filtering renormalization approach and symmetry-protected topological order. *Phys. Rev. B*, 80(15):155131, Oct 2009.
16. Zheng-Cheng Gu and Xiao-Gang Wen. Symmetry-protected topological orders for interacting fermions: Fermionic topological nonlinear σ models and a special group supercohomology theory. *Phys. Rev. B*, 90:115141, Sep 2014.
17. Jutho Haegeman, David Pérez-García, Ignacio Cirac, and Norbert Schuch. Order parameter for symmetry-protected phases in one dimension. *Phys. Rev. Lett.*, 109:050402, Jul 2012.
18. Masayuki Hagiwara, Koichi Katsumata, Ian Affleck, Bertrand I. Halperin, and J. P. Renard. Observation of S =1/2 degrees of freedom in an S =1 linear-chain heisenberg antiferromagnet. *Phys. Rev. Lett.*, 65:3181–3184, Dec 1990.
19. F. Duncan M. Haldane. Continuum dynamics of the 1-D heisenberg antiferromagnet: Identification with the O(3) nonlinear sigma model. *Physics Letters A*, 93:464, 1983.
20. M. B. Hastings. Lieb-schultz-mattis in higher dimensions. *Phys. Rev. B*, 69:104431, Mar 2004.
21. D. Hsieh, D. Qian, L. Wray, Y. Xia, Y. S. Hor, R. J. Cava, and M. Z. Hasan. A topological dirac insulator in a quantum spin hall phase. *Nature*, 452(7190):970–974, April 2008.
22. D. Hsieh, Y. Xia, D. Qian, L. Wray, J. H. Dil, F. Meier, J. Osterwalder, L. Patthey, J. G. Checkelsky, N. P. Ong, A. V. Fedorov, H. Lin, A. Bansil, D. Grauer, Y. S. Hor, R. J. Cava, and M. Z. Hasan. A tunable topological insulator in the spin helical dirac transport regime. *Nature*, 460(7259):1101–1105, July 2009.
23. C. L. Kane and E. J. Mele. Z_2 topological order and the quantum spin hall effect. *Phys. Rev. Lett.*, 95:146802, 2005.
24. Anton Kapustin, Ryan Thorngren, Alex Turzillo, and Zitao Wang. Fermionic symmetry protected topological phases and cobordisms. *ArXiv e-prints 1406.7329*, June 2014.
25. Tom Kennedy and Hal Tasaki. Hidden z2*z2 symmetry breaking in haldane-gap antiferromagnets. *Phys. Rev. B*, 45:304–307, Jan 1992.
26. Alexei Kitaev. Periodic table for topological insulators and superconductors. *AIP Conference Proceedings*, 1134(1):22–30, 2009.
27. Alexei Yu Kitaev. Unpaired majorana fermions in quantum wires. *PhysicsUspekhi*, 44(10S):131–136, 2001.
28. Markus König, Steffen Wiedmann, Christoph Brüne, Andreas Roth, Hartmut Buhmann, Laurens W. Molenkamp, Xiao-Liang Qi, and Shou-Cheng Zhang. Quantum spin hall insulator state in HgTe quantum wells. *Science*, 318(5851):766–770, November 2007.
29. Elliott Lieb, Theodore Schultz, and Daniel Mattis. Two soluble models of an antiferromagnetic chain. *Annals of Physics*, 16:407–466, December 1961.
30. J. E. Moore and L. Balents. Topological invariants of time-reversal-invariant band structures. *Phys. Rev. B*, 75:121306, 2007.
31. Tai-Kai Ng. Edge states in antiferromagnetic quantum spin chains. *Phys. Rev. B*, 50:555–558, Jul 1994.
32. B Pirvu, V Murg, J I Cirac, and F Verstraete. Matrix product operator representations. *New Journal of Physics*, 12(2):025012, 2010.
33. Frank Pollmann, Erez Berg, Ari M. Turner, and Masaki Oshikawa. Symmetry protection of topological phases in one-dimensional quantum spin systems. *Phys. Rev. B*, 85:075125, Feb 2012.
34. Frank Pollmann and Ari M. Turner. Detection of symmetry-protected topological phases in one dimension. *Phys. Rev. B*, 86:125441, Sep 2012.

35. Frank Pollmann, Ari M. Turner, Erez Berg, and Masaki Oshikawa. Entanglement spectrum of a topological phase in one dimension. *Phys. Rev. B*, 81:064439, Feb 2010.
36. Rahul Roy. Topological phases and the quantum spin hall effect in three dimensions. *Phys. Rev. B*, 79:195322, May 2009.
37. Andreas P. Schnyder, Shinsei Ryu, Akira Furusaki, and Andreas W. W. Ludwig. Classification of topological insulators and superconductors in three spatial dimensions. *Phys. Rev. B*, 78(19):195125–, November 2008.
38. Norbert Schuch, David Pérez-García, and Ignacio Cirac. Classifying quantum phases using matrix product states and projected entangled pair states. *Phys. Rev. B*, 84:165139, Oct 2011.
39. Ari M. Turner, Frank Pollmann, and Erez Berg. Topological phases of one-dimensional fermions: An entanglement point of view. *Phys. Rev. B*, 83(7):075102, Feb 2011.

Part V
Outlook

Chapter 11
A Unification of Information and Matter

Abstract In this book, our discussions on many-body quantum systems have been concentrated on gapped topological states. After the introduction of the concept of long-range quantum entanglement and the discovery of related mathematical theories (such as tensor category theory), a systematic understanding of all gapped states in any dimensions is emerging, which include topological orders, and SPT orders. However, our understanding of highly entangled gapless states is very limited. We do not even know where to start, to gain a systematic understanding of highly entangled gapless states. This will be the next big challenge in condensed matter physics. In this chapter, we will study some examples of highly entangled gapless states. We will show that long-range entangled qubits can provide a unified origin of light and electrons (or more generally, gauge interactions and Fermi statistics): light waves (gauge fields) are fluctuations of long-range entanglement, and electrons (fermions) are defects of long-range entanglement. Since gauge bosons and fermions represent almost all the elementary particles, the above results suggest that the space formed by long-range entangled qubits may be an origin of all matter. In other word, (quantum) information unifies matter. This happen to be the central theme of this book: a theory of quantum information and quantum matter.

11.1 Four revolutions in physics

We have a strong desire to understand everything from a single or very few origins. Driven by such a desire, physics theories were developed through the cycle of discoveries, unification, more discoveries, bigger unification. Here, we would like review the development of physics and its four revolutions[1]. We will see that the history of physics can be summarized into three stages: 1) all matter is formed by particles; 2) the discovery of wave-like matter; 3) particle-like matter = wave-like

[1] Here we do not discuss the revolution for thermodynamical and statistical physics.

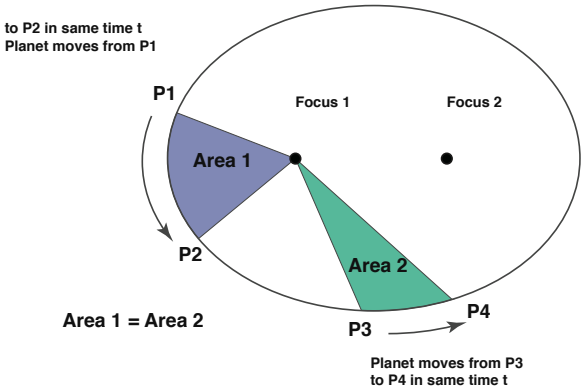

Fig. 11.1 Kepler's Laws of Planetary Motion: 1) The orbit of a planet is an ellipse with the Sun at one of the two foci. 2) A line segment joining a planet and the Sun sweeps out equal areas during equal intervals of time. 3) The square of the orbital period of a planet is proportional to the cube of the semi-major axis of its orbit.

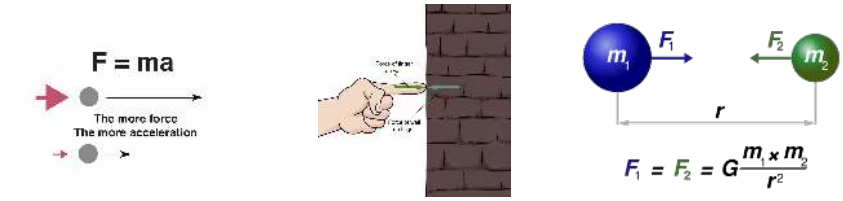

(a) (b) (c)

Fig. 11.2 Newton laws: (a) the more force the more acceleration, no force no acceleration. (b) action force = reaction force. (c) Newton's universal gravitation: $F = G\frac{m_1 m_2}{r^2}$, where $G = 6.674 \times 10^{-11}\,\frac{\mathrm{m}^3}{\mathrm{kg\,s}^2}$.

matter. It appears that we are now entering into the fourth stage: matter and space = information (qubits), where qubits emerge as the origin of everything.

11.1.1 Mechanical revolution

Although the down pull by the earth was realized even before human civilization, such a phenomena did not arose any curiosity. On the other hand the planet motion in the sky has arose a lot of curiosity and led to many imaginary fantasies. However, only after Kepler found that planets move in a certain particular way described by a mathematical formula (see Fig. 11.1), people started to wonder: Why are planets so rational? Why do they move in such a peculiar and precise way. This motivated Newton to develop his theory of gravity and his laws of mechanical motion (see Fig. 11.2). Newton's theory not only explains the planets motion, it also explains

Fig. 11.3 The perceived trajectories of planets (Mar and Saturn) in the sky. The falling of apple on earth and the motion of planet in the sky are unified by Newton theory.

the down-pull that we feel on earth. The planets motion in the sky and the apple falling on earth look very different (see Fig. 11.3), however, Newton's theory unifies the two seemingly unrelated phenomena. This is the first revolution in physics – the mechanical revolution.

Box 11.1 Mechanical revolution

All matter are formed by particles, which obey Newton's laws. Interactions are instantaneous over distance.

After Newton we view all matter as formed by particles, and use Newton's laws for particles to understand the motion of all matter. The success and the completeness of Newton's theory gave us a sense that we understood everything.

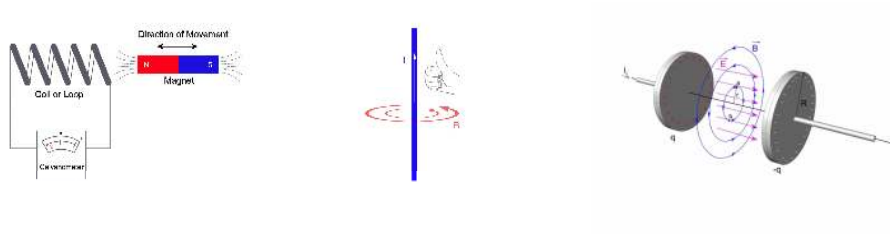

(a) (b) (c)

Fig. 11.4 (a) Changing magnetic field can generate an electric field around it, that drives an electric current in a coil. (b) Electric current I in a wire can generate a magnetic field B around it. (c) A changing electric field E (just like electric current) can generate a magnetic field B around it.

Fig. 11.5 Three very different phenomena, electricity, magnetism, and light, are unified by Maxwell theory.

11.1.2 Electromagnetic revolution

But, later we discovered that two other seemingly unrelated phenomena, electricity and magnetism, can generate each other (see Fig. 11.4). Our curiosity about the electricity and magnetism leads to another giant leap in science, which is summarized by Maxwell equations. Maxwell theory unifies electricity and magnetism and reveals that light is merely an electromagnetic wave (see Fig. 11.5). We gain a much deeper understanding of light, which is so familiar and yet so unexpectedly rich and complex in its internal structure. This can be viewed as the second revolution – electromagnetic revolution.

(a) (b) (c)

Fig. 11.6 (a) Magnetic field revealed by iron powder. (b) Electric field revealed by glowing plasma. (c) They form a new kind of matter: light – a wave-like matter

Box 11.2 Electromagnetic revolution

The discovery of a new form of matter – wave-like matter: electromagnetic waves, which obey Maxwell equation. Wave-like matter causes interaction.

However, the true essence of Maxwell theory is the discovery of a new form of matter – wave-like (or field-like) matter (see Fig. 11.6), the electromagnetic wave. The motion of this wave-like matter is governed by Maxwell equation, which is very different from the particle-like matter governed by Newton equation $F = ma$. Thus, the sense that Newton theory describes everything is incorrect. Newton theory does not apply to wave-like matter, which requires a new theory – Maxwell theory.

Unlike the particle-like matter, the new wave-like matter is closely related to a kind of interaction – electromagnetic interaction. In fact, the electromagnetic interaction can be viewed as an effect of the newly discovered wave-like matter.

11.1.3 Relativity revolution

After realizing the connection between the interaction and wave-like matter, one naturally ask: does gravitational interaction also corresponds to a wave-like matter? The answer is yes.

First, people realized that Newton equation and Maxwell equation have different symmetries under the transformations between two frames moving against each other. In other words, Newton equation $F = ma$ is invariant under Galileo transformation, while Maxwell equation is invariant under Lorentz transformation (see Fig. 11.7). Certainly, only one of the above two transformation is correct. If one believes that physical law should be the same in different frames, then the above observation implies that Newton equation and Maxwell equation are incompatible, and one of them must be wrong. If Galileo transformation is correct, then the Maxwell theory is wrong and needs to be modified. If Lorentz transformation is correct, then

the Newton theory is wrong and needs to be modified. Michelson-Morley experiment showed that the speed of light is the same in all the frames, which implied the Galileo transformation to be wrong. So Einstein choose to believe in Maxwell equation. He modified Newton equation and developed the theory of special relativity. Thus, Newton theory is not only incomplete, it is also incorrect.

Einstein has gone further. Motivated the equivalence of gravitational force and the force experienced in an accelerating frame (see Fig. 11.8), Einstein also developed the theory of general relativity.[14] Einstein theory unifies several seeming unrelated concepts, such as space and time, as well as interaction and geometry. Since the gravity is viewed as a distortion of space and since the distortion can propagate, Einstein discovered the second wave-like matter – gravitational wave (see Fig. 11.9). This is another revolution in physics – relativity revolution.

Box 11.3 Relativity revolution

A unification of space and time. A unification of gravity and space-time distortion.

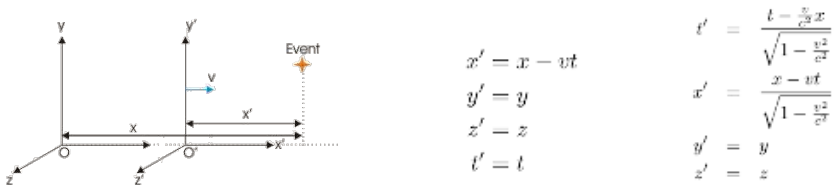

(a) (b) (c)

Fig. 11.7 (a) A rest frame and a moving frame with velocity v. An event is recorded with coordinates (x,y,z,t) in the rest frame and with (x',y',z',t') in the moving frame. There are two opinions on how (x,y,z,t) and (x',y',z',t') are related: (b) Galilean transformation or (c) Lorantz transformation where c is the speed of light. In our world, the Lorantz transformation is correct.

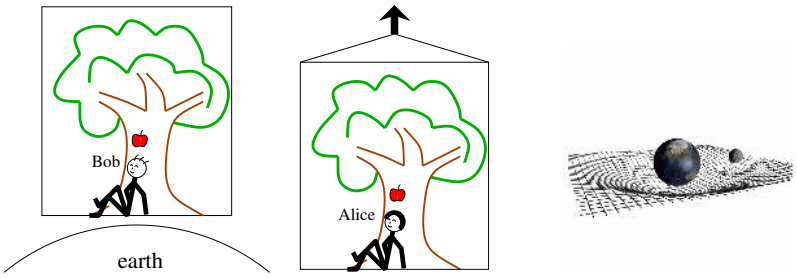

Fig. 11.8 The equivalence of the gravitational force of the earth and the force experienced in an accelerating elevator, leads to an geometric way to understand gravity: gravity = distortion in space. In other words, the "gravitational force" in an accelerating elevator is related to a geometric feature: the transformation between the coordinates in a still elevator and in the accelerating elevator.

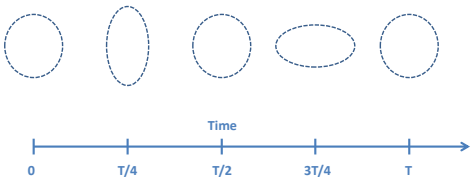

Fig. 11.9 Gravitational wave is a propagating distortion of space: a circle is distorted by a gravitational wave.

Fig. 11.10 A curved space can be viewed as a distortion of local directions of the space: parallel moving a local direction (represented by an arrow) around a loop in a curved space, the direction of the arrow does not come back. Such a twist in local direction corresponds to a curvature in space.

Motivated by the connection between interaction and geometry in gravity, people went back to reexamine the electromagnetic interaction, and found that the electromagnetic interaction is also connected to geometry. Einstein's general relativity views gravity as a distortion of space, which can be viewed as a distortion of local directions of space (see Fig. 11.10). Motivated by such a picture, in 1918, Weyl proposed that the unit that we used to measure physical quantities is relative and is defined only locally. A distortion of the unit system can be described by a vector field which is called gauge field. Weyl proposed that such a vector field (the gauge field) is the vector potential that describes the electromagnetism. Although the above particular proposal turns out to be incorrect, the Weyl's idea is correct. In 1925, the complex quantum amplitude was discovered. If we assume the complex phase is relative, then a distortion of unit system that measure local complex phase can also be described by a vector field. Such a vector field is indeed the vector potential that describes the electromagnetism. This leads to a unified way to understand gravity and electromagnetism: gravity arises from the relativity of spacial directions at different spatial points, while electromagnetism arises from the relativity of complex

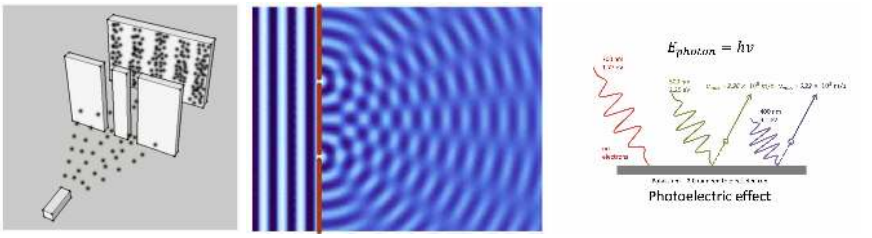

(a) (b)

Fig. 11.11 (a) An electron beam passing through a double-slit can generate an interference pattern, indicating that electrons are also waves. (b) Using light to eject electrons from a metal (the photoelectric effect) shows that the higher the light wave frequency (the shorter the wave length), the higher the energy of the ejected electron. This reveals that a light wave of frequency f can be viewed a beam of particles of energy $E = hf$, where $h = 6.62607004 \times 10^{-34} \frac{\text{m}^2\text{kg}}{\text{s}}$.

quantum phases at different spatial points. Further more, Nordström, Möglichkeit, Kaluza, and Klein showed that both gravity and electromagnetism can be understood as a distortion of space-time provided that we think the space-time as five dimensional with one dimension compactified into a small circle.[57, 34, 36] This can be viewed as an unification of gravity and electromagnetism. Those theories are so beautiful. Since that time, the geometric way to view our world has dominated theoretical physics.

11.1.4 Quantum revolution

However, such a geometric view of world was immediately challenged by new discoveries from microscopic world.[2] The experiments in microscopic world tell us that not only Newton theory is incorrect, even its relativity modification is incorrect. This is because Newton theory and its relativistic modification are theories for particle-like matter. But through experiments on very tiny things, such as electrons, people found that the particles are not really particles. They also behave like waves at the same time. Similarly, experiments also reveal that the light waves behave like a beam of particles (photons) at the same time (see Fig. 11.11). So the real matter in our world is not what we thought it was. The matter is neither particle nor wave, and both particle and wave. So the Newton theory (and its relativistic modification) for particle-like matter and the Maxwell/Einstein theories for wave-like matter cannot be the correct theories for matter. We need a new theory for the new form of existence: particle-wave-like matter. The new theory is the quantum theory that explains the microscopic world. The quantum theory unifies the particle-like matter and wave-like matter.

[2] Many people have ignored such challenges and the geometric view of world becomes the main stream.

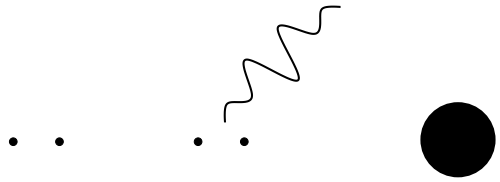

Fig. 11.12 To observe two points of distance l apart, we need to send in light of wave length $\lambda < l$. The corresponding photon has an energy $E = hc/\lambda$. If l is less than the Planck length $l < l_P$, then the photon will make a back hole of size larger then l. The black hole will swallow the two points, and we can never measure the separation of two points of distance less than l_P. What cannot be measured cannot exists. So the notion of "two points less than l_P apart" has no physical meaning and does not exist.

Box 11.4 Quantum revolution

There is no particle-like matter nor wave-like matter. All the matter in our world is particle-wave-like matter.

From the above, we see that quantum theory reveals the true existence in our world to be quite different from the classical notion of existence in our mind. What exist in our world are not particles or waves, but somethings that are both particle and wave. Such a picture is beyond our wildest imagination, but reflects the truth about our world and is the essence of quantum theory. To understand the new notion of existence more clearly, let us consider another example. This time it is about a bit (represented by spin-1/2). A bit has two possible states of classical existence: $|1\rangle = |\uparrow\rangle$ and $|0\rangle = |\downarrow\rangle$. However, quantum theory also allows a new kind of existence $|\uparrow\rangle + |\downarrow\rangle$. One may say that $|\uparrow\rangle + |\downarrow\rangle$ is also a classical existence since $|\uparrow\rangle + |\downarrow\rangle = |\rightarrow\rangle$ that describes a spin in x-direction. So let us consider a third example of two bits. Then there will be four possible states of classical existence: $|\uparrow\uparrow\rangle$, $|\uparrow\downarrow\rangle$, $|\downarrow\uparrow\rangle$, and $|\downarrow\downarrow\rangle$. Quantum theory allows a new kind of existence $|\uparrow\uparrow\rangle + |\downarrow\downarrow\rangle$. Such a quantum existence is entangled and has no classical analogues.

Although the geometric way to understand our world is a main stream in physics, here we will take a position that the geometric understanding is not good enough and will try to advocate a very different non-geometric understanding of our world. Why the geometric understanding is not good enough? First the geometric understanding is not self-consistent. It contradicts with quantum theory. The consideration based quantum mechanics and Einstein gravity indicates that two points separated by a distance less than the Planck length

$$l_P = \sqrt{\frac{\hbar G}{c^3}} = 1.616199 \times 10^{35}\text{m} \tag{11.1}$$

cannot exist as a physical reality (see Fig. 11.12). Thus the foundation of the geometric approach – manifold – simply does not exist in our universe, since manifold contains points with arbitrary small separation. This suggests that geometry is an

emergent phenomenon that appears only at long distances. So we cannot use geometry and manifold as a foundation to understand fundamental physical problems.

Second, Maxwell theory of light and Einstein theory of gravity predict light waves and gravitational waves. But the theories fail to tell us what is waving? Maxwell theory and Einstein theory are built on top of geometry. They fail to answer what is the origin of the apparent geometry that we see. In other words, Maxwell theory and Einstein theory are incomplete, and they should be regarded as effective theories at long distances.

Since geometry does not exist in our world, this is why we say the geometric view of world is challenged by quantum theory. The quantum theory tell us such a point of view to be wrong at length scales of order Planck length. So the quantum theory represents the most dramatic revolution in physics.

11.2 It from qubit, not bit

After realizing that even the notion of existence is changed by quantum theory, it is no longer surprising to see that quantum theory also blurs the distinction between information and matter. In fact, it implies that information is matter, and matter is information. This is because the frequency is an attribute of information. Quantum theory tells us that frequency is energy $E = hf$, and relativity tells us that energy is mass $m = E/c^2$. Both energy and mass are attributes of matter. So matter = information. This represents a new way to view our world.

Box 11.5 The essence of quantum theory
The energy-frequency relation $E = hf$ implies that matter = information.

The above point of view of "matter = information" is similar to Wheeler's "it from bit", which represents a deep desire to unify matter and information. In fact, such an unification has happened before at a small scale. We introduced electric and magnetic field to informationally (or pictorially) describe electric and magnetic interaction. But later, electric/magnetic field became real matter with energy and momentum, and even a particle associated with it.

However, in our world, "it" are very complicated. (1) Most "it" are fermions, while "bit" are bosonic. Can fermionic "it" come from bosonic "bit"? (2) Most "it" also carry spin-1/2. Can spin-1/2 arises from "bit"? (3) All "it" interact via a special kind of interaction – gauge interaction. Can "bit" produce gauge interaction? Can "bit" produce waves that satisfy Maxwell equation? Can "bit" produce photon?

In other words, to understand the concrete meaning of "matter from information" or "it from bit", we note that matter are described by Maxwell equation (photons), Yang-Mills equation (gluons and W/Z bosons), as well as Dirac and Weyl equations (electrons, quarks, neutrinos). The statement "matter = information" means that those wave equations can all come from qubits. In other words, we know that

elementary particles (*i.e.* matter) are described by gauge fields and anti-commuting fields in a quantum field theory. Here we try to say that all those very different quantum fields can arise from qubits. Is this possible?

All the waves and fields mentioned above are waves and fields in space. The discovery of gravitational wave strongly suggested that the space is a deformable dynamical medium. In fact, the discovery of electromagnetic wave and the Casimir effect already strongly suggested that the space is a deformable dynamical medium. As a dynamical medium, it is not surprising that the deformation of space give rise to various waves. But the dynamical medium that describe our space must be very special, since it should give rise to waves satisfying Einstein equation (gravitational wave), Maxwell equation (electromagnetic wave), Dirac equation (electron wave), *etc* . But what is the microscopic structure of the space? What kind of microscopic structure can, at the same time, give rise to waves that satisfy Maxwell equation, Dirac/Weyl equation, and Einstein equation?

Let us view the above questions from another angle. Modern science has made many discoveries and has also unified many seemingly unrelated discoveries into a few simple structures. Those simple structures are so beautiful and we regard them as wonders of our universe. They are also very myterious since we do not understand where do they come from and why do they have to be the way they are. At moment, the most fundamental mysteries and/or wonders in our universe can be summarized by the following short list:

Box 11.6 Eight wonders

(1) Locality.
(2) Identical particles.
(3) Gauge interactions.[87, 58, 95]
(4) Fermi statistics.[15, 12]
(5) Tiny masses of fermions ($\sim 10^{-20}$ of the Planck mass).[20, 59, 83]
(6) Chiral fermions.[42, 93]
(7) Lorentz invariance.[13]
(8) Gravity.[14]

In the current physical theory of nature (such as the standard model), we take the above properties for granted and do not ask where do they come from. We put those wonderful properties into our theory by hand, for example, by introducing one field for each kind of interactions or elementary particles.

However, here we would like to question where do those wonderful and mysterious properties come from? Following the trend of science history, we wish to have a single unified understanding of all of the above mysteries. Or more precisely, we wish that we can start from a single structure to obtain all of the above wonderful properties.

The simplest element in quantum theory is qubit $|0\rangle$ and $|1\rangle$ (or $|\downarrow\rangle$ and $|\uparrow\rangle$). Qubit is also the simplest element in quantum information. Since our space is a

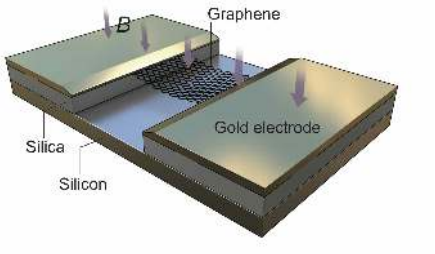

Fig. 11.13 Fractional quantum Hall states are new states of quantum matter formed by electrons traped at the interface of two semiconductors, or by electrons on a sheet of graphene, under a strong magnetic field B.

dynamical medium, the simplest choice is to assume the space to be an ocean of qubits. We will give such an ocean a formal name "qubit ether". Then the matter, *i.e.* the elementary particles, are simply the waves, "bubbles" and other defects in the qubit ocean (or quibt ether). This is how "it from qubit" or "matter = information".

Qubit, having only two states $|\downarrow\rangle$ and $|\uparrow\rangle$, is very simple. We may view the many-qubit state with all qubits in $|\downarrow\rangle$ as the quantum state that correspond to the empty space (the vacuum). Then the many-qubit state with a few qubits in $|\uparrow\rangle$ correspond to a space with a few spin-0 particles described by a scaler field. Thus, it is easy to see that a scaler field can emerge from qubit ether as a density wave of up-qubits. Such a wave satisfy the Eular eqution, but not Maxwell equation or Yang-Mills equation. So the above particular qubit ether is not the one that correspond to our space. It has a wrong microscopic structure and cannot carry waves satisfying Maxwell equation and Yang-Mills equation. But this line of thinking may be correct. We just need to find a qubit ether with a different microscopic structure.

However, for a long time, we do not know how waves satisfying Maxwell equation or Yang-Mills equation can emerge from any qubit ether. The anti-commuting wave that satisfy Dirac/Weyl equation seems even more impossible. So, even though quantum theory strongly suggests "matter = information", trying to obtain all elementary particles from an ocean of simple qubits is regarded as impossible by many and has never become an active research effort.

So the key to understand "matter = information" is to identify the microscopic structure of the qubit ether (which can be viewed as space). The microscopic structure of our space must be very rich, since our space not only can carry gravitational wave and electromagnetic wave, it can also carry electron wave, quark wave, gluon wave, and the waves that correspond to all elementary particles. Is such a qubit ether possible?

In condensed matter physics, the discovery of fractional quantum Hall states[76] (see Fig. 11.13) bring us into a new world of highly entangled many-body systems. When the strong entanglement becomes long range entanglement[10], the systems will possess a new kind of order – topological order[77, 78], and represent new states of matter. We find that the waves (the excitations) in topologically ordered states can

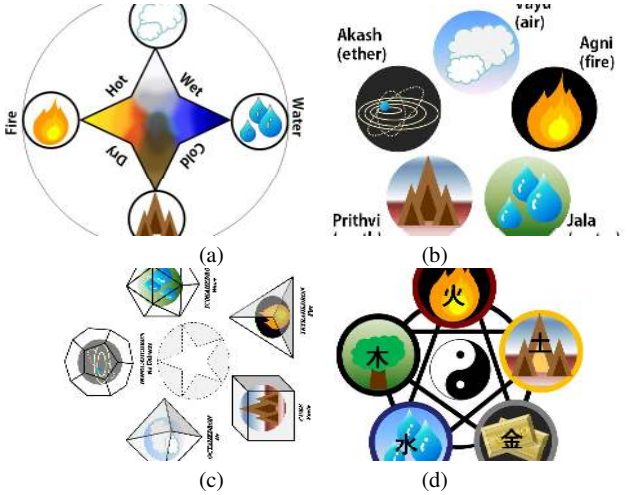

Fig. 11.14 Acient "atomic" theory of matter: (a) Aristotle's four-elements theory: all matter is formed by air, water, earth, and fire. (b) Ayurveda's five-elements theory: air, fire, water, earth, and ether (space). (c) Plato's five-elements theory: water, fire, earth, air, and universe. (d) Chinese five-elements theory: all matter is formed by five "features" gold, wood, water, fire, earth, which come from two more basic features ying (negtive) and yang (positive). Ying and yang come from the grand unifier Taiji (represented by the circle in the center).

be very strange: they can be waves that satisfy Maxwell equation, Yang-Mills equation, or Dirac/Weyl equation. So the impossible become possible: all elementary particles can emerge from long range entangled qubit ether.

We would like to stress that the above picture is "it from qubit", which is very different from Wheeler's "it from bit". As we have explained, our observed elementary particles can only emerge from long range entangled qubit ether. The requirement of quantum entanglement implies that "it cannot from bit". In fact "it from entangled qubits".

11.3 Emergence approach

11.3.1 Two approaches

In the reductionism approach, we try to understand various things by dividing them into smaller and smaller parts. If we assume the division has to end at a certain level, then we conclude that all things are formed by the parts that cannot be divided further. The indivisible parts are called "atoms" or elementary particles (see Fig. 11.14). So in the reductionism approach, we view all matter in our world as made of some simple beautiful building blocks, the elementary particles. A deeper understanding is gained if we find some elementary particles are not actually elementary

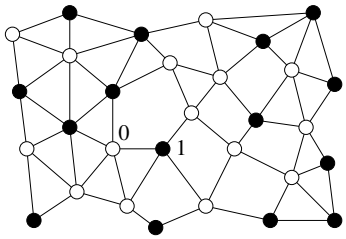

Fig. 11.15 In the emergence approach, there is only one form of "matter" – the space (the vaccum) itself, which is formed by qubits. What we regarded as matter are distortions and defects in this "space-matter".

and are formed by even smaller objects. A large part of science is devoted in finding those smaller and smaller objects, as represented by the discoveries of atoms, electrons and protons, and then quarks.

However, the reductionism approach that we followed in last 200 years may not represent a right direction. For example, phonons (the quanta of sound waves) in a solid is as particle-like as any other elementary particles at low energies. But if we look at phonons closely, we do not see smaller parts that form a phonon. We see the atoms that fill the entire space. The phonons are not formed by those atoms, the phonons are simply collective motions of those atoms.

This leads us to wonder that maybe photons, electrons, gravitons, *etc* , are also collective motions of a certain underlying structure that fill the entire space. They may not have smaller parts. Looking for the smaller parts of photons, electrons, and gravitons to gain a deeper understanding of those elementary particles may not be a right approach.

Here, we will use a different approach, emergence approach, to gain a deeper understanding of elementary particles. In the emergence approach, we view space as an ocean of qubits, *i.e.* a qubit ether (see Fig. 11.15). The empty space (the vacuum) corresponds to the ground state of the qubit ether, and the elementary particles (that form the matter) correspond to the excitations of the qubit ether.

As we have pointed out that the elementary particles in our world have very rich and strange properties. Can excitations of simple qubits have those rich strange properties? How to answer such an question? Here is our plan: due to the particle-wave duality in quantum theory, particles and waves are the same thing. So we can try to understand the rich strange properties of elementary particles by trying to understand the rich strange properties of waves.

11.3.2 Principle of emergence

One might think the properties of a material should be determined by the components that form the material. However, this simple intuition is incorrect, since all the materials are made of the same components: electrons, protons and neutrons, with

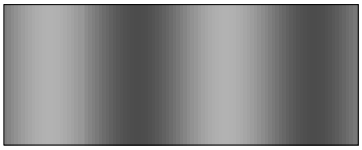

Fig. 11.16 Liquids only have a compression wave – a wave of density fluctuations.

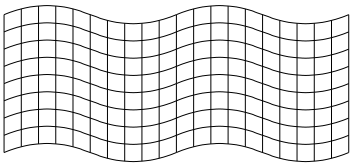

Fig. 11.17 Drawing a grid on a sold helps us to see the deformation of the solid. The vector u^i in eqn. (11.3) is the displacement of a vertex in the grid. In addition to the compression wave (*i.e.* the density wave), a solid also supports transverse wave (wave of shear deformation) as shown in the above figure.

about the same numerical density. So we cannot use the richness of components to understand the richness of the materials. In fact, the various properties of different materials originate from various ways in which the particles are organized. Different orders (the organizations of particles) give rise to different physical properties of a material. It is the richness of the orders that gives rise to the richness of material world.

Box 11.7 Principle of emergence
The physical properties of a many-body state mainly come from the organization (*i.e.* the order) of the degrees of freedom in the state.

We know that a deformation in a material can propagate just like the ripple on the surface of water. The propagating deformation corresponds to a wave traveling through the material. Since liquids can resist only compression deformation, so liquids can only support a single kind of wave – compression wave (see Fig. 11.16). (Compression wave is also called longitudinal wave.) Mathematically the motion of the compression wave is governed by the Euler equation

$$\frac{\partial^2 \rho}{\partial t^2} - v^2 \frac{\partial^2 \rho}{\partial x^2} = 0, \tag{11.2}$$

where ρ is the density of the liquid.

Solid can resist both compression and shear deformations. As a result, solids can support both compression wave and transverse wave. The transverse wave correspond to the propagation of shear deformations. In fact there are two transverse waves corresponding to two directions of shear deformations. The propagation of the compression wave and the two transverse waves in solids are described by the

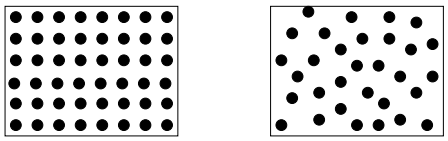

Fig. 11.18 (a) In a crystal, particles form a regular array (and break the continuous translation symmetry down to a discrete translation symmetry). (b) In a liquid, particles have a random fluctuating distribution (which do not break any symmetry).

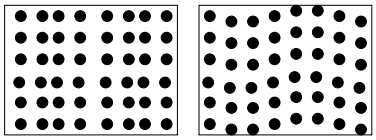

Fig. 11.19 The atomic picture of (a) the compression wave and (b) the transverse wave in a crystal.

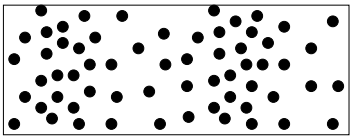

Fig. 11.20 The atomic picture of the compression wave in liquids.

elasticity equation

$$\frac{\partial^2 u^i}{\partial t^2} - T^{ikl}_j \frac{\partial^2 u^j}{\partial x^k \partial x^l} = 0 \tag{11.3}$$

where the vector field $u^i(x,t)$ describes the local displacement of the solid.

We would like to point out that the elasticity equation and the Euler equations not only describe the propagation of waves, they actually describe all small deformations in solids and liquids. Thus, the two equations represent a complete mathematical description of the mechanical properties of solids and liquids.

But why do solids and liquids behave so differently? What makes a solid to have a shape and a liquid to have no shape? What are the origins of elasticity equation and Euler equations?

To answer the above questions, we have to use the microscopic structure of liquids and solids: they are all formed by atoms. In liquids, the positions of atoms fluctuate randomly (see Fig. 11.18a), while in solids, atoms organize into a regular fixed array (see Fig. 11.18b).[3] It is the different organizations of atoms that lead to the different mechanical properties of liquids and solids. In other words, it is the different organizations of atoms that make liquids to be able to flow freely and solids to be able to retain its shape.

[3] The solids here should be more accurately referred as crystals.

How can different organizations of atoms affect mechanical properties of materials? In solids, both the compression deformation (see Fig. 11.19a) and the shear deformation (see Fig. 11.19b) lead to real physical changes of the atomic configurations. Such changes cost energies. As a result, solids can resist both kinds of deformations and can retain their shapes. This is why we have both the compression wave and the transverse wave in solids.

In contrast, a shear deformation of atoms in liquids does not result in a new configuration since the atoms still have the same uniformly random distribution. So the shear deformation is a do-nothing operation for liquids. Only the compression deformation which changes the density of the atoms results in a new atomic configuration and costs energies. As a result, liquids can only resist compression and have only compression wave. Since shear deformations do not cost any energy for liquids, liquids can flow freely.

We see that the properties of the propagating wave are entirely determined by how the atoms are organized in the materials. Different organizations lead to different kinds of waves and different kinds of mechanical laws. This point of view is called the principle of emergence.

In the above, we see that the Euler equation and elasticity equation originated from the different organizations of atoms. Elementary particles are described by Maxwell/Yang-Mills equations and Dirac/Weyl equations, or in other words they are described by quantum field theory (such as the standard model). But quantum field theory (*i.e.* the Maxwell/Yang-Mills equations and Dirac/Weyl equations) are effective theories like Euler/elasticity equations. They are not a complete description of physical systems, since they lack of description of the microscopic structure. We know that Euler/elasticity equations come from atoms. But what is the origin (*i.e.* the microscopic structure) of quantum field theory? The motion of what give rise to Maxwell/Yang-Mills equations and Dirac/Weyl equations? In the following, we like to show that the motion of particles or qubits can give rise both to Maxwell/Yang-Mills equations and Dirac/Weyl equations, as long as the particles/qubits have a proper organization. We will concentrate on how Maxwell and Dirac equations arise from the motion of particles/qubits.

11.3.3 String-net liquid of qubits unifies light and electrons

When Maxwell equation was first introduced, people firmly believed that any wave must corresponds to motion of something. So people want to find out what is the origin of the Maxwell equation? The motion of what gives rise electromagnetic wave?

First, one may wonder: can Maxwell equation comes from a certain symmetry breaking order? Based on Landau symmetry-breaking theory, the different symmetry breaking orders can indeed lead to different waves satisfying different wave equations. So maybe a certain symmetry breaking order can give rise to a wave that satisfy Maxwell equation. But people have been searching for ether – a medium that

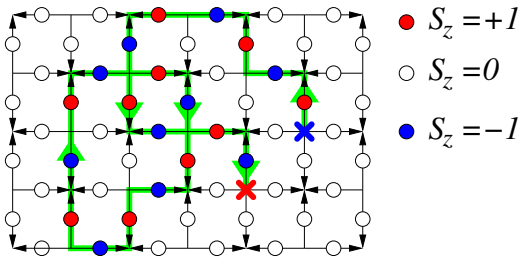

Fig. 11.21 Oriented strings from spin-1-qubits living on the links of a cubic lattice (only one slice is shown). A spin-1-qubit has three states $S_z = 0$ (open circle), $S_z = +1$ (red circle), $S_z = -1$ (blue circle). $S_z = 0$ corresponds to no string on the link, $S_z = +1$ a string with the same orientation of the link, $S_z = -1$ a string with the opposite orientation. (Oriented strings can also arise from atoms as oriented polymers.)

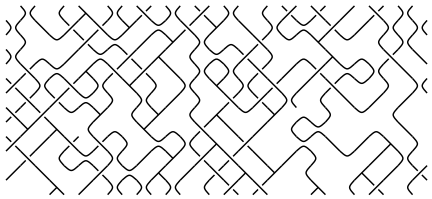

Fig. 11.22 A quantum ether: The fluctuation of oriented strings give rise to electromagnetic waves (or light). The ends of strings give rise to electrons. Note that oriented strings have directions which should be described by curves with arrow. For ease of drawing, the arrows on the curves are omitted in the above plot.

supports light wave – for over 100 years, and could not find any symmetry breaking states that can give rise to waves satisfying the Maxwell equation. This is one of the reasons why people give up the idea of ether as the origin of light and Maxwell equation.

However, the discovery of topological order [77, 78] suggests that Landau symmetry-breaking theory does not describe all possible organizations of particles/qubits. This gives us a new hope: Maxwell equation may arise from a new kind of organizations of particles/qubits that have non-trivial topological orders (or their gapless generalization, quantum orders).

In addition to the Maxwell equation, there is an even stranger equation, Dirac equation, that describes wave of electrons (and other fermions). Electrons have Fermi statistics. They are fundamentally different from the quanta of other familiar waves, such as photons and phonons, since those quanta all have Bose statistics. To describe the electron wave, the amplitude of the wave must be anti-commuting Grassmann numbers, so that the wave quanta will have Fermi statistics. Since electrons are so strange, few people regard electrons and the electron waves as collective motions of something. People accept without questioning that electrons are fundamental particles, one of the building blocks of all that exist.

Fig. 11.23 The fluctuating strings in a string liquid.

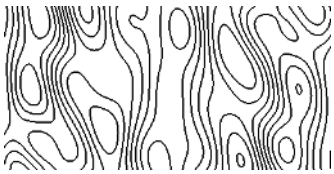

Fig. 11.24 A 'density' wave of oriented strings in a string liquid. The wave propagates in x-direction. The 'density' vector E points in y-direction. For ease of drawing, the arrows on the oriented strings are omitted in the above plot.

However, in a recent study [45, 47, 46], we find that if particles/qubits form large oriented strings (see Fig. 11.21) and if those strings form a quantum liquid state, then the collective motion of the such organized particles/qubits will correspond to waves described by Maxwell equation and Dirac equation. The strings in the string liquid are free to join and cross each other. As a result, the strings look more like a network (see Fig. 11.22). For this reason, the string liquid is actually a liquid of string-nets, which is called string-net condensed state.

But why the waving of strings produces waves described by the Maxwell equation? We know that the particles in a liquid have a random but uniform distribution. A deformation of such a distribution corresponds a density fluctuation, which can be described by a scaler field $\rho(x,t)$. Thus the waves in a liquid is described by the scaler field $\rho(x,t)$ which satisfy the Euler equation (11.2). Similarly, the strings in a string-net liquid also have a random but uniform distribution (see Fig. 11.23). A deformation of string-net liquid corresponds to a change of the density of the strings (see Fig. 11.24). However, since strings have an orientation, the 'density' fluctuations are described by a vector field $E(x,t)$, which indicates there are more strings in the E direction on average. The oriented strings can be regarded as flux lines. The vector field $E(x,t)$ describes the smeared average flux. Since strings are continuous (*i.e.* they cannot end), the flux is conserved: $\partial \cdot E(x,t) = 0$. The vector density $E(x,t)$ of strings cannot change in the direction along the strings (*i.e.* along the $E(x,t)$ direction). $E(x,t)$ can change only in the direction perpendicular to $E(x,t)$. Since the direction of the propagation is the same as the direction in which $E(x,t)$ varies, thus the waves described by $E(x,t)$ must be transverse waves: $E(x,t)$ is always perpendicular to the direction of the propagation. Therefore, the waves in the string liquid have a very special property: the waves have only transverse modes and no longitudinal mode. This is exactly the property of the light waves described by the Maxwell equation. We see that 'density' fluctuations of strings (which are

described be a transverse vector field) naturally give rise to the light (or electromagnetic) waves and the Maxwell equation [82, 83, 53, 27, 47, 46].

To understand how electrons appear from string-nets, we would like to point out that if we only want photons and no other particles, the strings must be closed strings with no ends. The fluctuations of closed strings produce only photons. If strings have open ends, those open ends can move around and just behave like independent particles. Those particles are not photons. In fact, the ends of strings are nothing but electrons (the blue $\times$ corresponds to an electron and the red $\times$ corresponds to a positron in Fig. 11.21).

Box 11.8 String density wave

String density wave in a quantum liquid of oriented strings is a divergence-free vector field, which give rise to a wave with only two transverse modes – an electromagnetic wave.

How do we know that ends of strings behave like electrons? First, since the waving of string-nets is an electromagnetic wave, a deformation of string-nets correspond to an electromagnetic field. So we can study how an end of a string interacts with a deformation of string-nets. We find that such an interaction is just like the interaction between a charged electron and an electromagnetic field. Also electrons have a subtle but very important property – Fermi statistics, which is a property that exists only in quantum theory. Amazingly, the ends of strings can reproduce this subtle quantum property of Fermi statistics [44, 45]: For string liquid state described by wave function

$$|\Phi\rangle = \sum_{\text{all conf.}} \left|\quad\right\rangle, \tag{11.4}$$

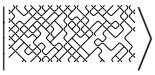

then the end of strings are bosons (*i.e.* Higgs bosons). For string liquid state

$$|\Phi\rangle = \sum_{\text{all conf.}} (-)^{\#\text{ of crossings}} \left|\quad\right\rangle, \tag{11.5}$$

then the end of strings are fermions. Here "# of crossings" is obtained by first project the 3D string configuration to a fixed 2D plan, then "# of crossings" is the number of string crossings  (for details, see Chapter 7). Actually, string-net liquids explain why Fermi statistics should exist.

We see that qubits that organize into string-net liquid naturally explain both light and electrons (gauge interactions and Fermi statistics). In other words, string-net theory provides a way to unify light and electrons [47, 46]. So, the fact that our vacuum contains both light and electrons may not be a mere accident. It may actually suggest that the vacuum is indeed a long-range entangled qubit state, whose order is described by a string-net liquid.

Box 11.9 A qubit unification of light and electrons

Q: Where do light and electrons come from?
A: Light and electrons come from the qubits that form the space.
Q: Why do light and electrons exist?
A: Light and fermions exist because the space-forming qubits form a string-net condensed state.
Q: What are light and electrons?
A: Light waves are collective motions of strings and electrons are ends of open strings in the string-net condensed state.

We would like to stress that the string-nets are formed by qubits. So in the string-net picture, both the Maxwell equation and Dirac equation, emerge from *local* qubit model, as long as the qubits form a long-range entangled state (*i.e.* a string-net liquid). In other words, light and electrons are unified by the long-range entanglement of qubits. Information unifies matter!

The electric field and the magnetic field in the Maxwell equation are called gauge fields. The field in the Dirac equation are Grassman-number valued field.[4] For a long time, we thought that we have to use gauge fields to describe light waves that have only two transverse modes, and we thought that we have to use Grassmann-number valued fields to describe electrons and quarks that have Fermi statistics. So gauge fields and Grassmann-number valued fields become the fundamental build blocks of quantum field theory that describe our world. The string-net liquids demonstrate that we do not have to introduce gauge fields and Grassmann-number valued fields to describe photons, gluons, electrons, and quarks. It demonstrates how gauge fields and Grassmann fields emerge from local qubit models that contain only complex scaler fields at the cut-off scale.

11.3.4 Evolving views for light and gauge theories

Our attempt to understand light has a long and evolving history. We first thought light to be a beam of particles (see Fig. 11.25a). After Maxwell, we understand light as electromagnetic waves (see Fig. 11.25b,c). After Einstein's theory of general relativity, where gravity is viewed as curvature in space-time, Weyl and others try to view electromagnetic field as curvatures in the 'unit system' that we used to measure complex phases. It leads to the notion of gauge theory. The general relativity and the gauge theory are two corner stones of modern physics. They provide a unified understanding of all four interactions in terms of a beautiful mathematical frame work: all interactions can be understood geometrically as curvatures in space-time

[4] Grassmann numbers are anti-commuting numbers.

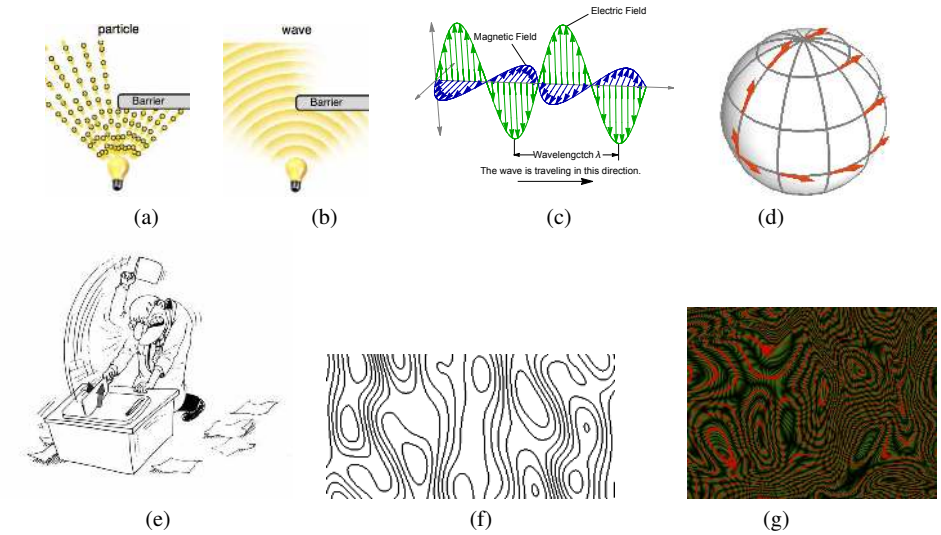

Fig. 11.25 The evolution of our understanding of light (and gauge interaction): (a) particle beam, (b) wave, (c) electromagnetic wave, (d) curvature in fiber bundle, (e) glue of partons, (f) wave in string-net liquid, (g) wave in long-range entanglement of many qubits.

and in 'unit systems' (or more precisely, as curvatures in the tangent bundle and other vector bundles in space-time, see Fig. 11.25d).

Later, people in high-energy physics and in condensed matter physics have found another way in which gauge field can emerge [11, 92, 6, 1]: one first cut a particle (such as an electron) into two partons (see Fig. 11.25e) by writing the field of the particle as the product of the two fields of the two partons. Then one introduces a gauge field to glue the two partons back to the original particle. Such a 'glue-picture' of gauge fields (instead of the fiber bundle picture of gauge fields) allow us to understand the emergence of gauge fields in models that originally contain no gauge field at the cut-off scale.

For long time, people think, by definition, gauge theories are theories with gauge symmetries (a kind of local symmetries). Since all interactions in our world are described by gauge theories (the abelian ones and non-abelian ones), gauge symmetry is regarded as a founding principle in our understanding of the world. The geometric fiber bundle picture of the gauge theory has stressed the gauge symmetry. However, some people are unhappy with the gauge-symmetry point of view for gauge theory, since it involves many unphysical quantities. An attempt to describe gauge theory only in terms physical quantities leads to a string-net picture of gauge theory [82, 45], which represent the third way to understand gauge theory (see Fig. 11.25f). Before the string-net theory of gauge interactions, string operators has appeared in the Wilson-loop characterization [91] of gauge theory. The Hamiltonian and the duality description of lattice gauge theory also reveal string

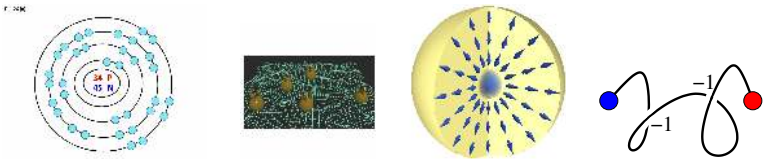

(a) (b) (c) (d)

Fig. 11.26 The evolution of our understanding of fermions: (a) elementary particles, (b) charge-flux bound state in 2D, (c) charge-monople bound state in 3D, (d) ends of string in quantum string liquids, with -1 factor for each string crossing (see eqn. (11.5)).

structures [39, 3, 38, 65], which lead to the string-net theory for all gauge interactions.

Lattice gauge theories are not local bosonic models since the strings are unbreakable in lattice gauge theories. String-net theory points out that we do not really need strings and qubits themselves are capable of generating gauge fields and the associated Maxwell/Yang-Mills equation. This is because even breakable strings can give rise to gauge fields [24]. This phenomenon was discovered in several qubit models [17, 6, 81, 55, 27] before realizing their connection to the string-net liquids [82]. In other words, opposite to our opinion that gauge symmetry is a founding principle of our world, in fact gauge symmetry is not important for gauge theory. A lattice gauge theory will always produce gauge interaction at low energies even if we break the gauge symmetry (by not too big amount) at lattice scale [17, 24]. So gauge theory does not need gauge symmetry! Since gauge field can emerge from local qubit models without gauge symmetry, the string picture evolves into the entanglement picture – the fourth way to understand gauge field: gauge fields are fluctuations of long-range entanglement (see Fig. 11.25g). String-net is only a description of the patterns of long-range entanglement.

We feel that the entanglement picture capture the essence of gauge theory. Despite the beauty of the geometric picture, the essence of gauge theory is not the curved fiber bundles. In fact, we can view gauge theory as a theory for long-range entanglement, despite the gauge theory is discovered long before the notion of long-range entanglement. The evolution of our understanding of light and gauge interaction: particle beam $\to$ wave $\to$ electromagnetic wave $\to$ curvature in fiber bundle $\to$ glue of partons $\to$ string-net density wave $\to$ wave in long-range entanglement (see Fig. 11.25), represents 200 year's effort of human race to unveil the mystery of universe.

Viewing gauge field (and the associated gauge bosons) as fluctuations of long-range entanglement has an added bonus: we can understand the origin of Fermi statistics in the same way: fermions emerge as defects of long-range entanglement, even though the original model is purely bosonic. Previously, there are two ways to obtain emergent fermions from purely bosonic model: by binding gauge charge and gauge flux in (2+1)D (see Fig. 11.26b [43, 88]), and by binding the charge and the monopole in a $U(1)$ gauge theory in (3+1)D (see Fig. 11.26c [74, 31, 89, 18, 41]). But those approaches only work in (2+1)D or only for $U(1)$ gauge field. Using long-

range entanglement and their string-net realization, we can obtain the simultaneous emergence of both gauge bosons (as string density waves) and fermions (as string ends) in *any* dimensions and for any gauge group (see Fig. 11.26d [44, 45, 47, 83]). This result gives us hope that maybe all elementary particles are emergent and can be unified using local qubit models. Thus, long-range entanglement offer us a new option to view our world: maybe our vacuum is a long-range entangled state. It is the pattern of the long-range entanglement in the vacuum that determines the content and the structures of observed elementary particles.

We would like to point out that the string-net unification of gauge bosons and fermions is very different from the superstring theory for gauge bosons and fermions. In the string-net theory, gauge bosons and fermions come from the qubits that form the space, and 'string-net' is simply the name that describe how qubits are organized in the ground state. So string-net is not a thing, but a pattern of qubits. In the string-net theory, the gauge bosons are waves of collective fluctuations of the string-nets, and a fermion corresponds to one end of string. In contrast, gauge bosons and fermions come from strings in the superstring theory. Both gauge bosons and fermions correspond to small pieces of strings. Different vibrations of the small pieces of strings give rise to different kind of particles. The fermions in the superstring theory are put in by hand through the introduction of Grassmann fields.

11.3.5 Where to find long-range entangled quantum matter?

In this book, we described the world of quantum phases. We pointed out that there are symmetry breaking quantum phases, and there are topologically ordered quantum phases. The topologically ordered quantum phases are a totally new kind of phases which cannot be understood using the conventional concepts (such as symmetry breaking, long-range order, and order parameter) and conventional mathematical frame work (such as group theory and Ginzburg-Landau theory). The main goal of this book is to introduce new concepts and pictures to describe the new topologically ordered quantum phases.

In particular, we described how to use global dancing pattern to gain an intuitive picture of topological order (which is a pattern of long-range entanglement). We further point out that we can use local dancing rules to *quantitatively* describe the global dancing pattern (or topological order). Such an approach leads to a systematic description of topological order in terms of string-net (or unitary fusion category theory) [45, 29, 10, 22] and systematic description of 2D chiral topological order in terms of pattern of zeros [84, 85, 63, 72, 8, 9, 4, 5, 50] (which is a generalization of 'charge-density-wave' description of FQH states [68, 7, 69, 66, 70, 2, 67, 16]).

The local-dancing-rule approach also leads to concrete and explicit Hamiltonians, that allow us to realize each string-net state and each FQH state described by pattern of zeros. However, those Hamiltonians usually contain three-body or more complicated interactions, and are hard to realize in real materials. So here we would

like to ask: can topological order be realized by some simple Hamiltonians and real materials?

Of cause, non-trivial topological orders – FQH states – can be realized by 2D electron gas under very strong magnetic fields and very low temperatures [76, 40]. Recently, it was proposed that FQH states might appear even at room temperatures with no magnetic field in flat-band materials with spin-orbital coupling and spin polarization [75, 73, 56, 71, 21]. Finding such materials and realizing FQH states at high temperatures will be an amazing discovery. Using flat-band materials, we may even realize non-Abelian fractional quantum Hall states [54, 80, 90, 60] at high temperatures.

Apart from the FQH effects, non-trivial topological order may also appear in quantum spin systems. In fact, the concept of topological order was first introduced [77] to describe a chiral spin liquid [33, 86], which breaks time reversal and parity symmetry. Soon after, time reversal and parity symmetric topological order was proposed in 1991 [64, 79, 51, 52], which has spin-charge separation and emergent fermions. The new topological spin liquid is called $\mathbb{Z}_2$ spin liquid or $\mathbb{Z}_2$ topological order since the low energy effective theory is a $\mathbb{Z}_2$ gauge theory. In 1997, an exactly soluble model [35] (that breaks the spin rotation symmetry) was obtained that realizes the $\mathbb{Z}_2$ topological order. Since then, the $\mathbb{Z}_2$ topological order become widely accepted.

More recently, extensive new numerical calculations indicated that the J_1-J_2-J_3 Heisenberg model on Kagome lattice [25, 96, 19]

$$H = \sum_{\text{1sf}} J_1 S_i \cdot S_j + \sum_{\text{2nd}} J_2 S_i \cdot S_j + \sum_{\text{3rd}} J_3 S_i \cdot S_j, \qquad J_2/J_1 \sim J_3/J_1 \sim 0.5, \tag{11.6}$$

has gapped spin liquid ground state. Such spin liquid is the chiral spin liquid.[33, 86]

The nearest neighbor Heisenberg model on Kagome lattice can be realized in Herbertsmithite $ZnCu_3(OH)_6Cl_2$ [26, 30]. Although J_1 is as large as 150K, no spin ordering and other finite temperature phase transitions are found down to 50mK. So Herbertsmithite may realize a 2D spin liquid state. However, experimentally, it is not clear if the spin liquid is a gapped spin liquid or a gapless spin liquid. Theoretically, both a gapped $\mathbb{Z}_2$ spin liquid [32, 94, 48, 49] and a gapless $U(1)$ spin liquid [23, 61, 28] are proposed for the Heisenberg model on Kagome lattice. The theoretical study suggests that the spin liquid state in Herbertsmithite may have some very interesting characteristic properties: A magnetic field in z-direction may induce a spin order in xy-plane [62], and an electron (or hole) doping may induce a charge $4e$ topological superconductor [37].

To summarize, topological order and long-range entanglement give rise to new states of quantum matter. Topological order, or more generally, quantum order have many new emergent phenomena, such as emergent gauge theory, fractional charge, fractional statistics, non-Abelian statistics, perfect conducting boundary, etc. In particular, if we can realize a quantum liquid of oriented strings in certain materials, it will allow us to make artificial elementary particles (such as artificial photons and artificial electrons). So we can actually create an artificial vacuum, and an artificial

world for that matter, by making an oriented string-net liquid. This would be a fun experiment to do!

References

1. Ian Affleck and J. Brad Marston. Large-n limit of the heisenberg-hubbard model: Implications for high-tc superconductors. *Phys. Rev. B*, 37:3774, 1988.
2. Eddy Ardonne, Emil J Bergholtz, Janik Kailasvuori, and Emma Wikberg. Degeneracy of non-abelian quantum hall states on the torus: domain walls and conformal field theory. *Journal of Statistical Mechanics: Theory and Experiment*, 2008(04):P04016, 2008.
3. T. Banks, R. Myerson, and J. B. Kogut. Phase transitions in abelian lattice gauge theories. *Nucl. Phys. B*, 129:493, 1977.
4. Maissam Barkeshli and Xiao-Gang Wen. Structure of quasiparticles and their fusion algebra in fractional quantum hall states. *Phys. Rev. B*, 79:195132, 2009.
5. Maissam Barkeshli and Xiao-Gang Wen. Classification of abelian and non-abelian multilayer fractional quantum hall states through the pattern of zeros. *Phys. Rev. B*, 82:245301, 2010.
6. G. Baskaran and P. W. Anderson. Gauge theory of high-temperature superconductors and strongly correlated fermi systems. *Phys. Rev. B*, 37:580–583, 1988.
7. E. J. Bergholtz, J. Kailasvuori, E. Wikberg, T. H. Hansson, and A. Karlhede. The pfaffian quantum hall state made simple–multiple vacua and domain walls on a thin torus. *Phys. Rev. B*, 74:081308, 2006.
8. B. Andrei Bernevig and F. D. M. Haldane. Fractional quantum hall states and jack polynomials. *Phys. Rev. Lett.*, 100:246802, 2008.
9. B. Andrei Bernevig and F. D. M. Haldane. Generalized clustering conditions of jack polynomials at negative jack parameter α. *Phys. Rev. B*, 77:184502, 2008.
10. Xie Chen, Zheng-Cheng Gu, and Xiao-Gang Wen. Local unitary transformation, long-range quantum entanglement, wave function renormalization, and topological order. *Phys. Rev. B*, 82:155138, 2010.
11. A. D'Adda, P. Di Vecchia, and M. Lüscher. *Nucl. Phys. B*, 146:63, 1978.
12. P. A. M. Dirac. On the theory of quantum mechanics. *Proc. Roy. Soc.*, A112:661, 1926.
13. Albert Einstein. On the electrodynamics of moving bodies. *Annalen der Physik*, 17:891, 1905.
14. Albert Einstein. The foundation of the general theory of relativity. *Annalen der Physik*, 49:769, 1916.
15. E. Fermi. Zur quantelung des idealen einatomigen gases. *Z. Phys.*, 36:902, 1926.
16. J. Flavin and A. Seidel. Abelian and non-Abelian statistics in the coherent state representation. *Phys. Rev. X*, 1:021015, 2011.
17. D. Foerster, Holger Bech Nielsen, and M. Ninomiya. Dynamical stability of local gauge symmetry – creation of light from chaos. *Phys. Lett. B*, 94:135, 1980.
18. A. S. Goldhaber. Electromagnetism, Spin, and Statistics. *Phys. Rev. Lett.*, 49:905 – 908, 1982.
19. S.-S. Gong, W. Zhu, L. Balents, and D. N. Sheng. Global phase diagram of competing ordered and quantum spin-liquid phases on the kagome lattice. *Phys. Rev. B*, 91(7):075112, February 2015.
20. David J. Gross and Frank Wilczek. Ultraviolet behavior of non-abelian gauge theories. *Phys. Rev. Lett.*, 30:1343, 1973.
21. A. G. Grushin, T. Neupert, C. Chamon, and C. Mudry. Enhancing the stability of fractional Chern insulators against competing phases. 2012.
22. Zheng-Cheng Gu, Zhenghan Wang, and Xiao-Gang Wen. A classification of 2D fermionic and bosonic topological orders. *Phys. Rev. B*, 91:125149, 2015.
23. M. B. Hastings. Dirac, Anderson, and Goldstone on the Kagome. *Phys. Rev. B*, 63:14413, 2000.

24. M. B. Hastings and Xiao-Gang Wen. Quasi-adiabatic continuation of quantum states: The stability of topological ground state degeneracy and emergent gauge invariance. *Phys. Rev. B*, 72:045141, 2005.
25. Y.-C. He, D. N. Sheng, and Y. Chen. Chiral Spin Liquid in a Frustrated Anisotropic Kagome Heisenberg Model. *Physical Review Letters*, 112:137202, April 2014.
26. J. S. Helton, K. Matan, M. P. Shores, E. A. Nytko, B. M. Bartlett, Y. Yoshida, Y. Takano, A. Suslov, Y. Qiu, J.-H. Chung, D. G. Nocera, and Y. S. Lee. Spin Dynamics of the Spin-1/2 Kagome Lattice Antiferromagnet $ZnCu_3(OH)_6Cl_2$. *Phys. Rev. Lett.*, 98:107204, 2007.
27. Michael Hermele, Matthew P. A. Fisher, and Leon Balents. Pyrochlore photons: The U(1) spin liquid in a S=1/2 three-dimensional frustrated magnet. *Phys. Rev. B*, 69:064404, 2004.
28. Michael Hermele, Ying Ran, Patrick A. Lee, and Xiao-Gang Wen. Properties of an algebraic spin liquid on the kagome lattice. *Physical Review B*, 77:224413, 2008.
29. S.-M. Hong. On symmetrization of 6j-symbols and Levin-Wen Hamiltonian. 2009.
30. T. Imai, M. Fu, T. H. Han, and Y. S. Lee. Local Spin Susceptibility of the S=1/2 Kagome Lattice in ZnCu3(OD)6Cl2. *Phys. Rev. B*, 84:020411, 2011.
31. R. Jackiw and C. Rebbi. Spin from Isospin in a Gauge Theory. *Phys. Rev. Lett.*, 36:1116 – 1119, 1976.
32. H. C. Jiang, Z. Y. Weng, and D. N. Sheng. DMRG numerical study of the kagom antiferromagnet. *Phys. Rev. Lett.*, 101:117203, 2008.
33. V. Kalmeyer and R. B. Laughlin. Equivalence of the resonating-valence-bond and fractional quantum hall states. *Phys. Rev. Lett.*, 59:2095–2098, 1987.
34. Theodor Kaluza. On the problem of unity in physics. *Sitzungsber. Preuss. Akad. Wiss. Berlin. (Math. Phys.)*, page 966, 1921.
35. A. Yu. Kitaev. Fault-tolerant quantum computation by anyons. *Ann. Phys. (N.Y.)*, 303:2–30, 2003.
36. Oskar Klein. Quantum theory and five dimensional theory of relativity. *Z. Phys.*, 37:895, 1926.
37. Wing-Ho Ko, Patrick A. Lee, and Xiao-Gang Wen. Doped kagome system as exotic superconductor with fractional quasiparticles. *Phys. Rev. B*, 79:214502, 2009.
38. J. B. Kogut. An introduction to lattice gauge theory and spin systems. *Rev. Mod. Phys.*, 51:659 – 713, 1979.
39. John Kogut and Leonard Susskind. Hamiltonian formulation of wilson's lattice gauge theories. *Phys. Rev. D*, 11:395, 1975.
40. R. B. Laughlin. Anomalous quantum hall effect: An incompressible quantum fluid with fractionally charged excitations. *Phys. Rev. Lett.*, 50:1395–1398, 1983.
41. K. Lechner and P. A. Marchetti. Spin-statistics transmutation in relativistic quantum field theories of dyons. *Journal of High Energy Physics*, 2000:12, 2000.
42. T. D. Lee and C. N. Yang. Question of parity conservation in weak interactions. *Phys. Rev.*, 104:254, 1956.
43. J. M. Leinaas and J. Myrheim. On the theory of identical particles. *Il Nuovo Cimento*, 37B:1, 1977.
44. Michael Levin and Xiao-Gang Wen. Fermions, strings, and gauge fields in lattice spin models. *Phys. Rev. B*, 67:245316, 2003.
45. Michael Levin and Xiao-Gang Wen. String-net condensation: A physical mechanism for topological phases. *Phys. Rev. B*, 71:045110, 2005.
46. Michael Levin and Xiao-Gang Wen. Quantum ether: photons and electrons from a rotor model. *Phys. Rev. B*, 73:035122, 2006.
47. Michael A. Levin and Xiao-Gang Wen. Photons and electrons as emergent phenomena. *Rev. Mod. Phys.*, 77:871, 2005.
48. Y.-M. Lu and Y. Ran. Z_2 spin liquid and chiral antiferromagnetic phase in Hubbard model on the honeycomb lattice: Duality between Schwinger-fermion and Schwinger-boson representations. *Phys. Rev. B*, 84:024420, 2011.
49. Y.-M. Lu, Y. Ran, and P. A. Lee. Z2 spin liquid in S=1/2 Heisenberg model on Kagome lattice: A projective symmetry group study of Schwinger-fermion mean-field states. *Phys. Rev. B*, 83:224413, 2011.

50. Yuan-Ming Lu, Xiao-Gang Wen, Zhenghan Wang, and Ziqiang Wang. Non-abelian quantum hall states and their quasiparticles: from the pattern of zeros to vertex algebra. *Phys. Rev. B*, 81:115124, 2010.
51. G. Misguich, C. Lhuillier, B. Bernu, and C. Waldtmann. Spin-liquid phase of the multiple-spin exchange hamiltonian on the triangular lattice. *Phys. Rev. B*, 60:1064, 1999.
52. R. Moessner and S. L. Sondhi. Resonating valence bond phase in the triangular lattice quantum dimer model. *Phys. Rev. Lett.*, 86:1881, 2001.
53. R. Moessner and S. L. Sondhi. Three-dimensional resonating-valence-bond liquids and their excitations. *Phys. Rev. B*, 68:184512, 2003.
54. G. Moore and N. Read. Nonabelions in the fractional quantum hall effect. *Nucl. Phys. B*, 360:362, 1991.
55. O. I. Motrunich and T. Senthil. Exotic order in simple models of bosonic systems. *Phys. Rev. Lett.*, 89:277004, 2002.
56. T. Neupert, L. Santos, C. Chamon, and C. Mudry. Fractional quantum Hall states at zero magnetic field. *Phys. Rev. Lett.*, 106:236804, 2011.
57. Gunnar Nordstrom and Uber die Moglichkeit. On the possibility of a unification of the electromagnetic and gravitational fields. *Physik. Zeitschr.*, 15:504, 1914.
58. W. Pauli. Relativistic field theories of elementary particles. *Rev. Mod. Phys.*, 13:203, 1941.
59. H. David Politzer. Reliable perturbative results for strong interactions? *Phys. Rev. Lett.*, 30:1346, 1973.
60. Iuliana P. Radu, J. B. Miller, C. M. Marcus, M. A. Kastner, L. N. Pfeiffer, and K. W. West. Quasiparticle tunneling in the fractional quantum hall state at $\nu = 5/2$. *Science*, 320:899, 2008.
61. Ying Ran, Michael Hermele, Patrick A. Lee, and Xiao-Gang Wen. Projected wavefunction study of spin-1/2 heisenberg model on the kagome lattice. *Phys. Rev. Lett.*, 98:117205, 2007.
62. Ying Ran, Wing-Ho Ko, Patrick A. Lee, and Xiao-Gang Wen. Spontaneous parity breaking and spin ordering of dirac spin liquid in a magnetic field. *Phys. Rev. Lett.*, 102:047205, 2009.
63. N. Read. Wavefunctions and counting formulas for quasiholes of clustered quantum hall states on a sphere. *Phys. Rev. B*, 73:245334, 2006.
64. N. Read and Subir Sachdev. Large-N expansion for frustrated quantum antiferromagnets. *Phys. Rev. Lett.*, 66:1773, 1991.
65. Robert Savit. Duality in field theory and statistical systems. *Rev. Mod. Phys.*, 52:453, 1980.
66. A. Seidel. Pfaffian statistics through adiabatic transport in the 1D coherent state. *Phys. Rev. Lett.*, 101:196802, 2008.
67. A. Seidel. S-duality constraints on 1D patterns associated with fractional quantum Hall states. *Phys. Rev. Lett.*, 105:026802, 2010.
68. Alexander Seidel and Dung-Hai Lee. Abelian and non-abelian hall liquids and charge density wave: Quantum number fractionalization in one and two dimensions. *Phys. Rev. Lett.*, 97:056804, 2006.
69. Alexander Seidel and Dung-Hai Lee. Domain wall type defects as anyons in phase space. *Phys. Rev. B*, 76:155101, 2007.
70. Alexander Seidel and Kun Yang. Halperin (m, m',n) bilayer quantum hall states on thin cylinders. 2008.
71. D. N. Sheng, Z.-C. Gu, K. Sun, and L. Sheng. Fractional quantum Hall effect in the absence of Landau levels. *Nature*, 2:389, 2011.
72. Steven H. Simon, E. H. Rezayi, and Nigel R. Cooper. Pseudopotentials for multi-particle interactions in the quantum hall regime. *Phys. Rev. B*, 75:195306, 2007.
73. K. Sun, Z.-C. Gu, H. Katsura, and S. D. Sarma. Nearly-flat bands with nontrivial topology. *Phys. Rev. Lett.*, 106:236803, 2011.
74. I. Tamm. *Z. Phys.*, 71:141, 1931.
75. Evelyn Tang, Jia-Wei Mei, and Xiao-Gang Wen. High temperature fractional quantum hall states. *Phys. Rev. Lett.*, 106:236802, 2011.
76. D. C. Tsui, H. L. Stormer, and A. C. Gossard. Two-dimensional magnetotransport in the extreme quantum limit. *Phys. Rev. Lett.*, 48:1559–1562, 1982.

77. Xiao-Gang Wen. Vacuum degeneracy of chiral spin state in compactified spaces. *Phys. Rev. B*, 40:7387, 1989.
78. Xiao-Gang Wen. Topological orders in rigid states. *Int. J. Mod. Phys. B*, 4:239, 1990.
79. Xiao-Gang Wen. Mean-field theory of spin-liquid states with finite energy gap and topological orders. *Phys. Rev. B*, 44:2664, 1991.
80. Xiao-Gang Wen. Non-abelian statistics in the FQH states. *Phys. Rev. Lett.*, 66:802, 1991.
81. Xiao-Gang Wen. Origin of gauge bosons from strong quantum correlations (origin of light). *Phys. Rev. Lett.*, 88:11602, 2002.
82. Xiao-Gang Wen. Artificial light and quantum order in systems of screened dipoles. *Phys. Rev. B*, 68:115413, 2003.
83. Xiao-Gang Wen. Quantum order from string-net condensations and origin of light and massless fermions. *Phys. Rev. D*, 68:065003, 2003.
84. Xiao-Gang Wen and Zhenghan Wang. Classification of symmetric polynomials of infinite variables: Construction of abelian and non-abelian quantum hall states. *Phys. Rev. B*, 77:235108, 2008.
85. Xiao-Gang Wen and Zhenghan Wang. Topological properties of abelian and non-abelian quantum hall states from the pattern of zeros. *Phys. Rev. B*, 78:155109, 2008.
86. Xiao-Gang Wen, F. Wilczek, and A. Zee. Chiral spin states and superconductivity. *Phys. Rev. B*, 39:11413, 1989.
87. Hermann Weyl. *Space, Time, Matter*. Dover, 1952.
88. F. Wilczek. Quantum mechanics of fractional-spin particles. *Phys. Rev. Lett.*, 49:957, 1982.
89. F. Wilczek. Remarks on Dyons. *Phys. Rev. Lett.*, 48:1146 – 1149, 1982.
90. R. Willett, J. P. Eisenstein, H. L. Strörmer, D. C. Tsui, A. C. Gossard, and J. H. English. *Phys. Rev. Lett.*, 59:1776, 1987.
91. Kenneth G. Wilson. Confinement of quarks. *Phys. Rev. D*, 10:2445, 1974.
92. E. Witten. *Nucl. Phys. B*, 149:285, 1979.
93. C. S. Wu et al. Experimental test of parity conservation in beta decay. *Phys. Rev.*, 105:1413, 1957.
94. S. Yan, D. A. Huse, and S. R. White. Spin Liquid Ground State of the $S = 1/2$ Kagome Heisenberg Model. *Science*, 332:1173 – 1176, 2011.
95. C. N. Yang and R. L. Mills. Conservation of isotopic spin and isotopic gauge invariance. *Phys. Rev.*, 96:191, 1954.
96. W. Zhu, S. S. Gong, and D. N. Sheng. Chiral and critical spin liquids in a spin-1/2 kagome antiferromagnet. *Phys. Rev. B*, 92(1):014424, 2015.